MEMO^2: MEthane goes MObile – MEasurements and MOdelling

MEMO^2 – 2nd Periodic Report

Period: 1 March 2019 – 28 February 2021

Lead author

Dr. S. Walter

Utrecht University, Institute for Marine and Atmospheric Research Utrecht (IMAU)

Princetonplein 5
3584CC Utrecht
The Netherlands

Phone: +31 (0)30 253 3167 /
Email : s.walter@uu.nl

Delivery month Annex I	50		
Actual delivery month	50		
Lead participant: UU	Work package: 5	Nature: R	Dissemination level: PU
Version: 1			

This project has received funding from the European Union's Horizon 2020 research and innovation programme under the Marie Sklodowska-Curie grant agreement No 722479.

Table of contents

Abbreviations

AirCore	Atmospheric Sampling System
AGH	Akademia Gorniczo-Hutnicza im. Stanislawa Staszics w Krakowie, Krakow, Poland
C_2H_6	Ethane
CH_4	Methane
CHIMERE	Multi-scale chemistry-transport model for atmospheric composition analysis and forecast
CoMet	Carbon Dioxice and Methane Mission
CRDS	Cavity Ring-Down Spectroscopy
D	Deliverable
DFB-QCL	Single-Mode QCL
DTU	Technical University of Denmark
ECCC	Environment and Climate Change Canada
EDGAR	Emissions Database for Global Atmospheric Research
EMPA	Eidgenössische Materialprüfungs, und Forschungsanstalt, Dübendorf, Switzerland
ESR	Early Stage Researcher
FTIR	Fourier-Transform Infrared Spectroscopy
GEOMAR	Helmholtz Centre for Ocean Research Kiel
GPS	Global Positioning System
GRAL	Graz Lagrangian Model
ICL	Interband Cascade Laser
ICOS	Pan-European research infrastructure for quantifying and understanding the greenhouse gas balance of Europe and its neighbouring regions
INCAS	National Institute for Aerospace Research "Elie Carafoli"
InGOS	Research infrastructure targeted at improving and extending the European observation capacity for non-CO_2 greenhouse gases
IRMS	Isotope Ratio Mass Spectrometry
LGR	Los Gatos Research
LMDz	Laboratoire de Météorologie Dynamique zoom, general circulation / global climate model
LU	Lunds Universitet, Lund, Sweden
MicroHH	Large-Eddy Simulation code
MS	Milestone
PPB	Parts Per Billion
PPM	Parts Per Million
Python	Programming language
QCL	Quantum Cascade Laser
R	Programming language / software environment for statistical computing and graphics
RANS	Reynolds-averaged Navier–Stokes equations
RHUL	Royal Holloway and Bedford New college, London, United Kingdom
RUG	Rijksuniversiteit Groningen, Groningen, The Netherlands
SLU	Swedish University of Agricultural Science
TNO MACC	Monitoring Atmospheric Composition and Climate – Emission data set (https://cordis.europa.eu/project/rcn/91167/factsheet/en)
TO-3	Transistor Outline, standardized metal semiconductor package incl. transistors, rectifiers and circuits
UAV	Unmanned Aerial Vehicle
UHEI	Ruprecht-Karls-Universität Heidelberg, Heidelberg, Germany
UU	Universiteit Utrecht, Utrecht, The Netherlands
UVSQ	Université de Versailles Saint-Quentin-en-Yvelines, Paris, France
WDCGG	World Data Center for Greenhouse Gases
WP	Work Package
WU	Wageningen Universiteit, Wageningen, The Netherlands

Figures and Tables are numbered continuously per chapter.

1. Overall summary

MEMO² ran smoothly and successfully and ended officially 28 February 2021. All beneficiaries and partner organisations were engaged and committed to the project. The consortium has not changed in this reporting period and consisted of 9 beneficiaries and 16 partner organisations. Scientifically, the third year was dedicated to continuing data collection, data evaluation and interpretation, and modelling activities. The fourth and final year focussed on further scientific evaluation and data publication and was also affected by the current Covid19-pandemic. As all ESR had sufficient data collected and most of them were close to the submission of their publications and theses, the impact of the pandemic was limited mainly on the celerity of data evaluation and progress in writing.

In total 16 deliverables and 8 milestones were due in the second reporting period. Except for one milestone all of them have been submitted respectively achieved. A few showed a slight delay such as those about improved isotopic source signatures or emission factors, European CH_4 emissions or related publications. The delay is - paradoxically - mainly caused by the high measurement activities and good data situation. Particularly for these deliverables the higher number of new data results in a better representativeness, e.g. for source signatures or emission factors. The implementation of these data increased the quality of the deliverables. The measurement and sample collection campaigns are described in the individual ESR reports (Chapter 6). Several data sets are published or close to publication, others are still under evaluation. As several ESRs are employed beyond the project lifetime, the publication of results is ongoing.

MEMO² is actively disseminating results and network activities by using several platforms, such as the project website, scientific conferences and social media (see Chapter 3). This is lasting also beyond the project.

The training activities are completed. All ESRs have made at least two secondments (Table 2.5), and have presented their results at least at two international conferences (Table 3.1). MEMO² aimed for an ensemble of training actions that should enable the ESRs to build-up a career either within the scientific community, or in the non-academic sector. Most of the ESRs at the end of the project have already defended their theses or are close to it, and several also found new positions inside and outside academia. Therefore, the training goals are considered to have been achieved.

Highlight of the second reporting period was a joint field campaign in Romania. ROMEO – ROmanian Methane Emissions from Oil & gas - was organised by the UU in collaboration with the MEMO² consortium. Executing such a campaign was one of the flagship activities the consortium was advised to implement by the SAB at the beginning of the project. The consortium decided to organise it in addition to the three intensive campaigns already executed in the Netherlands (MEMO²) and Poland (CoMet).

ROMEO aimed for the improvement of emission verification and offered an excellent opportunity for the MEMO² ESRs to learn about the complexity of logistical and scientific challenges when planning and executing a joint field campaign in collaboration with several research groups. The ROMEO data are unique and high-quality. They are implemented in the MEMO² data sets and used widely for the modelling activities, which is also a reason for the slight delay of the deliverables. As the campaign was highly successful, a follow-up was proposed and funded externally. However, the execution of the second campaign is delayed due to the current pandemic situation. More details about the campaigns are given in Chapter 2.2.1.2, Task 1.4.

Further results of MEMO², with respect to the recently released EU methane strategy and the implementation of independent verification of emissions by atmospheric measurements, are:

Urban CH4 emissions: CH_4 leaks in cities can be detected and quantified at the street-level with mobile high precision analysers. Studies have been carried out in >10 EU cities and, in collaboration with interested network operators, those measurements are ready to be rolled out at larger scale.

Emission attribution: MEMO² activities have significantly advanced the attribution of methane plumes from unknown sources by isotope and multi-tracer analysis, particularly in cities, but also regarding the evaluation of long-time isotope measurement time series, which were carried out within the project.

Coal mining: MEMO², in collaboration with CoMet, quantified the CH_4 emissions from the Upper Silesian coal mining area. The collaboration and its results contribute to the development of an independent and objective emission monitoring system.

Modelling: Micro-scale plume modelling has been significantly improved. Those models e.g. help to simulate a measurement day as we had during our field campaign in Romania and improve sampling and measurement strategies. Measurement strategies are also supported by detailed error estimations for common meso-scale models.

2. MEMO² – Explanation of work and overview of progress

2.1 Objectives

Within MEMO² we defined several objectives to target our main goals, which have not changed over time and were still valid in the second reporting period of the project.

The main scientific goals of MEMO² were to I) develop and apply innovative experimental and modelling tools, based on recently developed mobile analysers, on state-of-the-art isotope techniques, and on a hierarchy of models, including newly developed high-resolution dispersion models, II) to identify and quantify CH_4 emissions from local sources in Europe and use these updated emissions to III) improve estimates at the European scale. These tools enable the scientific and non-academic communities to improve the objective verification of CH_4 emission reduction strategies for specific source sectors.

The main training goal was to educate a generation of "cross–thinking" scientists that will be able to effectively develop and use novel measurement and modelling tools in an interdisciplinary and intersectoral context. A dedicated training program included original actions to reinforce the autonomy (learning by doing approaches) and the maturity (student autonomous virtual network) of the MEMO² early stage researchers (ESRs). This ensemble of training actions should help them to refine their career plan, either within the scientific community, or in the non-academic sector. As most of the ESRs at the end of the project either have already defended their theses or are close to it, and several also found new positions inside and outside academia, the training goals are considered to have been achieved.

The following **MEMO² objectives** were defined:

- Implementation of a mobile CH_4 measurement network across Europe that can be used for detection and quantification of sources, verification of mitigation measures, and for developing refined emission estimates
- Development of innovative new mobile CH_4 measurement systems (e.g. by using unmanned aerial vehicles (UAVs))
- Training of researchers to utilize and develop methods / tools for detection, quantification, and verification of greenhouse gases such as CH_4
- Augmentation of the established training programs at individual institutions with an innovative network training that incorporates direct links with non-academic partners
- Development and application of novel modelling tools to refine local emission estimates from mobile and isotope measurements
- Derivation of a new bottom-up CH_4 emission map, including isotopic information, across Europe
- Derivation of top-down emission estimates over Europe exploiting information acquired in MEMO².
- Fostering close collaboration between the academic and non-academic sector by joint activities

As in the years before the consortium continued I) the maintenance and further evolvement of measurement networks, II) the evaluation of developed measurement systems and modelling tools, and III) the continuation of training and collaboration activities inside and outside the consortium.

Scientifically, the second reporting period was dedicated to continue data collection, data evaluation and modelling activities towards the above-mentioned objectives, and to publish the results.

The following chapters describe the progress of MEMO² towards the goals and objectives in more detail.

2.2 General progress of the Work Packages

MEMO² was organised in five work packages (WPs): three scientific WPs, one training WP and one management WP. In the second reporting period of MEMO² only small changes or adjustments were made according to shifts in the secondments to ensure their usefulness for the ESRs. The changes had no significant impact on the project, neither scientifically nor administratively. The last year was affected by the current Covid19-pandemic. As all ESR had sufficient data collected and most of them were close to the submission of their publications and theses, the impact of the pandemic was limited.

2.2.1 WP1 – Mobile measurements of CH4 (Lead: Martina Schmidt, UHEI)

2.2.1.1 General WP overview and contribution of involved beneficiaries

Within WP1 – Mobile measurements of CH_4 (including primarily the ESRs 1-7 from the beneficiaries UHEI, RUG, AGH, LU, UVSQ, EMPA, and RHUL) – we aimed for identification, quantification, and monitoring of CH_4 plumes of major anthropogenic and natural CH_4 emitters in Europe from mobile platforms. The ESRs in WP1 further developed the instrumentation needed for mobile measurements and executed several (joint) measurement campaigns to gather data.

RUG performed a joint campaign together with TNO (ECN) at the Grijpskerk farm, NL, to quantify dairy farm CH_4 emissions in March 2019. Numerous flights downwind of the farm during the period from March 2017 to March 2019 have been used to calculate the CH_4 emission rates. Furthermore, the CH_4 emissions from manure on site were estimated, which allowed to estimate the CH_4 emissions per cow per year. The results will be published soon. Besides these activities, RUG participated in the ROMEO campaign and made 65 UAV flights downwind of 22 oil wells and oil facilities, from which CH_4 emissions have been determined using a mass balance approach. RUG also participated in a joint tracer release campaign together with EMPA and UHEI with drone-based active AirCore observations. RUG is collaborating with the UU, UHEI and AGH on scaling up the emissions to derive a total of basin-scale emissions.

UVSQ analysed the data from campaigns carried out during the second year of MEMO². The results have been implemented in a publication that has been recently accepted in Environmental Science & Technology in March 2021. Additional campaigns, e.g. on landfills and gas compressor stations were conducted in 2020 and all data were analysed and used for the PhD thesis of ESR5. UVSQ has also taken part in a release test organized by NPL. The aim was to compare and verify different methods used to quantify emissions. This will result in a publication as co-author for ESR5. Some of the results from the release experiment and the additional campaigns were also used in a publication about ethane:methane ratios (Defratyka et al. 2021, https://doi.org/10.5194/amt-2020-410, under discussion).

EMPA finalised the lightweight quantum cascade laser spectrometer for UAV based CH_4 measurements. The results were characterized and validated. In addition to the CH_4 concentrations, the instrument was equipped with sensors for temperature, pressure and GPS position. To improve the accuracy, a high-precision RTK GPS system was installed, and a battery powered ground station was developed. Real-time data transfer was implemented, which required the addition of a dedicated ground station antenna to provide a stable data link with the spectrometer. The instrument was extensively used by ESR6 during the ROMEO campaign (Oct/Nov 2019) in Romania and during a CH_4 release experiment (Feb 2020) at EMPA in Dübendorf. 56 mass balance measurements were performed on oil and gas wells in Romania. All data has been made available to the modellers of MEMO².

A publication on the laser spectrometer is published in Atmospheric Measurement Techniques (Tuzson et al. 2020, https://doi.org/10.5194/amt-13-4715-2020).

UHEI carried out mobile CH_4 and $^{13}CH_4$ measurement with AirCores in the region of Heidelberg with more than 20 site visits in 2019 and 2020. ESR1 participated in a CH_4 release experiment (Feb 2020) at EMPA in Dübendorf in order to test the OTM33a (Brantley et al. 2014) method. The main focus in the last year of the project was on the data evaluation to determine the CH_4 emissions with Gaussian plume model and OTM33a. The OTM33a method was applied for quantification of point sources like oil and gas wells during the ROMEO campaign (Oct/Nov 2019) in Romania. More than 100 determinations of CH_4 emission from oil and gas wells in Romania have been successfully computed. A joined publication together with AGH and UU is in preparation and will be submitted in 2021. In February 2020 UHEI organised the 3rd Annual Meeting of MEMO² and an associated ROMEO workshop.

RHUL focussed on mobile CH_4 measurement during UK city surveys (London, Swansea (ESR9), Birmingham (ESR7)), in conjunction with the UN CCACC Cities project, and in Bucharest (ESR9), in conjunction with the UN CCAC Romeo project. In the UK these surveys identified leaks in the gas distribution system as the main city source, with wastewater treatment plants and landfill sites becoming more important in peripheral areas, whereas in Bucharest the main sources are the city wastewater pipes. The second focus (ESR7) has been on waste CH_4 sources, primarily biogas plants and landfill sites. A paper on UK biogas plant CH_4 emissions has been published recently (Bakkaloglu, et al. 2021, https://www.sciencedirect.com/science/article/pii/S0956053X21000167). Surveys have been conducted downwind of 50 biogas sites, with 8 chosen for repeat multiple plume passes and flux calculations by the end of year 3. The ESR7 secondment with Viridor allowed access to 4 landfill sites in SW England, to assess differences before and after closure, during reopening of an old site, and seasonal variations in topsoil oxidation rates.

At **LU**, ESR4 focussed on CH_4 emissions from natural sources such as wetlands from the microscale to the landscape scale using different methods for quantification. These methods ranged from chamber measurements, mobile CH_4 measurements and eddy-covariance measurements to flight campaigns. Chamber measurements of CH_4 and CH_4 isotopes were conducted to quantify the spatial heterogeneity on the microscale on a wetland (Mycklemossen). ESR4 also measured CH_4 emissions in a subarctic environment (Abisko). Results have been published recently (Lakomiec et al. 2021, https://bg.copernicus.org/preprints/bg-2021-81/). During both campaigns bag samples were taken for analysis of isotopic signature, executed at the isotopic labs at RHUL and UU. ESR4 was joined by ESR6, who did his secondment with drone test flights at the ICOS station Hyltemossa and over Mycklemossen mire. ESR4 was seconded to Avfall Sverige to quantify CH_4 emissions and compare measurement methods over landfills. He also participated in the ROMEO campaign.

At **UU**, both ESRs were strongly involved in the CoMet campaigns and the ROMEO campaign. Data are currently in preparation for publication. ESR10 contributed to a paper by the COMET group from DLR that was published in 2019 (Fiehn et al., 2020, https://doi.org/10.5194/acp-20-12675-2020) and on the quantification of CH_4 emissions from the Munich Oktoberfest (Chen et al. 2020, https://doi.org/10.5194/acp-20-3683-2020). In collaboration with TNO and Staatstoezicht op de Mijnen, ESR10 participated in a campaign to investigate the status of CH_4 emissions from abandoned coal mining sites and closed oil and gas wells in the Netherlands. A paper on street level CH_4 emission estimates in Hamburg and Utrecht has been published recently (Maazallahi et al. 2021, https://doi.org/10.5194/acp-20-14717-2020). ESR8 characterised methane sources at several sites and published the results of Lutjewad (Menoud et al. 2020, https://doi.org/10.5194/acp-20-14717-2020), and established an isotope database which is publicly available (Menoud et al. 2021, http://doi.org/10.5281/zenodo.4062356). Two publications on the long-term isotope dataset from Krakow and the measurements during the ROMEO campaign are prepared (on in review, one under co-author review).

At **AGH**, ESR3 focussed on the performance tests of analyser signals including a wide calibration range for CH_4 concentration, water cross-sensitivity, the influence of the ethane concentration on the

measured CH_4 concentration, and comparisons between instruments (Picarro G2201i and LGR MGGA918). ESR3 constructed a simple, low weight static chamber. The chamber, together with a portable LGR analyser, was deployed in order to determine the CH_4 release rate at e.g. coal mine waste dumps. ESR3 carried out measurement campaigns with vehicles to determine emissions from coal mine shafts in the USCB. She also visited coal mining locations in the Ruhrgebiet (Germany) and LSCB (Poland) regions. CH_4 isotope signatures of the plumes from the coal mining shafts were carried on at 38 individually localized CH_4 sources (23 ventilation shafts and 15 hard coal mining waste dumps). During the last year ESR3 focused on the data evaluation and publication.

2.2.1.2 Progress of WP tasks

Task 1.1 Surface-based mobile CH_4 measurements on vehicles (Lead: UHEI, Martina Schmidt)

ESRs 1-5 & 7 will use mobile CH_4 analysers on vehicles to monitor and quantify the main emitters in their respective hosting countries, (DE, NL, FR, PL, UK, SE), by performing regular measurement campaigns, in cooperation with non-academic partners. This includes tracer release experiments and multi-tracer analysis. Methodology, data and findings will be shared among the ESRs to assess the EU scale. Event samples will be collected and analysed for $^{13}CH_4$ and CH_3D at RHUL or UU (cooperation with WP2). ESRs from UVSQ, UHEI and AGH will also carry out in-situ $^{13}CH_4$ source signature measurements.

All ESRs within this task performed several campaigns measuring CH_4 concentrations downwind of different CH_4 emitters. Fig. 2.1 summarises the regions, campaigns and the CH_4 source types, which were visited with mobile measurement equipment by the individual ESRs. ESR3 focused on measurements in Poland, mainly in the region of Upper Silesia, whereas ESR4 made measurements at wetlands in Sweden. With this setup, we were able to cover many European regions and many typical CH_4 sources like wetland, farms, landfills, biogas plants, as well as coal mines, gas compressor stations and oil and gas wells.

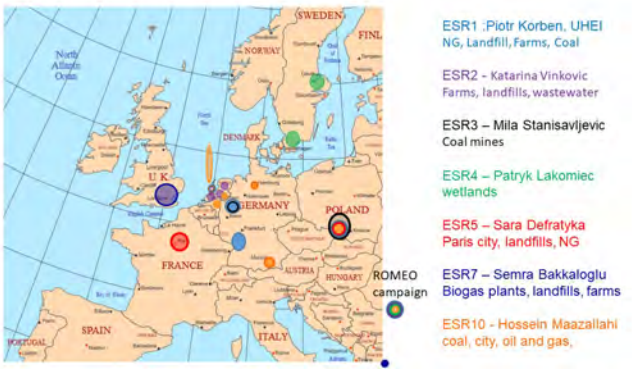

Fig. 2.1: Map of mobile CH_4 measurement performed by 7 MEMO² ESRs

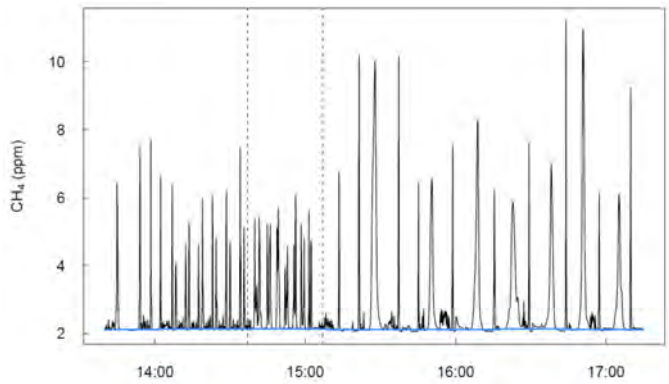

Fig. 2.2: Measurements of CH_4 plume crossings of a farm with a biogas plant close to Heidelberg.

In addition, systematic screening of city emissions has been carried out in e.g. Paris, London, Birmingham, Swansea, Hamburg, Utrecht, Groningen, Katowice, and Bucharest. ESR1 focused on CH_4 sources in the region around Heidelberg and participated to the ROMEO campaign in Romania. UHEI monitored the CH_4 enhancements downwind of a landfill, a biogas plant two gas compressor stations, and two farms in the region of Baden Württemberg. More details about the executed campaigns are given in the individual ESR reports (Chapter 6).

Fig. 2.2 shows a typical measurement, performed close to a farm with a biogas plant in the region of Heidelberg. When a peak is detected, several crossings are performed to get a better statistic. Here ESR1 measured during 4 hours with the goal to monitor also temporal variations. During the first half, the CH_4 concentration varies between 4 and 7 ppb, later between 6 and 10 ppb. A detailed evaluation of the data collected within the last two years is in progress and will be published in papers and respective PhD theses.

A different strategy has been applied during city measurements. Fig. 2.3 shows an example of surveys in the city of Paris, performed by ESR5. Initial surveys were used to identify areas of the greatest elevated CH_4 concentrations, designated as 'hot spots'.

Two hot spot areas were identified: 1) on the west-south part of inner Paris (Fig. 2.3, area A), and 2) hot spot area B on west-south suburbs (Fig. 2.3, area B).

Five days of repeated surveys focused on both hot spots A and B (respectively three and two days). In total, hot spots A and B represent respectively 16 % (118 km) and 25 % (183 km) of the total surveys' mileage.

The developed guideline of good practice (D1.5) and the collaboration between students during secondments and joint campaigns helped a lot to harmonise the performance of measurements in the field. After four years of MEMO², a large number of data has been collected and stored on the ICOS data base. In 2020/2021 the students focused on the data evaluation and the calculation of emission factors for each source category (see also Task 1.5).

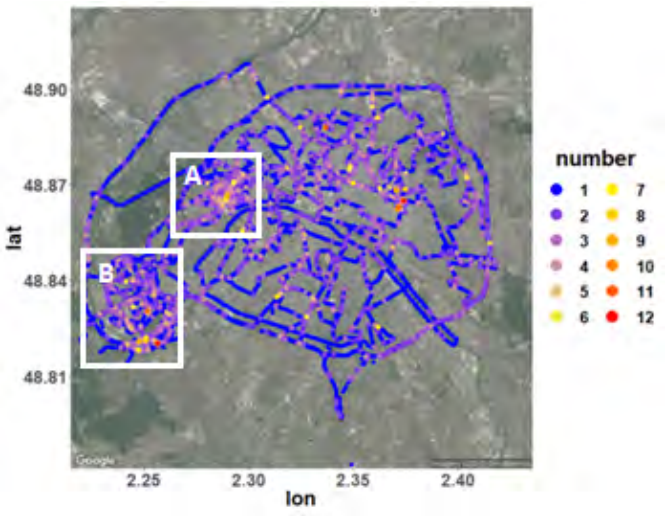

Fig. 2.3: Number of a revisit of the particular area during Paris surveys; A - hot spot area A, B – hot spot area B

Task 1.2 Airborne measurements of CH4 on airplanes and UAVs (Lead: LU, Jutta Holst)

Natural CH_4 emissions from wetlands and lakes will be monitored in Sweden using a small research aircraft from LU. Inflow and outflow CH_4 concentrations of a major source area will be determined at different times throughout the year to derive total CH_4 emissions. Air samples and AirCore (see Task 1.3) samples will be collected using UAVs to map CH_4 plumes. The lightweight CH_4 spectrometer (Task 1.3) will be deployed on a UAV by Empa to study CH_4 emissions of rivers and lakes in Switzerland. Air samples will be collected on the aircraft and on UAVs for isotope analysis (cooperation with WP2).

The focus of the airborne campaigns in 2019 was on the seasonal variation of CH_4 fluxes from a smaller wetland (Florarna, Uppland) close to the ICOS research sites Norunda, approx. 100 km north of Stockholm and a post forest fire area in the centre of Sweden close to Ljusdal (Kårböle, Hälsingland). The fire in 2018 affected 23475 acres of forest. Due to the reduced active biomass, an increase in water table depth and soil moisture was expected that will influence the microbial activity in the soil. Depending on the severity of the damage to the soil and microbial community, CH_4 fluxes were expected to increase in the years after the forest fire, but the lowered water table led to a reduction of both summertime CO_2 uptake and CH_4 emission, and annual exchange of these GHGs (Rinne et al. 2020, http://dx.doi.org/10.1098/rstb.2019.0517).

The airborne measurement campaign in July 2019 was a first inventory of the situation on the landscape scale. Follow-up flights were planned for 2020 and 2021 (part of the video taken during the research flight on 2019-07-20 is available via https://www.youtube.com/watch?v=DhQqZwgxw-Q). The measurement campaigns were performed in collaboration with several research projects focusing on the post forest-fire ecological development, greenhouse gas (GHG) and energy fluxes at the site scale as well as respiration and BVOC exchange on the microscale using chambers. The area of airborne measurements covered a typical Swedish landscape with coniferous dominated forest and imbedded smaller patches of wetland. A thorough footprint analysis was done to disaggregate the influence of the different landcover types. Identical flight patterns were flown on three consecutive days. Depending on the weather conditions, one flight in the early morning hours and one flight in the early afternoon were scheduled. Due to the expected small source and the large heterogeneity of the area the mass balance

approach could not be applied. Instead, long straight horizontal flight paths at constant height for direct calculation of the GHG and energy fluxes at three different heights were performed.

Measurements over the wetland Florarna were performed once per month from early (June) to late (September) summer 2019. The observed CH_4 fluxes were low, close to the detection limit of the system. Florarna was as large parts of Sweden strongly affected by the drought in 2018 resulting in very low water table depths, which only slowly came back to normal in autumn 2019. It was thus expected that the CH_4 fluxes have still been reduced in 2019 due to the weather conditions in 2018.

The analyses of the airborne data were the focus of 2020. Follow-up flights and measurement campaigns were strongly influenced by the situation due to covid-19 pandemic. In the end of the measurement season, the CH_4 analyser was sent to the manufacturer in the US for the exchange of valves. Due to the lock-down in the US, it is unclear when the analyser can be returned to Sweden.

The results on CH_4 emissions from wetland and lakes in Sweden has been published recently (Lakomiec et al. 2021, https://bg.copernicus.org/preprints/bg-2021-81/). A short overview report about the outcomes has been submitted as deliverable D1.2.

Task 1.3 Development of lightweight sensors and AirCore (Lead: Empa, Lukas Emmenegger)

Partner Empa will develop a lightweight high-precision CH_4 sensor-based quantum cascade lasers (QCL) and interband cascade lasers (ICL) for UAV application. High-precision 3-D measurements of CH_4 will be developed at RUG using a lightweight active AirCore aboard a UAV. The lightweight spectrometer and the active AirCore will be simultaneously deployed on UAVs and compared during a joint measurement campaign.

A lightweight, high-precision CH_4 spectrometer based on a quantum cascade laser (QCL) has been developed at Empa and deployed in several studies in collaboration with MEMO² ESRs (Fig. 2.4). The open-path absorption spectrometer is based on a single-mode quantum cascade laser (DFB-QCL) and includes a novel circular, segmented multi-pass cell with an optical path length of 10 m. The instrument weighs 2.1 kg (including battery) and has an average power consumption of 18 W. Low heat dissipation is achieved by intermittent continuous wave laser driving and a system-on-chip FPGA data acquisition module. The spectrometer is equipped with additional sensors for pressure, temperature and relative humidity, as well as a GPS receiver and an optional module for real-time data transmission. Therefore, it is possible to use the device aboard any drone, regardless of its specific communication protocol.

The sensor reaches a precision significantly below 1 ppb after 10 – 1000 s integration and has been regularly flown on a commercial drone (DJI Matrice 600). The open-path design allows very fast sampling, and absorption spectra are measured at > 10 kHz. This gives a wide flexibility in terms of the required precision and time resolution. For more details, see deliverable D1.1.

Fig. 2.4: Photograph of the CH_4 laser spectrometer with (left side) and without (right side) the protecting cover.

A lightweight active AirCore system that is capable of simultaneous measurements of CH_4, CO_2, and CO has been developed at RUG, which subsequently has been flown downwind of a dairy farm in Grijpskerk, NL, to quantify CH_4 emissions. Besides the profile measurements, the collected air samples were also used for CH_4 isotopic composition measurements by ESRs in Utrecht and London. Furthermore, collaborations with ESRs at Empa and in Wageningen on both field campaigns and modelling work have been executed.

In the last 12 months, both the lightweight CH4 spectrometer and the active AirCore system have been successfully used during individual regional measurement campaigns, the ROMEO campaign and the Dübendorf release Experiment.

Task 1.4 Intensive campaigns (Lead: RUG, Huilin Chen)

Two intensive campaigns involving all ESRs and numerous instruments will be carried out to train the ESRs and improve methodologies to quantify CH_4 emissions. The first campaign (month 12) will be performed at an agricultural farm in Dronten, The Netherlands, with very simple topography and easy logistics. The second campaign (month 30) will be carried out at the European CH_4 emission hotspot upper Silesia (Poland), an industrialized region with a dense network of coalmines.

The two campaigns took place in the first reporting period and have been submitted as milestone MS2, and deliverable D1.3. Although this task was formally completed, the consortium decided to execute a third one - ROMEO. Executing such a campaign was one of the flagship activities the consortium was advised to implement by the SAB at the beginning of the project.

The **ROMEO** campaign (**RO**manian **M**ethane **E**missions from **O**il and Gas), organised and executed by the UU, offered an excellent opportunity for the MEMO² ESRs to learn about the complexity of logistical and scientific challenges, planning and executing a joint field campaign, and to gain unique and high-quality data in collaboration with several research groups. The organisation and execution of ROMEO was funded through the Climate and Clean Air Coalition (CCAC) international methane science studies (https://www.ccacoalition.org/en/activity/oil-and-gas-methane-science-studies), administered through the United Nations Environment Program. Final results of several groups / ESRs are close to submission.

According to UNFCCC statistics, Romania is one of the European Countries that reported highest emissions of CH_4 from the oil and gas sector to the atmosphere, in particular related to CH_4 production and end use. However, the estimates reported by Romania are derived using non-country specific emission factors and there are only very few observations which investigate whether the reported emissions are realistic.

The measurements carried out provide an experimental quantification of CH_4 emissions from the oil and gas sector in Romania and can help in devising emission mitigation strategies. CH_4 emission quantifications were executed on three different scales - the exploration basin scale, the well scale and the city scale – by using different mobile platforms such as aircrafts, drones, and cars. The practical part of ROMEO took place 02 - 07.08.2019 (city scale part) and 30.09. – 20.10.2019 (basin & well scale part). Due to the administrative and logistical complexity of the campaign and the very narrow time frame for the practical part, the organisation of ROMEO started already in February 2019. The evaluation and publication of data is ongoing and will last beyond MEMO².

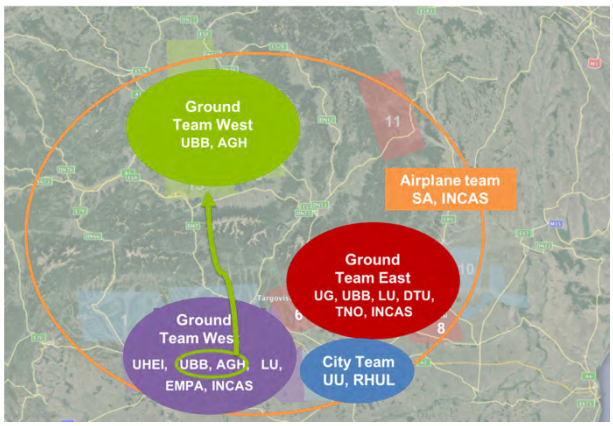

Fig. 2.5: distribution of teams in the field and the measurement areas

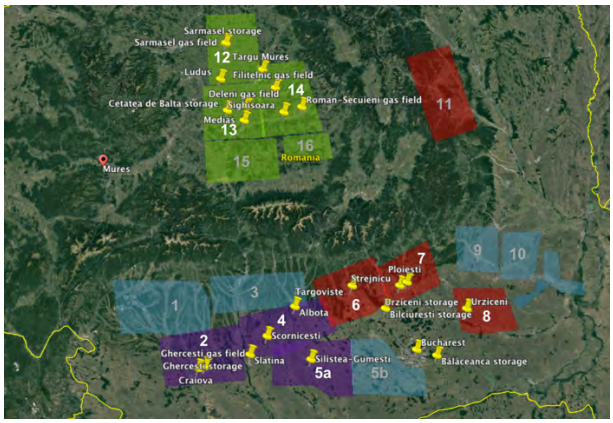

Fig. 2.6: Overview of the measurement areas

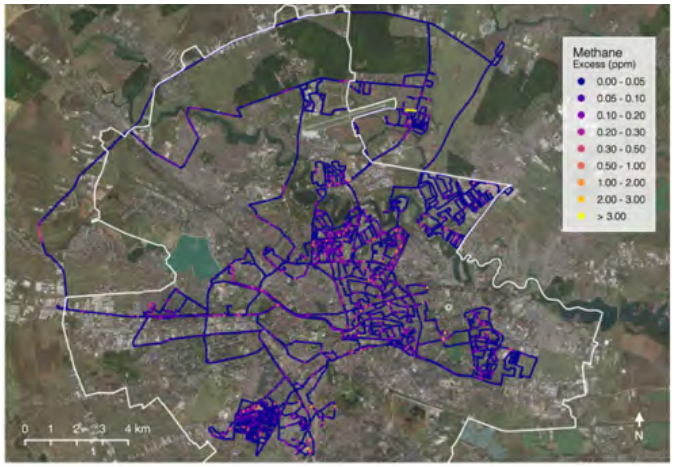

Fig. 2.7: Single data set of RHUL. Data sets of RHUL, UU and INCAS will be combined after evaluation.

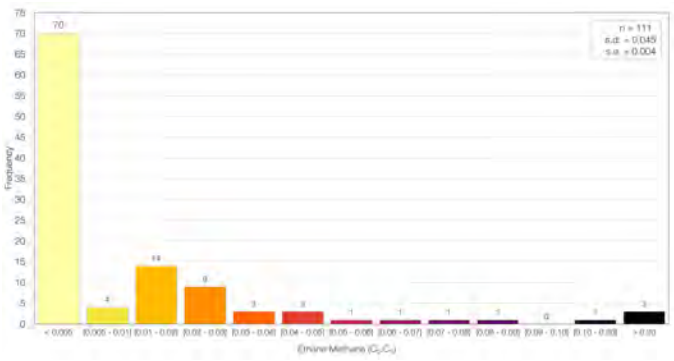

Fig. 2.8: Distribution of ethane:methane ratios for elevations encountered during the Bucharest city survey. Most of the elevations do not show ethane, indicating the dominance of biogenic sources in Bucharest

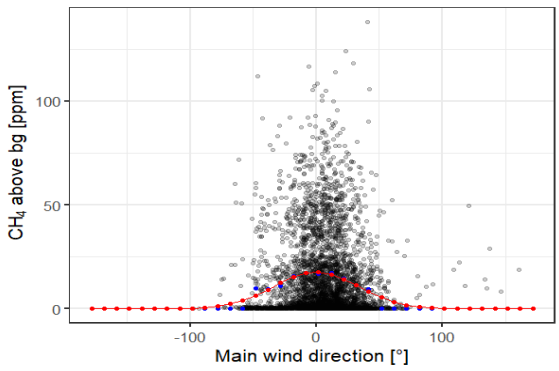

Fig. 2.9: Example of an OTM33A measurement during the ROMEO campaign Black points are individual measurements, blue dots are averages and red are the model results.

In total more than 80 participants of 18 institutes and universities contributed to the campaign, of which 75% in the field and 25% remote, including the MEMO² consortium and all ESRs. Fig. 2.5 gives an overview of the distribution of teams in the field and Fig. 2.6 about the measurement areas. The measurement areas were defined on the basis of public and confidentially available facility locations provided by the operator, and a-priori bottom-up inventories. The inventories were based on TNO's emission databases including all sources. The selected areas had an average size of 40x60 km, were logistically reachable within the constraints of ROMEO and suitable for the applied methods during the campaign.

The participants of the ground-based teams were distributed over two groups (Group West and Group East), each group with 6 teams. Each ground-based group measured at pre-selected facilities within 3 dedicated areas, whereas Group West split during the last week to also cover some of the northern parts in Transylvania. The airplane teams from Scientific Aviation and INCAS covered the areas 2, 4, and 5a as well as 6, 7, and 8. Additionally, one flight was made above mud volcanos between area 7 and 11.

The **City team** measured already in August 2019 due to logistical reasons. The teams from RHUL and UU joined our local partner from INCAS in Bucharest and the city was surveyed by three cars simultaneously. The INCAS team continued with measurements in Ploiesti.

Data from all surveys were combined to produce whole city maps of the emission locations. The data are uploaded to the ICOS carbon portal (https://www.icos-cp.eu). and a publication has been submitted for internal review by CCAC.

Fig. 2.7 shows the coverage of mobile measurements in the city of Bucharest. Methane enhancements of more than 3 ppm were observed. Besides the mobile measurements, spot samples for isotopic analysis and source attribution of methane elevations were taken in Bucharest and its suburbs, and also from Ploiesti. Results from the attribution using ethane:methane rations and isotopic composition demonstrate that the waste and wastewater system is the main source of methane in the city of Bucharest.

Figure 2.8 shows the results of the ethane:methane ratios. The majority of the samples shows no ethane content, indicating biogenic sources. This is supported by isotopic analysis of the collected bag samples. In Bucharest biogenic sources are also the source of larger methane elevations, whereas in Hamburg the lagest elevations originatd only from fossil sources.

During the main campaign in the oil and gas production region in Southern Romania, the **ground-based teams** visited more than 1000 individual facilities, of which 200 were quantified. All measurement data are available on the ICOS carbon portal (https://www.icos-cp.eu). All ground teams executed calibration measurement to be used in the data evaluation for correction and intercomparison of the data. Used methods were mass balance and Gaussian plume approaches, OTM33A (see Fig. 2.9 as an example), and Tracer gas dispersion models.

The evaluation of the data is finished. Two manuscripts are under co-author review and a third one is being prepared. At several facilities simultaneous measurements using different quantification methods were executed to be able to combine all quantifications into one dataset. The concentration elevations vary between one and several thousand ppm at distances between several meters to several ten meters away from the facility (Fig. 2.10 as an example). There is almost no gas flaring in the regions that we have visited, and often the visited methane collection infra-structure at production / separation / storage sites are visibly not in good state.

Fig. 2.10: Elevation of CH_4 at several oil & gas facilities (measured 1 Oct. 2019, area 6)

The **drone teams** performed more than 120 flights at individual facilities. CH_4 emission fluxes were mainly deter-mined using the mass balance method, e.g. by combining measured CH_4 mole fractions with the wind data obtained from the 3D sonic anemometer. Geostatistical interpolation (Kriging) of the measured CH_4 molar fractions was performed to spatially fill the gaps as illustrated in Fig. 2.12, for a flight with the QCLAS-drone system downwind of a given source perpendicular to the main wind direction at various altitudes above ground (Fig. 2.11). In this particular example, the emission flux computed is 1.53 g/s.

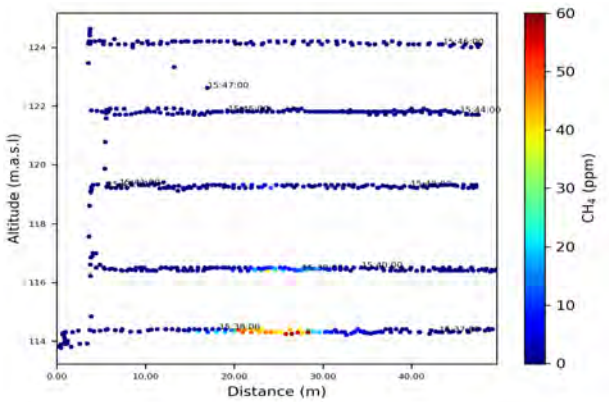

Fig. 2.11: Gridded measured CH_4 molar fractions (by drone)

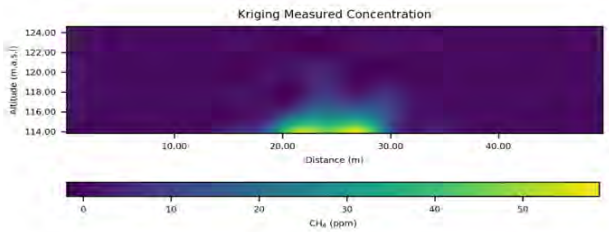

Fig. 2.12: Spatially filled measured CH_4 molar fractions (Kriging)

The component level measurements show detectable methane emissions with the FLIR camera (Fig. 2.13) at roughly half of the individual wells, in agreement with the facility scale estimates. In general, observations at the smaller facilities such as oil and gas wells and compressor stations showed that emissions were frequently due to open pipes or not properly closed valves and partly due to leaking equipment (flanges, pressure gauges). These leaks might be fixed relatively easy. Oil wells with H_2S emissions are much better maintained and show fewer leaks. The collection manifolds were generally in good state and showed only few leaks.

Fig. 2.13: leak detection and quantification using a FLIR camera (taken from ROM location 229, 6 October 2019)

The **airplane teams** conducted more than 20 flights, including regional mass balance and facility-cluster quantifications and raster flights (Fig 2.14). The aircraft measurements show significant methane enhancements at altitudes of hundred to several hundred meters close to production clusters, in qualitative agreement with the facility scale measurements. The generally low winds during the campaign made airborne quantification challenging, but nevertheless methane emissions estimates were obtained for several clusters in the areas 4, 5a, 6, 7, and 8, and for the entire region 7. Data analysis provide merged files of raw data, kmls of flight paths and chemical species.

Under the low wind conditions the raster flights alone do not allow for quantification, and comparison with three different atmospheric models are underway to facilitate more quantitative evaluation of the raster flights.

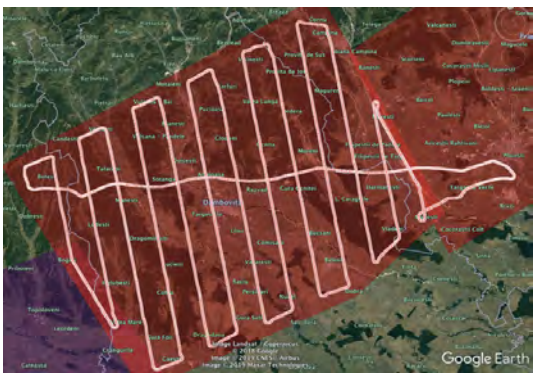

Fig. 2.14: Example of flight pattern, executed in area 6

In Strejnic, the CH_4 column concentration was measured by FTIR at more than 10 days, together with other species (CO, CO_2, H_2O and O_2).

The comparison of the EM27sun CH_4 column data with in situ data from Picarro is in progress. From preliminary results, a significant leakage at a facility storage in area 8 has been identified. It has also been observed that the elevation of methane emissions from a landfill was stronger than the ones observed in highly dense clusters. The identification of methane sources from raster flights is on-going and teams are collaborating on the analyses.

Task 1.5 Emission factor estimates with dispersion models (together with WP3) (Lead: UVSQ, Camille Yver-Kwok)

Dispersion models will be evaluated and applied to derive emission rates from mobile CH_4 measurements performed in Task 1.1, 1.2 and 1.4 (cooperation with WP3). This top-down approach will used to improve national Emission factors used for UNFCC reporting.

Since the MEMO² plume modelling workshop held in October 2018 in Heidelberg, all ESRs progressed well in setting up their methods to derive methane emission factors. Various methods were applied by the ESRs of WP1 and WP3 to transform the CH_4 concentration measurements to CH_4 emissions and emission factors. Several examples are given below, a more detailed description is presented in the deliverable D1.4.

ESR 5 used equipment to apply a dual tracer flux ratio measurement. The tracer acetylene (C_2H_2) is released near to the suspected emission source with a known flow rate. A mobile analyser records the resulting downwind enhancements of methane and C_2H_2 during plume transects. The ratio of the measured enhancements of methane and acetylene can be used together with the known release rate of C_2H_2 to determine the unknown CH_4 emission rate.

The advantage of this method is that it does not require knowledge of atmospheric stability and transport. This method was applied at a gas compression site and a landfill during the project.

Another approach is based on Gaussian Plume modelling or other dispersion models. Several ESRs applied a Gaussian Plume approach, which was studied in detail during the MEMO² workshop on plume modelling. The model is based on a simple Gaussian equation together with Pasquill stability classes and Briggs equations. Gaussian plume models efficient in computation. ESR12 applied a more complex model (GRAL), which simulated a trace gas using a Gaussian plume model - formulated with a dispersion parameterization scheme based on the Monin-Obukhov Similarity Theory. This included dispersion coefficients in the horizontal and vertical direction. On the other hand, Lagrangian forward dispersion simulations were also conducted using GRAL by prescribing the location of the source and the evolution of the air parcels were followed within the modelling domain. The method was also applied to a landfill site in Ile-de-France where previous studies had been made. A rate of 62kg/h was calculated. Compared to the first survey, made in 2016, the estimated emission rate decreased by a factor four. The observed reduction is likely an effect of the mitigation actions implemented on this landfill, such as the extension of the collection network (implemented between September and November 2016) and covering the filled parts with geomembranes (implemented between November and December 2016).

ERS5 also used the Gaussian model hosted on the Polyphemus platform to estimate the emission rates of two gas compression sites in Ile-de-France. Using data from several campaign days, the emission rates were estimated to be between 0.8 to 2 kg/h. It should be noted that the atmospheric pressure can highly affect methane emissions during landfill measurements. In low pressure conditions, landfill gas is transported by the air turbulence and CH_4 emissions increase. Thus, the emission rate calculated during one mobile measurement cannot be extrapolated to annual emission by simply multiplying the calculated rate by time. More regular surveys should be done to estimate the emission rate of sites over a year.

ESR3 focused on the CH_4 emissions from coal mines in Poland and derived emission rates for 12 coal mines the emission from mobile CH_4 measurements combined with Gaussian plume modelling (see Fig. 2.15). A publication about these results is in preparation and will be submitted in May 2021.

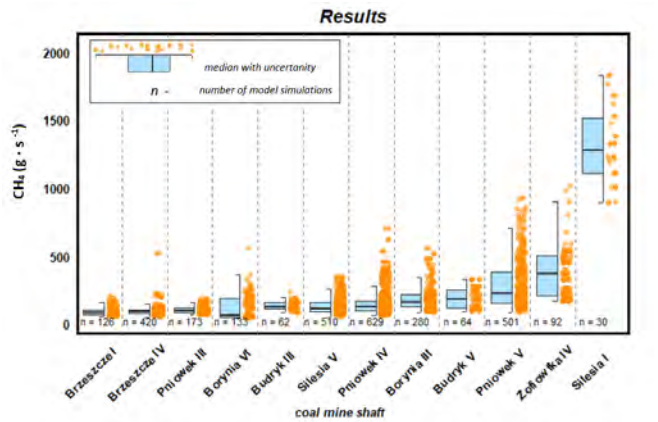

Fig. 2.15: CH_4 emission from Upper Silesian coal mines derived from mobile measurements and Gaussian plume modelling

For point source emissions, especially for the ROMEO campaign, the EPA other test method (OTM33A), which produces facility-level methane emissions estimates, was tested and applied. This method uses measured concentration of CH_4 and meteorological conditions at a stationary location in the emissions plume downwind of the emission location. The parallel CH_4 and 3-D wind measurements were performed stationary at one place during 20 – 40 min, 20 - 200 m downwind a point source. During the ROMEO campaign ESR1 and ESR10 applied this method.

ESR2 applied a mass balance approach using UAV measurements. The CH_4 concentration time series measured from an AirCore that was filled during a UAV flight through the emission plume (8 - 15 minutes) was used model the emission plume in the horizontal and vertical directions. These data are then spatially interpolated, and the effects of different interpolation techniques were studies in detail. Using this approach, during the period from March 2017 to March 2019, four measurement campaigns were carried out at a Dutch farm. A total of 17 flights were performed, 8 of them were suitable for further analysis.

2.2.2 WP2 – Source identification by isotopic characterization (Lead: Dave Lowry, RHUL)

2.2.1.1 General WP overview and contribution of involved beneficiaries

Significant progress has been made in measuring the isotopic signatures of methane and reporting them to a common scale. Inter-comparison between RHUL and UU showed that the two IRMS groups are reporting to the same carbon isotopic scale (D2.1) and this has been extended to the CRDS isotope groups. This inter-comparison has been pushed further by joint measurement and sampling campaigns by multiple partners (see Task 2.2 results), and by comparison of the results from co-located sampling and multi-laboratory measurement (milestone MS7). The addition of the ROMEO campaign (joint with UN CCAC) has added significantly more isotopic data.

Task 2.2 (D2.2) database has been compiled by source category and country and was completed by month 42. D2.3 has been submitted in month 48, publications related to task 2.3 are continuing, as the expected output from this task is greater than first envisaged, with at least 4 manuscripts on urban methane emissions and isotopic discrimination, either published or in the process of being written. Task 2.4 is completed with measurements made at 2 sites in 2017-19 and the first of 2 papers published in 2020, the second submitted in 2021. D2.4 was submitted in month 48. Task 2.5 (D2.5) has been most affected by delays to other tasks as this requires the database of measurements and source localities to produce maps and to model the data. The amount of data required to validate inventories at a national scale proved to be beyond the scope of this project, but in focussed areas, such as cities that were intensively surveyed, or for the footprints of fixed monitoring sites, it has allowed discrepancies with inventories to be identified. The development and purchase of new instrumentation and the additional funding from UNCCAC means that tasks 2.1 to 2.4 will deliver more than was expected for MEMO².

The **UU** have reached milestone MS7, and the scale inter-comparison work is fully completed. Progress has continued on all other WP2 tasks. A publication on the continuous CH_4 isotope measurements at Lutjewad, NL, has been published in the journal Tellus B (Menoud et al. 2020). ESR8 was responsible for the continuous isotope measurement campaign at AGH university, Krakow, with the UU IRMS installed there from September 2018 to March 2019. The goal was to get a clearer picture of the main CH_4 sources in the Krakow region, and especially to evaluate the influence of emissions from the Silesian coal mines. It was carried out in parallel with sampling campaigns in Silesia during the CoMet campaign. Isotope measurement from sources in the vicinity of the monitoring site were collected in order to characterize the surrounding sources. The data were then interpreted with the help of model calculations of MEMO² partner UVSQ. A manuscript was published in ACPD in 2021. A second publication, focussing in more detail on the isotope modelling, is in preparation by the UVSQ group. ESR8 has also analysed more than 300 samples collected during the ROMEO campaign in the city of Bucharest and oil and gas fields for $\delta^{13}C$ and δD. This identified the samples collected during flight and ground surveys to be dominantly of thermogenic origin, therefore fossil fuel rather than waste or animal sources. The isotope data have been interpreted in relation to C_2H_6 : CH_4 ratio measurements collected in Romania by UU (ESR10) and MEMO² partner TNO and will be published in a special issue on ROMEO in the journal Elementa – Science of the Anthropocene.

RHUL successfully completed task 2.6 / milestone MS8 (by month 20), which was the organisation of a 3-day methane isotope workshop, and organised and prepared inter-comparison cylinders for exchange between RHUL and UU, resulting in an accepted C-isotope scale for methane in the range -61 to -38 ‰ (D2.1). Progress has continued on WP2 tasks, particularly task 2.2 and 2.3. ESR7 and ESR9 have made measurements at waste, fossil fuel and biogenic sites. In particular the rapidly expanding biogas sector has been isotopically characterised in the SE of England, cow barn emissions sampled in the north of England, landfill plumes have been sampled across England, with 4 sites studied in more detail from the SW of England. Fugitive gas distribution measurements have been measured across England and South Wales, with a focus on city leaks in London, Birmingham and Swansea. Progress has been delayed in the final year with the laboratory and department being closed to research for 4 months during first Covid-19 lockdown.

Focus shifted toward compilation of the isotopic database for D2.2, with significant contributions by ESR7 and ESR 9, who between them provided information on more than 50 % of measured CH_4 sources. Work progressed on manuscripts, with ESR7 submitting an isotopic paper on UK landfill site oxidation (Bakkaloglu et al. 2021). ESR9 continued to process data from London city surveys completed in February 2020, but has focussed on processing Bucharest data for the ROMEO project and a manuscript is now close to submission, both of which contribute to D2.3.

Other work has focussed on compilation of a UK database for the carbon isotopes of CH_4 adding a further 120 source signatures for pre-2017 surveys and other recent project data to the 300 UK signatures included in D2.2 database. This information has contributed to maps forming part of D2.5 and form part of a publication on UK CH_4 isotopes.

2.2.2.2 Progress of WP tasks

Task 2.1: Isotope inter-calibration and calibration service (LEAD: RHUL, Dave Lowry)

Exchange of standards between isotope ratio mass spectrometry (IRMS) groups (UU, RHUL). UU and RHUL will provide calibration services to those ESRs that operate mobile CRDS isotopic analysers (UVSQ, UHEI, AGH-UST). This task will be undertaken by WP2-focussed students and lead to deliverable D2.1.

This task was completed with deliverable D2.1 and milestone MS7, but UU and RHUL have continued to exchange samples to maintain the integrity of the common isotopic scale. The intercalibration was extended so that the partners with laser-based isotopic instruments could inter-compare their measurements to the IRMS scale. Now 3 CRDS partners have reported their isotopic values for the tanks (Table 2.1). These show a stretching of the isotopic scale, that can be corrected for by the intercalibration.

Table 2.1: Inter-comparison results for 5 circulated cylinders of air. Total offset of CRDS instruments (UHEI, UVSQ and AHG) over a 23 ‰ range varies from 3.6 to 5.2 ‰.

Sample ID	RHUL (‰)	RHUL (1 SD)	UU (‰)	UU (1 SD)	Agreed value (‰)	UHEI (‰)	Offset (‰)	UVSQ* (‰)	Offset (‰)	UVSQ (1 SD)	UVSQ C_2H_6 c	AHG (‰)	AHG (1 SD)	Offset (‰)
Air 2 ppm	-48.07	0.01	-48.09	0.03	-48.1	-48.0	+0.1	-47.7	+0.4	3.5	-52.0	-50.1	3.5	-2.0
Gas 2 ppm	-39.64	0.02	-39.61	0.07	-39.6	-36.9	+2.7	-37.0	+2.6	3.4	-39.9	-40.7	3.5	-1.1
Gas 10 ppm	-38.21	0.01	-38.17	0.07	-38.2	-36.0	+2.2	-35.2	+3.0	0.7	-37.8	-41.7	0.8	-3.5
LF 2 ppm	-59.73	0.05	-59.80	0.10	-59.8	-61.9	-2.1	-60.4	-0.6	3.9	-60.8	-63.2	4.5	-3.6
LF 10 ppm	-60.93	0.04	-60.91	0.05	-60.9	-63.9	-3.0	-61.4	-0.5	0.7	-61.1	-66.0	0.8	-5.1

Intercomparison Results for 2 IRMS labs and 3 mobile Picarro instruments.

Precisions <±0.1 ‰ for all concentrations for IRMS measurements, ±0.7 ‰ for Picarro at 10 ppm, ±3.5 ‰ for Picarro at 2 ppm

* Without ethane correction

Sample ID	RHUL (‰)	UU (‰)	UHEI (‰)	Offset (‰)	UVSQ (‰)	Offset (‰)	AHG (‰)	Offset (‰)
Air 2 ppm	-48.1	-48.1	-48.1	+0.0	-48.1	+0.0	-48.1	+0.0
Gas 2 ppm	-39.6	-39.6	-37.0	+2.6	-37.4	+2.2	-38.7	+0.9
Gas 10 ppm	-38.2	-38.2	-36.1	+2.1	-35.6	+2.6	-39.7	-1.5
LF 2 ppm	-59.7	-59.8	-62.0	-2.2	-60.8	-1.0	-61.2	-1.6
LF 10 ppm	-60.9	-60.9	-64.0	-3.1	-61.8	-0.9	-64.0	-3.1

New offsets when fixing ambient air at -48.1 ‰.

Task 2.2: Isotopic characterisation of significant CH_4 sources (LEAD: RHUL, Dave Lowry)

Air samples will be collected and analysed for CH_4 isotopic composition by UU or RHUL. ESRs from WP1 will sample source plumes identified by mobile measurements for isotope analysis. Links to innovation in WP1 (UAV sampling and AirCore sampling) for vertical profiling of isotopic signature through plumes. Strong collaboration with mobile CRDS – based isotope measurements in WP1.

This task was completed with the submission of D2.2 in Month 40, which is the database of methane sources and their isotopic signatures from mobile surveys and sampling carried out by partners during the 2017-2020 period. The database contains significant source numbers for large regions of the UK (ESR7, ESR9 and other projects), Romania (ESR8 and 9), plus smaller regions of Netherlands (ESR8), France (ESR5), Germany (ESR1), Poland (ESR3) and Sweden (ESR4).

This process has been aided by multi-partner isotopic campaigns:

- CoMet, Silesia – May-June 2018 (AGH, UU, UHEI, UVSQ)
- Southern England – June – July 2018 (RHUL, UU, UVSQ)
- Hamburg – Oct 2018 (UU, RHUL)
- ROMEO, Bucharest – Aug - Sept 2020 (UU, RHUL)
- ROMEO gas fields – Oct 2020 (whole MEMO²)

Additional data comes from ESR secondments such as ESR9 to UVSQ in March 2019 to sample Paris sources and from individual ESRs sending samples to UU and RHUL for high-precision analysis by mass spectrometry. Measurements of samples from several MEMO² students were carried out by the UU and RHUL groups, particularly ESRs 2, 3, 4 and 5. Additionally, isotopic measurements were made using new CRDS instruments to a lower precision during mobile campaigns by UHEI, AGH and UVSQ. These contribute 80 sources out of a total of 816 sources characterized for $\delta^{13}C$ of CH_4.

The signatures of source plumes are calculated using Keeling or Miller-Tans plots, whereby the excess CH_4 over background for multiple sample points in an emission plume plot as a mixing line between background and source end members. This allows one signature per source to be entered into the database.

Samples were collected during mobile surveys, often also aiming at the detection and quantification of the emissions. Several vehicles could be used, from bicycles to aircraft. A cavity ring down spectrometer (CRDS) in the vehicles provided real-time values of CH_4 mixing ratio to identify emission plumes from sources. The samples that were to be measured in the lab were collected in either Flexfoil bags, Tedlar bags, glass flasks or stainless-steel canisters. Direct isotopic measurements were also performed using isotopic CRDS instruments.

Table 2.2: Survey days and results per country

Country	Number of survey days	Number of isotopically characterized sources
United Kingdom	70	303
Romania	24	196
Poland	23	98
The Netherlands	26	71
Germany	33	78
France	17	47
Sweden	2	21
Turkey	1	2
TOTAL	**196**	**816**

The campaigns were made in 8 different countries. Table 2.2 shows the distribution of the surveys and results per country.

Fig. 2.16 shows the locations that were characterized, and the different source categories. Many are in the UK and the Netherlands due to the proximity with the measurement labs. However, the 2 intensive campaigns that involved several MEMO² beneficiaries, CoMet and ROMEO, contributed significantly to extending the geographical range of the dataset.

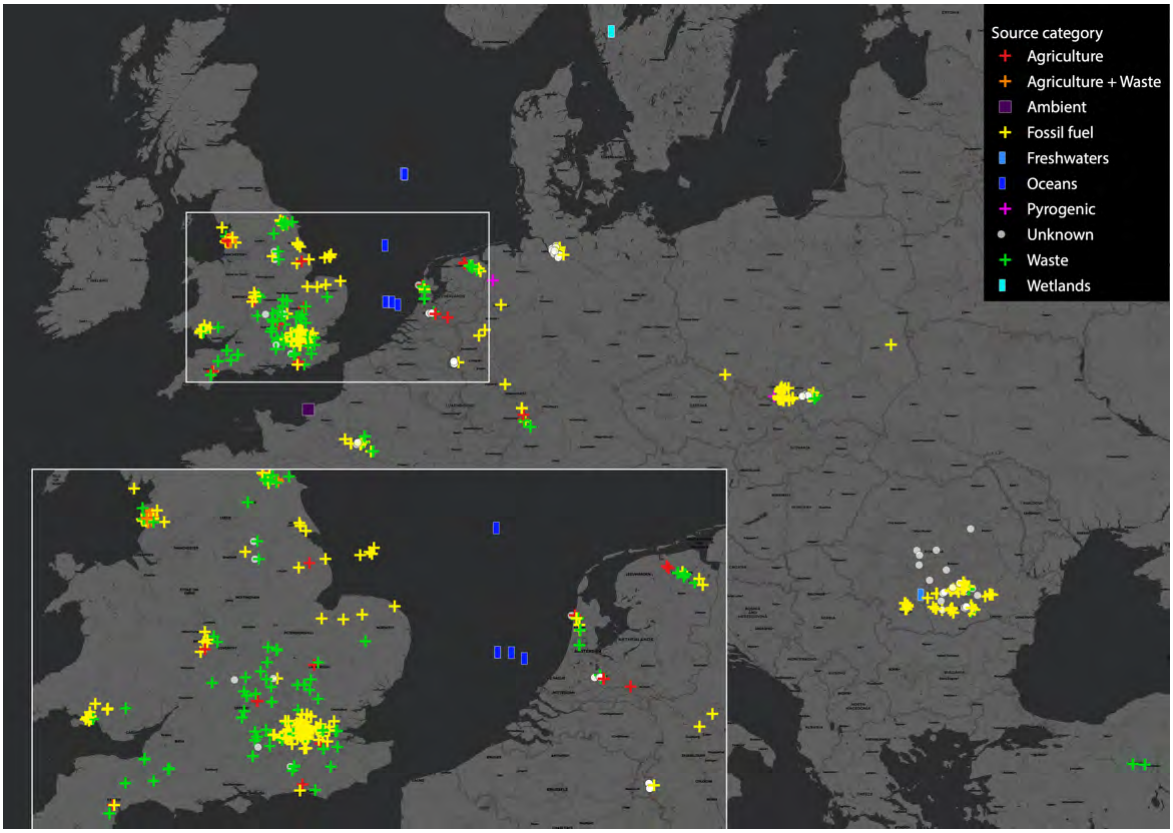

Fig. 2.16: Map of all locations that were sampled and characterized for $\delta^{13}C$ and/or δD, and reported in the database. When identified, the emissions were classified into 8 source categories.

Task 2.3: Deciphering mixed urban and industrial emissions (LEAD: RHUL, Dave Lowry)

Samples will be collected when CH_4 plumes are identified by grid-pattern mobile measurement surveys in complex areas with small to medium-sized urban / industrial sources. Isotope data will improve understanding of source contributions (D2.3). CRDS groups (WP1) will directly measure the $^{13}CH_4$ during these surveys for direct comparison with IRMS technique.

This task has been significantly aided by additional funding from UN CCAC to study fossil fuel infrastructure emissions in cities, and using C_2H_6 and isotopic proxies can distinguish fossil fuel and combustion sources from biogenic sources during mobile surveys. Isotopic measurements to back-up mobile methane mapping have been completed for the following cities: Hamburg and Utrecht (ESR10, aided by ESR8 and ESR9), Bucharest (ESR9 aided by ESR8 and ESR10), London (Fig. 2.17), Birmingham and Swansea (ESR9 aided by ESR7), Paris (ESR5 aided by ESR8 and ESR9), Heidelberg (ESR1) and Katowice (ESR3), with additional work in the Groningen and Alkmaar regions of NL. Deliverable D2.3 (Month 36) was delayed, partly by the additional requirement of the ROMEO project to conduct surveys in Romania, and latterly by lockdown restrictions impacting on final surveys and subsequent data processing.

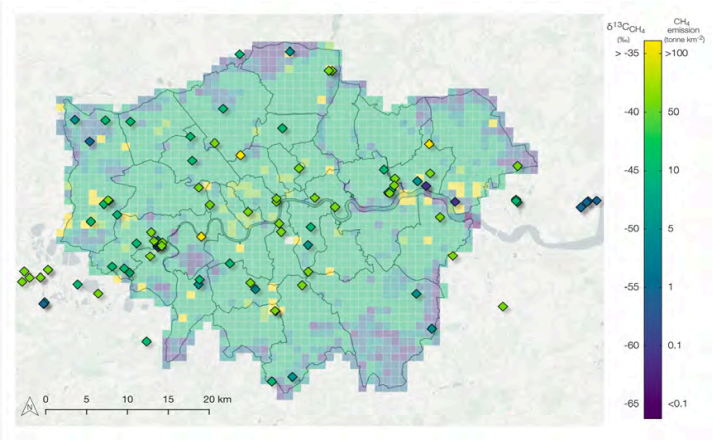

Fig. 2.17: Calculated $\delta^{13}C_{CH4}$ source signatures (diamonds) from samples collected during 2018-2019. Greater London 2018 National Atmospheric Emission Inventory (NAEI) methane estimates (grid, tonnes y^{-1} km^{-2}) form the base map.

Task 2.4: Isotope monitoring at fixed sites (LEAD: UU, Thomas Röckmann)

The IRMS and isotopic CRDS instruments from WP1 and WP2 will make co-located continuous isotope measurements at fixed sites. This will provide important information on temporal and meteorological variations in isotope source signatures that will be interpreted with regional models from WP3. This task will lead to deliverable D2.4.

Continuous isotope measurements were made at the Lutjewad site for 6 months during 2017 and in Krakow for 6 months during 2019.

Lutjewad data for $\chi(CH_4)$, $\delta^{13}C$ and $\delta D\text{-}CH_4$ were analysed using Keeling plots applied on a moving window over the time series. The main conclusions, presented in Menoud et al. (2020), are that CH_4 sources were mostly biogenic, mainly from dairy farms and also from landfills, according to the anthropogenic activities of this region. Some pollution had a higher thermogenic component when the wind came from the east, pointing towards the Groningen gas extraction region or more distant sources in Germany. The emissions from the North Sea oil and gas platforms were not detected from the coast during the time of the measurements. This can be due to the distance and the prevalence of southern winds.

The time series from Krakow were analysed with a similar algorithm. Fig. 2.18 shows the Krakow data series, together with model calculations that were carried out with two different inventories. The data were evaluated to calculate the contributions of different methane source types to the excess over background using the changes in isotopic signals observed during elevated methane events.

The isotopic source signatures from the two sites are shown in Fig. 2.19, and clearly demonstrate that the CH_4 sources in the two regions are isotopically very different.

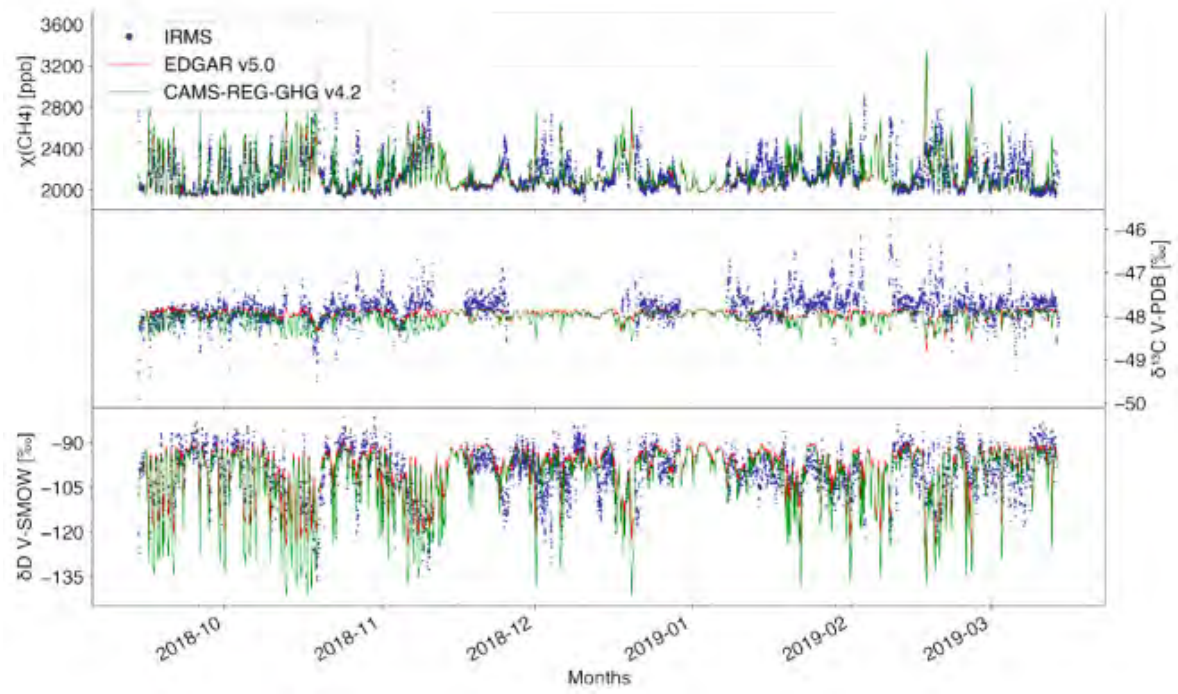

Fig. 2.18: Example of a high-resolution isotope time series (>2500 measurements of δD and $\delta^{13}C$ each) in Krakow, Poland, and related modeling, using two different emission inventories. The differences between measurements and model results point to discrepancies in the inventories. For Krakow, this suggests a mis-representation of sources from coal mining waste in the category "waste" in the CAMS-REG-GHG v4.2 inventory.

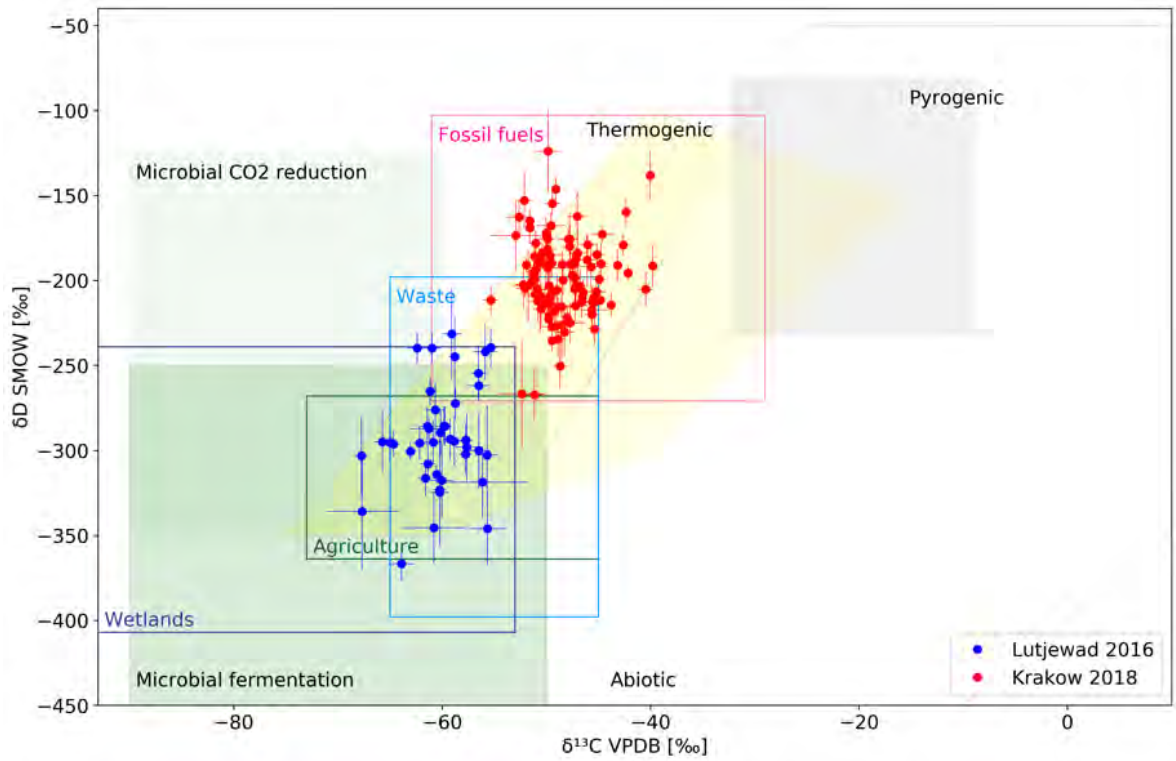

Fig. 2.19: Dual isotope plot showing the isotopic composition of CH_4 produced from different processes and in different regions. Shaded areas indicate the reported ranges in isotopic composition of CH_4 produced from different geophysical processes (thermogenic, pyrogenic and biogenic). Areas surrounded by coloured lines indicate reported isotope signatures from specific source categories (wetlands, agriculture, waste, fossil fuels). Blue and red symbols show isotope source signatures assigned to methane plumes observed in long-time measurement periods in the Netherlands (Lutjewad) and Poland (Krakow).

Task 2.5: Validation of inventories at grid scale (LEAD: UU, Thomas Röckmann)

The isotopic signature of each major source will be constrained at regional to EU-wide scale (D2.2) for use in models (WP3). ESRs from WP2 and WP3 will use data from Tasks 2.2-2.4 to produce maps of isotopic source signatures contributing to the validation of inventories (D2.5, due month 42).

Deliverable 2.5 originally scheduled for Month 42 required that the database of isotopic values (D2.2) was completed. The database was completed by month 42 allowing use of the data for the understanding of changing source signatures across NW Europe. This has been complemented by the single site isotopic footprint evaluations performed by ESR8 for Task 2.4 and previously published in Röckmann et al. (2016). Measuring the isotopic signature at a fixed site some distance from sources can point towards source regions (based on wind sector analysis) that have greater or less biogenic to fossil fuel components. Interpretation of such measurements also requires measurement of typical source signatures in the regional footprint to validate national inventories at kilometre grid scale. Fixed site measurements become more relevant when comparison is made with models where the inventory is at 0.1 x 0.1° scale and representative of site footprints.

In other regions, it proved difficult to gather sufficient isotopic data for sources to be able to show that the inventories are correct or not. One region of England was surveyed on 32 days over the 2017-2020 period and sources were located only in 46 out of 208 1x1 km grid squares (Fig. 2.20). Inventories capture the general distribution of sources and highlight dominant fossil fuel and combustion sources in urban areas and biogenic sources in rural areas on a larger grid scale. The main finding provided by isotopic characterisation is that gas pipelines and installations in rural areas do not form part of inventory emissions, but often leaks go unnoticed and so are not repaired (Lowry et al., 2020).

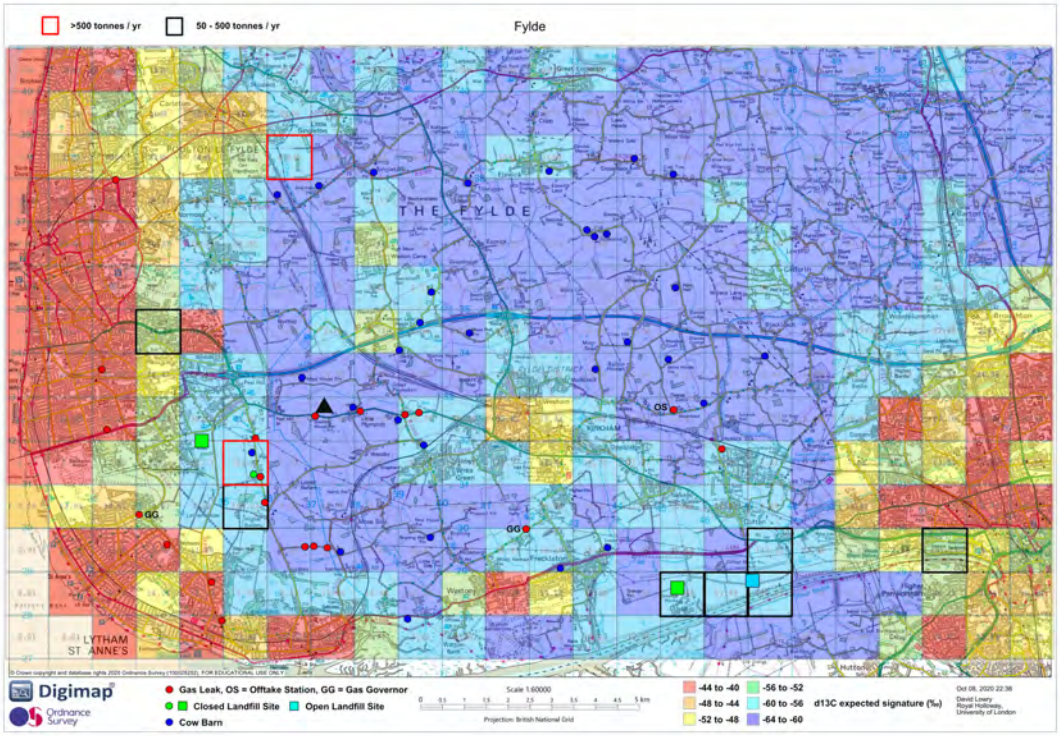

Fig. 2.20: UK emissions mapping inventory (NAEI) data for the Fylde region of NW England has been converted to a source mix isotopic signature for each 1 x 1 km grid square. Red is dominated by gas supply leaks and blue by agricultural emissions. The red coloured dots are located gas leaks, the blue coloured dots are emissions from cow barns. Squares are landfill site emissions. There is good correspondence between red dots in red squares and blue dots in blue squares, except for red dots in blue squares which are leaks in gas infrastructure crossing the agricultural areas. Black triangle is an unconventional gas well.

Task 2.6: Isotope workshop at RHUL (LEAD: RHUL, Dave Lowry)

Sessions aimed at helping WP1 students interpret the isotopic measurements from their mobile campaigns, and in discussing with WP3 students the suitability of data to incorporate into their models.

This task was milestone MS8 and has been successfully completed. A report on the workshop was submitted to the Project Officer.

2.2.3 WP3 – Modelling: A multi-scale interpretation framework for CH_4 observations (Lead: Maarten Krol, WU)

2.2.3.1 General WP overview and contribution of involved beneficiaries

In this WP the ESRs focussed on modelling on different spatio-temporal scales, the link with measurements, and the use of isotopes to better constrain European methane sources.

The multi-scale framework for interpreting CH_4 observations has been addressed by three ESRs. ESR11 **(WU)** addressed the smallest scale, targeting dispersion of plumes right after emissions. The numerical tools that were used were Direct Numerical Simulation (DNS) and Large Eddy Simulation (LES). A main conclusion from this project is that LES with realistic atmospheric conditions has proven to be a good tool for reproduction of conditions encountered in the field.

Close to a source, variability of the observations (and simulations) is mostly due to meandering wind patterns that sweep the plume over a measurement device. Thus, observations are characterized by a strong “on-off” nature: either the plume is sampled or not. Further away from the source, atmospheric turbulence has had the time to disperse the concentrated plume patches further. This behaviour can be well quantified using numerical models, and this basic understanding is important for the interpretation of field measurement.

The numerical tools have been applied to measurements made during the ROMEO campaign. By constraining the local meteorological situation (wind speed, direction) to observations, the tool provides a useful addition to more conventional models to estimate the source strength, such as Gaussian Plume models.

ESR12 **(EMPA)** developed a novel strategy of CH_4 flux quantification with the use of unmanned aerial vehicle (UAV) equipped with a CH_4 sensor. This was pioneered in a tracer release experiment in Dübendorf, CH. Using drone observations, different estimation methods have been tested, with different interpolation methods, and different assumptions for the wind. These studies clearly show that wind conditions and sampling distance are crucial parameters for drone quantification methods to be successful.

The results of the fast methane measurements were compared to results obtained with AirCore sampling, a technique further employed by ESR2 **(RUG).** It was found that, next two the expected smoothing of sharp concentrations in the AirCore due to diffusion, AirCore measurements were also temporally shifted. Correcting for this time shift is important to obtain accurate source estimates. Results of the emission quantification using drones was also compared to the so-called OTM33A approach, with a stationary measurement location downwind of the source. This was the method of choice for many source locations during the ROMEO campaign in 2019. Results show that both approaches lead to source estimations that are close to the true-release. This showcases that the drone-based quantification technique has great potential.

ESR13 **(UVSQ)** worked on European inversions, in which measurements of CH_4 mole fractions and isotopologues can be used to infer emission magnitudes and the responsible source sectors. In contrast to ESR11 and ESR12, models are used with relatively coarse grid resolution. This implies that individual point sources are not resolved by the model, and measurements are used that are collected further away from big sources. This is the measurement strategy within the ICOS measurement program. The studies of ESR13 mostly offer insights into how inversion frameworks should be configured and what the essentials are to reliably estimate CH_4 emissions at the European scale. It has for instance been shown that a detailed error characterisation (emission errors, model errors) is important. The project computed CH_4 mixing ratios, as well as $\delta^{13}C$ and $\delta^{2}H$ isotope ratios, over the European domain. To quantify emissions errors, two anthropogenic emission inventories were used and their impact on mixing ratios and isotope ratios was investigated. Thanks to collaboration with other ESRs, detailed new information on isotope source signatures could be used for these simulations. The studies show that isotopologue measurements of CH_4 are a great asset for determining the origin of atmospheric CH_4. ESR13 also investigated, through experiments with synthetic data, the importance of (potentially new) high-frequency measurements of $\delta^{13}C$ and $\delta^{2}H$ in better constraining CH_4 emission estimates. Although these high-frequency measurements are not yet available at sufficient locations, this study draws the important conclusion that a precision of at least 1 ‰ for $\delta^{2}H$ analyses and 0.05 ‰ for $\delta^{13}C$ analyses would be needed to discriminate methane sources at most ICOS sites.

Within WP3 as a whole, not all promised goals have been reached. For instance, ESR11 was supposed to contribute to European emission estimates though inverse modelling. Likewise, ESR12 would provide better constraints on the European CH_4 source mixture based on CH_4 isotope measurements, and ESR13 was supposed to do actual inversions. Reasons for this are diverse, and mostly related to the very busy programs of the ESRs within the project and the involvement of ESRs in the ROMEO measurement campaign, which was given priority. Through this, the ESRs in WP3 worked with real data collected by the other ESRs, which made them appreciate the great effort it takes to collect and analyse data with a good underlying plan.

Cutting-edge science has been delivered on two important aspects. On the use of local scale measurements to infer emission rates of strong point sources, the importance of atmospheric turbulence and conditions for measurement collection have been studied in great detail and with advanced numerical tools. On the estimation of CH_4 sources over Europe, the potential role of $\delta^{13}C$ and $\delta^{2}H$ isotope measurements has been quantified, based on the assumed measurement precision. This provides important information for the measurement community.

2.2.3.2 Progress of WP tasks

Task 3.1: Interpretation mobile observations (LEAD: WU, Maarten Krol)

Dispersion of emissions will be modelled using the newest Large Eddy Simulation tools, in which detailed land-use maps, roughness elements, and surface heterogeneity can be taken into account. This approach will be compared to the dispersion model approach (WP1). Modelling will also assist in planning of the mobile measurements and intensive campaigns.

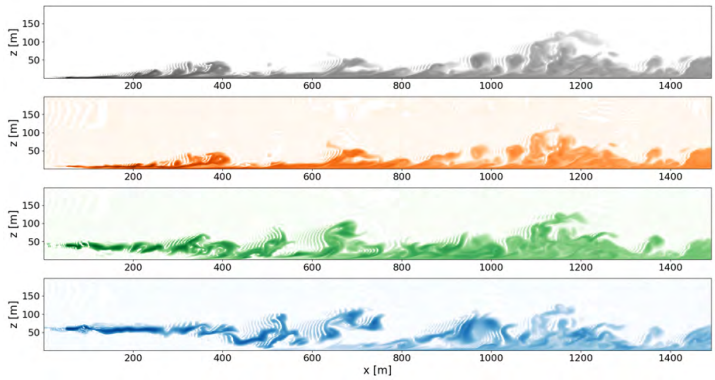

Fig. 2.21: Snapshots of x-z transects of four plumes taken at the plume centreline for different emissions heights. From top to bottom emission heights are: 1, 7, 39, 60 m.

To help the interpretation of mobile measurements, WU was using the CFD code MicroHH (www.microhh.org). Simulations have been performed of the time-dependent dispersion from a single point source. The aim was to validate the Gaussian Plume Model approaches, such as OTM33a and drive-bys. Simulations are shown in Fig. 2.21.

Fig. 2.22 shows an hourly averaged top view of the plume that should be comparable to the GPM. However, we found that lateral dispersion of the GPM is much faster. This is due to the larger dispersion coefficients, which are based on Briggs (according to the OTM33a protocol).

According to this, source strength estimates using OTM33a would highly overestimate sources strengths, at least compared to this simulation. In our analysis we found that dispersion of a plume can be described by two processes: turbulent mixing and plume meandering. The first process is the "classical" turbulent mixing, in which eddies slowly mix down the plume in a diffusion-like process (when averaged). The second process represents the movement of the whole plume by the larger eddies in the flow. Near the source (OTM33a) the meandering seems to dominate. Thus, close to the source the plume is keeping its shape dictated by the shape of the source itself and the dispersion of the plume might be too small to use methods which rely on the GPM (Fig. 2.22).

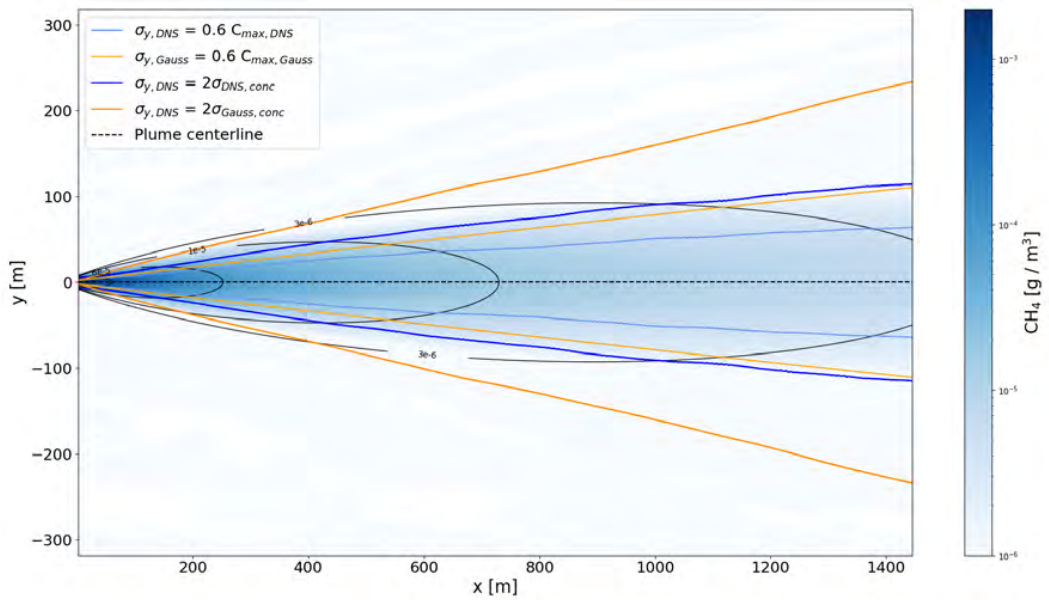

Fig. 2.22: One-hour time-averaged DNS plume at 60 m height. Isopleths of concentration show the GPM result at the same height with the mean wind at the release height. Straight lines denote the edges of the two plumes.

In support of the ROMEO campaign, the drive-by strategy was also tested. Fig. 2.23 shows the main result. From the results it is clear that integrating the downwind concentration pattern can result in a correct source estimate. However, at least five drive-by experiments should be averaged to correctly infer the source strength.

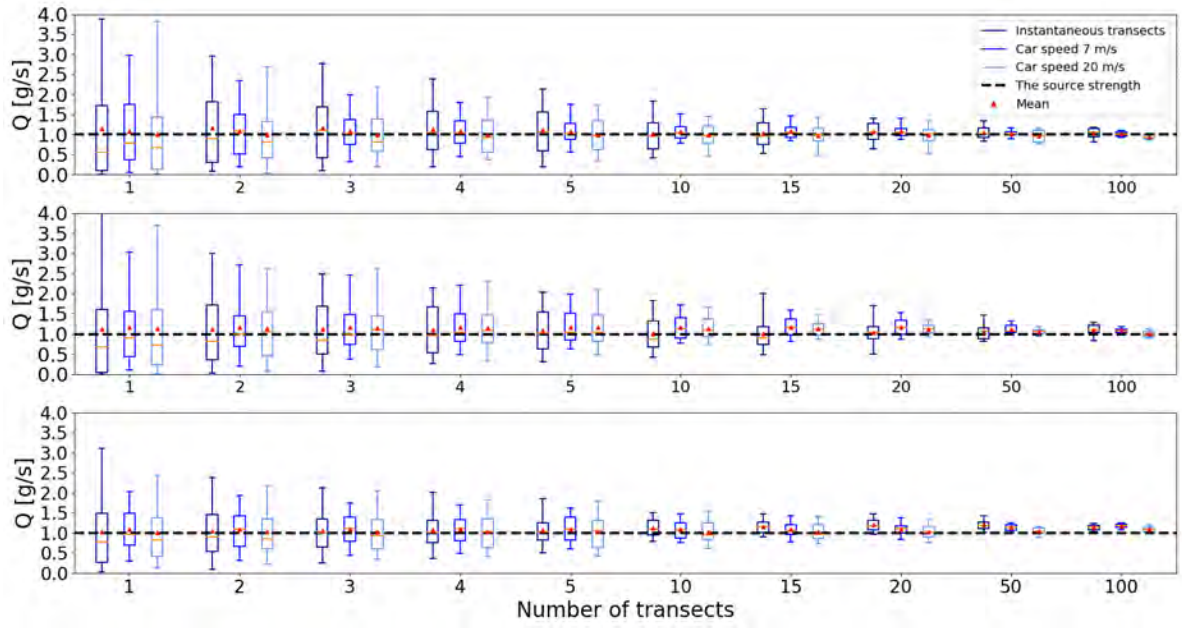

Fig. 2.23: Estimation of the source strength of 1-100 drive-by experiments. The emission height was 60 m, and different speeds of the sampling device were tested. Boxes show interquartile range, the whiskers span from 5 to 95 percentile, the orange lines are the median. Distances from the source: (top) 225 m, (middle) 454 m, (down) 1213 m.

As MicroHH simulations in the above described set-up were not able to simulate observed plume meandering, on which the OTM33a technique relies, the use of MicroHH in LES mode has been started. The main goal was to better understand dispersion of methane from point sources in the atmosphere. High-resolution simulations are an invaluable tool in studying plume dispersion in great detail. Early studies using Large Eddy Simulations (LES) and Direct Numerical Simulations (DNS) mostly focused on idealized channel flows and mostly lack the connection to atmospheric boundary layers encountered when measuring plumes in the field. The use of these tools in interpreting atmospheric plumes is an emerging science field, because more and more sensors become available that can sample atmospheric concentrations downwind of point sources with high accuracy. The ROMEO campaign was therefore a good target. During the campaign, about 40 plume transects were measured downwind of an oil well. To verify the CH_4 emissions, a known source of N_2O was emitted at the source location. Moreover, the wind characteristics were measured.

To illustrate the difficulty in estimating source strength in the field, Fig. 2.24 shows snapshots of LES simulations. Due to a lack of large-scale forcing (i.e. low wind speed), the simulated plumes behave in a rather chaotic way. To solve this issue, plumes calculated with fixed background wind were rotated in order to match the observed wind speed and direction. After this, the source strength is determined using the mass-balance approach. Fig. 2.25 shows the half-hourly averages of the measured N_2O and CH_4 transects, as well as the corresponding LES results for passive tracer dispersion (here there is no difference between N_2O and CH_4). The red line is the average of the four half-hourly values.

The insets show the measured and modelled wind-speed and direction. Note here that specifically the wind direction is different (by design of the numerical experiment in which the background wind direction was forced to 270 degrees). Using mass-balance, the source strength of the N_2O source was estimated as 0.53 g s^{-1}, which is ~10 % smaller than the true source strength of 0.59 g s^{-1}. The mass-balance estimate for the CH_4 source amounts to 1.11 g s^{-1} (corrected for the N_2O-based underestimate: Q_{CH4} = 1.23 g s^{-1}).

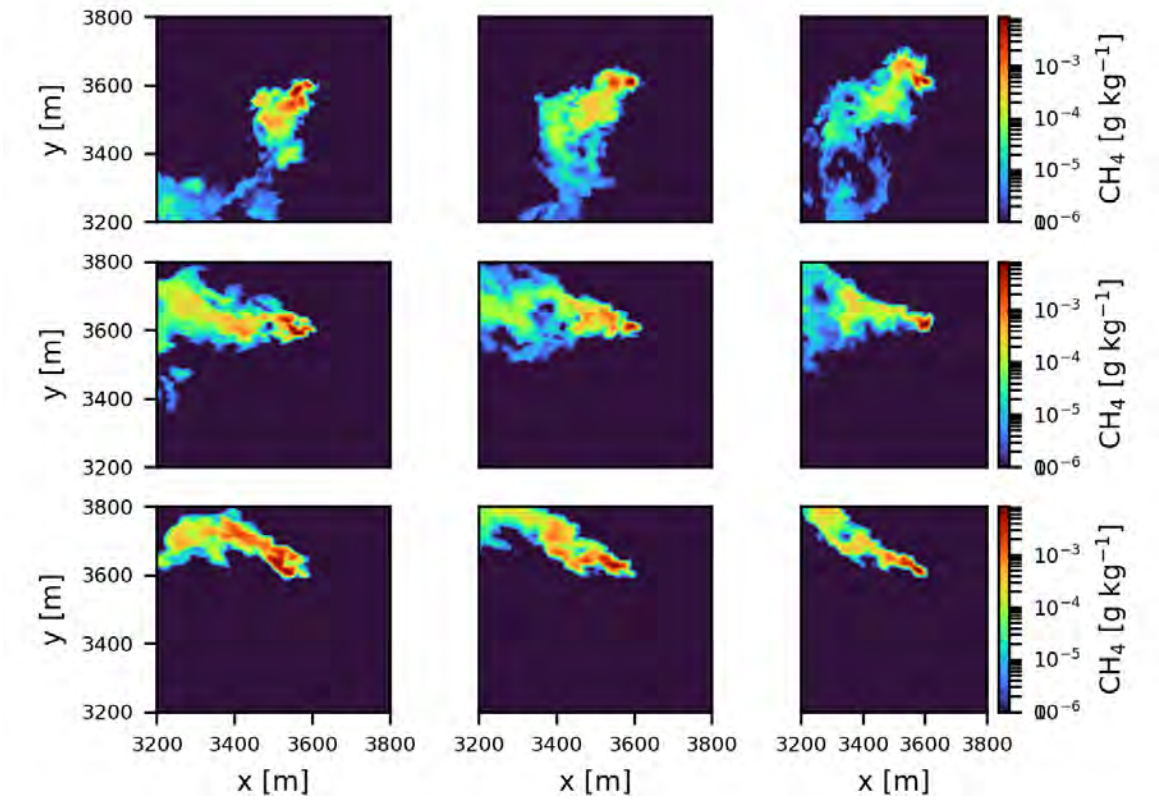

Fig. 2.24: LES simulation (resolution 5m x 5m x 2m) of the dispersion of methane from a gas well point source located at (x,y) = (3600m,3600m). Plumes were sample at z = 3m.

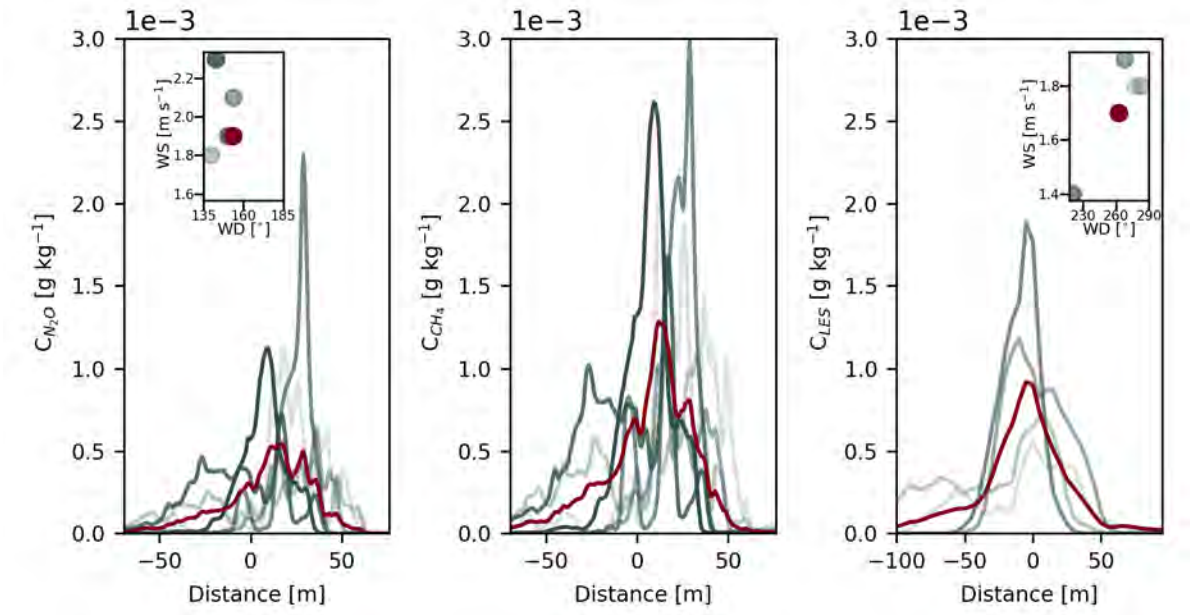

Fig. 2.25: Averages of instantaneous plumes over periods of half hour from (left) measured N_2O, (middle) measured CH_4 and (right) simulated LES tracer. LES transects were taken at 3 m height and 78 m downwind from the source. Plumes are shown with a color gradient corresponding to the half-hour increments i.e. lightest gray plume is the average of plumes measured in 11.30 - 12.00 UTC, dark grey is the average over 14.00 - 14.30 UTC. The insets show horizontal wind speed and direction for the corresponding half-hour averages in (left) measurements and (right) LES. Over-plotted in red are the averages of all the plumes.

This example from the ROMEO campaign shows that LES simulations can be used to quantify source strengths, even when no co-emitted tracer is available.

ESR11 further works on a theoretical framework to analyse different measurement strategies, like OTM33A and drive-bys. In this framework, LES simulations are used to separate dispersion processes into relative dispersion and dispersion caused by plume meandering due to larger-scale forcing. Findings show that close to the source, meandering is the driving mechanism, and that relative dispersion becomes prevalent further away from the source. The distance at which dispersion becomes dominant is important for designing measurement strategies.

Plans for the future include analysis of city-scale dispersion observations in collaboration with ESR10. We already identified suitable measurements for further interpretation from the Hamburg campaign.

The work on EU-scale methane inversions using TM5-4DVAR has not been performed. The involvement in the ROMEO campaign and the interaction between WP3 with the other WPs were considered and have proven more important and beneficial for the overall outcome of MEMO².

Task 3.2: Construction of new bottom-up emission maps, including isotopes (LEAD: TNO, Hugo Denier v. Goon)

The mobile measurements that become available in MEMO² will be used to construct updated high-resolution emission maps for the EU domain. For modelling purposes, the isotopic signature of the CH_4 sources will be included in the inventories.

The MEMO² project benefited strongly from concomitant societal and scientific developments and projects as regards detection and quantification of CH_4 emissions from various sources and source areas. The idea behind the workflow of this task, leading towards deliverable D3.2, was that the novel techniques deployed in MEMO² can facilitate a measurement-based emission assessment which can be compared against the traditional inventory guidebook approach of combining emission factors and activity data. The result would be an improved, more certain emission map. The greatest opportunity to apply this workflow opened through the United Nations - initiated study on methane emission detection, quantification and attribution in cities, with special focus on leaks from the urban natural gas networks. MEMO² partners were able to take on key roles in this project and from our consortium we covered the following cities in Europe:

- Hamburg, Germany (Maazallahi et al., ACP, 2020)
- Utrecht, Netherlands (Maazallahi et al., ACP, 2020)
- Paris, France (Defratyka et al., Environmental Science and Technology, in press, 2021)
- Bucharest, Romania, (Fernandez et al, Atmospheric Environment, ready for submission)
- London, UK, (Fernandez et al., in preparation)
- Groningen, Netherlands (Vinkovic et al., in preparation)
- Katowice, Poland (Stanisavljević et al., in preparation)
- Swansea, UK, (Fernandez et al., in preparation)
- Birmingham, UK (Bakkaloglu et al., in preparation)

This MEMO² set represents 9 of the 13 cities (EU plus Toronto, Canada) that are presently evaluated as part of a synthesis study on methane emissions from European cities. Since the MEMO² project strongly evolved in this direction, much of the work related to improved European CH_4 emissions (deliverable D3.2) is directed to the city scale. MEMO² partner organisations such as TNO and ECCC are closely involved in preparing the publication for synthesis, led by the former MEMO² PI Felix Vogel (now ECCC and leading the EU cities intercomparison study).

TNO and UU are presently providing the city scale inventory data, based on official country reporting and spatial distribution for this synthesis report. The availability of the measurement based (bottom-up) estimates and the currently used national scale top-down estimates allow us to evaluate differences and deliver a set of improved bottom-up estimates for city emissions in Europe (D3.2).

A second part of inventory related work is associated with the international ROMEO measurement campaign (again, co-funded by UNEP), organised by the UU and carried out in 2019 by the MEMO²

consortium. The evaluation of these data is in full swing, but will take longer than the operational period of MEMO², mainly due to delays associated with the COVID pandemic. The workflow as outlined above for the city data towards production of improved emissions for other emission categories cannot be completed as initially planned. For generating the improved emissions, we are in contact with the group that is responsible for the Romanian greenhouse gas inventory reports. This work will be continued and finished within the associated ROMEO project by the end of October 2021, and by this last beyond the lifetime of MEMO². The improved bottom-up European CH_4 emissions will concentrate on city emissions (to be covered in the upcoming D3.2). This will provide an excellent example how techniques and abilities developed under MEMO² can directly support policy relevant products like emission inventories. The information in this deliverable will be part of a peer-reviewed publication to ensure dissemination of the knowledge. As indicated above, emission estimates for the Romanian oil and gas production regions will be completed after MEMO² in the associated ROMEO project, but linked to and disseminated by MEMO².

Task 3.3: Forward simulations of CH_4 and CH_4 isotopes (LEAD: UVSQ, Philippe Bousquet)

Two meso-scale transport models with up to km-scale resolution will be used to simulate CH_4 and its isotopic composition over Europe with the aim to predict how different sources with different isotopic signatures (e.g. from an urban environment) blend into larger-scale concentration fields. Comparison to new and existing "background" observations will be performed.

Atmospheric inversions make it possible to obtain top-down emissions which represent the best knowledge, including the information from both bottom-up emission inventories and atmospheric measurements. To prepare for atmospheric inversions, much effort has been dedicated to the error estimates. These errors are important, because they will finally determine how much information can sensibly be extracted from measurements, depending on the sampling location, and the capability of the model to simulate the measurement in that location. Using a dedicated set of simulations, the following errors are determined:

- The representation error ε_{repr}: error of a model not perfectly representing the measured values due to the difference between a grid cell in the model and the actual scale at which a measurement is representative.
- The boundary condition error ε_{LBC}: the background error associated with the lateral boundary conditions (LBCs), due to the choice of the lateral (sides and top of the domain) and initial conditions.
- The transport error ε_{transp}: error that is due to discretizing the model of the fundamental equations of the atmospheric transport used in a model.
- The emission induced error ε_b: error that is due to the misrepresentation of emissions on the spatial and temporal grid of the model.

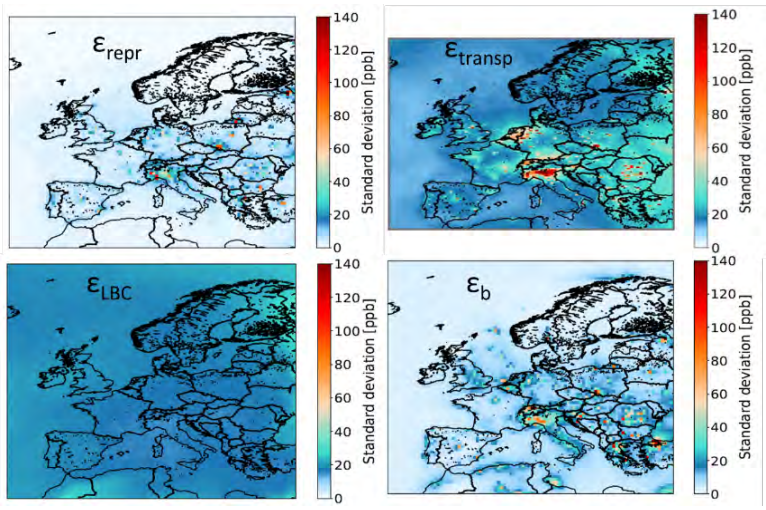

Fig. 2.26: Annual mean standard deviation of the estimated errors over the European domain for 2015

In a first study, ESR13 (UVSQ) used several bottom-up anthropogenic emission inventories of CH_4 to simulate the atmospheric mixing ratio of CH_4 over Europe (Fig. 2.26).

The simulations are used for estimating errors for atmospheric inversions of CH_4 emissions over Europe. A second study targets other possible causes for misfits between measured and simulated atmospheric CH_4 mixing ratios, as well as isotopic ratios $\delta^{13}C$ and $\delta^{2}H$.

This work demonstrates that information gained from isotopic measurements within MEMO², in addition to measurements of CH_4 mixing ratios, can be valuable for evaluating emission inventories and estimating emissions by atmospheric inversions. Isotopologues are useful to discriminate sector contributions of CH_4 emissions as the isotopic composition varies highly depending on the source type. For instance, the signature is different depending on whether CH_4 is produced by thermogenic (e.g. natural gas), biogenic (e.g. domestic animals, landfills, wetlands) or pyrogenic (combustion) sources. As a result, comparing the measured and simulated CH_4 mixing ratios and isotopic composition can provide additional information about the sources that contribute to a particular measurement. Finally, a third study focusses on the required precision of $\delta^{13}C$ and $\delta^{2}H$ measurements to constrain European methane sources. Thus, the overall aim of this task is to study how the various CH_4 sources, with different isotopic signatures, in different areas and environments in Europe, such as the regional or city scale, blend into larger-scale concentration fields.

The workhorse for ESR13 was the CHIMERE model. With this model, time series of atmospheric $\delta^{13}C$ and $\delta^{2}H$ isotope ratios are computed with an hourly temporal resolution based on simulated CH_4 mixing ratios for the four main CH_4 source categories: agriculture, waste, fossil fuel related emissions and wetland emissions.

As an example, Fig. 2.27 shows the results of the sectoral discrimination at Lutjewad. For this figure, we took the simulated CH_4 mixing ratios from the anthropogenic and wetland emission sources, as well as the total CH_4 mixing ratios without taking the background into account. We then compared the contribution of each emission sector to the total contribution in relative terms, which showed that 40-60% of the simulated mixing ratios above the background is due to the agriculture sector.

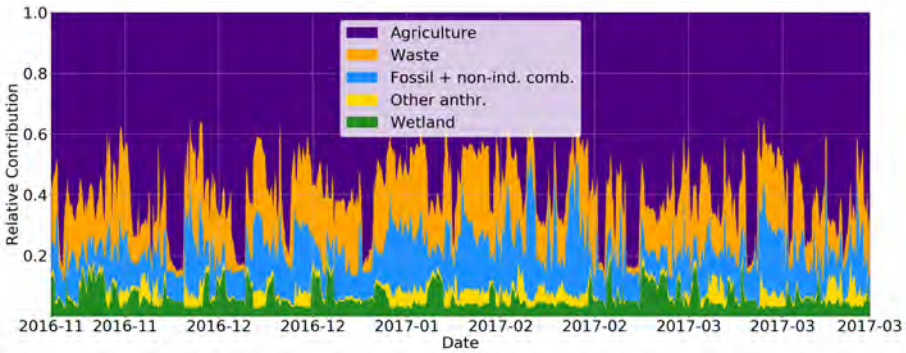

Fig. 2.27: Sectoral discrimination of CH_4 mixing ratios above background at Lutjewad. The emissions from TNO-MACC_III were used to simulate the sectoral contributions of CH_4 by CHIMERE that are shown in this figure.

Fig. 2.28 presents some of the results of the CHIMERE simulations in the form of Miller-Tans plots. It compares the simulated mixing ratios (with respect to the background) and isotope ratio to observations. Two emission inventories are compared. Further analysis revealed that the shift of the model relative to the observations is likely due to the boundary conditions used for the CHIMERE model.

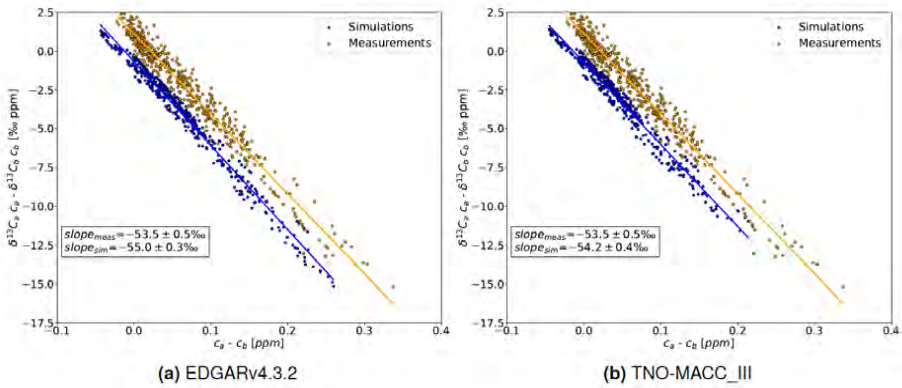

Fig. 2.28: Miller-Tans plots based on measured and simulated CH_4 mixing ratios and $\delta^{13}C$ isotopic ratios for the period November 2016 -- March 2017

In a further study it was investigated, through experiments with synthetic data, what could be the added value of high-frequency $\delta^{13}C$ and $\delta^{2}H$ data to be assimilated in atmospheric inversions, alongside with

CH_4 mixing ratios, to improve CH_4 emission estimates. The analysis reveals that the 0.2 ‰ and 5 ‰ precisions for $\delta^{13}C$ and $\delta^{2}H$ (WMO recommended targets) are sufficient for detecting sources only from large emitting areas, such as the Po-Valley in Italy or the Silesian coal basin in Poland, during about six months of the year (Fig. 2.29, showing an example using the TNO-MACC_III inventory for simulations).

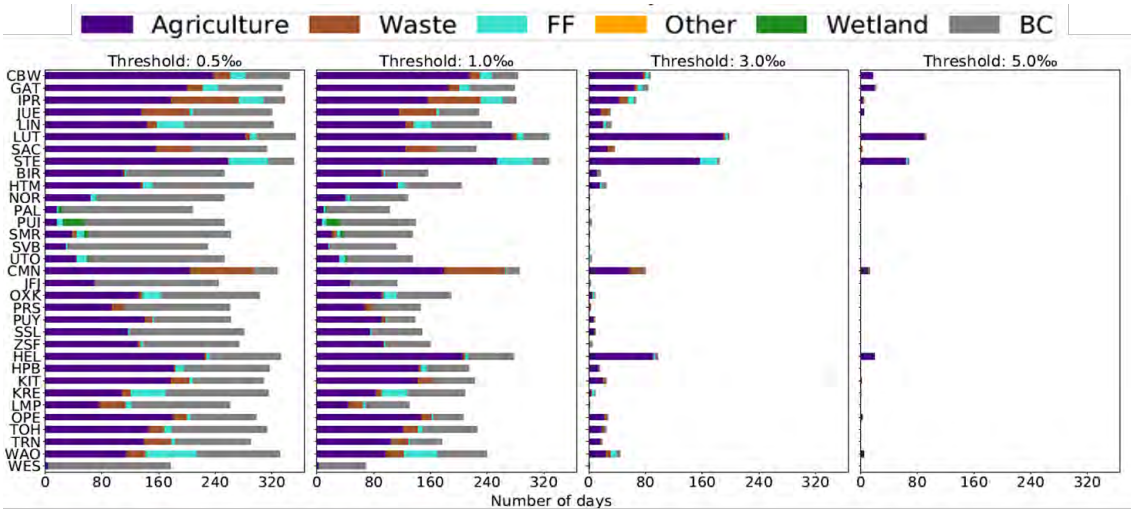

(a) $\delta^{2}H$, TNO-MACC_III

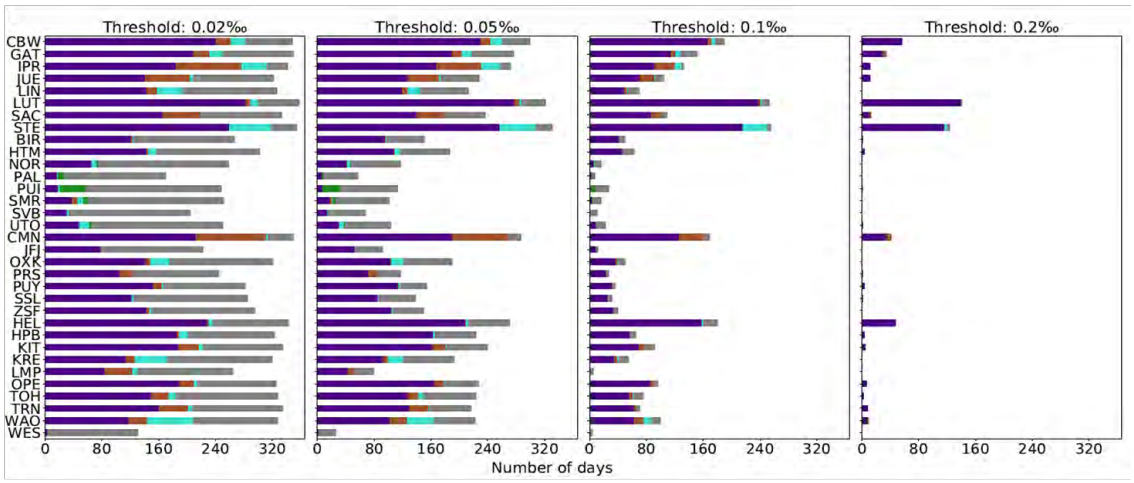

(b) $\delta^{13}C$, TNO-MACC_III

Fig. 2.29: Number of days in the study year when simulated daily source contributions to (**a**) $\delta^{2}H$ and (**b**) $\delta^{13}C$ at ICOS sites are above given thresholds, computed from standard deviations over the 3-day running windows, for the TNO-MACC_III inventory in the domain covering whole Europe. Colours indicate detectable source types.

The analyses demonstrate that mainly background and agricultural sources would be detectable at most ICOS sites (Fig. 2.29). The sites Steinkimmen (DE), Cabauw (NL), Lutjewad (NL) and Ispra (IT) have been implied by simulations with both inventories as potential sites for signal detection during at least six months in a year. However, areas around the first three sites are known for large emissions originating from agricultural activities and thus the main detectable confirmed source at these sites is agriculture. At Ispra, waste sources are the dominant detectable source. The sites Krešín u Pacova (CZ) and Lindenberg (DE) appear to be promising for the detection of fossil fuel related sources for about a month.

In conclusion, $\delta^{2}H$ and $\delta^{13}C$ data sets can be implemented in atmospheric inversions of CH_4 emissions over Europe, once a sufficient amount of $\delta^{2}H$ and $\delta^{13}C$ data with sufficient instrument precision are available. However, as studies of ESR13 showed, even higher precisions than 0.02 ‰ for $\delta^{13}C$ and 0.5 ‰ for $\delta^{2}H$ may be necessary to detect sources. This may be the case especially for wetland and fossil fuel related sources.

The original aim was to incorporate MEMO² measurements in providing improved emission estimates. This proved to be difficult. Performing and calibrating measurements takes time, as does setting up model simulations. Nevertheless, MEMO² measurements have played an important role in validating the model results, e.g. at Lutjewad. Furthermore, the simulations with synthetic observations of isotope ratios are very valuable for the measurement community. Detailed work has been performed on error characterisation of the CHIMERE inverse modelling framework, and benchmarked current emission estimates.

Task 3.4: Top-down estimates of EU emissions (LEAD: EMPA, Dominik Brunner)

Two meso-scale transport models with up to km-scale resolution will be used to infer EU-scale CH_4 emissions, and these estimates will be compared to products of the Copernicus services. The updated emission maps of task 3.2 will form the starting point of inverse modelling. EMPA will employ Lagrangian dispersion models to analyse the small-scale dispersion.

Overall, this task focussed on the quantification of CH_4 emissions from facility-scale sources such as landfills and oil and gas production facilities. It aimed to improve or validate bottom-up emission inventories using high-resolution dispersion simulations of CH_4 for the investigation of single sources. Moreover, a novel strategy of methane flux quantification with the use of unmanned aerial vehicle (UAV) equipped with a CH_4 sensor has been developed. The methods were evaluated in tracer release experiments with known emission rates and applied to quantify emissions from oil and gas wells in Romania as measured during the ROMEO campaign in October 2019. The task deviated slightly from the proposed work-plan. In the original plan it was proposed to use Lagrangian Particle Dispersion Models (LPDM) to simulate effects of point sources at European scale, and to perform atmospheric inversions. Moreover, it was planned to compare the LPDM results to LES simulations of ESR11 (WU). Concerning the use of LPDMs, simulation results from FLEXPART-COSMO were compared with observed ambient CH_4 isotopic composition (e.g. at Lutjewad, NL). Results indicate qualitative agreement between in-situ measurements of isotopic composition of CH_4 in ambient air and simulated CH_4 isotopic composition using FLEXPART-COSMO. The agreement between the measured and simulated values is a proof-of-concept that continuous high-resolution isotopic data is applicable to constrain source type information on a regional scale better.

In this task, use is made of Lagrangian dispersion modelling (GRAL). In order to benchmark the performance of GRAL, a tracer gas simulation using a Gaussian plume model was performed. Dispersion coefficients in the horizontal and vertical direction were prescribed by taking 5-minute averages of standard deviation of wind velocity fluctuations in crosswind horizontal and vertical direction. Using GRAL, Lagrangian forward dispersion simulations were conducted by prescribing the location of the source and the meteorological conditions. From the comparison in Fig. 2.30 it is clear that the dispersion parameters of the GPM lead to a too fast horizontal and vertical dispersion, similar to findings in Task 3.1.

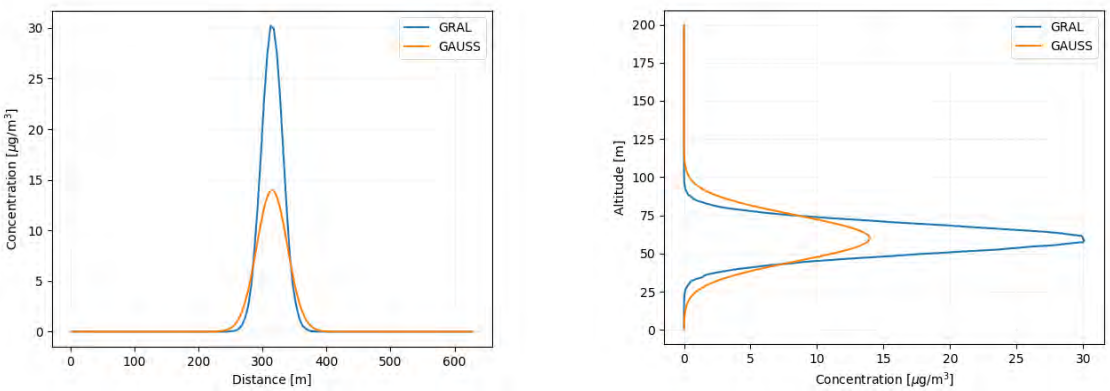

Fig. 2.30: Comparison of concentrations 100 m downwind of a source using GRAL (Blue) and the Gaussian plume model (GPM) (Orange).

To optimally exploit measurements with unmanned aerial vehicles, GRAL has been applied to the problem of source estimation. Unmanned vehicles allow a complete mapping of the spatial and temporal variability of emission plumes within a short period. A drone equipped with a QCLAS system was employed to sample a controlled release downwind.

Illustrated in Fig. 2.31 is an example of a flight measurement performed using this measurement setup. The UAV equipped with a methane sensor was flying 35 meters downwind of the source. Moreover, the plume was sampled at five different altitudes: 2.5, 5.0, 7.5, 10.0, and 12.5 meters above the ground. Each sampling height was measured twice before moving on to the next height.

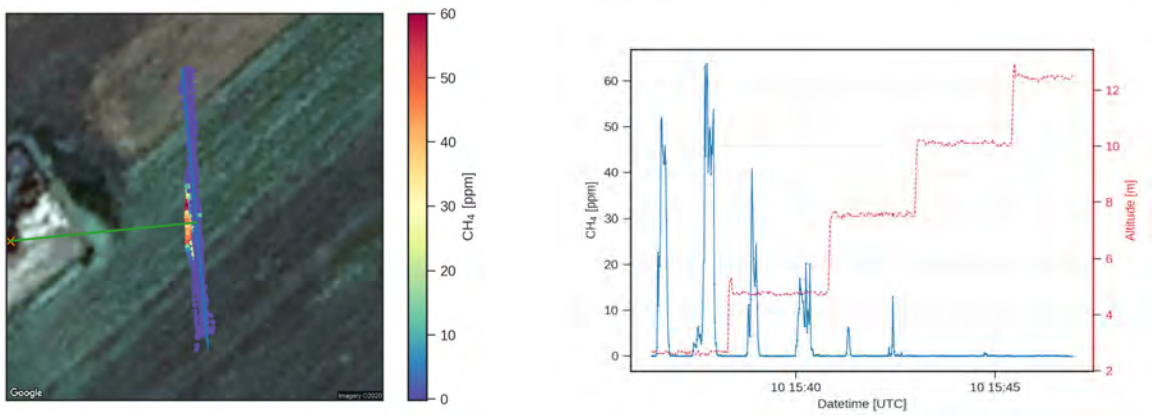

Fig. 2.31: Downwind sampling pattern of an UAV equipped with methane sensors. The left panel shows the source location and in colour the observed CH_4 enhancements. The right panel shows the sampling strategy: the plume was sampled twice at each measurement level.

In a next step, the measured mole fractions were gridded in a single plane, and geostatistical interpolation (Kriging) was applied in the plane, as shown in Fig. 2.32, to spatially fill the gaps within the plane. After filling in the gaps the source strength was estimated, using the cross-sectional area (m^2) and mean streamwise wind profile (m/s) obtained from the 3D sonic anemometer.

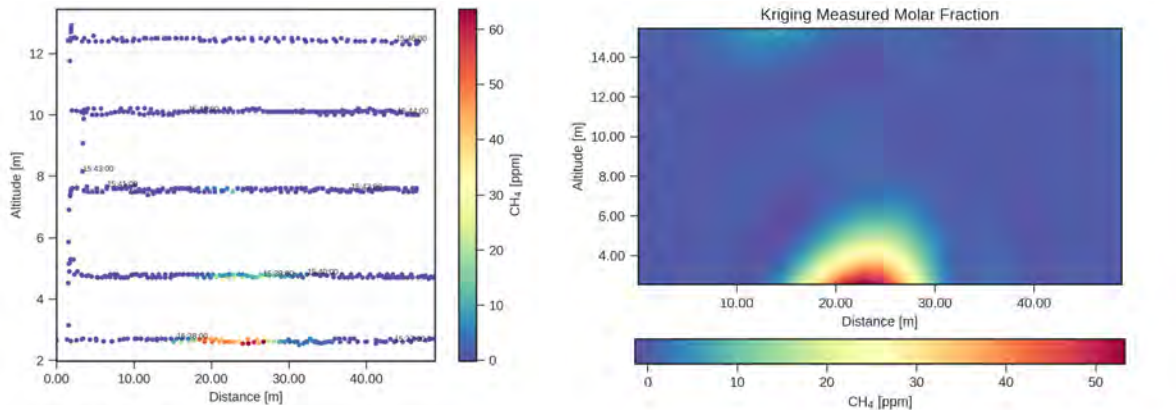

Fig. 2.32: Gridded measured methane mole fractions obtained from drone (left) and spatially filled measured methane mole fractions using Kriging (right).

The method was further tested and employed for source estimation. An extensive tracer release experiment was organized in Dübendorf, Switzerland from 23 Feb. to 14 Mar. 2020 to develop, optimize, and evaluate the quantification method.

Some results from the UAV measurements are given in Fig. 2.33. Cluster Kriging methods were developed to interpret the observations. In total six methods were compared to estimate the source strength. These methods differ in the Kriging method and the use of observed wind variables to calculate the source strength.

It was found that the Cluster-Kriging Projected-Wind (CK-PW) method gave the best estimate of the source strength (underestimate the true-release by ~5 % with a mean absolute error of 55 %). One of the reasons for the still large error is that it is difficult to capture the whole extent of the plume during the flights. For the UAV quantification method, it is recommended to fly at windspeeds > 2 m.s-1, and at downwind distances between 10 and 75 m.

Fig. 2.33:

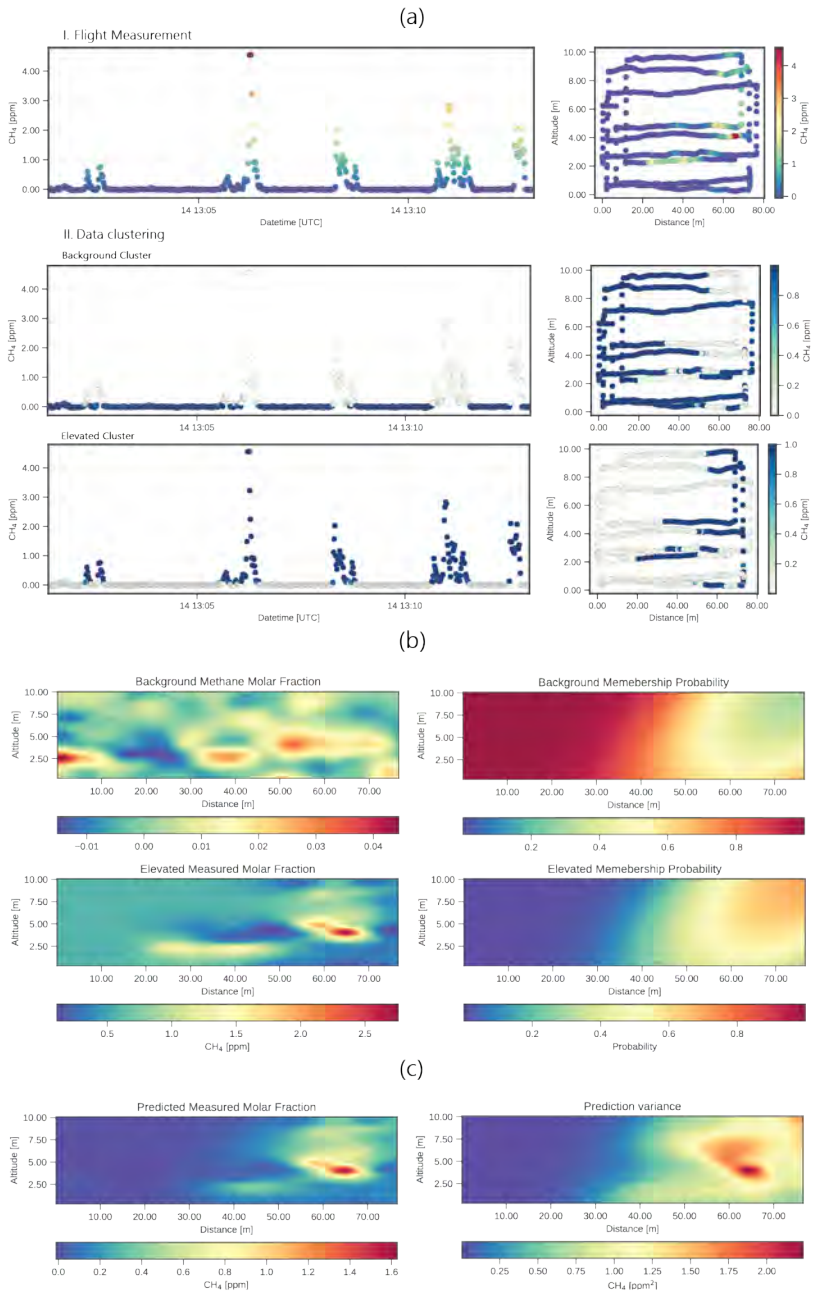

(a) Results from artificial tracer release experiment DüREx:314_02. Upper panel shows the measurement as a function of time and as a cross-wind direction/vertical plot. These measurements are analysed using a Gaussian Mixture Model (GMM) analysis. This model separates the background from the data points influences by the source.

(b) Kriging prediction and membership probabilities of each spatial point within the domain of interest for background and elevated clusters.

(c) Expected value and variance of CH_4 molar fractions after combining kriging prediction of the two clusters and their respective membership probabilities

The experiment also involved ESR2 (RUG) to compare the measurements from the fast in-situ drone analyser of Empa with the AirCore-system of the University of Groningen. In addition, the source quantifications from the drone were compared for selected cases with results from stationary measurements applying the OTM33A method as carried out by ESR1 (UHEI).

An AirCore collects air during flight in a thin tube, which is pushed through a gas-analyser after landing. A comparison is shown in Fig. 2.34. For the AirCore measurement it is expected that some diffusion within the tube occurs. This diffusion can be quantified. It was also found that a time-shift occurs, which gets longer towards the end of the flight. Correcting for this time shift is very important for a correct quantification of the source strength using AirCore. This cooperation shows a clear synergy within MEMO².

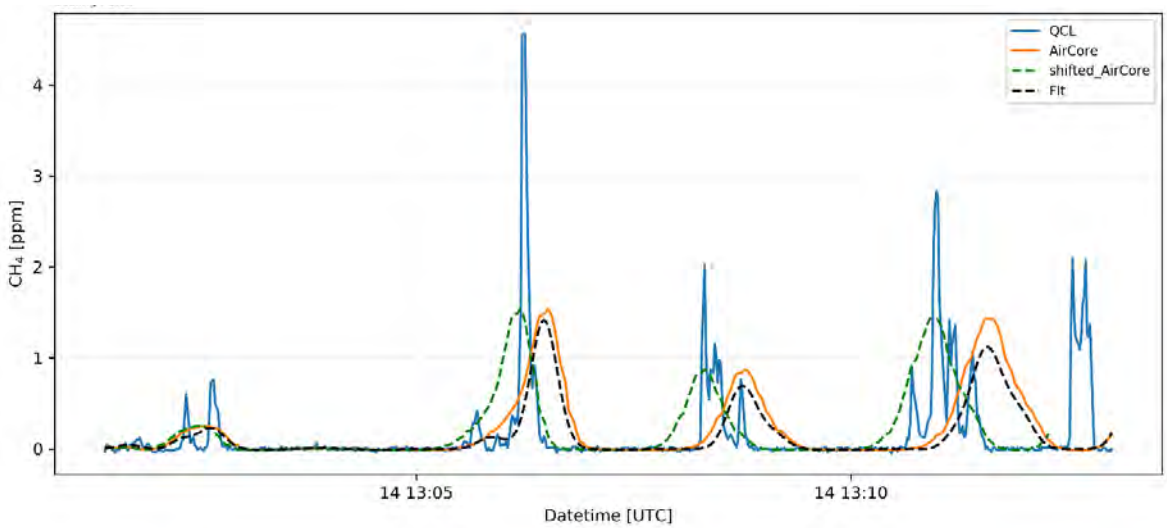

Fig. 2.34: Comparison between measurements with the QCL system and AirCore. The blue line shows the QCL measurements, which are smoothed (green) and shifted (orange) to match the AirCore (black). In this way, the required smoothing and time shifts have been determined.

The gained knowledge was also implemented in the evaluation of data from the ROMEO campaign. In collaboration with UHEI the OTM33A estimation was compared to the UAV-based quantification, using known release rates. It was found that the estimates agree within the errors. However, errors of both quantification methods remain substantial (~50 %). Fig. 2.35 compares the estimated source strength from different targets. Results of the CK-PW UAV and AirCore are shown.

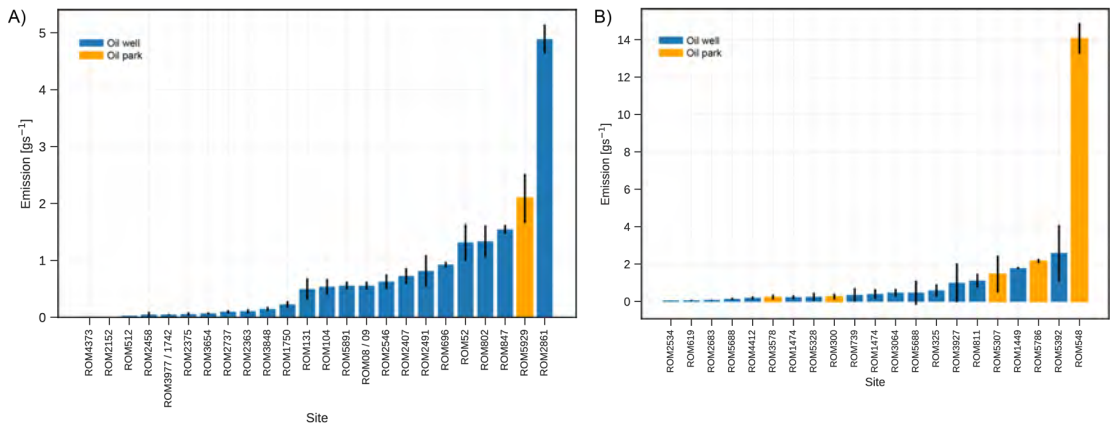

Fig. 2.35: Estimated emission rates from oil and gas wells of visited sites in Romania. Reported uncertainty is the standard deviation (1σ) of multiple quantified emissions per site (N>=2) and estimated uncertainty of individual flight (N=1) A) Empa UAV B) Groningen University AirCore.

Currently, all quantification estimates from different ground-based measurement techniques performed during ROMEO are further analysed. As a major outcome of MEMO², this will provide a robust estimate of oil and gas emissions in Romania.

Within this project also the model FLEXPART-COSMO was used on European scale. FLEXPART-COSMO is a model version of FLEXPART, an offline Lagrangian Particle Dispersion Model (LPDM), which uses the output of the mesoscale numerical weather prediction model COSMO as the driving meteorology. In this model version, all meteorological fields are preserved on the original COSMO vertical grid which, compared to other versions of FLEXPART, strongly reduces interpolation errors. Top-down CH4 emission estimates for whole Europe for the years 2005-2017 have been produced in the framework of the VERIFY project using FLEXPART-IFS and are currently being adapted on inversions with FLEXPART-COSMO.

Using this model, continuous timeseries of CH_4 mole fraction as well as the isotopologues $\delta^{13}C\text{-}CH_4$ and $\delta D\text{-}CH_4$ in ambient air at the Lutjewad station located in the Netherlands were simulated. Fig. 2.36 shows an example in which measurements are compared to simulation results using three different emission inventories (co-operation with ESR12). The figure shows a qualitative agreement between in-situ measurements of isotopic composition of methane in ambient air and simulated CH_4 isotopic composition using FLEXPART-COSMO. The agreement between the measured and simulated values is a proof-of-concept that continuous high-resolution isotopic data can be used to better constrain source type information on a regional scale.

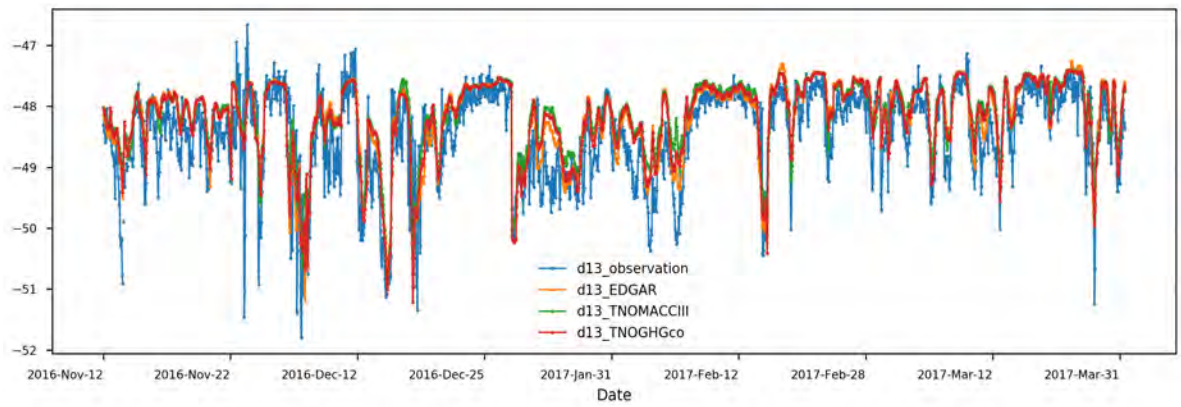

Fig. 2.36: Simulated isotopic composition of methane ($\delta^{13}C\text{-}CH4$) compared to observed values obtained from the Lutjewad station in the Netherlands.

Task 3.5: Workshop on top-down emission estimates (LEAD: WU, Maarten Krol)

A workshop was planned for around project month 30, but postponed due to the participation of the MEMO² ESRs to the ROMEO campaign. It was then scheduled in September 2020, associated to the ICOS conference in Utrecht. Unfortunately, based on the pandemic situation the conference was held remotely. As the topic of the workshop was not relevant for all ESRs, being already part of the individual training of several of them, and an informal introduction had also given during the ROMEO campaign, there was at this stage in the project no general benefit of the workshop for the ESRs. Thus, time was dedicated to support ESRs individually at the host institutions to finalize their data evaluation and prepare the publications.

2.2.4 WP4 – Training (Lead: Philippe Bousquet, UVSQ)

2.2.4.1 General WP overview and contribution of involved beneficiaries

This WP involved all beneficiaries and non-academic partners of MEMO². All activities scheduled in WP4 continued as planned. ESRs updated their individual Career Development Plan (CDP, D4.5) during the 3rd Annual Meeting, held in February 2020 at UHEI. This was the last update of the CDPs.

The main, not only scientific but also training highlight of this period was the ROMEO campaign, organised in collaboration with MEMO², where all ESRs were directly or indirectly involved. The campaign offered an excellent opportunity for ESRs to learn about the complexity of logistical and scientific setting-up and executing a joint field campaign, next to jointly gaining unique and high-quality data.

2.2.4.2 Progress of WP tasks

Task 4.1: Monitoring and quality assurance of training goals (LEAD: UVSQ, Philippe Bousquet)

Training of ESRs will be organized on an individual and a network level as described in detail in chapter 1.2 of the GA. The individual training will be specified in the CDPs for each ESR, which are updated on an annual basis. The progress of the ESRs will be monitored by the supervisors / co–supervisors. A more detailed description of the quality assurance procedure is given in chapter 3.2.4 of the GA.

The monitoring of training goals was performed both at local and project scales. At local scale, the supervisors of the ESRs took care that their students i) have access to useful training courses in local universities/institutions to support her/his career development plan and ii) attend to the relevant international conferences and workshops. At the project scale, the career development plan (CDP) and the table of secondments were the key elements of the monitoring. The CDPs were implemented as living documents, adapting to the present and future activities and plans of the ESRs. The last update of the CDPs had been executed at the 3rd Annual meeting and was submitted as D4.5.

The secondments (Table 2.5) were an important part of the student work, and included a research and a training dimension. All ESRs have done at least 2 secondments (D4.3). With respect to the work planning and the additional ROMEO field campaign, some secondment periods had slightly been shifted compared to the original plan. This was to ensure that the spent secondment time was used efficiently and beneficial regarding the project objectives. Due to travel restrictions and safety issues several secondments planned for the last year of the project were executed remotely.

ESRs were encouraged to report about their secondments as blogs, published on the website as those blogs do not only reflect the work done but also enhance the writing skills of the ESRs towards a public audience, and disseminate the project and its outcomes. Their blogs are available on the project website (https://h2020-memo2.eu/category/blog/).

Task 4.2: Organisation of network training events (LEAD: UU, Thomas Röckmann)

The network training will be coordinated by the UU and locally organized by dedicated PI´s and their groups. A list of the training events is given in Table 1.2.1c of the GA. The network training events are mandatory for the ESRs. The project meetings are part of the training (see WP5).

During the second reporting period, no dedicated network training courses were organised. Training took place by local supervision, network meetings and the (international) conferences and field campaigns the ESRs participated in. The training included e.g. presenting their work to other supervisors and ESRs by oral presentations, participating in the ROMEO joint field campaign, practice with instruments, or joint data analysis and writing scientific publications.

Several ESRs presented their results at scientific conferences as given in Table 3.1. A final MEMO² conference, associated to the final meeting was initially planned to be organised in collaboration with ICOS. Due to the pandemic situation the UU together with the ICOS headquarter decided to organise the conference remotely.

2.2.5 WP5 – Project Management (Lead: Thomas Röckmann, UU)

The Project Management and the work done are described in detail in Chapter 4.

2.2.6 WP6 – Ethics (Lead: Thomas Röckmann, UU)

Within WP6 - Ethics – two deliverables (D6.1 and D6.2) have been submitted. The ethical aspects of the project, with focus on the use of drones, will be applied throughout the project lifetime as described.

2.3 Deliverables

Within the second reporting period 16 deliverables and 8 milestones were due. Several deliverables were delayed. The main reason for this was the organisation of and participation in the ROMEO field campaign as these data were implemented in the MEMO² data sets and used e.g. for modelling work. The ROMEO field campaign was an additional campaign on top of the initial planning. A brief overview of the campaign is given in Chapter 2.2.1.2, Task 1.4. Table 2.3 gives an overview of all project deliverables and their actual status.

Table 2.3: overview of project deliverables and their actual status

Scientific Deliverables

No.	Deliverable Title	Lead	Due Date	Status*
D1.1	Lightweight CH_4 sensor and Air-Core developed and deployed on UAV	RUG	24	Approved
D1.2	Report / publication on CH_4 emissions from wetland and lakes in Sweden	LU	30	Submitted
D1.3	Report / publication of results from the campaign in Silesia, Poland	AGH	36	Approved
D1.4	Improved emission factors for different source categories from mobile measurements	UHEI	42	Submitted
D1.5	Report on harmonized method for mobile CH_4 and $^{13}CH_4$	UHEI	18	Approved
D2.1	Isotopic measurements linked to common scale	RHUL	18	Approved Additionally the inter-comparison tanks were circulated around the mobile laser-based mobile isotopic measurement groups to link them to the common scale in addition to UU and RHUL.
D2.2	Improved isotopic source signatures of local and regional CH_4 emissions	UU	36	Submitted In month 39 after delays due to additional survey requirements (ROMEO project).
D2.3	Publications on the use of isotopes for CH_4 source attribution in urban / industrial regions	RHUL	36	Submitted In month 48 after delays due to additional survey requirements (ROMEO project). Publications for Paris (ESR5), Bucharest (ESR9 and ESR 10), London (ESR9) and Hamburg (ESR10) are published or in preparation.
D2.4	Publication on temporal / meteorological influences on CH_4 at fixed sites	RHUL	42	Submitted In month 48. The data from 2 fixed sites in Netherlands and Poland has been evaluated. ESR 8 has published a paper on the NL site and a second manuscript has been submitted.
D2.5	Report providing isotopic maps at grid scale from inventories and atmospheric measurements	UU	42	Submitted In month 48. The required data from D2.2 and D2.3 were needed to form the database to produce these maps.
D3.1	New tools to estimate CH_4 source strengths from point sources, including mobile measurements	WU	24	Approved
D3.2	Improved bottom-up European CH_4 emissions	UU	30	Submitted In month 48. During the previous reporting periods the focus was laid on measurement campaigns to ensure a solid data base. The task of constructing high-resolution emission maps and including the isotopic signatures will continue beyond MEMO².
D3.3	Forward modelling simulations of CH_4 and isotopologues	UVSQ	30	Approved
D3.4	Top-down estimates of EU-scale CH_4 emissions	Empa	42	Submitted Top-down CH_4 emission estimates for whole Europe for the years 2005-2017 have been produced in the framework of the VERIFY project using FLEXPART-IFS and is being adapted on inversions with FLEXPART-COSMO.
Management, Training, Recruitment and Dissemination Deliverables				
D4.1	Individual Career Development Plan for each ESR	UVSQ	12	Approved
D4.2	Annual update of the CDP for each ESR	UVSQ	24	Approved
D4.3	Two secondments for each ESR completed	UU	30	Submitted

D4.4	Two MEMO² schools organized	UU	30	Approved
D4.5	Annual update of the CDP for each ESR	UVSQ	36	Approved
D4.6	Two conference participations for each ESR completed	UU	42	Submitted
D5.1	MEMO² consortium agreement	UU	1	Approved
D5.2	Project Management Plan (PMP)	UU	6	Approved
D5.3	Data management, Dissemination & Exploitation Plan (DDEP)	UU	6	Approved
D5.4	Recruitment of ESRs finished	UU	9	Approved
D5.5	Project meetings organized (UU, Empa, RUG, RHUL, UHEI)	UU	48	Submitted Meetings organized: Kickoff (UU), 1st Annual Meeting (Empa), 2nd Annual Meeting (UVSQ), 3rd Annual Meeting (UHEI)
D5.6	Reports approved by Supervisory Board and sent to EC	UU	48	Submitted
D5.7	Communication infrastructure established – interactive website including public dissemination	UU	6	Approved
D5.8	Progress Report	UU	13	Approved
D5.9	Mid-term Review Report	UU	22	Approved
D5.10	Supervisory Board of the network	UU	2	Approved
D6.1	NEC – Requirement No.1	UU	6	Approved
D6.2	EPQ – Requirement No.2	UU	6	Approved

***Note:** The status "In Progress" may differ between this table and the status given in the ESR reports (in the attachment). This is due to the differing involvement of ESRs into the planning and execution of deliverables.

2.4 Milestones

Within the 2nd reporting period 8 milestones were due.

Table 2.4: overview of milestones in the project and their actual status

Nr.	Milestone Title	Lead	Due date	Status / Report
M1	ESRs trained at host institute with mobile equipment	UHEI	10	Achieved (see D5.8)
M2	First intensive campaign with training in the Netherlands	RUG	12	Achieved (MS2 report submitted)
M3	Workshop on Gaussian plume and dispersion models	UHEI	15	Achieved (MS3 report submitted)
M4	Lightweight CH_4 sensor and Air-Core developed and deployed on UAV	RUG	24	Achieved (see D1.1)
M5	Second intensive campaign in Silesia (Poland)	AGH	30	Achieved (see D1.3) As indicated in the Midterm Report, an additional intensive campaign was organised (ROMEO, see Chapter 2.2.1.2, Task 1.4)
M6	ESRs trained at host institute to measure/interpret isotope data	RHUL	12	Achieved (see D5.8)
M7	Comparative isotopic scale for project groups established	UU	15	Achieved (see D2.1) The comparison between groups is continuing to gain a better understanding of laboratory measurement differences during exchange of different types of air bag samples, when there is very good agreement for samples in stainless steel cylinders. Completion of Deliverable 2.1 has allowed continuing comparison of the results from co-located sampling and exchange of sample bags between UU and RHUL. This has focused on samples collected during surveys in Bucharest and Paris.
M8	Workshop on isotope measurement techniques and data interpretation	RHUL	20	Achieved (MS8 report submitted)
M9	Isotopic maps at grid scale produced from inventories and atmospheric measurements	RHUL	36	Achieved (D2.2 / D2.3) A variety of maps have been produced from the MEMO² isotopic database (D2.2) and an allied and extended UK isotopic database. These have been used to construct distribution maps of CH_4 sources with isotopic measurements at European and national scale, but these highlight the very localised nature of measurements, that are focussed around measurement labs or in the regions of the intensive MEMO² / COMET / UNCCAC campaigns. Isotopic measurement is not yet routine and performed by all project partners. In areas with enough measurement (London, Bucharest), isotopic maps of city

				sources have been produced. Enough measurements have been made in England and Wales over the last decade that C-isotopic signatures can be applied to the national inventory (NAEI) and produce predicted isotopic maps that assume the estimated emissions are correct. For Greater London, which has been heavily surveyed and sampled (D2.3), this has allowed comparison between real sample isotopes and predictions.
M10	Large Eddy Simulation Tools ready for campaign & workshop	WU	12	Achieved (MS10 report submitted)
M11	First updated CH_4 emission map EU	UU	30	Achieved (see D3.2)
M12	Workshop on top-down emission estimates	UVSQ	30	Partly achieved The milestone was initially postponed due to the ROEMO campaign, but then jeopardized by the pandemic. As the topic of the workshop was not relevant for all ESRs, already part of the individual training of several of them, and an informal introduction also given during the ROMEO campaign, there was at this stage in the project no general benefit of an additional workshop for the ESRs (see Chapter 2.2.3.2, Task 3.5)
M13	Two secondments for each ESR completed	UU	30	Achived (see D4.3)
M14	Two MEMO² schools organized	UU	30	Achieved (see D4.4)
M15	Two conference participations for each ESR completed	UU	42	Achieved Conference participations are given in Table 3.1
M16	Communication infrastructure established – interactive website including public dissemination	UU	6	Achieved (see D5.7)
M17	Planned recruitments completed and recruited fellows enrolled in PhD programme	UU	12	Achieved (see D5.4)
M18	Project meetings organized (UU, Empa, RUG, RHUL, UHEI)	UU	48	Achieved Meetings organized: Kickoff (UU), 1st Annual Meeting (Empa), 2nd Annual Meeting (UVSQ), 3rd Annual Meeting (UHEI), Final Meeting (UU, remotely associated to the 4th ICOS Science Conferenc)

2.5 Impact

MEMO² aimed on impact on different levels such as personal levels for the ESRs (career perspective and employability), structural training levels (national / international training) and scientific levels (provision of data and contribution to the evaluation of EU greenhouse gas emission reduction policies). All expected impacts as described in the Midterm Report were relevant throughout the project, and the consortium successfully implemented them.

All ESRs have done at least two of their secondments (deliverable D4.3) and reported about them by public blogs on the project website (https://h2020-memo2.eu/category/blog/). As mentioned before, the secondment schedule as described in the Grant Agreement needed some adjustments to ensure them as efficient as possible for the ESRs. This was necessary e.g. due to the late recruitment of several ESRs, the execution of several mobile measurement campaigns which often depended on circumstances such as weather conditions or unexpected delays in sample measurements. The last secondment of ESR11 was delayed and took place remotely due to the Corona pandemic. Table 2.5 gives an overview executed secondments.

Table 2.5: Overview of executed secondments

ESR	Secondments executed / ongoing
ESR1: Piotr Korben (UHEI)	AGH (22.05.18 – 10.06.18, 31.10.18 – 9.11.18), https://h2020-memo2.eu/2018/08/16/1056/ LSCE (02.2019 – 03.2019), https://h2020-memo2.eu/2020/01/30/piotr-korben-is-paris-a-romantic-city-or-a-city-of-methane/
ESR2: Katarina Vinkovic (RUG)	ECN (26.08. – 07.09. 2018, 29.10. 2018. – 25.01. 2019), https://h2020-memo2.eu/2019/06/19/katarina-vinkovic-are-the-cow-farts-real-threat/ Empa (14.02. – 16.03.2020), https://h2020-memo2.eu/2020/07/10/katarina-vinkovic-drone-race-with-covid-19/
ESR3: Mila Stanisavljevic (AGH)	PGI (short preparation visit 18.10. - 20.10.2017) PGI (01.08.-01.10.2019) UHEI (13.01.-10.02.2018), https://h2020-memo2.eu/2020/05/14/mila-stanisavljevic-adventurous-month-in-germany/

	UU (15.05.-01.06.2019), https://h2020-memo2.eu/2020/01/31/mila-stanisavljevic-the-isotopic-signature-of-methane-from-coal-mines-facilities/
ESR4: Patryk Lakomiec (LU)	Afvall Sverige - Single preparation days Afvall Sverige (28.10.-15.11.2019), https://h2020-memo2.eu/2020/06/09/patryk-lacomiek-quantification-of-landfill-methane-emissions-a-method-comparison-study/ RHUL (19.11.-30.11.2018), https://h2020-memo2.eu/2018/12/06/patryk-lakomiec-swedish-air-goes-britain/ ROMEO in collaboration with Empa (30.09.-13.10.2019), https://h2020-memo2.eu/2020/05/14/romeo-afterwards-impressions/
ESR5: Sara Defratyka (UVSQ)	RHUL (17.06.-13.07.2018), https://h2020-memo2.eu/2018/12/05/sara-defratyka-aircores/ NPL (03.09.-17.09.2019), https://h2020-memo2.eu/2020/05/15/sara-defratyka-unobvious-side-of-science-secondment-at-npl/
ESR6: Badrudin Stanicki (EMPA)	No secondments due to resignation
ESR6b: Jonas Ravelid (EMPA)	LU (26.08.-15.09.2019) ROMEO in collaboration with UHEI (30.09.-20.10.2019)
ESR7: Semra Bakkaloglu (RHUL)	RUG (17.09.-26.10.2018), https://h2020-memo2.eu/2019/02/01/semra-bakkaloglu-what-an-adventurous-secondment/ UU (27.05.-07.06.2019), Viridor (07.05. – ongoing), https://h2020-memo2.eu/2020/05/15/semra-bakkaloglu-what-happens-to-my-garbage/
ESR8: Malika Menoud (UU)	AGH (16.05.-30.05.2018, to be continued), https://h2020-memo2.eu/2018/09/21/installation-of-a-cf-irms-and-methane-extraction-system/ AGH (15.03.-27.03.2019) RHUL (18.06.-14.07.2018), https://h2020-memo2.eu/2019/02/09/malika-menoud-secondment-at-royal-holloway-university-of-london/ UVSQ (17.02.-13.03.2020), https://h2020-memo2.eu/2020/04/21/malika-menoud-lets-play-with-the-isotopic-signatures/
ESR9: Julianne Fernandez (RHUL)	UU (24.09.-21.10.2018), https://h2020-memo2.eu/2019/02/10/julianne-fernandez-the-isotopic-signature-of-urban-methane-emissions/ UVSQ (12.02.-23.03.2019) ELEMENTAR (23.09.27.09.2019, 14.10.-19.10.2019)
ESR10: Hossein Maazallahi (UU)	TNO (01.2018 – ongoing), https://h2020-memo2.eu/2019/02/11/hossein-maazallahi-my-collaboration-with-tno/ AGH (05-06 2018, CoMet campaign)
ESR11: Anja Raznjevic (WU)	Empa (26.03.-27.04.2018), https://h2020-memo2.eu/2018/11/07/anja-raznjevic-modeling-dispersion-of-methane/ Wiffle (fall 2020)
ESR12: Randulph Morales (EMPA)	UVSQ (29.10.-23.11.2018), https://h2020-memo2.eu/2020/02/05/randulph-morales-a-research-visit-with-an-unexpected-road-trip-secondment-at-lsce/ WU (10.11.-07.12.2019), https://h2020-memo2.eu/2020/02/05/randulph-morales-being-closer-to-the-environment-in-wageningen/
ESR13: Barbara Szenasi (UVSQ)	WUR (19.02.2018–19.03.2018), https://h2020-memo2.eu/2018/09/05/ barbary-szenasi-my-research-visit-at-wageningen-university/ TNO (17.06.-12.07.2019), https://h2020-memo2.eu/2020/04/20/barbara-szenasi-secondment-in-the-exceptionally-sunny-netherlands/ UU (09.-20.12.2019), TNO (13.-24.01.2020), https://h2020-memo2.eu/2020/04/20/barbara-szenasi-secondment-in-the-exceptionally-sunny-netherlands/

Table 2.6: Overview of total sample collection days per ESR

ESR	Number of measurement days
1	89
2	58
3	30
4	54
5	87
6	14 / 62
7	60
8	74
9	60
10	113
11	6
12	59
13	6

Impact for the ESRs is not only created by the executed secondments but also by giving them the chance to visit international conferences and present their projects and results. An overview is given in the next chapter in Table 3.1 about the dissemination activities within MEMO².

For the project as a whole, general impact is also created by available data sets. The consortium continued producing and providing high-quality data sets. As described in the Data Management Plan (D5.3), data are collected on the ICOS data portal and will be public available after the project. The activities for data collection are listed in the individual ESR reports in Chapter 6 and an overview of executed measurement days per ESR is given in the in Table 2.6.

The description of the scientific impact is implemented in the task reporting of the WPs and is highlighted and summarized in the final report.

2.6 Evaluation of the Action by the external Supervisory Board (SB)

In the third year the Scientific Advisory Board was extended by Bill Hirst as we highly appreciated his scientific contribution to the project. He was already participating in the project as representative of Shell before, but retired last year.

As for the first years, the SAB has general access to all relevant documents via the internal SURFDrive folders, e.g. to the Grant Agreement, previous reports, and deliverables. The advice and suggestions given by the SAB at the 2nd Annual Meeting have been implemented as much as possible. One of the main suggestions of the SAB was to make use of the unique data sets by synthesizing and implementing them in the forward and also backward modelling to get realistic emission estimates. This has been realised in working towards the related deliverables but also towards peer-reviewed publications. Other suggestions were to focus on interdisciplinarity, collaboration, and to ensure that the interdisciplinary expertise will be capitalized such that MEMO² offers added value to the scientific community.

This has been continued and extended e.g. by organising and executing the ROMEO campaign (see Chapter 2.2.1.2, Task 4). The ROMEO campaign also worked towards the SAB suggestion that the training should include stimulating scientific thinking and scientific creativity to ensure that ESRs are able to plan projects themselves and become experts in their field. Most ESRs were participating in the field part of the campaign, the rest was participating remotely or was involved in data evaluation and implementation. By this the ESRs had the opportunity to develop a deep understanding of good measurement practices, including uncertainties and intercomparison, and the measurement needs depending on the aim of the research. Beside this, the consortium was continuously communicating about the project to keep the recognition and visibility of the project on a high level.

The progress of the project was demonstrated during the 3rd Annual meeting as a general overview, an overview per WP and by oral presentations of the ESRs. During the meeting Alex Vermeulen (ULUND) and Bill Hirst (Shell, retired) represented the SAB. As the last year was mainly focussed on the organisation and execution of the ROMEO campaign and as data are still under evaluation, the SAB was invited to get an update about the progress but not requested to participate physically in the meeting.

As an outcome of the 3rd Annual Meeting, the SAB stated to be impressed by the progress and the results, and advised the consortium to keep up the good work. Especially the enthusiastic collaboration within the consortium on all levels, the impressive amount of data, and the progress in CH_4 modelling was emphasised. As the project went in the critical phase of harvesting, the SAB suggested to prepare an overview about achievements, how to use and disseminate them, e.g. create a kind of “cooking book” with recipes for different CH_4 sources, how to deal with measurements, emission and model factors. It is important that data are publicly available in the future and that the consortium ensures exploitation of them for the long-term impact of MEMO². This is ongoing and lasting beyond the project lifetime. It was also suggested to consider a follow-up project to keep the momentum and continue the work on this highly relevant topic.

Regarding the timeline of the project the final year was important for the ESRs to finish, with the requirement of producing meaningful and sustainable data. The main topics for the last year suggested by the SAB were:

- Ensure that all data are high quality and available on the ICOS server
- Ensure that data already available are used and additional data are collected where needed, e.g. additional isotope data for modelling
- Implement a kind of roadmap for MEMO² and its activities to ensure that the interdisciplinary expertise will be capitalized and that MEMO² offers added value to the scientific community
- Continue communicating and disseminating MEMO² and its results
- Finalise the deliverables and milestones on a high-quality level so that they offer added value to the community and increase the long-term impact of MEMO².

The consortium implemented the recommendations so far as much as possible as they are crucial for long-term impact of the project. Several suggestions will also last beyond MEMO², e.g. data evaluation, publication of results, and communication and dissemination activities regarding the project.

3. Communication, dissemination and exploitation

The consortium continued to actively communicate and disseminate MEMO² as an EU project in general and by presenting results of the individual ESR projects. The consortium is using different platforms to approach different target groups, aiming on increasing the impact of the consortium as such and the understanding of the project type H2020-ITN-ETN in general. As scientific platforms conferences are used to not only communicating the individual scientific projects within MEMO² and their results, but also MEMO² as itself. Table 3.1 shows the dissemination activities of MEMO² (mainly ESR) at the scientific platforms so far.

Table 3.1: Dissemination activities of MEMO²

Nr.	Conference name	Location	Date	Type	Title of presentation	Authors / Conveners	Link
1	EGU 2017	Vienna, Austria	24-28 April 2017	Poster	MEMO2: Methane goes MObile – MEsurements and MOdelling – Part 1	Walter, S., Röckmann, T., and the MEMO² team:	http://meetingorganizer.copernicus.org/EGU2017/EGU2017-13442.pdf
2	EGU 2017	Vienna, Austria	24-28 April 2017	Poster	MEMO2: Methane goes MObile – MEsurements and MOdelling – Part 2	Röckmann, T., Walter, S., and the MEMO² team	http://meetingorganizer.copernicus.org/EGU2017/EGU2017-15754.pdf
3	EGU 2017	Vienna, Austria	24-28 April 2017	Splinter meeting SMP6	MEMO2: Methane goes MObile – MEsurements and MOdelling	Walter, S. and Röckmann, T.	http://meetingorganizer.copernicus.org/EGU2017/session/25151
4	Industrial Methane Measurement Conference – PEFTEC 2017	Antwerp, Belgium	29-30 November 2017	oral	Short duration, high precision methane flux measurements: Implications for annual CH_4 emission reporting and CH_4 mitigation strategies	Denier van der Gon, H., Arzoumanian, E., Bouchet, C., Jonkers, S. Kelly, R., Morin, D.	https://www.ilmexhibitions.com/peftec/abstracts/Short+duration%2C+high+precision+methane+flux+measurements%3B+Implications+for+annual+CH4+emission+reporting+and+CH4+mitigation+strategies/223/
5	Industrial Methane Measurement Conference – PEFTEC 2017	Antwerp, Belgium	29-30 November 2017	oral	Identification and validation of methane sources using carbon-13 measurements	Fisher, R., Lowry, D., Zazzeri, G., al-Shalaan, A., France, J., Brownlow, R.	https://www.ilmexhibitions.com/peftec/abstracts/Identification+and+validation+of+methane+sources+using+carbon-13+measurements/210/
6	Industrial Methane Measurement Conference – PEFTEC 2017	Antwerp, Belgium	29-30 November 2017	oral	Validating methane measurement techniques	Robinson, R.	https://www.ilmexhibitions.com/peftec/abstracts/Validating+methane+measurement+techniques/224/
7	Industrial Methane Measurement Conference – PEFTEC 2017	Antwerp, Belgium	29-30 November 2017	oral	Methane source attribution: Methane and ethane analysis using a portable battery-powered Picarro Cavitiy Ring-Down spectrometer	Winkler, R.	https://www.ilmexhibitions.com/peftec/abstracts/Methane+source+attribution%3A+Methane+and+Ethane+Analysis+Using+a+portable+Battery-powered+Picarro+Cavity+Ring-down+Spectrometer/238/
8	Industrial Methane Measurement Conference – PEFTEC 2017	Antwerp, Belgium	29-30 November 2017	oral	A new technique for detecting gas emissions and estimating the locations and mass emission rates of sources	Hirst, B., Randell, D.	https://www.ilmexhibitions.com/peftec/abstracts/A+new+technique+for+detecting+gas+emissions+and+estimating+the+locations+and+mass+emission+rates+of+sources./241/

9	Industrial Methane Measurement Conference – PEFTEC 2017	Antwerp, Belgium	29-30 November 2017	poster	Methane source distribution in the complex landscapes of the United Kingdom: isotopic characterisation, seasonal variation and inventory validation	Lowry, D.	https://www.ilmexhibitions.com/peftec/abstracts/Methane+source+distribution+in+the+complex+landscapes+of+the+United+Kingdom%3A+isotopic+characterization%2C+seasonal+variation+and+inventory+validation/284/
10	Industrial Methane Measurement Conference – PEFTEC 2017	Antwerp, Belgium	29-30 November 2017	poster	MEMO²: MEthane goes MObile - MEasurements and MOdelling	Walter, S., Röckmann, T.	https://www.ilmexhibitions.com/peftec/abstracts/MEMO2%3A+MEthane+goes+MObile+-+MEasurements+and+Modelling/214/
11	Industrial Methane Measurement Conference – PEFTEC 2017	Antwerp, Belgium	29-30 November 2017	poster	Isotopic composition of methane from exhausts of mines and gas fields in South Poland	Necki, J., Zimnoch, M., Jasek, A., Chmura, L., Lakomiec, P., Korben, P., Wolkowicz, W.	https://www.ilmexhibitions.com/peftec/abstracts/Isotopic+composition+of+methane+from+exhausts+of+mines+and+gas+fields+in+South+Poland./229/
12	EGU 2018	Vienna, Austria	8-13 April 2018	poster	Starting an EU project – lessons learnt from the first year of MEMO²	Walter, S.	https://presentations.copernicus.org/EGU2018-7406_presentation.pdf
13	EGU 2018	Vienna, Austria	8-13 April 2018	poster	MEMO²: MEthane goes MObile – MEsurements and MOdelling	Walter, S., Röckmann, T., and the MEMO² team	https://meetingorganizer.copernicus.org/EGU2018/posters/26398
14	EGU 2018	Vienna, Austria	8-13 April 2018	Splinter meeting SMP1	MEMO²: Methane goes MObile – MEsurements and MOdelling	Walter, S. and Röckmann, T.	https://meetingorganizer.copernicus.org/EGU2018/session/29051
15	EGU 2018	Vienna, Austria	8-13 April 2018	Short Course SC3.13	How to apply for the MSCA grants IF and ETN	Walter, S., Ingrin, J., Henkel, D., Padrón-Navarta, J.A.	https://meetingorganizer.copernicus.org/EGU2018/session/28965
16	EGU 2018	07. – 12.04. 2018.	Vienna (Austria)	poster	Bottom – up methane budget estimation from the sources over Upper Silesian Coal Basin	M. Stanisavljevic, J. Necki, M. Zimnoch, L. Chmura, M. Galkowski, W. Wolkowicz, P. Lakomiec	https://meetingorganizer.copernicus.org/EGU2018/EGU2018-14798.pdf
17	EGU 2018	Vienna, Austria	8-13 April 2018	poster	Modeling CH_4 dispersion using three modeling techniques to prepare a field campaign on methane emissions	A. Ražnjević , C. van Heerwaarden , M. Krol	https://meetingorganizer.copernicus.org/EGU2018/EGU2018-13940.pdf
18	EGU 2018	Vienna, Austria	8-13 April 2018	poster	Atmospheric monitoring of methane emission at the European scale	B. Szénási, I. Pison, G. Broquet, M. Saunois, P. Bousquet, A. Berchet	https://presentations.copernicus.org/EGU2018-14964_presentation.pdf
19	3rd ICOS Science Conference	Prague (Czech Republic)	10. – 14.09. 2018	poster	Quantification of methane emissions from dairy cows in the Netherlands	K.Vinkovic,T.Andersen, M.de Vries, W. Peters, A. Hensen, H. Chen	https://conference.icos-ri.eu/wp-content/uploads/2018/08/ICOS-SC-Programme.pdf
20	3rd ICOS Science Conference	Prague (Czech Republic)	10. – 14.09. 2018	poster	Using the PicarroG2301-m for airborne eddy covariance measurements of GHG fluxes	Lakomiec, P., Peltola, O., Holst, J., Rinne, J.	https://conference.icos-ri.eu/wp-content/uploads/2018/08/ICOS-SC-Programme.pdf
21	3rd ICOS Science Conference	Prague (Czech Republic)	10. – 14.09. 2018	poster	Mobile measurement of CH_4 isotopes in urban, mining and industrial environments	S. Defratyka, C. Yver Kwok, A. Hensen, J. Necki, D. Lowry, J.-D. Paris, P. Jagoda, P. Bousquet	https://conference.icos-ri.eu/wp-content/uploads/2018/08/ICOS-SC-Programme.pdf
22	3rd ICOS Science Conference	Prague (Czech Republic)	10. – 14.09. 2018	poster	MEMO²: Methane goes MObile – MEsurements and MOdelling	Walter, S. and Röckmann, T.	https://conference.icos-ri.eu/wp-content/uploads/2018/09/ICOS2018SC_Book_of_Abstracts.pdf
23	3rd ICOS Science Conference	Prague (Czech Republic)	10. – 14.09. 2018	poster	Waste Source in the UK	S. Bakkaloglu + D. Lowry, R. Fisher, E. Nisbet	https://conference.icos-ri.eu/wp-content/uploads/2018/09/ICOS2018SC2424_Book_of_Abstracts.pdf

24	3rd ICOS Science Conference	Prague (Czech Republic)	10. – 14.09. 2018	poster	Isotopic characterization of methane from mine shafts in the Silesia region	M. Menoud, H. Maazallahi, M. Stanisavljevic, T. Röckmann, J. Necki	https://www.researchgate.net/publication/327655309_Isotopic_characterisation_of_methane_from_mine_shafts_in_the_Silesia_region
25	3rd ICOS Science Conference	Prague (Czech Republic)	10. – 14.09. 2018	poster	Methane Emission Mapping and Evaluation across Utrecht City, the Netherlands	H. Maazallahi, M. Menoud, C. van der Veen, H. Denier van der Gon, T. Röckmann	https://conference.icos-ri.eu/wp-content/uploads/2018/09/ICOS2018SC_Book_of_Abstracts.pdf
26	3rd ICOS Science Conference	Prague (Czech Republic)	10. – 14.09. 2018	poster	Combining airborne and ground based remote sensing (lidar, spectrometer) as well as in-situ techniques to determine CH4 emissions of a European CH4 emission hot spot area – initial results from COMET	H. Bovensmann and the CoMet team	https://conference.icos-ri.eu/wp-content/uploads/2018/09/ICOS2018SC_Book_of_Abstracts.pdf
27	3rd ICOS Science Conference	Prague (Czech Republic)	10. – 14.09. 2018	poster	Airborne measurements of GHG fluxes over northern wetlands	J. Holst, P. Lakomiec, J. Rinne	https://conference.icos-ri.eu/wp-content/uploads/2018/09/ICOS2018SC_Book_of_Abstracts.pdf
28	Flair conference	Assisi, Italy	12.09.2018	oral	A compact QCL absorption spectrometer for mobile, high-precision methane measurements aboard drones	B. Stanicki, B. Tuzson, L. Chang, M. Graf, P. Scheidegger, H.Looser, L. Emmenegger	https://fox.ino.it/flair/FLAIR%202018%20-%20Scientific%20Program.pdf
29	NAC	Utrecht, NL	21.-22.03.2019	Poster	Isotopic characterization of methane sources across Europe	M.Menoud, C. van der Veen, B. Szenasi, H. Maazallahi, B. Scheeren, H. Chen, J. Necki, P. Bousquet, T. Röckmann	https://www.nwo.nl/actueel/nieuws/2019/04/succesvol-verloop-van-aardwetenschappelijk-congres-nac2019.html
30	NAC	Utrecht, NL	21.-22.03.2019	Poster	MEMO2: MEthane goes MObile -- MEasurements and Modelling	S. Walter, T. Röckmann	https://www.nwo.nl/actueel/nieuws/2019/04/succesvol-verloop-van-aardwetenschappelijk-congres-nac2019.html
31	EGU 2019	Vienna, Austria	7-12 April 2019	Splinter meeting SMP7	MEMO²: MEthane goes MObile – MEsurements and MOdelling	Walter, S. and Röckmann, T.	https://meetingorganizer.copernicus.org/EGU2019/session/33411
32	EGU 2019	Vienna, Austria	7-12 April 2019	Pico	MEMO²: MEthane goes MObile – MEsurements and MOdelling	Walter, S. and Röckmann, T.	https://meetingorganizer.copernicus.org/EGU2019/EGU2019-4798.pdf
33	EGU	Vienna, Austria	08/04/19-12/04/19	PICO	Methane source mapping in Paris urban area from mobile measurement of mole fraction and isotopic composition	S. Defratyka, C. Yver-Kwok, J.-D. Paris, P. Bousquet	https://sharebox.lsce.ipsl.fr/index.php/s/avpXcncjQTXVIfO
34	EGU	Vienna, Austria	08/04/19-12/04/19	PICO	Using continuous high-precision isotope measurements over several months to characterize sources of atmospheric methane at various European locations	M. Menoud, C. van der Veen, B. Szenasi, B. Scheeren, H. Chen, J. Necki, P. Bousquet, T. Röckmann	https://meetingorganizer.copernicus.org/EGU2019/EGU2019-15656.pdf
35	EGU	Vienna, Austria	08/04/19-12/04/19	PICO	Mapping, emission quantification, and attribution of methane enhancements across two European cities; Utrecht, NL and Hamburg, DE	H. Maazallahi, D. Zavala-Araiza, S. Schwietzke, M. Menoud, J. Fernandez, R. Fisher, D. Lowry, E. Nisbet, H. Denier van der Gon, T. Röckmann	https://meetingorganizer.copernicus.org/EGU2019/EGU2019-17678-2.pdf
36	EGU	Vienna, Austria	08/04/19-12/04/19	PICO	Investigations of Methane Emissions from the Munich Oktoberfest 2018	J. Chen, F. Dietrich, H. Maazallahi, D. Winkler, A. Forstmaier, M. Hofmann, H. Denier van der Gon, T. Röckmann	https://meetingorganizer.copernicus.org/EGU2019/EGU2019-15485-1.pdf

37	EGU	Vienna, Austria	08/04/19-12/04/19	oral	Tidal dynamics control microbial methane oxidation in the water column above an active cold seep (Doggerbank, North Sea)	T. de Groot, H. Maazallahi, T. Röckmann, S. Walter, M. Menoud, B. Meijninger, C. Mesdag, D. Rush, H. Niemann	https://meetingorganizer.copernicus.org/EGU2019/EGU2019-5523-1.pdf
38	EGU	Vienna, Austria	08/04/19-12/04/19	PICO	Evaluation of methane emission inventories at the European scale by comparing atmospheric transport models and measurements	B. Szenasi, I. Pison, A. Berchet, G. Broquet, P. Bousquet, M. Saunois, H. Denier van der Gon, A. Segers, R. Morales, D. Brunner	https://meetingorganizer.copernicus.org/EGU2019/EGU2019-14884.pdf
39	EGU	Vienna, Austria	08/04/19-12/04/19	PICO	Characterising methane emissions from North Sea gas production using δ13C in CH4 and C2H6:CH4 ratios	M. Coleman, R. Fisher, D. Lowry, J. France, M. Lanoiselle, J. Fernandez	https://meetingorganizer.copernicus.org/EGU2019/EGU2019-14892.pdf
40	EGU	Vienna, Austria	08/04/19-12/04/19	Oral	A Tale of Three Cities: Mobile Methane Measurement and Isotopic Characterisation in London, Kuwait and Hong Kong	D. Lowry, R. Fisher, G. Zazzeri, J. Fernandez, A. al-Shalaan, M. Lanoisellé, J. France, S. Bakkaloglu, E. Nisbet	https://meetingorganizer.copernicus.org/EGU2019/EGU2019-7975.pdf
41	EGU conference	Vienna, Austria	08/04/19-12/04/19	Oral	Combining airborne remote sensing (lidar, spectrometer) of CH4 as well as in-situ data to determine CH4 emissions of a European CH4 emission hot spot area – initial results from the COMET campaign	H. Bovensmann, S. Krautwurst, A. Fiehn, A. Roiger, K. Gerilowski, J. Borchardt, S.-L. Meyer, A Fix, N. Necki, J. Swolkień, A. Amediek, P. Jöckel, M. Gałkowski, C. Gerbig and the COMET Team*	https://meetingorganizer.copernicus.org/EGU2019/EGU2019-15249-2.pdf
42	EGU	Vienna, Austria	08/04/19-12/04/19	Oral	Airborne in-situ measurements of CO2 and CH4 and their interpretation using WRF-GHG: results from the HALO CoMet 1.0 campaign	M. Galkowski, C. Gerbig, J. Marshall, F.-T. Koch, J. Chen, S. Baum, A. Jordan, A. Fiehn, A. Roiger, P. Jöckel, A.-L. Nickl, M. Mertens, H. Bovensmann, J. Necki, J. Swolkien, G. Ehret, C. Kiemle, A. Amediek, M. Quatrevalet, A. Fix and the COMET Team*	https://meetingorganizer.copernicus.org/EGU2019/EGU2019-14091.pdf
43	EGU	Vienna, Austria	08/04/19-12/04/19	Pico	Quantifying methane emissions using mobile FTIR spectrometry during CoMeT	A. Luther and the COMET Team*	https://meetingorganizer.copernicus.org/EGU2019/EGU2019-10182.pdf
	Journées de Spectroscopie Moléculaire JSM 2019	Paris, France	21.-23.05.2019	Oral	Quantum cascade laser spectroscopy for high- precision measurements of atmospheric trace-gases and their isotopes	L. Emmenegger B. Tuzson, J. Mohn, K. Kantnerova, M. Hundt, F. Kapsalidis, M. Shahmohammadi, P. Scheidegger, O. Aseev, H. Looser, J. Faist	https://jsm-creteil2019.sciences-conf.org/data/pages/RECUEIL_DES_RESUMES_JSM_2022.pdf
44	PEFTEC 2019	Rotterdam, The Netherlands	22.-23.05.2019	Poster	Stable isotopic signature of methane from biogas sources in the UK and the Netherlands	S. Bakkaloglu, D. Lowry, R. Fisher, C. Huilin, E. Nisbet	
45	PEFTEC 2019	Rotterdam, The Netherlands	22.-23.05.2019	Poster	Isotopic signatures of urban methane emission in London	Fernandez J.M., D. Lowry, R. Fisher, E. Nisbet, JL France, Colman, S. Bakkaloglu	
46	PEFTEC 2019	Rotterdam, The Netherlands	22.-23.05.2019	Oral	Methane Emission Mapping and Evaluation across Utrecht City, the Netherlands	H. Maazallahi, J. M. Fernandez, M. Menoud, R. Fisher, D. Zavala Araiza, Z. D. Weller, S. Schwietzke, J. C.	https://www.ilmexhibitions.com/methane/speakers-list/

						von Fischer, H. Denier van der Gon, T. Röckmann	
47	PEFTEC 2019	Rotterdam, The Netherlands	22.-23.05.2019	Oral	Building mobile measurement and modelling capacity to detect and quantify methane leakages from gas production and distribution in Europe: the MEMO2 project	T. Röckmann and the MEMO² team	https://www.ilmexhibitions.com/methane/abstract/Building+mobile+measurement+and+modelling+capacity+to+detect+and+quantify+methane+leakages+from+gas+production+and+distribution+in+Europe%3A+the+MEMO2+project/807/
48	NCGG8	Amsterdam, The Netherlands	12/06/19-14/06/19	Oral	MEMO²: MEthane goes MObile – MEsurements and MOdelling	Walter, S., Röckmann, T.	
49	NCGG8	Amsterdam, The Netherlands	12/06/19-14/06/19	Poster	Using long-term high-precision isotope measurements to characterise sources of atmospheric methane at various European locations	M. Menoud, C. van der Veen, B. Scheeren, H. Chen, J. Necki, D. Brunner, R. P. Morales, T. Röckmann	
50	NCGG8	Amsterdam, The Netherlands	12/06/19-14/06/19	oral	Isotopic signatures of urban methane emissions in London, UK	Fernandez JM, D. Lowry, R. Fisher, E. Nisbet	
51	NCGG8	Amsterdam, The Netherlands	12/06/19-14/06/19	Poster	Mobile in situ measurements of methane mixing ratio over Upper Silesian Coal Basin	M. Stanisavljević, J. Necki, H. Maazallahi, M. Menoud, K. Vinkovic, Piotr Korbeń, M. Schmidt, L. Chmura, J. Bartyzel, M. Gałkowski, W. Wołkowicz, G. Florczyk, S. Defratyka	
52	NCGG8	Amsterdam, The Netherlands	12/06/19-14/06/19	Oral	Mobile measurement of methane in Ile de France region – source mapping, isotopic composition & emission estimation	S. Defratyka, C. Yver-Kwok, J.-D. Paris, P. Bousquet	https://sharebox.lsce.ipsl.fr/index.php/s/0EIdZUPvNs163Hq
53	NCGG8	Amsterdam, The Netherlands	12/06/19-14/06/19	Oral	Methane Emission Mapping and Evaluation across Utrecht City, the Netherlands	H. Maazallahi, J. M. Fernandez, M. Menoud, R. Fisher, D. Zavala Araiza, Z. D. Weller, S. Schwietzke, J. C. von Fischer, H. Denier van der Gon, T. Röckmann	
54	NCGG8	Amsterdam, The Netherlands	12.06.-14.06.2019	Poster	High precision isotope measurements to characterise waste source of atmospheric methane	S. Bakkaloglu, D. Lowry, R. Fisher, C.Huilin, E. Nisbet	
55	NCGG8	Amsterdam, The Netherlands	12.06.-14.06.2019	Poster	Methane, Ethane and Nitrous oxide transect mapping using mobile measurements	Dinther, D. van	
56	NCGG8	Amsterdam, The Netherlands	12.06.-14.06.2019	oral	Monitoring the methane emission from different sources around Heidelberg, Germany	P. Korben, A. Hoheisel, J. Kammerer, J. Wietzel, M. Schmidt	https://www.ncgg.info/ncgg8/proceedings
57	NCGG8	Amsterdam, The Netherlands	12.06.-14.06.2019	Poster	Quantification of methane emissions from dairy cows in the Netherlands	K.Vinkovic, T.Andersen, M.deVries, W.Peters, A.Hensen, H.Chen	https://www.ncgg.info/ncgg8/proceedings
58	NCGG8	Amsterdam, The Netherlands	12.06.-14.06.2019	oral	Quantifying localized methane source emissions from mobile sensors using an obstacle-resolving Lagrangian dispersion model	R. Morales, L. Emmenegger, D. Brunner	https://www.ncgg.info/ncgg8/proceedings

59	NCGG8	Amsterdam, The Netherlands	12.06.-14.06.2019	Oral	Atmospheric monitoring of methane emissions at the European scale	B. Szenasi, I. Pison, A. Berchet, G. Broquet, P. Bousquet, M. Saunois, H. Denier van der Gon, A. Segers, R. Morales, D. Brunner	https://www.ncgg.info/ncgg8/proceedings
60	NCGG8	Amsterdam, The Netherlands	12.06.-14.06.2019	Oral	Methane/ethane used to split fossil and non-fossil methane emissions	Dinther, D. van	https://www.ncgg.info/ncgg8/proceedings
61	NCGG8	Amsterdam, The Netherlands	12.06.-14.06.2019	Oral	Offshore gas & methane emission measurements at the North Sea	Maazallahi, H., Ilona Velzeboer	https://www.ncgg.info/ncgg8/proceedings
62	NCGG8	Amsterdam, The Netherlands	12.06.-14.06.2019	Oral	A high-precision mid-IR methane laser spectrometer for UAVs	Emmenegger, Lukas	https://www.ncgg.info/ncgg8/proceedings
63	NCGG8	Amsterdam, The Netherlands	12.06.-14.06.2019	Oral	Methane emission verification for the Upper Silesia coal basinin Poland using earth observation data	H. Denier van der Gon, J. Hullegie, A. Segers, S. Pandey, P. Sadavarte, J. Landgraf, S. Houweling, M. Krol, I. Aben	https://www.ncgg.info/ncgg8/proceedings
64	NCGG8	Amsterdam, The Netherlands	12.06.-14.06.2019	Oral	Airborne in-situ observations during the CoMet campaign 2018: Quantification of CH4emissions from coal mining activities in Upper Silesia, Poland	A. Roiger, A. Fiehn, J. Kostinek, M. Eckl, P. Jöckel, M. Mertens, A. Nickl, A. Fix, A. Butz, M. Schmidt, T. Röckmann, H. Maazallahi, C. Gerbig, M. Galkowski, J. Swolkien, J. Necki	https://www.ncgg.info/ncgg8/proceedings
65	NCGG8	Amsterdam, The Netherlands	12.06.-14.06.2019	Oral	CH4 lidar measurements during the CoMet 2018 airborne field campaign	A. Fix, A. Amediek, C. Büdenbender, G. Ehret, C. Kiemle, M. Quatrevalet, M. Wirth, S. Wolff, H Bovensmann, A. Butz, C. Gerbig, P. Jöckel, J. Marshall, J. Nęcki, K. Pfeilsticker, A. Roiger, J. Swolkień, M. Zöger, and the CoMet team	https://www.ncgg.info/ncgg8/proceedings
66	45th Congress of Polish Physicists	Cracow, Poland	13.09.-18.09.2019	poster	Isotopes measurements and methane emissions from different sources in Germany and Poland	P. Korbeń, H. Krümpelmann, M. Schmidt	
67	2nd Nordic ICOS Symposium	24.10.2019-25.10.2019	Gothenburg, Sweden	Poster	Methane emissions from a palsa-mire underlayed by sporadic permafrost under rapid degradation	P. Łakomiec, J. Holst, J. Rinne	http://www.icos-sweden.se/symp/Abstract_Lakomiec.pdf
68	AGU	09. – 13.12.2019	San Francisco, US	Poster	The greenhouse gas methane emissions from waste sources in the UK	S. Bakkaloglu, D. Lowry, R. Fisher, C.Huilin, E. Nisbet	https://agu.confex.com/agu/fm19/meetingapp.cgi/Home/Paper/499625
69	AGU	09. – 13.12.2019	San Francisco, US	Poster	Fugitive methane emissions from UK onshore gas distribution: geo-chemical characterisation and inventory verification	D. Lowry, R. Fisher, J.L. France, M. Coleman, J. Fernandez, M. Lanoisellé, G. Zazzeri, E. G. Nisbet, J. Shaw, G. Allen J. R. Pitt	https://agu.confex.com/agu/fm19/meetingapp.cgi/Home/Paper/501580
70	AGU	09. – 13.12.2019	San Francisco, US	Poster	Charactistics of urban methane emissions in London: the determination of small leaks in a large city	J. Fernandez, D. Lowry, R. Fisher, E. G. Nisbet, J. L France, P. Nisbet-Jones, M. Coleman, M. Lanoisellé, S. Bakkaloglu	https://agu.confex.com/agu/fm19/meetingapp.cgi/Home/Paper/580804
71	AGU	9th -13th Dec 2019	San Francisco, CA, USA	Poster	Characteristics of Urban Methane Emissions in London: The	Fernandez J.M., D. Lowry, R. Fisher, E. Nisbet, JL France, P. Nisbet-Jones, M.	

					Determination of Small Leaks in a Large City	Colman, S. Bakkaloglu, M. Lanoiselle	
72	NAC	12.-13.2020	Utrecht, Netherlands	Oral	Methane Emission Mapping and Evaluation across Utrecht City, the Netherlands	H. Maazallahi, J. M. Fernandez, M. Menoud, R. Fisher, D. Zavala Araiza, Z. D. Weller, S. Schwietzke, J. C. von Fischer, H. Denier van der Gon, T. Röckmann	https://nacgeo.nl
73	NAC	12.-13.2020	Utrecht, Netherlands	Oral	Characterisation of methane sources in Lutjewad, NL, using high temporal resolution isotopic composition mesurements	M. Menoud, C. van der Veen, B. Scheeren, H. Chen, B. Szenasi, R. Morales, D. Brunner, T. Röckmann	https://nacgeo.nl
74	NAC	12.-13.2020	Utrecht, Netherlands	Poster	MEMO²: MEthane goes MObile – MEsurements and MOdelling	Walter, S. and Röckmann, T.	https://nacgeo.nl
75	EGU2020	04.-09.05.2020	online	Display format	Emissions of CH4, CO2, C2H6, CO and isotopic signatures in thde Upper Silesian Coal Basin, Poland	A. Fiehn, J. Kostinek, M. Eckl, M. Galkowski, J. Chen, C. Gerbig, T. Röckmann, H. Maazallahi, M. Schmidt, P. Korben, J. Necki, N. Wildmann, C. Mallaun, T. Klausner, R. Bun, A. Fix, A. Roiger	https://meetingorganizer.copernicus.org/EGU2020/EGU2020-19119.html
76	EGU2020	04.-09.05.2020	online	Display format	Methane emissions from coal mines ventilation shafts in Upper Silesia, Poland	M. Stanisavljevic, J. Nęcki, P. Korbeń, H. Maazallahi, M. Menoud, S. Defratyka, K. Vinkovic, C. van der Veen, Ł. Chmura, D. Zieba, M. Schmidt, W. Wołkowicz, T. Röckmann, J. Wietzel, J. Swolkień	https://meetingorganizer.copernicus.org/EGU2020/EGU2020-15165.html
77	EGU2020	04.-09.05.2020	online	Display format	Isotopic characterisation of methane emissions from oil and gas operation in Romania	M. Menoud, C. van der Veen, H. Maazallahi, J. Fernandez, P. Korben, A. Calcan, J. France, D. Lowry, M. Schmidt, T. Röckmann	https://meetingorganizer.copernicus.org/EGU2020/EGU2020-13643.html
78	EGU2020	04.-09.05.2020	online	Display format	Methane emission from dairy farm located in north of Heidelberg	P. Korben, J. Kammerer, J. Wietzel, M. Schmidt	https://meetingorganizer.copernicus.org/EGU2020/EGU2020-20442.html
79	EGU2020	04.-09.05.2020	online	Display format	Methane emissions from a palsa-mire underlayed by sporadic permafrost under rapid degradation	P. Łakomiec, J. Holst, J. Rinne	https://meetingorganizer.copernicus.org/EGU2020/EGU2020-4748.html
80	EGU2020	04.-09.05.2020	online	Display format	Estimating local methane sources from drone-based laser spectrometer measurements by mass-balance method	R. P. Morales, J. Ravelid, K. P. Brennan, B. Tuzson, L. Emmenegger, D. Brunner	https://meetingorganizer.copernicus.org/EGU2020/EGU2020-14778.html
81	EGU2020	04.-09.05.2020	online	Display format	Characterization and Quantification of Methane Emissions from Waste in the UK	S. Bakkaloglu, D. Lowry, R. Fisher, J. France, M. Lanoiselle, J. Fernandez	https://meetingorganizer.copernicus.org/EGU2020/EGU2020-17839.html
82	EGU2020	04.-09.05.2020	online	Display format	Characteristics of urban street level methane emissions in Bucharest, Romania	J. Fernandez, J. France, M. Menoud, H. Maazallahi, M.-P. Corbu, T. Röckmann, R. Fisher, D. Lowry	https://meetingorganizer.copernicus.org/EGU2020/EGU2020-21759.html
83	EGU2020	04.-09.05.2020	online	Display format	Methane Source Attribution Challenges in the Surat Basin, Australia	X. Lu, S. J. Harris, R. E. Fisher, D. Lowry, J. L. France, J. Hacker, B. Neininger, T. Röckmann, C. van der Veen, M. Menoud, S. Schwietzke, B. F.J. Kelly	https://meetingorganizer.copernicus.org/EGU2020/EGU2020-12508.html
84	EGU2020	04.-09.05.2020	online	Display format	Atmospheric satellite-based and in situ surface observations on summertime trace gases (CO, CO2,	M.-P. Corbu, A. Calcan, I. Vizireanu, D. E. Moaca, R.-V. Chiritescu, T. Röckmann, H. Maazallahi, J. M. Fernandez, J, France, G. Iorga	https://meetingorganizer.copernicus.org/EGU2020/EGU2020-4930.html

					CH4) over the metropolitan area of Bucharest		
85	EGU2020	04.-09.05.2020	online	Display format	Temporal water column dynamics control microbial methane oxidation above an active cold seep (Doggerbank, North Sea)	T. de Groot, M. Menoud, T. Röckmann, H. Maazallahi, D. Rush, C. Mesdag, B. Meijninger, H. Niemann	https://meetingorganizer.copernicus.org/EGU2020/EGU2020-5366.html
86	EGU2020	04.-09.05.2020	online	Display format	Methane Emission Source Attribution and Quantification for Munich Oktoberfest	J. Chen, F. Dietrich, S. Lober, K. Krämer, G. Legget, H. Denier van der Gon, I. Velzeboer, C. van der Veen, T. Röckmann	https://meetingorganizer.copernicus.org/EGU2020/EGU2020-18919.html
87	EGU2020	04.-09.05.2020	online	Display format	MEMO2: MEthane goes MObile – MEasurements and Modelling	S. Walter, T. Röckmann and the MEMO² team	https://meetingorganizer.copernicus.org/EGU2020/EGU2020-6760.html
88	EGU2020	04.-09.05.2020	online	Display format	ROMEO – ROmanian Methane Emissions from Oil and Gas	T. Röckmann and the ROMEO team	https://meetingorganizer.copernicus.org/EGU2020/EGU2020-18801.html
89	4th ICOS	15-17 Sep. 2020	Online	Oral	Atmospheric transport model analysis of methane emissions from oil- and gas-production in Romania observed during the ROMEO campaign in 2019	Brunner, D. Steiner, M., Jähn, M., Mertens, M., Jöckel, P., Ardelean, M. Calcan, A., Schwietzke, S., Lauvaux, T., Maazallahi, H., Röckmann, T.	https://www.icos-cp.eu/sc2020/abstracts#170
90	4th ICOS	15-17 Sep. 2020	Online	Oral	Spatio-temporal kriging in estimating local methane sources from drone-based laser spectrometer measurements	Morales, R., Ravelid, J., Vinkovic, K., Tuzson, B., Emmenegger, L., Brunner, D.	https://www.icos-cp.eu/sc2020/abstracts#178
91	4th ICOS	15-17 Sep. 2020	Online	Oral	Comparison of large eddy simulation of a point source methane plume in a slightly convective atmosphere with measurements from MEMO² campaign	Raznjevic, A., van Heerwaarden, C., Krol, M., Hensen, A., van den Bulk, P., Velzeboer, I.	https://www.icos-cp.eu/sc2020/abstracts#175
92	4th ICOS	15-17 Sep. 2020	Online	Oral	Effect of the 2018 drought on methane and carbon dioxide exchange of northern mire ecosystems	Rinne, J., Tuovinen, J.-P., Klemedtsson, L., Aurela, M., Holst, J., Lohila, A., Weslien, P., Vestin, P., Peichl, M., Tuittila, E.-S., Heiskanen, L., Laurila, T., Li, X., Alekseychik, P., Mammarella, I., Ström, L., Crill, P., Nilsson, M.	https://www.icos-cp.eu/sc2020/abstracts#195
93	4th ICOS	15-17 Sep. 2020	Online	Poster	Quantification of methane emission from oil and gas wells using Other Test Method 22a during ROMEO campaign	P.Korben P.Jagoda, H. Maazallahi, J.Necki, J.Bartyzel, A. Radovici, M.Schmidt,, T.Roeckmann	https://www.icos-cp.eu/sc2020/abstracts#196
94	4th ICOS	15-17 Sep. 2020	Online	Poster	Isotopic composition of methane from Swedish wetlands	Łakomiec, P., Bakkaloglu, S., Fernandez, J., Fisher, R., Holst, J., Lanoiselle, M., Lowry, D., Menoud, M., Röckmann, T., Ström, L., White, J., Rinne, J.	https://www.icos-cp.eu/sc2020/abstracts#186
95	4th ICOS	15-17 Sep. 2020	Online	Oral	Local-scale atmospheric inversion for the estimation of the location and rate of CH4 and CO2 controlled releases using mobile and fixed-point measurements	Kumar, P., Broquet G., Caldow C., Laurent O., Yver-Kwok C., Cropley F., Defratyka S., Gichuki S., Lauvaux T., Rivera R., Zheng B., Berthe G., Martin F., Noirez S., Duclaux O., Juery C., Bouchet C., Ramonet M., and Ciais P.	https://www.icos-cp.eu/sc2020/abstracts - 129

96	4th ICOS	15-17 Sep. 2020	Online	Poster	Characterization of natural gas compressor stations in Ile-de-France region: CH_4 emissions rate, C_2H_6:CH_4ratio, and isotopic signatures ($\delta^{13}CH_4$)	Defratyka, S., Yver-Kwok, C., Paris, J.-D., Lozano, M., Broquet, G., Kumar, P., Menoud, M., Röckmann, T., and Bousquet, P.	https://www.icos-cp.eu/sc2020/abstracts#167
97	4th ICOS	15-17 Sep. 2020	Online	Poster	Characterisation of methane sources in Krakow, Poland, using high temporal resolution isotopic composition measurements	Menoud, M., van der Veen, C.,Necki, J., Szenasi, B., Pison, I., Bousquet, P., Röckmann, T.	https://www.icos-cp.eu/sc2020/abstracts#150
98	AGU 2020	1-17 December 2020	Online	Oral	Quantification of methane emissions from UK biogas plants	Bakkaloglu, S., Lowry, D., Fisher, R., France, J.L., Brunner, D., Chen, H., and Nisbet, E.G	https://agu.confex.com/agu/fm20/webprogram/Paper702158.html
99	AGU 2020	1-17 December 2020	Online	Poster	Importance of utilizing multiple methane source tracers when measuring European cities	Fernandez, J.M., France, J.L., Menoud, M., Corbu, M.-P., Fisher, R.E., Lowry, D., Röckmann, T., and Nisbet, E.G.:	https://agu.confex.com/agu/fm20/meetingapp.cgi/Paper/735587
100	EGU2021	19-30 April 2021	Online	vPICO	UK landfill methane emissions: Use of mobile plume measurements and carbon isotopic characterisation to reassess oxidation rates for open and closed sites	Bakkaloglu, S., Lowry, D., Fisher, R., France, J., and Nisbet	https://meetingorganizer.copernicus.org/EGU21/EGU21-8192.html
101	EGU2021	19-30 April 2021	Online	vPICO	Isotopic characterisation of cola mine methane in the Upper Silesian Coal Basin, Poland	Fiehn, A., Kostinek, J., Eckl, M., Galkowski, M., Gerbig, C., Röckmann, T., Menoud, M., Maazallahi, H., Schmidt, M., Korben, P., Necki, J., Stanisavljevic, M., Swolkien, J., Nickl, A.-L., Winterstein, F., Mertens, M., Jöckel, P., Fix, A., and Roiger, A.	https://meetingorganizer.copernicus.org/EGU21/EGU21-6056.html
102	EGU2021	19-30 April 2021	Online	vPICO	Evaluation of the performance of different short-range atmospheric dispersion models for the monitoring of CH4 emissions from industrial facilities	Fontanier, B., Kumar, P., Broquet, G., Caldow, C., Laurent, O., Yver-Kwok, C., Cropley, F., Shah, A., Lozano, M., Defratyka, S., Gichuki, S., Lauvaux, T., Berthe, G., Martin, F., Noirez, S., Duclaux, O., Juery, C. Bouchet, C., Ciais, P., and the TRACE team	https://meetingorganizer.copernicus.org/EGU21/EGU21-13010.html
103	EGU2021	19-30 April 2021	Online	vPICO	The extent of methane emission associated with the natural gas industry in southeastern Poland	Jagoda, P., Nęcki, J., Bartyzel, J., Korbeń, P., Kud, M., Florczyk, G., and Król, S.	https://meetingorganizer.copernicus.org/EGU21/EGU21-12214.html
104	EGU2021	19-30 April 2021	Online	vPICO	Local-scale atmospheric inversions to monitor CH4 emissions from industrial sites using mobile and/or fixed-point measurements	Kumar, P., Broquet, G., Caldow, C., Laurent, O., Yver-Kwok, C., Cropley, F., Fontanier, B., Shah, A., Lozano, M., Defratyka, S., Gichuki, S., Lauvaux, T., Rivera, R., Berthe, G., Martin, F., Noirez, S., Duclaux, O, Juery, C., Bouchet, C., Ciais, P., and the TRACE team	https://meetingorganizer.copernicus.org/EGU21/EGU21-12743.html
105	EGU2021	19-30 April 2021	Online	vPICO	Estimating coal mine methane emissions using ground-based FTIR spectrometry, WRF driven Lagrangian dispersion modelling, and a regularized inversion approach	Luther, A., Kleinschek, R., Kostinek, J., Stanisavljevic, M., Dandocsi, A., Forstmaier, A., Defratyka, S.,Scheidweiler, L., Wildmann, N., Dubravica, D., Hase, F., Frey, M., Chen, J., Dietrich, F., Knote,	https://meetingorganizer.copernicus.org/EGU21/EGU21-12751.html

						C., Nęcki, J.,Roiger, A., and Butz, A.	
106	EGU2021	19-30 April 2021	Online	vPICO	Detection and quantification method inter comparison of methane emission from natural gas distribution network leaks in Hamburg, Germany	Maazallahi, H., Delre, A., Buth, L., Fredenslund, A.M., Nagler, I., Scheutz, C., Schwietzke, S., Denier van der Gon, H., and Röckmann, T.	https://meetingorganizer.copernicus.org/EGU21/EGU21-16140.html
107	EGU2021	19-30 April 2021	Online	vPICO	Isotopic characterisation of methane emissions from Krakow, Poland	Menoud, M., van der Veen, C., Necki, J., Stanisavljevic, M., Szénási, B., Pison, I., Bousquet, P., and Röckmann, T.	https://meetingorganizer.copernicus.org/EGU21/EGU21-10697.html
108	EGU2021	19-30 April 2021	Online	vPICO	Spatial and temporal variation of 13C-signature of methane emitted by a temperate mire ecosystem	Rinne, J., Łakomiec, P., Vestin, P., Weslien, P., Kelly, J., Liljebladh, B., Xie, X., Kljun, N., Ström, L., and Klemedtsson, L.	https://meetingorganizer.copernicus.org/EGU21/EGU21-12559.html
109	EGU2021	19-30 April 2021	Online	vPICO Highlight	MEMO2: MEthane goes MObile – MEasurements and MOdelling	Walter, S., Röckmann, T., and the MEMO team	https://meetingorganizer.copernicus.org/EGU21/EGU21-3244.html

*MEMO² participants in the CoMet team: H. Chen, P. Korben (ESR1), H. Maazallahi (ESR10), M. Menoud (ESR8), J. Necki, T. Röckmann, M. Schmidt, M. Stanisavljevic (ESR3)

* MEMO² participants in the ROMEO team: H. Chen, M. Schmidt, D. Brunner, M. Menoud (ESR8), H. Maazallahi (ESR10), P. Lakomiec (ESR4), S. Walter, K. Vincovic (ESR2), C. Scheutz, A. Delre, A. Hensen, P. van der Bulk, I. Velzeboer, H. Denier van der Gon, P. Korben (ESR1), R. Morales (ESR12), J. Ravelid (ESR6), L. Emmenegger, D. Brunner, J. Necki, J. Fernandez (ESR7), R. Fisher, D. Lowry, D. Zavala-Araiza

All ESRs have finalised the practical work and are now focussing on data evaluation and preparation of their scientific publications. Several publications have been published already, more are close to submission (see list below, MEMO² participants in bold, * mark datasets):

1. **Bakkaloglu, S., Lowry, D., Fisher, R.E.,** France, J.L., **Brunner, D., Chen, H., and Nisbet, E.G.:** *Quantification of methane emissions from UK biogas plants,* Waste Management, 124, 82-93, https://www.sciencedirect.com/science/article/pii/S0956053X21000167, 2021
2. Chen, J., Dietrich, F., **Maazallahi, H.,** Forstmaier, A., Winkler, D., **Hofmann, M. E. G., Denier van der Gon, H., and Röckmann, T.**: *Methane emissions from the Munich Oktoberfest,* Atmos. Chem. Phys., 20, 3683–3696, https://doi.org/10.5194/acp-20-3683-2020, 2020
3. **Defratyka, S.** M., Paris, J.-D., **Yver-Kwok, C.**, Loeb, D., France, J., Helmore, J., Yarrow, N., Gros, V., and **Bousquet, P.:** *Ethane measurement by Picarro CRDS G2201-i in laboratory and field conditions: potential and limitations*, Atmos. Meas. Tech. Discuss. [preprint], https://doi.org/10.5194/amt-2020-410, under review, 2020
4. **Defratyka, S.,** Paris, J.-D., **Yver-Kwok, C., Fernandez, J.M., Korben, P., and Bousquet, P.:** *Mapping urban methane sources in Paris*, France, Environm. Sci. Techn., in preparation
5. **Delre, A., Hensen, A., Velzeboer, I., van den Bulk, P., and Scheutz, C.:** Fugitive methane and ethane emission quantifications from onshore oil and gas sites in Romania, using a tracer gas dispersion method, Elementa Science, in preparation
6. **Fernandez, J.M., Maazallahi, H.,** France, J.L., **Menoud, M.,** Corbu, M., Ardelean, M., Calcan, A., van der Veen, C., **Röckmann, T., Fisher, R.E., Lowry, D., and Nisbet, E.G.:** Street-level methane emissions of Bucharest, Romania and the influence of urban wastewater, Atmospheric Environment, in preparation
7. Fiehn, A., Kostinek, J., Eckl, M., Klausner, T., Gałkowski, M., Chen, J., Gerbig, C., **Röckmann, T., Maazallahi, H., Schmidt, M., Korben, P., Neçki, J.,** Jagoda, P., Wildmann, N., Mallaun, C., Bun, R., Nickl, A.-L., Jöckel, P., Fix, A., and Roiger, A.: *Estimating CH_4, CO_2 and CO emissions from coal mining and industrial activities in the Upper Silesian Coal Basin using an aircraft-based mass balance approach*, Atmos. Chem. Phys., 20, 12675–12695, https://doi.org/10.5194/acp-20-12675-2020, 2020
8. Hoheisel, A., Yeman, C., Dinger, F., Eckhardt, H., and **Schmidt, M.:** *An improved method for mobile characterisation of δ13CH4 source signatures and its application in Germany*, Atmos. Meas. Tech., 12(2), 1123-1139, https://doi.org/10.5194/amt-12-1123-2019, 2019
9. **Korben, P.,** Jagoda, P., **Maazallahi, H.,** Kammerer, J., **Necki, J.M.,** Bartyzel, J., Radovici, A., **Schmidt, M., Röckmann, T.,** and other ROMEO team members: Quantification of methane emission from oil and gas wells using Other Test Method - 33a and Gaussian Plume Model during ROMEO campaign, Romania, in preparation
10. **Łakomiec, P., Holst, J.,** Friborg, T., Crill, P., Rakos, N., Kljun, N., Olsson, P.-O., Eklundh, L., and **Rinne, J.:** Field-scale CH_4 emission at a sub-arctic mire with heterogeneous permafrost thaw status, Biogeosciences

Discuss. [preprint], https://doi.org/10.5194/bg-2021-81, in review, 2021. NOTE: a summary of this paper was submitted as deliverable D1.2

11. Lu, X., Harris, S.J., **Fisher, R.E.,** France, J.L., **Nisbet, E.G., Lowry, D, Röckmann, T.,** van der Veen, C., **Menoud, M.,** Schwietzke, S., and Kelly, B.F.J.: Isotopic signatures of major methane sources in the coal seam gas fields and adjacent agricultural districts, Queensland, Australia, Atmos. Chem. Phys. Discuss. [preprint], https://doi.org/10.5194/acp-2021-76, in review, 2021
12. Luther, A., Kleinschek, R., Scheidweiler, L., **Defratyka, S.**, **Stanisavljevic, M.**, Forstmaier, A., Dandocsi, A., Wolff, S., Dubravica, D., Wildmann, N., Kostinek, J., Jöckel, P., Nickl, A.-L., Klausner, T., Hase, F., Frey, M., Chen, J., Dietrich, F., **Nęcki, J., Swolkień, J.**, Fix, A., Roiger, A., and Butz, A.: *Quantifying CH_4 emissions from hard coal mines using mobile sun-viewing Fourier transform spectrometry*, Atmos. Meas. Tech., 12, 5217–5230, https://doi.org/10.5194/amt-12-5217-2019, 2019.
13. **Maazallahi, H., Fernandez, J.M. , Menoud, M., Zavala-Araiza, D.,** Weller, Z.D., Schwietzke, S., von Fischer, J.C., **Denier van der Gon, H., and Röckmann, T.:** *Methane mapping, emission quantification, and attribution in two European cities: Utrecht (NL) and Hamburg (DE)*, Atmos. Chem. Phys., 20, 14717–14740, https://doi.org/10.5194/acp-20-14717-2020, 2020
14. **Menoud, M.,** van der Veen, C., Scheeren, B., **Chen, H., Szénási, B., Morales, R.P., Pison, I., Bousquet, P., Brunner, D., and Röckmann, T.:** *Characterisation of methane sources in Lutjewad, The Netherlands, using quasi-continuous isotopic composition measurements*, Tellus B: Chemical and Physical Meteorology, 72, 1–19, https://doi.org/10.1080/16000889.2020.1823733, 2020
15. ***Menoud, M., Röckmann, T., Fernandez, J., Bakkaloglu, S., Lowry, D., Korben, P., Yver Kwok, C.:** mamenoud/MEMO2_isotopes: v8.1 complete (Version v8.1.0) [Data set]. Zenodo. http://doi.org/10.5281/zenodo.4062356, 2020
16. **Menoud, M.,** van der Veen, C., **Maazallahi, H., Hensen, A., Velzeboer, I.,** van den Buk, P., **Delre, A., Korben, P.,** Schwietzke, S., Ardelean, M., Calcan, A., Baciu, C., **Scheutz, C., Schmidt, M., and Röckmann, T.:** CH_4 isotopic signatures of emissions from oil and gas extraction sites in Romania, in preparation
17. **Nisbet, E.G., Fisher, R.E., Lowry, D.**, France, J.L., Allen, G., **Bakkaloglu, S.**, Broderick, T.J., Cain, M., Coleman, M., **Fernandez, J.**, Forster, G., Griffiths, P.T., Iverach, C.P., Kelly, B.F.J., Manning, M.R., Nisbet-Jones, P.B.R., Pyle, J.A., Townsend-Small, A., al-Shalaan, A., Warwick, N., and Zazzeri, G.: *Methane Mitigation: Methods to Reduce Emissions, on the Path to the Paris Agreement*;Reviews of Geophysics, 58, e2019RG000675, https://doi.org/10.1029/2019RG000675, 2020
18. **Ražnjevic, A., van Heerwaarden, C.,** van Stratum, B., **Hensen, A., Velzeboer, I,,** van den Bulk, P., **and Krol, M.:** Large-eddy simulation of a point source methane plume in a realistic convective atmospheric boundary layer, in preparation
19. **Ražnjevic, A., van Heerwaarden, C., and Krol, M.:** Evaluation of OTM33A and car sampling plume measurement strategies under neutral conditions using direct numerical simulation, in preparation
20. **Rinne, J.,** Tuovinen, J.-P., Klemedtsson, L., Aurela, M., **Holst, J.,** Lohila, A., Weslien, P., Vestin, P.,**Łakomiec,** P., Peichl, M., Tuittila, E.-S., Heiskanen, L., Laurila, T., Li, X., Alekseychik, P., Mammarella, I., Ström, L., Crill, P., and Nilsson, M.B.: *Effect of the 2018 European drought on methane and carbon dioxide exchange of northern mire ecosystems*, Phil. Trans. R. Soc. B, 375: 20190517, http://dx.doi.org/10.1098/rstb.2019.0517, 2020
21. **Stanisavljević, M., Nęcki, J., Swolkień, J.,** Gałkowski, M., **Maazallahi, H., Korbeń, P., Menoud, M.,** van der Veen, C., **Röckmann, T., Schmidt, M.,** Wietzel, J., **Vinković, K., Defratyka, S.,** Zieba, D., Chmura, L., and Wołkowicz, W.: Determination of methane emission rates and isotopic signatures from coal mine ventilation shafts in Upper Silesia, Poland, in preparation
22. **Szénási, B.,** Berchet, A., **Pison, I., Broquet, G., Menoud, M.,** van der Veen, C., Scheeren, B., **Chen, H., Röckmann, T., and Bousquet, P.**: What can we learn about methane emissions from the comparison of measured and simulated methane isotopic ratios at a coastal monitoring site?, in preparation
23. Tuzson, B., Graf, M., **Ravelid, J.,** Scheidegger, P., Kupferschmid, A., Looser, H., **Morales, R. P., and Emmenegger, L.:** *A compact QCL spectrometer for mobile, high-precision methane sensing aboard drones*, Atmos. Meas. Tech., 13, 4715–4726, https://doi.org/10.5194/amt-13-4715-2020, 2020.
24. **Vinkovic, K.,** Andersen, T., de Vries, M., Kers, B., van Heuven, S., Peters, W., **Hensen, A., and Chen, H.:** Quantification of methane emissions from dairy cows using an Unmanned Aerial Vehicle (UAV) based active AirCore system and mobile van, in preparation
25. Xinyi, L., Harris, S.J., **Fisher, R.E.,** France, J.L., **Nisbet, E.G., Lowry, D., Röckmann, T.,** van der Veen, C., **Menoud, M.,** Schwietzke, S., and Kelly, B.F.: *Isotopic Signatures of Major Methane Sources in the Coal Seam Gas Fields and Adjacent Agricultural Districts, Queensland, Australia;* ACP discussions preprint discussion started: 5 February 2021, https://doi.org/10.5194/acp-2021-76

Except for the position of ESR6, all ESRs have either already defended their thesis (ESR5, ESR9, and ESR13) or envisaged a date within the coming months.

- ESR5 - Sara Defratyka: Characterization of CH_4 emissions in urban environments (Paris), Universite Paris Saclay, 19 January 2021, http://www.theses.fr/s186567
- ESR9 – Semra Bakkaloglu: will be public available 3 months after defense
- ESR13 – Barbara Szénási: Atmospheric monitoring oft he CH_4 emissions at European scale, Universite Paris Saclay, 17 December 2020, http://www.theses.fr/s189587

To reach out to a broader audience, internet-based platforms such a dedicated project website (https://h2020-memo2.eu) and social media are used (users and increase related to the last reporting period), such as:

- LinkedIn (https://www.linkedin.com/groups/13506528/, 31 (+7) members)
- ResearchGate (https://www.researchgate.net/project/MEMO2-MEthane-goes-MObile-MEsurements-and-MOdelling, 102 (+20) followers)
- Instagram https://www.instagram.com/h2020_memo2/, 300 (+136) followers)
- Facebook (https://www.facebook.com/H2020MEMO2/), 106 followers
- Twitter (https://twitter.com/H2020_MEMO2, 108 (+76) followers)

All participants were encouraged to contribute either by uploading posts themselves, or send information or links to the coordinator and the ESRs. As the ESRs were strongly encouraged to blog about their secondments, additional to general blogs about campaigns and training events, more than 30 MEMO² blogs have been published in the meantime (https://h2020-memo2.eu/category/blog/).

Fig. 3.1 shows that the project website clearly contributes to the visibility of the project. As a mean, the website had almost 2000 views per month during the recruitment period. After closing the recruitment, the mean amount of views was around 600 per month. For the website, a correlation in increasing user or view numbers were seen for more detailed reporting as e.g. about the ROMEO campaign, but not for single tweets. MEMO² participants published more than 90 tweets, which reached a mean of more than 800 views per tweet. Beside this, Empa recently published a short youtube video about their drone-based laser spectrometer (https://www.youtube.com/watch?v=fuQnPOCagI0&feature=youtu.be), and a professional campaign video has been published about the MEMO² / ROMEO activities in Romania (https://www.youtube.com/watch?v=IceCnEM0x5U&t=5s).

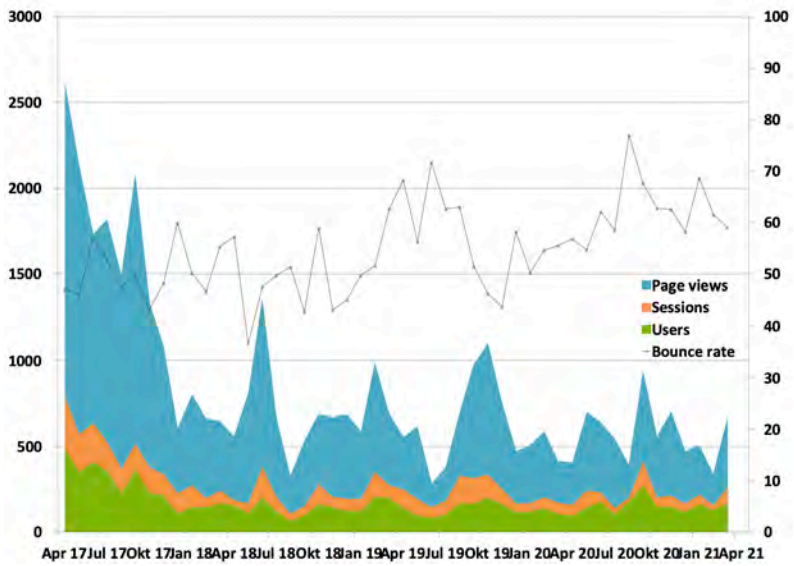

Fig. 3.1: Visibility of the P-TRAP project website, based on data from Google Analytics

Due to the numerous dissemination activities and joint measurement campaigns MEMO² attracts more and more attention, indicated by e.g. increasing numbers of followers, reads, likes, and retweets on social media, mentioning the project activities in newsletters or highlighting them. Some examples are e.g.

- https://www.nature.com/articles/d41586-020-00987-5
- https://doi.org/10.1029/2020EO143214
- https://twitter.com/AGU_Eos/status/1254055173904834561?s=20.

- http://www.scientificaviation.com/next-stop-romania/
- https://www.the-sniffers.com/wp-content/uploads/2020/02/Case-Study-ROMEO-Project-Methane-Emission-Quantification-for-the-Romanian-Oil-Gas-Industry-1.pdf
- https://c2sm.ethz.ch/news/newsletter/c2sm-newsletter-vol-29.html#empa
- https://www.egu.eu/publications/highlight-articles/?limit=10&sortby=&page=&keywords=methane&journal

Unfortunately, MEMO² or the EU funding was not consequently mentioned or included in acknowledgements. ESRs and beneficiaries were attended on this for the upcoming activities.

To ensure exploitation, MEMO² data are stored at the ICOS Carbon Portal https://fileshare.icos-cp.eu/login and will be public available after the project (see also D5.3.). Where possible, data are already shared with collaborating colleagues outside the consortium, e.g. by public data sets (Menoud et al. 2020, http://doi.org/10.5281/zenodo.4062356).

4. Management of MEMO²

4.1 General overview of the management

The management of MEMO² has not been changed in the 2nd reporting period of the project. It was organised and implemented based on the Grant Agreement and the Consortium Agreement (D5.1), and described in D5.2 (Project Management Plan) and D5.3 (Data Management, Dissemination & Exploitation Plan).

4.2 Consortium

The initial consortium has not changed since the last reporting. All 9 beneficiaries and 16 partner organisations were involved and part of the consortium, the project was running smoothly. In total about 60 researchers and staff members participated in MEMO².

Due to the commitment indicated in the proposal some partner organisations were more active in the first reporting period than others, e.g. by supervising ESRs, organising network events, giving advice or access to their properties. All partner organisations functioned as external mentors for the ESRs and were in contact with them.

During the second reporting period, the focus of the consortium laid on finalising the practical work, evaluating the data and start writing. This resulted in a shift of contact intensity as e.g. partner organisations committed to training were less involved whereas others as e.g. DTU had increased their activities due to their participation to the joint campaign ROMEO. Also, most secondments have been executed, which led to joint data evaluation and publications.

4.3 Meetings

As MEMO² required a high level of collaboration, regular meetings (for an overview see Table 4.1) were implemented right from the beginning of the project and on all levels within the consortium. The general meeting strategy as described earlier has not changed.

I) Consortium Meetings: The 3rd Annual Meeting of MEMO² was held mid-February 2020 in Heidelberg, organised by the UHEI in association with a ROMEO meeting. Two full days were scheduled to update the CDPs (D4.2) and internally review the project. The WP leader updated the consortium about the achievements of their work packages, the general progress of the project and its deliverables was evaluated and the next steps within MEMO² were discussed. The consortium also discussed possible follow-up projects. The ROMEO Meeting aimed on presenting the preliminary data from the measurement campaign in Romania, and discuss the results and future plans. All involved ESRs presented their data at either one or both meetings. The Final Meeting of MEMO² was scheduled associated to the ICOS conference, aiming to discuss the overall outcome of MEMO² and possible follow-up actions. As

the ICOS conference was held online with respect to the pandemic situation, the MEMO² meeting had been shortened to a half day in October, focussing on ESR presentations, deliverable updates, and brainstorming about future proposals.

II) 3-monthly tele-conferences: Next to the Annual Meeting, the Network Supervisory Board (NSB) held only three regular tele-conferences during the second reporting period mainly. Focus laid on updating the consortium about ongoing activities and inform them about organisation and implementation of ROMEO.

III) ESR skype meetings: The ESRs continued with their regular Skype meetings and kept the project manager informed about the outcome. In total 12 ESR meetings were held during the reporting period. As several ESRs´ contracts are close to end, the regular meetings stopped in project month 42.

IV) WP meetings: The WP leaders were in close email contact with the participants of their WPs, e.g. due to organising joint measurements, data exchange, and coordinating writing activities. The frequency was on request accordingly.

Table 4.1: overview of MEMO² meetings

Meeting	Date / Location	Organizer	Work Package	Invited participants
Kickoff Meeting	23–24 March 2017, Utrecht, The Netherlands	UU	All	All project participants
1st Annual Meeting	21 – 22 March 2018, Dübendorf, Switzerland	Empa	All	All project participants
2nd Annual Meeting	21 – 22 February 2019, Paris, France	UVSQ	All	All project participants, Project Officer, external reviewer(s)
3rd Annual Meeting	10 – 11 February 2020, Heidelberg, Germany 12 – 13 February 2020: Associated ROMEO meeting	UHEI	All	All project participants MEMO² and ROMEO consortium
4th Annual Meeting	14 September 2020	UU	All	All
Tele-Conferences	15 June 2017 15 September 2017 13 December 2017 1 June 2018 12 October 2018 16 May 2019 5 June 2020 12 October 2020	UU	All	Representatives of all beneficiaries and partner organisations, ESR representatives
WP Tele-Conferences	On request of WP leader	Respective WP leader	Respective WP	WP participants (PIs + ESRs)
ESR Tele-Conferences	14 November 2017 14 December 2017 13 March 2018 19 April 2018 23 May 2018 27 June 2018 16 July 2018 21 August 2018 22 November 2018 11 December 2018 29 January 2019 20 March 2019 25 April 2019 29 May 2019 2 July 2019 13 August 2019 7 November 2019 5 December 2019 19 March 2020 21 April 2020 20 May 2020 30 June 2020 27 August 2020	ESRs	All	ESRs

4.5 Communication infrastructure

The communication infrastructure had been described in detail in deliverable D5.7 and had not been changed since the last reporting. Email, phone and web-based meeting tools were the main communication channels.

4.6 Risk assessment and faced difficulties

A detailed overview of possible risks is listed and described in Chapter 7 of the Project Management Plan (submitted as deliverable D5.2). In the second reporting period of MEMO² we faced no issues impacting the project in general, but we faced some individual risks and general difficulties.

Risk 6: Personal conflicts

As already indicated during the Midterm Meeting, personal conflicts were spotted between one ESR and her supervisor. The coordinator and co-supervisor tried to mediate in the conflict, but could not improve the situation. So, in agreement with everyone involved a daily supervisor from another but related faculty was appointed. This works well and the ESR continued with her work.

A general difficulty was that the schedule towards a PhD is very tight, with many obligations. As mentioned above, this was very good for the interaction - network-building among the ESRs and their supervisors was excellent – but the publication of scientific papers is lagging behind for most ESRs. This is a point of concern, and the supervisors and co-supervisors are working hard to help ESRs in the writing process. However, the contractual restrictions to three years in combination with intensive data production / measurement campaigns and mandatory network activities created a kind of time pressure which works counter-productive for time-consuming creative processes such as writing scientific publications.

The pandemic situation also affected the project, but only marginal as most ESRs finished already their data collection and focussed on evaluation and publication of them.

5. Outlook

MEMO² was an extraordinary success for the consortium, not only regarding data collection and general outcome but also in setting up a stable network within the scientific community. Although MEMO² ended in February, the consortium is still in contact for further publications and follow-up activities such as measurement campaigns (ROMEO II) or a new MSCA proposal.

6. ESR individual progress reports

This chapter demonstrates the individual scientific progress of the ESRs, and includes a cumulative overview of general activities within the project.

6. Individual ESR reports

6.1 ESR1 - Monitoring the methane emissions from different sources in Germany

ESR1

Monitoring the methane emissions from different sources in Germany

ESR	Piotr Korben, pkorben@iup.uni-heidelberg.de
Supervisor	Martina Schmidt, martina.schmidt@iup.uni-heidelberg.de
Co-supervisor	Thomas Roeckmann, t.roeckmann@uu.nl
Non-Academic mentor	Bill Hirst, bill.hirst@shell.com
Official start – end date	1.1.2018 – 31.12.2020

6.1.1. Scientific progress

6.1.1.1 Project introduction and objectives

Methane (CH_4) is one of the greenhouse gases (GHG) like CO_2 or water vapor, but with a larger greenhouse gas potential. Methane has natural but also anthropogenic sources. The main natural sources are wetlands and wild ruminants. Anthropogenic sources are agriculture (ruminants and rice cultivation), landfills, biomass burning, extraction and transport of fossil fuel (natural gas, oil, coal). In Germany the major methane sources are ruminants, waste and wastewater treatment, and transport and storage of natural gas.

In this project we monitored different methane sources with different measurement techniques. We used analysers like CRDS or OF-CEAS and some additional tools like AirCore. These instruments were installed in a vehicle, and during regular measurement campaigns we were able to measure the methane mole fraction and the isotopic composition ($^{13}CH_4$). It allowed us to determine some temporal and/or spatial variability of methane emission. Collected data were analysed with some simple models to estimate the emission. We used the Gaussian Plume Model (GPM) and the Other Test Method 33a (OTM33a) as our main methods to transfer the measured concentration in emissions. Results given by models and data analysis were compared to inventories for Germany and for other European countries. This project focuses originally on EU emission from natural gas, but due to additional sources around Heidelberg, and the ROMEO campaign to oil and gas fields in Romania, our research focus was extended to get more information about methane emission in these regions.

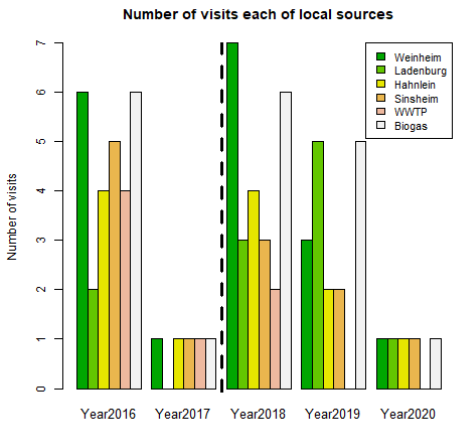

Fig. 6.1.1: Frequency of measurement campaigns around Heidelberg at two farms (green), landfill and waste water treatment plant (orange), gas compressor station (yellow), and biogas plant (white). Data before 2018 were collected by A. Hoheisel.

6.1.1.2 Project results

6.1.1.2.1 Third year

In the third year of the project I focused on measurement campaigns around Heidelberg and a three-week campaign in Romania (ROMEO).

It was planned to perform 1 - 2 measurement campaigns each month to visit different CH_4 sources in the surrounding of Heidelberg. Measurements have been performed at several farms, landfills, gas compressor

stations and biogas plants. The number of site visits per year is presented in Fig. 6.1.1. These campaigns were focused on $^{13}CH_4$ source signature with the goal to account for possible seasonal or temporal variation. Prior to each campaign all equipment was prepared and weather conditions were checked. Especially wind direction and wind speed are important information for the campaign planning as due to available roads the CH_4 emitters can only be measured downwind under specific conditions. Collected data will be used for estimating methane emission from visited sources.

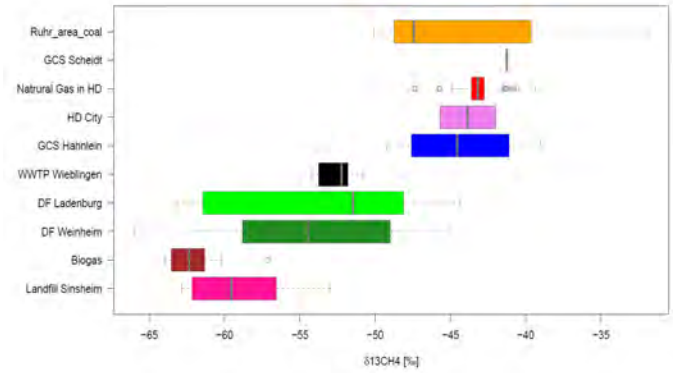

Fig. 6.1.2: Methane source signature evaluation for measurement campaigns carried out between 2016 and 2020.

Fig. 6.1.2 shows a summary the source signatures. In total, 17 samples from the Ruhr area, 3 for a gas compressor station in Scheidt, 109 sample bags for natural gas in Heidelberg, 5 for Heidelberg, 29 for a gas com-pressor station in Hahnlein, 12 for a waste water treatment plant in Wieblingen, 26 for a dairy farm in Ladenburg, 75 for a dairy farm in Weinheim, 70 for a biogas plant in Kircheim, and 37 for a landfill in Sinsheim were analysed.

The campaigns allowed to not only collect data, but also to perform release tests and to test additional methods for emission estimates like OTM-33a. Fig. 6.1.3 shows the results from the Gaussian Plume Model (GPM) Polyphemus to analyse data from a dairy farm in Weinheim. Analyses based on the comparison between the measured peak surface and the modelled peak surface are shown.

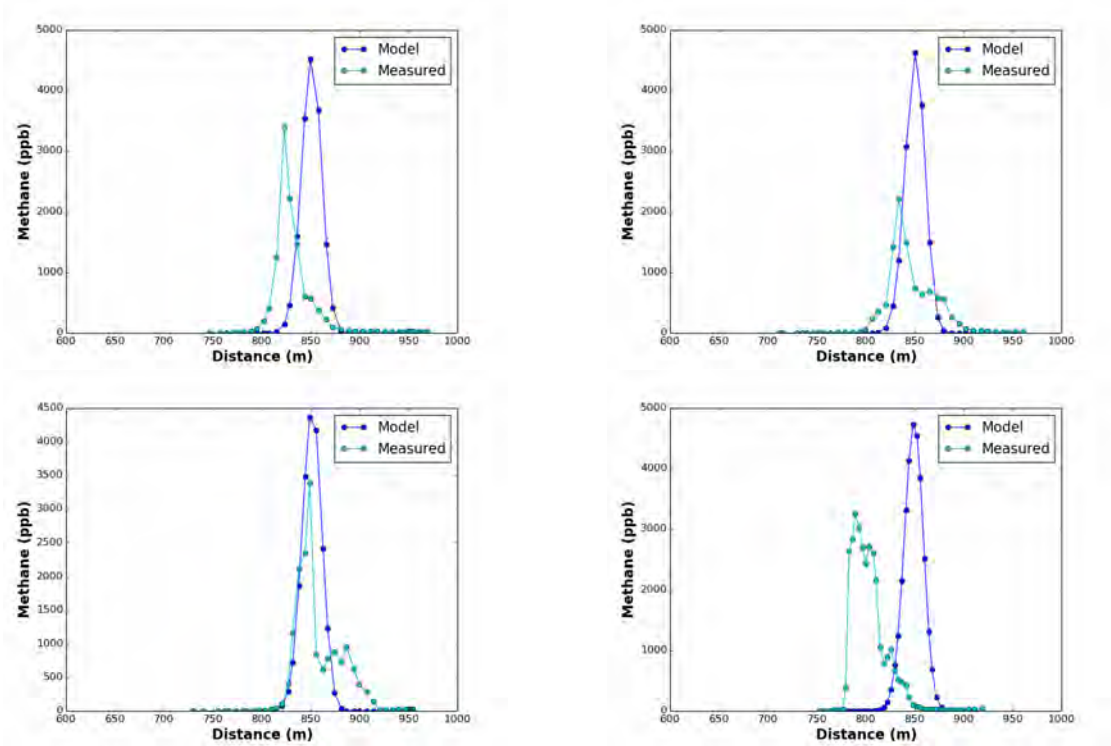

Fig. 6.1.3: Results of Polyphemus analysis for dairy farm in Weiheim (transect nr: 2,3,5 and 18)

Fig. 6.1.4 shows results of applying the OTM-33a method for a biogas plant in Kircheim. Based on the measured methane concentration, wind speed, horizontal and vertical dispersion coefficients we were able to calculate emissions using equation 1.

$$CH_4 = 2\pi \cdot \sigma_Y\,[m] \cdot \sigma_Z\,[m] \cdot U\,[m/s] \cdot C\,[g/m^3] \quad (1)$$

Two instruments were compared to check if a slower instrument with a data acquisition of only 0.4 Hz can be used instead of a 1 Hz analyser.

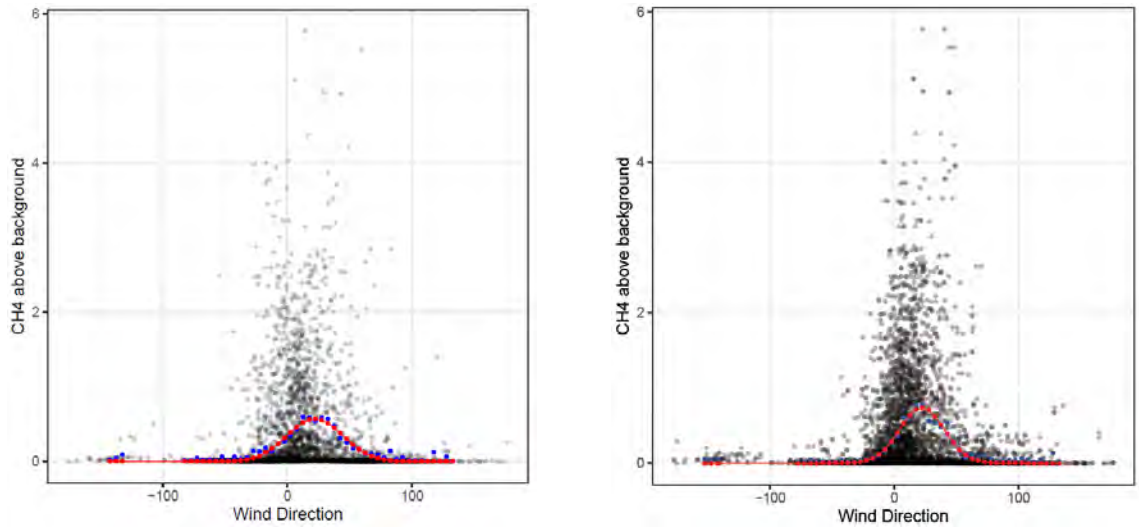

Fig. 6.1.4: OTM-33a data application using 0.4 Hz data (on left) and 1 Hz data (on right). Computed CH4 emission for this test was 1.49 g/s and 1.67 g/s respectively. This method was also tested later.

The participation in the ROMEO campaign in Romania was a huge achievement in the reporting period. In collaboration with other MEMO² partners (UG, UL, UU, EMPA, AGH), local teams of UBB and INCAS, and several other partners mobile measurements were carried out over 3 weeks. I performed measurements close to oil and gas wells using the OTM-33a method and Gaussian Plume Modelling. Additionally, I collected sample bags for analyses in the laboratory. Together with all partners we visited over 1000 oil and gas wells and quantified around 150 – 200 of them. First results of the CH_4 emissions are shown in Fig. 6.1.5. A more detailed analysis will follow during the next months.

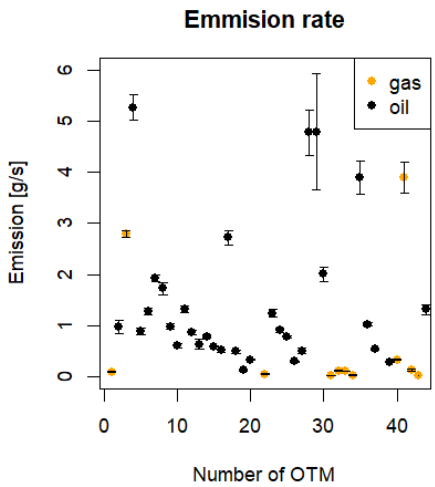

Fig. 6.1.5: Preliminary results for OTM-33a places during ROMEO campaign provided by UHEI team.

6.1.1.2.2 Fourth year

Release experiment in Dübendorf

The release experiments were carried out at various distances from the source in order to check as many parameters as possible. The figure below shows the places where the controlled gas release took place (red), and where the released gas was measured (yellow). Performing this test helped to understand the emission estimation method as well as the whole data analysis process. The longest release test lasted 3 hours and was an ideal test case, as the data can be divided into shorter time intervals. One of the conclusions of this release experiment is the repeatability. It is better to do more tests with a short time frame (15-20 min) than one long one. The derived emission under or overestimate between - 17% and + 56% the released one.

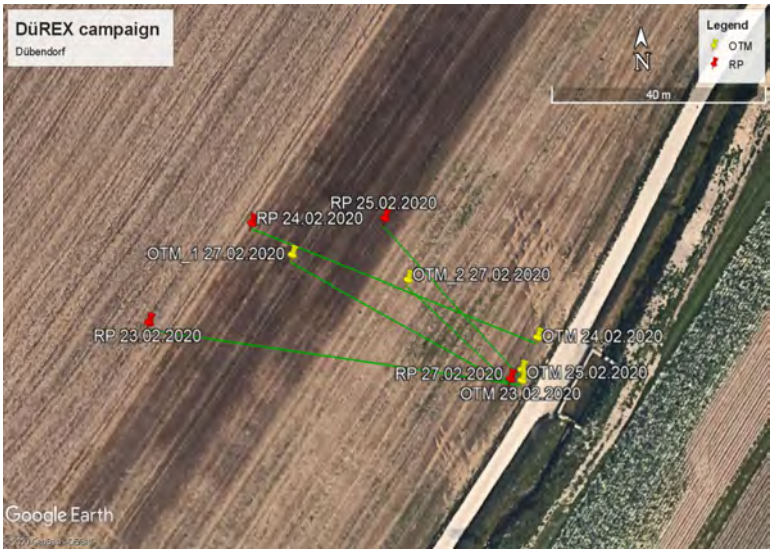

Fig. 6.1.6: Release test in Dübendorf, CH, data from March to May were evaluated

An important element of the data analysis was the uncertainty analysis. In the original version, only the uncertainty of Gaussian fit to the methane concentration data divided into wind bins was used to calculate the uncertainty.

The analysis shows that if the exact distance of the receiver from the source is not known (it is not measured with a laser), it is necessary to use additional components of uncertainty, namely the uncertainty of wind speed and the distance on the basis of which the dispersion coefficients are calculated. Then the uncertainty of the estimated emission increases up to +/- 50%, which corresponds to the OTM33a accuracy of the methods presented in the literature.

Data analysis of the ROMEO campaign

As outlined above, the ROMEO campaign was a flagship project involving several MEMO² members such as UG, UL, UU, EMPA, AGH. Also Romanian research teams from UBB and INCAS collaborated to carry out mobile measurements both on the ground and in the air.

Additional to the ground measurements, the OTM33a and Gaussian Plume Model (GPM) methods were used. In total, about 1500 sites with oil or gas wells were visited (Fig. 6.1.7), however, due to the unfavorable wind conditions, only 140 quantifications were made.

As shown below, most of them took place south-west of Bucharest (region 5a), due to the terrain and the accessibility of individual sites. At the same time, most of the quantifications have been done on the oil wells that are still producing. The estimated emission using GPM and OTM is in the range from 0.03 (±0.01) to 25.85 (±8.49) g CH_4 / s.

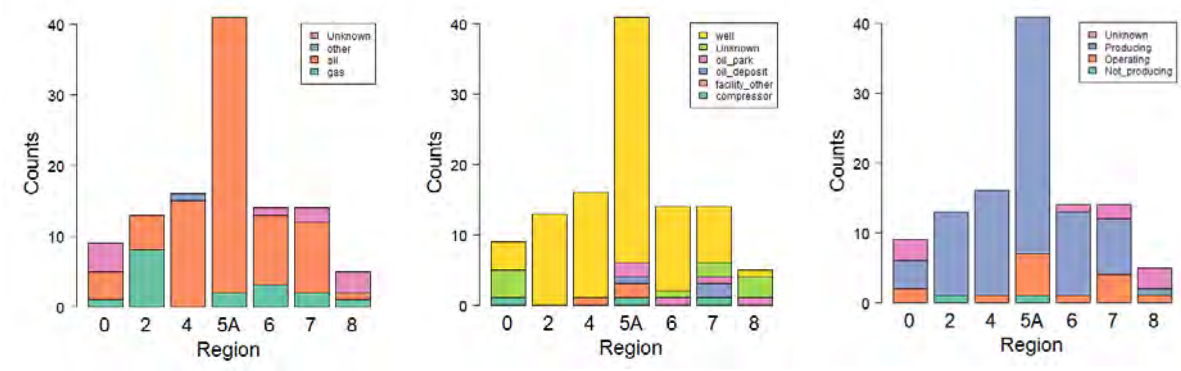

Fig. 6.1.7: Distribution of visited sites during ROMEO campaign. On the left based on the type of source (oil or gas), in the middle based on type of installation, on the right based on status of the site. An overview of the regions: https://h2020-memo2.eu/romeo-a-brief-history-before-it-became-real/

Fig. 6.1.8 shows the results of the analysis performed with the non-parametric bootstrap method. On the left the CH_4 emission is plotted for each visited region. In red, the average emissions are marked with 95 % confidence intervals. The Y axis is a logarithmic scale. The number of samples measured in a given region is written on the top of the graph. The lowest methane emissions were determined in region 2 around Craiova, with a higher proportion of gas wells. This is also the case with oil wells, where gas is a by-product and methane is released directly into the atmosphere. The fact of higher methane emissions for gas wells is also confirmed by the image on the left (bottom). The results will be published soon.

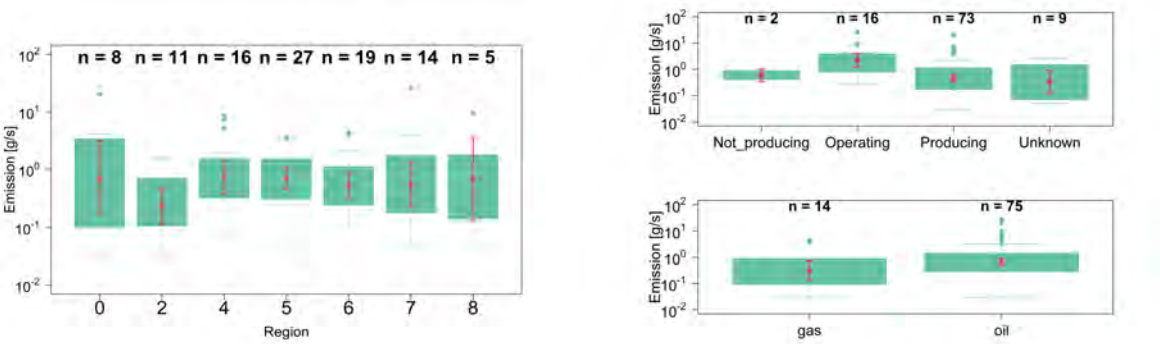

Fig. 6.1.8: Estimated emission per region (on the right) and per status and type of site (on the left) with means and 95% confidence intervals (marked in red).

In the reporting period, two further release tests were performed in which GPM and OTM were tested, and the case of gas emission in the urban area was simulated. Both of the above tests are currently being analyzed and discussed by the local group that is working on them. The conclusions obtained on their results allowed for a better analysis of data for local methane sources, which were mainly quantified using GPM.

6.1.1.3 Future plans and expected results

Based on the collected data, it is planned to write 3 publications. The subject of the first one is methane emission from oil and gas wells in Romania using GPM and OTM methods. This is a summary of the analysis of data collected during the ROMEO campaign (September - October 2019). The first draft of this publication has already been prepared and is in the process of verification by co-authors. The next two publications refer to local methane emissions from various sources in the vicinity of Heidelberg, and qualitative measurements using GPM and OTM methods, respectively. The first of these will be the result of the work of the last 3 years on local methane emissions, while the second will summarize the results obtained during the 3 release tests, made to check the accuracy of the used methods.

Writing a doctoral dissertation is at the stage of data analysis, which includes data analysis for the ROMEO campaign, which will postpone the defence of the PhD thesis compared to the previous assumptions, but the planned completion of the writing and defence process should end in June 2021. After defending PhD thesis, it is planned to take part in another project as a post-doc.

6.1.1.4 Collaborations (internal / external)

During the ROMEO campaign (October / November 2019) I cooperated with other MEMO^2 students but also with teams from the University Cluj and INCAS. I was responsible for the application of the OTM-33a method to measure emissions from oil & gas wells in Romania. After the campaign, close cooperation's are ongoing with the MEMO^2 partners UU, AGH, and RUG in order to prepare a publication.

In February 2020 I visited EMPA in Dübendorf to participate on a CH_4 release experiment. The main goal was to compare different measurements and analysis methods in cooperation with K. Vinkovic (RUG), R. Morales and J. Ravelid.

Several short meetings focussing on ROMEO data analyses with AGH team took place. The MEMO^2 annual meeting and ROMEO workshop was hosted in Heidelberg in February 2020.

During the fourth year, a number of meetings were held on the results of the ROMEO campaign. They were attended by other members of the project, including MEMO2 (UG, UU, AGH, EMPA, TNO, DTU) and also from outside MEMO2 (EDF). Partners from AGH took part in the release test carried out in September 2020, the results of which can be used to write another publication

6.1.1.5 Risks and difficulties

Due to the additional measurement campaign in Romania, and the COVID-19 pandemic the third secondment at UU was cancelled and replaced by close cooperation in data analyses and paper writing. Despite the restrictions due to the pandemic, final measurements were executed and results are under evaluation.

6.1.2 Deliverables

ESR1 is involved in the following deliverables: D1.4 / D1.5 / D2.2 / D2.3. There is no contribution planned to D1.1, this is a typing error in the description of work.

D1.4 - Improved emission factors for different source categories from mobile measurements (month 42)

In addition to the Gaussian Plume model (GPM) evaluation we added a second method (OTM-33a) to quantify CH_4 emissions from point sources. This method was evaluated during a release experiment and successfully applied at the ROMEO campaign. The fourth year I was more focused on analysing the data from the ROMEO campaign. It helped to improve the emission factor from oil and gas sources and it gave new information on emission from oil and gas sector. However, local sources were also visited again and the GPM method was applied to estimate methane emissions. Two additional release tests were also performed to better understand the data analysis method and, if possible, to adjust and to improve the data analysis process. The release tests concerned both the GPM and OTM methods, and some of them concerned the emission of measurements in the urban area, on which one of my colleagues is working. The collected data (3-5 release tests) will probably be used to write a publication on the comparison of different methods of methane emission estimation.

D.1.5 - Report on harmonized methods for mobile CH_4 and $^{13}CH_4$ measurements (month 18)

The deliverable has been submitted and accepted.

D.2.2 - Improved isotopic source signature of local and regional CH_4 emissions (month 36)

Analysis with in-situ $^{13}CH_4$ analyser started in January 2018 in the Heidelberg region and were continued during the project. As was mentioned before, around Heidelberg it is possible to measure different isotopic source signatures, including biogenic and thermogenic isotopic signature. Together with data from previous studies, we have 5 years of source signature evaluation of 8 sources in the Heidelberg region. The isotopic source signatures collected will be part of PhD thesis and will be compared to their respective sources from elsewhere where samples were collected by other MEMO2 partners.

The deliverable has been submitted.

D.2.3 - Publications on the use of isotopes for CH_4 source attribution in urban / industrial regions (month 36)

Data collection started in 2018 and is ongoing. This data collection is used to write a publication about different methane sources around Heidelberg in cooperation with members of the local research group

(IUP) and other partners from the MEMO² project. They will also be the main part of a written doctoral dissertation.

The deliverable has been submitted.

6.1.3 Training and network activities

6.1.3.1 General training events

Event	Date (start – end)	Location (Host)	Objective / expected skills	ECTS points	Contribution
MEMO² TrainingSchool	5.02.2018 – 16.02.2018	Schoorl, Netherlands (UU)	Knowledge about chemistry of atmosphere,	6	Presenting a poster, and oral presentation, participating in measurements campaign
I MEMO² Annual Meeting	22.03.2018 – 23.03.2018	Duebendorf, Switzerland (EMPA)	Progress of work from other PhD and other work package		Oral Presentation
Isotope Workshop	17.09.2018 – 19.09.2018	Egham, UK (RHUL)	Improve knowledge about isotopes and measurements techniques		Oral presentation,participation to lecture and training
Plume Workshop	9.10.2018 – 10.10.2018	Heidelberg, Germany (UHEI)	Getting knowledge about different models and how use them		Participation to lecture and exercises
Institute seminar	11.01.2018 - now	Heidelberg, Germany (UHEI)	Lectures about environmental physics, knowledge about other topics from science / other groups	2 (SWS)	participating
Group meeting	8.01.2018 - now	Heidelberg, Germany (UHEI)	Meeting where problems and progress of each member is discussed. Discussion of scientific publications.	2 (SWS)	Participating, giving presentations
COMET workshop	09.01.2019 – 11.01.2019	Zakopane, PL	Summary of work on COMET data collected in May/June 2018		Presentation
III MEMO² Annual Meeting	10.02.2020 – 11.02.2020	Heidelberg, DE	Summary of work of all ESRs involved in MEMO² , update of results		Presentation
ROMEO workshop	12.02.2020 – 13.02.2020	Heidelberg, DE	Preliminary results of ROMEO campaign		Presentation
Virtual Workshop	07-08.10.2020	Helsinki Finland	Partnering Science and Law for Effective Climate Action		Participating, Getting knowledge about legislation process and different activities connected to Climate Action
Virtual Workshop	29.11.2020	Krakow, Poland	Workshop about: Correct argumentation, the art of public speaking, principles of the Oxford debate and culture of discussion		participating

6.1.3.2 Secondments

Secondment	Date (start – end, planned (when))	Location	Host	Description of work / deviations	Scientific / training (skills) objective	Results and future plans
AGH	22.05.18 – 10.06.18, 31.10.18 – 9.11.18	Cracow, Poland	AGH UST in Krakow	Participation in CoMet campaign with other students and different research group on coal mines area on Silesia, Poland /.	Improving measurements campaign organization skills, measurements isotopic composition of methane from coal mines, cooperation with other groups and other instruments, creating scientific network	Work on data is still in process. Coal mines, landfill and dairy farm were visited during this campaign. Methane isotopic composition ($\delta^{13}C$) for coal mines showed values from – 64 to – 43 ‰. It is a big range, and during campaign days methane could come from different depth. Cooperation with aircrafts helped to construct vertical profile for methane on Silesia area.
LSCE	02.2019 – 03.2019	Paris, France	LSCE	Measurement campaign on urban area and work with Polyphemus model	Getting knowledge about Polyphemus model	

6.1.3.3 Conferences

Conference name	Date (start – end, planned (when))	Location	Presentation (oral / poster)	Title of presentation	Authors (main author + co-authors)	Public available (yes / no) / web link
NCGG-8 Symposium	12.06.2019 – 14.06.2019	Amsterdam, NL	Oral Presentation	Monitoring the methane emission from different sources around Heidelberg, Germany	P. Korben, A. Hoheisel, J. Kammerer, J. Wietzel, M. Schmidt	Yes https://www.ncgg.info/ncgg8/proceedings
45th Congress of Polish Physicists	13.09.2019 – 18.09.2019	Cracow, PL	Poster	Isotopes measurements and methane emissions from different sources in Germany and Poland	P. Korbeń, H. Krümpelmann, M. Schmidt	No
ICOS	15-17.09.2020	Utrecht	Poster	Quantification of methane emission from oil and gas wells using Other Test Method 22a during ROMEO campaign	P.Korben, P.Jagoda, H. Maazallahi, J. Necki, J.Bartyzel, A. Radovici, M. Schmidt, T. Roeckmann	YES https://www.icos-cp.eu/sites/default/files/2020-09/ICOS%20Science%20Conference%202020%20-%20BoA_11.09.2020.pdf
EGU	04-08.05.2020	Vienna	Oral	Methane emission from dairy farm located in north of Heidelberg	P. Korben + J. Kammerer, J. Wietzel, M.Schmidt	NO

6.1.3.4 Measurement / sampling campaigns

Campaign	Date (start – end, planned (when))	Location	Host	Description of work	Scientific objective	Samples (nature/ number of AirCores)	Results and future plans
I	10.01.2018	Heidelberg and surrounding area (Weinheim, Hähnlein, Kirchheim)	UHEI	Mobile measurements using CRDS Analyzer Picarro G2201-i	Measurements isotopic composition of methane from different sources to check seasonal variations	Dairy farm, gas compressor station, biogas plant / 10	Values of isotopic composition of methane from visited sources, calculate emission factor
II	26.10.2018	Heidelberg and surrounding area (Kirchheim, Sandhausen)	UHEI	Mobile measurements using CRDS Analyzer Picarro G2201-i	Measurements isotopic composition of methane from different sources to check seasonal variations	Biogas plant, gas compressor station, city / 12	Values of isotopic composition of methane from visited sources, calculate emission factor
III	9.02.2018 – 12.02.2018	Schoorl, Netherlands	UU	Measurements campaign and release experiment in Schoorl and surrounding area	Learning about campaign organization, measurements different sources in Netherlands	Landfill, dairy farms, gas compressor station, city / 17	Values of isotopic composition of methane from visited sources, cooperation with other groups
IV	26.03.2018 – 27.03.2018	Heidelberg and surrounding area (Hähnlein, Kirchheim, Scheidt)	UHEI	Mobile measurements using CRDS Analyzer Picarro G2201-i	Measurements isotopic composition of methane from different sources to check seasonal variations	Gas compressor stations, biogas plant / 15	Values of isotopic composition of methane from visited sources, calculate emission factor
V	26.04.2018	Heidelberg and surrounding area (Weinheim, Ladenburg, Sinsheim)	UHEI	Mobile measurements using CRDS Analyzer Picarro G2201-i	Measurements isotopic composition of methane from different sources to check seasonal variations	Dairy farms, landfill / 13	Values of isotopic composition of methane from visited sources,

							calculate emission factor
VI	22.05.2018 – 10.06.2018	Upper Silesia, coal mines area	AGH	Mobile measurements using CRDS Analyzer Picarro G2201-I / CoMet campaign	Methane and isotopic composition of methane measurements from coal mines	Coal mines, landfill, dairy farm / 75	Values of isotopic composition of methane from coal mines on Silesia area, vertical profile of methane concentration in cooperation with aicrafts
VII	4.07.2018 – 6.07.2018	Heidelberg and surrounding area (Weinheim, Ladenburg, Ludwigshafen, Hähnlein)	UHEI	Mobile measurements using CRDS Analyzer Picarro G2201-I and release experiment	Measurements isotopic composition of methane from different sources to check seasonal variations	Dairy farms, landfill, gas compressor station / 10	Values of isotopic composition of methane from visited sources, calculate emission factor
VIII	24.08.2018	Heidelberg and surrounding area (Weinheim, Sinsheim, Kirchheim)	UHEI	Mobile measurements using CRDS Analyzer Picarro G2201-i	Measurements isotopic composition of methane from different sources to check seasonal variations	Dairy farm, landfill / 17	Values of isotopic composition of methane from visited sources, calculate emission factor
IX	25.10.2018	Heidelberg and surrounding area (Weinheim, Ladenburg, Hähnlein)	UHEI	Mobile measurements using CRDS Analyzer Picarro G2201-i	Measurements isotopic composition of methane from different sources to check seasonal variations	Dairy farms, gas compressor station / 18	Values of isotopic composition of methane from visited sources, calculate emission factor
X	29.03.2019	Heidelberg and surrounding area (Kircheim)	UHEI	Mobile measurements using CRDS Analyzer Picarro G2201-i	Measurements isotopic composition of methane from different sources to check seasonal variations		Values of isotopic composition of methane from visited sources, calculate emission factor
XI	02.04.2019	Heidelberg and surrounding area (Weinheim)	UHEI	Mobile measurements using CRDS Analyzer Picarro G2201-i	Measurements isotopic composition of methane from different sources to check seasonal variations	Dairy farm / 10	Values of isotopic composition of methane from visited sources, calculate emission factor
XII	10.05.2020	Heidelberg and surrounding area (Sinsheim, Hahnlein)	UHEI	Mobile measurements using CRDS Analyzer Picarro G2201-i	Measurements isotopic composition of methane from different sources to check seasonal variations	Landfill / 10 Gas compressor station / 2	Values of isotopic composition of methane from visited sources, calculate emission factor
XIII	3.07.2019 23.07.2019 - 31.07.2019	Heidelberg and surrounding area (Ladenburg, Sinsheim, Hahnlein, Kircheim, Heidelberg)	UHEI	Mobile measurements using CRDS Analyzer Picarro G2201-i	Measurements isotopic composition of methane from different sources to check seasonal variations Test of OTM-33a method	Landfill / 5 Dairy farm / 7 Gas compressor station / 2 Biogas / 7 + 1 OTM	Values of isotopic composition of methane from visited sources, calculate emission factor
XIV	09.09.2019 – 10.09.2019 23.09.2019	Heidelberg and surrounding area (Weinheim, Ladenburg, Kirchheim)	UHEI	Mobile measurements using CRDS Analyzer Picarro G2201-I and LGR	Test of OTM-33a method	Dairy farm / 2 Dairy farm / 2 Biogas /1	Calculate methane emission
XV	30.09.2019 – 20.10.2019	Romania ROMEO campaign	INCAS	Mobile measurements using LICOR 7810	Application of OTM-33a method and GPM, collecting sample bags	44 OTM 15 GPM Sample bags 68	Calculate emission from oil & gas wells

XVI	13.12.2019	Heidelberg and surrounding area (Ladenburg)	UHEI	Mobile measurements using LICOR 7810	Application og GPM model	Dairy farm Transect 20	Calculate methane emission
XVII	29.01.2020 – 31.01.2020	Heidelberg and surrounding area (Sinsheim, Hahnlein, Kircheim, Ladenburg, Weinheim)	UHEI	Mobile measurements using LICOR 7810	Application og GPM model	Landfill: Transect 12 Gas compressor station: Transect 21 Biogas: Transect 15 Dairy farm: Transect 21 Dairy farm: Transect 21	Calculate methane emission
XVIII	23.02.2020 – 27.02.2020	Dubendorf	EMPA	Release experiment using LICOR 7810	Different test for OTM 33a	Many hours of measurements	Calculate methane emission from release
XVIIII	13.03.2020	Heidelberg and surrounding area (Hähnlein)	UHEI	Mobile measurements, using OF-CEAS Analyzer, LI-7810	Measurements of methane concentration for estimating methane emission	Gas compressor station (31)	Methane emission
XX	07-11.09.2020	Heidelberg and surrounding area (Ladenburg, Kirchheim)	UHEI	Mobile measurements, using OF-CEAS Analyzer, LI-7810	Measurements of methane concentration for estimating methane emission	Dairy farm, biogas plant {30}	Methane emission
XXI	07-11.09.2020	Mannheim	UHEI	Release test using OF-CEAS Analyzer, LI-7810 and LGR	Measurements of methane concentration for estimating methane emission and checking accuracy of the method	Several GPM transects in different distance + several 20-30 minutes period for OTM33a	Intercomparison paper
XXII	22.10.2020	Mannheim	UHEI	Release test using OF-CEAS Analyzer, LI-7810	Measurements of methane concentration for estimating methane emission and checking accuracy of the method	Several GPM transects in different distance + several 20-30 minutes period for OTM33a	Intercomparison paper

6.1.4 Dissemination activities

6.1.4.1 Scientific publications

The ESR is involved in the following publications:

Defratyka, S.M., Paris, J.-D., Yver-Kwok, C., Fernandez, J.M., Korben, P., Bousquet, P.: Mapping urban methane sources in Paris, France; Environmental Science & Technology, in preparation

Fiehn, A., Kostinek, J., Eckl, M., Klausner, T., Gałkowski, M., Chen, J., Gerbig, C., Röckmann, T., Maazallahi, H., Schmidt, M., Korben, P., Neçki, J., Jagoda, P., Wildmann, N., Mallaun, C., Bun, R., Nickl, A.-L., Jöckel, P., Fix, A., and Roiger, A.: Estimating CH_4, CO_2, and CO emission from coal mining and industrial activities in th eUpper Silesian Coal Basin using an aircraft-based mass balance approach, Atmos.Chem.Phys., 20, 12675-12695, https://doi.org/10.5194/acp-20-12675-2020, 2020

6.2 ESR2 - Quantifying CH_4 emissions using measurements on cars and UAVs in the Netherlands

ESR2

Quantifying CH_4 emissions using measurements on cars and UAVs in the Netherlands

ESR	Katarina Vinkovic (k.vinkovic@rug.nl)
Supervisor	Prof.dr. Huilin Chen (huilin.chen@rug.nl)
Co-supervisor	Prof.dr. Wouter Peters (wouter.peters@wur.nl)
Non-academic mentor	Dr. Arjan Hensen (arjan.hensen@tno.nl)
Official start-end date	01.10.2017 – 30.04.2021

6.2.1. Scientific progress

6.2.1.1 Project introduction and objectives

The aim of the ESR2 project is to quantify CH_4 emissions using atmospheric concentration and isotopic composition measurements, with a focus on the agriculture CH_4 emissions (cattle and manure) that account for ~ 67% of the total emissions in the Netherlands in 2015 (Coenen et al., 2017). Spatial and temporal variations of CH_4 concentrations near major sources will be obtained on two different mobile platforms, a vehicle (car/van) and unmanned aerial vehicle (UAV). Additional trace gas measurements (e.g. NH_3, CO, $^{13}CH_4$ and CDH_3) on the vehicle enable us to identify the source type, whereas 3D mapping of the CH_4 plumes using an active UAV AirCore system will allow an accurate estimate of the source strength when combined with a Gaussian plume model as well as large eddy model simulations in collaboration with other researchers within the same project.

6.2.1.2 Project results

During the reporting period, ESR2 focussed on three different subjects: quantifying methane emissions from the Grijpskerk dairy cow farm (section 6.2.1.2.1.), quantifying methan emissions from oil and gas facilities from Romania (section 6.2.1.2.2.) and the CH4 trace release experiment (section 6.2.1.2.3.).

6.2.1.2.1 The Grijpskerk dairy cow farm

The CH_4 mole fraction measurements from an unmanned vehicle (UAV) based active AirCore system (8 – 15 minutes) were used to determine the CH_4 enhancement of the downwind against the upwind from a dairy cow farm, ~ 20km NW of the city of Groningen, the Netherlands. During the period from March 2017 to March 2019, four measurement campaigns were carried out on the farm (Fig.6.2.1).

The first three campaigns were performed using an UAV based active AirCore system from the University of Groningen (UG). The last campaign was a joined campaign between UG and The Netherlands Organisation for applied scientific research (TNO), where measurements were obtained using two different mobile platforms, a mobile van and an UAV.

In all four measurement campaigns, the CH_4, CO_2 and CO mole fractions were measured downwind of the farm, nearly perpendicular to

Fig. 6.2.1: The flight location of downwind flights conducted for this study: (a) 27th March 2017, (b) 3rd May 2018, (c) 10th October 2018, (d) 29th March 2019. The red arrow indicated the wind direction for each campaign. The distance is measured from the stable (1), where adult cows are housed.

the wind direction. A total of 17 flights were performed, of these only 8 were suitable for further analysis. We used a combination of different approaches to quantify CH_4 emissions from the farm.

A three-dimensional plot showing CH_4 concentrations distributed in the space (Fig.6.2.2 a), together with interpolated data in a two-dimensional plane (Fig.6.2.2 b), which were used to estimate a flux with a mass balance method. To integrate the enhanced CH_4 mole fraction, data need to be spatially interpolated to equally distributed grids in a plane.

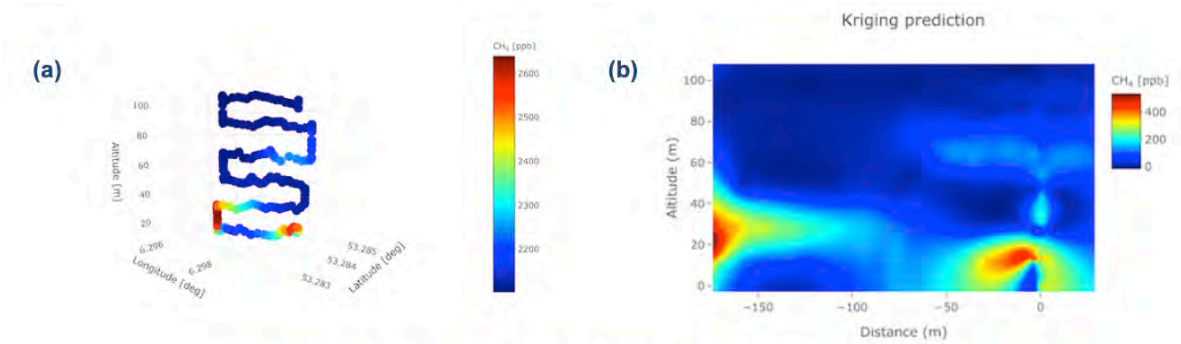

Fig. 6.2.2: 3D plot of CH_4 concentration, March 27th 2017: a) Downwind flight; b) Interpolated data.

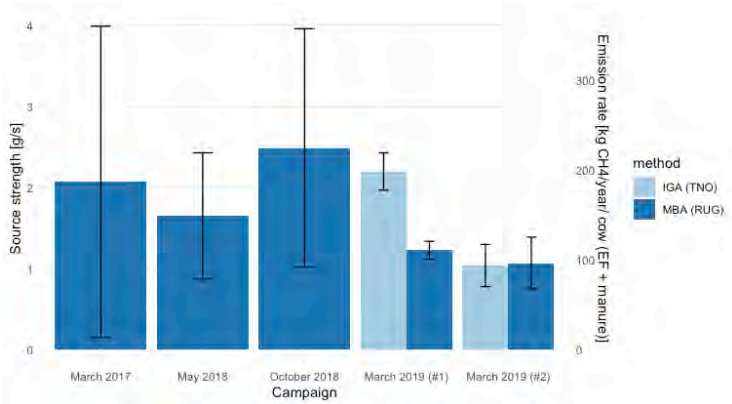

Fig. 6.2.3: Estimated source strength and emission rates of the Grijpskerk farm for the flights during the period March 2017 – March 2019, using a mass balance approach (MBA) and an inverse Gussian approach (IGA).

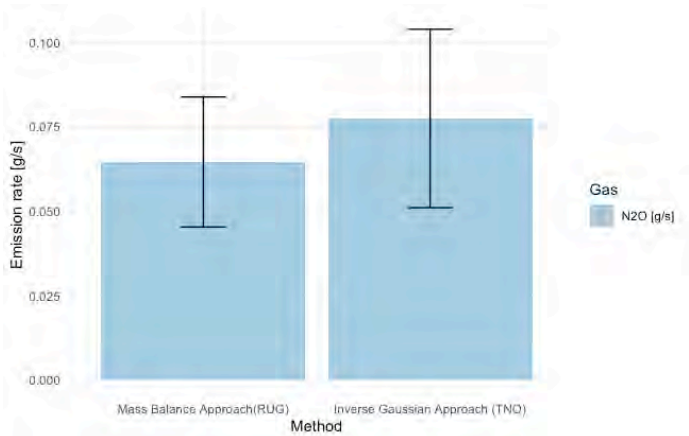

Fig. 6.2.4: The estimated emission rate of a controlled N_2O tracer release experiment, using two different inversion methods, a mass balance approach (RUG) and inverse Gaussian approach (TNO).

The total CH_4 emission rates from the farm, determined using a mass balance approach and inverse Gaussian approach are shown in Fig. 6.2.3 for each campaign.

The estimated emission rates vary by a factor of ~2.5, in the range of 1.1 – 2.5 g/s and the average emission rate over all quantifications is (1.7 ± 0.6) g/s. The sources of CH_4 include both the cows and the manure in storage on the farm. Since the manure is stored under the stables, the emissions from the manure and from the cows are basically collocated and cannot be distinguished from downwind CH_4 measurements.

Furthermore, an N2O tracer release experiment (Fig. 6.2.4) was performed during the last campaign on 29 March 2019, with a known release rate of 0.08 gs-1 in the immediate vicinity of the cow stables (1) and (2).

The emission rates of controlled N_2O tracer release experiment agree within 78 % for a mass balance approach (RUG), and within 96 % for

the Gaussian plume model (TNO) when compared to the known release rate. The estimates from 29 March 2019 (Table 6.2.1) were corrected based on the model run using the N_2O tracer data. The difference shows the effect of having or not having a tracer available in this kind of tests. In that case, the emission levels need to be corrected by factor 1.22 and 1.04, respectively.

Table 6.2.1: Overview of estimated N_2O emission rates for the UAV-based active AirCore and mobile van measurements, 29th March 2019

29th March 2019	UAV			VAN		
	CH_4 [g/s]		N_2O [g/s]	CH_4 [g/s]		N_2O [g/s]
	Flight #1	Flight #2	Flight #2	Crossover #1	Crossover #2	Van #2
1st order estimate	1.2 ± 0.1	1.1 ± 0.3	0.07 ± 0.02	2.2 ± 0.2	1.0 ± 0.3	0.08 ± 0.02
N_2O corrected	X	1.3 ± 0.4	0.08 ± 0.02	x	1.1 ± 0.3	0.08 ± 0.02

A) Background analysis

Significant variations have been observed in the CH_4 background between the flights.

To understand the cause of those variations, a thorough analysis had to be done. Therefore, we decided to compare measured CH_4 concentrations from the farm with continuous measurements from the nearby atmospheric station Lutjewad. The station (Fig. 6.2.5) is located ~ 15 km N from the farm on the northern coast of the Netherlands, directly next to the Wadden Sea dike, where CO_2 and CH_4 are continuously monitored at the 60-m high tower. The goal of this study was to investigate and understand how the observed background variations affect the final emission estimate, taking the magnitude of the observed source into account.

Fig. 6.2.5: The location of the Grijpskerk farm and the Lutjewad station (left side); the Lutjewad station (right side)

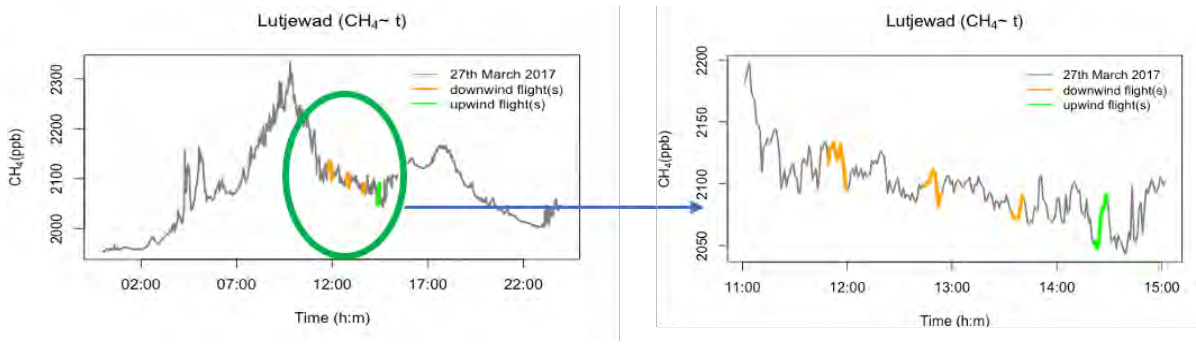

Fig. 6.2.6: The continuous CH_4 measurements from the atmospheric tower at 60 m. The green highlighted periods indicate the time span for downwind flights, while orange highlighted periods upwind flight, 27th March 2017.

For each flight 1st, 5th, 10th, and 15th percentiles were calculated to study background variations, and afterward compared with the Lutjewad station data. Only the analysis for 27th March 2017 is being presented in this report as an example when in total 5 flights were conducted, while only 4 of them were suitable for the background analysis.

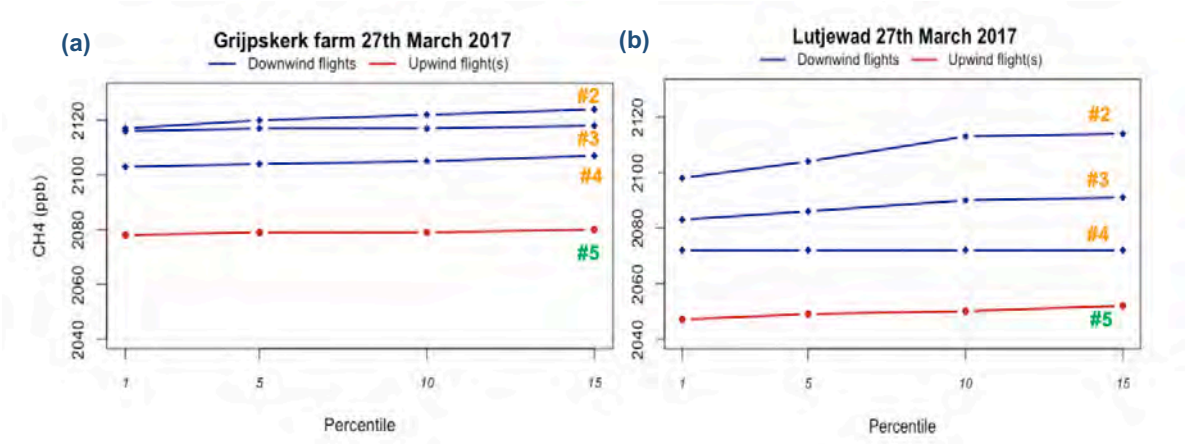

Fig. 6.2.7: 1st, 5th, 10th, and 15th percentiles of upwind and downwind flights, 27th March 2017, a) the Grijpskerk farm, b) the Lutjewad station

Table 6.2.2: Estimated emission rates of the background

Campaign	Downwind flight	Upwind flight	Flux* [g/s]	
	Background 10th perc. [ppb]	Background mean [ppb]	Background 10th perc.	Background mean upwind
March 2017	2105	2086	3.36	4.47
May 2018	1958	1952	2.19	2.31
October 2018	1970	1961	2.40	2.72
March 2019	2124	-	1.82	-
	1990	-	1.35	-

*The non-enteric emissions are not subtracted

Fig. 6.2.7a and 6.2.7b indicate that the background variations on both locations follow the same trend. That indicated that the background is influenced by the regional processes. Furthermore, the calculated 10th percentile is compared with the mean upwind value to see how it affects the final emission estimate (Table 6.2.2). From this study, we can see that is more correct to use the 10th percentile to estimate the background since the variations between the flights are significant what in the end can cause the overestimated flux using the upwind flight as the background.

B) Altitude analysis

Since the drone altitude is based on the ambient pressure measured on the drone, the reported drone altitude drift over the period of a flight, likely due to the warm up of the pressure sensor. We were unable to download the original pressure measurements of the drone; however, the ambient pressure was also observed with a pressure sensor within the active AirCore system. We assume that the pressure measurements by two sensors drift in a similar way, and developed a pressure correction procedure to correct for the drifts.

The pressure correction procedure includes the following steps (Fig. 6.2.8 a - d):

a) Apply a 1st linear regression to the pressure measurements immediately before and after the flight.

b) Subtract the background to get a pressure difference.

c) With a 2nd linear regression predicted pressure difference based on the drone altitude.

d) As the final step, convert predicted pressure difference to altitude.

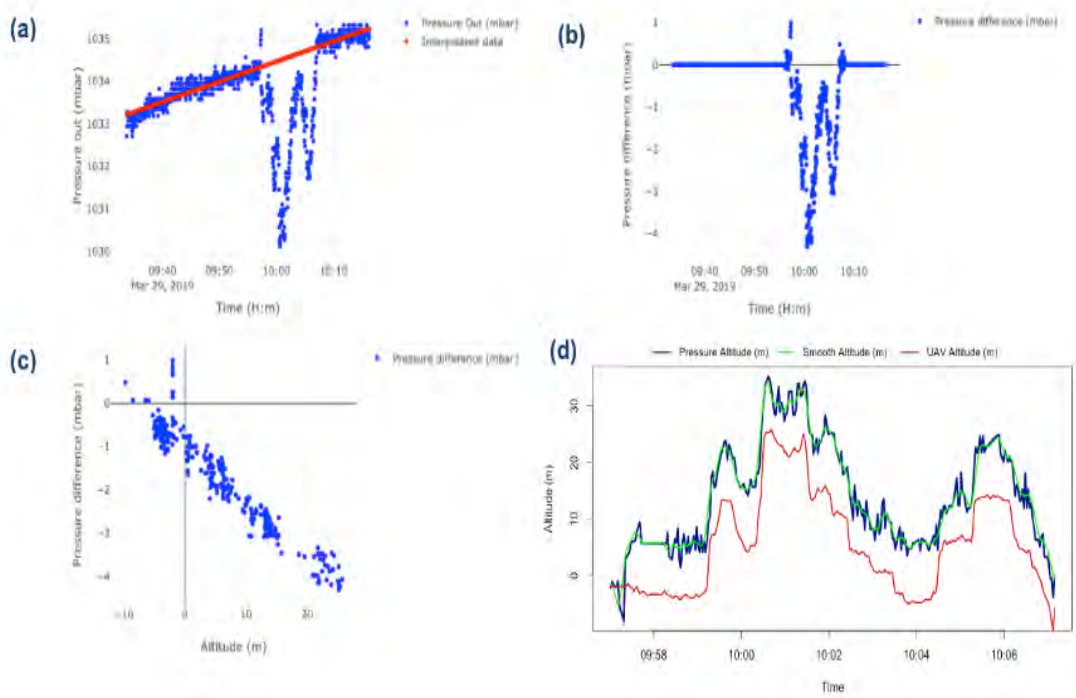

Fig. 6.2.8: The pressure correction procedure of the altitude measurements, 29th March 2019 - (a) Step 1 – 1st linear regression applied to the pressure background; (b) Step 2 – Pressure difference; (c) Step 3 – 2nd linear regression predict pressure difference to a respect of the drone altitude (d) Step 4 – Pressure corrected altitude. The red line presents the drone altitude, while the blue pressure corrected altitude and green smoothed pressure corrected altitude with a moving average to reduce the noise.

It is important to have as much as possible accurate altitude measurements, because it affects the uncertainty of the final emission estimate, and the plume itself (Fig. 6.2.9). As shown in Fig. 6.2.9b the pressure corrected altitude overestimates (Table 6.2.3) due to the noise in the signal, compared to the drone altitude (Fig. 6.2.9a). However, smoothing it with a moving average some of the atmospheric variability effects are being eliminated from the signal.

Table 6.2.3: Estimated CH_4 emission rates of different altitudes.

Campaign	Flux* [g/s]		
	The drone altitude	Pressure corrected altitude	Smoothed pressure corrected altitude
March 2019	1.62	1.82	1.60

*The non-enteric emissions are not subtracted

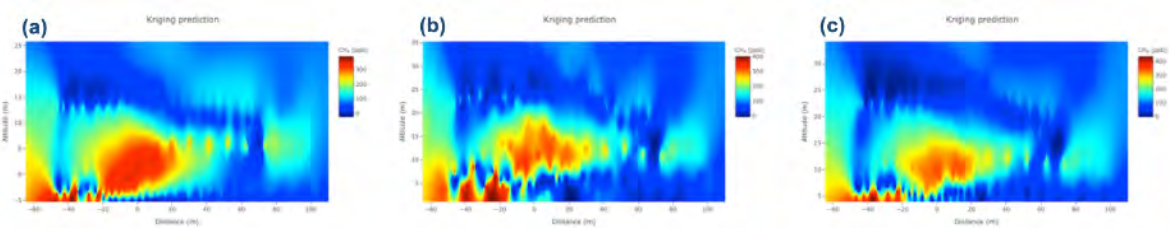

Fig. 6.2.9: Interpolated data, 29th March 2019 - (a) The drone altitude; (b) Pressure corrected altitude; (c) Smoothed pressure corrected altitude

6.2.1.2.2 Oil and gas facilities (ROMEO campaign)

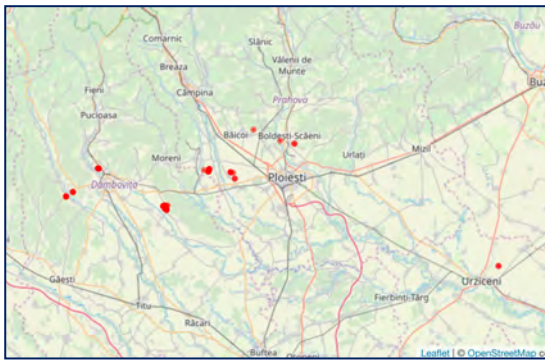

Fig. 6.2.10: Overview of quantified sites during the ROMEO campaign, October 2019

Fig. 6.2.11: The flight location of downwind flights with its surroundings, conducted on the site A and B, ROMEO campaign 2019. The red dots indicated the location of the source (area), while the green dots indicated the location of the 3D sonic anemometer. The orange arrows indicate the wind direction for each site.

Table 6.2.4: Emission rates

Location	Source estimate [g/s]			
	Flight #1	Flight #2	Flight #3	Mean
Site A	0.42	0.11	0.50	0.34
Site B	0.46	0.16	-	0.31

Besides continuously working on UAV measurements from a dairy cow farm, ESR2 also participated in the international ROMEO campaign – ROmanian Methane Emissions from Oil & gas, which was held in Romania, ~70 km N from the city of Bucharest. The fieldwork took place from 29th September until 20th October 2019. The main goal of this campaign was to quantify CH_4 emissions from oil and gas facilities using the Active AirCore system. The collected data are the basis for the 2nd publication of ESR2.

In total, 65 UAV flights at 22 different locations were performed. By this, 18 oil wells and 4 oil parks were quantified (Fig. 6.2.10). In this report, two different sites will be presented, an oil well (site A) and oil park (site B). On the site A 3 flights were conducted, while on the site B 2 flights (Fig. 6.2.11). The same methodology was applied as in section 6.2.1.2.1. All flights were performed downwind of the source, nearly perpendicular to the wind direction. Prior to a flux estimate, the data needs to be interpolated (Fig.6.2.12) since it is unequally distributed in the space. CH_4 emission rates from sites A and B are determined using the mass balance approach. The discrepancy in the flux estimates (Table 6.2.4) between the flights is mainly caused by very variable wind, i.e. atmospheric variability, which was present almost during the whole campaign, and sources that may not leak continuously in time. Preliminary results of the sites A and B are presented in Figure 6.2.13. CH_4 emission rates of visited sites determined using the mass balance approach are presented in Figure 6.2.14.

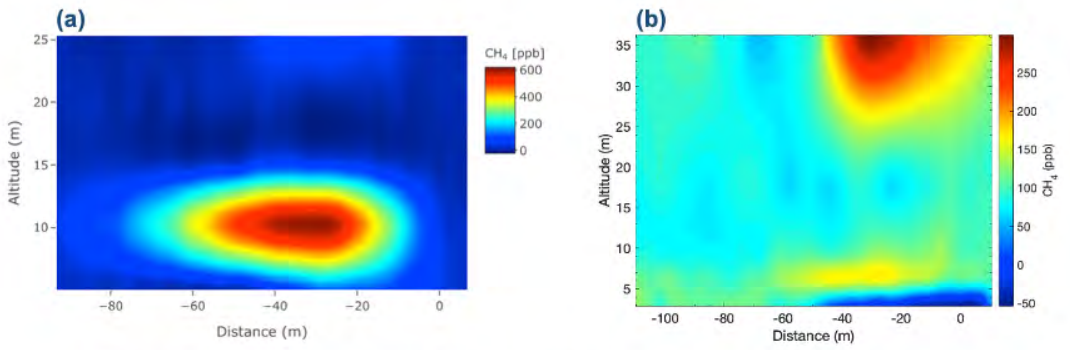

Fig. 6.2.12: Interpolated data; a) the site A, flight #1, b) the site B, flight #1

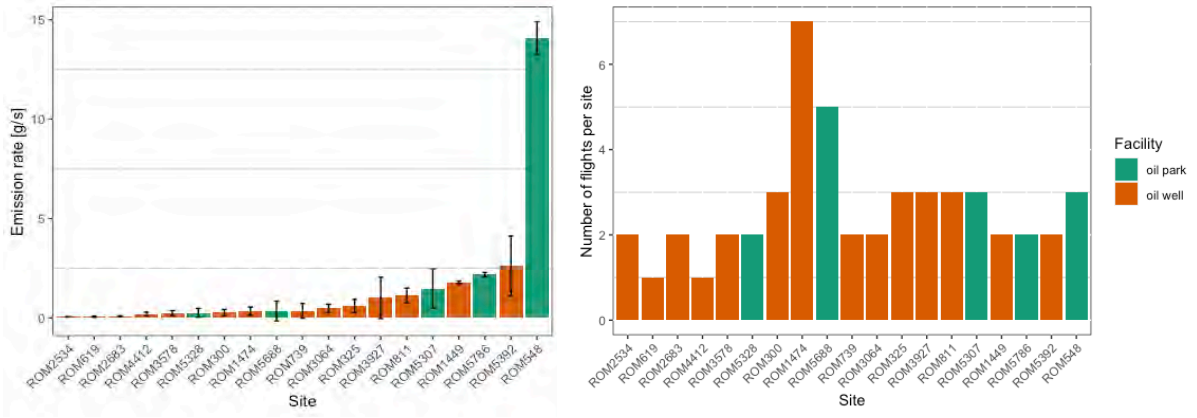

Fig. 6.2.13: (a) Overview of quantified emission rates per visited site, where the uncertainties are presented as standard deviation (1-sigma) of the multiple quantified emissions per site (N>=2) or the estimated uncertainty of individual flight (N=1). **(b)** The number of flights that were performed per site during the ROMEO campaign.

6.2.1.2.3. The CH4 trace release experiment

ESR2 participated in multiple drone-based measurement campaigns that took place during her secondment at the Swiss Federal Laboratories for Materials Science and Technology (EMPA) in February 2020, together with ESR1 and ESR12. The aim of this experiment was to compare two different Unmanned Aerial Vehicle (UAV) platforms, the Active AirCore System (UG) with EMPA's QCLAS system. The main difference between those two systems is that EMPA has an in-situ instrument, while UG's Active AirCore system is collecting air samples using ~ 50 m long coil. The CH_4 controlled release experiment was performed on an open field nearby Dübendorf (Switzerland), where in total 30 flights have been conducted with both systems mounted to the drone (Fig. 6.2.14.a) during 12 days of measurements.

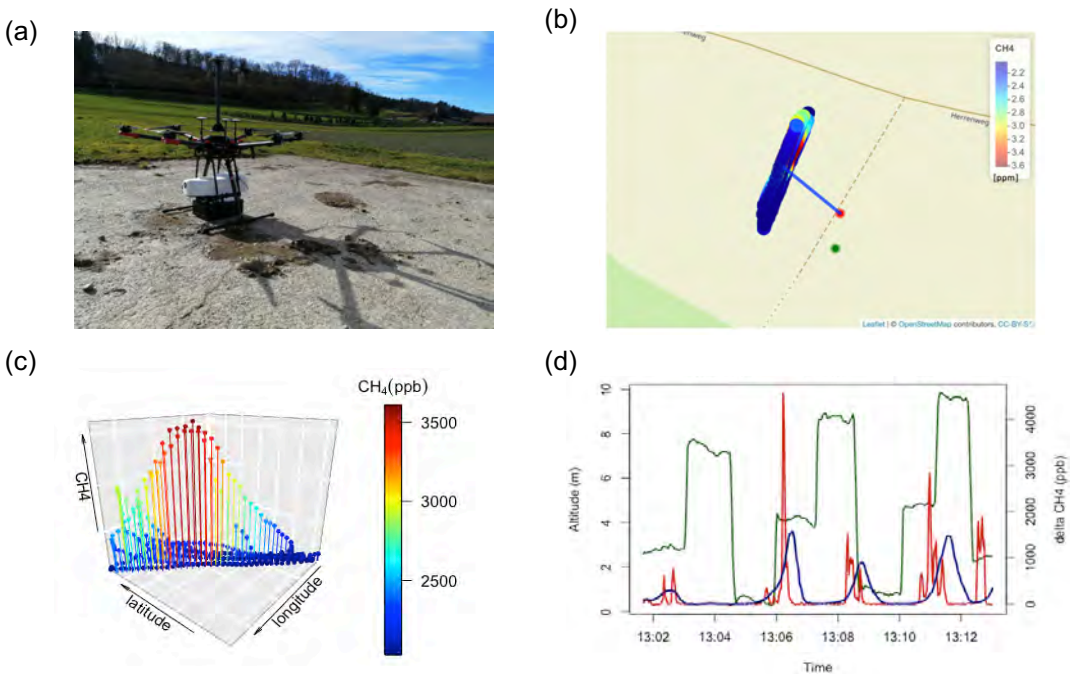

Fig. 6.2.14: (a) The Active AirCore (UG) and QCLAS (EMPA) systems mounted to the drone. **(b)** The flight location of downwind flight, March 14th 2020. The red dot indicates the location of controlled CH_4 release experiment, while the green dot the location of 3D sonic anemometer. **(c)** 3D plot of CH_4 concentrations, March 14th 2020. **(d)** Enhanced CH_4 profiles, March 14th 2020. The red line represents the EMPA's CH_4 profile, while the blue line UG's CH_4 profile, and the green line the altitude.

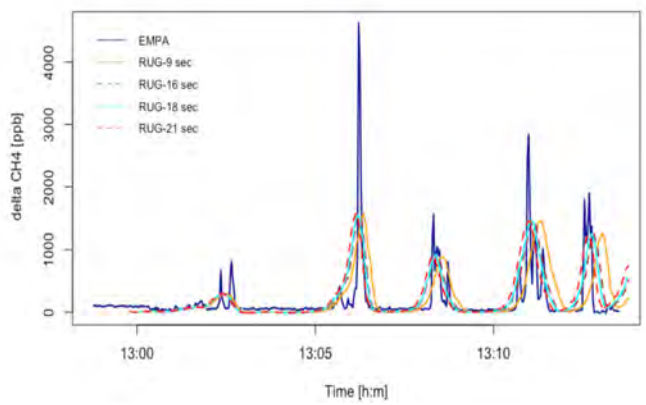

Fig. 6.2.15: The correction of the starting point of UG's Active AirCore CH_4 signal between 9 – 21 seconds. The flight has been conducted on March 14th, 2020.

During the data analysis, it has been discovered that the Active AirCore signal is more stretched towards the end in comparison to QCLAS signal (Fig. 6.2.14 d). Therefore, it has been investigated whether the starting point has been determined correctly. By shifting the starting point backward between 9 and 21 seconds the CH_4 profile is less stretched because it contains more points. From Fig. 6.2.15 it can be seen that the correction of 18 seconds eliminates the stretching effect from the AirCore profile. However, the same analysis needs to be applied to the remaining UG flights in the coming months.

6.2.1.3 Future plans and expected results

Following the final report, the ESR2 will mainly focus on the publications and the dissertation. Unfortunately, the ESR2's last campaign (planned April – May 2020) was affected by an unexpected outbreak of the coronavirus in Europe, and therefore, was cancelled.

Planned publications:

1st publication: Methane emissions from a dairy farm in the Netherlands

(data collected: March 2017 – March 2019)

2nd publication: Methane emissions from oil and gas facilities in Romania

(data collected: October 2019, ROMEO campaign)

6.2.1.4 Collaborations (internal / external)

In December 2019 we started a collaboration with ESR1 (University of Heidelberg - UHEI) about screening data, which was collected during the ROMEO campaign in Romania (September – October 2019). The idea is that the ESR1 and ESR2 together analyse the screening data, and afterward find the best approach to upscale emissions from oil and gas facilities.

Furthermore, in February 2020, we started a collaboration with ESR12 (EMPA) and ESR1 (University of Heidelberg – UHEI) through the ESR2 secondment (February – March 2020). During the secondment, multiple drone-based field measurement campaigns were performed on an open field nearby Dübendorf, Switzerland. The study focused on comparison and evaluation using different methodologies, a mass balance approach and otm33A respectively. The obtained data will result in a future scientific publication between the above-mentioned parties.

6.2.1.5 Risks and difficulties

During the whole project, there were no difficulties related to the beneficiary's administration or country legislation. Our potential issues were more related to the experimental part of our work, in a sense, that we may experience possible technical failure of the instruments or the availability of our technicians. However, our last campaign (planned April - May 20220) has been affected by the outbreak of the coronavirus.

6.2.2 Deliverables

ESR 2 is involved in the following deliverables: D1.1 / D1.2 / D1.4 / D1.5 / D2.2 / D2.3.

D1.1 – Report on harmonized method for mobile CH_4 and $^{13}CH_4$ measurements (month 18)

Approved

ESR2 contributed to a number of mobile measurement campaigns, and was responsible for the assessment of these data during her secondment at TNO (October 2018 – January 2019).

D1.2 – Lightweight CH_4 sensor and AirCore developed and deployed on UAV (month 24)

Submitted

ESR2 contributed to the development of the active AirCore system and a low-cost methane sensor. The development work has been completed and reported.

D1.5 – Report and public on improved emission factors for different source categories from mobile measurements (month 42)

Approved

ESR2 performed UAV-based CH_4 concentration measurements and analyzed mobile van-based measurements by TNO to improve the emission factors of dairy cows.

D2.2 – Improved isotopic signatures of local and regional CH_4 emissions (month 36)

Submitted

Being part of mobile measurement campaign for one day in Groningen, the Netherlands, during the secondment of ESR7 (September – October 2018).

During the 2nd Grijpskerk campaign, three air samples were collected from drone flights, and later analyzed for isotopic compositions at UU by ESR8.

D2.3 – Publication on the use of isotopes for CH_4 source attribution in urban / industrial regions (month 36)

Submitted

ESR2 was not involved in urban/industrial CH_4 studies, but contributed to oil & gas facilities studies.

6.2.3 Training and network activities

6.2.3.1 General training events

Event	Date (start – end)	Location (Host)	Objective / expected skills	ECTS points	Contribution	Comments
PhD Introductory Event	09. – 10.11. 2017.	University of Groningen (RUG)	To get acquainted with other PhD students, and the university.	1	attended	Training programme for a PhD students.
Mastering your PhD	1st meeting: 19.02.2018. 2nd meeting: 22.05.2018.	University of Groningen (RUG)	Project management, time management.	2	attended (2 meetings out of 6)	Training programme for a PhD students (new meeting every 6 months).
1st MEMO^2 School	05.02. – 16.02. 2018.	Schoorl (The Netherlands)	Two-week thematic school on CH_4 including courses, practical exercises, field campaigns, and data analysis.	6	poster, presentation	-
1st MEMO^2 annual meeting	21.03. – 23.03. 2018.	EMPA (Switzerland)	Meet and update each other about the project, discuss and evaluate the progress of the first year and give an outlook to the second year.	2	poster, presentation	-
English Academic Writing Skills	01.05. – 21.06. 2018.	University of Groningen (RUG)	Focus on academic writing.	1	written essay	-
Gaussian Plume Modelling workshop	09. – 10.10. 2018.	University of Heidelberg (UHEI)	The workshop included lectures and hands-on practical exercises.	2	attended	-
Publishing in English	28.01. – 26.03. 2019.	University of Groningen (RUG)	Improve academic writing skills.	2	draft of 1st manuscript	

Global Change course	February – April 2019	University of Groningen (RUG)	Various causes of climate change, global water and carbon cycle, stable isotope analysis methods, IPCC.	-	teaching assistant	-
2nd MEMO² School	18.02. – 22.02. 2019.	University of Versailles-St-Quentin en Yvelines (UVSQ)	Meet and update each other about the project, discuss and evaluate the progress of the second year and give an outlook to the third year.	4	poster, presentation	-
Global Change course	February – April 2019	UG	Various causes of climate change, global water and carbon cycle, stable isotope analysis methods, IPCC.	-	Teaching assistant.	-
NCGG 2019	12. – 14.06. 2019.	Amsterdam (NL)	Presented ongoing research about methane emissions from dairy cows in the Netherlands.	2	Attended + poster.	International conference.
Scientific Integrity	1st meeting: 10.12.2019. 2nd meeting: 25.02.2020.	UG	The storage, interpretation and presentation of research data, for example, the question of authorship in co-authored articles, or the use of other scientists' work in your own publication.	2	Attended + essay.	-
Mastering your PhD	1st meeting: 19.02.2018. 2nd meeting: 22.05.2018. 3rd meeting: 17.01.2020	UG	Project management, time management.	2	Attended (3 out of 6 meetings)	Training programme for PhD students (new meeting every 6 months).
3rd MEMO² annual meeting	10.02. – 11.02.2020	UHEI	Meet and update each other about the project, discuss and evaluate the progress of the second year and give an outlook for the last year.	1	Attended + presentation.	-
ROMEO meeting	12.02. – 13.02.2020	UHEI	Meet and update each other about the preliminary results, discuss and evaluate both the progress and future plans.	1	Attended + presentation.	-
EMPA secondment	14.02. – 16.03.2020	EMPA	Participate in joint campaigns, together with UHEI and EMPA. Comparison of EMPA's in-situ device with UG's Active AirCore system.	2	1 month visit	International research experience / exchange visit, 0.5 ECTS/week.
Climate System and Atmosphere	April – June 2020	UG	Various causes of climate change, understanding of anthropogenic and natural forcing, and the feedbacks. Overall, understanding the earth climate system.	-	Teaching assistant.	-
EMPA secondment	14.02. – 16.03.2020.	EMPA	Participate in joint campaigns, together with UHEI and EMPA. Comparison of EMPA's in-situ device with UG's Active AirCore system.	2	1 month visit	International research experience / exchange visit, 0.5 ECTS/week.
MEMO² progress meeting	12.10.2020.	Virtual meeting	Meet and update each other about the project, discuss and evaluate the progress of the third year and give an outlook for the last year.	2	Attended + presentation.	-

6.2.3.2 Secondments

Secondment	Date (start – end, planned (when))	Location	Host	Description of work / deviations	Scientific / training (skills) objective	Results and future plans
Energy research Centre of the Netherlands (ECN)	26.08. – 07.09. 2018.	Petten (The Netherlands)	ECN	Analyse data from 1st MEMO² school (Feb. 2018) and make a poster for 3rd ICOS conference.	Gaussian plume model.	Poster for 3rd ICOS conference, and continue to work on Gaussian plume model.
Energy research Centre of the Netherlands (ECN)	29.10. 2018. – 25.01. 2019.	Petten (The Netherlands)	ECN	Modify Gaussian plume model for a drone, and participate in campaigns.	Gaussian plume model, CH_4 and N_2O emissions from cow farms in the Netherlands.	In progress.
Swiss Federal Laboratories for Materials Science and Technology (EMPA)	14.02. – 16.03.2020.	Dübendorf (Switzerlnad)	EMPA	Joint multiple campaigns between EMPA, UG and UHEI with CH4 trace release.	Data analysis and evaluation and comparison of mass balance approach and OTM33a method.	Joint publication between EMPA, UHEI and RUG.

6.2.3.3 Conferences

Conference name	Date (start – end, planned (when))	Location	Presentation (oral / poster)	Title of presentation	Authors (main author + co-authors)	Public available (yes / no) / web link
BBOS Symposium 2017	25. – 27.10. 2017.	Berg en Dal (The Netherlands)	no	-	-	-
Industrial Methane Measurement Conference – PEFTEC 2017	29. – 30.11. 2017.	Antwerp (Belgium)	no	-	-	-
3rd ICOS Science Conference	11. – 13.09. 2018.	Prague (Czech Republic)	poster	Quantification of methane emissions from dairy cows in the Netherlands	K.Vinkovic + T.Andersen, M.de Vries, W. Peters, A. Hensen, H. Chen	no
BBOS Symposium 2018	25. – 26.10.2018.	Soesterberg (The Netherlands)	poster	Quantification of methane emissions from dairy cows in the Netherlands	K.Vinkovic + T.Andersen, M.de Vries, W. Peters, A. Hensen, H. Chen	no
NCGG 2019	12. – 14.06. 2019.	Amsterdam (NL)	Poster	Quantification of methane emissions from dairy cows in the Netherlands	K.Vinkovic + T.Andersen + M.deVries + W.Peters + A.Hensen + H.Chen	no
AGU 2020	01. – 17.12.2020.	San Francisco (USA)	Virtual Poster Session	Quantification of methane emissions from a dairy cow farm in the Netherlands	K.Vinkovic + T.Andersen + M.deVries + B. Kers + S. Heuven + W.Peters + A.Hensen + H.Chen	no

6.2.3.4 Measurement / sampling campaigns

Campaign	Date (start – end, planned (when))	Location	Host	Description of work	Scientific objective	Samples (nature / number)	Results and future plans
1st Grijpskerk campaign	27th March 2017	Grijpskerk (The Netherlands)	RUG	Drone measurements at the Grijpskerk cow farm.	Quantify CH_4 emissions.	-	Material for 1st publication.
1st MEMO2 School	9th – 11th February 2018	North Holland (The Netherlands)	ECN	Van measurements across the North Holland province.	Design, plan and run field campaigns to measure atmospheric CH_4 at site scale.	-	Some of the results presented on 3rd ICOS conference in Prague.
2nd Grijpskerk campaign	3rd May 2018	Grijpskerk (The Netherlands)	RUG	Drone measurements at the Grijpskerk cow farm.	Quantify CH_4 emissions.	bag samples / 3	Material for 1st publication.

3rd Grijpskerk campaign	19th October 2018	Grijpskerk (The Netherlands)	RUG	Drone measurements at the Grijpskerk cow farm.	Quantify CH_4 emissions.	bag samples / 4	Material for 1st publication.
4th Grijpskerk campaign	29.03.2019.	Grijpskerk (The Netherlands)	RUG	Drone measurements at the Grijpskerk cow farm, together with TNO, that performed van measurements and N2O trace release test.	Quantify CH_4 emissions.	-	Material for 1st publication.
ROMEO	29.09. – 20.10. 2019.	(Ploiesti, Urziceni) Romania	INCAS	Drone measurements of oil and gas facilities.	Quantify CH_4 emissions.	bag samples / 44	Material for 2nd publication.
Trace release campaign	17.02. – 16.03. 2020.	Dübendorf (Switzerlnad)	EMPA	The CH_4 trace release experiment.	Quantify CH_4 emissions.	-	Joined publication between EMPA, UHEI and RUG.

6.2.4 Dissemination activities

Two publications are in progress, but except for the contributions to the conferences further no scientific publications or other dissemination activities so far from the ESR.

6.3 ESR3 - Validating CH_4 inventories over intense mining area, natural and anthropogenic emissions

ESR3

Validating CH_4 inventories over intense mining area, natural and anthropogenic emissions

ESR	Mila Stanisavljevic (mila.stanisavljevic@gmail.com)
Supervisor	Justyna Swolkien (swolkien@agh.edu.pl), Jaroslw Necki (necki@agh.edu.pl)
Co-supervisor	Martina Schmidt (martina.schmidt@iup.uni-heidelberg.de)
Non-Academic mentor	Wojciech Wolkowicz (wwola@pgi.gov.pl)
Official start – end date	16.10.2018 - 15.10.2020

6.3.1 Scientific progress

6.3.1.1 Project introduction and objectives

The main objective of the ESR3 project is to investigate methane emissions from industrial sites, primarily coal mining. The areas of interest are:

- Upper Silesia Coal Basin (USCB), the region reaches with active underground coal mine explanation and/or abandoned coal mines,
- the Lublin Coal Basin (LB), the region of active underground coal mine explanation,
- Lower Silesia (LSCB), the region of abandoned coal mines and
- Ruhr region, Germany, region of recently closed coal underground coal mining.

Existing high precision equipment enables measurement of CH_4 emission and its isotopic signatures staying outdoor of facility gates. Such a deployment introduces a new measurement methodology to reduce the uncertainty of CH_4 release.

The aim of such a study was the characterisation of emissions from the abandoned coal mines. For such a task, simple static chambers were deployed. We measured not only CH_4 mole fraction and fluxes but also the CH_4 isotopic signature ($\delta^{13}C$-CH_4 and δD- CH_4), from all above-described regions. This technique was used to confirm the sources of the CH_4 enhanced concentration by analysing the air with Picarro CRDS and CF-IRMS.

Finally, the Gaussian plume model supplemented by WRF wind simulation (Weather Research and Forecasting model) was deployed to determine CH_4 release rate from the measured mole fraction over the mining regions in Europe. During the project timeframe, we were focused on the single-site study. In addition to each investigation site, the uncertainty of each estimated CH_4 emission rate has been assigned.

The CH_4 emission results have been compared with available databases (E-PRTR 2017, CoMet v4.0), while CH_4 isotopic data have been compared with studies done over the same coal regions or compared with the other world coal regions.

6.3.1.2 Project results

6.3.1.2.1 Third year

All results ESR3 achieved can be connected to one of the three types of activity:

A) Testing of instruments in the laboratory conditions prior to field measurements

B) Measurements of CH_4 concentrations supplemented by data analysis

C) Measurement of methane isotopes ($\delta^{13}CH_4$ and δD), by different techniques

A) Testing of instruments in the laboratory conditions prior to field measurements

Under the scope of the ESR3 project, we have been used different equipment: Picarro G2201-i CRDS, LGR, CF-IRMS and static chambers. The following list gives a short overview of experiments aimed at improving the analyser performance:

- Calibration of CH_4 concertation: (Picarro and LGR).
- Water cross-sensitivity to all measured species (Picarro).
- Influence of the ethane concentration on the measured methane concertation (Picarro).
- CF- IRMS and CRDS comparison (CF-IRMS and Picarro).

The calibration of all the instruments was performed regularly under laboratory conditions during the project time. The main purpose of this activity is to eliminate systematic errors and/or evaluate data on the same level (since we use different instruments for the concentration measurements of the same compounds). Since all our instruments have a linear response, the typical procedure follows the recommendation from *Richardson et al. (2017)*. The air mixtures of methane from four different cylinders (one by one, for 30 minutes) were measured.

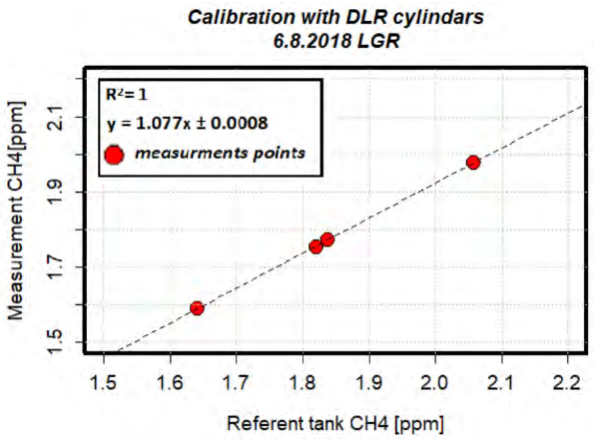

Fig. 6.3.1: Typical calibration curve for the LGR instrument

As all of the volumes have to be flushed with new mixture every time it is connected, the first 10 minutes of measurement were rejected due to the questionable quality of the measurements.

Using the data from the next 20 minutes of the measurements, simple statistics moments were calculated: mean and standard deviation.

Fig. 6.3.1 illustrates the construction of typical calibration function. After the calibration, the necessary correction was applied to the results.

Water cross-sensitivity tests: According to *Rella et al. (2015)*, the changes of water vapor content in a sample might have an influence on the results of measurements of other compounds (CH_4, CO_2, $\delta^{13}CH_4$). The experimental procedure was designed based on the recommendation of the Heidelberg group contacted during the secondment.

The cooling trap (to hold and release the water vapour) was installed between the laboratory standard and the Picarro CRDS instrument. Firstly, only dry air with a known methane mixing ratio passed through the cooling trap (for approximately half an hour). After ½ h, we introduce distilled H_2O. Even though our instruments have automatic correction still, experiment proofed the effect (Fig. 6.3.2).

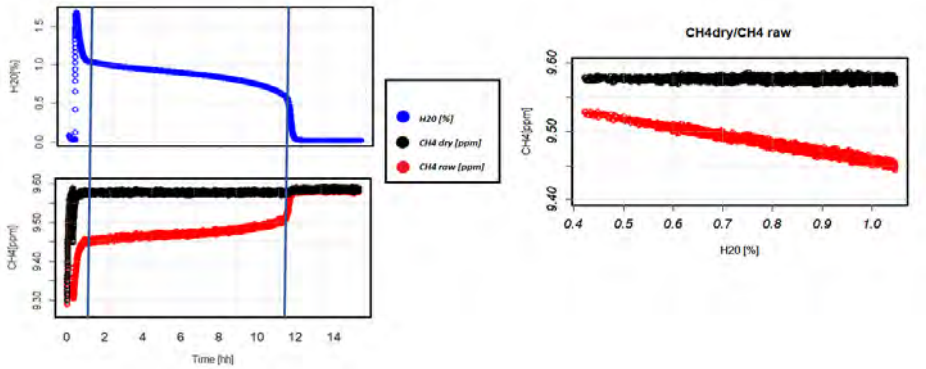

Fig. 6.3.2: CH_4 cross-sensitivity to H_2O. The left panel illustrates the concentration of H_2O (blue), CH_4 without water vapor correction (red), and CH_4 with water vapor correction (black). Panel b) CH_4 concentration as a function of H_2O mixing ratio.

The data has been separated into two parts: with water vapor in a range of 0 – 0.16 % and from 0.16 % to 2.5 %. This also fit to real field conditions since our plume of interested (methane from the coal ventilation shafts) are enriched with water vapor. The isotopic composition of $\delta^{13}CH_4$ in humidity range between 0.16 to 2.5 % revealed a change in the recorded values. The relative error may reach up to 10 % of measured value. In this case, drying of the humid samples prior to the measurements in the field or laboratory is highly recommended.

Ethane influence onto CH_4, H_2O, CO_2, $\delta^{13}CH_4$: Usually the release of the methane from the industrial facilities is accompanied by the emission of ethane and other hydrocarbons. We examined changes in the response of the analyser to CH_4, H_2O, CO_2, and $\delta^{13}CH_4$ due to increased C_2H_6 concertation in the samples.

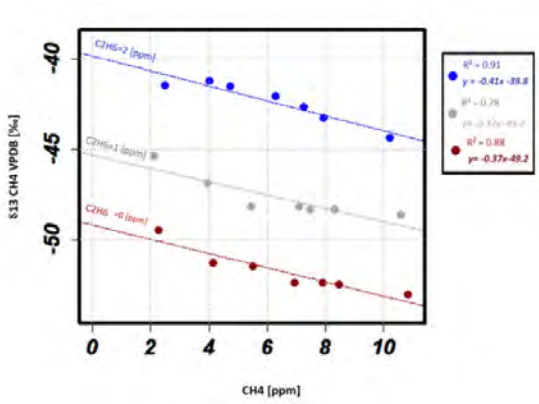

Fig. 6.3.3: The dependency of $\delta^{13}CH_4$ due to changes of C_2H_6 concentration

For the purpose of the experiment, we prepared three cylinders with the same CH_4 mixing ratio but different amounts of C_2H_6. The initial CH_4 concertation of 10 ppm was diluted into different known proportions by adding zero air to the mixture. The ethane in a range of 0 to 2 ppm does not change the results of the measurements of CH_4 and CO_2. In case of $\delta^{13}CH_4$, we can clearly see that C_2H_6 introduce an isotopic shift. In our case from -47 ‰ to – 39 ‰ (Fig. 6.3.3). Samples containing high concentration of ethane (e.g. natural gas) should be analysed for the concentration of C_2H_6 and subsequently the isotopic composition needs to be appropriately corrected. Indeed, the ESR3 project is based on methane from coal industry. Naturally coal do not contain significant amounts of ethane and other hydrocarbons, hence we do not apply spatial correction for our measured samples.

Comparison CRDS – IRMS: During the secondment at Utrecht University, ESR 3 had the opportunity to measure bags samples (collected over the USCB area) using a high precision isotope ratio mass spectrometer CF-IRMS. Beside $\delta^{13}CH_4$, we measured δD inside the samples. Picarro CRDS can determine $\delta^{13}CH_4$ with the precision of 2 ‰ (*Picarro, 2019*) while the precision of IRMS is 0.02 % *(Brass et al., 2010)*. More details about the δD results can be found in the section 6.3.1.2.2. The Fig. 6.3.4 illustrates the comparison of both instruments. 28 bag samples were examined.

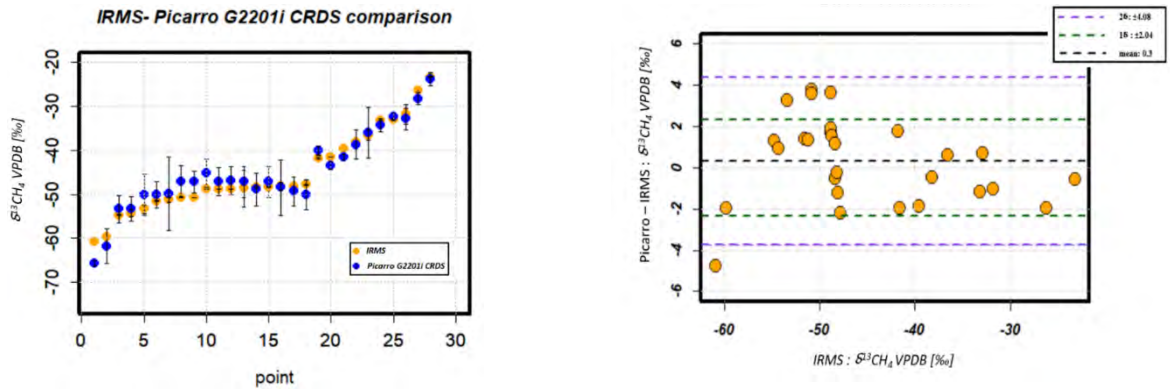

Fig. 6.3.4: left panel illustrates the comparison of IRMDS and CRDS measured values. In total, 28 samples were examined. The right panel illustrates statistical approaches for having a closer look at the difference: y-axis presents the Picarro – IRMS difference

We can see that our results are in a relatively good agreement. The standard deviation of difference between the measurement results are in order of 2 per mills. The Picarro instrument can be applied for a field condition analyses of a high concentration samples, rather than for the precise analysis.

B) Measurements of CH_4 concentrations supplemented by data analysis

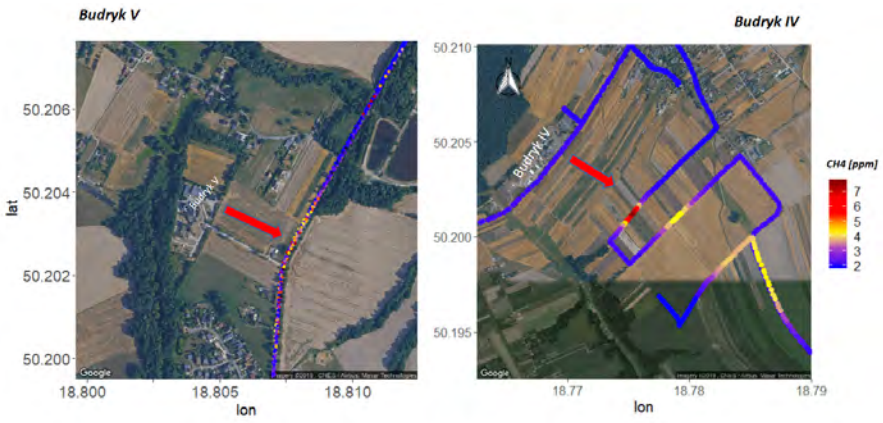

Fig. 6.3.5: One typical coal mine ventilation shaft. Left: passing a road a few times, right: passing road of interest on the different distances

Beside a laboratory testing of the equipment, we performed field measurements. For this purpose, we used Picarro G2201i CRDS analyser installed in a car. A 2D wind sensor was installed on the roof of our car, as well as the GPS system.

We performed multiple cross-sections of the methane plumes from the coal mine shafts using public roads approximately perpendicular to the plume direction, downwind from the source. When possible, the plumes were intersected several times at different distances as Fig. 6.3.5 illustrates. During reporting period, we revisit some points over USCB, LB, vested new spots at Ruhr and LSCB regions. The measurements procedure and data analyses were performed at the same way.

We are able to pass the roads at distances up to 1 km from the coal mine shafts, as distances are limited by the Gaussian plume model applied for a flux estimation. To quantify the emissions, each peak was analysed separately. Below are the basic steps performed to fit our measured CH_4 concertation to the Gaussian plume model (Fig. 6.3.6).

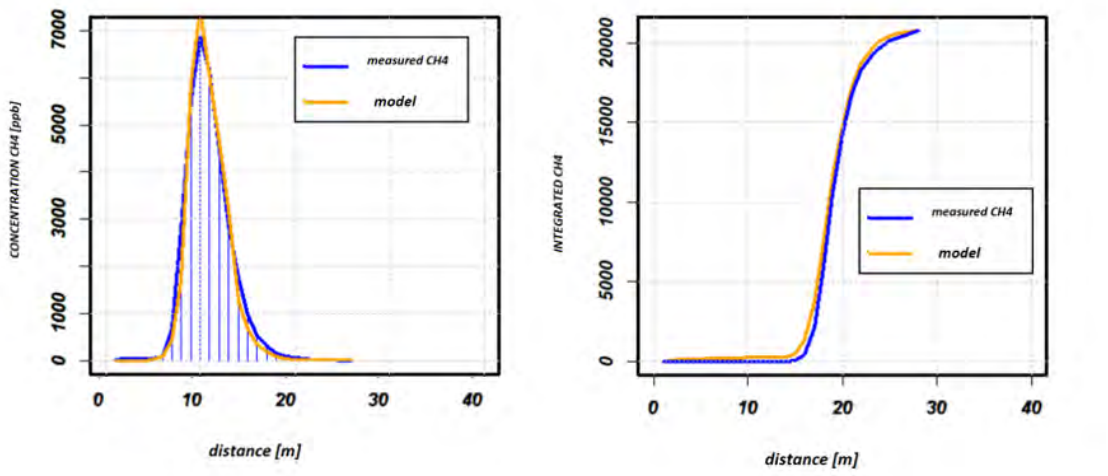

Fig. 6.3.6: Gaussian plume cross-section: measured CH_4 concentration and Gaussian curve fitted by the model(left); comparison of the total area under the peak of measurements and modelling

The model based on a simple Gaussian equation together with Pasquill stability classes and Briggs equations for the plume reflected from the ground *(Turner, 1994):*

$$C(x,y,z,H) = \frac{Q}{2u\pi\sigma_{y\sigma_z}} e^{\frac{-y^2}{2\sigma y^2}} \left(e^{\frac{-(z-h)^2}{2\sigma_z{}^2}} + e^{\frac{-(z+h)^2}{2\sigma_z{}^2}}\right) \quad \left[\frac{g}{s}\right] \qquad (1)$$

where C is the concertation of methane [ppb], Q is the release rate applied in the model [g/s], σ_y is the standard deviation of plumes in a vertical dimension [m], σ_z is the standard deviation of plumes in a horizontal dimension [m], h is the height of the source [m], z is the height of the measurement [m], and u is the wind speed along the plume [m/s]. The emissions are calculated in two major steeps. After setting up all necessary parameters, e.g. source strength, meteorological data; wind speed, wind direction, stability classes we can run our model. The modelling is repeated using different parameter values to establish the sensitivity of calculation on variability of the parameters.

Fitting procedure bases on comparison of the total area under the peak of methane recorded experimentally during the transects and the modelled data along the same path. (Fig. 6.3.6, right panel) Equation 2 described the final step in our approach.

$$Q = \frac{\int mesured,CH4}{\int model,CH4} * source\ strenght \left[\frac{g}{s}\right] \qquad (2)$$

Under the MEMO² project, we have estimated methane emissions from 23 independent sources over USCB. The summary of data is illustrated in Fig. 6.3.7. In this figure we have integrated the fluxes obtained from all exhaust ventilation shafts belonging to 13 facilities. Typically, one coal mine has 2 or 3 exhaust shafts.

Calculated data were compared with the available database E-PRTR for the years 2017 and 2018. For 13 mines visited by ESR3 the total emission from the database is ascribed to 197.5 kt CH_4 per year, while our calculation gives the release rate 204 kt CH_4 per year. These values are statistically in agreement as the uncertainty of our estimates is larger than 20%. In the following period ESR3 will work more on the uncertainties in order to have statistical correct data.

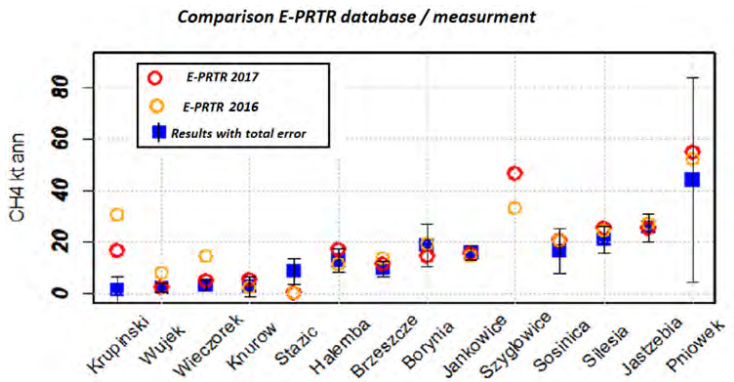

Fig. 6.3.7: Upper Silesia measurement: comparison with E-PRTR database

C) Methane isotopic signatures

The study of ^{13}C and D isotopes abundance in the CH_4 were carried on at 38 individually localized CH_4 sources (23 ventilation shafts and 15 hard coal mining waste dumps).

Bag samples from coal mine ventilation shafts*:* The data were collected through a series of mobile surveys (May/Jun 2018, Jun 2019). When the methane enhancement was strong enough (more than 0.5 ppm above background), we performed a sampling and subsequent the isotopic measurements. At the majority of coal ventilation shafts.

As Fig. 6.3.8 illustrates, we are using the Keeling method to infer the $\delta^{13}CH_4$ or δD signatures from each source every time we are able to visit the facilities. The intercept value of the regression line illustrated at Fig. 6.3.8 constitutes the isotopic signature of the source.

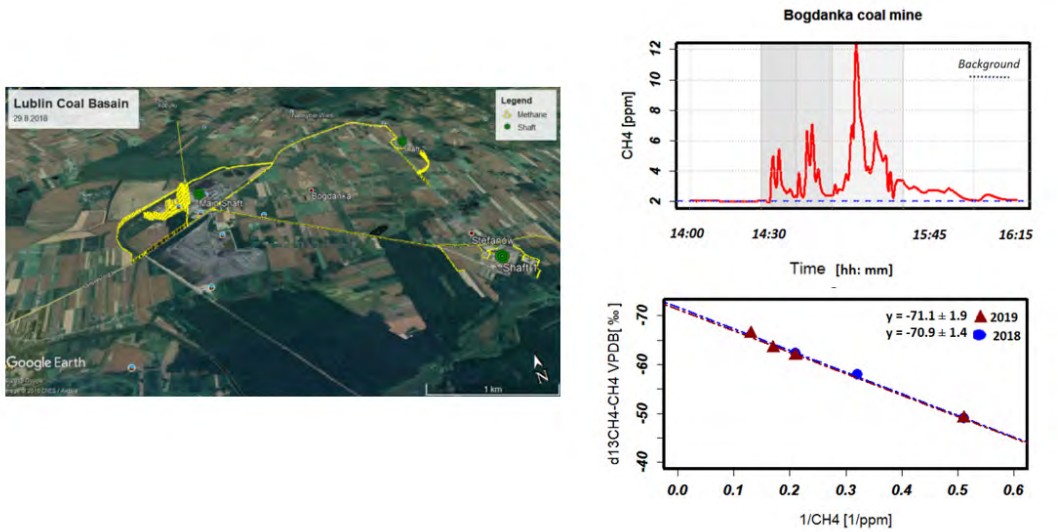

Fig. 6.3.8: Bogdanka mine investigation. Left: sampling procedure - we are driving near-source through the available public roads circling around the ventilation shafts. Right: methane concentration record and the sampling results.

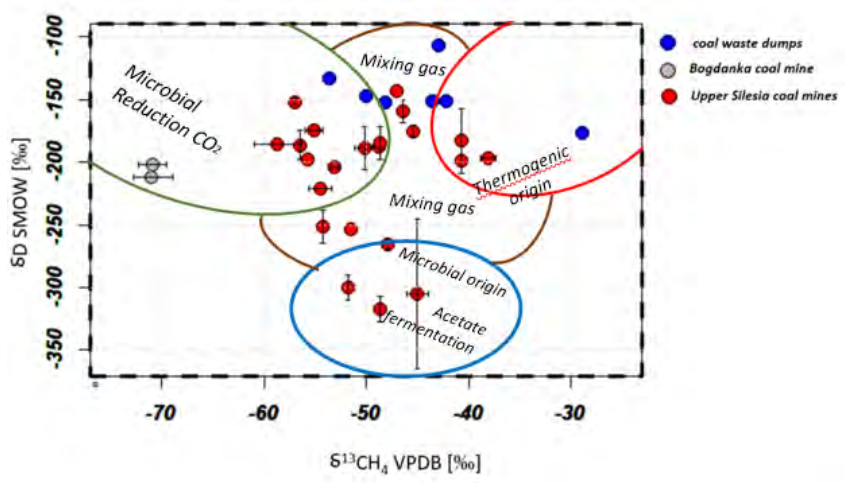

Fig. 6.3.9: Characterization of coal bed gases from USCB, LSCB, and LSCB with δD versus $\delta^{13}CH4$ plot. Diagnostic fields are taken from Whituchret al 1986.

We have estimated the signatures of both methane isotopes. Fig. 6.3.9 illustrates an overview of our results.

In conclusion, we can say that the methane isotopic signature over the coal mining regions can be qualified to different groups of originations: biogenic, thermogenic, or even mixed. In this case, assignment whole methane to the category „coal mine source" is wrong. The results are in range between -72 to -29 ‰ VPDB or -310 to -110 ‰ SMOW for δD or $\delta^{13}CH_4$ retrospectively. According to results each region and even the sub regions, need to be characterize separately.

Bag samples from the coal mine waste dumps: According to the actives over the examined sites, we grouped all existing coal waste dumps as

- active (sites where mining activities such as dumping are still present),
- abandoned (where mining activities are not presents, and sites are left as they are) or
- burning (sites where burning of matters occurs).

Since the coal mine waste damps have steep slopes which are difficult to access, we didn't apply the plume sampling technique. Instead, we collect direct samples from the small cracks in the heaps or from the static chambers (detailed description in section 6.3.1.2.4).

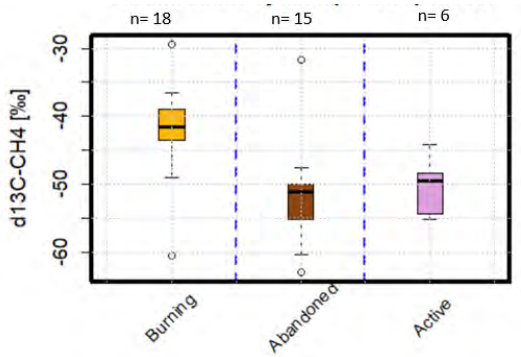

Fig. 6.3.10: Methane isotopic signatures of $\delta^{13}CH_4$ from 3 categories of waste dump.

The methane isotopic signature is ranging from -29.49 to -63.11 ‰ VPDB (Fig. 6.3.10). The methane emission from the coal mine waste dump is confirmed, however its origination is different in each group. On active dumps methane kept in pores of coal is diffusing. In case of abandoned dumps more likely, the methane emission follows the organic matter cracking, or is produced by the microorganism living on coal waste dump (Fabiańska et al. 2013). Burning coal dumps release the methane of thermogenic origin.

D) Static chamber technique: measurements of CH_4 concentrations over coal waste dumps

During the second year of the project ESR3 performed measurements on coal waste dumps. The IPCC report (IPCC, 2019) describes methane emissions from the coal:

1) Coal ventilation shafts

2) Coal transport and storage

3) From abandoned coal shaft and coal piles (dumps)

Emissions from the second and third category are small in comparison to the first category (Kriche at all, report ~ 1Tg CH_4 $year^{-1}$).

Fig. 6.3.11: Static chambers. a) the main part of chambers 1. Plastic sealing, 2. Inlet 3. Outlet b) static chamber deployed with LGR analyser. Additional feature is 4. Thermometer

Static chambers, together with the portable LGR analyser, were deployed in order to determine the methane release rate by the area of a coal mine waste dumps. ESR3 constructed a simple, low weight static chambers (Fig. 6.3.11). The plastic sealing 1cm width allowed for a better adjustment of the chamber to uneven measurement surface. External chamber surface is covered by the aluminium tape in order to reflect Sun radiation and reduce the heating of the gas volume. Inlet and outlet are on the opposite sides of the chamber. Together with LGR analyser, a whole system is working in a close loop of the gas flow.

Fig. 6.3.12: Spatial distribution of methane over coal mine waste dump

According to the Central Mining Institute (Katowice, Poland), over USCB there is 200 different coal mine waste dumps. Some of them are re-cultivated, some still actively used by the mines and some are burring inside. During the project time, we did measurements over 15 sites. Some of them release significant amount of methane. Before the measurements using the static chamber, we did a detail mapping of the methane concentration over the dump area. LGR analyser together with GPS was used by ESR3 walking on the top of the heap (Fig. 6.3.12).

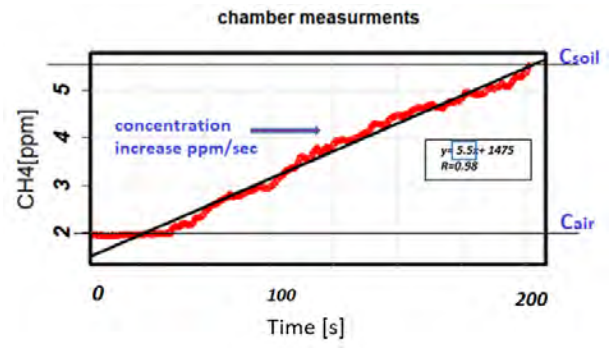

Fig. 6.3.13: Accumulation of methane under the static chamber.

Table 6.3.1: Summary of estimated fluxes for coal mine waste dumps

Sites	Flux [µg /s · m²]	No*
Burning	$(0.6 \pm 0.5) \cdot 10^6$	7
Active	220 ± 190	4
Abandoned	180 ± 64	4

*Number of vested sites under the group

We prepared than the spatial distribution map of methane sources. In the representative locations, the static chambers were placed on the ground and increase of methane concentration was observed. Enclosure lasted for 2 minutes or longer if the flux was not strong enough to observe the significant change in methane mixing ratio. An example of the recorded data is shown on Fig 6.3.13 The measurements of air temperature (T) and pressure (p) are necessary for flux calculations with use a linear model. The model assumes a constant concertation change dC/dt read from Fig. 6.3.13 as a slope of linear regression. To provide a rough estimate of the methane flux rate from the coal mine waste dumps, gas flux results were scaled up onto the whole site using the kriging procedure. As we are looking at a difference between 3 types of waste dump (active, abandoned, burning) the Table 6.3.1 and Fig. 6.3.14 illustrate the summary of the results. Extremely high fluxes of methane were observed on waste dumps which were burning. The average value of the flux for sites where coal heaps were burning is three orders of magnitude higher than from active or abandoned sites. Active or abandoned coal heaps indicate nearly the same methane flux (Table 6.3.1).

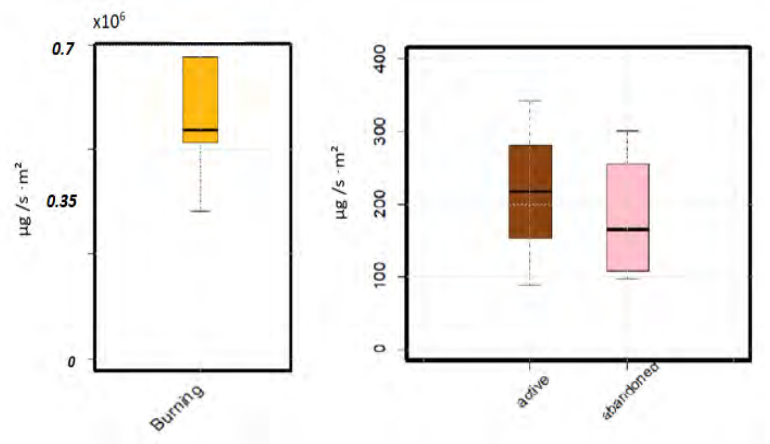

Fig. 6.3.14: Fluxes from coal waste dumps: left burning sites right active or abandoned sites

The static chambers applied to estimation of the methane flux worked well. However, the presence of a high concentration of water vapour could lead to underestimation of the calculated fluxes. Even if only one percent of the area of all coal mine waste dumps over USCB is burning and only 1 % of each heap is still burning the total flux from USCB reaches approx. 60 kt CH_4 per year. Unfortunately, only 15 sites (USCB and LSCB) were investigated. To extrapolate the results for a whole USCB and LSCB regions, more measurements are necessary.

6.3.1.2.2 Fourth year

During the fourth year of the MEMO² project, no additional measurements/ experiments were conducted and ESR3 continued working on the dataset collected in the previous years of the MEMO² project. The main focus was on finalizing the results from the CoMet campaign (Carbon Dioxide and Methane Mission) and individual measurements conducted during 2018 and 2019.

The work was divided into four major steps:

- Wind Simulation using WRF (Weather Research and Forecasting model) tool
- Improvement of already established Gaussian Plume model (GPM)
- Comparison of the results estimated by GPM with publicly available databases
- Comparison of CH_4 isotopic signatures with literature available datasets.

A) Wind Simulation using WRF tool

To estimate the CH_4 emission rate using GPM, accurate wind information is essential. Since GPM CH_4 modeling approach requires precise wind data at a particular location, we simulated wind over the USCB (Fig. 6.3.15).

Wind data used in this study were simulated by the Weather Research and Forecasting model coupled with chemistry (WRF-Chem, v3.9) with a GHG (Greenhouse Gas) module, run with 2 km x 2 km horizontal resolution and 1h of temporal sampling. The simulation domain was centered over the USCB, a domain spanning continental Europe. A more detailed description of the modeling system can be found in (*Galkowski et al. 2021*).

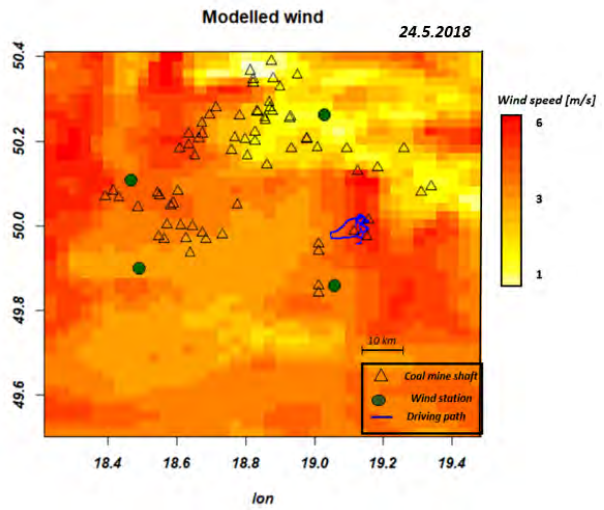

Fig. 6.3.15: Spatial distribution of wind speed across Silesia. The plot demonstrates the capability of the WRF- Chem v3.9 model to simulate wind data near measurements routes (blue line)

In situ measurements of wind speed were made using three tower-mounted sonic anemometers at 10m height above the surface. The 1h averaged measurements were used to check the validity of modeled wind. To assess the uncertainty in wind data, vertical wind speeds simulated by WRF-Chem v3.9 model are compared with in situ measurements (Weather Forecast & Reports - Long Range & Local, 2019) at 4 publicly available wind stations (Fig. 6.3.15; green dots).

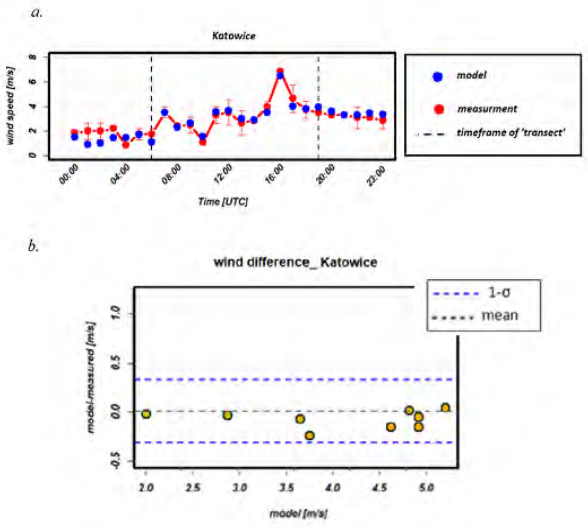

Fig. 6.3.16: a) Comparison WRF Chem v.3 model simulation (blue dots) with synoptic data (red dots). b) Difference between simulated and in situ data.

Here we illustrate one example over the 24 h comparison during one day's measurements. (24.5.2018). Note that Fig. 6.3.16 illustrates an example from the station Katowice (19.0291; 50.2690). However, we show only one example with the detailed description, but the same approach has been applied to all station.

The analysis assumes that differences between simulated and in situ data come from minor data differences (Giovarna, 2015). For every station simulated, using WRF- Chem v3.9 model wind data (during time frame 07:00 to 20:00 h UTC), and results were plotted against the difference between simulated and in situ data. If the 2σ range corresponds to the results range (blue dashed line- Figure 2b.), the methods are in statistical agreement. These differences (2σ) were used for wind uncertainty evaluation by running the Gaussian Plume model. However, such an approach has been applied to each CH_4 measurement day.

B) Improvement of already established Gaussian Plume model (GPM)

The data processed during the reported period were collected during 2018 and 2019 on already established measurement techniques (mobile car platform equipped with CRDS and GPS was cycling through the routes perpendicular to wind direction; more details are available in previous progress reports). In total, 100 different transects (near 12 different coal mine shafts) were simulated by GPM for different scenarios (for the different WRF simulated wind speed, wind direction, stability class). The medina value with corresponded uncertainty (as an interquartile range) was reported among all measurements and simulations near one coal mine shaft (Fig. 6.3.17). More details about the GPM approach can be found in studies (Hensen et al., 2016)

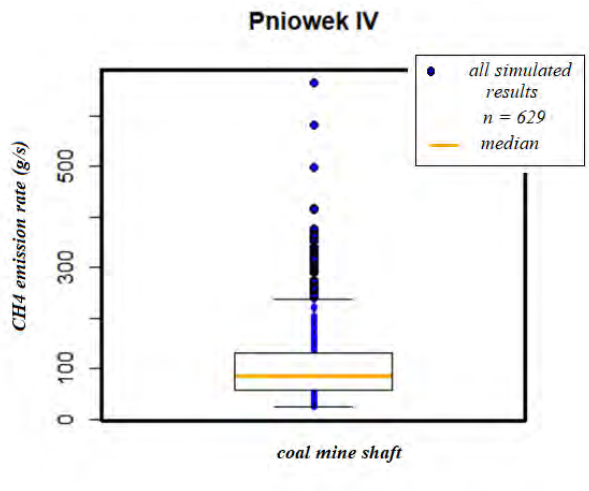

Fig. 6.3.17: Results of the CH_4 estimation at location Pniowek IV

As can be seen in Fig. 6.3.17, the CH_4 emission rate is highly variable. Since this figure is a summary of different wind and other metrological scenarios, we can conclude that CH_4 emission level of a coal mine shaft is variable in time. The study Luther (Luther et al. 2019) performed at the same coal region report an increase in CH_4 emission of almost factor 2, while observed the same coal mine ventilation shaft. This, together with the study (Swolkień 2020) confirms that CH_4 emission rate reported here can be considered representative for a short emission snapshot. More frequent measurements are needed to obtain a daily, monthly, or annual CH_4 emission rate.

The emission rates with corresponding uncertainties of 12 surveyed coal mine ventilation shafts are shown in figure 6.3.18. We obtained a broad range of CH_4 emission estimates: (20 ± 135) to (1722 ± 1405) $g \cdot s^{-1}$. The study was designed to cover only a part of the total coal mine ventilation shafts operating in the USCB. Careful analysis of the values of CH_4 emission estimate makes it evident that one coal mine shaft exceeded 1700 $g \cdot s^{-1}$. These coal mine shafts contribute 50 % of the total emissions estimates. This particular coal mine shaft will be described separately.

In addition, a slight enhancement in the number of coal mine ventilation shafts with estimated CH_4 emissions was found in the range 50 – 200 $g \cdot s^{-1}$, but the shafts were spread across all studied sites. Finally, two studied shafts have the emission lower than 50 $g \cdot s^{-1}$. The fact that we did not detect a large population of smaller CH_4 emissions across the USCB suggested that majority of coal mine shafts emits CH_4 in the range 50 - 200 $g \cdot s^{-1}$.

A variation in the CH_4 emissions existed in the observed coal mine shaft within the same coal mine facilities: e.g. Inside the Pniowek coal mine there are three ventilation shafts with CH_4 emission rates of (180 ± 224) $g \cdot s^{-1}$; (57 ± 30) $g \cdot s^{-1}$; and (86 ± 72) $g \cdot s^{-1}$, respectively. In the Pniowek coal mine, one shaft has an estimated CH_4 emission rate almost 50% different from the other. Such a difference illustrating the importance of CH_4 emission study on coal mine shaft level.

As it can be seen in Fig. 6.3.18 (n - number of simulations), each coal mine shaft has a different n number. This number varies due to a number of transect differences, simulated wind, and stability class variability. However, in Fig. 6.3.18 one coal mine shaft has a low number of simulations (n = 30) followed by a significantly higher CH_4 emission rate than the rest.

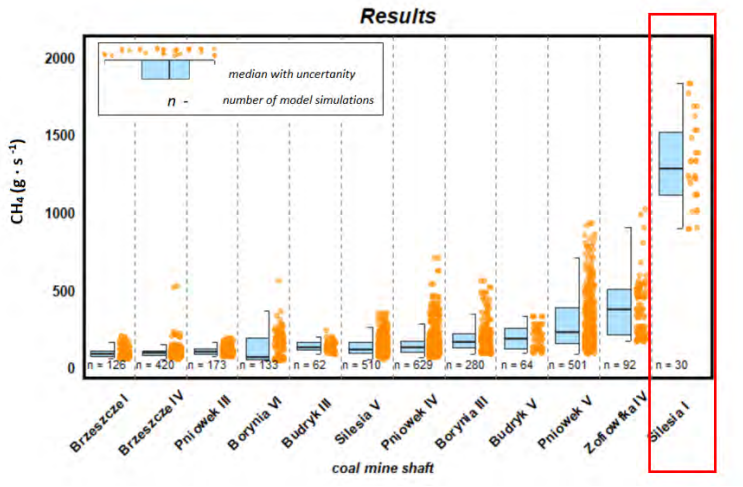

Fig. 6.3.18: Boxplot distribution of CH_4 emissions with corresponding uncertainties for 12 individual coal mine shafts in the USCB. Vertical grey dashed lines indicate the separation between different coal shafts, while orange dots indicate the variation in simulated/ measured results. Below each boxplot (n) the number of simulations is indicated.

Such a low number of simulations corresponds to only two transects performed during one measurement day. However, this high emission number might be addressed to the specific operation held inside of company gate (or potential company problem). Here is important to underline that this estimated number cannot be representative of a total emission rate such as a high CH_4 emission rate. Therefore, it is not clear is there a strict needed to quantify source variability at the scale of our measurements (second). We thus expect changes in CH_4 emission rate at the scale of the day, month, year to be reflected in what we treated as transect to transect variability. More transect allows a CH_4 emission rate to be calculated with more accuracy.

The additional limitation in CH_4 emission rate estimates which might affect the results is the modeled wind speed. However, our modeled wind speed is 1h snapshot since our measurements are performed on the second level.

In addition to the above conclusions, the significant differences between individual coal mine shafts and coal mines indicate considerable differences in the underground mining activities, including exploration, excavation of different coal seams, ventilation of "completed" seams, etc. occurs in various mining areas. Information at such a detailed level is not available in any public database. This finding also implies that the CH_4 emissions in the USCB likely vary in time within coal mine facilities and individual shafts, which could be investigated by quantifying emissions regularly. However, when a large number of shafts is investigated during a relatively short period, as during the CoMet campaign, this likely represents a typical distribution of CH_4 emissions from the entire basin on a short timescale.

C) Comparison of the results estimated by GPM with publicly available databases

Generally, the bottom-up inventories report CH_4 emissions for the USCB at different spatial and temporal resolutions (E-PRTR, 2017; Crippa et al., 2018). In order to compare our measurements with databases, only E-PRTR and CoMet v4.0 were used for comparison (E-PRTR, 2017, CoMet v4.0).

In this study, instead of comparing the absolute emission estimates with the database (either E-PRTR or CoMet v4.0) we report the ratio R to quantify the model - data agreement:

$$R = \frac{Q_{estimates}}{Q_{database}} \pm \Delta R \qquad (3)$$

where ($g \cdot s^{-1}$ CH_4) is the result of our estimates using the GPM evaluation, and $Q_{database}$ ($g \cdot s^{-1}$ CH_4) is the emissions estimate from the corresponding database, the uncertainty in the emission estimate is transferred to uncertainty in the ratio, ΔR.

When comparing the results of our study with databases, it is essential to emphasize that the comparisons are on the coal mine level and on the coal mine shaft level. Those differences appear due to public databases such as E-PRTR which do not contain information on emissions at coal ventilation shaft level. Accordingly, data from CoMet v4.0 and E-PRTR database are analysed separately, in order to gain better knowledge about CH_4 emission rates. Fig. 6.3.19 shows the ratio of measured CH_4 emission at coal mine facilities versus and emissions from the databases. For single coal mine shafts, the ratios of measured versus reported (CoMet v4.0) emission rate (orange rectangles, Fig. 6.3.19) vary between (0.09 ± 0.87) (Brzeszcze II- mani shaft) and (0.7 ± 0.78) (Borynia VI).

For the E-PRTR database, we compared coal mine facilities since there is no available data on the single coal mine shaft level (blue dots, Fig. 6.3.17). In this case, the ratios vary between (0.9 ± 0.3) (Pniowek) and (4.8 ± 0.1) (Knurow) (Fig. 6.3.17).

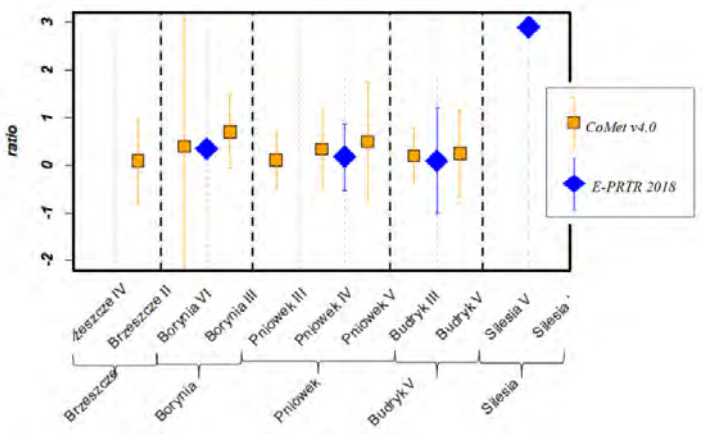

Fig. 6.3.19: Comparison: Ratio of measured emission rate relative to E-PRTR database (blue points) and CoMet v3.0 database (orange points). Note that blue points detonate comparison between coal mine since orange illustrate comparison with coal mine shafts

Despite the large uncertainties for estimate emission rate, we found that one coal mine difference of observed CH_4 emissions differed from the reported database (Silesia coal mine, different by factor 2.9). The largest differences are observed at the Brzeszcze coal mine shaft and Silesia coal mine (Figure 3; while comparing to E-PRT and CoMe v4.0 retrospectively).

To conclude section B) and C): Ground-based mobile and fast response measurements of CH_4 were used together with Gaussian plume modeling to derive CH_4 emission rates from 12 coal mine ventilation shafts in the USCB. The results showed a substantial variation in CH_4 emissions from different shafts. These findings imply that the emissions rate at the USCB varies within coal mine facilities and within different coal mine shafts. The emission rate of comparable shafts only partly agrees with reported emission estimates from the bottom-up E-PRTR and CoMet v4.0 inventories. Such a difference might be due to different reported scales. Our measurements provide information on the second level since E-PRTR database report only yearly emission rate, while CoMet v4.0 database time reporting is different than our measurements. This indicates that coal mine emissions might be well understood and monitored by the provider of CoMet 4.0 data. For coal mines, however, the agreement is worse, and the emission rates quantified in this study can be up to a factor 2.9 or more different from the inventories. This discrepancy between our measurement and bottom-up inventories may be due to the temporal variability of emissions from individual shafts, which cancels out over the entire basin. More frequent measurements are needed to fully understand the variability and errors related to the temporary variability of sources.

D) Comparison of CH_4 isotopic signatures with literature available datasets

In addition to the CH_4 emission estimation, ESR3 worked on the CH_4 isotopic signatures. During the project time, 23 different coal mine shafts (across the USCB) were sampled and compared with already existing literature. The main goal of this approach was to fill a gap in knowledge about CH_4 origin (since different coal mine shafts can have different CH_4 isotopic signatures) and to assign a isotopic signature to the USCB region (and particular coal mine shafts).

All isotopic signatures have been calculated using Keeling plot approach (Keeling, 1964). To aggregate all estimated CH_4 signatures into one value, the weighted average approach has been used (Fisher et al 2017). Such results have been compared with other studies carried out at the USCB or with the studies in other world coal regions.

Accordingly, Fig. 6.3.20 shows our results of the isotope analysis for the examined coal mine shafts in the USCB. As can be seen, $\delta^{13}C$-CH_4 values ranged from (-58.7 ± 2.5) to (-41.6 ± 0.9) ‰ VPDB and δD values from (-267.2 ± 60) to (-143 ± 1.5) ‰ SMOW (Fig. 6.3.20, right side). Such a high variability of isotopic signatures reflect multiple origins of gases: thermogenic (13%), microbial (56%), and mixing (34%) (Sherwood et al. 2017, Whiticar 1990).

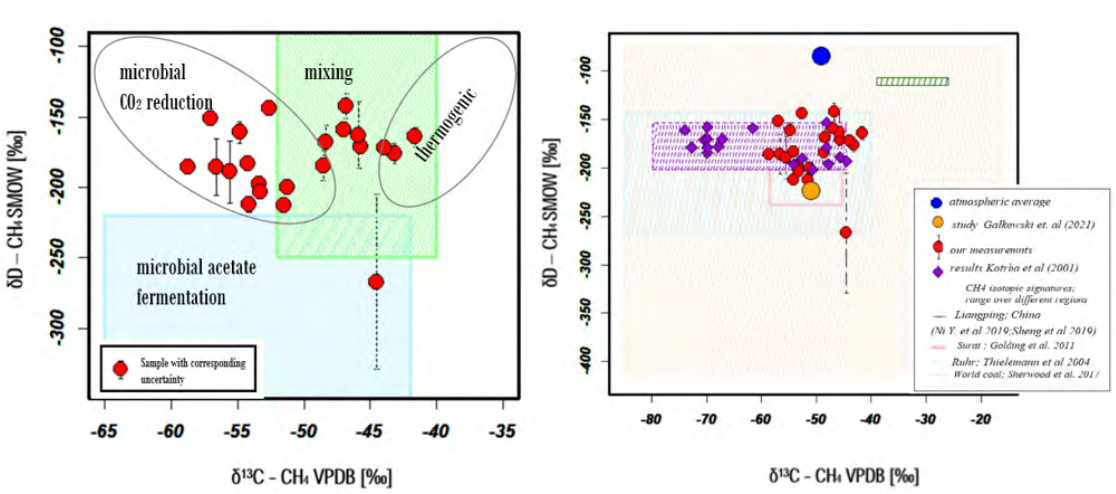

Fig. 6.3.20: Left: Combination of carbon and hydrogen isotope ratio of CH_4 to characterize the various CH_4 origin (Whiticar 1990). Sorce signatures (USCB) with associated uncertainty together with literature ranges related to origin (color boxes); Right: Source signatures at the USCB (red dots) compared with literature (Kotarba 2001; Thielemann 2004; Gałkowski et al 2021)

Also, one Figure 6.3.20 (left side), one sample from the coal mine shaft display depleted δD ((-267 ± 62) ‰ SMOW) source signature in comparison to others. Here, an isotopic shift from the rest of the samples suggests the influence of physical processes such as the inflow of fresh, meteoric water (Kotrba 2001). The origin of CH_4 with such isotopic value is identified as microbial acetate fermentation. It proves that the genetic origin of CH_4 is not unique in the USCB

To have a better comparison of results obtained during this study and Fig. 6.3.20 show the main ranges of these coal basin signatures together with samples collected during the MEMO^2. As can be seen the values during this study (red dots) fall into typical range for all World coal data (orange rectangle; reported by Swerwood et al 2017) (Fig. 6.3.20, right side).

The weighted average isotopic signature (CH_4 signatures weighted by fluxes) for the USCB derived in our study ($\delta^{13}C$ of CH_4 (-49.03 ± 5.28) ‰) is statistically identical to the signature reported by Gałkowski et al. (2021; orange dot, Figure 6b), Kotrba (2001, violet rectangle, Fig. 6.3.20), Thielemann (2004) (Ruhr region; Germany; green rectangle – Fig. 6.3.20), global coal reported by Sherwood et al. (2017; orange rectangle; Fig. 6.3.20 right side) (-49 ‰) or to value of the bulk atmosphere (-48.8 ‰, (Sherwood et al. 2017); blue dot, Fig. 6.3.20 right side). However, the study Thielemann (2004) focused on the isotopic signatures over the Ruhr region (Germany) since Kotraba (2001) and Gałkowski et al (2021) reported values for the USCB. Here is important to emphasise the Gałkowski study of CH_4 isotopic signatures at the free troposphere (data collected by airplane) since Kotarba study is 20 years old. However there the major difference between all results has not been observed. Here we can conclude that $\delta^{13}C$ over the USCB is well understood.

The δD signature found in the USCB (δD = (-163 ± 22) ‰) is distinct from emissions in other main world sources, such as coal deposits in Australia (Surat Basin), where δD values are much lower (-202 to -238 ‰) than those determined in the USCB during this study (range: (-143 ± 1.5) to (-267 ± 60) ‰). The δD values found in the USCB region also differ from Chinese coal mines (Liangping region), where isotopic signatures are more enriched than at the USCB, revealing a clearly dominant thermogenic origin in China. Such variability in origin significantly differs from other world coal regions such in China or Australia, can be due to unique processes related to different coal basins (primary generation and/or secondary migrations process followed by mining operations) (Kotraba 2001; Ni Y 2019; Golding et al 2011). However, in the present study, we added more valuable information to the available data on δD from the coal mining sector. Here we can conclude that study on the δD - CH_4 isotopes is a useful tool for distinguished signatures within different coal regions.

However, our finding on the total CH_4 isotopic signatures (weighted average $\delta^{13}C$-CH_4 = (-49 ± 5) ‰ and δD = (-163 ± 22) ‰) can be used in future modeling studies or for comparison with other aircraft data. To conclude, a high amount of sampling sites proved more representative isotopic signatures for use in CH_4 budget assessment at sites, regional and global scales. More detailed description about this topic will be available at ESR3 PhD, authors or coauthors manuscripts.

6.3.1.3 Future plans and expected results

The collected results are part of the scientific publication: 'Determination of methane emission rate and isotopic signatures Upper Silesia Coal Basin, Poland' (currently in preparation). In addition, the part of the dataset (collected in the 1^{sta} and 2nd year of the MEMO^2 project) is shared with different research groups (e.g. Utrecht of DLR- Germany Aerospace Centre). The aim of data share is to contribute to the new scientific publications, where ESR3 will be a co-author.

Furthermore, the data collected over LB and Ruhr are specific and open new research question: 'methane study over closed coal mine regions'. Such quality researches question to open the possibility of writing additional scientific manuscripts. Depend on the next ESR career path, the study on the above-mentioned question might be continued through new projects.

Currently ESR3 is working on the final PhD theses draft in order to submit ready PhD in the following months. The date of PhD defense is under discussion.

6.3.1.4 Collaborations (internal / external)

During the reporting period, ESR3 collaborated with the PGI institute. The scientific mentor supported the AGH team with equipment - providing access to Picarro CRDS and GC. One measurement campaign has been organized in cooperation with PGI.

The second project supervisor is from UHEI, and the ESR continuously collaborated with this group. ESR1 and ESR3 cooperated a lot during secondments, and are finalising the manuscript as the outcome of CoMet measurements.

ESR3 also collaborated with the UU group. Under the project realisation, ESR 8 and ESR 3 cooperated in a term of methane isotopic signature estimates. The ESR performed sample collection (during March 2019, for a propose of ESR 8 project). Also, ESR8 help with δD measurements during the secondment as UU have unique instruments for such purpose.

Another important collaboration raised within the AGH University - with Faculty of Mining. With the help of this group, ESR3 learned a lot about miner's way of methane measurement and had the opportunity to compare parts of the MEMO^2 data with data obtained directly from the mining companies.

Due to corona difficulties, all collaborations were conducted on the online level.

6.3.1.5 Risks and difficulties

The ESR has experienced language issues during the daily work, as e.g the administration in Poland does not speak English, mining companies do not want to cooperate (foreign student), attending lectures recommended for PhD students is partly possible, as lectures are mostly in Polish language. Teaching duties is not possible to fully performed – not enough English classes.

During the project time, ESR3 was forced to conduct the teaching activates (all project years) and attend the classes. Both dues were partly performed in the Polish language and were not subject to payment for the ESR3 4th PhD year of study. The same issue brings a very limited time for ESR3 data collection and experimental work. In combination with the limited laboratory access, ESR3 faced a big delay with scientific manuscript and PhD theses defense.

As additional issues, ESR3 reports the administration problems. At the end of the ESR 3 project (October 2020); ESR3 got information about the potential suspension of PhD studies by AGH University. The main reason for such an action was ESR origin (non-EU citizenship) and running out of MEMO² project. However, during the official PhD submitting procedure ESR3 expects similar difficulties.

6.3.2 Deliverables

ESR 3 is involved in the following deliverables: D1.1 / D1.3 / D1.5 / D2.2 / D2.3 / D2.5.

D.1.1 – Report on harmonized method for mobile CH_4 and $^{13}CH_4$ measurements (month 18)

Approved.

D1.3 – Report and publication of the results from the campaign in Silesia (month 36)

Approved

During the project time ESR3 together with other ESR worked on data collection. The data are in the final stage of preparation.

Publication about results from the campaign in Silesia is under correction. ESR3, with cooperation to ESR1, ESR2, ESR8, ESR 10, and supervisors, made a significant effort to write a publication draft, did the first round of corrections. Submission is expected in the following months

D1.5 – Report and public on improved emission factors for different source categories from mobile measurements (month 42)

Approved

With cooperation with ESR8, ESR 3, ESR1 performed collaboration measures. The collaboration measurements rely on measurement over Ruhr region, measurement over South Germany on various sources (during secondments, small amount). Besides measurements during project time, ESR3 working together with other ESR onto CoMet data in order to create a unique data template.

As CH_4 isotopic data have been measured at UU University using CF-IRMS techniques, ESR3 measured part of samples at AGH University using CRDS techniques. The comparison and main conclusion have been described in the previous progress report as well as in the PhD theses.

All data has been uploaded on the ICOS server accordingly.

D.2.2 – Improved isotopic signatures of local and regional CH_4 emissions (month 36)

Submitted

During project time, ESR3 collected data with cooperation with ESR8 or alone. Since AGH faculty has the opportunity to measure only $\delta^{13}CH_4$ isotope, the δD measurement has been conducted at UU. All data are part of section 6.3.1.2.

D.2.3 – Publication on the use of isotopes for CH4 source attribution in urban/industrial Regions (month 36)

Submitted

Since the data set is quite large, the data are shared between different groups. ESR3 included CH_4 isotope data together with CH_4 emission data in the scientific publication (see D1.3). Furthermore, the same dataset will be part of the additional researcher publications (currently under preparation of other researcher groups)

D.2.5 – Report providing isotopic maps at grid scale from inventories and atmospheric measurements
The isotopic data collected over different part of Poland are distributed to MEMO2 community. The work is in progress.

6.3.3 Training and network activities

6.3.3.1 General training events

Event	Date (start – end)	Location (Host)	Objective / expected skills	ECTS points	Contribution	Comments
Applied geology	16.10.2017 – 20.1. 2018.	AGH University	Be familiar with complex Polish coal geology	6	attended	Courses are obligator for PhD students in Poland.
Ecological economics in global change	16.10.2017 – 20.1. 2018..	AGH University	Get a knowledge about Ecological economics in global change	3	attended	Courses are obligator for PhD students in Poland.
Physics	16.10.2017 – 20.1. 2018..	AGH University	Improve physics skills	5	attended	Courses are obligator for PhD students in Poland.
Introduction to statistics and data handling	1.3- 1.7. 2018	AGH University				Courses are obligator for PhD students in Poland
1st MEMO^2 School	05.02. – 16.02. 2018.	Schoorl (The Netherlands)	Two-week thematic school on CH_4 including courses, practical exercises, field campaigns, and data analysis.	6	poster, presentation	-
1st MEMO^2 annual meeting	21.03. – 23.03. 2018.	EMPA (Switzerland)	Meet and update each other about the project, discuss and evaluate the progress of the first year and give an outlook to the second year.		poster, presentation	-
Isotopic workshop	17. – 19.09. 2018.	Royal Holloway University of London	Learning about isotopic skills and methods	-	presentation	-
Gaussian Plume Modelling workshop	09. – 10.10. 2018.	University of Heidelberg (UHEI)	The workshop included lectures and hands-on practical exercises.	-	attended	-
Air Pollution	October 2018– January 2019	AGH University	Get a knowledge about non methane air pollution substance	-	In progress	-
2nd MEMO^2 School	18.02. – 22.02. 2019.	University of Versailles-St-Quentin en Yvelines (UVSQ)	Meet and update each other about the project, discuss and evaluate the progress of the second year and give an outlook to the third year.	??	poster, presentation	-
				/	ESR3 performed laboratory classes	Classes were performed with

Lectures	February 2019-Jun 2019	AGH	Teaching activates		for the student of 1year	cooperation to dr Orzehowska
seminar	September 2019	AGH	Presenting results in front of the scientific committee	/	ESR3 prepared overview of obtained results	The presentation was in front of AGH scientists. During the event, the scientist asked different questions related to the topic
seminar	May 2020	AGH	Presenting results in front of the scientific committee	/	ESR3 will prepare an update of results in order to present scientific progress	Once per year, each Ph.D. student has an obligation to update AGH scientific committee about results and future planes
Lectures	February 2020-Jun 2020	AGH	Teaching activates	/	ESR3 performed laboratory classes for the student of 1year	Classes will be performed with cooperation to dr Orzehowska
MEMO2 project meeting	February 2020	UHEI	Project meeting	/	ESR3 present results in front of MEMO2 colleagues, also participate in an interactive discussion	ESR support each other with ideas, comments on presentation and existed results
MEMO2 project meeting	September 2020	UU	Project meeting	/	ESR3 will prepare a presentation with overview results	The final meeting is obligatory for all MEMO2 students where we will present our data with high-level scientific conclusions
	PhD seminar	AGH	Update AGH University about the current state of PhD	2	Presentation	ESR3 has an obligation to participate in the PhD seminar
classes	Laboratory classes (Physic)	AGH	ESR3 had an obligation to preformed teaching activities due to the PhD studies	/	ESR3 organized laboratory classes and entered test to the students of the 1year at AGH	Due to corona issues, the classes have been modified to online. All teaching activates have been performed with cooperation to Dr. Aleksandra Orzechowska

6.3.3.2 Secondments

During the reporting period, two secondments have been performed: 1. At UU University, where ESR3 with cooperation with ESR8. A short description of activates is listed at the table below. Also, results are part of this progress report, and they are listed above (section 6.3.1.2). The secondment was conducted under the timeframe of GA.

2. Implementation of PGI secondments faced problems during project time. Initially, PGI was planned for 1year as part of the preparation to CoMet measurements. Unfortunately, only 2month of secondments has been conducted during project time. ESR 3 faced with problem of reorganization of PGI institute, hence secondment was limited.

Due to the ROMEO measurements, PGI secondment, we cut off onto two parts, with the goal to link them. Unfortunately, it was not possible to perform. The data and results obtained during two months of secondments are listed at table below and described at section 6.3.1.2.

Secondment	Date (start – end, planned (when))	Location	Host	Description of work / deviations	Scientific / training (skills) objective	Results and future plans
UHEI	13.1. – 10.02. 2019.	Heidelberg Germany	UHEI	Laboratory teste (calibration), field transect (AirCore, post mining emission)	New system: AirCore system Cross Calibration Ethane	ESR will be able to perform ethane calibration in Poland
UU	15 May- 1Jun 2019	UU	UU	A prior to secondments, ESR3 organized the sampling collection over USCB. In total, 36 bags of samples have been collected and sent to UU. During the secondments, ESR8 shows basing princes of CF-IRMS working	Usage of CF-IRMS technique extended knowledge on methane isotopic compositions	The results are described in section 1.2.2 Additionally, results will be part of the ESR3 Ph.D. thesis, as well as part of ESR8 publication. Possible publication on methane isotopic compositions from the coal industry. The possibility of publication is still under discussion
PGI	1Agust- 1 October 2019	Warszawa	PGI	The main goal of secondments was to examine ethane and other hydrocarbons in samples collected from coal waste dumps. The main technique was GC, Picarro CRDS, LGR. Prior to laboratory work, we collected bag samples over USCB and LSCB. In addition, waste dump measurements we performed one small measurement over the closed oil field. The same technique, as describes above, has been used. Beside we investigate possible influence of ethane to methane measurements using CRDS	Coal waste dumps are investigated places. Worldwide. As it is described above, the cola waste dump could be active, abandoned, or burning. During this project, we tried to use our equipment (CRDS, LGR, CF-IRMS, GC, static chambers) in order to extend our knowledge. Second part – abandoned gas well measures have been performed in order to obtain knowledge of methane from abandoned gas filed(by taking soil samples)	All results have been described in previous sections 1.2.1 and 1.2.3. The part of cola waste dump investigation on ethane and other hydrocarbons were unsuccessful. Unfortunately, inside samples, we did not find the number of hydrocarbons suitable for GC analysis. Other results will be part of PhD thesis, and they are described through this progress report.

6.3.3.3 Conferences

Conference name	Date (start – end, planned (when))	Location	Presentation (oral / poster)	Title of presentation/poster	Authors (main author + co-authors)	Public available (yes / no) / web link
Industrial Methane Measurement Conference – PEFTEC 2017	29. – 30.11. 2017.	Antwerp (Belgium)	Poster	Isotopic composition of methane from exhausts of mines and gas fields in Southern Poland" -	J. Necki, M. Zimnoch, A. Jasek, L. Chmura, M. Galkowski, W. Wolkowicz, P. Lakomiec, P. Korben, M. Stanisavljevic	no
EGU 2018	07. – 12.04. 2018.	Vienna (Austria)	poster	Bottom – up methane budget estimation from the sources over Upper Silesian Coal Basin		no
				Mobile in-situ measurements of methane mixing ratio over Upper	**M. Stanisavljević** , J. Necki , H. Maazallahi, M. Menoud, K. Vinkovic, P.	

NCGG 2019	May 2019	Amsterdam, Netherlands	poster	Silesian Coal Basin	Korbeń, M. Schmidt, Ł. Chmura, J. Bartyzel, M. Gałkowski, W.Wołkowicz, G. Florczyk, S. Defratyka	No
EGU	May 2020	online	Picco	Methane emission from coal mines ventilation shafts in Upper Silesia, Poland	M.Stanisavljevic, J.Necki, P.Korben,H.Maazallahi, S. Defratyka, K. Vinkovic, C. Veen, L. Chmura, D. Zieba, M. Schmidt, W. Wolkowicz, T. Rockmann, J Wietzel, J. Swolkien	https://meetingorganizer.copernicus.org/EGU2020/EGU2020-15165.html

6.3.3.4 Measurement / sampling campaigns

Campaign	Date (start – end, planned (when))	Location	Host	Description of work	Scientific objective	Samples (nature / number)	Results and future plans
Belhatow coal mine	19.10.2017	Poland		Checking methane emission from non-point source			
1st MEMO2 School	9th – 11th February 2018	North Holland (The Netherlands)	ECN	A van measurements across the North Holland province.	Design, plan and run field campaigns to measure atmospheric CH_4 at site scale.	-	-
Lublin coal Basin	28.8.2018	Poland Silesia					
Post mining emission	13.9.2018 1.10.2018	Poland Silesia		Checking methane emission from closed mines			
Samplings from mine shafts		Poland Silesia		Collecting of bag samples directly from mines shafts		10	
USCB	28.2.-29.2	USCB	AGH	Regularly checking of selected coal ventilation shafts. Additionally, three abandoned coal mine spots were investigated	The main goal of these measurements is to supplement measurement conduct during 2018.	We measured methane fluxes using CRDS. In total four sources were revisited, and three sources were new	The results are part of this report (described above). Also, the results will be part of ESR3 PhD thesis
Krakow and USCB	March 2019	Krakow city and USCB	AGH	In proposing to collect bag samples to ESR8, we performed measurement over Krakow city and USCB	ESR8 conducts long term measurements at AGH. (Continuously measurement of ambient air using CF-IRMS). As a supplement to this measurement ESR3 help with bag samples collection in order to distinguish various sources	Bag samples, collected on a method described in section 1.2. ESR8 measured them using CF-IRMS	As the sampling was part of the ESR8 project, she is responsible for carrying on the main part of the research.
USCB	March 2019	USCB	AGH	Abandoned mines measurements. We investigate old miners' work, to cheek potential methane leaking. Coal waste dumps, and closed ventilation	While reading IPCC reports, ESR3 found out that abandoned coal mine and waste dump measurement of greenhouse gases are missed. In order to collect data over USCB, ESR3	The first stage conducted during March were: to find spots of interest and performed the first measurements. We use Picarro CRDS or static	The results allowed us to estimate the first methane fluxes from selected sites. Results have been described above at section 1.2 and

				shafts were investigated.	performed a few small measures	chambers with LGR, temperature measurements, pressure measurements	also will be part of ESR3 PhD thesis
USCB	April 2019	USCB	AGH	Waste dump measurements. During April, we just continue our measures, which we start during March. The same aim can be applied.	The scientific objectives are following previous descriptions.	The measurements were conducted using LGR, static chambers. During this period first bag samples were collected and measured for methane isotopic compositions	The results are the following description from previous measurement (conducted during March 2019). Also, all results will be part of ESR3 PhD theses
USCB	May 2019	USCB	AGH	Bag sampling measurements. A prior to CF-IRMS measurement we collected bag samples necessary for isotopic investigation	Methane isotopes signature from USCB investigated. Work follows the previous bag collection conduct by ESR8 (during CoMet)	In 2 days of sampling, we collected 36 bags in total. The amount was enough for □D and □$^{13}CH_4$ measurements	The results are Extended knowledge about methane isotopic signature from USCB region. The data has been described above in section and also will be part of the ESR3 PhD thesis. The part of data will be the publication of ESR8
USCB	July 2019	USCB	AGH	Regularly checking of selected coal ventilation shafts	During the reporting period, some of the ventilation shafts were revisited or we visited new (where we do not have information). During July we visited Budryk coal mine, mine with the highest methane emission over USCB region (1kgCH4/s in total, E-PRTR 2019)	Typically CRDS measurement was conducted. Picarro CRDS installed into the van together with GPS system.	The data are part of this progress report. Also, data will be part of ESR3 PhD thesis and scientific publication about USCB
Lublin region	August 2019	Lublin region	PGI	Abandoned oil field measurements. Soil samples collections. Water samples collections	After closing the oil fracking filed, the amount of methane can be trapped into the ground. Since after oil farcing, the filed is free for people usage, the possible dangerous consequences might occur	Soil gas samples collected inside bags. 1l water samples collected into transparent bottles	The results are part of this report and also used for PGI project propose
Lublin region	August 2019	Bogdanka coal mine	AGH	Methane isotopic measurements. During August 2019, we collected bag samples of methane plume near Bogdanka coal mine.	Bogdanka coal mine is an underground hard coal mine. The mine is in the Lublin coal region. Since now, there is no proof about methane released to the atmosphere. However, around ventilation shafts, roads are 'hard to access'; hence we just collected bag samples form	Since roads are really hard to access, ESR3 collected only bag samples. The samples have been sent to UU, for □D analysis as well	The result has been part of this report. Also, the results will be part of the ESR3 PhD thesis. The key founding about isotopes from this coal mines is: results indicate biogenic origin – untypical for

					methane isotopic characterizations		underground coal mines
USCB	September 2019	USCB	AGH	Coal waste dump measurements. During this measurement, ESR3 revisited some sources and also vested one new. The measurements are the same as we performed during March	The objectives and goals are the same as described for March measurements	The sampling strategy is the same as for March measurements: ESR3 used LGR, static chambers, CRDS and collected bags	The results are part of this report and will be part of ESR3 PhD thesis
LSCB	September	Lower Silesia	AGH, PGI	Coal waste dump measurements. Abandoned coal mine measurements	LSCB is a hard coal region of Poland where miner activates stopped approximately 20 years ago. In order to check methane emissions, we performed measurements over the region in cooperation with PGI	We performed experiments on 2 different approaches: driving around sources (we did not found out methane enrichment above background) or collected samples over waste dumps. Key founding: some of the waste dumps are burning. In total, we collected ten bag samples	Outcomes from these measurements are the isotopic characterization of the LSCB region. The data are described above (this progress report) and will be part of ESR3 PhD thesis
USCB	13-16 October	USCB	AGH	Coal waste dump measurements. During this measurement, ESR3 revisited some sources and also vested one new. The measurements are the same as we performed during March	The objectives and goals are the same as described for March measurements	The sampling strategy is the same as for March measurements: ESR3 used LGR, static chambers, CRDS and collected bags	The results are part of this report and will be part of ESR3 PhD thesis

6.3.4 Dissemination activities

ESR3 is co-author of the following publication:

Luther, A., Kleinschek, R., Scheidweiler, L., **Defratyka, S., Stanisavljevic, M.**, Forstmaier, A., Dandocsi, A., Wolff, S., Dubravica, D., Wildmann, N., Kostinek, J., Jöckel, P., Nickl, A.-L., Klausner, T., Hase, F., Frey, M., Chen, J., Dietrich, F., **Nęcki, J., Swolkień, J.**, Fix, A., Roiger, A., and Butz, A.: Quantifying CH_4 emissions from hard coal mines using mobile sun-viewing Fourier transform spectrometry, Atmos. Meas. Tech., 12, 5217–5230, https://doi.org/10.5194/amt-12-5217-2019, 2019. https://www.atmos-meas-tech.net/12/5217/2019/

6.4 ESR4 - Assessing CH_4 emission from wetlands and other sources by use of mobile measurements

ESR4

Assessing CH_4 emission from wetlands and other sources by use of mobile measurements

ESR	Patryk Lakomiec, patryk.lakomiec@nateko.lu.se
Supervisor	Janne Rinne, janne.rinne@nateko.lu.se
	Jutta Holst, jutta.holst@nateko.lu.se
Co-supervisor	Dominik Brunner, dominik.brunner@empa.ch
Non-academic mentor	Johan Fagerqvist, johan.fagerqvist@avfallsverige.se
Official start-end date	01.08.2017 – 31.07.2021

6.4.1 Scientific progress

6.4.1.1 Project introduction and objectives

The main focus of the ESR4 project was the quantification of CH_4 emissions in Sweden with focus on spatial variations within wetlands and lakes by use of mobile measurements from a small research aircraft, tower measurements and chambers system. Airborne measurements will allow for direct assessment of vertical CH_4 exchange between surface and atmosphere as well as the vertical structure of CH_4 concentration within the atmospheric boundary layer at landscape scale. Footprint based analyses of eddy-covariance measurements allow the analyses of variations in methane emissions on ecosystem scale. ICOS Sweden data from Abisko-Stordalen has been used to quantify the annual budget from Swedish wetlands with permafrost gradient thaw. Additionally, controlling factors of methane emission have been investigated. Emissions evaluated from chambers systems enable to catch differences of methane fluxes at very small scale. As the isotopic signatures of CH_4 varies depending on the origin, air samples for isotopic analyses in the lab and in situ field measurements will be taken at specific points of interest to be able to identify sources of measured CH_4. Isotopic signals from these sources will be assessed by comparison with the analysis of samples from these source categories collected by WP1 students in trans-European mobile measurement campaigns.

The project work included:

- Analysis of methane flux data from ICOS station Abisko-Stordalen
- Field measurement to specify ^{13}C signatures of methane emission from wetlands,
- Analysis of existing airborne flux data,
- Airborne flux measurement campaign to gather additional data over wetland

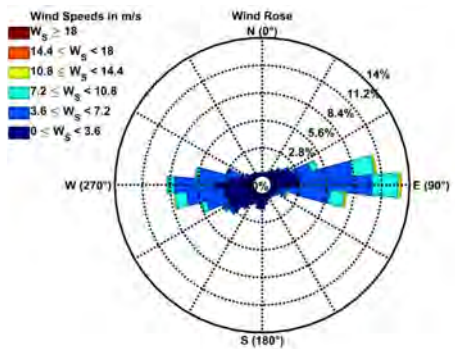

Fig. 6.4.1: Distribution of wind speed and direction for Abisko-Stordalen for the years 2014-2016, based on 30 min averages.

6.4.1.2 Project results

6.4.1.2.1. Third year

6.4.1.2.1.1 Analysis of methane fluxes from ICOS Sweden – Abisko-Stordalen

Abisko-Stordalen mire, with its bimodal wind direction (Fig. 6.4.1) offers a unique opportunity to conduct flux studies where one flux system is used to monitor two ecosystem types. While previous studies at Abisko-Stordalen have compared open water surfaces to thawed fen (Jackowicz-Korczynski et al. 2010, Jammet et al., 2015, 2017), no comparison of field-scale CH_4 emission from permafrost peat plateau and thaw fen have been conducted.

In this study, we compare field-scale CH_4 emissions from the two main source areas of the greenhouse gas fluxes at the Abisko-Stordalen sub-arctic mire (footprint). The source area to the west of the measuring mast is dominated by a permafrost plateau (palsa), while the footprint area to the east is dominated by thaw fen, forming together a thaw gradient. Aims of this study are to estimate the annual methane emission from this thaw gradient exposed to the same environmental factors, and to analyse differences in controlling factors for these two different source areas.

Analysis has been done on data from years 2014 - 2016. Eddy covariance measurements of CH_4 fluxes were done with use of a close-path fast greenhouse gas analyser (LGR Fast Greenhouse Gas Analyzer model GGA-24EP) combined with a sonic anemometer (SA-Metek uSonic-3 CLASS A). Methane fluxes have been calculated with EddyPro 6.2.1 (LICOR Environment, USA). Fluxes have been partioned by wind direction and undergone a thorough quality control. Daily averages of fluxes (Fig. 6.4.2) have been calculated, when at least 10 of 48 half hourly data points per day were available. This averaging based on the limited numbers of data points was possible because no diurnal cycle has been observed.

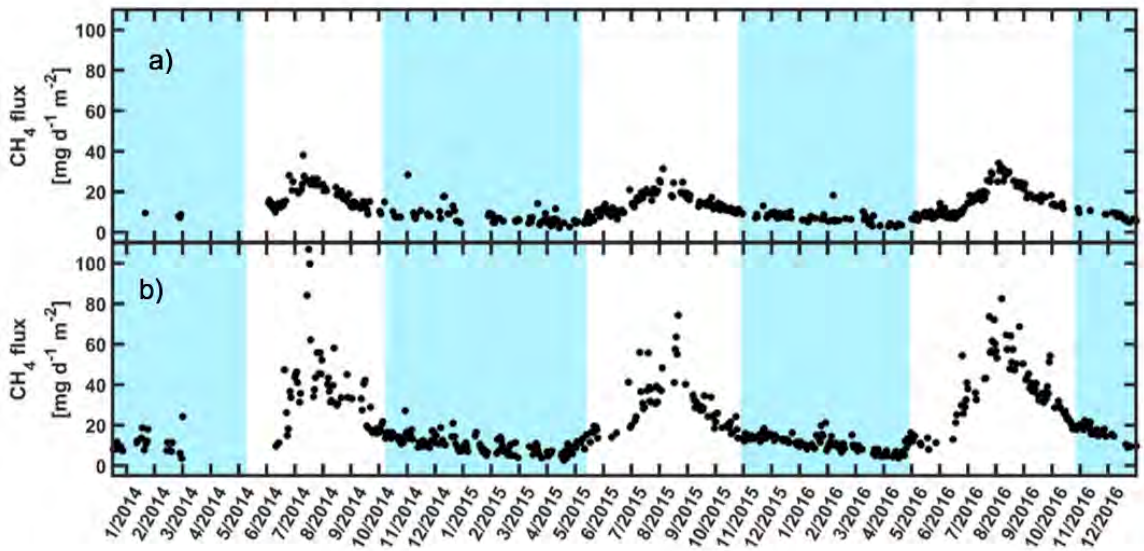

Fig. 6.4.2: Time series for daily averaged CH_4 fluxes for a) the western area of footprint (Palsa), and b) the eastern area of footprint (fen). Shaded blue area is frozen period.

Due to data partioning with respect to wind direction and other factors (e.g. sensor fail or inadequate conditions for using the eddy covariance method for flux calculations) gaps in the time series have to be filled before the calculation annual budgets of CH_4. Four different gap filling methods have been tested, for both wind directions: (1) look-up tables (Jena-gap filling tool, Wutzler et al 2018), (2) 5- day moving mean (Jammet et al 2017), (3) artificial neural network (Jammet et al 2015,2017) and (4) general linear model (Rinne et al 2018). Annual budgets calculated with different gap filling methods have been presented on Fig. 6.4.3.

Three years of eddy covariance measurements showed differences in methane emission from two wetlands ecosystem with different permafrost status. Both ecosystems had similar seasonal cycles, with maximum appearing in the same time but with various emission. Seasonal cycles were characterized with gentle rise up and drop down of methane fluxes, without any burst events close to melt-down and freeze-in periods. Frozen intervals had positive fluxes and emission from those times has significant input to annual budget.

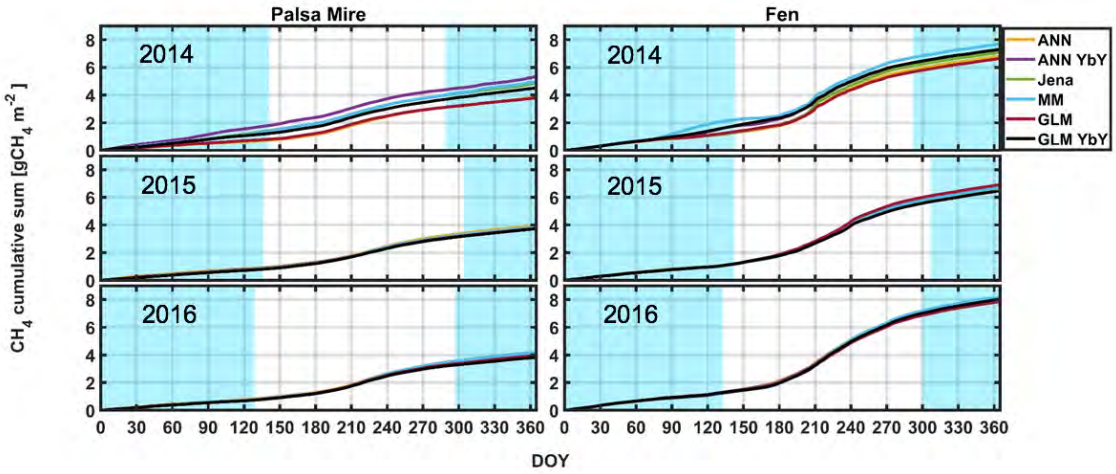

Fig. 6.4.3: Cumulative sum of CH_4 fluxes at Abisko-Stordalen for the source areas palsa mire and fen during the years 2014 - 2016.

Controlling factors for CH_4 emission were examinated using a general linear model. The most important factor was peat temperature, already reported by many different studies (Christensen et al. 2003, Jackowicz-Korczyński et al. 2010, Bansal et al. 2016, Pugh et al. 2017, Rinne et al. 2018). Exponential relationship was found like in the previous studies. Water table level was checked for fen as controlling factor. No clear relationship has been found. Soil water content (SWC) was checked for palsa mire during the unfrozen period. Negative exponential relationship was found between SWC and methane emissions. Gross primary production was checked as controlling factor for both source areas. Preliminary results showed high correlation with CH_4 fluxes. Temperature normalization of CH_4 fluxes decreased this correlation. This drop down of correlation shows that gross primary production was correlated with temperature information hidden in the CH_4 fluxes.

Palsa mire and fen had differences in controlling factors. Like in different studies about wetlands, peat temperature is the most important factor, but the highest correlation with CH_4 fluxes appear on different depth. Relationship between CH_4 emission and water table level were checked but did not show any significant correlation. This information supports the theory that in fully saturated wetland ecosystems variation in water table level in a certain range are not important for the CH_4 emissions.

6.4.1.2.1.2 ^{13}C signature of methane from an ombrotrophic hemiboreal peatland

We have measured the ^{13}C signature of CH_4 from an ombrotrophic hemiboreal peatland in South-Western Sweden in microtopographic and field scales. The measurements in microtopographic scale were carried out by static chambers and those in field scale by nocturnal boundary-layer accumulation method. In both cases ^{13}C-CH_4 was measured by online CRDS analyser. Isotopic signature was obtained using the Keeling formula. In addition to isotopic signatures, we have also measured CH_4 emission both at field scale using the eddy covariance method, and at microtopographic scale using automated chambers.

ESR4's task has been to calculate CH_4 fluxes and their isotopic composition from the automatic chamber system. Samples were taken from automatic chamber system for result comparison between CRDS analyser and IRMS (isotopic ratio mass spectrometer) systems.

6.4.1.2.1.3 Gen composition on wetlands with different permafrost status

In this study, we have investigated three peatlands under different stages of permafrost thaw. Kattejokk, where the permafrost has completely disappeared, Storflaket, where the permafrost is degrading slowly and Kursflaket, currently undergoing rapid permafrost loss. With this motivation in mind we investigated

how the microbial, vegetation and physical dynamics of these peatland ecosystem respond the permafrost degradation.

We will again combine data from in-situ measurements (metagenomics, stable isotope, flux measurements, plus additional environmental parameters) to investigate the relationship between below ground microbial activity and above ground CH_4 emissions.

ESR4 part of this project is the isotopic analysis of CH_4 and preliminary results are presented on Fig. 6.4.4. Isotopic composition of carbon from CH_4 is different for different wetlands and it can vary inside one wetland. Different isotopic composition is linked with different pathway of CH_4 production and probably with different microbial communities. CH_4 on wetlands with different permafrost status could be produced in different reactions.

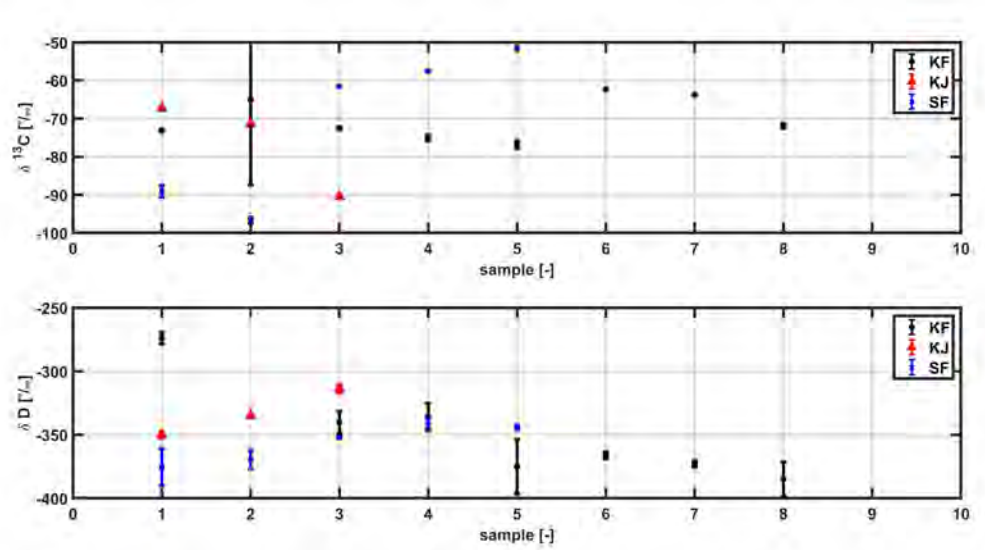

Fig. 6.4.4: Preliminary results of isotopic composition of CH_4 for three wetlands, obtained as the zero-intercept of a Keeling plot.

6.4.1.2.1.4 Landfill campaign

The temporal and spatial variability of surface emissions from landfills results in challenging conditions for accurate measurement of the emissions. Not only are the emissions a result of internal parameters of the landfill, such as waste type, depth, leachate, landfill shape and cover, but also the atmospheric conditions have a significant impact on the emissions rates variation.

This study, commissioned by Technical University of Denmark (DTU), Lund University, Sweco Environment, FORCE Technology, and ReSource, has been designed to provide detailed methane emission data using tracer gas dispersion technique, UAV-based plume measurements, ground-based plume measurements and surface flux chambers at three landfill sites (one closed and two operational) located in Sweden. The measurement campaigns were carried out during the last week in October 2019 and the first week in November 2019. Results including the comparative analysis of the different methods will be presented in a report to be published by Avfall Sverige.

The overall aim is to recommend a method for standardizing measurements of fugitive methane emissions from landfills in Sweden. Hence, the aim of this study is to compare different measurement techniques in terms of CH_4 flux quantification, duration of measurement, uncertainties, suitability for different kinds of landfills and practicability.

6.4.1.2.1.5 ROMEO campaign

ROMEO was a large measurement campaign to investigate CH_4 emissions from oil and gas production in Romania. The campaign was initiated by the European H2020 project MEMO² and was funded through the Climate and Clean Air Coalition (CCAC) international methane science studies, administered through the United Nations Environment Program.

During the campaign 14 research teams from The Netherlands, UK, Denmark, Germany, Romania, US, Switzerland, Poland, and Sweden were in the field to measure CH_4 and other atmospheric parameters using instruments placed on two aircraft from Scientific Aviation and INCAS, but also on drones, and in cars.

ESR4 was responsible for ground-based measurements. On his duty was a screening area for leak detection and if it was possible to quantify them using OTM 33A (Other Test Method 33A).

6.4.1.2.2 Fourth year

The fourth year was dedicated to further evaluation of the data described above and to prepare the respective manuscripts.

6.4.1.2.2.1 Analysis of methane fluxes from ICOS Sweden – Abisko-Stordalen

The Artic area is exposed to faster temperature changes than other places on Earth. Constantly increasing temperature will lead to melting permafrost and changing in the CH_4 emissions from wetlands. One of the places exposed to those changes is Abisko-Stordalen Mire in northern Sweden, where climate and vegetation studies are going from the 1970s.

In our studies, we analyzed field-scale CH_4 emissions measured by an eddy covariance method in this place for three years (2014-2016). The site is a subarctic mire mosaic of palsas, thaw-fens, and open water bodies. A bidirectional wind pattern (Fig. 6.4.5) prevalent at the site provides an ideal opportunity to measure mire patches with different permafrost statues with one flux measurement system.

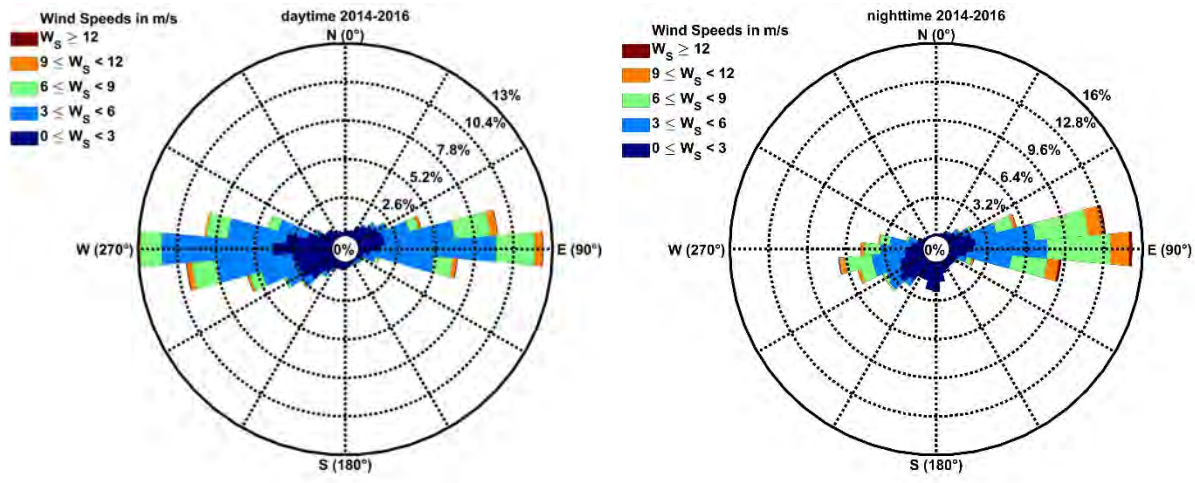

Fig. 6.4.5: Distribution of wind speed and direction for Abisko-Stordalen for the years 2014-2016, based on 30 min averages for the daytime (left panel) and nighttime (right panel).

Additionally, those patches were exposed to the same environmental conditions, so unique responses for them were checked. The flux footprint is dominated by an elevated palsa plateau in easterly winds. While the flux footprint from the westerly winds is almost equally distributed between palsa plateau and thawing sectors (Fig. 6.4.6).

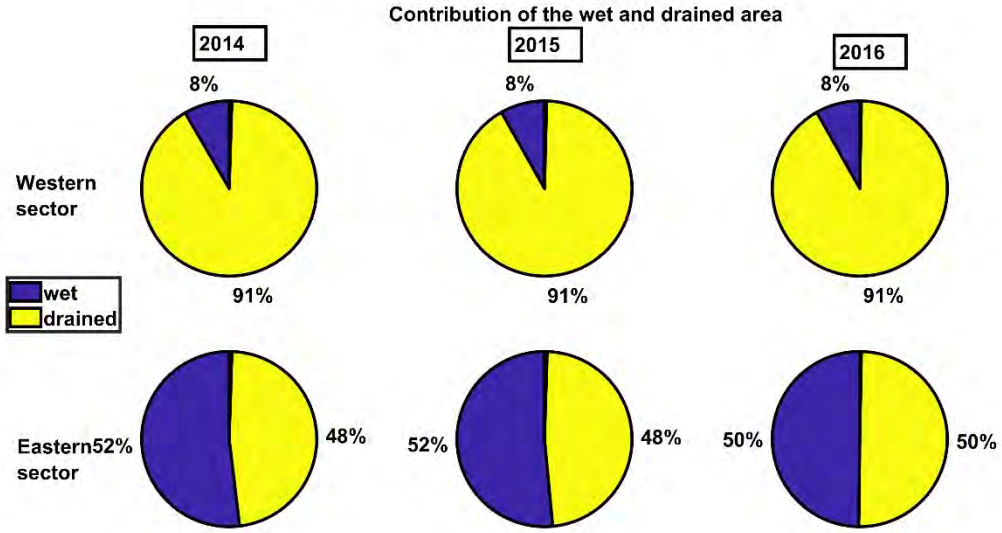

Fig. 6.4.6: Contribution of the wet and drined area for eastern and western sector.

The CH_4 fluxes followed a similar annual cycle over the three years, with a gentle rise during spring and decrease during autumn, with not emission burst at either end (Fig. 6.4.7). Peak season emission from the mire with two permafrost statuses was significantly different, palsa mire emitting 24 mg CH_4 m^{-2} d^{-1} and thawing wet sector 56 mg CH_4 m^{-2} d^{-1}.

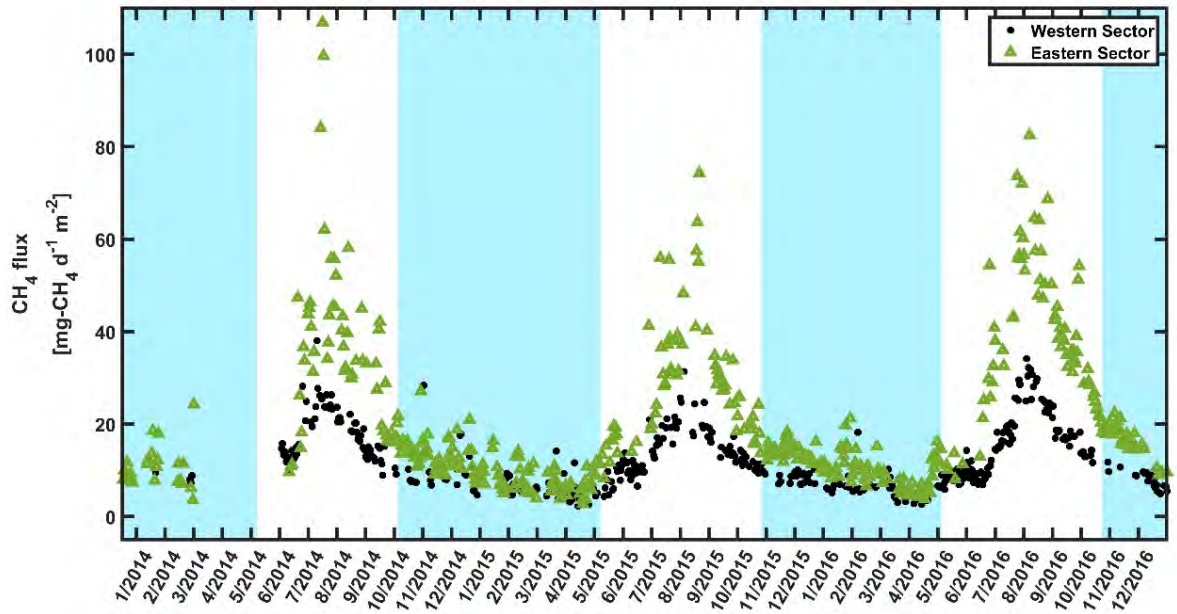

Fig. 6.4.7: Time series for non-gap-filled CH_4 daily averaged fluxes for the western sector and the eastern sector, where the shaded light blue area is frozen period.

Factors controlling the CH_4 emission were analyzed by the generalized linear models. The main driver for the CH_4 fluxes was peat temperature for both types of mires. Soil water content emerged as an explanatory variable for the three years for western sectors and the year 2016 in the eastern sector. Water table level showed a significant correlation with CH_4 emission for the year 2016 as well. Gross primary production did not show a significant correlation with CH_4 emission.

Annual emissions were estimated with the use of four different gap-filing methods. It was important to check four methods, independents between each other's because the available data-set was smaller due to portioning. The different methods were tested generally resulted in very similar annual emissions. The mean annual emission based on all models was (4.2 ± 0.4) g CH_4 m^{-2} a^{-1} for palsa mire and (7.3 ± 0.7) g CH_4 m^{-2} a^{-1} for the thawing wet sector (Fig. 6.4.8). Winter fluxes were relatively high contributing 27 - 45 % to the annual emissions.

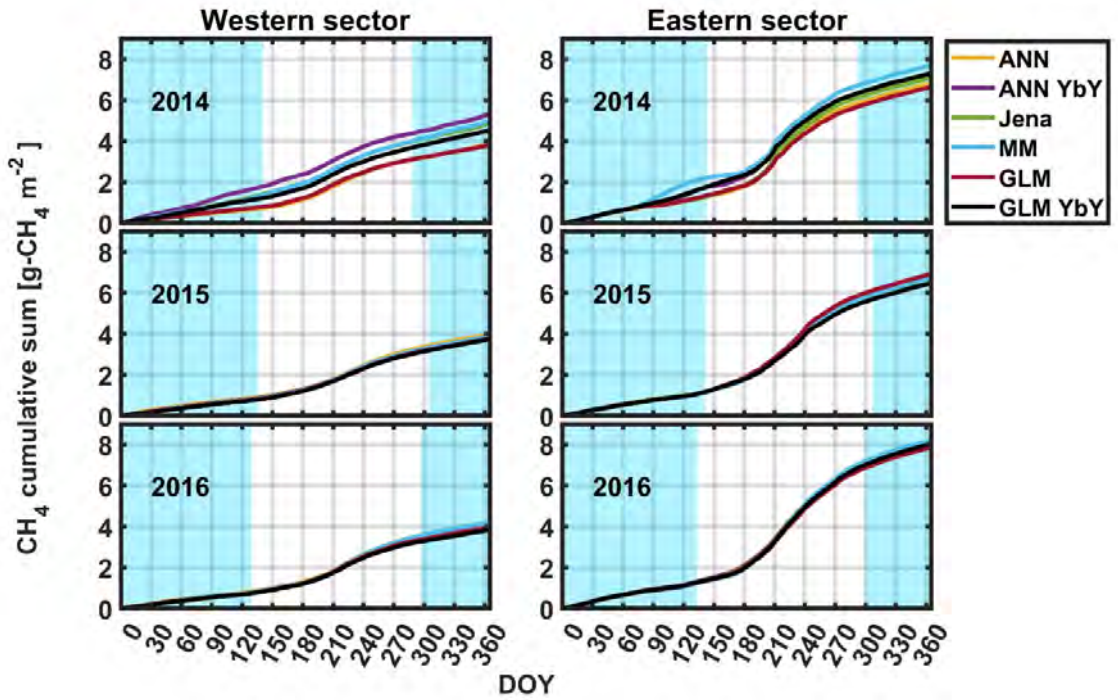

Fig. 6.4.8: The cumulative sum of CH_4 fluxes for the years 2014-2016 for western and eastern sectors calculated with the different gap-filling methods. ANN - the artificial neural network for all years, ANN YbY - artificial neural network each year separately, Jena - Jena online gap-filling tool, MM - moving mean with 5-day moving window, GLM- the general linear model for all years, GLM YbY - the general linear model for each year separately. The shaded light blue area is frozen period.

6.4.1.2.2.2 ^{13}C signature of CH_4 from an ombrotrophic hemiboreal peatland

We have measured the ^{13}C signature of CH_4 from an ombrotrophic hemiboreal peatland in South-Western Sweden at microtopographic and field scale. The measurements in microtopographic scale were carried out by static chambers and those at field scale by nocturnal boundary-layer accumulation method. In both cases ^{13}C-CH_4 was measured using an online cavity-ring-down-spectroscopy (CRDS) analyzer Picarro G2201-i (Picarro, Inc., Santa Clara, CA). Isotopic signature was obtained using the Keeling plot approach (Keeling, 1958). In addition to isotopic signatures, we have also measured CH_4 emission both at field scale using the eddy covariance method, and at microtopographic scale using automated chambers (Fig. 6.4.9).

ESR4's task has been to calculate CH_4 fluxes and their isotopic composition from the automatic chamber system. Bag samples were taken from the automatic chamber system for analyses in the lab using IRMS (isotopic ratio mass spectrometer) systems. Differences in the results of the two methods, online (CRDS) and offline (IRMS), were quantified.

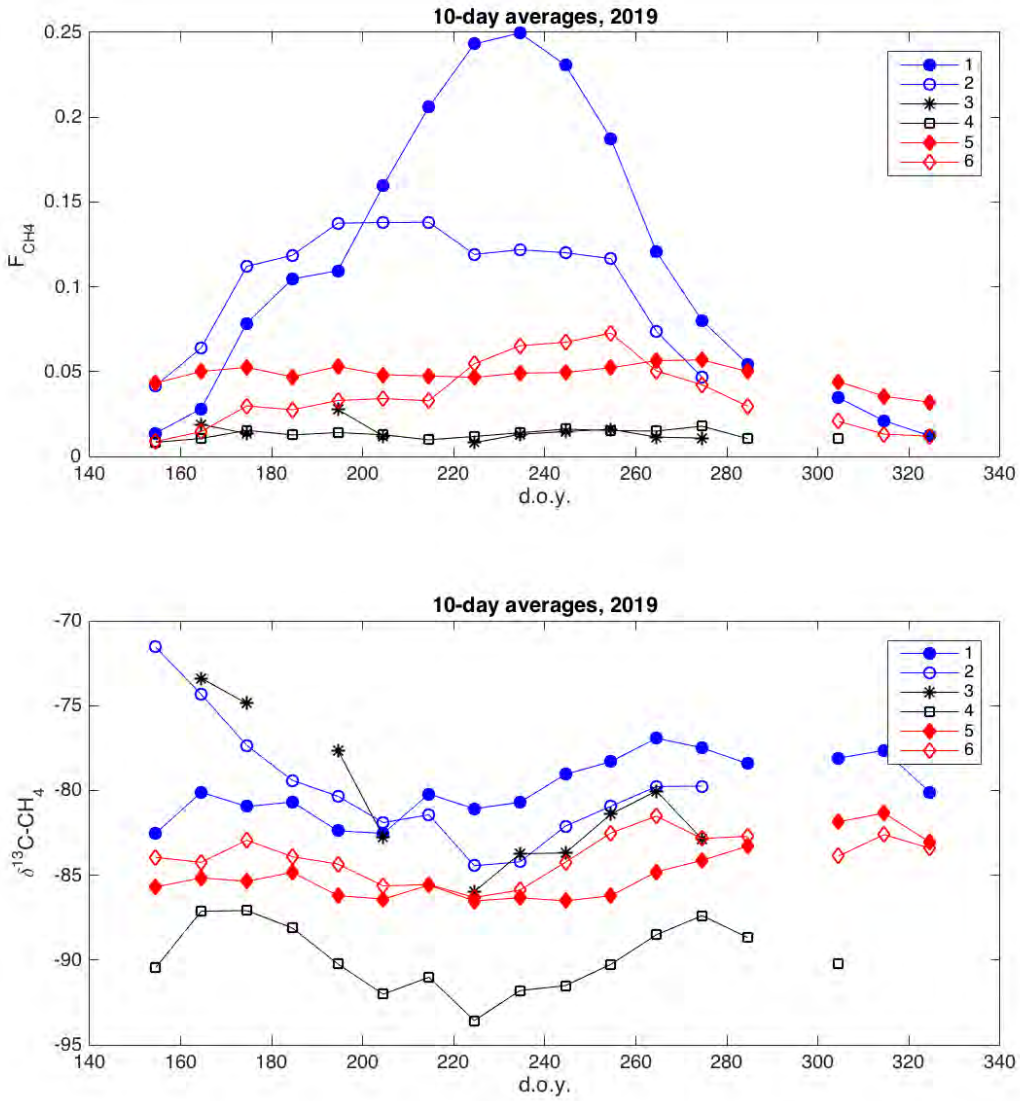

Fig. 6.4.9: 10-day average of CH_4 fluxes and isotopic composition for six chambers at Mycklemossen (Skogaryd catchment, https://www.fieldsites.se/sv-SE/forskningsstationer/skogaryd-32286094) between June and December 2019.

6.4.1.2.2.3 Gen composition on wetlands with different permafrost status

The isotopic composition of carbon from CH_4 is different for different wetlands and it can vary inside one wetland. Different isotopic composition is linked with different pathway of CH_4 production and probably with different microbial communities We investigated how the microbial, vegetation and physical dynamics of these peatland ecosystem respond the permafrost degradation. To obtain this we have investigated three peatlands under different stages of permafrost thaw. Kattejokk, where the permafrost has completely disappeared, Storflaket, where the permafrost is degrading slowly and Kursflaket, currently undergoing rapid permafrost loss.

Data from different in-situ measurement approaches (metagenomics, stable isotope, flux measurements, plus additional environmental parameters) will be combined to investigate the relationship between below ground microbial activity and above ground CH_4 emissions.

ESR4 part of this project is the isotopic analysis of CH_4; preliminary results are presented on Fig. 6.4.10. The isotopic composition of carbon from CH_4 is different for different wetlands and it can vary inside one wetland. Different isotopic composition is linked with different pathway of methane production and probably with different microbial communities. CH_4 on wetlands with different permafrost status could be produced in different reactions. Based on Whiticar et al. 1999, Chanton et al. 2005 and Milkov and Etiope 2018 CH_4 pathway production are:

- Hydrogenotrophic methanogens (HM), range $\delta^{13}C$ = −110 ‰ to −60 ‰ and δD = −250 ‰ to −170 ‰
- Acetoclastic methanogens (AM), range $\delta^{13}C$ = −60 ‰ to −50 ‰ and δD = −400 ‰ to −250 ‰
- Fermentation process (FM), range $\delta^{13}C$ = −90 ‰ to −50 ‰ and δD = −450 ‰ to −250 ‰

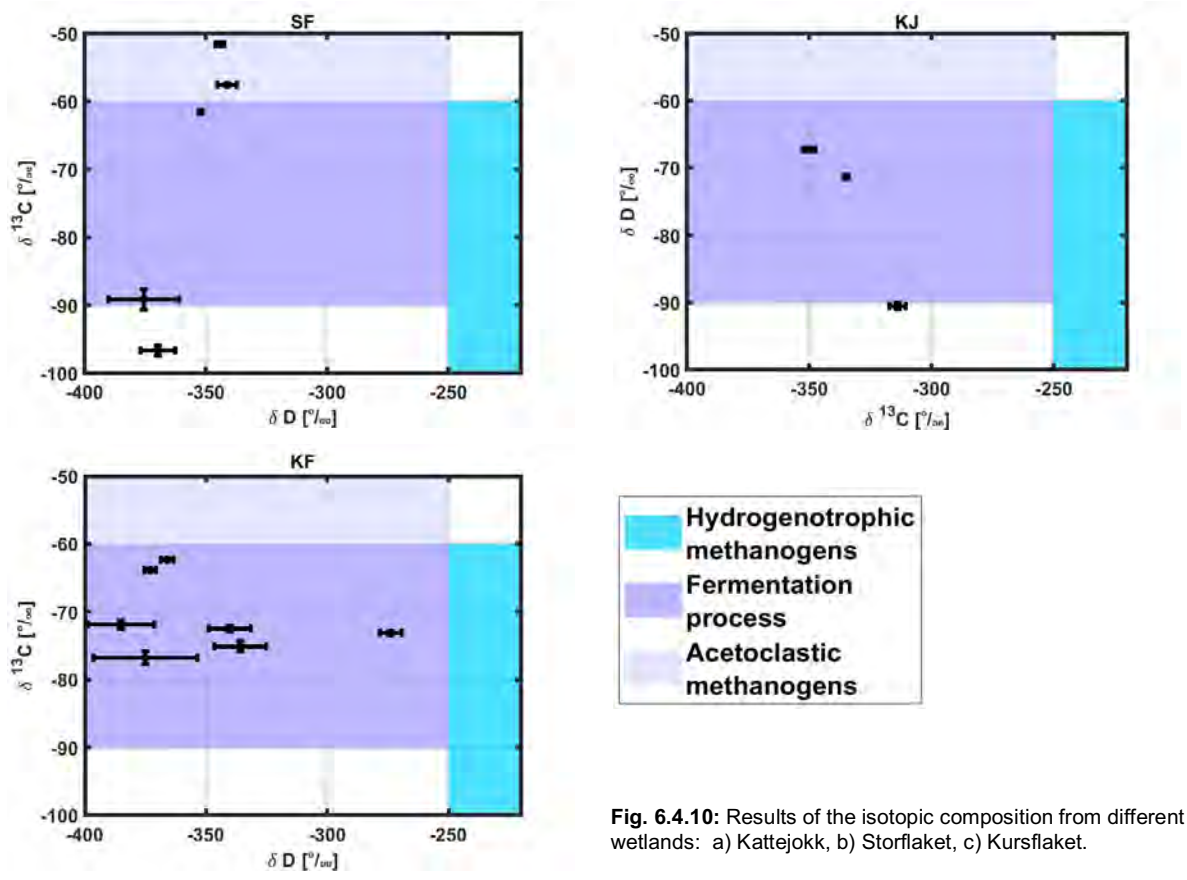

Fig. 6.4.10: Results of the isotopic composition from different wetlands: a) Kattejokk, b) Storflaket, c) Kursflaket.

6.4.1.3 Future plans and expected results

A first paper co-authored by ESR4 has been published https://doi.org/10.1098/rstb.2019.0517. A manuscript about the analysis of methane fluxes from ICOS Sweden – Abisko-Stordalen is ready to submit. A manuscript about the analysis ^{13}C signature of methane from an ombrotrophic hemiboreal peatland is in preparation. ESR4 will be a co-author of this paper. The manuscript about the analysis of gen composition on wetlands with different permafrost status is slightly delayed due to the CoVID-19 virus, but in progress. The defence of the thesis is planned for the late spring 2022. It will be later than initially planned, due to delays caused by the restrictions related to the covid-19 pandemic and parental leave of the ESR in summer 2021.

6.4.1.4 Collaborations (internal / external)

The collaboration with the Avfall Sverige has started. Few joint measurement campaigns have been done. Additional partners during campaigns with Avfall Sverige were Technical University of Denmark (DTU), Sweco Environment (https://www.sweco.se/en/our-offer/water-and-environment/), FORCE Technology (https://forcetechnology.com/sv/om-force-technology), and ReSource (www.resource.is). Within this collaboration, the ESR were focused to develop a better method to monitor leaks on landfills. ESR gained work experience with non-academic partners.

Collaboration with Joel White and Didac Pascual, from Department of Physical Geography and Ecosystem Science, Lund University, about the gen composition on wetlands with different permafrost status was continued. Results of the collaboration will be published jointly.

6.4.1.5 Risks and difficulties

Due to the restrictions connected to the covid-19 pandemic, lab access as well as fast communication channels have been limited. This has slowed progress to a certain extent.

6.4.2 Deliverables

D1.2 - Report & publication on seasonal variation of CH_4 emissions from wetland and lakes in Sweden (month 30)

The report has been submitted as report, extracted from the manuscript. The publication will be submitted soon.

D1.4 - Improved emission factors for different source categories from mobile measurements (month 42)

The ongoing measurements in collaboration with Avfall Sverige / SWECO on landfills will provide additional data material to receive improved emission factors. ESR4 also contributed to the ROMEO campaign, of which data are used for D1.4.

D1.5 - Report on harmonized method for mobile CH_4 and $^{13}CH_4$ (month 18)

Approved

D2.2 - Improved isotopic source signatures of local and regional CH_4 emissions – month 36

ESR collected bag samples from wetland in western Sweden for isotopic analyses at RHUL and UU. This data was compared with results from isotopic CRDS analyzer.

ESR collected bag samples from wetlands in north Sweden for isotopic analyses. Data contained air from wetlands with different permafrost status. Isotopic composition will be linked with genes composition for better understanding methanogenesis.

D3.4 - Top-down estimates of EU-scale CH_4 emissions – Month 42

Problems with the methane analyser to be used in the aircraft led to delays and finally fewer flight campaigns than planned. The measurements made concentrated on the estimation of emission factors on the local scales and were not optimised for using the data for top-down modelling.

6.4.3 Training and network activities

6.4.3.1 General training events

Event	Date (start – end)	Location (Host)	Objective / expected skills	ECTS points	Contribution	Comments
Biosphere-Atmosphere interaction	28.08.2017-27.10.2017	Lund University and Hyltemossa ICOS station, Sweden	Extend knowledge about biosphere-atmosphere interactions	15	participating	
Greenhouse gases GHG - biogeochemistry and measurement techniques in ecosystems and landscapes	3.09.2017-9.09.2017	Örtagaarden and Skogaryd, Sweden	Extend knowledge about biogeochemistry and measurement techniques in ecosystems scale	5	participating	

PhD Introduction Course	9.01.2018-19.01.2018	Lund University, Sweden	Gain knowledge about phd studies at Lund University	3	participating	
MEMO² Summer School	5.02.2018-16.02.2018	Schoorl, Nederlands	Extend knowledge about methane mobile measurements	6	participating	
Advanced Analysis of Atmosphere-Surface Interactions and Feedbacks	5.03.2018-16.03.2018	Hyytiälä, Finland	Extend knowledge about atmosphere-surface interactions	5	participating	
MEMO² Workshop on Methane Isotopes	17.09.2018-19.09.2018	RHUL, United Kingdom	Extend knowledge about methane isotopes measurements techniques		participating	
MEMO² Workshop on Gaussian plum modelling	9.09.2018-10.09.2018	UHEI, Germany	Gain knowledge about Gaussian plum modelling		participating	
Genral Physical Geography	09.01.2019-20.03.2019	Lund University, Sweden	Get knowledge about different spheres of physical geography.	4	participating	Mandatory course on the department
Problem analysis	23.04.2019	Lund University, Sweden	Literature review on PhD topic and presentation of findings	8	Participating	Mandatory course on the department
Drone workshop	2nd May	Lund University School of Aviation (LUSA)	Basic knowledge about drone law in Sweden	0	participating	
Half-time seminar	15.10.2020	Lund University	Summary of the current progress of PhD	1.5	ESR presented results from his PhD studies	mandatory course at Lund University

6.4.3.2 Secondments

Secondment	Date (start – end, planned (when))	Location	Host	Description of work / deviations	Scientific / training (skills) objective	Results and future plans
RHUL	19.11.2018-30.11.2018	RHUL, Egham	RHUL	Analysing isotopes composition air from wetlands	Mass spectrometer training	
Afvall Sverige	Single preparation days	Lund	Avfall Sverige	Single preparation days for measurements	Practical skills	
Afvall Sverige	28.10.2019-15.11.2019	Gotland, Helsingborg, Hässleholm	Avfall Sverige	Landfill campaign where different method of methane quantification were tested	Test of different quantification methods	Report has been written and will be published by Avfall Sverige
ROMEO campaing	30.09.2019-13.10.2019	Romania	INCAS	Quantification methane emission from oil and gas sector	Learned and applied other test method 33A (OTM 33A)	

6.4.3.3 Conferences

Conference name	Date (start – end, planned (when))	Location	Presentation (oral / poster)	Title of presentation	Authors (main author + co-authors)	Public available (yes / no) / web link
3rd ICOS Science conference	10-13 Sep 2018	Prague, CZ	poster	Using the PicarroG2301-m for airborne eddy covariance measurements of GHG fluxes	Lakomiec, P., Peltola, O., Holst, J., Rinne, J.	no
MEMO annual meeting	22-23 Mar 2018	Zurich, CH	oral + poster	Airborne methane fluxes from wetlands	Lakomiec, P.	
2nd Nordic ICOS Symposium	24.10.2019-25.10.2019	Gothenburg, Sweden	Poster	Methane emissions from a palsa-mire underlayed by sporadic permafrost under rapid degradation	Patryk Łakomiec, Jutta Holst, Janne Rinne	http://www.icos-sweden.se/symp/Abstract_Lakomiec.pdf

EGU 2020	4.05-8.05 2020	virtual	Poster	**Methane emissions from a palsa-mire underlayed by sporadic permafrost under rapid degradation**	**Patryk Łakomiec, Jutta Holst, Janne Rinne**	no
ICOS Science Conference 2020	15.09-17.09 2020	virtual	Poster	**Isotopic composition of methane from Swedish wetlands**	**Patryk Łakomiec, Semra Bakkaloglu, Julianne Fernandez, Rebecca Fisher, Jutta Holst, Mathias Lanoiselle, David Lowry, Malika Menoud, Thomas Röckmann, Lena Ström, Joel White, Janne Rinne**	no

6.4.3.4 Measurement / sampling campaigns

Campaign	Date (start – end, planned (when))	Location	Host	Description of work	Scientific objective	Samples (nature / number)	Results and future plans
Bag sampling	12.10.2018	Skogaryd Mycklemosse, wetlands, 58°21'52.85"N, 12°10'16.71"E.		Samples were taken from automatic chambers system on wetlands	Spatial distribution of isotopic composition	Wetlands/ around 120 from 6 chambers	
Bag sampling	11.08.2019-17.08.2019	Abisko	Abisko Scientific Research Station	Samples were taken from chambers	Estimate isotopic composition of methane for wetlands with different permafrost status	Around 50 samples from three different wetlands	Plan for publication where isotopic composition of methane will be connected with microbial activity
Aircraft campaign	27.06.2019-30.06.2019	Norunda	Lund University	Test flight around wetlands near Norunda ICOS Sweden station	Equipment test		
Aircraft campaign	19.07.2019-21.07.2019	Ljusdal	Lund University	Flight over burned forest	Estimation of methane fluxes form burned forest and wetlands area		
Aircraft campaign	23.08.2019-25.08.2019 13.09.2019-15.09.2019	Norunda	Lund University	Florarna wetland, several flights	Estimation of methane fluxes from wetland, obtained by several flights over the same area		
Afvall Sverige	28.10.2019-15.11.2019	Gotland, Helsingborg, Hässleholm	Avfall Sverige	Landfill campaign where different method of methane quantification were tested	Test of different quantification methods		Report has been written and will be published by Avfall Sverige
ROMEO campaign	30.09.2019-13.10.2019	Romania	INCAS	Quantification methane emission from oil and gas sector	Learned and applied other test method 33A (OTM 33A)		

6.4.4 Dissemination activities

Rinne, J., Tuovinen, J.-P., Klemedtsson, L., Aurela, M., Holst, J., Lohila, A., Weslien, P., Vestin, P.,Łakomiec, P., Peichl, M., Tuittila, E.-S., Heiskanen, L., Laurila, T., Li, X., Alekseychik, P., Mammarella, I., Ström, L., Crill, P., and Nilsson, M.B.: Effect of the 2018 European drought on methane and carbon dioxide exchange of northern mire ecosystems, Phil. Trans. R. Soc. B, 375: 20190517, http://dx.doi.org/10.1098/rstb.2019.0517, 2020

6.5 ESR5 - Characterizing CH_4 emissions in urban environments (Paris)

ESR5

Characterizing CH_4 emissions in urban environments (Paris)

ESR	Sara Defratyka sara.defratyka@gmail.com
Supervisor	Philippe Bousquet philippe.bousquet@lsce.ipsl.fr
	Camille Yver-Kwok Camille.yver@ilsce.ipsl.fr
	Jean-Daniel Paris jean-daniel.paris@lsce.ipsl.fr
Co-supervisor	David Lowry D.Lowry@rhul.ac.uk
Non-academic mentor	Rod Robinson Rod.Robinson@npl.co.uk
Official start-end date	01.10.2017 – 30.09.2020

6.5.1 Scientific progress

6.5.1.1 Project introduction and objectives

On a global scale, CH_4 emissions are relatively well estimated. However, characterization of local scale CH_4 sources is still not clear and require further analysis (Dlugokencky et al., 2011). According to the IPCC report, the anthropogenic CH_4 emission is partly associated with urban areas (IPCC, 2006). Urban and sub-urban areas contribute from 30 % to 40 % anthropogenic greenhouse gas emission and concentrate more than 50 % of the global population. However, those areas cover 2 % of the Earth's surface. According to the predictions, urban population will double by 2050 (Satterthwaite, 2008; Duren and Miller, 2012). Moreover, an urban ecosystem is a complex case, where many different sources coexist: oil and natural gas networks, heating / cooling system, landfills and waste treatment, wastewater and road transport (Gioli et al., 2012; Townsend-Small et al., 2012; Zazzeri et al., 2017). In case of different cities in the United States like Los Angeles, Boston and Washington, the dominant CH_4 sources are leakages of fossil fuels (Townsend-Small et al.,2012; Jackson et al., 2014; McKain et al., 2015). The similar situation has been observed in Florence, in Italy (Gioli et al., 2012). However, in the case of London, landfills and the waste treatment sector are the major sources of CH_4 (Lowry et al., 2001; Fisher at al., 2006). The significant but not well-determined contribution to global emissions of urban CH_4 requires detailed measurement.

One of the significant urban CH_4 sources can be the Ile-de-France (IDF) region (number of inhabitants:12,14 million, Paris contributing to 18 % population). Due to this, CH_4 emissions in IDF region need independent estimations, source by source, from atmospheric measurements. The main purpose of my PhD study is to characterize the spatio – temporal variations of mole fraction and isotopic signature of CH_4 in Île-de-France region and to infer from that, CH_4 emissions from site to city scale. The main approach to achieve this goal is the design, realization and analysis of field campaigns, taking benefit of laser-based continuous and mobile instruments. The chosen strategy leads to atmospheric CH_4 characterization followed by emission estimations using tracer dispersion method and modeling tools. The study is conducted at city and site scale, as small-scale measurements play a key role to explain sectoral uncertainties and can help improve CH_4 regional budget. This objective is a necessary and important step to improve estimates of CH_4 sources in the IDF region. As a consequence, these objectives aim at contributing to the improvement of emission inventories, to gap reduction between top-down and bottom-up studies and to give insights to design more efficient mitigation actions.

6.5.1.2 Project results

6.5.1.2.1 Third year

6.5.1.2.1.1 Paris city measurements

The end of the last reporting period was focused on the mobile surveys in Paris. Due to that, at the beginning of this year, I analysed the collected data and prepared a publication about the CH_4 sources in Paris. Results, presented in the article draft, were obtained from 17 surveys conducted between 07.09.2018 and 07.03.2019 in the city of Paris, including its west and south suburbs (mostly Boulogne-Billancourt and Issy-les-Moulineaux), which have been extensively covered. Overall, we collected over 720 km of measurements (includes some overlap represented by the colour code in Fig. 6.5.1). Measurements analysed during this study were made using cavity ring-down spectrometers (CRDS) manufactured by Picarro (Santa Clara, California). During 16 of the surveys, a CRDS type G2201-i measuring $^{12}CO_2$, $^{13}CO_2$, $^{12}CH_4$, $^{13}CH_4$ and H_2O was used. Moreover, during 4 surveys, a Los Gatos Research (LGR) analyser (San Jose, California) model MGGA was also used. All measurements are time-corrected to account for the delay induced by the travel time from the inlet to the analysers. Delays vary between 15 s and 30 s. The inlet was situated on the roof of the car. During measurement periods, a 3-point concentration and isotopic composition calibration was done. Additionally, a known gas was measured for 20 minutes before and after 11 surveys to check analyser stability and the influence of switching on/off the analyser for the obtained CH_4 and $\delta^{13}CH_4$ values. In both cases, the analyser was stable and no detectable influence of switching on/off instrument was observed. Also, the LGR MGGA analyser was tested and a calibration factor was applied to this instrument.

To obtain higher precision for in-situ measurements of the isotopic composition, the G2201-i analyser was also included in a so-called AirCore setup (Rella et al. 2015). This 50 m sampling tube used in "replay mode" allows for better time resolution. Replay mode is equivalent to increasing the sampling frequency by a factor of 3. When this is applied to a detected CH_4 peak, accuracy of isotopic signature is improved by sqrt (3). We measured isotopic signatures using AirCores only for 'significant' CH_4 enhancements. We define a CH_4 enhancement as significant if its maximum mole fraction is greater than 500 ppb above local background. Local background values were calculated as the mean CH_4 mole fraction measured immediately before and after each peak. In total, 28 peaks from 17 different sites were significant, mainly in downtown Paris (Trocadero) and the west and south suburbs (Boulogne-Billancourt and Issy-les-Moulineaux). Isotopic signatures were calculated using the Miller-Tans approach without C_2H_6 correction. The Miller-Tans plot requires to subtract the background value, both for CH_4 and $\delta^{13}CH_4$ (Miller and Tans 2003). Here, we only report the isotopic $\delta^{13}CH_4$ signature of peaks where the Miller-Tans approach yields a 1-sigma uncertainty less than 10 ‰ and a correlation coefficient $R^2 > 0.85$. 12 of the 28 AirCores samples fulfilled the criteria, with 2 AirCores measuring the same peak.

Initial surveys were used to identify areas of the greatest elevated CH_4 concentrations, designated as 'hot spots'. Two hot spot areas were identified: 1) on the west-south part of inner Paris (Fig. 6.5.1 area A), and 2) hot spot area B on west-south suburbs (Fig. 6.5.1 area B). Five days of repeated surveys focused on both hot spots A and B (respectively three and two days). In total, hot spots A and B represent respectively 16 % (118 km) and 25 % (183 km) of the total surveys' mileage.

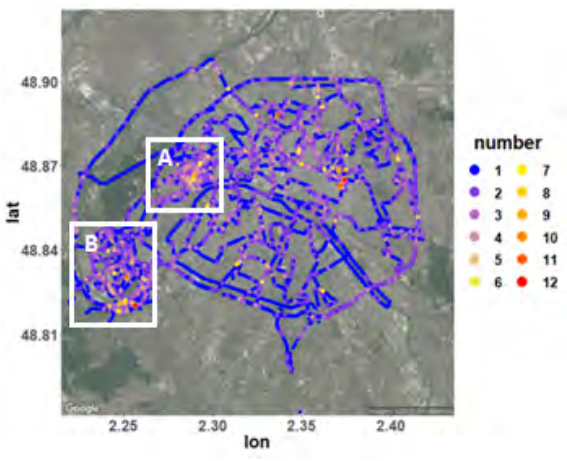

Fig. 6.5.1: Number of a revisit of the particular area during Paris surveys; A - hot spot area A, B – hot spot area B

We collected additional measurements by foot using an LGR MGGA portable analyser to find the exact position of the sources causing peak concentrations. This protocol was implemented twice in the hot spot area A, once in hot spot area B, and once in the central and north-east part of Paris.

In order to exploit also smaller peaks and to separate them from slow background changes, we define a typical baseline variation. Daily background values were calculated for each day separately using the 1st percentile of the CH_4 mole fraction observed during one measurement day in the Paris area. The CH_4 baseline was calculated for each day separately after removing significant CH_4 peaks (higher than 500 ppb). Over the 17 days, daily backgrounds varied between 1926 ppb and 2058 ppb. The maximum variability of the CH_4 baseline, calculated as a CH_4 baseline standard deviation, was equal to 50 ppb. As a consequence, we define a peak detection threshold as 3 times the maximum CH_4 baseline variation (i.e. 150 ppb). Hereafter, CH_4 is expressed as an enhancement above daily background. Depending on their maximum CH_4 enhancement, peaks are defined as small, medium, and large (ranging respectively between150-500 ppb, 500-1000 ppb, and higher than 1000 ppb).

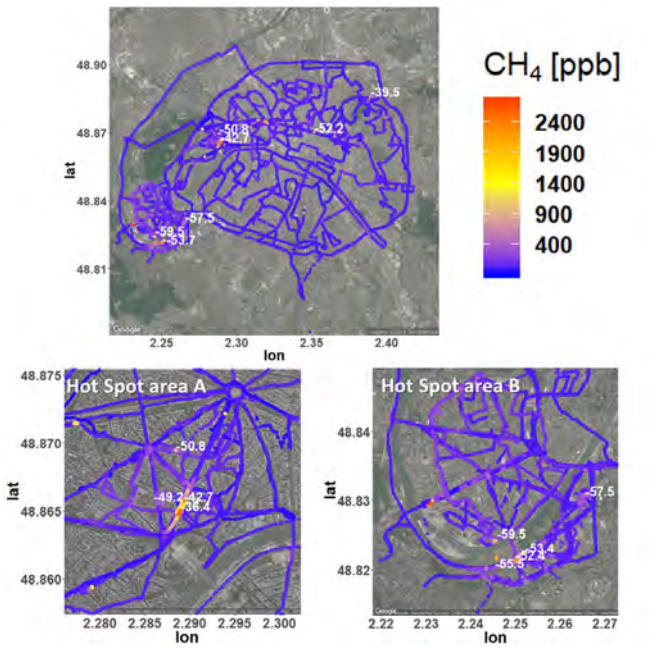

Fig. 6.5.2: Paris enhancement above background with $\delta^{13}CH_4$ signature determined for 11 peaks selected by criteria: 1-sigma uncertainty less than 10 ‰ and a correlation coefficient $R^2 > 0.85$ from Miller-Tans plot. Top – whole measured Paris area. To make a map of the whole area of interest more legible, part of peaks in hot spots area A and B are treated as one peak with one averaged value shown on the map, bottom – zoom on hot spot area A and B.

Fig. 6.5.2 is a map of CH_4 mixing ratio enhancement measured in Paris also reporting the isotopic composition of medium and large peaks. It includes zooms on hot spots A (Trocadero area) and B (west-south suburbs).

Overall, observed CH_4 enhancements above background are within a relatively low range (0–2700 ppb). 95 % of measurements correspond to enhancements lower than 133 ppb. In total, 91 peaks were detected. Typically, crossing the peaks took 4-8 seconds. 69 % of these peaks are small, whereas 16 % and 14 % of the detected peaks are classified as medium and large peaks, respectively. 30 % of observed peaks come from hot spots area A and 27 % from hot spots area B, although these areas represent only 16 % (area A) and 25 % (area B) of the total surveyed area. The two largest enhancements were observed in hot spot area A and B and reached 2500 ppb and 2700 ppb, respectively.

The characterization of isotopic composition allows distinguishing the type of source for medium and large peaks, and walking observations allow for more precise locations of emission sources. In hot spot area B, 4 medium and 5 large peaks have been found. All isotopic signatures associated with these peaks fall within the range of -59.5 ‰ - -52.4 ‰. This suggests a microbial origin of the emissions. As the area has no landfills, these peaks are likely assigned to the sewage emissions. Walking measurements were used during one measurement day (27.02.2019) in hot spot area B using the portable LGR MGGA. That day only medium and large peaks were observed and no small size peaks occurred. Walking measurements observed CH_4 enhancement from sewage ground covers, but no CH_4 from natural gas ground covers. These LGR MGGA measurements confirmed results obtained using the approach based on isotopic signatures. During this day small peaks did not occur, therefore it is not possible to determine the source of the small peaks in hot spot area B.

A contrasting situation is found for hot spot A (7 medium and 5 large peaks). The range of isotopic signatures observed for medium and large peaks in hot spot area A is between -50.8 ‰ and -36 ‰. These values are distinctly higher than those for hot spot B. The isotopic signature range of these peaks are compatible with thermogenic sources. The most likely release of thermogenic CH_4 in the area would be natural gas leaks and nonindustrial combustion associated with heating systems. In the latter category, individual sources are expected to be localized to boiler room ventilation exhaust of buildings.

During two days of walking measurements in hot spot area A, one CH_4 peak was observed from a sewage ground cover. However, several CH_4 peaks were observed from the ground covers of natural gas networks and from ventilation grates of buildings' boiler rooms, which is consistent with measured isotopic signatures. Walking measurements also provided a validation of our isotopic approach together with an identification of the precise location of the emission. Peaks identified by the combination of the determination of the isotopic signature and CH_4 enhancement observed by walking measurements are presented in Fig. 6.5.3. Walking measurements with the LGR MGGA observed emissions from grids of buildings' boiler rooms ventilation. These are not reported, to our knowledge and in other studies focused on urban environment. The highest concentration measured directly from the boiler room ventilation was equal to 40 ppm. This ventilation system is separated from general building ventilation. Also, walking measurements combined with determined isotopic signature showed a contribution of sewage sector to urban CH_4 emission, what was neglected (not found) in some previous studies (von Fischer et al. 2017; Lamb et al. 2016; Phillips et al. 2013) or only briefly mentioned (Townsend-Small et al. 2012; Zazzeri et al. 2017).

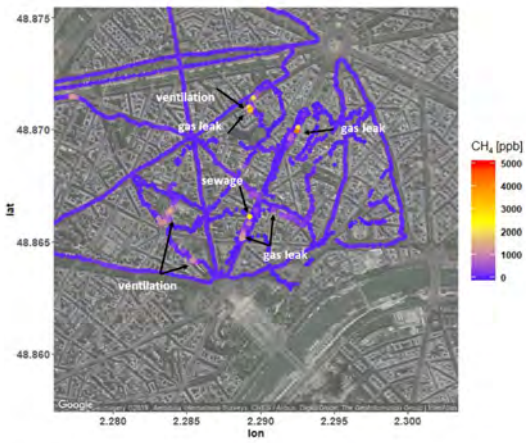

Fig. 6.5.3: Type of sources detected in hot spot area A, Enhancement above daily background in the range of 0-5000 ppb, source type defined using isotopic composition and detected CH_4 emission directly from ground covers (both sewage and natural gas network) and buildings boiler room ventilation (on figure names "ventilation").

An isolated small CH_4 (238 ppb above local background) peak detected in the central part of Paris city, has $\delta^{13}CH_4$ isotopic signature of (-52.2 ± 8.1) ‰. This is compatible with a leak in the natural gas network, but a possible mix with other sources cannot be ruled out due to the large uncertainty. This should be verified with additional observations. Another isolated peak observed in the north-east part of Paris has an isotopic signature of (39.5 ± 5.0) ‰. Compatible with thermogenic sources. It is interpreted to come from a natural gas leak or from the ventilation of a buildings' boiler rooms.

6.5.1.2.1.2 Synthesis

Table 6.5.1 shows the distribution of peaks by the type of origin. Gas leaks and boiler room ventilation accounted for 68 % of the medium and large peaks. The sewage sector contributed to 32 % of the medium and large peaks.

Table 6.5.1: Number of detected peaks classified by source type and size.

source	small	medium	large
Gas leaks and house ventilation	60	11	8
sewage	1	4	5
landfill	1	0	0
cement factory	1	0	0

Small peaks of unidentified origin are assumed to be related to emissions from gas leaks and building's boiler room ventilation, while peaks from landfill and cement factory are categorized by visual inspection of the surrounding environment when detected (Table 6.5.1). On average, 87% of detected peaks in Paris city and its west-south suburbs come from the gas leaks or the building's boiler room ventilation,

with contributions of this sector, equalling 93 % and 76 %, in area A and B, respectively. Although, in hot spots of area B, all peaks classified as medium or big peaks come from the sewage sector, reducing gas contribution below Paris average. Overall, the gas leaks and boiler room ventilation give together 0.11 peaks per km, calculated as a total number of peaks from this sector (79 peaks) divided by a number of driven kilometres in the area of interest (720 km). 76 % of peaks classified as gas leaks and boiler room ventilation are classified as small peaks (150-500 ppb), whereas 50 % of the sewage peaks (less numerous) are classified as large peaks.

Here, we do not report mobile sources from road transport. A fraction of the bus fleet in Paris uses natural gas and biogas as fuel, which can cause additional emission of CH_4. According to the AIRPARIF inventory (AIRPARIF 2005), road transport contributed to 8 % of CH_4 emission in Paris for the year 2000. In our study, we determine CH_4 emission coming from road transport if the detected peak does not occur during the second passing of the same street in a short time. Using this approach, only one peak is associated with road transport emissions and has been excluded from the analysis.

Moreover, outside of the Paris city, surveys were focused on 3 natural gas compressor stations, located in Ile-de-France region: Beynes (BNS) (48.844155°N, 1.873789°E), Fontenay-Mauvoisin (FM) (48.95059°N, 1.638410°E) and Limoges-Fourches (LF) (48.639016°N, 2.659842°E). 10 surveys in those areas of interest were conducted (BNS – 3, FM – 4, LF – 3). During first surveys, focused on recognition of infrastructure and road access, CRDS G2203 was used. During subsequent measurements, G2201-i was used. Additional surveys were also focused on two landfills: Butte-Bellot (BB) (48.641306°N, 2.74011°E) and Gonesse (GNS) (49.025175°N, 2.408130°E). 6 surveys in those areas of interest were conducted (BB – 4, GNS - 2), using CRDS G2201-i. As in the case of the Paris measurements results are corrected and calibrated according to the laboratory tests.

Both for compressor station and landfill surveys, during mobile measurements with G2201-i, when a CH_4 peak was observed and its maximum was at least 500 ppb higher than values of daily background (which is calculated as a quantile 0.01), measurement of isotopic composition δC^{13} was made with tool so-called AirCore (Rella et al. 2015). Depending on meteorological conditions and observed CH_4 enhancement, for each site from 2 to 7 AirCores were taken. For some surveys, bag samples were also taken. These samples will be analysed further in Utrecht University to determine isotopic composition (both δC^{13} and δD) using IRMS analyser.

Moreover, using additional measured C_2H_6 value during part of the surveys, ratio C_2H_6/CH_4 was calculated for gas compressor station measurements. C_2H_6 is the second component of the natural gas, however it is not observed in biogenic CH_4 sources (Lopez et al. 2017). Due to that, using C_2H_6/ CH_4 ratio is an additional method to distinguish CH_4 sources. As C_2H_6 absorption line interferes with ^{13}C absorption line, CRDS G2201-i has possibility to measure C_2H_6 (Rella et al. 2015). However, as it is an additional control value, it is necessary to make laboratory tests to calibrate and correct values obtained by G2201-i (Assan et al. 2017; Rella et al. 2015). To obtain information about C_2H_6/CH_4 ratio, the car was stopped in the middle of the peak and stationary measurement was conducted for 35 minutes. To obtain wind data, Gill Windmaster anemometer, which is a precise 3D-axis sonic anemometer with U, V, W vector and sonic temperature outputs, was used. Data are saved with 20 Hz rata in range 0-50 m/s and 0-359°. During further analysis, meteorological data will be used as an input data to the model to calculate emission rate for observed sites.

This reporting period was focused on collecting data from CH_4 sources (gas compressor stations and landfills, see also Fig. 6.5.22). In the next step, transects and wind data collected on all observed station will be used with model to estimate emission rate from every site. In this case, the Polyphemus model (http://cerea.enpc.fr/polyphemus/), which is a Gaussian Eulerian model, will be used. Additionally, in case of one of the sites, another model will be also used. The second model, called GRAL, is based on

Lagrangian approach. Obtained results will allow to compare models which based on different approach (Eulerian and Lagrangian).

6.5.1.2.1.3 Beynes (BNS)

Natural gas compressor station with underground storage facilities is located in Beynes town, west of Paris (48.844155 °N, 1.873789 °E). This site is surrounded by forest on the north, west and south with access to the small road on the east. This site is bigger than the two others.

During measurements on 27.05.2019, 4 peaks were detected, where one is bigger than others (Fig. 6.5.4). That survey was focused on isotopes measurements (both AirCore and bag samples) and C_2H_6 measurements (48.842765 °N, 1.87688 °E - location where the biggest peak that day was observed).

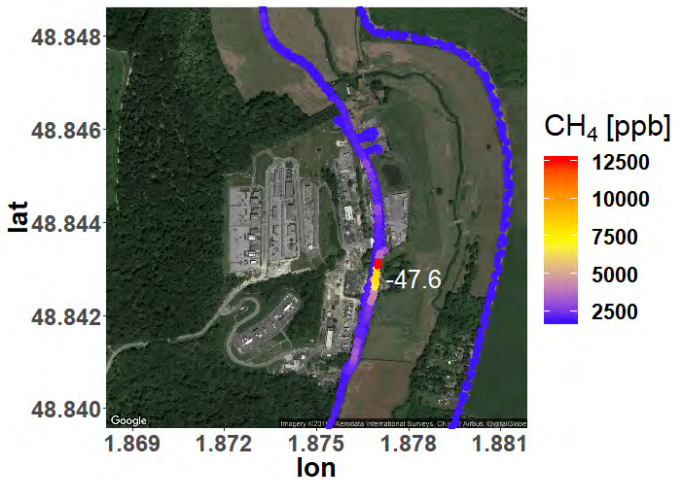

Fig. 6.5.4: Survey 27.05.2019 on BNS gas station

Measurement made on 15.07.2019 let suspect that this bigger peak is a combination of the two sources, localized close to each other (first source – 48.843106°N, 1.877027°E; second source – 48.842745°N, 1.876771°E).

That day only one peak was observed, where detected concentration was smaller than previously. Survey made on 15.07.2019 was focused on isotopes measurements (only AirCore), C_2H_6 measurements (3 location) and transects to use with model to estimate emission (Fig. 6.5.5). General information about measurements carried out so far, are presented in Table 6.5.2.

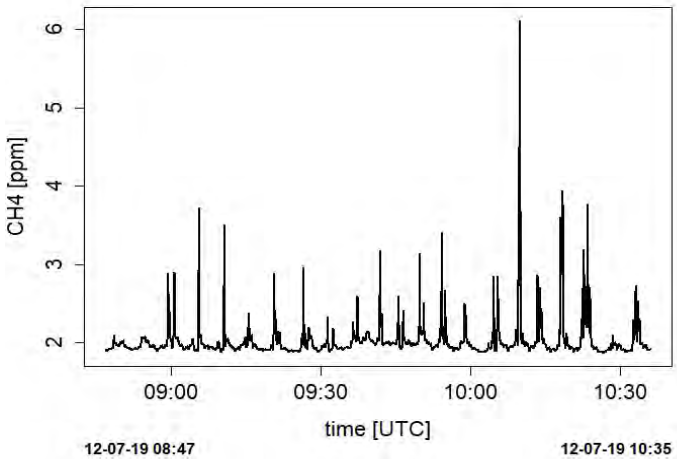

Fig. 6.5.5: Survey 28.05.2019 on FM gas station made transects

Table 6.5.2: Surveys on BNS

Date	AirCore	Bag samples	transects	comment
19.01.2019	No data	No data	No data	First attempt – to localize site
27.05.2019	-47.6 ± 1.6	collected	No data	C_2H_6 measurements
12.07.2019	collected	No data	20	C_2H_6 measurements

6.5.1.2.1.4 Fontenay-Mauvoisin (FM)

Fig. 6.5.6: Gas compressor station plan

This natural gas compressor station is situated close to Fontenay Mauvoisin (north-west of Paris) with possibly two sources of CH_4 inside the station. Around the site there is farmland and on the south-west side a small forest. Gas compressor station position is: 48.95059N, 1.638410E. Possible localization of CH_4 source: first source: 48.953563°N, 1.640052°E – main source peaks observed during every survey and second source: 48.953971°N, 1.638634°E, small peak, observed depending of the meteorological condition (not during all surveys). However, this peak can also come from area 2 showed on the plan of the site (Fig. 6.5.6). Surveys conducted on this site are presented in Table 6.5.3.

Table 6.5.3: Surveys on FN

Date	AirCore	Bag samples	transects	comment
10.01.19	No data	No data	No data	First attempt – to localize site
28.02.19	-40.8 ± 5.7 (peak 1) -45.2 ± 6.2 (peak 2)	Collected	38	no wind data
28.05.19	-48.9 ± 5.6	Collected	30	no wind data
29.05.19	No samples	No data	30	no isotopic data

Maps with isotopic concentration are presented on Fig. 6.5.7 (28.02.2019) and on Fig. 6.5.8 (28.05.2019). On Fig. 6.5.9 are presented results from 29.05.2019 when survey was focused on making transects to use later with model to estimate CH_4 emission from the site.

Fig. 6.5.7: Survey 28.02.2019 on FM gas station

Fig. 6.5.8: Survey 28.05.2019 on FM gas station

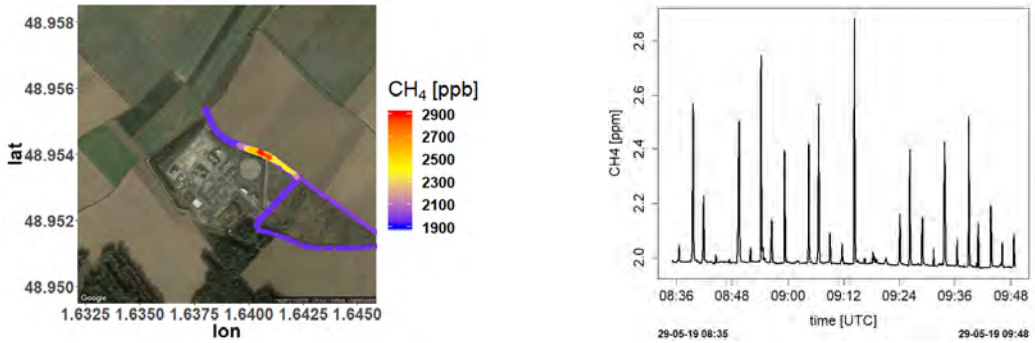

Fig. 6.5.9: Survey 28.05.2019 on FM gas station, left side: CH_4 mixing ratio along the transect

6.5.1.2.1.5 Limoges-Fourche (LF)

This natural gas compressor station is situated south of Paris, close to Limoges Fourche (48.853319°N, 2.348702°E). The site is surrounded by farmlands and only possible access is on road on the south-west side of the station.

On 10.01.2019, when one peak was observed, survey was focused on isotopic measurements (AirCore and bag samples) (Fig. 6.5.10).

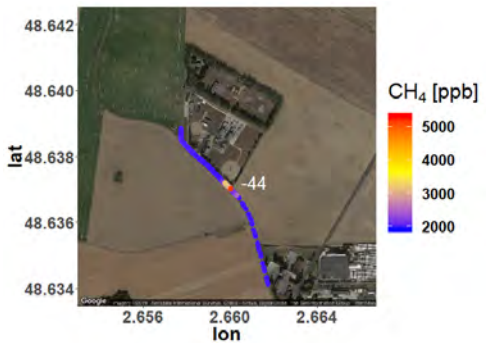

Fig. 6.5.10: Survey 10.01.2019 on FM gas station

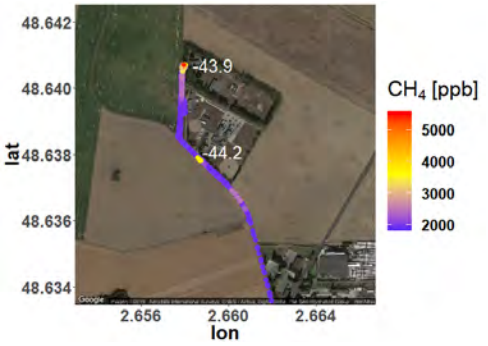

Fig. 6.5.11: Survey 16.05.2019 on FM gas station

On 16.05.2019 (Fig. 6.5.11), when survey was conducted also on part of a private company road, two peaks were detected, when one probably come from the same source as peak observed during previous measurement. This survey was focused on isotopes measurements (both AirCores and bag samples) and C_2H_6 measurements. The last survey so far, was conducted on 15.07.2019 and it was focused on isotopes (only AirCore), C_2H_6 and transects collecting (Fig. 6.5.12). The survey was conducted on the same road as 10.01.2019 so only one peak was observed. General information about measurements carried out so far, are presented in Table 6.5.4.

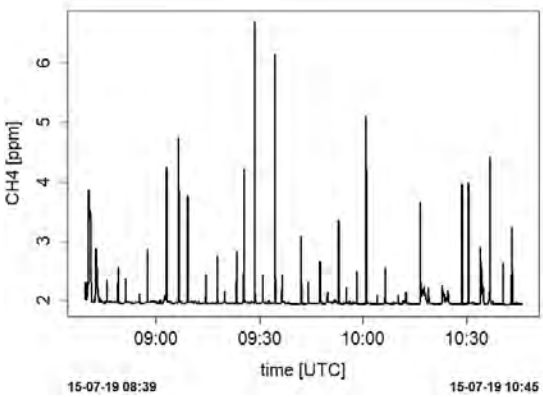

Fig. 6.5.12: Survey 15.07.2019 on LF gas station made transects

Table 6.5.4: Surveys on LF

Date	AirCore	Bag samples	transects	comment
10.01.2019	-44.2 ± 4.1	-45.8	No data	no wind data
16.05.2019	-43.9 ± 1.6 -44.2 ± 4.3	collected	No data	C_2H_6 measurements
15.07.2019	collected	No data	40	C_2H_6 measurements

Table 6.5.5: C_2H_6/CH_4 ratio from observed natural gas compressor station – calculated parameters

	1 sec averaging time			1 min averaging time		
	Slope	Intercept	R^2	Slope	Intercept	R^2
BNS	0.089 ± 0.001	0.030 ± 0.001	0.83	0.090 ± 0.003	0.030 ± 0.004	0.982
FM	0.092 ± 0.011	0.037 ± 0.002	0.03	0.11 ± 0.03	0.035 ± 0.004	0.33
LF	0.058 ± 0.004	0.022 ± 0.002	0.14	0.050 ± 0.014	0.025 ± 0.006	0.323

6.5.1.2.1.6 Butte-Bellot (BB)

Table 6.5.6: Surveys on BB

Date	AirCore	Bag samples	transects
27.11.2019 inside	-63.3 ± 1.5	-63.0	10
10.01.2019 outside	-62.5 ± 1.1	-62.9	10
16.05.2019 outside	No	-64.4	no
15.07.2019 outside	3 samples	No	no

This landfill is situated south of Paris, close to Limoges Fourche (48.641306N, 2.74011E). Only possible access is on road on the south side of the station. From the road, one peak from the active part of the landfill is observed and, depending on the meteorological condition, it is also possible to observe second, a smaller peak from already closed part of the landfill. On 27.11.2018 survey was focused on the fieldwork inside the landfill. That day isotopic measurements (AirCore and bag samples) and transect to calculate emission were collected. On 10.01.2019 (the same measurement protocol was applied, but outside of the landfill, where measurements were made on the public road (Fig. 6.5.13). The next two surveys (16.05.2019 and 15.07.2019) were focused only on isotopic measurements carried outside of the landfill. General information about measurements carried out so far are presented in Table 6.5.6.

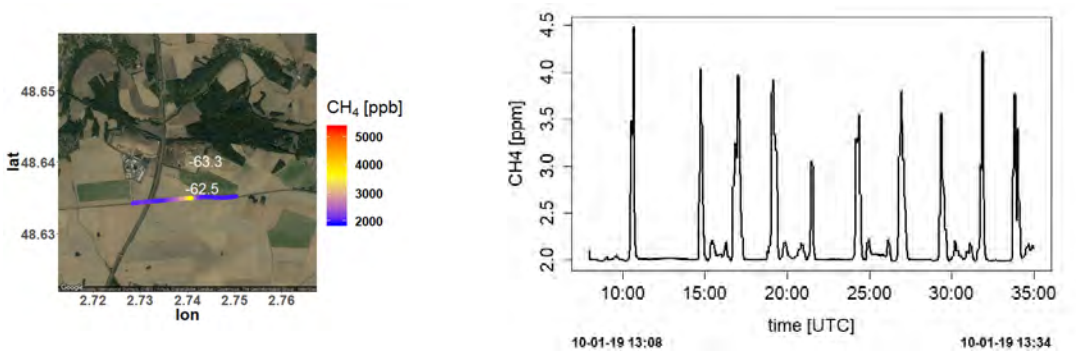

Fig. 6.5.13: Survey on BB landfill on 10.01.2019 (left side); Survey 10.01.2019 on FM gas station made transect (right side)

6.5.1.2.1.7 Gonesse GNS

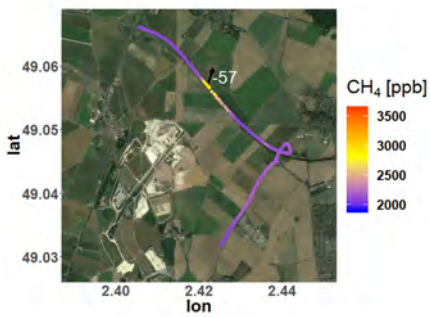

Fig. 6.5.14: Survey on GNS landfill, 25.01.2019

This landfill is situated north of Paris, close to Gonesse (49.025175N, 2.408130E). The best roads to make measurements are situated on the east and south side of the landfill. This landfill is larger than the previous one and more peaks are observed from the roads. On 25.01.2019 survey was focused both on isotopic measurements (AirCore) and transect to calculate emission (Fig. 6.5.14). However, due to technical problems with the car, that survey had to be stopped. The second, more successful survey was conducted 01.03.2019.

That day isotopic measurements (AirCore and bag samples) and transect to calculate emission were collected (Fig. 6.5.15). General information about measurements carried out so far are presented in Table 6.5.7.

Table 6.5.7: Surveys on GNS

Date	AirCore	Bag samples	transects	comment
25.01.19	-57.5 ± 4.1	no	8	Car problems – canceled survey
01.03.19	-58.0 ± 3.2	-57.5	20	

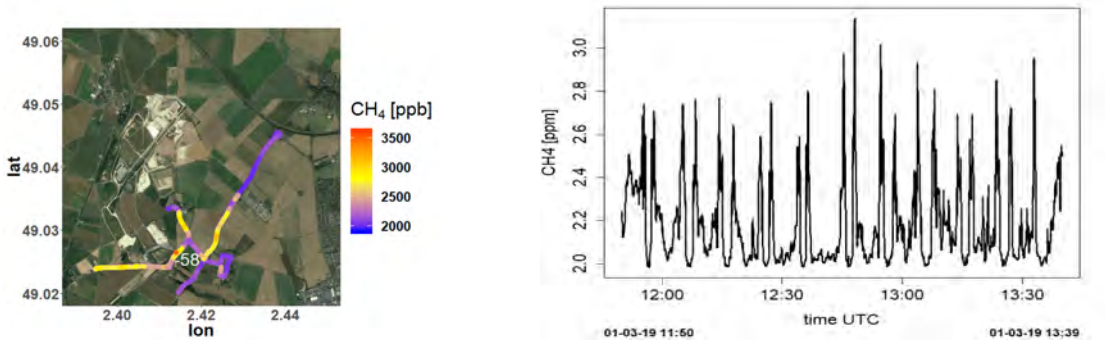

Fig. 6.5.15: Survey on GNS landfill, 25.01.2019 (left side); Survey 25.01.2019 on GNS landfill made transect (right side)

6.5.1.2.1.8 MEMO² tanks intercomparison

As a part of the laboratory tests, 5 MEMO² tanks were measured. Those tanks going from laboratory to laboratory, participating in the MEMO² project, allow to compare used methods and instruments. The tanks were measured by CRDS 2072 G2201-i. This instrument is normally used to conduct mobile measurements during surveys. The measured MEMO² tanks:

- Ambient EGH air 12/09/2018 1,976 ppm 22 psi gauge 2,43 UU 6/11/2018,
- Lab Gas 25/07/2018 1,957 ppm 25 psi gauge 2.64 bar UU 6/11/2018,
- Lab Gas 20/07/2018 10,19 ppm 24 psi gauge 2,46 bar UU 6/11/2018,
- Landfill Gas 25/07/2018 10,073 ppm 28 psi gauge 2,86 bar UU 6/11/2018,
- Landfill Gas 25/07/2018 1,777 ppm 25 psi gauge 2,64 bar UU 6/11/2018.

The measurement of MEMO² tanks was conducted 23.08.2019 and in total it lasted 6 hours. Measurement of MEMO² tanks was conducted according to the ICOS ATC calibration procedure. 5 tanks where measured alternatively for 20 minutes. Between each cycle, LSCE tank was also measured for 20 minutes. This cycle was repeated 3 times. 10 minutes from the 20-minutes measurement period was used for further analysis (9 minutes from the beginning of measurements and 1 minute from the end of measurement were removed). For every 10 minutes' measurement period, mean value and the standard deviation (used for errors calculation) were calculated for every species. The final value for each tank was measured as a mean value of 3 measured cycles and the standard deviation is treated as a mean of the standard deviation of the 3 cycles (Table 6.5.8).

Table 6.5.8: MEMO² tanks CRDS results

name.id	CO_2	u(CO^2)	CH_4	u(CH_4)	$\delta^{13}CH_4$	u($\delta^{13}CH_4$)	C_2H_6	u(C_2H_6)	H_2O	u(H_2O)
1	1.11	0.29	1970.1	1.6	-37.0	3.4	0.16	0.05	0.0045	0.0015
2	2.61	0.14	10091.3	3.0	-35.2	0.7	0.63	0.06	0.0055	0.0006
3	422	0.13	1960.6	0.3	-47.7	3.5	-0.18	0.05	0.8574	0.0011
4	1.99	0.07	1775.8	0.3	-60.4	3.9	0.04	0.05	-0.0001	0.0004
5	8.45	0.09	9986.8	2.2	-61.4	0.7	-0.08	0.05	0.0015	0.0004

Table 6.5.9: MEMO² tanks – CRDS vs IRMS results

source	CH4 [ppm]	IRMS [‰]	$CRDS_{calib}$ [‰]	IRMS-CRDS [‰]
natural gas	2	-39.6	-37.0 ± 3.4	**-2.6**
natural gas	10	-38.2	-35.2 ± 0.7	**-3**
air	2	-48.1	-47.7 ± 3.5	-0.4
landfill	2	-59.8	-60.4 ± 3.9	0.6
landfill	10	-60.9	-61.4 ± 0.7	0.5

In the next step, results obtained by CRDS analyser were compared with IRMS isotopic signature (agreed value between Utrecht University and Royal Holloway University of London). Results are presented in Table 6.5.9 and Fig. 6.5.16. In the case of ambient air and landfill air, the values are in good agreement. However, in the case of natural gas air CRDS analyser value are higher than IRMS values. This discrepancy can be caused by instrument specification or by not good enough calibration for enriched $^{13}CH_4$ value.

6.5.1.2.1.9 Trace release experiment in the collaboration with NPL and RHUL

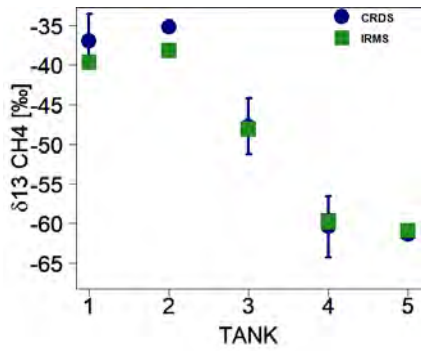

Fig. 6.5.16: MEMO² tanks – Comparison $\delta^{13}CH_4$ value IRMS and CRDS, with CRDS 2072 calibration, all uncertainties are marked

Between 09.09.2019 and 13.09.2019 the trace release experiment in Bedford (100 km North from London) was conducted by National Physical Laboratory (NPL). This experiment was focused on the controlled emission of CH_4 and C_2H_6. Over the experiment time, the emission rate, C_2H_6/CH_4 ratio and emission height were changed. The isotopic composition did not change over the experiment. Part of emissions was conducted with known values (emission rate and C_2H_6/CH_4 ratio) and part was conducted as a blind test. Participating in the test allowed to verify the methods used during my PhD thesis (emission calculation using transects and Polyphemus model, isotopic value using AirCore tool, C_2H_6/CH_4 ratio observed standing inside the peak). The conducted releases and made observations are presented in Table 6.5.10. Due to technical problems with batteries, no measurements were conducted during the first day of the experiment (09.09.2019) and over the first release on 10.09.2019. Collected data will be analyzed and results obtained by CRDS analyzer will be compared with results obtained by RHUL team.

Table 6.5.10: Schedule of trace release experiment and observation made by CRDS G2201-i

day	time UTC	emission flux	C_2H_6/CH_4	high	AirCore	C_2H_6	transects
20190909	12:27-13:15	70l/min	0.00	4 m	0	0	0
	13:40-14:22	70l/min	0.00	0 m	0	0	0
20190910	10:01-10:45	70l/min	0.03	0 m	0	0	0
	11:28-12:20	70l/min	0.03	4 m	2	19 min	0
	12:45-12:32	70l/min	0.07	4 m	2	15 min	0
	13:58-14:53	70l/min	0.07	0 m	3	11 min	0
	15:00-15:38	35l/min	0.07	0 m	2	7 min	0
	15:40-16:22	35l/min	0.07	4 m	2	10 min	0
20190911	09:13-09:56	blind	blind	4 m	0	0	10/10/10
	10:16-10:58	blind	blind	0 m	0	0	10/10/10
	11:23-12:10	blind	blind	0 m	2	17 min	0
	12:26-13:10	blind	blind	4 m	2	20 min	0
	14:43-15:25	blind	blind	4 m	0	0	10/10/10
	15:30-16:10	blind	blind	0 m	0	0	10/10/10
20190912	08:56-09:47	blind	blind	0 m	2	11 min	0
	09:50-10:35	blind	blind	4 m	2	11 min	0
	10:45-11:27	blind	blind	4 m	0	0	10/10/10
	11:40-12:24	blind	blind	0 m	0	0	10/10/10
	13:00-13:42	blind	blind	0 m	0	0	10/10/10
	13:49-14:29	blind	blind	4 m	0	0	10/10/10
	14:37-15:20	blind	blind	4 m	2	15 min	0
20190913	09:25-10:10	70l/min	0.00	0 m	2	17 min	0
	10:15-10:45	70l/min	0.00	4 m	2	12 min	0

6.5.1.2.2 Fourth year

Between March 2020 and February 2021, I was focused on the last data analysis based on surveys made during previous reporting periods, writing 2 draft of articles and preparing my PhD defense. Finally, I defended my PhD on 19.01.2021 and was awarded my PhD title.

The reported results are partly updating the results of the third year.

6.5.1.2.2.1 C_2H_6 study

One article was dedicated to the verification of potential and limitations of Picarro CRDS G2201-i to field C_2H_6 measurement. This draft was submitted to Atmospheric Measurements Techniques and after open discussion, it is currently in the review process (DOI:10.5194/amt-2020-410). There, the work is divided into three parts: first, the laboratory tests to determine instrument noise and precision are described. Then the results from the controlled gas release experiment are shown. Finally, the results from in-situ mobile near-source measurements are presented. Also, the CRDS G2201-i is compared to other instruments dedicated for C_2H_6 measurement.

During laboratory tests, I determined the instrument CMR and Allan variance by measuring a working gas for 24 hours. Using the CRDS G2201-i, the corrected and calibrated value is steadily equaling (33.2 ± 1.7) ppb over the 24-hour duration. It was also measured by GC-FID coupled to a preconcentrator, and its C_2H_6 mixing ratio equals 2.2 ppb. This value suggests a bias of the CRDS instrument of 31 ppb at low C_2H_6 concentrations.

As the result of the 24-hour test, CMR and Allan deviation (Fig. 6.5.17) are calculated for target gases with different C_2H_6 mixing ratios: low mixing ratio, 100 ppb and 1000 ppb. In all cases, increasing the C_2H_6 mixing ratio does not affect the determined CMR and Allan deviation. Looking at raw data (one data point every 3.7 s) for different mixing ratios, CMR and Allan deviation are about 50 ppb and 25 ppb, respectively. Increasing averaging time improves these parameters and for 1-minute average, all achieve about 13 ppb.

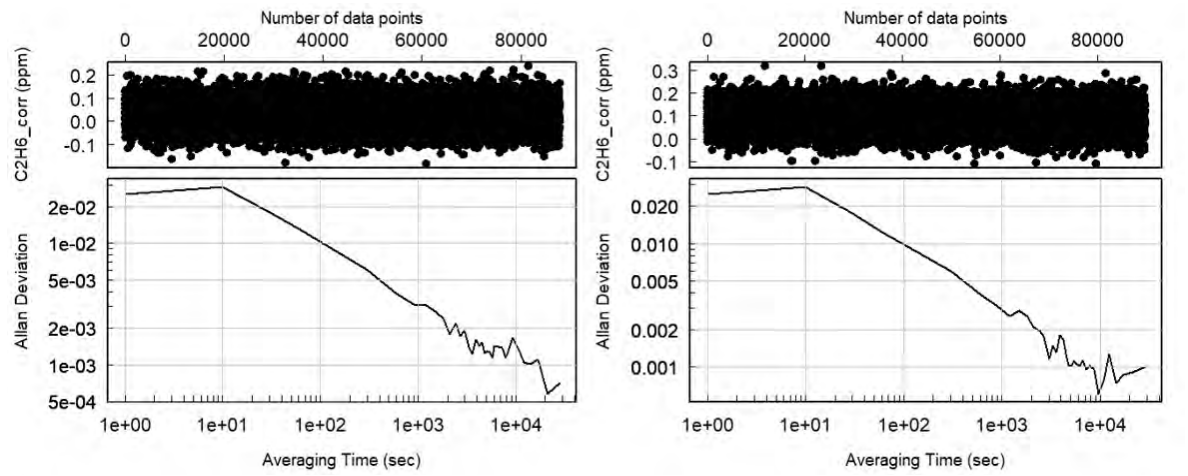

Fig. 6.5.17: Allan deviation for corrected and calibrated C_2H_6. Left: Measurement of working gas with negligible C_2H_6 mixing ratio, right: measurement of the mixture of working gas with ~100 ppb of C_2H_6.

With 30 ppb bias and a CMR of 50 ppb, the CRDS G2201-i cannot be used to measure C_2H_6 absolute value. However, this instrument can be used to observe C_2H_6 enhancement near the source and to estimate C_2H_6 to CH_4 ratios. From these numbers, we can deduct that the smallest enhancement that the analyzer can measure with significant precision at the highest possible data acquisition frequency is 50 ppb.

This value was obtained both for gas with a low and high C_2H_6 mixing ratio (~100 ppb and ~1 ppm). We can assume that a C_2H_6 enhancement is significant when the maximum C_2H_6 mixing ratio in the peak is higher than 2xSD, i.e., 100 ppb above background.

Fig. 6.5.18 shows C_2H_6 to CH_4 ratios measured in situ during the controlled release experiment. In September 2019, during five days, a gas release experiment was conducted by the National Physical Laboratory (NPL, UK) and the Royal Holloway University of London (RHUL, UK). The experiment took place in Bedford Aerodrome, UK. The description of the experimental setup configuration can be found in Gardiner et al. (2017). The goal was to evaluate the methods for calculating C_2H_6:CH_4 ratios, emission flux and isotopic composition during local mobile measurements. Each release lasted about 45 minutes. During the experiment, the parameters of each release: C_2H_6:CH_4 ratio (0.00 to 0.07), emission flux (until 70 L/min) and the source height (ground or ~4 m source) could vary. Seven releases were measured using the mobile setup (AirCore and standing in the plume) to determine C_2H_6 to CH_4 ratio. During measurements, air was dried before entering the analyzer using a magnesium perchlorate cartridge. Due to the limited time of the releases, the time of standing inside the plumes was in the range of 15 to 20 minutes.

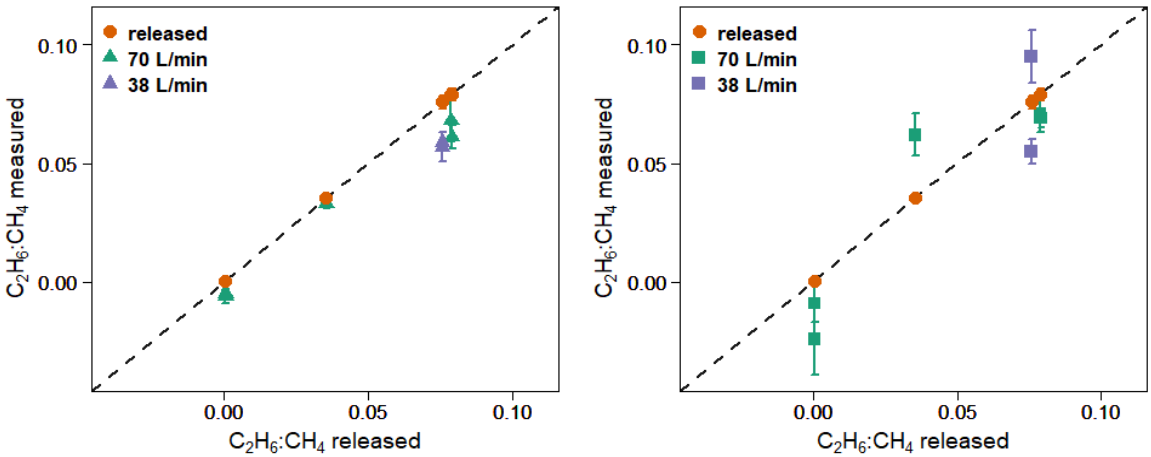

Fig. 6.5.18 C_2H_6:CH_4 ratio observed using G2201-i as a part of a mobile setup. Left: measured standing inside the plumes. Right: measured using AirCore. Red points: known released C_2H_6:CH_4 ratio. Error bars represent 1 standard deviation. The uncertainties of released values are invisible on the graph.

The measurement set-up used here is the same as in the field. The general principle of the setup is comparable to the previous works (e.g., Hoheisel et al., 2019; Lopez et al., 2017; Rella et al., 2015). As the instrument is not dedicated to C_2H_6 measurements, the vibrations induced by the motion of the car cause noise in the instrument readouts. Such a constraint can be overcome using two approaches. First, by stopping the car and standing some time inside the plume. Second, by accumulating air in the AirCore (Karion et al. 2010; Rella et al. 2015; Lopez et al. 2017) while moving through the plume and eventually reinjecting the AirCore's air into the analyzer while stopped. For all mobile measurements, the background mixing ratios are calculated as the 1st percentile of the data sampled just before and just after the plumes, both for CH_4 and C_2H_6. Then the data with CH_4 enhancements above background are further analyzed. The C_2H_6:CH_4 ratio is calculated for each release as the slope of the linear regression of C_2H_6 against CH_4.

During the 7 analyzed releases, the C_2H_6:CH_4 ratio was set to ~0.032 for one release, ~0.00 for two releases and ~0.07 for four releases. For measurements with the car stopped inside the plume, most of the data from the CRDS G2201-i are found lower than known emitted C_2H_6:CH_4 ratio, (mean absolute deviation = 0.011, standard deviation = 0.004) with residuals in the range -0.018 to -0.002 for raw data (Table 6.5.11).

The observed underestimation can be caused by an insufficient number of measurement points (15-20 minutes of measurement). For AirCore measurements, there is more discrepancy than for the plume standing situation, with residuals in the range -0.025 to 0.027 (mean absolute deviation = 0.017, standard deviation=0.009). The plume standing set-up shows less noisy data and a smaller range of residuals than AirCore results. Moreover, the plume standing approach has a (small) regular bias (mean bias = -0.011), higher than in the AirCore approach (mean bias = -0.004). These results show that in the case of C_2H_6:CH_4 ratio measurements, standing inside the plume gives results closer to the reality than AirCore sampling.

Table 6.5.11: C_2H_6:CH_4 ratio observed using G2201-i as a part of a mobile setup, during standing inside the plume or from AirCore measurements. * Small amount of C_2H_6 impurity in the CH_4

Emitted C_2H_6:CH_4	emitted CH_4 flux [L/min]	Source height [m]	nn	C_2H_6:CH_4 [ppm/ppm]	Residuals C_2H_6:CH_4	C_2H_6:CH_4 [ppm/ppm] AirCore	Residuals C_2H_6:CH_4 AirCore
0.0355 ± 0.0011	70	4	382	0.033 ± 0.002	-0.002	0.062 ± 0.009	0.027
0.0788 ± 0.0025	72	4	149	0.068 ± 0.009	-0.011	0.071 ± 0.008	-0.008
0.0790 ± 0.0025	73	0	220	0.061 ± 0.005	-0.018	0.069 ± 0.004	-0.010
0.0758 ± 0.0028	38	0	142	0.059 ± 0.004	-0.017	0.055 ± 0.005	-0.020
0.0758 ± 0.0028	38	4	191	0.057 ± 0.006	-0.018	0.095 ± 0.011	0.019
0.0005 ± 0.0006*	70	0	350	-0.005 ± 0.001	-0.005	-0.024 ± 0.015	-0.025
0.0005 ± 0.0006*	70	4	202	-0.006 ± 0.003	-0.007	-0.009 ± 0.008	-0.010
Mean residuals					**-0.011**		**0.004**

As a final step, the CRDS G2201-i was evaluated in real field conditions. Measurements were collected in the Paris area downwind of three gas compressor stations (referred to as A, B, C) and one landfill (D). All measurements were done stationary inside the plume. Surveys where air was not dried before measurements or CH_4 enhancement was smaller than 1 ppm above background, are rejected from further analysis. Results from remaining surveys are presented in Fig. 6.5.19.

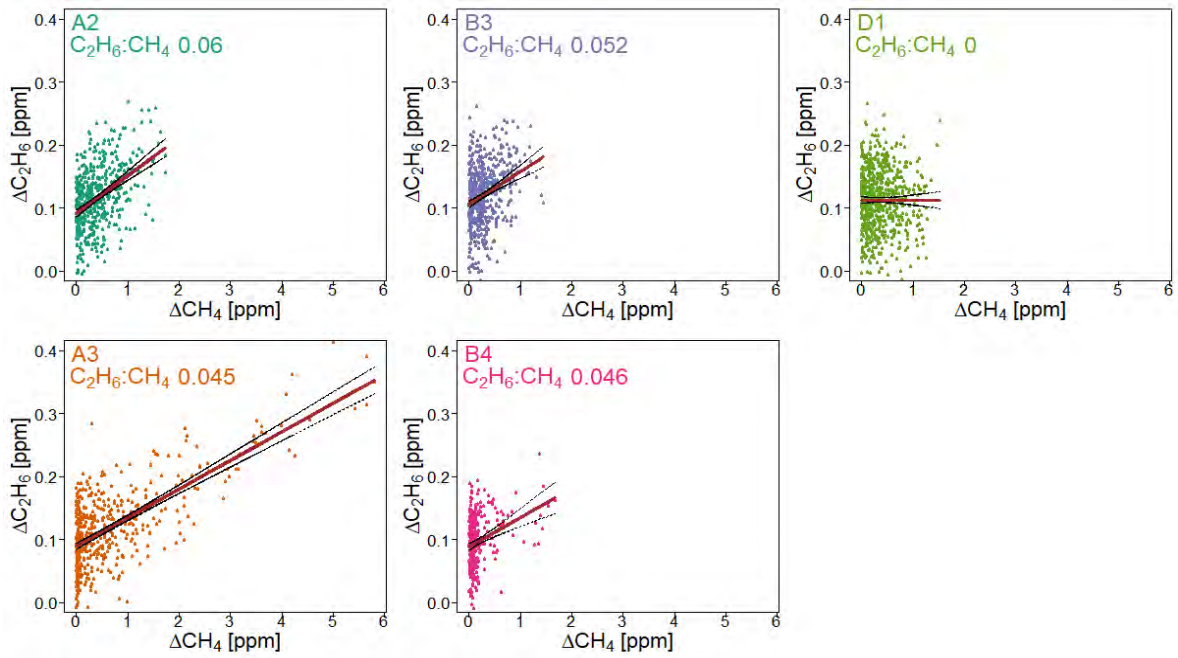

Fig. 6.5.19: C_2H_6:CH_4 ratio for gas compressor stations (A and B) and the landfill (D), calculated for non-averaged data. Linear fitting (red line) with confidence intervals (black lines)

Table 6.5.12. Comparison of results obtained by CRDS G2201-i with the values from the operator company.

id	CRDS 1s C_2H_6:CH_4 ratio	Operator data C_2H_6:CH_4 ratio	Residuals C_2H_6:CH_4 ratio	Date
A2	0.060 ± 0.005	0.051	0.009	16.05.2019
A3	0.045 ± 0.002	0.049	-0.004	15.07.2019
B3	0.052 ± 0.007	0.052	0.000	12.07.2019
B4	0.046 ± 0.008	0.052	-0.006	12.07.2019
D1	0 ± 0.006	NA	NA	16.05.2019

Also, we compared the observed ratios with the values provided by the owner of the gas compressor stations (Table 6.5.12). The residuals between values measured by CRDS and values provided by the owner (considered as the "true" values) are in the range -0.006 to 0.009. This range is more symmetrically distributed around the released value than for the controlled release experiment (-0.018 to 0.002). The uncertainty of C_2H_6:CH_4 ratio measured using the CRDS G2201-i in the field conditions is smaller than the differences between the ratios of CH_4 sources (e.g., biogenic sources C_2H_6:CH_4 ~0.00, natural gas leaks and compressors stations ~0.06, processed natural gas liquids ~ 0.30). These results clearly show that C_2H_6:CH_4 ratio measured by the CRDS G2201-i can be used to portion the origin of the CH_4 during mobile measurements.

6.5.1.2.2.2 Measurements inside Paris city

Also, during the reporting period, I finished working on the second article, which is focused on mobile measurements made on the city scale. The article was submitted to Environmental Science & Technology and it is currently in the review process. Here, I am focused on Paris city, which is the densest area in Metropolitan France and reached 20,000 people km^{-2}. Its population is about two mln people (INSEE 2019). Mobile measurements in Paris city allow defining direct city CH_4 emissions (scope 1).

Between September 2018 and March 2019, 17 surveys were made in the Paris city and its south-west suburbs using a CRDS analyzer with the AirCore tool. The base of our mobile set-up is the CRDS G2201-i which was used for sixteen of the surveys. This instrument measures CO_2, $\delta^{13}CO_2$, CH_4, $\delta^{13}CH_4$, and H_2O, with a gas flow of ~160 sccm and a frequency of ~0.27 Hz. $\delta^{13}CH_4$ is reported using the international standard Vienna Pee Dee Belemnite (VPDB, $^{13}C/^{12}C$ $_{VPDB}$=0.0112372)(Craig 1957) and CH_4 using the WMO X2004A scale. Our CRDS G2201-i has a $\delta^{13}CH_4$ precision of ~ 3.5 ‰ for ambient air CH_4 mixing ratios, but as CH_4 mixing ratios increase to ~10 ppm, $\delta^{13}CH_4$ precision improves to 0.7 ‰. During surveys, the CH_4 mixing ratio was observed in situ. The background was calculated as 2 minute moving average. Leak indications are defined as a CH_4 enhancement larger than the threshold (10 % above background CH_4).

In locations where CH_4 enhancement reached more than 500 ppb above background, the isotopic signature was sampled using the AirCore tool. In total, 28 leak indications from 17 different locations were found significant. Isotopic signatures were calculated using the Miller-Tans approach (Miller and Tans 2003; C. W. Rella et al. 2015), offering comparison possibilities with previous studies. Fitting of the observations were calculated as a linear regression type II using the ordinary least squares method, while data was grouped in 50 ppb bins. Here, we only report the isotopic $\delta^{13}CH_4$ signature of leak indications where the Miller-Tans approach yields a 1-sigma uncertainty less than 10 ‰ and with a correlation coefficient $R^2 > 0.85$. Twelve of the 28 AirCores samples fulfilled the criteria, with two AirCores measuring the same leak indication (Table 6.5.13). Additionally, during four days, walking measurements using LGR MGGA were made, which allowed determining the exact position of some CH_4 leak indications observed from the car. In total, 500 km out of the 1800 km roads in Paris and suburbs were driven. Part of the streets was passed multiple times (2-5). Overall, 90 leak indications were observed and the origin of 27 of them was determined based on the isotopic signature or walking measurements.

Table 6.5.13. Determined isotopic signature using AirCore

Date	CH_4 [ppb]	$\delta^{13}CH_4$ [‰]	r^2	latitude	longitude	n	source
31-01-2019	4170	-42.7 ± 1.8	0.95	48.86571	2.28928	1	furnaces
12-02-2019	2316	-52.2 ± 8.1	0.95	48.86996	2.35164	1	sewage
13-02-2019	2794	-49.2 ± 8.9	0.86	48.86573	2.28594	1	gas leak
13-02-2019	4000	-36.4 ± 2.6	0.95	48.86503	2.28892	2	furnaces
13-02-2019	2707	-50.8 ± 6.0	0.92	48.86949	2.28842	1	sewage
26-02-2019	3098	-55.5 ± 3.4	0.97	48.8202	2.24547	1	sewage
26-02-2019	2727	-57.5 ± 6.8	0.92	48.83062	2.26566	1	sewage
26-02-2019	3982	-52.4 ± 3.1	0.96	48.82142	2.25007	1	sewage
27-02-2019	2953	-59.5 ± 8.1	0.92	48.82453	2.24583	1	sewage
27-02-2019	3222	-53.4 ± 2.2	0.97	48.82251	2.25216	1	sewage
07-03-2019	2805	-39.5 ± 5.0	0.86	48.88578	2.38904	1	furnaces

Three main CH_4 sources were observed: natural gas distribution network leaks, sewage network leaks and building's venting grids.

The emission from venting grids was observed during walking measurements and was not reported in previous studies. As the emission observed from venting grids probably come from leaking heating installation, this category is further called "furnaces". The biggest contribution comes from natural gas leaks. Fifteen leaks were observed from this source. Two clusters with a denser spatial distribution of CH_4 leak indications were observed (Fig. 6.5.20). Cluster A is situated in west Paris, and six defined leak indications were observed there. Cluster B is located in the south-west suburbs of Paris, and 15 defined leak indications occurred there. In Cluster A majority of defined leaks come from furnaces (3 leaks). In contrast, in cluster B, emissions were attributed to gas leaks (9 leak indications) or sewage (6 leaks).

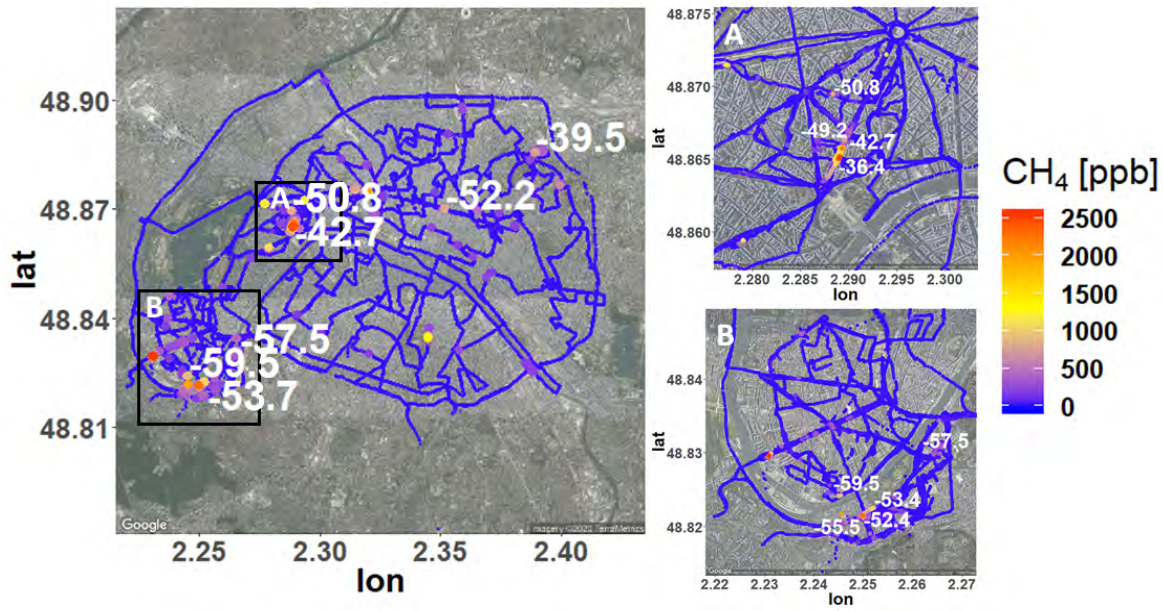

Fig. 6.5.20: Paris CH_4 enhancements above background with $\delta^{13}CH_4$ signature (white numbers) determined for 11 leak indications. Left panel – whole measured area. To make the map more legible, part of leak indications in cluster areas A and B are treated as one leak indication with an averaged value. Right panel – zoom of cluster area A (top right) and B (bottom right). Base map provided by Google Maps

It was not possible to determine the origin of 63 remaining leak indications. Their enhancement was too small to take isotopic samples, and the instrument to make walking measurements was not available. Part of these leak indications was observed once and part of them multiple times. Seven unknown leak indications are localized in Cluster A and 17 in Cluster B.

The remaining 39 unknown leak indications were found outside of clusters A and B. A simple assumption was made based on the detected leaks with the known origin to attribute unknown leak indication to Paris' CH_4 sources. 66% of leak indications in Paris come from gas leaks (natural gas distribution network and furnaces) and 34% from sewage network. This distribution of source categories is propagated to the 63 leaks of unknown origin determined during mobile measurements and 41 additional leaks are considered as coming from gas leaks and 22 as sewage network leaks (Fig. 6.5.21). Using this assumption, the gas leak indications rate (gas leak indications/ unique kilometers) is equal to 0.11 km^{-1}.

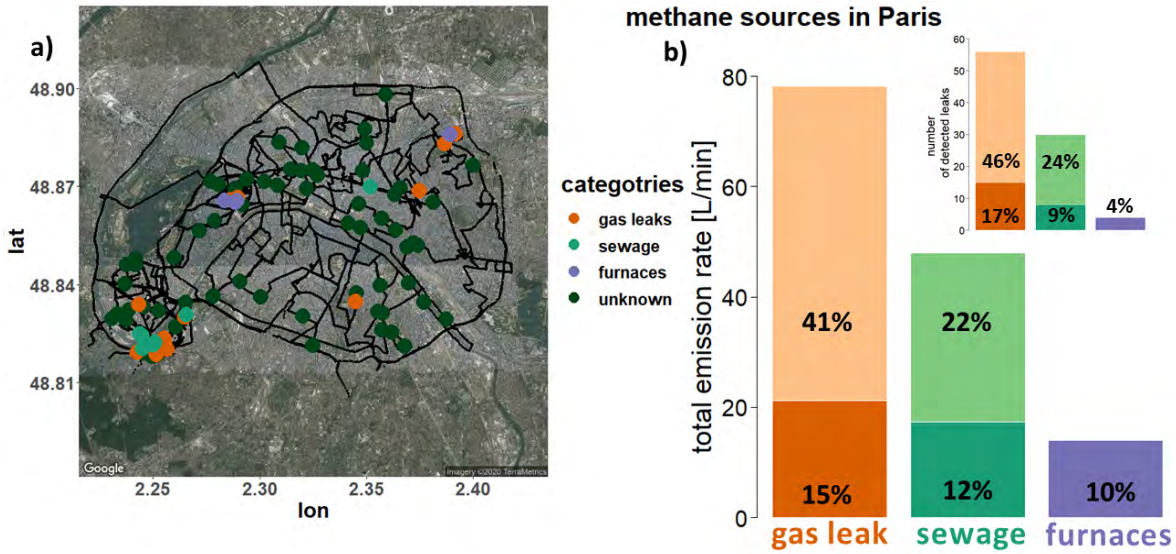

Fig. 6.5.21: CH_4 leak indication categories detected in the Paris area. a) Map of the surveyed area with positions of the detected sources. b) Distribution of the emission of the leak indication categories in the Paris area, inner figure: number of detected leaks. Paler colors represented unknown leaks attributed to gas leaks (orange) or sewage (green), based on the percent of defined leak indication. Base map provided by Google Maps.

Based on von Fisher et al. (2017) and Weller et al. (2019), the emission rate of individual leaks was calculated, using a statistical calibration model:

$$\ln(M\ CH_4) = -0.988 + 0.817 \cdot \ln(CH_4 \text{ emission rate}) \quad (1).$$

M is the maximum CH_4 enhancement above the background of the leak indication [ppm], and emission rates are estimated in L/min.

For the natural gas distribution leak indications, indicated using $\delta^{13}CH_4$ or walking measurement, the mean estimated emission rate for an individual leak location is equal to 1.4 L/min (range 0.5 – 3.87 L/min). They are categorized as small leaks (< 6 L/min), according to the categorization proposed by von Fischer et al. (2017). The mean estimated emission rate for an individual location is equal to 2.2 L/min (0.7 to 6.5 L/min) for the sewage sector. In this case, seven leak indications are in the small leak category, and one leak indication is in the medium category. The mean emission rate for an individual location is equal to 3.5 L/min (0.7 to 5.9 L/min) for the furnace sector. For the remaining 63 leak indications, the mean estimated emission rate is equal to 1.4 L/min (0.5 – 10.5 L/min). Only one is categorized as a medium, and it reached 10.5 L/min. Thus, the emission rate for individual leaks is skewed for lower emission rates with a median value equals to 0.8 L/min. Overall, on a unique 500 km, the accumulated emission rate is equal to 140 L/min. The gas sector contributes 56% under the attribution assumption. The sewage sector and furnaces contribute 34% and 10%, respectively. After upscaling to the Paris road length, the city emission rate is equal to 500 L/min (190 t/yr).

Based on these surveys, Paris is in the middle to low range compared to U.S cities, according to von Fischer et al. (2017) leak size categories. Overall, the results for the leak rate in Paris are two to four times smaller than the rates calculated for the cities with an old pipeline system in the U.S. and two to forty times higher than cities with a modern pipeline system in the U.S.(von Fischer et al. 2017).

6.5.1.2.2.3 Industrial sites study

Along results presented in two submitted articles, I was working on analyzing data from surveys made on industrial site scale in IDF (Fig. 6.5.22). Surveys were focused on

- three natural gas compressor stations
  - A (Limoges-Fourche (LF), see also chapter 6.5.1.2.1.5)
  - B (Beynes (BNS), see also chapter 6.5.1.2.1.3)
  - C (Fontenay-Mauvoisin (FM), see also chapter 6.5.1.2.1.4)
- Landfills
  - D (Butte-Bellot (BB), see also chapter 6.5.1.2.1.6)
  - E (Gonesse (GNS), see also chapter 6.5.1.2.1.7)

To obtain wind data, the Gill Windmaster, 3D-axis sonic anemometer with U, V, W vector and sonic temperature outputs, was used. Data are saved with 20 Hz rata in the range 0-50 m/s and 0-359°. Meteorological data are used as model input to calculate the emission rates of observed sites.

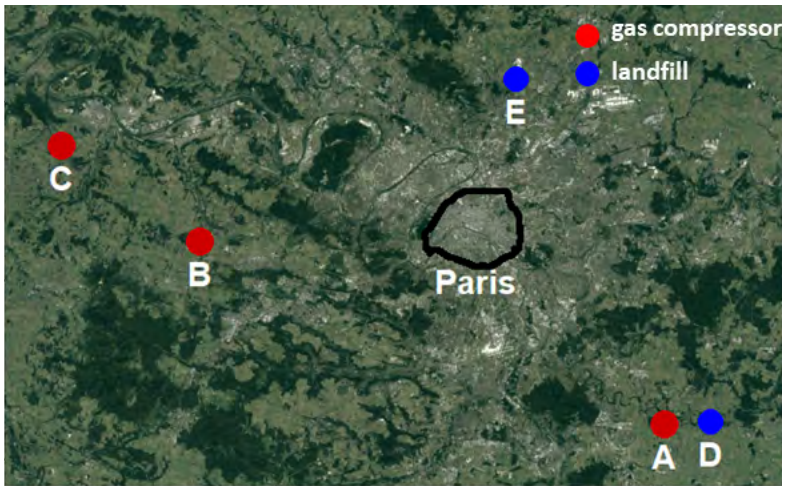

Figure 6.5.22: The location of landfills and gas compressors surveyed during the Ph.D. study

The study was mostly focused on determination of isotopic signature, and they are contributing to MEMO² isotopic database (Menoud et al. 2020). Moreover, during some surveys, emission rate for individual sites was also determined. During mobile measurements, isotopic signatures were determined using CRDS G2201-i with the AirCore tool. The plume from one site was typically crossed several times (between 3 and 7) during one survey. Then, data were treated using the Miller-Tans approach (Miller and Tans 2003) and linear regression type II, which accounts for uncertainty in x and y (Sokal and Rohlf 1995). If the coefficient correlation r^2 remains below 0.85 and uncertainty determined as one standard deviation of linear regression is above 10 ‰, the data are rejected for further analysis. Then, the isotopic signature of the site for the individual day is calculated as the mean of the remaining samples.

Additionally, during part of the measurements, bag samples were taken to measure isotopic signature afterward in the laboratory on IRMS instruments. Typically, three bag samples were taken inside the CH_4 plume, and one bag sample was taken outside as a background sample. Most often, bags were sent to UU (Utrecht University). There, the IRMS instrument can measure $\delta^{13}CH_4$ and δDCH_4 (Röckmann et al. 2016). Moreover, during two surveys, additional bag samples were taken and sent to RHUL (Royal Holloway University of London) to measure $\delta^{13}CH_4$ on IRMS(Fisher et al. 2006). This protocol allowed comparing the results from CRDS with the AirCore tool and two IRMS instruments for measurements of $\delta^{13}CH_4$.

For the emission rates, I used the Gaussian plume model in the Polyphemus platform to estimated CH_4 emission rates from gas compressor stations A and C. The Gaussian model is a common air pollution model, which is based on a simple formula that describes the three-dimension concentration field given by a point source (Mallet et al. 2007; Roscioli et al. 2015; Yacovitch et al. 2015; Rella et al. 2015; Caulton et al. 2017). It considers a Gaussian distribution of mean concentration in the horizontal and vertical directions during homogeneous and steady-state meteorological conditions. The concentration C in the location x, y, z is given by:

$$C(x,y,z) = \frac{Q}{2\pi\sigma_y\sigma_z\bar{u}} exp\left[\frac{-(y-y_s)^2}{2\sigma_y^2}\right] \cdot \left\{exp\left[\frac{-(z-z_p)^2}{2\sigma_z^2}\right] + exp\left[\frac{-(z+z_p)^2}{2\sigma_z^2}\right]\right\} \quad (2)$$

where:

Q is the emission rate of the source (mass per second),

$\bar{u}$ is the mean wind speed,

σ_y and σ_z are the Gaussian plume standard deviations in the horizontal and vertical directions,

x is the downwind distance from the source,

y is the horizontal crosswind coordinate,

y_s is the source coordinate in the horizontal direction,

z is the vertical coordinate,

z_p is the plume height above ground.

The Gaussian plume standard deviations, σ_y and σ_z, are the sum of the spread due to turbulence, plume rise and the diameter of the source. Different empirical schemes are used to estimate these standard deviations. In my study, I used the Briggs parametrization, based on the Pasquill – Turner stability classes, with six stability classes to establish σ_y and σ_z. These classes are determined by wind speed and solar irradiance. They vary from extremely unstable class A to extremely stable class F, while class D is a neutral one. Classes E and F are dedicated for the nighttime observation (Pasquill 1961).

Gas compressor station A (Limoges-Fourche (LF), see also chapter 6.5.1.2.1.5)

The gas compressor station A is situated about 35 km southeast of Paris, in a rural area with small villages and small industrial sites. On the station, two compressors and two venting zones are located. CH_4 plume emitted from the gas compressors is visible only from the street situated on the south side of the site (Fig. 6.5.23). On gas compressor station A, the surveys were conducted three times. Each time, the isotopic signature was measured using CRDS with AirCore tool.

Table 6.5.14: $\delta^{13}CH_4$ observed for gas compressor station A. CRDS results in this study are determined using the AirCore tool. For IRMS measurements, bag samples were taken and sent to UU.

Date	CRDS [‰]	Number of CRDS samples	IRMS [‰]	source
10.01.2019	-44.0 ± 4.1	2	-45.8 ± 0.5	Plume 1
16.05.2019	-44.2 ± 4.3	3	-44.3 ± 1.0	Plume 1
16.05.2019	-43.9 ± 1.6	6	-	Plume 2
15.07.2019	-43.0 ± 2.9	4	-	Plume 1

$\delta^{13}CH_4$ isotopic signature ranged between (-44.0 ± 4.1) ‰ and (-43.0 ± 2.9) ‰ using CRDS with AirCore tool (Table 6.5.14) for the plume coming from the venting zone. Also, the isotopic signature of the second plume did not differ statistically from the first one. Additionally, during two surveys (10.01.2019 and 16.05.2019), bag samples were taken and analyzed afterward on IRMS at Utrecht University (UU). $\delta^{13}CH_4$ isotopic signature reached (-45.8 ± 0.5) ‰ during first day and (-44.3 ± 1.0) ‰ during the second day. Isotopic signature obtained by CRDS with the AirCore tool are in good agreement within uncertainty with the results obtained from IRMS. The uncertainty of results from IRMS is smaller than for CRDS with AirCore tool.

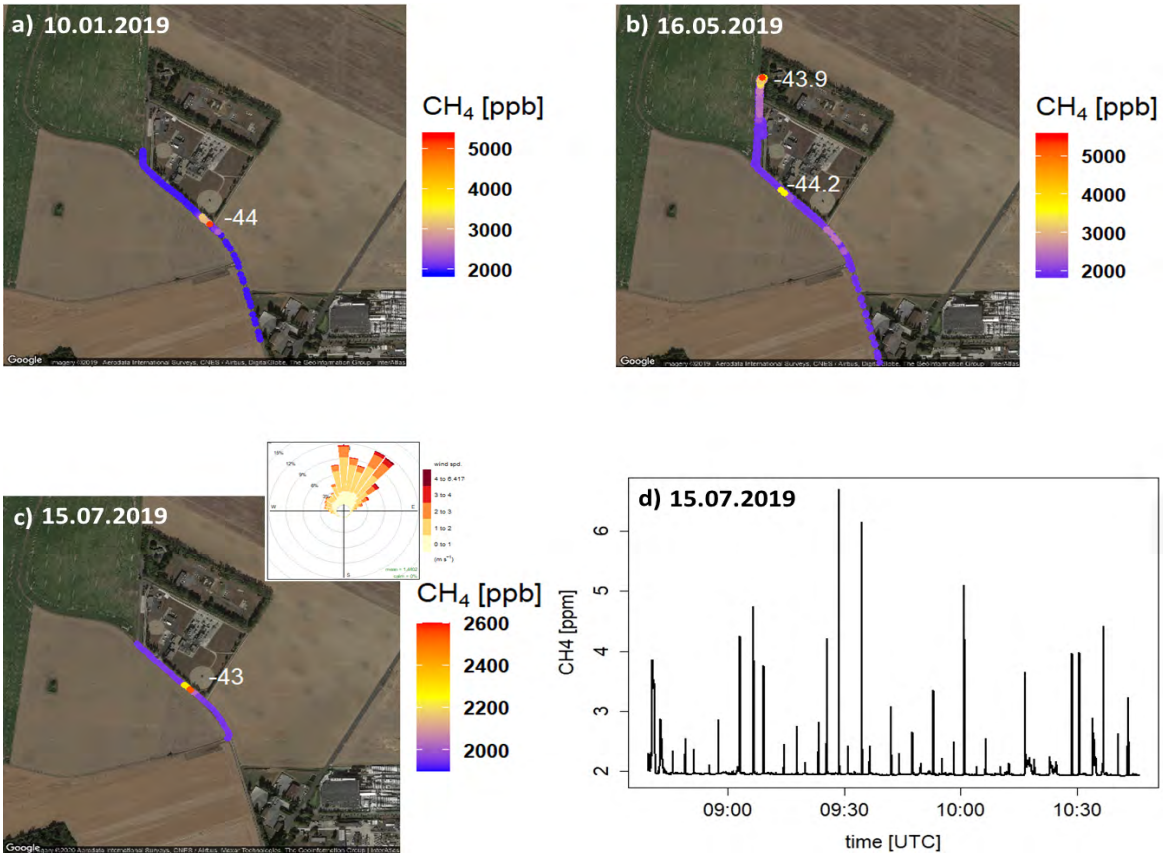

Fig. 6.5.23: Gas compressor A. Observed CH_4 mixing ratio. The white number indicate $\delta^{13}CH_4$ [‰]. Background is not subtracted. c) and d) present CH_4 mixing ratio on 15.07.2010 when the emission rate was estimated. d) multiple crossing of the CH_4 plume.

During the last survey (15.07.2019), when one plume was observed, the emission rate was calculated using the Gaussian model. The plume was crossed 30 times. The wind station was situated outside of the site. Due to the challenge to identify a single stability class, the emission rate was calculated using two stability classes: A and B. For both stability classes, in the model 0.2 g CH_4 s^{-1} (0.73 kg CH_4 h^{-1}) was used as an input emission rate.

Fig. 6.5.24 presents model output for a transect. Before comparing the observed and modeled CH_4 mixing ratio, the background was subtracted. The background was calculated separately for each plume as the 1st percentile of the observed CH_4 mixing ratio. The ratio of measured to modeled summed concentration was calculated and input CH_4 emission was multiplied by the averaged ratio to calculate the emission rate. That day, for the gas compressor A, the CH_4 emission rate is equal to (2.45 ± 0.50) kg CH_4 h^{-1} for stability class A and (1.68 ± 0.34) kg CH_4 h^{-1} using stability class B.

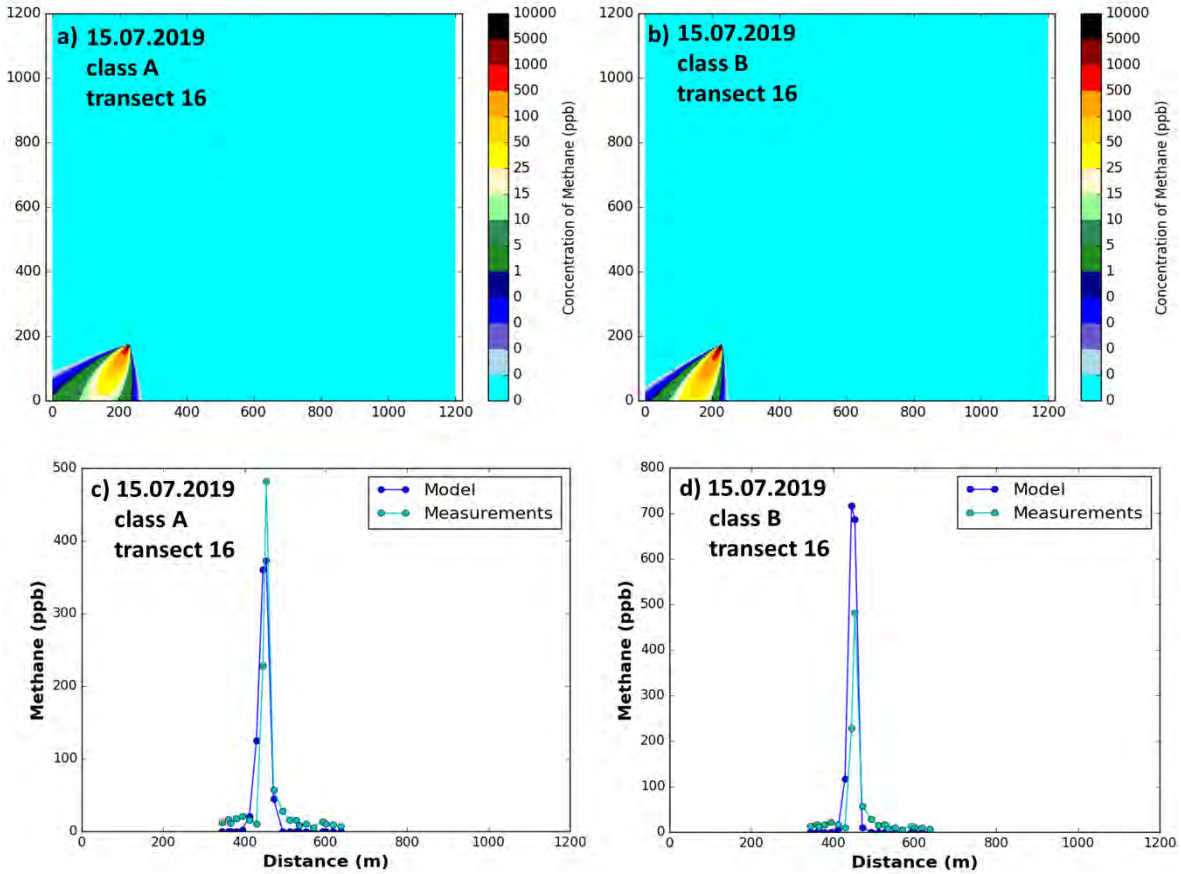

Fig. 6.5.24: Gaussian model results for transect 16th, gas compressor A, 15.07.2019, Top: Spatial dispersion of CH_4 concentration, bottom: Comparison of model and observation. a) and c) stability class A b and d) stability class B

Gas compressor station B ((Beynes (BNS), see also chapter 6.5.1.2.1.3)

The gas compressor B is situated about 40 km east of Paris. This is the biggest gas facility studied here and it includes not only gas compressors, but also gas storage tanks. Additionally, access around this site is much more limited compared to gas compressor stations A and C. The only available small road is on the east. Likely, on gas compressor B, venting zone, gas storage tubes and above ground pipelines are possible sources of CH_4 released to the atmosphere (Fig. 6.5.25).

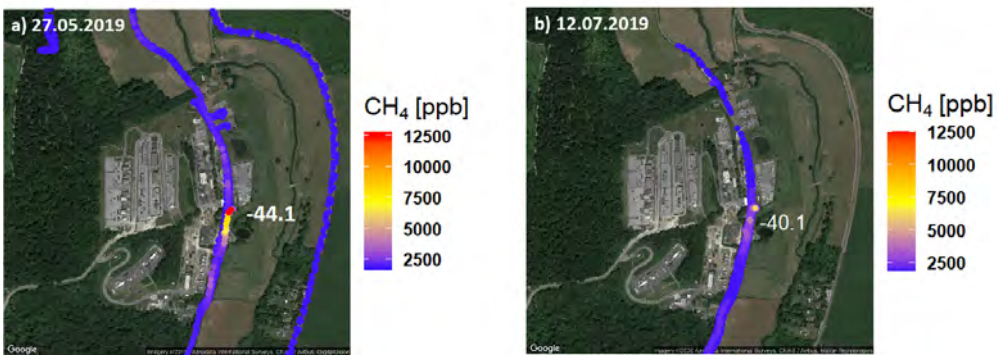

Fig. 6.5.25: Gas compressor station B observed CH_4 mixing ratio. The white number indicates $\delta^{13}CH_4$ [‰]. Background is not subtracted.

During two surveys, the isotopic composition was determined using CRDS with the AirCore tool. During the first survey (27.05.2019), $\delta^{13}CH_4$ was equal to (-44.1 ± 1.9) ‰ using CRDS instrument and (-43.9 ± 0.4) ‰ using IRMS (Table 6.5.15). These values are statistically in good agreement. The uncertainty of the value obtained from CRDS during AirCore sampling is lower than in the gas compressor A. It is caused by a higher observed CH_4 mixing ratio on site B than A. This value was obtained for the biggest plume observed that day. This value is also in good agreement with the value obtained in December 2015, when the isotopic signature was measured for gas storage in this area ((-43.4 ± 0.5) ‰) (Xueref-Remy et al. 2019).

During the second survey, $\delta^{13}CH_4$ was determined only using CRDS. The isotopic signature was more enriched and reached (-40.1 ± 3.9) ‰. In this case, the $\delta^{13}CH_4$ uncertainty is higher, as the maximum CH4 enhancement above background did not exceed 1000 ppb during AirCore sampling. More enriched value suggests that natural gas of a different origin, but still thermogenic (i.e. extracted in different region) was processed that day on the gas compressor station B.

Table 6.5.15: $\delta^{13}CH_4$ observed for gas compressor B. CRDS results in this study are determined using the AirCore tool. For IRMS measurements, bag samples were taken and sent * to RHUL or ** to UU.

Date	CRDS [‰]	Number of CRDS samples	IRMS [‰]	source
7.12.2015	-		-43.4 ± 0.5*	Gas storage (Xueref-Remy et al. 2019)
27.05.2019	-44.1 ± 4.1	5	-43.9 ± 0.5**	Plume 1
12.07.2019	-40.1 ±3.9	3	-	Plume 1

Gas compressor station C (Fontenay-Mauvoisin (FM), see also chapter 6.5.1.2.1.4)

The gas compressor station C is the last studied gas facility in IDF. It is situated 60 km north-west of Paris. Similar to gas compressor A, it is located in a rural area. This site hosts two compressors and one venting zone. Four surveys were conducted on this site, three to determine the isotopic composition and one to determine the emission rate.

During the first survey, the isotopic composition of the two plumes was measured. Likely, one plume came from venting zone and the second from area where two compressors are located. Two AirCore samples were taken for each plume. Averaged isotopic signature was equal to (-40.8 ± 5.7) ‰ for the first plume and (-45.2 ± 6.2) ‰ for the second plume (Fig. 6.5.26).

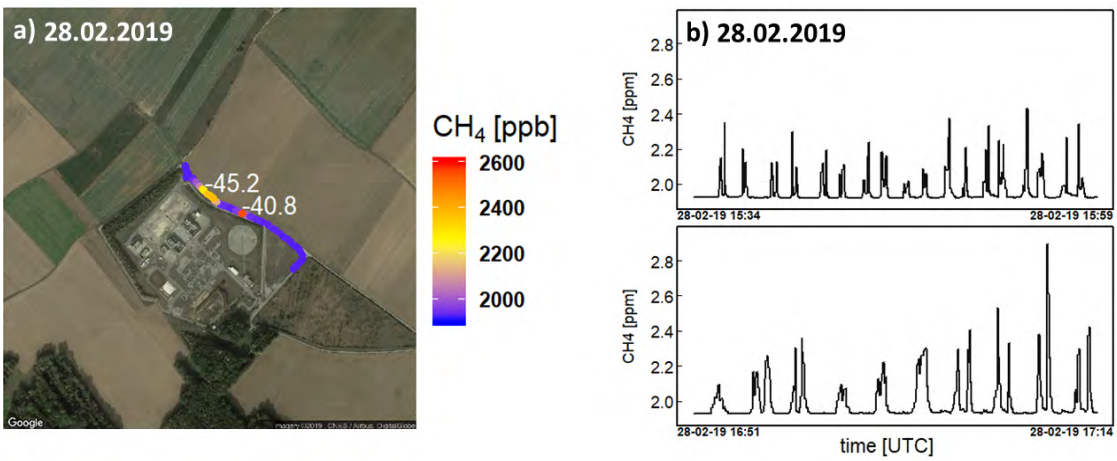

Fig. 6.5.26: Gas compressor station C. Observed CH_4 mixing ratio above background. The white numbers indicate $\delta^{13}CH_4$. Background is not subtracted. b) multiple crossing of the CH_4 plume.

That day, bag samples were also collected and sent to RHUL and UU to measure with IRMS. The $\delta^{13}CH_4$ was equal (-41.0 ± 3.5) ‰ and (-43.5 ± 1.2) ‰, at RHUL and UU, respectively (Table 6.5.16). Results obtained by the two IRMS instruments differ and have much bigger uncertainty (calculated as the uncertainty of the fitting regression in the Keeling method) than during studies on gas compressor stations A and B and landfills D and E. Even though, the results still agree statistically within 1 sigma uncertainty.

Table 6.5.16: $\delta^{13}CH_4$ observed for gas compressor C. CRDS results in this study are determined using the AirCore tool. For IRMS measurements, bag samples were taken and sent * to RHUL or ** to UU.

Date	CRDS [‰]	Number of CRDS samples	IRMS [‰]
28.02.2019	-40.8 ± 5.7 (plume 1; venting zone)	2	-41.0 ± 3.5*
	-45.2 ± 6.2 (plume 2; compressors)	2	-43.5 ± 1.2**
28.05.2019	-49.6 ± 5.4	1	-43.9 ± 0.4 **
12.03.2020	-		-43.8 ± 0.2**

There are two possible explanations of the observed bigger uncertainties. First of all, the observed CH_4 enhancement was small (< 600 ppb above background) for isotopic samples. During AirCore sampling, the maximum observed CH_4 enhancement above background reached 450 ppb. This relatively small enhancement is below CRDS limit to measure isotopic signature and cause larger uncertainty of detected value, as for isotopic sampling CH_4 enhancement should reach at least 500 ppb (e.g., Lopez et al. 2017; Hoheisel et al. 2019; Defratyka et al. 2020). Also, during bag samples collecting, CH_4 concentration varied between 1950 ppb and 2140 ppb, which is bellow required 500 ppb enhancement above background. Second, that day the wind was quite strong and changing over time, which caused the mixing of these two plumes in different proportions and during part of transects, only one plume was observed. Fig. 6.5.26b presents changes in the shapes of observed CH_4 plumes and their overlapping during part of transects. Unfortunately, during that day, the wind station did not work, so it is impossible to provide any detailed information.

Three months later (28.05.2019), four AirCore samples were measured on the gas compressor station C. However, due to low CH_4 enhancement, three were rejected from further analysis as it caused large uncertainty and low r^2 coefficient correlation. $\delta^{13}CH_4$ isotopic signature determined from remaining sample was equal to (-49.6 ± 5.4) ‰, with $r^2 = 0.95$.

On 28.05.2019 bag samples were also taken to analyze later at IRMS. Isotopic signature from IRMS reached (-43.9 ± 0.4) ‰ and it is more enriched than isotopic signature from CRDS instrument ((-49.6 ± 5.4) ‰). The isotopic signature from IRMS is similar to the other values, observed during summer 2019 in gas compressors A ((-43.0 ± 2.9) ‰) and B ((-40.1 ± 3.9) ‰). Moreover, an isotopic signature of (-49.6 ± 5.4) ‰ obtained from CRDS analyzer is more depleted than other isotopic signatures determined for gas facilities in IDF both in this study and in the study made by Xueref-Remy et al. (2019). It suggests that, the value from CRDS should be rejected and could be caused by some instrumentation problems (e.g., leaking tubing in the mobile set-up).

Finally, the last survey to measure the isotopic composition was conducted on 12.03.2020. That day, the CRDS G2201-i was not available, and only bag samples were collected to measure on IRMS at UU. That day, determined $\delta^{13}CH_4$ was in good agreement with results from the second survey and reached (-43.8 ± 0.2) ‰.

In addition to measurements of the isotopic composition, one day (29.05.2019) was dedicated to estimating CH_4 emission rate of the gas compressor station C. That day only one CH_4 plume was observed, and 30 transects were made (Fig. 6.5.27). The meteorological conditions were similar to the conditions on gas compressor station A during the survey dedicated to making multiple transects. The wind speed varied between 0.01 m/s and 3 m/s with mean wind speed of 1.3 m/s, and the insolation was moderate.

Similar to gas compressor station A, due to the challenge to identify a single stability class, the emission rate was calculated using two stability classes: A and B. The emission rates were calculated in the same way as for gas compressor station A. For that day, the calculated emission rate reached 0.81 ± 0.13 kg CH_4 h^{-1} using stability class A and 0.55 ± 0.09 kg CH_4 h^{-1}, using stability class B. As plumes from stability class A match better to plumes from observations, possibly estimations using stability class A are closer to reality.

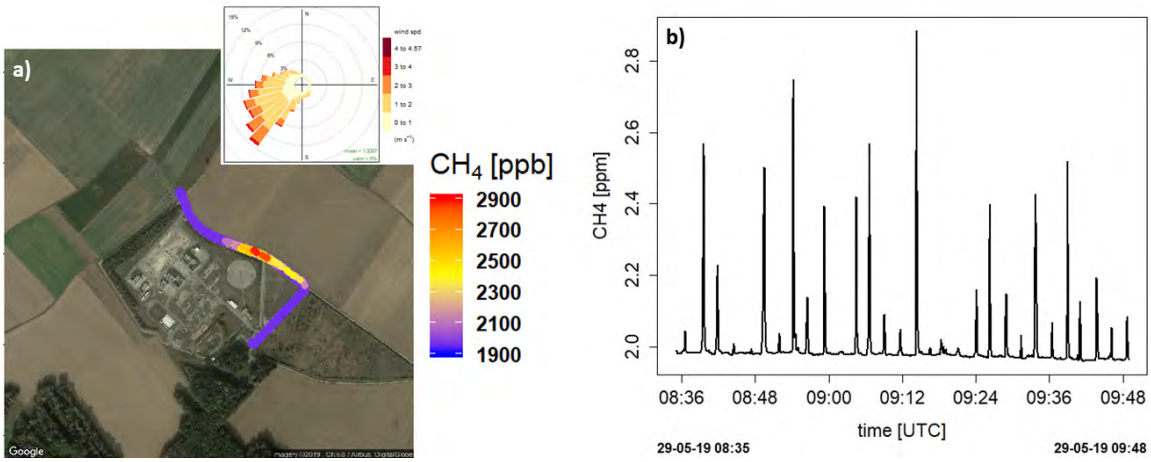

Fig. 6.5.27: Gas compressors C, 29.05.2019. a) Observed CH_4 mixing ratio with rose wind b) multiple crossing of the CH_4 plume. Background is not subtracted

Landfill D (Butte-Bellot (BB), see also chapter 6.5.1.2.1.6)

Landfill D is situated about 35 km south-west of Paris, in a rural area with small villages and small industrial sites. The only possible access is on the road on the south side of the landfill (Fig. 6.5.28). Typically, from the road, one CH_4 plume from the active part of the landfill is observed. Depending on the meteorological conditions, it is also possible to observe a second, smaller plume from a close-by already closed landfill.

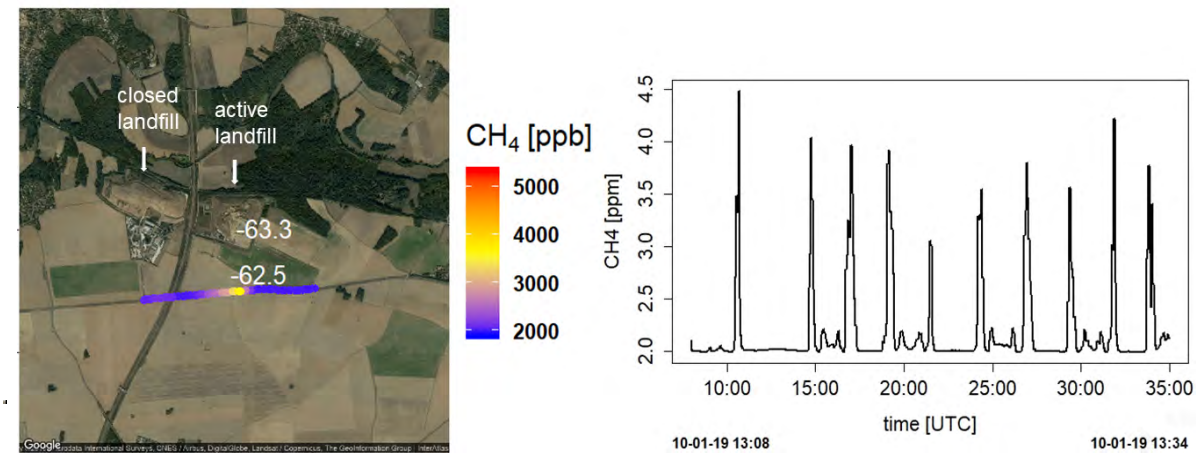

Fig. 6.5.28: Landfill D, 10.01.2019. a) Observed CH_4 mixing ratio above background. The white numbers indicate $\delta^{13}CH_4$ measured inside landfill (27.11.2018) and outside landfill (10.01.2019). b) multiple crossing of the CH_4 plume. Background is not subtracted

On 27.11.2018 and 10.01.2019, the isotopic composition was determined using a CRDS analyzer with an AirCore tool on the mobile platform and taking bag samples. Bag samples were analyzed afterward on IRMS at UU (Table 6.5.17).

Table 6.5.17: $\delta^{13}CH_4$ observed for landfill D. CRDS results in this study are determined using the AirCore tool, *** measured during crossing plume. For IRMS measurements, bag samples were taken and sent * to RHUL or ** to UU.

Date	CRDS [‰]	Number of CRDS samples	IRMS [‰]	References
08.12.2015	-		-63.2 ± 0.1*	Xueref-Remy et al. 2019
02.12.2016	-60.0 ± 1.3***	8	-	Assan 2017
27.11.2018	-63.3 ± 1.5	3	-63.0 ± 0.9**	this study
10.01.2019	-62.5 ± 1.1	3	-62.9 ± 0.5**	this study
16.05.2019	-		-64.4 ± 1.0**	this study

During the first day, measurements were made inside the landfill, while during the second day they were made outside the landfill. Using these two methods, obtained isotopic signatures are in good agreement and reached (-63.3 ± 1.5) ‰ during the first survey and (-62.5 ± 1.1) ‰ during the second survey, using CRDS analyzer. $\delta^{13}CH_4$ from CRDS are in good agreement with $\delta^{13}CH_4$ observed by IRMS instrument. They are also in good agreement the value obtained in 2015 by Xueref-Remy et al. (2019). $\delta^{13}CH_4$ from my study and study made by Xueref-Remy et al. (2019) are more depleted than the isotopic signature determined in 2016 by Assan (2017), equaled to (-60.0 ± 1.3) ‰. During study of Assan (2017), the $\delta^{13}CH_4$ was calculated from data obtained during crossing eight times a CH_4 plume, so when the car was in motion. As the motion of the car increases the fluctuation of measured $^{13}CH_4$, it could affect the measured $\delta^{13}CH_4$.

Finally, the last measurement of $\delta^{13}CH_4$ was made on 16.05.2019. During this survey, only bag samples were taken and isotopic signature was determined from IRMS measurements. The observed value was equal to (-64.4 ± 1.0) ‰. It was the only survey conducted in summer instead of winter. The value from summer survey is a bit more depleted than from surveys made during winter. However, they are still in good agreement within uncertainties.

Landfill E ((Gonesse (GNS), see also chapter 6.5.1.2.1.7)

Landfill E is situated 20 km north of Paris. This landfill is bigger than landfill D. The CH_4 plumes can be observed from different roads around the landfill, which suggest multiple sources of CH_4 inside the landfill and complex dispersion patterns (Fig. 6.5.29). The landfill is situated in a rural area with small villages. Two surveys were made on this landfill: on 25.01.2019 and on 01.03.2019 (Table 6.5.18).

During both surveys, the isotopic composition was determined using CRDS with the AirCore tool. In January 2019, $\delta^{13}CH_4$ was equal to (-57.4 ± 4.1) ‰, and in March 2019, it was equal to (-58.0 ± 3.2) ‰.

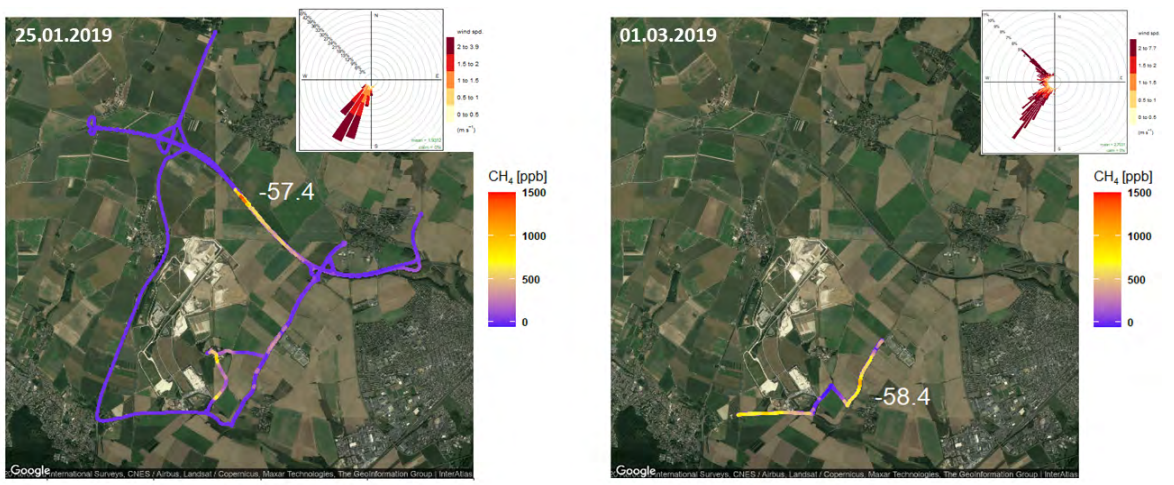

Fig. 6.5.29: Landfill E, observed CH_4 mixing ratio above background. The white numbers indicate $\delta^{13}CH_4$ [‰]. Inert plots - rose wind.

Moreover, in March, bag samples were also taken and measured afterward on IRMS at RHUL and UU. The obtained results are not statistically different within 1 standard deviation as from CRDS and reached (-58.1 ± 0.3) ‰ at RHUL and (-57.5 ± 0.4) ‰ at UU. The isotopic signature is in good agreement with the one determined in December 2015 (-58.2 ± 0.3‰) (Xueref-Remy et al. 2019). The isotopic signature of the landfill E is more enriched than for landfill D. It can be explained by the different waste composition (Liptay et al. 1998; Zazzeri et al. 2015). Additionally, CH_4 on landfill E could be partly oxidized. CH_4 oxidation by methanotrophic bacteria occurs when CH_4 produced in deep layers of landfill travels to topsoil. As ^{12}C is more preferably oxidized, emitted remaining CH_4 is more ^{13}C enriched (Chanton and Liptay 2000).

Table 6.5.18: $\delta^{13}CH_4$ observed for landfill D. CRDS results in this study are determined using the AirCore tool. For IRMS measurements, bag samples were taken and sent * to RHUL or ** to UU.

Date	CRDS [‰]	Number of CRDS samples	IRMS [‰]	References
10.12.2015	-		-58.2 ± 0.3*	Xueref-Remy et al. 2019
25.01.2019	-57.4 ± 4.1	1	-	this study
01.03.2019	-58.0 ± 3.2	2	-58.1 ± 0.3* -57.5± 0.4**	this study

Also, δDCH_4 can be used as an additional proxy to determine CH_4 source during mobile measurements. Currently, it can be done by collecting bag/flask samples and analyzed in the laboratory afterward. Here, for part of measurements sites, when bag samples were measured and sent to UU, δDCH_4 was also calculated (Table 6.5.19). δDCH_4 is reported in the international standard of Vienna Standard Mean Ocean Water (VSMOW). The bag samples are measured with the precision of 5 ‰ on IRMS (Röckmann et al. 2016). To determine δDCH_4, three bags were collected inside CH_4 plume and one bag outside, as a background sample. The same bag samples were analyzed to determine δDCH_4 and $\delta^{13}CH_4$ and Keeling approach (Pataki et al. 2003) was used for both isotopic signature.

Table 6.5.19: δDCH_4 observed in IDF. Bag samples were taken and sent to UU.

Type	site	date	δDCH_4 [‰]
Gas compressor	A	10.01.2019	-175.9 ± 3.7
	A	16.05.2019	-183.0 ± 3.6
Gas compressor	B	27.05.2019	-157.40 ± 0.66
Gas compressor	C	28.02.2019	-185.3 ± 11.0
	C	28.05.2019	-143.0 ± 17.0
	C	12.03.2020	-176.5 ± 8.3
Landfill	D	27.11.2018	-307.1 ± 1.2
	D	10.01.2019	-314.4 ± 1.7
	D	16.05.2019	-316.5 ± 4.1
Landfill	E	01.03.2019	-214.2 ± 2.7

In the case of gas compressor station A-C, δDCH_4 ranged from (-185 ± 11) ‰ to (-143 ±17) ‰, which is a bit less depleted than global average for thermogenic sources (-197‰) (Sherwood et al. 2017). In fact, the two extreme values come from gas compressor station C. Moreover, for site C, δDCH_4 uncertainties are typically one order of magnitude larger than for other sites (A, B, D, E). Likely, larger fluctuation and uncertainties are caused by relatively low CH_4 enhancement above background observed on site C. On the contrary, at gas compressor station A, CH_4 enhancement reached more than 1000 ppb and only a small difference was observed between δDCH_4 from the two surveys ((-175.9 ± 3.7) ‰ versus (-183.0 ± 3.6) ‰). Considering biogenic sources, on a global scale, δDCH_4 varies between -442 ‰ and -281 ‰ with average equals to -317 ‰ (Sherwood et al. 2017). For Landfill D, δDCH_4 was analyzed three times and varied between (-316.5 ± 4.1) ‰ and (-307.1 ± 1.2) ‰. The most enriched value was observed during first measurements on 27.11.2018. For the two remaining surveys, made 10.01.2019 and 16.05.2019, δDCH_4 did not change significantly. Overall, δDCH_4 of landfill D is similar to global average δDCH_4 for biogenic sources.

A different situation was observed for landfill E. Here, δDCH_4 reached (-214.2 ± 2.7) ‰, which is out of range from biogenic samples collected so far over the world. Emission of CH_4 with more enriched $\delta^{13}CH_4$ and δDCH_4 can be caused by CH_4 oxidation. The process occurs when CH_4 is produced in deep layers of landfill and travels to the topsoil (Chanton and Liptay 2000). Access to information about waste composition and age accumulated on landfill E would empower better data interpretation.

6.5.1.3 Future plans and expected results

First of all, I plan to resubmit two articles which are currently in the reviewing process and require some additional corrections. Then, I will contribute as co-author in four articles which are currently in preparation. First of them will present results from controlled release experiment, where I participated in 2019 as my secondment in the NPL. The second article will be a synthesis work about urban CH_4 emissions, based on the collaboration within Climate and Clean Air Coalition Methane Study. The third article will be based on the study made during CoMet campaign in 2018 about CH_4 emissions from coal mining in Upper Silesia. It will be focused on isotopic signature and emission rates estimated for individual venting shafts in the Upper Silesia region. The last article, where I contribute so far, will present results of mobile measurements made on one of landfills in the Île-de-France region.

6.5.1.4 Collaborations (internal / external)

During the reporting period, I participate in trace release experiment conducted by RHUL (James France) and NPL (Jon Helmore). That test allowed for verification of the methods used during my PhD. Part of the results will be included in my second paper. The main part of data will be published in the collaborative paper about this experiment. At the beginning of October, I helped my team during the TADI experiment made conducted by TOTAL.

We collaborated with GRTgaz company (National French Gas Transmission company), focused on estimation of emission rate for gas compressor stations. Based on it, a Master internship was made and resulted in a confidential Master Thesis “Estimation des émissions de méthane liées au transport du gaz naturel: comparaison d'approches top-down et bottom-up à l'échelle du site de compression” (Lozano 2020). Also, during the reporting period, I collaborated with GRTgaz, RHUL and NPL to prepare the article about C_2H_6 measurements using CRDS G2201-i.

6.5.1.5 Risks and difficulties

I had my defense 19.01.2021 and most of work connected with project is finished. So, I do not see any possible risks and difficulties.

6.5.2 Deliverables

D1.4 - Improved emission factors for different source categories from mobile measurement (month 42)

During the reporting period, I conducted numerous mobile measurements campaigns inside Paris city, on gas compressor stations and landfills. Both CH_4 mixing ratio and $\delta^{13}CH_4$ were in-situ measured during these surveys. During the secondment of ESR1 and ESR9 at LSCE, we were working with Polyphemus model to calculate emission from FM compressor station.

D1.5 - Report on harmonized method for mobile CH_4 and $^{13}CH_4$ (month 24)

Approved

D2.1 - Isotopic measurements linked to common scale (month 18)

Approved – isotopic measurements are ongoing

D2.3 - Publications on the use of isotopes for CH_4 source attribution in urban / industrial regions (month 36)

Submitted

17 surveys in Paris are already analyzed and described in the paper (waiting for the review from UNEP). Map of the concentration with isotopic composition of 11 sources was made (Paris with its west-south suburb). Location and source type of big and medium peaks were determined by the isotopic composition and walking measurements. Over summer time 5 additional measurements were made to determine seasonal variation.

Publication about measurements made in Paris, including ^{13}C isotopic signature is under review in Environmental Science & Technology.

D2.5 - Report providing isotopic maps at grid scale from inventories and atmospheric measurements (month 42)

Isotopic compositions of CH_4 sources are already calculated and presented in the first paper (paper in the review process). Isotopic compositions of landfills and gas compressor in the Ile-de-France region are already calculated and they will be published in the third paper and are contributing to the MEMO^2 isotopic database.

D3.2 - Improved bottom – up European emissions (month 30)

Surveys on gas station and landfills were made. The emission rates from these sites were estimated. Based on mobile measurements, the first estimations of ground-level CH_4 emissions in Paris city were made. Data will be used to improve bottom-up emission.

D3.3 - Forward modelling simulations of CH_4 and isotopologues (month 30)

Approved – improving of modeling simulations ongoing

6.5.3 Training and network activities

6.5.3.1 General training events

Event	Date (start – end)	Location (Host)	Objective / expected skills	ECTS points	Contribution
course	7.11.2017-30.01.2018	Universite Paris-Sud	Practical Data Analysis	30 h	participating
Language course	Whole time since november2017	LSCE	French course		Participating
1st MEMO2 school	05.02.2018 - 16.02.2018		physics and chemistry connected with greenhouses gases	160 h/ 6 ECTS	Participating
Isotopic workshop	17.09.2018-19.09.2018	RHUL	Measurement and data treatment of isotopic composition		Participating
Plume modeling workshop	09.10.2018-10.10.2018	UH	Plume modeling		Participating
2nd MEMO2 school	18.02.2018-22.02.2018	LSCE	Methane and society		Participating
Master internship	23/04/2019-31/08/2019	LSCE	Supervising, transfer of knowledge, teaching		supervision
2st follow up meeting	19/09/2019	LSCE	Presentation and discussion about results, ideas for next working year		Oral presentation
Workshop Scientific writing	12/11/2019-13/11/2019	Campus d'Orsay	Improve skills necessary for scientific writing	14h	participation
UNEP meeting	14/11/2019-15/11/2019	UNEP	Presentation of the results, international collaboration		oral presentation
GRTgaz meeting	29/11/19	GRTgaz	Start of the collaboration with French National natural gas company		oral presentation
Intensive French course	13/01/2020-24/01/20202	Sorbonne Universite	Improve French language	30h	participation
GRTgaz meeting	30/01/2020	LSCE	collaboration with French National natural gas company		Oral presentation
MEMO^2 meeting	12.10.2020	UU – online meeting	Annual MEMO^2 meeting to summarize last year progress	-	presentation

6.5.3.2 Secondments

Secondment	Date (start – end, planned (when))	Location	Host	Description of work / deviations	Scientific / training (skills) objective	Results and future plans
	17.06.2018-13.07.2018	Egham	RHUL	campaign for isotope measurements of CRDS (UVSQ) and IRMS (RHUL)/ comparison of	Build and using storage tube AirCore, calculation isotopic composition from in situ measurements	Plume mapping and source isotopic comparison, in the future - further comparison of obtained results

				measurements done by CRDs and IRMS		
NPL secondment	03/09/2019 – 17/09/2019	Egham/ Bedford	NPL	On the site: Preparation of the instrument, conduction of measurements, in LSCE: data treatment	Collaborative campaign, methods validation	publication

6.5.3.3 Conferences

Conference name	Date (start – end, planned (when))	Location	Presentation (oral/poster)	Title of presentation	Authors (main author + co-authors)	Public available (yes / no) / web link
3rd ICOS science conference	11.09.2018-13.09.2018	Prague	poster	Mobile measurement of CH_4 isotopes in urban, mining and industrial environments	Sara Defratyka, Camille Yver Kwok, Arjan Hensen, Jaroslaw Necki, Dave Lowry, Jean-Daniel Paris, Pawel Jagoda, Philippe Bousquet	no
EGU conference	08/04/19-12/04/19	Vienna, Austria	PICO session	Methane source mapping in Paris urban area from mobile measurement of mole fraction and isotopic composition	Sara Defratyka, Camille Yver-Kwok, Jean-Daniel Paris, Philippe Bousquet	Yes https://sharebox.lsce.ipsl.fr/index.php/s/avpXcncjQTXVlfO
NCGG8 conference	12/06/19-14/06/19	Amsterdam, Netherlands	Oral presentation	Mobile measurement of methane in Ile de France region – source mapping, isotopic composition & emission estimation	Sara Defratyka, Camille Yver-Kwok, Jean-Daniel Paris, Philippe Bousquet	Yes https://sharebox.lsce.ipsl.fr/index.php/s/0EIdZUPvNs163Hq
ICOS conference	15.09.2020-17.09.2020	online	poster	Characterization of natural gas compressor stations in Ile-de-France region: CH_4 emissions rate, C_2H_6:CH_4 ratio, and isotopic signatures ($\delta^{13}CH_4$)	Sara Defratyka, Camille Yver-Kwok, Jean-Daniel Paris, Mathis Lozano, Gregoire Broquet, Pramod Kumar, Malika Menoud, Thomas Röckmann, Philippe Bousquet	Available via SurfDrive

6.5.3.4 Measurement / sampling campaigns

Campaign	Date (start – end, planned (when))	Location	Host	Description of work	Scientific objective	Samples (nature / number)	Results and future plans
landfill	06.102017	Butte-Bellot, France	LSCE	Mobile measurement using acetylene as tracer	Estimation of emission from source	Mobile measurement with 20 transects	Estimated emission from landfill
MEMO² school	05.02.2018 - 16.02.2018	Netherlands		Continuous measurement from common inlet by CRDS analyzers from different PhD students, 3 mobile campaigns	Comparison of obtained value, first attempt to harmonize different methods	3 days of mobile surveys, one with using acetylene, continuously measurement 05.02-09.02	Estimated emission from landfill, further work with Polyphemus model on obtained data
Gas compressor station	19.01.2018	Beynes, France	LSCE	First attempt to measure site in Ile de France	Primary survey to optimize condition for further measurement	Mobile measurement	No further plans
Gas compressor station	05.03.2018	Limoges-Fourches, France	LSCE	First attempt to measure site in Ile de France	Primary survey to optimize condition for further measurement	Mobile measurement	No further plans
Gas compressor station	13.03.2018	Fontenay-Mauvoisin, France	LSCE	First attempt to measure site in Ile de France	Primary survey to optimize condition for further measurement	Mobile measurement	No further plans

CoMet	23.05.2018-10.06.2018	Sielsia, Poland	DLR, AGH	Mobile measurement in mining area: around mining shafts and in urban area	Better understanding of emission from mining industry in Poland, urban area source mapping	10 days of mobile measurement around mining shafts, 6 nighttime measurement of urban area	Urban source mapping, future plans – find probably emission source in Silesia urban area
secondments	17.06.2018-13.07.2018	South of United Kingdom	RHUL	Mobile campaigns with in situ measurement of isotopic composition, nighttime measurement from common inlet by CRDS and IRMS	Calculated isotopic composition of different source, comparison of results obtained by CRDS and IRMS	5 measurement campaign,4 with using storage tube, 3 nighttime measurement,	Plume mapping and source isotopic comparison, in the future - further comparison of obtained results
Paris urban area	07.09.2018, 25.09.2018, 26.09.2018	Paris	LSCE	Mobile measurement in Paris urban area	Source mapping in Paris urban area	3 measurement days	Not significant sources detected
Landfill	01/03/19, 29/05/19	Gonesse)	LSCE	Isotopic measurements and transects to calculate emission	Estimation of emission from source/ isotopic composition	3 AirCores, bag samples, 30 transects	Estimated emission further work with Polyphemus model on obtained data
Gas compressor	28/05/19, 29/05/19	Fontenay Mauvasin	LSCE	Isotopic measurements and transects to calculate emission	Estimation of emission from source/ isotopic composition	6 AirCores, bag samples, 40 transects	Estimated emission further work with Polyphemus model on obtained data
Gas compressor	05/03/19,16/05/19, 15/07/19	Limoges Fourche	LSCE	Isotopic measurements and transects to calculate emission	Estimation of emission from source/ isotopic composition	7 AirCores, bag samples, 30 transects	Estimated emission further work with Polyphemus model on obtained data
Gas compressor	27/05/19,12/07/19	Beynes	LSCE	Isotopic measurements and transects to calculate emission	Estimation of emission from source/ isotopic composition	14 AirCores, bag sample, 30 transects	Estimated emission further work with Polyphemus model on obtained data
city	05/03/19, 06/03/19, 07/03/19, 06/06/19, 07/06/19, 11/07/19, 16/07/19, 22/07/19	Paris	LSCE	Mobile measurement in Paris urban area	Source mapping/ isotopic composition	12 AirCores	Map of CH4 sources in Paris, analysis of seasonal variation

6.5.4 Dissemination activities

Type of scientific publication	Title of scientific publication	DOI	Authors	Title of journal or equivalent	Number of journal, month and	Year of publication	Relevant pages	Public/private publication	Peer review [yes/no]	Open access [yes/no],
article in journal	Quantifying CH4 emissions from hard coal mines using	https://doi.org/10.5194/a	Luther, A., Kleinschek, R., Scheidweiler, L., Defratyka, S.,	Atmospheric Measurement Techniques	Atmos. Meas.	2019	14	yes	yes	yes

	mobile sun-viewing Fourier transform spectrometry	mt-12-5217-2019, 2019	Stanisavljevic, M., Forstmaier, A., Dandocsi, A., Wolff, S., Dubravica, D., Wildmann, N., Kostinek, J., Jöckel, P., Nickl, A.-L., Klausner, T., Hase, F., Frey, M., Chen, J., Dietrich, F., Nęcki, J., Swolkień, J., Fix, A., Roiger, A., and Butz, A		Tech., 12, 5217–5230					
[article in journal]	Ethane measurement by Picarro CRDS G2201-i in laboratory and field conditions: potential and limitations	10.5194/amt-2020-410	Sara M. Defratyka, Jean-Daniel Paris, Camille Yver-Kwok, Daniel Loeb, James France, Jon Helmore, Nigel Yarrow, Valérie Gros, and Philippe Bousquet	Atmospheric Measurements Techniques Discussion		-		24	Yes	yes
[thesis]	Characterization of CH_4 emissions in urban environments (Paris)	2021UPASJ002	Sara Defratyka			2021	Université Paris Saclay	171	Yes	yes

Dissemination activity	Name	Date	Location	Type of audience	Size of audience
Blog note on MEMO^2 website	MEMO^2 at CoMet	25.06.2018	https://h2020-memo2.eu/category/blog/	general	

6.6 ESR6 - Mid-infrared laser spectroscopy for three dimensional CH4 mapping by unmanned aerial vehicles (UAV)

ESR6

Mid-infrared laser spectroscopy for three dimensional CH_4 mapping by unmanned aerial vehicles (UAV)

ESR	Jonas Ravelid, jonas.ravelid@empa.ch
Supervisor	Lukas Emmenegger, lukas.emmenegger@empa.ch
Co-supervisor	Huilin Chen, huilin.chen@rug.nl
Non-academic mentor	N.A.
Official start-end date	02.12.2018 – 31.05.2020

6.6.1 Scientific progress

6.6.1.1 Project introduction and objectives

One limitation for field measurements of methane is the currently available methane detectors. They are mostly large and bulky, requiring a car or at best a case being carried in the field, meaning that measurements are restricted to ground level and where driving or walking is permitted/possible.

A platform for scientific instrumentation that has gained prominence over the last decade is unmanned aerial vehicles (UAVs), or drones. Their capability to lift heavier objects is still very limited however, and there are currently very few methane detectors that are light enough to be mounted on a drone while simultaneously offering high quality methane detection.

To fill this niche, Empa is developing a Quantum-Cascade Laser Absorption Spectrometer (QCLAS), for detection of methane, within the MEMO^2 consortium. The device should allow ppb precision and simultaneously be light enough (<2 kg) to be mounted on a drone. It also needs to fulfil other criteria related to drone flights, such as low power consumption and, ideally, instantaneous wireless transfer of data. In short, the instrument should allow in-situ measurements with real-time concentration reporting in three spatial dimensions.

6.6.1.2 Project results

The past reporting period has been dominated by two important MEMO^2 collaborations; the ROMEO campaign and a secondment at Lund University (LU). Furthermore, many local tests and improvement have been carried out at the host institution, Empa. Finally, Empa recently hosted ESR2 during one month of secondment. This occurred in conjunction with the local measurement campaign, which was named Dübendorf Release Experiment (DüReX).

While the Lund University secondment had to be cut short due to issues with the drone system and yielded little scientifically reliable data, both the ROMEO and the DüReX campaign, provided a wealth of valuable results.

6.6.1.2.1 Third year

6.6.1.2.1.1 Secondment at Lund University – Wetlands Measurements

The Lund University secondment took place in September 2019 in Sweden, in collaboration with ESR 4 at LU. The aims of the secondment were the following:

- Perform an altitude profile, investigating the local CH_4 concentration altitude gradient and comparing the results with the LU Picarro system, which is connected to gas inlets at several altitudes on a mast located close to a wetland at the Hyltemosse research station.
- Investigate the feasibility of drone-based CH_4 concentration measurements over bogs as a way of identifying CH_4 hot-spots, possibly connecting detected hot-spots to local variations in bog characteristics and/or flora. This test was to be performed over the Mycklemosse bog.

- Use the drone during an intercomparison measurement campaign, organized by MEMO² partner Avfall Sverige, measuring methane release from landfills.

Due to issues with the drone system and the QCLAS, as well as problematic weather, none of the three goals was fully achieved.

The first experiment, at the Hyltemosse research station, was made impossible by a lightning strike in the mast on the first day, damaging the Picarro on site. Therefore, no comparison could be made. Furthermore, a faulty update of the drone software rendered vital drone flying aids defunct, making flying the system difficult at best, hazardous at worst.

The second experiment still suffered from the drone flying problems but was more forgiving when it came to flight location (open marshland instead of a small open space in dense forest). On the other hand, the QCLAS performance had deteriorated significantly during the travel from Switzerland to Sweden and with no tools available to diagnose the cause and readjust the system, the precision of the instrument remained significantly below its potential.

During the Mycklemossen measurements, the instrument precision was on the order of tens of ppb. Originally, the expected methane concentration fluctuations were expected to be at least one order of magnitude larger than that. The observed fluctuations were, however, on the same order of magnitude as the instrument precision. Consequently, no conclusions could be drawn from these measurements except for the methane concentration of the Mycklemossen bog being more homogenous than expected. To illustrate this, a heat map from one of the measurements is displayed in Fig. 6.6.1. The precision for this particular measurement is 10 ppb, given by the Allan deviation at 1 Hz from a pre-flight reference measurement taken over five minutes just before the flight.

Fig 6.6.1: The detected CH_4 concentration, above background, over the Mycklemossen bog is displayed.

The hope was that the drone-based measurements would allow for the localization of methane concentration hotspots over the bog. However, the detected methane concentration fluctuation was smaller than expected, especially compared to the uncharacteristically large Allan deviation of the QCLAS, for the flight shown here approximately 10 ppb. This, in conjunction with difficult flying conditions leading to poor realization of the desired grid-based sampling pattern, let to the results being discarded as too unreliable. No conclusions about hotspots were made. After three days spent at Mycklemossen, the decision was made to terminate prematurely to allow more time to solve the problems experienced during the secondment, ahead of the start of the ROMEO campaign in October-November 2019, which was deemed more important to the project as a whole. Consequently, the QCLAS did not take part in the Avfall Sverige campaign.

6.6.1.2.1.2 ROMEO Campaign

The problems encountered during the secondment at LU were addressed in the second half of September. Then, Empa took part in the ROMEO campaign in October-November 2019.

A total of 35 sites, mainly oil wells, were measured using a mass balance approach where curtains were flown 30-70 m downwind of the site, probing the CH_4 plume to allow ESR 12 to estimate a facility emission rate.

The total number of measurements were 56 mass balance curtains and 21 measurements using OTM 33A (Assuming 20 min OTM 33A per measurement). The total measurement time for OTM 33A was 7 hours, 10 minutes.

Apart from minor field tests conducted in Switzerland, this was the first real field test of the system for source quantification and detection of a large range of CH_4 concentrations. In fact, the concentrations encountered during ROMEO were sometimes significantly larger than expected. One exemplary case is shown in Fig. 6.6.2, which illustrates the extremely wide dynamic range of the QCLAS, resolving peaks from a few ppm to over 400 ppm.

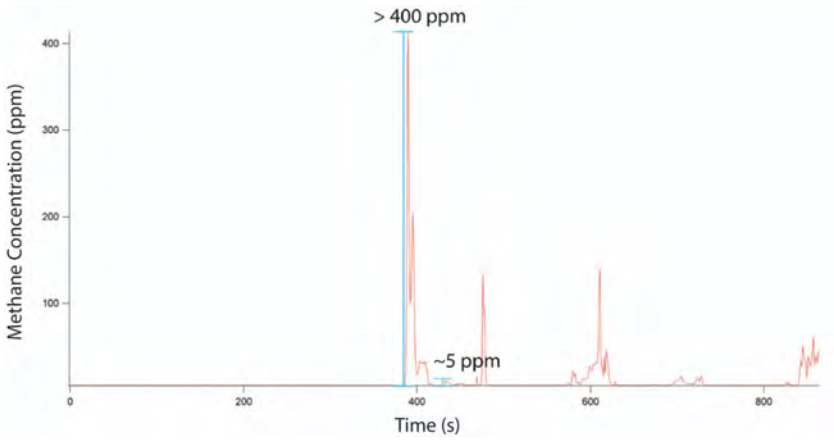

Fig. 6.6.2: A methane concentration measurement illustrating the wide range of concentrations the QCLAS can detect accurately. Marked in blue are two peaks, the high peak and a (comparatively) low peak just after. Both are easily distinguishable from background fluctuations.

Additionally, the CH_4 concentration detected during another facility measurement, at different altitudes, are shown in Fig. 6.6.3 to give an overview of how a standard facility measurement was performed. Note that the x-axis is time and the plume was probed at each altitude twice, as the drone was flown back and forth, downwind of the source and perpendicular to the wind direction, before increasing the altitude.

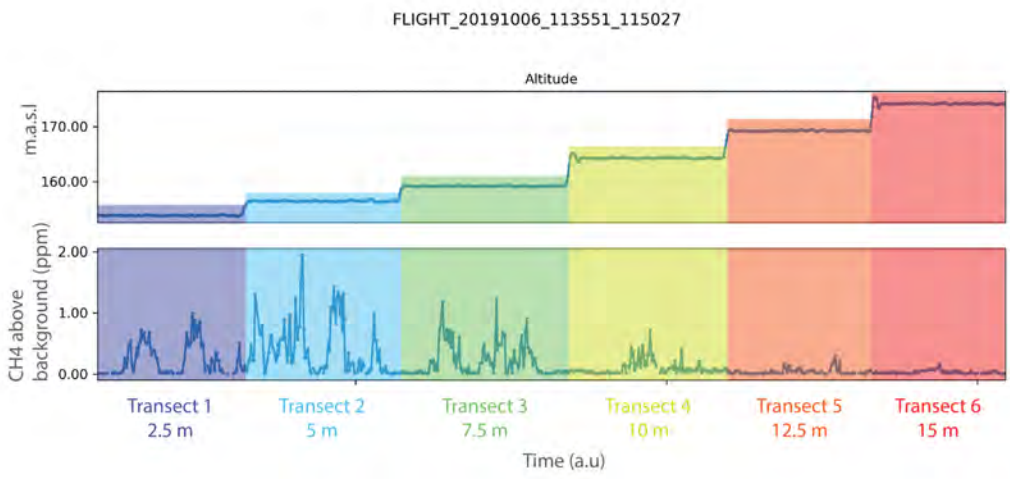

Fig. 6.6.3: The altitude (top) and detected concentration (bottom) during a mass balance measurement from the ROMEO campaign are plotted against time. Furthermore, each pair of horizontal transects of the plume at a specific altitude is shaded with a distinct color, with its corresponding altitude above ground given underneath, in the same color. The performance of the device is, in this case, good enough to distinguish peaks in methane concentration down to a few hundred ppb, more than enough to properly quantify the emissions from this facility.

Apart from producing high-quality data with the QCLAS system, the ROMEO campaign gave an opportunity to investigate some other aspects of the measurement regime: the altitude precision of the drone system and the feasibility of on-board wind measurements on the drone.

The conclusion drawn for altitude reporting was that the altitude precision inherent in the drone system was inadequate for precise source release quantification and that alternatives should be investigated. On-board wind measurements are not dismissed but there are a number of challenges that have to be investigated. This includes the inherent difficulty in accounting for drone movement and the influence of turbulence from drone propellers.

Originally, the altitude was originally taken from the drone manufacturer's (DJI) algorithm which is not transparent and includes GPS data and pressure measurements. To increase efficiency and obtain more reliable location and altitude data, a so-called RTK GPS system was integrated, which offers outstanding accuracy. The system is in the final stages of implementation.

The investigation of drone-based wind measurements is ongoing. First results indicate disagreement with tests performed by other parties and thus require more in-depth investigation.

6.6.1.2.1.3 DüReX Campaign

The DüReX campaign took place in February-March 2020 and involved the drone QCLAS system, the AirCore system from the University of Groningen and the LGR system from the University of Heidelberg (UHEI). ESR 2 visited Switzerland for a full month of secondment and ESR 1 visited from Heidelberg for one week. Additionally, ESR 12 contributed to the fieldwork and is responsible for the emission rate estimations based on the measurement data.

The research question to be answered was the following: How well can the release rate of a natural gas source, with a known release rate, be estimated using the techniques applied during ROMEO? The techniques to be investigated were the mass balance approach utilized by both Empa and University of Groningen, and the OTM 33A technique used by the group from University of Heidelberg.

6.6.1.2.2 Fourth year

The employment of ESR 6, Jonas Ravelid, ended on May 31, 2020. Therefore, only 3 month (01.03.2020 – 31.05.2020) are reported for the fourth year.

The last time period of ESR3 focussed on further evaluation and publication of data. Also, an additional validation campaign was performed in Beromünster, Switzerland (Fig. 6.6.4).

Beromünster is a unique location in the Swiss midlands. It is located in a moderately hilly environment at the southern border of the Swiss Plateau. Here, a former radiotower (47_ 1102300 N, 8_ 1003200 E, 212:5m tall, base at 797ma.s.l.) is equipped with air inlets at 12, 44, 71,131 and 212 m. A cavity ringdown spectrometer (CRDS; G2401, Picarro Inc., USA) monitors the mole fractions of CH_4 at these five different heights sequentially, sampling each height for 3 min. Therefore, this tower allows the validation of the mobile measurements under real field conditions in comparison with a high-performance reference instrument that is calibrated with traceable reference gases. The field test took place on a day with stable atmospheric conditions, when methane accumulates during night-time in a shallow nocturnal boundary layer near the ground. Fig. 6.6.4 shows drone flights at the Beromünster tower and the CH_4 time series provided by the CRDS analyser for the selected day. Consistent with our expectations, the data indicate a pronounced gradient among the inlet heights during the time period before sunrise. This concentration build-up then slowly disappears after sunrise due to breakup of the nocturnal boundary layer by convective vertical mixing. The sensor's precision was adequate to easily resolve the vertical gradients of atmospheric methane. The CH_4 mole fractions typically varied between 1940 and 2200 ppb, with some exceptional cases, when sudden increase in CH_4 mole fractions of up to 3200 ppb were observed close to ground over time periods of tens of minutes. These short-term spikes can be attributed to pollution events, due to emissions from the farmsteads (ruminants) in the close vicinity (200 m) of the tower.

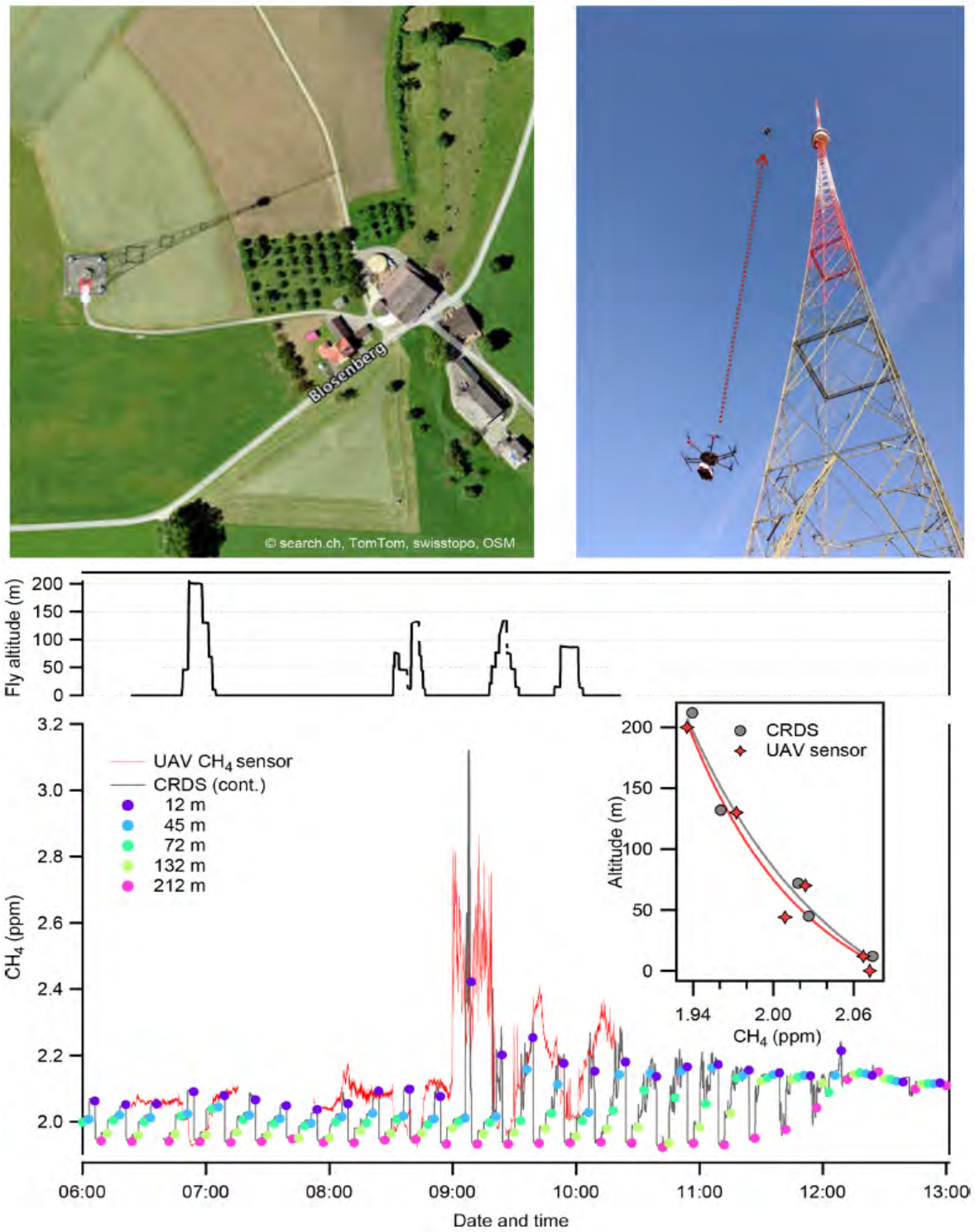

Fig. 6.6.4: Satellite image of the area used for profiling (top left). Photograph of the drone flying at various heights in the vicinity the radio tower (212 m) at Beromünster (top right). Vertical profile measurements of atmospheric methane (bottom). The concentration gradient is clearly observable until noon, when the nocturnal boundary layer is broken up by convective vertical mixing. The gray trace represents the continuous, while the colored dots indicate the mean CH_4 concentration values at various heights as measured by a ground-based CRDS analyzer. The UAV methane instrument (red trace) performed four flights covering the altitude span between 0 and 200 m. The inset shows the comparison of the profile data collected by the two analyzers. The concentration gradient is well captured in both cases

6.6.1.3 Future plans and expected results

The ESR's employment contract finished at the end of May 2020. Therefore, contributions to MEMO^2 were finishing the data post-processing from the DüReX campaign, documentation and knowledge transfer. On more general terms, the results from the measurements performed during this reporting period are expected to lead to the following scientific publications:

- Description and validation of the QCLAS system, to be submitted in March.
- Scientific publications resulting from the ROMEO campaign, specifically those involving drone-based measurements.
- Performance review of the mass balance measurement methodology, mainly based on the DüReX campaign.

6.6.1.4 Collaborations (internal / external)

In addition to the ROMEO campaign, where almost all members of MEMO2 were involved, intensive collaboration involved ESR 1, 2 and 12, as described above. A joint campaign with Avfall Sverige and DTU had also been planned for the second half of the LU secondment but participation was cancelled, as explained above.

6.6.1.5 Risks and difficulties

No significant risks and difficulties beyond the ones described above

6.6.2 Deliverables

D1.1 - Lightweight CH_4 sensor and AirCore developed and deployed on UAV (month 24)

Approved – activities are ongoing

ESR 6 was responsible for the lightweight CH_4 sensor development. This goal has been fully met or even exceeded. The sensor has been validated on the UAV, it has exceeded the original specifications, and it has provided reliable results in several campaigns, and in validation excercises which also included the AirCore.

Although approved, the deliverable was further developed. While the spectroscopic performance of the instrument has remained nearly constant, relevant improvements have been made to several relevant sub-systems. Progress has been made in in the overall design of the instrument, e.g. by redesigning the structure covering the instrument to allow for better cooling and ventilation and by constructing a new detector mounting, as the old mounting was noted to be structurally unstable enough to affect the performance of the instrument. Finally, a more precise GPS-module has just been implemented, and the feasibility of on-board wind measurements is being investigated.

Apart from this, a lot of surrounding infrastructure has been developed over the past reporting period to allow for smoother and more efficient in-situ measurements in many aspects. Most notably, drone batteries can now be charged in the field, to allow a larger number of consecutive flights.

D1.2 - Report/publication on CH_4 emissions from wetland and lakes in Sweden (month 24)

ESR 6 has performed several measurement campaigns during his secondment at Lund Universitiy as described above. For several reasons (drone technology, sensor failure, weather conditions), the drone measurements were strongly limited, and did not contribute to the quantification of wetland emissions.

D1.4 - Improved emission factors for different source categories from mobile measurements (month 42)

All of the ROMEO data and meta-data has been finalized, documented and published in the corresponding channels. The drone measurements did strongly contribute to the quantification of different sources in the oil and gas industry in Romania. The corresponding results are to be described and published separately.

6.6.3 Training and network activities

6.6.3.1 General training events

Event	Date (start – end)	Location (Host)	Objective / expected skills	ECTS points	Contribution	Comments
Laboratory seminar	13.09.2017 – 14.09.2017	Sigriswil	Team building event	-		
Aquatic Chemistry group retreat	29.11.2017 – 31.11. 2017	Waltensburg	networking activities and general PhD training course, workshop on scientific writing	-	Short presentation of project	
Drone training (theory)	07.12.2017	Empa, Dübendorf	Theoretical introduction for using a UAS	-		Realised by Koller Engineering
Drone training (practice)	15.12.2017	Zwillikon	Practical training on how to fly a drone	-		Realised by Koller Engineering
MEMO² School	05.02.2018 – 16.02.2018	Schoorl, Netherlands	Methane measurements and modeling	6	preparation of a poster and the analyses of data	
Annual Memo2	22.03.2018	Empa, Dübendorf	Networking event		Presentation, poster	
PhD congress	06.04.2018	Institute of Biogeochemistry and Pollution Dynamics at ETH Zurich	Phd congress for networking		Poster	
Drone training	07.06.2018	Empa, Dübendorf	Practical training with the Matrice 600 drone			Realised by Koller Engineering
Presentation Course	Feb 2019-July 2019	Empa	Improved skills in presenting research results efficiently	-	Participation	Participation aborted due to secondment and ROMEO

6.6.3.2 Secondments

Secondment	Date (start – end, planned (when))	Location	Host	Description of work / deviations	Scientific / training (skills) objective	Results and future plans
Secondment at Lund University	20190826 - 20190915	Sweden	Lund University	Bringing the QCLAS and drone system to Sweden. Do measurement flights to investigate the questions posed earlier. Measurement campaign at landfill with Avfall Sverige and DTU had to be cut due to aborted secondment on the 15:th.	Altitude gradient comparison with Hyltemosse research station Picarro and feasibility test for using drone-based measurements for hot-spot localization over wetlands at Mycklemossen.	Unexpectedly small concentration range at Mycklemossen identified. Value of results very limited due to lacking data quality and drone problems. Therefore, the secondment was ended prematurely.
Secondment with UHEI during ROMEO	20190930 - 20191020	Romania	INCAS	Driving between oil- or gas facilities in rural Romania and doing drone flights, measuring methane in order to allow a quantification estimation	Assist in the ROMEO campaign and measure chosen facilities, based on facility screening done by ESR 1 and UHEI.	All data sent to ESR 12 after post-processing to be used for facility release rate estimations. Furthermore, ESR 1 has gotten access to all data relating to OTM 33A from the campaign.

6.6.3.3 Conferences

The ESR has not participated in conferences due to the reduced contract.

6.6.3.4 Measurement / sampling campaigns

Campaign	Date (start – end, planned (when))	Location	Host	Description of work	Scientific objective	Samples (nature / number)	Results and future plans

MEMO² School*	05.02.2018 – 16.02.2018	Schoorl, Netherlands	RUG	Mobile measurements with cars, methane release experiment	For training purpose		
Test Flight 1*	2018.08.10	Empa, Dübendorf	Empa	Test flight with mobile methane spectrometer	First test for the assessment of measurement characteristics during flight conditions.	CH4 concentration with 2Hz resolution, additional: H2O conc., T, p, GPS pos.	Results can be used for quantifying and improving the stability of the spectrometer, further test flights are planned
Test Flight 2*	2018.10.10	Empa, Dübendorf	Empa	Test flight with mobile methane spectrometer	Testing a slightly modified setup and the observation of artificial methane release.	CH4 concentration with 2Hz resolution, additional: H2O conc., T, p, GPS pos.	Results can be used for quantifying and improving the stability of the spectrometer, further test flights are planned
ROMEO	20190930 - 20191020	Romania	INCAS	Drone measurements at oil- or gas facilities in rural Romania for emission quantification.	Assist in the ROMEO campaign	Total number of sites: 35 Mass balance measurements: 56 OTM 33A Measurements: 21 (7 h 10 min) All sites include wind data as well as GPS-position, temperature and pressure of the QCLAS.	All data sent to ESR 12 after post-processing to be used for facility release rate estimations.
DüReX	20200213 - 20200316	Dübendorf, Switzerland	Empa	Create a set-up with a controlled release for natural gas in the field. Fly the QCLAS and AirCore systems on the drone a large number of times.	Investigate the performance of the mass balance approach as well as OTM 33A, at different distances and at different source flows.	Mass balance measurements: 35	Post-processing still ongoing. Should result in a publication on the performance of the mass balance approach.

*Executed by the previous ESR6

6.6.4 Dissemination activities

Type of scientific publication	Title of scientific publication	Authors	Title of journal or equivalent	Place of publication	Year of publication	Peer review [yes/no]	Open access [yes/no]
Oral presentation	Quantum cascade laser spectroscopy for high-precision measurements of atmospheric trace-gases and their isotopes	L. Emmenegger et al.	Journées de Spéctroscopie Moléculaire	Paris, France	2019	No	No
Oral presentation	Recent developments in environmental trace gas sensing using quantum cascade lasers	L. Emmenegger et al.	Research Seminar at MIT	Boston, USA	2019	No	No
Oral presentation	A high-precision mid-IR methane laser spectrometer for UAVs	L. Emmenegger et al.	Non-CO_2 Greenhouse Gas Conference	Amsterdam, NL	2019	No	No
Oral presentation	Environmental and industrial trace gas sensing using quantum cascade lasers	L. Emmenegger et al.	Optical Sensors and Sensing Congress	San Jose, USA	2019	No	No

Oral presentation	Tracking molecules from the ground to the sky. Multi-wavelength QCLs in mobile analyzers	B. Tuzson et al.	PhotonIcs & Electromagnetics Research Symposium (PIERS)	Rome, It	2019	No	No		
Oral presentation	A high-precision laser spectrometer for methane monitoring aboard UAVs	B. Tuzson et al.	Industrial Methane Measurement Conference (IMMC)	Rotterdam, NL	2019	No	No		
Oral presentation	A compact QCL absorption spectrometer for mobile, high-precision methane measurements aboard drones	B. Tuzson et al.	EGU	Vienna, Au	2019	No	No		
article in journal	A compact QCL spectrometer for mobile, high-precision methane sensing aboard drones	10.5194/amt-13-4715-2020		Tuzson, B., Graf, M., Ravelid, J., Scheidegger, P., Kupferschmid, A., Looser, H., … Emmenegger, L.	Atmospheric Measurement Techniques	13(9), 4715-4726	Copernicus		2020
publication in conference proceedings / workshop	Quantum cascade laser spectrometers for mobile trace-gas sensing			L. Emmenegger, M. Graf, P. Scheidegger, H. Looser, J. Ravelid, A. Kupferschmid, B. Tuzson	OSA High-brightness Sources and Light-driven InteractionsCongres	MTh5C.2	OSA Publishing		2020
publication in conference proceedings / workshop	Cought in Flight			Cornelia Zogg	Empa Quarterly	May 2020	OSA Publishing	Düben dorf	2020

6.7 ESR7 - CH_4 from waste: constraints on captured and fugitive emissions from isotopic analysis

ESR7

CH_4 from waste: constraints on captured and fugitive emissions from isotopic analysis

ESR	Semra Bakkaloglu (semra.bakkaloglu@rhul.ac.uk)
Supervisor	Dave Lowry (d.lowry@rhul.ac.uk)
Co-supervisor	Huilin Chen (huilin.chen@rug.nl)
Non-academic mentor	Stuart Davies (SDavies@viridor.co.uk)
Official start-end date	08/01/2018- 30/09/2020

6.7.1 Scientific progress

6.7.1.1 Project introduction and objectives

As mitigation of climate change is a key scientific and societal challenge, CH_4 emissions are a major contributor to Europe's global warming impact and emissions are not well quantified yet. There are significant discrepancies between official inventories of emissions and estimates derived from direct atmospheric measurement. Effective emission reduction can only be achieved if sources are properly quantified, and mitigation efforts are verified. Globally, human activities produce over 60 % of total CH_4 emissions, with 22 % of emissions from the energy sector and 10 % from the waste sector.

CH_4 from waste is dominantly of biogenic origin and can vary with temperature and production process, which results in variation of emissions with time of day and time of year. In addition, the waste sites now commonly produce and combust this biogas, and emissions from each component can be identified by analysing the CH_4 isotopic composition, as different source types are characterized clearly by distinct $\delta^{13}C$ signatures. For landfill sites in particular a percentage of the CH_4 produced is oxidised by soil cap or oxygen in upper-levels of less-compacted waste and this results in a different isotopic signature to non-oxidised CH_4 in the gas extraction system.

This project includes the measurement and modelling the plume of CH_4 originated from waste processing sites at different times of year under different meteorological conditions, using mobile equipment. Moreover, off-site plume samples will be collected for isotopic characterization. Selected sites will be studied in more detailed using isotopic characterization of emission plumes from individual site components such as active and remediated landfill cells, gas combustion plants, anaerobic digestion cells. Gas wells will be sampled to characterize un-oxidized CH_4 to aid in the understanding of on-site oxidation rates.

The main objectives of this project are:

- Estimate the biogas emission rates and characterize their ^{13}C isotopic signature depending on different kind of feeding material.
- Sample CH_4 plumes and gas wells on sites of project partner Viridor and use the isotopic difference to assess the role of oxidation of fugitive emission considering the seasonal variation.
- Characterize the waste sources isotopically by collecting offsite plume samples from individual site components such as sewage emission, active and remediated landfill cells, biogas plants for selected sites.

6.7.1.2 Project results

6.7.1.2.1 Third year

6.7.1.2.1.1 Characterization and Quantification of Biogas Plant Emissions in the UK

In the UK, the waste sector contributed 36% of total CH_4 emission in 2017 [1]. Fugitive emissions from major sources are not yet well quantified. Most of the biogas plants have started operation in the last few years and a significant number of them have not been included in emissions inventories. During March 2019 to March 2020, ESR7 investigated 55 biogas plants in the UK to detect CH_4 emissions. However, 37 of the biogas plants have no emission on the survey day because it was not possible to get close enough to 8 of them and the wind direction and plume location could not be properly transacted by the public road for 7 other plants. Of the remaining 22 where wind direction was suitable and distance from installation small, these may not have been emitting at the time of survey. Emission plumes were encountered from 18 of 53 biogas plants, eight biogas plants were not taken into account for emission rate calculation because they were close to other CH_4 sources such as landfill and composting facilities and the plume shape was not suitable for Gaussian plume modelling. Therefore, ten of the biogas plants with suitable plume emissions were selected for further research and repeat surveys in this study shown in Table 6.7.1.

Table 6.7.1: Surveyed Biogas Plants

Number	Biogas Plant	Main Substrate(s)	Total feedstock (tonnes)	Gas Utilization	Day of Measurement	Number of Gaussian Plume
1	Arla AD	Commercial Food Waste	50000	BtG&CHP	06-12-2018 01-11-2019	5
2	Greentye AD	Vegetable outgrades	10000	CHP	06-12-2018 01-11-2019	6
3	Buttermilk	Maize Sludge	20000	CHP	06-12-2018 01-11-2019	3
4	Mapledurham	Maize silage & cattle manure	56400	CHP	17-12-2018 01-11-2019 20-01-2020	6
5	Stanley's Quarry	Animal manures, food waste & organic fraction of MSW	50000	CHP	11-03-2019 20-01-2020	3
6	Home Farm (Cranford) AD	Maize silage & Grass silage	2964	CHP	23-05-2019	3
7	Fernbrook AD	Food Waste	49000	CHP	23-05-2019	2
8	Biogen by grave	Food Waste	45000	CHP	13-05-2018 06-12-2018 01-11-2019 30-01-2020	6
9	Frogmary Green Farm	Farm Feed: cattle slurry, chicken manure, cattle manure, maize silage, sugar beet, grass silage (agricultural waste and energy crops)	43900	BtG& CHP	18-02-2020	6
10	Stuchbury Farm	Farm Feed: Animal slurries, maize and grass silage	200	CHP	05-03-2020	9

The biogas plants surveyed at least two times to ensure constant CH_4 emission from plants and collect air samples to further isotope analysis. The emission rate results are given in Table 6.7.2.

The measured CH_4 emission rates varied between 0 and 375 kg CH_4/h. CH_4 losses ranged between 0 to 40% relative to calculated production rates. The emission rates were calculated under different conditions because the facility properties are not reported publicly, and in-situ measurements were not available. Therefore, emission rate estimations were calculated for a range of source release heights from the tallest height of facility where known and 15 meters for unknown facilities, 10, 5m, 2m, and ground-level to take into consideration any pipe, pump, or valve leakages at lower levels.

Also, the expected uncertainty for wind speed data was taken as 50% as recommended in Caulton et al. 2018. As seen in Table 6.7.2, none of those biogas plant emissions are included in the NAEI for 2017.

Table 6.7.2: Surveyed Biogas Plants Results

Nr.	Biogas Plant	Capacity (kWe)	Biomethane Capacity (Nm^3/hr)	Measured Total CH_4 Emission (kg/h)	CH_4 Loss relative to Calculated Production Rate (%)	Availability in NAEI	Isotopic Signature, $\delta^{13}C$ (‰)
1	Arla AD	1410.7	990	[1.5 – 5.3]	[0.3 – 0.6]	No	-51.5±0.4 -61.8±0.3
2	Greentye AD	500	N/A	[11.3 – 31.3]	[5.3 – 14.6]	No	-54.8±0.2
3	Buttermilk	989	N/A	[10.5 – 20.3]	[2.5 – 4.8]	No	-47.8 ± 0
4	Mapledurham	487	N/A	[3.3 – 25.0]	[0.8 – 5.7]	No	-45.1±1.1
5	Stanley's Quarry	2000	N/A	[8.5– 375]	[1.0 – 44]	No	-56.2±0.5
6	Home Farm (Cranford) AD	500	N/A	[0.2 – 0.7]	[0.1 – 0.4]	No	-64.8±1.3
7	Fernbrook AD	1519	N/A	[0.01 – 0.2]	[0.0 – 0.3]	No	-63.9±2.8
8	Biogen Bygrave	2600	N/A	[5.0 – 25.3]	[0.5– 2.6]	No	-60.6±0.1 (Winter) -56.9±0.4 (Summer)
9	Frogmary Green Farm	450	550	[8.3 – 44.6]	[2.1 – 11.3]	No	-57.9 ± 0.3
10	Stuchbury Farm	2000	N/A	[7.8 – 45.2]	[4 – 21.6]	No	-54.0 ± 1.6

The total CH_4 emission rates from 10 biogas plants varied between 56.4 to 573 kg/hr and 448 to 4553 kilotonne annually. The average $\delta^{13}C_{CH4}$ isotopic signature of biogas plants was (-56.0 ± 0.8) ‰. Food waste biogas plants gave an average $\delta^{13}C_{CH4}$ emission value of (-58.6 ± 1.1) ‰ and agricultural biogas plants emitted CH_4 averaging (-54.1 ± 0.8) ‰. Moreover, the maize, C4 type of agricultural biogas plants had more enriched signature (-46.5 ± 0.6) ‰, which results in an overall enriched isotopic signature for agricultural biogas plants compared to food waste.

6.7.1.2.1.2 Landfill Oxidation Rate Calculation

ESR 7 also worked with Viridor company for landfill surveys. Four Viridor landfill sites were chosen for investigation of landfill oxidation rate. Also, Dimmer landfill site was selected for seasonal surveys.

CH_4 from a landfill site can be emitted to the atmosphere by flowing through the gas well or pipeline leaks, through cracks or fissures in the soil cap, through uncovered, active areas and the cover soil. To determine the total amount of oxidation of CH_4 from the entire landfill site, the isotopic source signature of CH_4 in the landfill plume is calculated using equation 1 (Chanton et al. 1999) from air samples collected, upwind (background), downwind and transecting the CH_4 plume from the landfill site.

$$\text{Calculated source signature} = \frac{\delta^{13}C_{measured}[CH4]_{measured} - \delta^{13}C_{upwind}[CH4]_{upwind}}{[CH4]_{measured} - [CH4]_{upwind}} \quad \text{eq. (1)}$$

A Keeling plot is a plot of $\delta^{13}C$ against 1/concentration and is a graphical method of determining the source isotopic signature in measurements of CH_4 in ambient air, derived using the principles of conservation of mass.

I) Dimmer Landfill (Seasonal Survey)

Dimmer Landfill opened in 1967, since then it has landfilled 4.6 million tonnes of material mainly domestic and industrial waste. It has active site, passive site, composting area, leachate pond. Dimmer landfill was surveyed for summer 2019, fall 2019 and winter 2019. The spring survey has been cancelled due to Covid-19 pandemic. The overall results are given in Table 6.7.3 and Table 6.7.4.

Table 6.7.3: Seasonal Results of Dimmer Landfill

	Site-1	Site-2	Composting	Leachate
Summer	-53.3 ± 0.4 ‰	-59.5 ± 0.5 ‰	-53.0 ± 1.6 ‰	-58.0 ± 1.2 ‰
Fall	-52.6 ± 1.5 ‰	-58.6 ± 0.7 ‰	-51.0 ± 0.5 ‰	-55.7 ± 0.4 ‰
Winter	-56.2 ± 0.1‰	-59.6 ± 0.1 ‰	-55.5 ± 0.5 ‰	No emission

Table 6.7.4: Oxidation Rate of Dimmer Landfill

	Oxidation Rate Site-1	Oxidation Rate Site-2
Summer(25 °C)	15.9	3.6
Fall(20 °C)	17.6	9
Winter(10 °C)	4.2	2.8

Isotopic signature of CH_4 emission from active sites in the landfill are in the range –59.6 to -58.6 ‰ with 2.8 – 9 % oxidation rate. Closed sites are characteristically more enriched in $\delta^{13}C$ than active sites and more oxidation compared to the active site in the landfill. During winter season, more CH_4 mole fraction, more depleted isotopic signature and smaller oxidation rate were observed from this landfill area.

The survey maps and keeling plots are shown in Fig. 6.7.1 through Fig. 6.7.6 regarding to seasonal changes with their source of keeling plots.

Fig. 6.7.1: Survey Map of Winter Survey (17/02/2019)

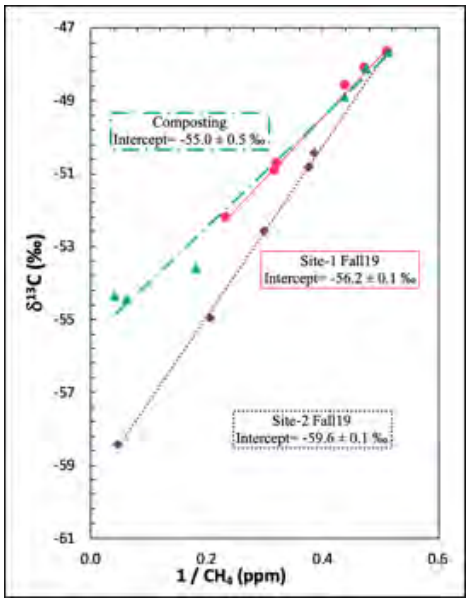

Fig. 6.7.2: Keeling Plot of Winter Survey (17/02/2019)

Fig. 6.7.3: Survey Map of Fall Survey (05/11/2019)

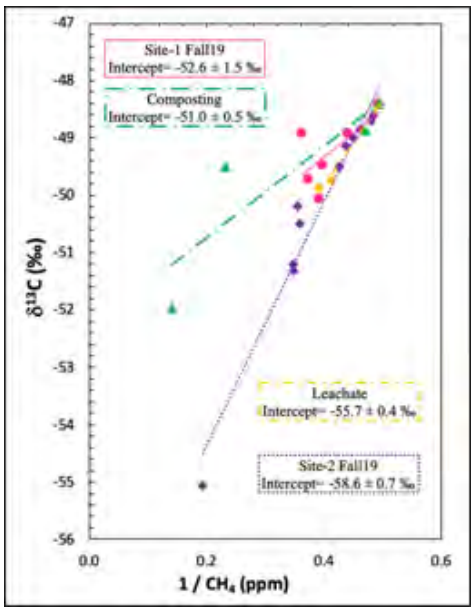

Fig. 6.7.4: Keeling Plot of Winter Survey (05/11/2019)

Fig. 6.7.5: Survey Map of Summer Survey

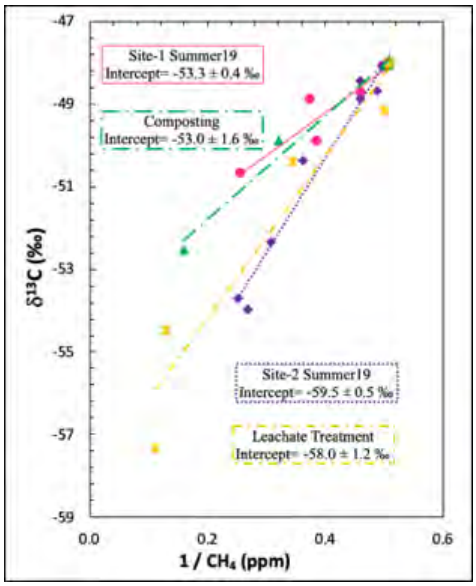

Fig. 6.7.6: Keeling Plot of Summer Survey

For Dimmer Site-1 (Closed) Gas well results (Table 6.7.5):

- Interquartile range (IQR) has been applied to the data set and outliers was eliminated to calculate average isotopic signature and statistically compare by t-test.
- Average gas well isotopic signature: -55.5 per mil, Standard Deviation (STD): 1.9
- There were statistically significant differences in the data between isotopic signature and gas well depth and any compound concentration, $p<0.05$, which means there was no relationship between isotopic signature and gas well properties.

Table 6.7.5: Results of Dimmer Site-1 Gas Well Samples

Gas Well Name	$\delta^{13}CH_4$	Base Level (mbgl)	CH_4 (%)	CO_2 (%)	O_2 (%)	CO (ppm)	H_2S (ppm)
1DM026CV*	-46.77	1.85	22.5	22.7	8.9	6	0
1DM137CV	-57.49			23.1	0.4	4	22
1DM006CV	-57.01	10.15	70.3	31.5	0.3	5	0
1DM105CV	-56.64	5.58	63.7	30.9	0.7	4	12
1DM041CV	-55.73	11.29	1	1.9	18.2	1	0
1DM100CV	-55.21	6.04	68	33.7	0.2	3	2
1DM021CV	-54.18	7.82	64.9	32.8	0.3	5	4
1DMAREA5	-52.04	13.88	29.3	15.8	10.6	2	2

*outlier was not included to mean calculation

For Dimmer site-2 (Active) Gas well Results (Table 6.7.6):

- Interquartile range (IQR) has been applied to the data set and outliers was eliminated to calculate average isotopic signature and statistically compare by t-test.
- Average gas well isotopic signature: -60.2 per mil, Standard Deviation (STD): 0.6
- There were statistically significant differences in the data between isotopic signature and gas well depth and any compound concentration, $p<0.05$, which means there was no relationship between isotopic signature and gas well properties.
- Gas engine isotopic signature is -58.7 ± 0.1 per mil.

Table 6.7.6: Results of Dimmer Site-2 Gas Well Samples

Gas Well Name	$\delta^{13}CH_4$	Base Level (mbgl)	CH_4 (%)	CO_2 (%)	O_2 (%)	CO (ppm)	H_2S (ppm)
2DM247CV*	-62.50	10.6	17.7	12.7	5.5	45	0
2DM293CV*	-61.65	11.9	62.9	39	0	22	57
2DM341CV	-60.94	9.35	55.8	40.5	0.2	57	93
2DM297CV	-60.79	7.78	64.1	34.9	0.2	6	0
2DM323CV	-60.45	10.36	59.1	40.3	0.2	18	265
2DM265CV	-60.18	6.9	59.1	35.4	0.9	29	83
2DM338CV	-60.16	10.94	64.1	38.2	0	21	21
2DM215CV	-59.99	3.5	64.9	28	0.1	7	0
2DMnewwell	-59.77	-	-	-	-	-	-
2DM279CV	-59.41	5.05	-	-	-	-	-
2DM280CV	-59.34	9.5	59.5	32.1	1.4	23	65
2DM320CV*	-57.70	7.34	59.1	39	0.3	18	98

*outliers were not included to mean calculation

The extent of CH_4 oxidation is a major uncertainty in estimating the extent of landfill CH_4 emission. Oxidation of CH_4 by methanotrophic bacteria in landfill cover soil causes isotopic fractionation of the carbon in CH_4. Methanotrophs preferentially utilise the lighter $^{12}CH_4$, leaving the remaining CH_4 relatively enriched in $^{13}CH_4$. The amount of oxidation of CH_4 can be determined by comparing the carbon stable isotopic composition ($\delta^{13}C$) of CH_4 in the anoxic zone with that of CH_4 emitted to the atmosphere from the landfill site.

$$f_o = \frac{\delta E - \delta A}{(\alpha_{ox} - 1) * 1000} \qquad \text{eq. (2)}$$

δE, $\delta^{13}C$ of CH_4 emitted from a landfill and CH_4 in the anoxic zone, δA are known, the fraction of CH_4 oxidised (f_o) can be calculated using equation (1) (Liptay et al.). This equation assumes that CH_4 transports advectively through the cover soil. α_{ox} is a fractionation factor and depends on temperature and soil type.

The selection of the constant α in equation 2 was calculated from the equation derived by Börjesson et al. (2009) following measurements in a Swedish landfill site (Börjesson et al. 2009).

$$\alpha = 1.0251 - 0.000313*T \quad \text{eq. (3)}$$

Where T (°C) is the mean soil temperature measured. The isotopic composition of anoxic CH_4 was taken from gas wells. It was assumed that gas wells have uniform conditions such as same temperature, pH and moisture content.

II) Broadpath Landfill (Closure Impact)

Broadpath was opened in 1998 and was closed in 2019. It was filled with 4.3 million tonnes of material: 47 % domestic waste, 35% industrial and commercial waste, 11 % cover soil, remaining contaminated soil, sludge & sewage and difficult waste.

Table 6.7.7: Oxidation Rate and Isotopic Signature Results of Broadpath Landfill

	Isotopic Signature	Oxidation Rate, f_o (%)
When Active(25 °C)	-57.3 ± 0.6 ‰	13.7
After Closure (10 °C)	-55.9 ± 0.3 ‰	17.1

Broadpath landfill was surveyed two times when it was active and after it was closed to see the closure impact on oxidation and mole fraction changes. The results are given in Table 6.7.7.

Because of the weather conditions and works on the landfill, we could not survey the whole landfill on February 2020 as we did in July 2019. As seen in the Fig. 6.7.18 the highest mole fraction was around 3 ppm on February 2020 which was lower than July 2019 surveys. The closure impact can be seen clearly with lower mole fraction, more enriched isotopic signature and highest oxidation rate.

After Closure (17/02/2020): During this survey high CH_4 concentrations were not observed due to wind direction and road conditions. Ambient air isotopic signature after it was closed is given in Keeling plot in Fig. 6.7.7.

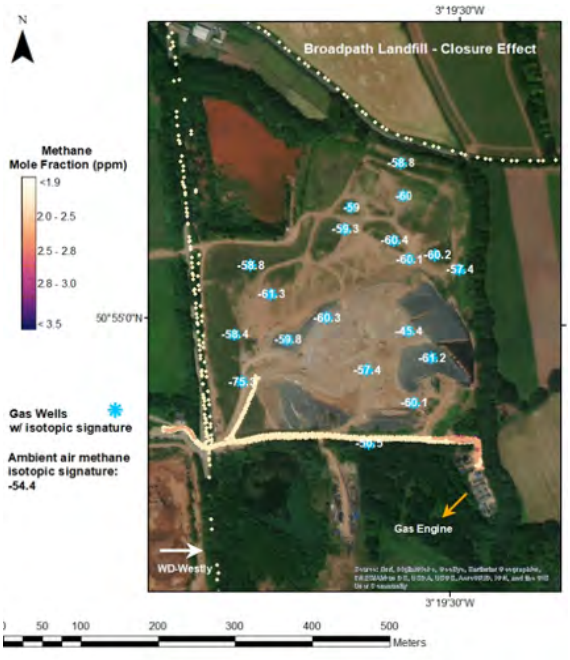

Fig. 6.7.7: Broadpath Landfill Survey Map after closed

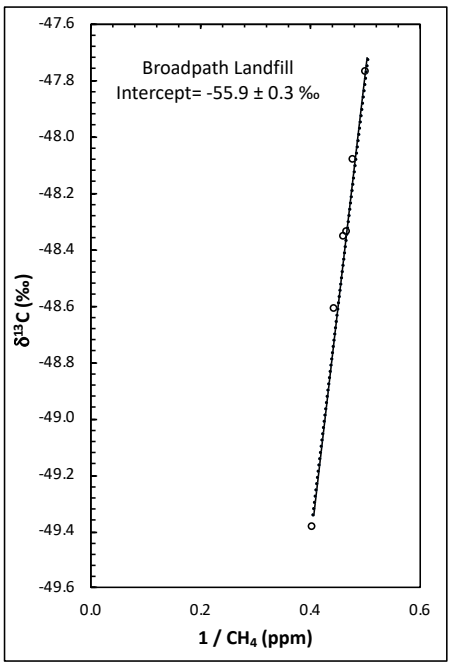

Fig. 6.7.8: Keeling Plot of Broadpath Landfill after closed

When Active (23/07/2019): Mobile Broadpath landfill survey with 19 gas well sampling isotopic signature is given in Fig. 6.7.9 when it was still dumping with waste.

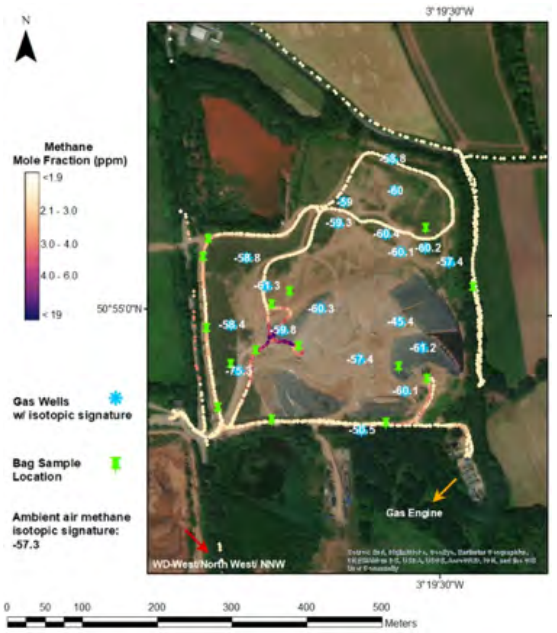

Fig. 6.7.9: Broadpath Landfill Survey Map when it was active

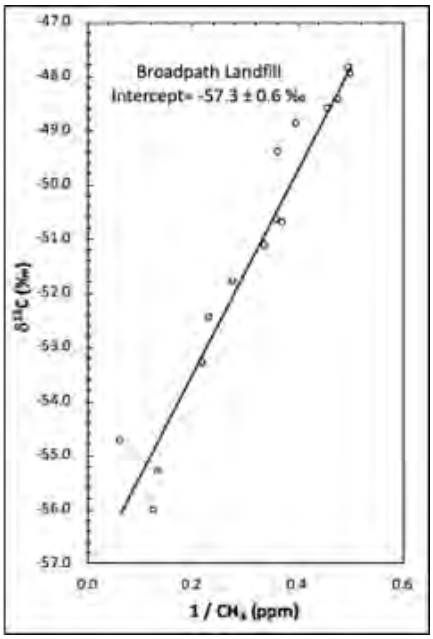

Fig. 6.7.10: Keeling Plot of Broadpath Landfill- Active

Table 6.7.8: Broadpath Landfill Gas Well Results

Gas Well Name	$\delta^{13}CH_4$	Base Level (mbgl)	CH_4 (%)	CO_2 (%)	O_2 (%)	CO (ppm)	H_2S (ppm)
1BP021OW	-57.39	17.86	33.6	26	0	72	0
1BP070OW	-50.46	29.43	4.6	17.1	1	49	2
1BP422CV	-61.28	14.78	49.7	49.2	0.1	100	4
1BP521CV	-59.32	24.55	52.2	39.2	1.5	99	0
1BP526CV	-59.99	20.84	25.3	18	10.8	81	0
1BP543CV	-75.34	17.76	3.2	4.5	16	9	0
1BP549CV	-58.40	21.7	43.1	41.7	0.1	41	0
1BP563CV	-58.95	18.62	60.5	42.5	0.1	150	0
1BP568CV	-60.35	31.5	46	38.7	0.1	85	0
1BP570CV	-60.16	13.54	51.2	38.9	0.1	78	0
1BP578CV	-58.82	60	38.2	42.8	0.6	76	0
1BP580CV	-60.09	34.27	52	40.8	0.2	85	0
1BP596CV	-61.24	N/A	50.4	41.9	0.1	112	5
1BP608CV	-60.30	N/A	58.9	41.4	0.1	76	80
1BP612CV	-60.11	N/A	59.4	41.8	0.1	94	270
1BP5-2ALM	-59.78	N/A	71.3	29.9	0.1	73	0

The outliers and leachate wells were not included in the average isotopic value calculation. Interquartile range (IQR) has been applied the data set except leachate wells and outliers was eliminated to calculate average isotopic signature and statistically compare by t-test.

- Average gas well isotopic signature: -59.9 per mil, Standard Deviation (STD): 0.9
- There were statistically significant differences in the data between isotopic signature and gas well depth and any compound concentration, $p<0.05$, which means there was no relationship between isotopic signature and gas well properties.
- Gas engine isotopic signature is (-60.5 ± 0.05) per mil.

III) Heathfield Landfill (Process Impact)

Heathfield Landfill was opened in 1986 and then mothballed in 2016, with plans for to reopen in August 2019. When operational, Heathfield landfilled 9.4 million tonnes of material.

Heathfield landfill was surveyed three times. Mobile measurements were performed on 20/08/2019 for observing cap stripping impact shown in Fig. 6.7.11, 16/07/2019 in Fig. 6.7.12 and 5/07/2018 in Fig. 6.7.13. Also, gas well sampling was mainly done on 16th and 17th of July 2019 and 6 more gas wells were sampled on 20/08/2019.

Fig. 6.7.11: Heathfield Landfill Survey in August 2019

Fig. 6.7.12: Heathfield Landfill Survey in July 2019

Fig. 6.7.13: Heathfield Landfill Survey in July 2018

Keeling Plot Approach:

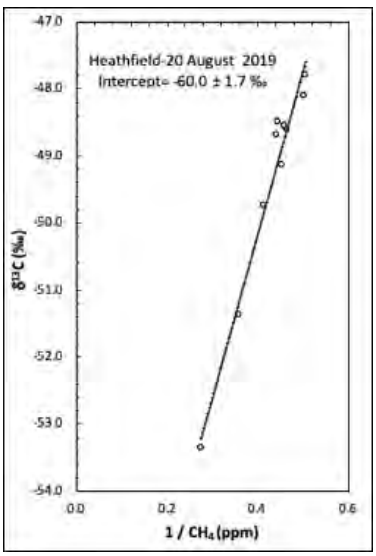

Fig. 6.7.14: Keeling Plot for 20/08/2019 Survey

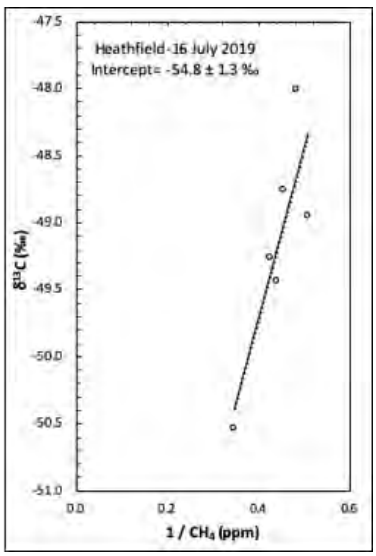

Fig. 6.7.15: Keeling Plot for 16/07/2019 Survey

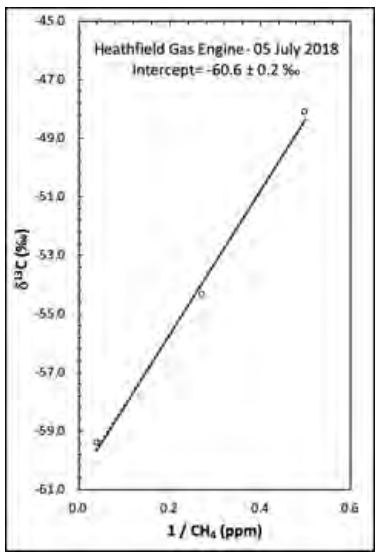

Fig. 6.7.17: Keeling Plot for 05/07/2018 Survey- Gas Engine

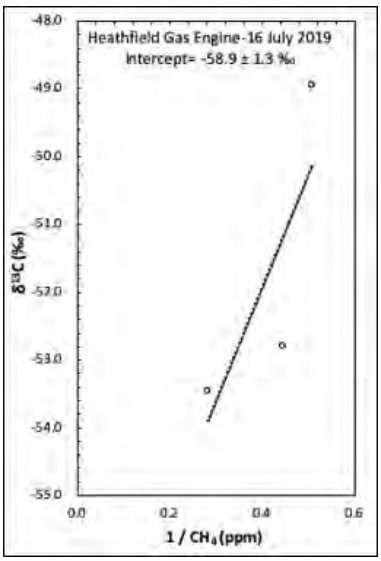

Fig. 6.7.16: Keeling Plot for 16/07/2019 Survey (Air was collected near the gas engine)

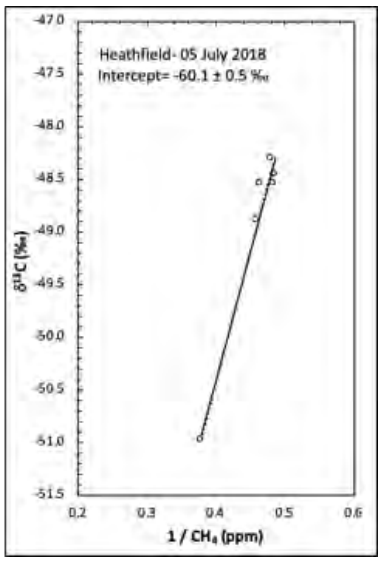

Fig. 6.7.18: Keeling Plot for 05/07/2018 Survey

Table 6.7.9: Heathfield Landfill Gas Well Results

Gas Well Name	$\delta^{13}CH_4$	Base Level (mbgl)	CH_4 (%)	CO_2 (%)	O_2 (%)	CO (ppm)	H_2S (ppm)
1HF003CV	-60.49	11.29	45.2	33.2	0	0	7
1HF004CV	-63.91	13.31	19.1	22	2.8	0	0
1HF004CV*	-61.46	13.31	9.9	21.1	0.3	0	0
1HF008CV	-62.56	9.66	62.3	38.1	0.2	0	287
1HF037CV	-61.54	21.63	39.8	32	0.3	29	8
1HF039CV	-61.47	18.17	47.5	35.4	0	29	7
1HF051CV	-61.02	14.56	47.2	34.5	0.6	328	29
1HF063CV	-50.74	6.04	32.6	25	0	0	11
1HF069CV	-59.49	10.09	58.9	39.7	0	83	10
1HF072CV	-60.12	5.73	58.7	34	0	69	31
1HF079CV	-61.69	8.56	60.3	37.3	0	0	10
1HF123CV	-60.47	10.88	54.9	38.7	0	44	72
1HF124CV	-61.46	11.45	62.2	39.1	0	1	29
1HF165CV*	-59.46	5.24	9.9	21.1	0.3	0	0
1HF193CV*	-60.04	7.83	64.6	36.1	0	0	27
1HF220CV	-55.78	14.06	40.4	23.1	0	0	9
1HF221CV	-57.14	16.7	41.3	18.4	1.3	31	0
1HF224CV	-59.17	10.32	59.8	38.1	0	0	105
1HF352PW	-47.92	4.13	46.7	34	0	0	27
1HF352PW*	-55.41	4.13	31.5	23.3	2.6	0	0
1HF707CV*	-55.23	11.85	48.8	27.4	0.4	0	0
1HF720CV	-58.50	13.1	49.1	30.3	3.7	0	73
1HF734CV	-59.35	20.98	43	32.4	0	0	46
1HF747CV	-60.45	20.31	23.1	27.8	0	0	14
1HF751CV	-58.09	22.91	56.8	39.3	0	0	77
1HF767CV	-47.40	22.01	18.5	23	0	0	5
1HF778CV	-59.86	25.83	56.7	39.4	0.4	0	166
1HF789CV	-59.51	19.9	46.8	35.9	0	206	174
1HF25BLM	-60.30	N/A	63	54.2	0	1861	1605

*sampled on August 20, 2019 Survey

Outliers and leachate wells were not included in the average isotopic value calculation.

- Interquartile range (IQR) has been applied the data set except leachate wells and outliers was eliminated to calculate average isotopic signature and statistically compare by t-test.
- Average gas well isotopic signature: -60.1 per mil, Standard Deviation (STD): 1.1

- There were statistically significant differences in the data between isotopic signature and gas well depth and any compound concentration, $p<0.05$, which means there was no relationship between isotopic signature and gas well properties.
- Gas engine isotopic signature is (-59.9 ± 0.1) per mil from July 2019 survey and (-60.5 ± 0.1) per mil from July 2018 survey.

However, the ambient air isotopic signature value from July 2019 was suspicious, therefore the August 2019 value of -59.96 was taken to calculate oxidation rate given in Table 6.7.10. Because Heathfield landfill was closed longer than Dimmer and Broadpath landfills, the oxidation rate for it was lower than Dimmer and Broadpath landfills.

Table 6.7.10: Oxidation Rate of Heathfield Landfill on August 2019

T(°C)	10	15	20	22	25	30
$\propto$	1.0220	1.0204	1.0188	1.0182	1.0173	1.0157
f_o (%)	0.73	0.79	0.86	0.89	0.93	1.03

IV) Walpole Landfill

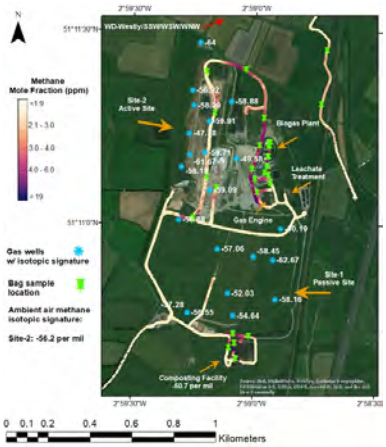

Fig. 6.7.19: Walpole Landfill Survey Map

Walpole Landfill has been opened in 1989, since then it has landfilled 5,513,511 tonnes of material, mainly industrial and commercial waste. Walpole landfill has both passive (site-1) and active (site-2) sites with biogas plants, leachate treatment and composting facilities shown in Fig. 6.7.19.

Keeling Plot Approach: Due to wind direction on the available road, the ambient air could not be sampled for site 1. So, keeling plot of site-2, biogas plants and composting facilities are shown in Fig. 6.7.20 – 6.7.22.

Table 6.7.11: Oxidation Rate of Site-2

T(°C)	10	15	20	22	25	30
$\propto$	1.022	1.020	1.019	1.018	1.017	1.016
f_o (%)	11.4	12.3	13.3	13.8	14.5	16

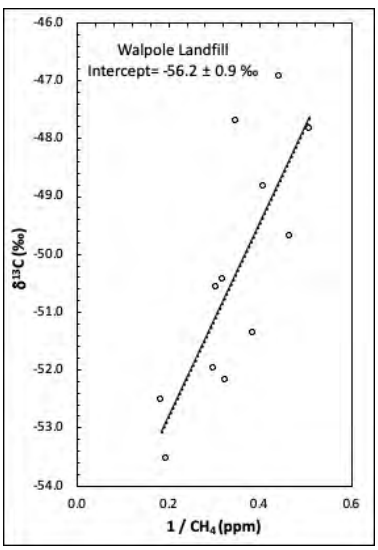

Fig. 6.7.20: Walpole Landfill Keeling Plot (Site-2)

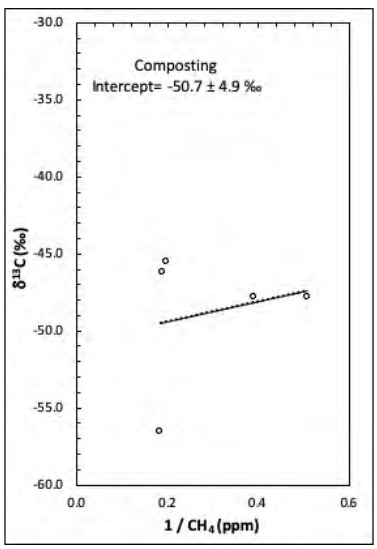

Fig. 6.7.21: Composting Area Keeling Plot

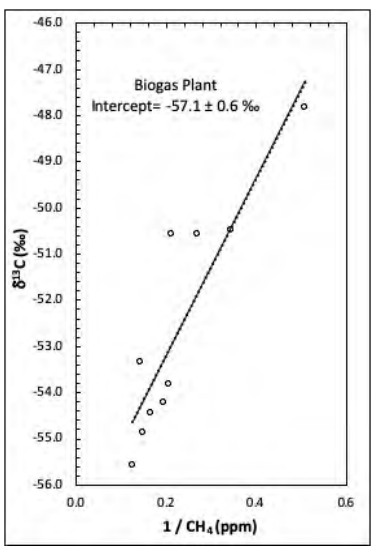

Fig. 6.7.22: Biogas Plant Keeling Plot

Walpole Site-1 Gas Well Results:

- Interquartile range (IQR) has been applied in the data set and outliers was eliminated to calculate average isotopic signature and statistically compare by t-test.
- Average gas well isotopic signature: -57.8 per mil, Standard Deviation (STD): 1.3
- There were statistically significant differences in the data between isotopic signature and gas well depth and any compound concentration, $p<0.05$, which means there was no relationship between isotopic signature and gas well properties.

Table 6.7.12: Walpole Landfill Site-1 Gas Well Results

Gas Well Name	$\delta^{13}CH_4$	Base Level (mbgl)	CH_4 (%)	CO_2 (%)	O_2 (%)	CO (ppm)	H_2S (ppm)
1WP009CV	-56.68	2.22	60.5	37.6	0.2	6	11
1WP023CV*	-61.67	10.97	49.3	33.5	0.1	8	114
1WP029CV	-57.28	7.06	56.9	31.2	0.1	2	16
1WP041CV	-56.55	4.68	45.8	32.5	2.5	2	0
1WP074CV	-58.45	10.96	6.9	5.9	15	6	1
1WP091CV	-60.19	7.96	30.5	20.6	2.5	4	1
1WP094CV*	-62.67	13.22	29.2	22.2	0.2	4	101
1WP109CV	-57.06	8.02	42.6	29.1	0.1	4	74
1WP111CV*	-52.03	8.66	41.9	29.1	0.6	2	0
1WP115CV*	-54.64	5.65	70	29	0.1	5	308
1WP116CV	-58.16	7.22	42.9	28.7	0.3	5	1
1WP009CV	-56.68	2.22	60.5	37.6	0.2	6	11

* outliers were not included the average isotopic value calculation.

Walpole Site-2 Gas Well Results

- Interquartile range (IQR) has been applied in the data set and outliers was eliminated to calculate average isotopic signature and statistically compare by t-test.
- Average gas well isotopic signature: -58.7 per mil, Standard Deviation (STD): 1.0
- There were statistically significant differences in the data between isotopic signature and gas well depth and any compound concentration, $p<0.05$, which means there was no relationship between isotopic signature and gas well properties.
- Gas engine isotopic signature is (-59.1 ± 0.04) per mil.

Table 6.7.13: Walpole Landfill Site-2 Gas Well Results

Gas Well Name	$\delta^{13}CH_4$	Base Level (mbgl)	CH_4 (%)	CO_2 (%)	O_2 (%)	CO (ppm)	H_2S (ppm)
2WP010CV	-56.92	7.52	41.3	28.7	0.1	21	77
2WP018CV	-58.18	12.71	59.2	37.1	0.2	9	57
2WP028CV*	-47.78	9.4	51.5	34.4	0.1	21	43
2WP034CV	-58.29	11.68	56.7	34.9	0.2	18	169
2WP060CV	-59.71	12.1	55.9	38.5	0.3	18	95
2WP065CV	-59.09	6.78	41.6	32.7	0.3	11	18
2WP069CV	-59.91	9.95	41.6	32.7	0.3	11	18
2WP072WM**	-64.00	NA	7.7	15	1.9	6	2
2WP073CV	-58.88	6.65	47	37.7	0.1	30	137
2WPCH*	-49.58	NA	57.9	41.8	0.2	20	535

* outliers and monitoring well (**) were not included the average isotopic value calculation.

6.7.1.2.1.3 Waste Sources Isotopic Signature Inventory

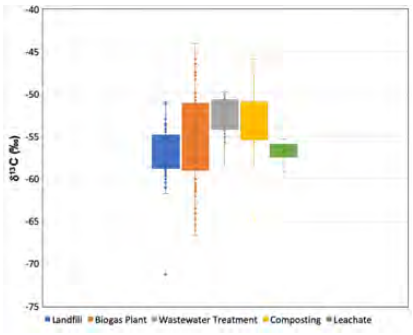

Fig. 6.7.23: Waste Sources Isotopic Signature Differences

ESR 7 aimed to characterize waste sources shown in Fig. 6.7.23 Twenty-four landfills, 25 biogas plants, 12 wastewater treatment plants, four composting facilities and two leachate source isotopic signatures were measured. Because of the various feeding materials, biogas plants isotopic signatures have a larger range than the other waste types.

Biogas emissions have a fairly varied isotopic signature (-43 to -67‰) compared to other waste sources given in Fig. 6.7.24. Agricultural waste type (maize) biogas plants (-50 to -43 ‰) are more enriched compared to other biogas plants, which depend on the waste type and anaerobic digestion process.

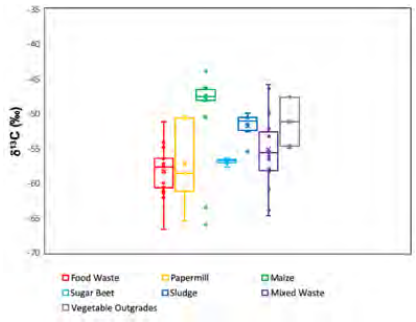

Fig. 6.7.24: Biogas Plants Isotopic Signature depending on Different Feeding Material

6.7.1.2.1.4 Birmingham City Survey

ESR 7 joined the city surveys for over 5 days. It was aimed to measure city CH_4 emissions for 1x1 km^2 shown in Fig. 6.7.25. The main CH_4 emissions originated from gas leaks in the city, with landfill, sewage treatment works and a farm in peripheral regions. Their isotopic signatures are given in Table 6.7.14. Results are under evaluation and will be submitted soon.

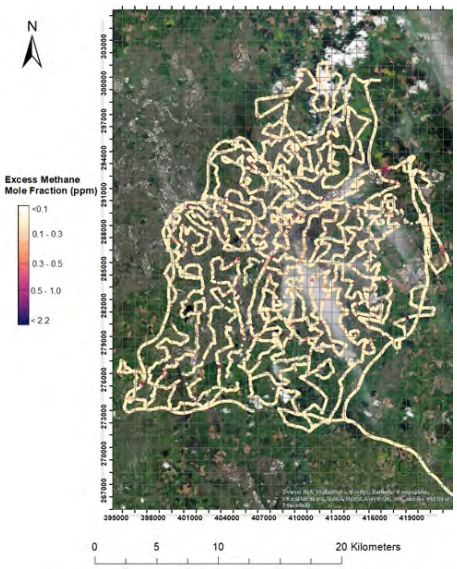

Fig. 6.7.25: Birmingham City Survey Map

Table 6.7.14: Summary of Main CH_4 Sources in Birmingham City

Sources Name	$\delta^{13}C$ (‰) ±SE
Gas leaks	-39.5 ± 0.5
Suez Landfill	-57.9 ± 0.7
Minworth Sewage	-51.1± 0.2
Gay Hill Farm	-69.3 ± 3.3

6.7.1.2.2 Fourth year

The fourth year was dedicated to further data collection, data evaluation and publication. The following chapter is partly an update of and based on what has been reported before.

6.7.1.2.2.1 Quantification of CH_4 emissions from UK biogas plants

The emission rates, losses and emission factors for 10 biogas plants were calculated by mobile instruments and Gaussian plume modelling.

Overall, the measured CH_4 emission rates varied between 0.1 and 58.7 kg CH_4 h^{-1}, and CH_4 losses ranged between 0.02 and 8.1%, with the average being 3.7 % (see Table 6.7.15). These results are comparable with those of Scheutz and Fredenslund (2019), who found losses of 0.4 to 14.9 % with an average of 4.6 % of the CH_4 production gas at 23 biogas plants. The results are also comparable to Flesch et al.'s (2011) results, which estimated an average loss of 3.1 % of CH_4 production for a Canadian biodigester. Baldé et al. (2016) also found a wide range of emission rates of 0 to 97 kg CH_4 h^{-1}. It is important to reiterate that we measured the total CH_4 emissions from the plants on the public road with the limited information about the processes. Therefore, it is hard to pinpoint the sources of the emissions in the biogas plants.

Table 6.7.15: Estimated CH_4 emissions rates obtained from Gaussian plume modelling, CH_4 losses relative to calculated production rates and emission factors calculated as annual emission rates divided by annual feedstock amount.

Name	Biomethane capacity (Nm^3/hr)	Calculated average CH_4 production rate (kg CH_4 h^{-1})	Estimated total CH_4 emissions (kg CH_4 h^{-1})	CH_4 loss relative to calculated production rates (%)	Emission factors (kg CH_4 emitted/ tonnes of feedstock)
A	N/A	970 [b,c]	12.6 ± 3.8	1.3 ± 0.4	2.5 ± 0.7
B	N/A	861 [a,c]	58.7 ± 25	6.8 ± 2.9	10.3 ± 4.4
C	N/A	654 [a,c]	0.1 ± 0.02	0.02 ± 0.003	0.02 ± 0.004
D	990	709	2.8 ± 0.8	0.4 ± 0.1	0.5 ± 0.1
Plant average CH_4 loss and EF, **food waste**: 2.1% and 3.3, respectively Production weighted average CH_4 loss and EF, **food waste**: 2.3% and 3.4, respectively					
E	550	394	21.9 ± 6.2	5.6 ± 1.6	10.0 ± 2.8
F	N/A	425 [a]	14.3 ± 4.2	3.4 ± 1.0	6.3 ± 1.8
G	N/A	215 [a,c]	17.5 ± 3.7	8.1 ± 1.7	15.3 ± 3.2
H	N/A	198 [a]	0.5 ± 0.1	0.3 ± 0.1	1.5 ± 0.3
I	N/A	439 [a,c]	14.0 ± 3.9	3.2 ± 0.9	2.2 ± 0.6
J	N/A	209 [a,c]	16.6 ± 4.1	7.9 ± 0.02	11.4 ± 2.8
Plant average CH_4 loss and EF, **farm waste**: 4.8% and 7.8, respectively Production weighted average CH_4 loss and EF, **farm waste**: 4.5% and 6.1, respectively **All biogas plants** Plant average CH_4 loss and EF, all: 3.7% and 6.0, respectively Production weighted average CH_4 loss and EF, all: 3.1% and 4.4, respectively					

[a] results estimated by interpolation; [b] results found in public reports; [c] CH_4 content of 60% and normal conditions (25^{0}C and 1 atm); CH_4 density = 0.7157 kg/Nm^3 at normal conditions (25^{0}C and 1 atm); EF: emission factor; plant average is equal to the sum of CH_4 losses divided by the number of the plants and weighted average is equal to the sum of the all estimated CH_4 emissions rates divided by the sum of calculated production rates.

The biogas plants selected for this study were of two types based on feedstock material: farm and waste. The farm types include slurry, manure, and purpose-grown crops such as maize, silage and grain. The waste types are mainly food waste. In general, CH_4 losses from farm biogas plants E, F, G, H, I and J were higher (0.5 to 21.9 kg CH_4 h^{-1} and 0.3 to 8.1 % relative to calculated production rates) than from food waste biogas plants A, C and D (0.1 to 12.6 kg CH_4 h^{-1} and 0.02 to 6.8 % relative to calculated production rate), yet the latter all had a higher capacity than the farm plants. At four of the 10 biogas plants, the calculated CH_4 loss was higher than the average of 3.7 % (Fig. 6.7.26). Of these four plants, three were farm biogas plants except plant B which can be considered as an outlier due to its large emission rate uncertainty. The farm biogas plants E, G and J that emitted more than 3.7% had the lowest level of calculated biogas production, capacity (KWe) and total feedstock amount excluding Plant H whose emission loss is also lower.

Altogether, it seemed that there was a negative correlation between the CH_4 loss and the size of the biogas plant as Scheutz and Fredenslund suggested in 2019. The reason for this outcome cannot be determined owing to limited knowledge of the plants' operating conditions and properties. One reason may be that larger facilities are generally better maintained and that investment in modernization, operations and monitoring plans are higher.

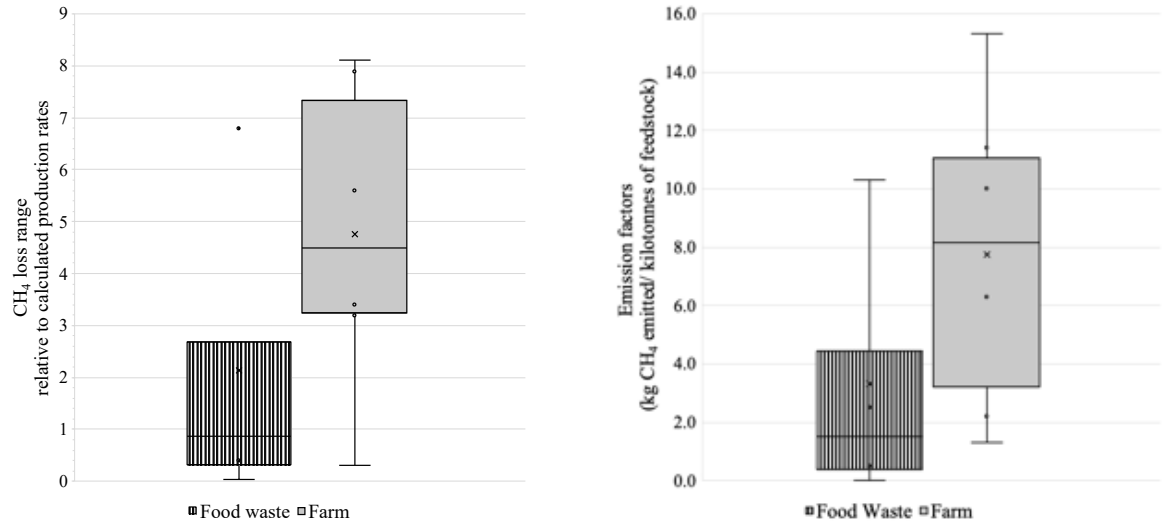

Fig. 6.7.26: Representation of emission factors with respect to different feedstock material

Projection of fugitive CH_4 emissions from UK biogas plants

The British anaerobic digestion market comprises 660 operational biogas plants, with 148 and 338 being waste and farm feedstocks, respectively (ADBA, 2019). The inventories are not all regularly updated for the biogas plants whose numbers have linearly increased since 2009 (ADBA, 2019). In this study, 31 of 148 waste and 25 of 338 farm feed biogas plants were surveyed as mentioned earlier. It is critical to estimate how much total CH_4 emission might come from biogas plants in the UK to underline the importance of fugitive CH_4 emission from biogas plants.

Upscaling results to study the impact on total UK fugitive CH_4 emissions was performed using two hypotheses. In hypothesis A, we assume that the 22 biogas plants, for which we could not detect a measurable emission, had in fact zero emissions. We thus use the ten biogas plants with noticeable emission rates (see Table 6.7.15) and 22 biogas plants with zero emission for upscaling of overall emissions, which we consider as the lower bound of CH_4 emissions from UK biogas plants.

In hypothesis B, the emission rates of the ten biogas plants are upscaled for the total farm and waste biogas plants, which we consider as the upper bound of the total emission rate. The estimated emission rates in Table 6.7.15 were extrapolated to the UK anaerobic digestion market information using a linear fit for the electrical capacity (KWe), feedstock amount (kilotonne), the number of biogas plants and biogas production amount ($Nm^3\,hr^{-1}$). The extrapolated inventory can give a guideline for assessing the different level of CH_4 emissions for both farm and waste type of biogas plants, and overall emission range.

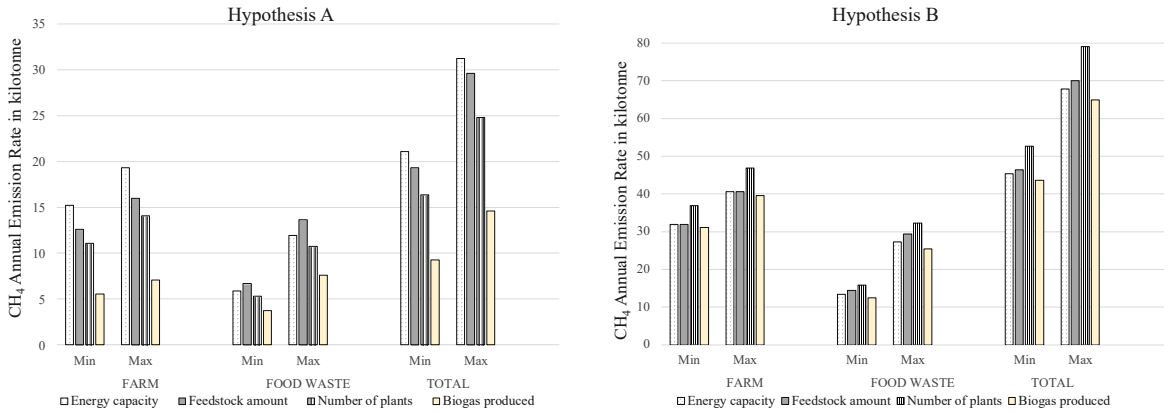

Fig. 6.7.27: a) Extrapolation of farm, food waste and total annual fugitive emissions from surveyed biogas plants to all UK biogas plants, based on four parameters: energy capacity, feedstock amount, number of biogas plant and produced biogas amount. Total mean emission rates of 10 biogas plants and zero emission rates of 22 biogas plants were scaled up to observe the possible emission range in the UK. The standard error was taken into consideration to estimate minimum and maximum values of emission. The maximum and minimum extrapolated emissions were obtained from the energy capacity and amount of biogas production, respectively. **(b)** Emission estimation based on hypothesis B. The maximum and minimum emissions were based on the number of biogas plants and the amount of biogas production, respectively.

The total CH_4 emission of ten biogas plants was estimated as (159 ± 27) kg CH_4 hr^{-1}, which varied between 1.1 and 1.7 kilotonnes annually. In particular, the overall estimated CH_4 emissions from four food waste biogas plants and six farm biogas plants ranged from 0.4 to 0.9 kilotonnes and 0.7 to 0.8 kilotonnes, respectively. The most recent published NAEI inventory reports that total annual UK CH_4 emission is 2,079 kilotonnes in 2018.

In hypothesis A, the reported sum of all 486 biogas plants excluding the sewage sludge and other type biogas plants in the UK can be projected as between 9.3 and 31.3 kilotonnes (see Fig. 6.7.27 a) in various scaled-up categories to justify the extrapolation of emission range. Specifically, the overall projected CH_4 emission from 12 food waste biogas plants and 20 farm biogas plants range from 3.7 to 13.6 kilotonnes, and 5.5 to 19.3 kilotonnes, respectively. In hypothesis A, biogas plants may account for 0.4 to 1.5 %, with the average being 1 % of the total CH_4 emission in the UK. In hypothesis B, the extrapolation of emissions from the ten biogas plants to the total number of biogas plants for the different upscaling parameters gives emissions in the range of 43.6 to 79.1 kilotonnes annually (Fig. 6.7.27 b).

In hypothesis B, biogas plants may account for 2.1 to 3.8 %, with the average being 2.8 %, of the total CH_4 emissions in the UK. Note that the figure of 3.8 % of the total UK emissions is an upper bound, as it is assumed that all plants resume operations and constantly emit in the same manner as the surveyed plants.

Hence, these hypotheses illustrate that biogas plant CH_4 emissions excluding sewage sludge biogas plants might be as low as 0.4% or as much as 3.8% of the total CH_4 emissions in the UK for 2018. On average, 1.9 % of the UK CH_4 emissions can come from the biogas plants. We also highlight that CH_4 emissions from biogas plants may have intermittent emission patterns or highly unpredictable leaks, leading to an underestimate or overestimate of emission rates (Duren et al. 2019). This might be the reason of measuring no emission from 22 of the visited biogas plants.

The NAEI (2020) estimated CH_4 emission from anaerobic digestion processes as 7.7 kilotonnes in 2018 under the waste category rather than manure management using IPCC Tier 2 methodology, which is the 0.4% of total UK emissions. As observed in Fig. 6.7.27, the estimated lower range of CH_4 emissions from hypothesis A is very close to the NAEI (2020) inventory calculation. But it should be noted that anaerobic digestion from agricultural residuals is considered in the agricultural category. The CH_4 emissions from manure management were reported as 158.7 kilotonne by NAEI (2020) except excreta

and waste of horses, goats and deer, but it is not clearly identified how much of these CH_4 emissions are coming from the anaerobic digestion process.

Additionally, it has been recommended that landfilling of biodegradable wastes should be banned across the UK by 2025 and more food and garden waste will be diverted to the anaerobic digestion and composting facilities (CCC, 2020), which can cause more CH_4 emissions from anaerobic digestion in the coming years. The Committee on Climate Change's Net Zero report (CCC, 2019) predicts the rise in CH_4 emissions from anaerobic digestion will be to 9.0 kilotonnes by 2050. Thus, regular monitoring of biogas plant emissions is absolutely essential to quantify and reduce CH_4 emissions and achieve the net zero aim by 2050.

6.7.1.2.2.2 Carbon isotopic characterisation and oxidation of UK landfills CH_4 emissions

This study was conducted at four landfill sites (A,B,C & D) in southwest England. In this chapter, the results for landfill A, B, C, and D correspond the results of Dimmer, Heathfield, Broadpath, and Walpole landfill sites, respectively. Mobile mole fraction measurement at the four sites was coupled with Flexfoil bag sampling of air for high-precision isotope analysis. CH_4 samples were also collected from gas well collection systems to estimate landfill oxidation rate.

The amount of CH_4 oxidation in a landfill site can be determined by comparing the $\delta^{13}C$-CH_4 of CH_4 from the anoxic zone with that of CH_4 emitted into the atmosphere. To calculate the fraction oxidized, it is assumed that the CH_4 mole fraction is well mixed in the porous soil media and that the system is open, f_0 (Börjesson et al., 2007; Chanton et al., 1999):

$$f_0 = \frac{\delta E - \delta A}{(\alpha_{ox} - \alpha_{trans})1000} \qquad \text{eq. (3)}$$

The $\delta^{13}C$ of CH_4 emitted from the landfill (δE) and the CH_4 in the anoxic zone (δA) are known, so the fraction of CH_4 oxidised (f_0) can be calculated using equation (4) (Chanton and Liptay, 2000; De Visscher et al., 2004; Liptay et al., 1998). This equation assumes that CH_4 is transported advectively through the cover soil. α_{ox} is a fractionation factor that depends on temperature and soil type. It is determined mainly by the incubation of soil cover samples. The constant, α_{ox} in equation (4) was taken from that derived by Börjesson et al. (2009) from measurements in a Swedish landfill site.

$$\alpha_{ox} = 1.0251 - 0.000313*T \qquad \text{eq. (4)}$$

where T (°C) is the mean soil temperature measured. Although detailed defence of this method of calculating the oxidation rate is beyond the scope of this paper, we consider that our results illustrate the lower limit of CH_4 oxidation.

The isotopic composition of anoxic CH_4 was taken from the operational gas wells. The interquartile range (IQR) was calculated for the collected gas well samples for each site and the 1.5 IQR was applied to the data set, and outliers were eliminated to calculate the average isotopic signature. It was assumed that conditions in the gas wells were uniform, with the same temperature, acidity and moisture content.

Seasonal variation in Landfill A

Mobile CH_4 measurement and air and gas-well sampling for $\delta^{13}C_{CH4}$ analysis of Landfill A were carried out between summer 2019 and winter 2020. A more detailed mobile survey could only be performed during dry July 2019, owing to the restricted vehicle access on the muddy soil surface during the autumn and winter surveys.

The survey plot of the excess CH_4 mole fraction above the background demonstrates a seasonal trend, with slightly lower values in the autumn. In addition to the prevailing wind direction and temperature

changes, rainfall in autumn and winter fills the pores of the gas exchange, which may cause lower emissions. Maximum excess CH_4 mole fractions (around 29 ppm) were recorded during the winter survey on the active site and east side of Landfill A, in an area downwind of a closed (historical) site where a leaking gas well was identified. Due to operations on the active site during the winter measurement, we were unable to survey the Site 2 road as in other seasons. Following the winter survey, the higher excess CH_4 mole fraction above the background was assessed during the summer survey. In particular, in summer, active, uncovered areas produced more excess CH_4 mole fraction than other areas of the landfill, apart from leaking or leachate gas wells. The high mole fraction to the far west of the landfill, representing the upwind edge of the active site, may also be influenced by variations in wind direction and speed during the analysis period.

Table 6.7.16: Seasonal variations in $\delta^{13}C_{CH4}$ measurement for Landfill A with $\delta^{13}C_{CH4}$ of mean gas well samples and oxidation rate estimate. The errors are calculated as one standard deviations.

δ^{13}C-CH_4 (‰)	Site 1 (closed)	Site 1 oxidation rate[3]	Site 2 (active)	Site 2 oxidation rate[3]
Summer 2019[1]	-53.9 ± 0.6	11.6 ± 1.3 %	-59.6 ± 0.1	4.1 ± 0.5 %
Autumn 2019[1]	-53.6 ± 0.3	11.3 ± 1.2 %	-58.7 ± 0.1	7.8 ± 0.5 %
Winter 2019[1]	-54.6 ± 0.02	6 ± 1.2 %	-59.6 ± 0.04	3.2 ± 0.5 %
Gas well samples[2]	-55.9 ± 1.2 (10)	–	-60.3 ± 0.5 (10)	–

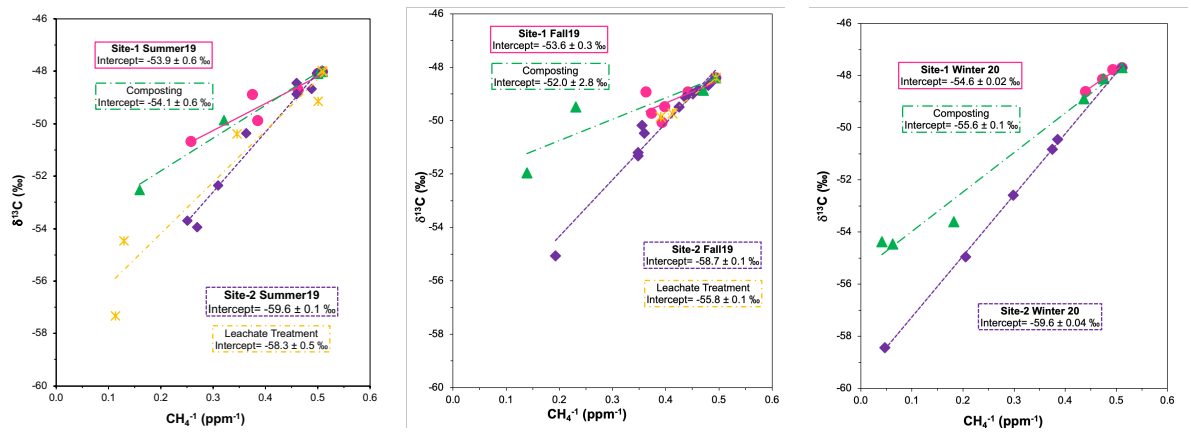

Fig. 6.7.28: Keeling plots for seasonal survey of Landfill A.

There was strong underlying variation in the δ^{13}C-CH_4 signatures calculated for downwind plumes between the closed and active sites at Landfill A, with a minimum δ^{13}C-CH_4 emission value of -59.6 ‰ in summer active site and up to a maximum δ^{13}C-CH_4 emission value of -53.6 ‰ in autumn in the closed site (Table 6.716, Fig. 6.7.28). High precision measurements found a maximum 1 ‰ difference between seasonal emission signatures.

The mean δ^{13}C-CH_4 of CH_4 emitted into the atmosphere ranged from (-59.3 ± 0.5) ‰ in the active part of the site to (-54.0 ± 0.5) ‰ in the closed part of the landfill. The CH_4 emissions from older, closed sites were characteristically more enriched in δ^{13}C than emissions from active sites. The isotopic signatures of landfill emissions from covered areas have been shown to differ from those in uncapped active tipping areas, owing to oxidation mediated by methanotrophic bacteria in the cover soil (Bergamaschi et al., 1998). Bergamaschi et al. (1998) obtained highly enriched values of (−45.9 ± 8) ‰ in covered areas compared with samples from uncovered areas ((−55.1 ± 5.2) ‰).

A similar trend was observed for the isotopic signatures for the anoxic zone gas wells of both active and closed sites. The closed site isotopic signatures were more enriched in ^{13}C than the active sites, presumably because they were much older and further along the CH_4 generation curve, so residual CH_4 might be more enriched.

Older waste may produce CH_4 that is more ^{13}C-enriched because the easier-to-decompose ^{12}C has already been preferentially used by methanogens in earlier decomposition soon after waste deposition. Another reason might be a change in waste composition as it evolved and matured over time which might produce a higher proportion of degradable organic matter in the older waste and variation in methanogenic communities. Also, over time there may have been differences in the composition of the input waste mixture in various parts of the landfill.

The oxidation rate was higher in the closed part of the site than in the active site in all seasons. During the winter season, a more depleted isotopic signature and a lower oxidation rate were observed from the closed cell owing to a decrease in the oxidizing ability of methanotrophs in soil cover during cold weather. Autumn produced the highest oxidation rates of (11.3 ± 1.2) % and (7.8 ± 0.5) % for the closed and active sites of Landfill A, respectively. Chanton et al. (1999) found the highest oxidation in autumn ((21 ± 2.7) %) and summer ((15.9 ± 4.5) %). These results are also consistent with Czepiel et al.'s (1996) finding of less oxidation in winter owing to an increase in precipitation and soil moisture, which limits the rate of CH_4 delivery to methanogenesis. In summary, the annual oxidation rate at Landfill A was approximately 7.3%, being (9.6 ± 3.2) % for the closed site, and (5.0 ± 2.4) % at the active site.

Impact of partial cap stripping on Landfill B

Landfill B was opened in 1986, mothballed in 2016, and partially reopened in August 2019. It was surveyed three times between July 2018 and August 2019. It was assessed to understand the impact of cap stripping on CH_4 emissions and $\delta^{13}C$-CH_4.

The widest plume and highest mole fraction of CH_4 were recorded from Landfill B during the July 2019 survey. The recorded maximum excess CH_4 over background on site was 3.5 ppm, 10 ppm and 6.5 ppm for July 2018, July 2019 and August 2019 surveys, respectively. Hot spots were located mostly downwind of leaking gas wells and the landfill gas engine area.

Landfill B has calculated $\delta^{13}C$-CH_4 emission signatures of (-56.8 ± 0.1) ‰, (-55.7 ± 0.1) ‰ and (-57.3 ± 0.2) ‰ for July 2018, July 2019 and August 2019, respectively (Fig. 6.7.29). In general, the July 2019 survey results revealed a higher CH_4 mole fraction with emitted CH_4 being more enriched in ^{13}C. The isotopic signatures of emitted plumes at different parts of the site were similar even after the partial cap stripping process. The placement of fresh waste in the next few weeks after stripping would not yet have been producing much CH_4 under the higher atmospheric pressure and ambient temperature. Downwind of cap stripping areas, we did not observe any CH_4 plumes. The average $\delta^{13}C$-CH_4 of 18 gas well isotopic samples was (-60.1 ± 1.1) ‰, with oxidation rates of (26.6 ± 1.1) % and (16.9 ± 1.1) % in July and August 2019, respectively.

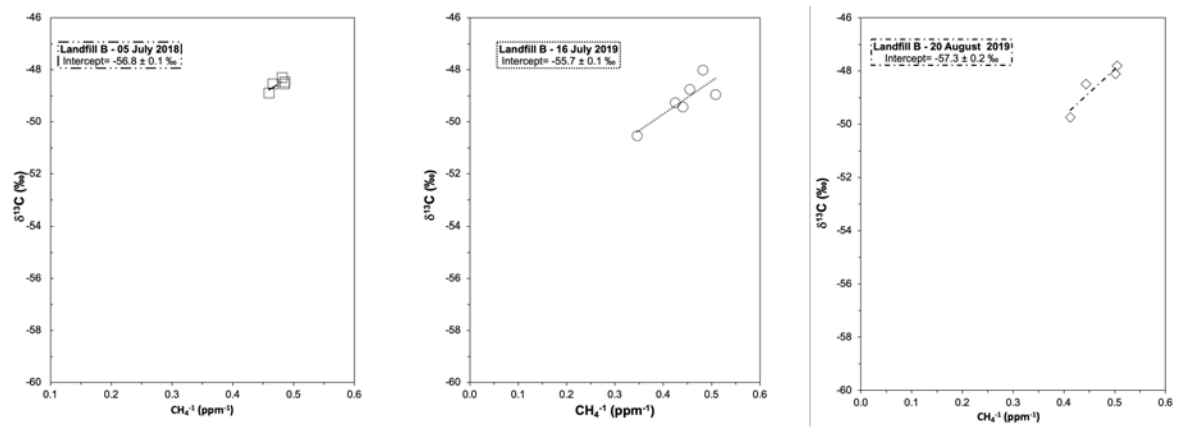

Fig. 6.7.29: Keeling plots for Landfill B.

Because all the gas wells were sampled in 2019, the oxidation rate for the 2018 survey was not estimated. Landfill B, with the hottest landfill temperature, gave the highest oxidation rate of the sites studied. Czepiel et al. (1996) suggested continuous increase in temperature limits the methanotrophs' enzymatic activity which causes a decrease in oxidation rate.

Impact of closure on Landfill C

Landfill C was surveyed in July 2019 and February 2020. There was freshly placed waste during the first survey, and there was a significant (almost 18.7 times) observable difference between the CH_4 mole fraction measured when active, compared to after closure. The excess CH_4 mole fraction above the background was up to 28 ppm while it was active, owing to direct CH_4 emissions into the atmosphere from uncapped active areas. After closure, the excess CH_4 mole fraction above the background dropped dramatically to 1.5 ppm. Due to the winter weather conditions, accessible roads to drive around the landfill site were limited. In previous studies of sources, CH_4 emissions can be still measured up to 4-5 km downwind of the largest landfill plumes (Lowry et al., 2020; Zazzeri et al., 2015), but in this case a wide plume was not detected at 600-650 meters downwind of Landfill C during the winter survey. The small plume measured around the gas engine site where the CH_4 was converted to electricity was due to gas engine work during the survey.

The $\delta^{13}C$-CH_4 signatures of CH_4 emissions from Landfill C were found to be between (-57.5 ± 0.2) ‰ and (-55.9 ± 0.02) ‰ (see Fig. 6.7.30), with a more depleted ^{13}C signature while the site was still active, and 1.6 ‰ more enriched in ^{13}C after the closure.

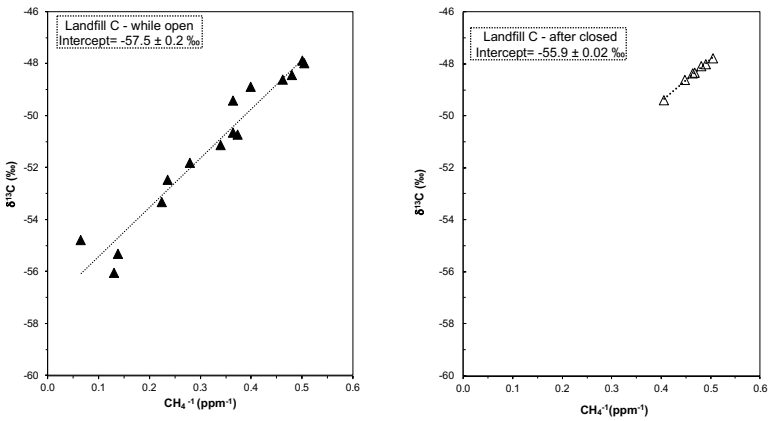

Fig. 6.7.30: Keeling plots for Landfill C.

The average $\delta^{13}C$-CH_4 signature of the 15 gas well samples were (-59.7 ± 1.1) ‰. The oxidation rate was estimated at (12.5 ± 1.1) % while waste was actively being placed, and (17.1 ± 1.1) % after the site was closed. The ambient air results indicate that the oxidation rate of CH_4 from the landfill site increased by 4.6 % after it was closed, because a build-up of surface vegetation, an increase in the organic layer and microorganism in the soil may have led to increased organic decomposition and microbial competition (Czepiel et al., 1996).

Landfill D site

Landfill D is similar to Landfill A with respect to the waste depth, the number of gas wells and cover soil type. They have also both active and closed sites. Therefore, the comparison of the two landfills can clearly show how the waste type and age affects the isotopic signature of CH_4.

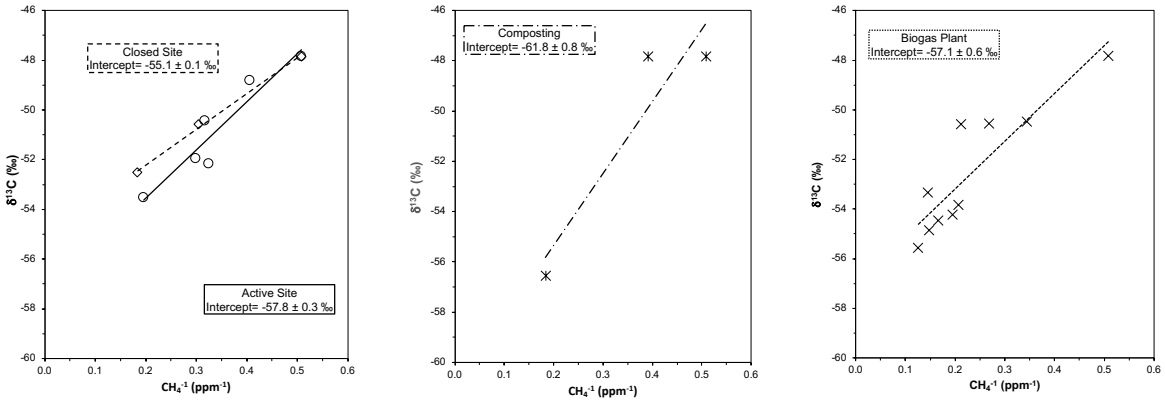

Fig. 6.7.31: Keeling plots for Landfill D.

Table 6.7.17: Ambient air samples, gas well samples and estimated oxidation rate at 25^{0}C for Landfill D. The errors are calculated as one standard deviations.

Landfill D	Site 1 (closed)	Site 2 (active)
Ambient air, δ^{13}C-CH$_4$ (‰)	-55.1 ± 0.1	-57.8 ± 0.3
Gas well samples, δ^{13}C-CH$_4$ (‰)[1]	-57.8 ± 1.3 (7)	-59.0 ± 0.7 (7)
Oxidation rate (%)	15.4 ± 1.3	7.0 ± 0.8

Notes: [1]The interquartile range (IQR) was applied to the collected gas well data set, and outliers were eliminated to calculate the average isotopic signature. The average of gas well samples is reported. The number of gas well samples is in brackets.

The δ^{13}C-CH$_4$ isotopic signatures observed for the Landfill D (Table 6.7.17, Fig. 6.7.31) are (-57.8 ± 0.3) ‰ and (-55.1 ± 0.1) ‰ for active and closed sites, respectively. In the closed parts of Landfills, A and D, δ^{13}C-CH$_4$ ranged from (-55.1 ± 0.1) ‰ to (-53.9 ± 0.6) ‰, indicating greater enrichment in ^{13}C than in the active parts, where values varied between (-59.6 ± 0.1) ‰ and (-57.8 ± 0.3) ‰.

The closed site of Landfill D was more depleted in ^{13}C relative to atmospheric background compared to the closed site of Landfill A. The difference between Landfill D and Landfill A may be due to differences in methanogenic communities, temperature differences and/or the age and composition of waste.

Because the closed site of Landfill D is younger than the closed site of Landfill A, methanogenesis in landfill D may have generated more-depleted, isotopically lighter CH$_4$ in the presence of excess substrate. On the other hand, CH$_4$ from the active site of Landfill A was more depleted in ^{13}C in comparison to Landfill D active site. Because Landfill A had a higher ratio of domestic waste compared to industrial and commercial waste, placed in the active site, and food waste is diverted to the anaerobic digestion plant located at Landfill D site, thus the lighter isotopic value may reflect easier degradation of domestically sourced organic matter.

In general, at Landfills A and D, the fraction of CH$_4$ oxidised at closed sites, as identified in the plumes, was higher (average (11.1 ± 3.9) %) than at active sites (average (5.4 ± 2.2) %) and much of the CH$_4$ emitted into the atmosphere from the active sites was from operational areas with daily cover only. However, it is possible that some oxidation may also occur in areas with temporary caps but very little cover soil in active zones of Landfills A and D.

The δ^{13}C-CH$_4$ in CH$_4$ emitted at active sites ranged from -59.6 to -57.5 ‰, with an averaged value of (-58.6 ± 1.0) ‰. In closed sites δ^{13}C-CH$_4$ varied from -57.3 to -53.6 ‰, with an average of (-55.4 ± 1.3) ‰ indicating more enrichment in ^{13}C compared to active sites (Table 6.7.18). These trends are in line with the findings of Börjesson et al. (2007) and Lowry et al. (2020). Anoxic zone samples were also more depleted in ^{13}C than the emissions to the atmosphere at all sites, and CH$_4$ from the anoxic zones of the older closed parts of Landfills A and D was less depleted in ^{13}C than the δ^{13}C-CH$_4$ in the anoxic zones of active sites.

Table 6.7.18: Summary of average ambient air signature, gas well isotopic signature and estimated oxidation rate of overall landfill sites. The errors are calculated as one standard deviations.

Site Name	Range of ambient air isotopic signature, $\delta^{13}C\text{-}CH_4$ (‰)	Average gas well isotopic signature, $\delta^{13}C\text{-}CH_4$ (‰)[1]	Range of estimated oxidation rate (%)	Emissions in 2018 NAEI (tonnes yr^{-1}, NAEI, 2020)
Landfill A - active	-59.6 to -58.7	-60.3 ± 0.5(10)	3.2 to 7.8	0.07
Landfill A - closed	-54.6 to -53.6	-55.9 ± 1.2 (10)	6 to 11.6	
Landfill B	-57.3 to -55.7	-60.1 ±1.1(18)	16.9 to 26.6	0.14
Landfill C	-57.5 to -55.9	-59.7 ±1.1(15)	12.5 to 17.1	N/A
Landfill D - active	-57.8 ± 0.3	-59.0 ±0.7(7)	7	0.05
Landfill D - closed	-55.1 ± 0.1	-57.8 ±1.3(7)	15.4	
Active cells of Landfills A, D and C while active: -59.6 to -57.5‰ and 3.2 to 12.5%				
Closed cells of Landfills A, D, B and C while closed: -57.3 to -53.6‰ and 6 to 26.6%				

Notes: [1] The number of gas wells are given in the brackets. N/A: Not Available

This may be attributable to several factors, including changes through maturation of waste composition, variations in decomposition rates for different types of waste, depth of burial, and the temperature and moisture content of the soil.

The oxidation rates for these four landfills varied across active and closed sites (see Table 6.7.16), as well as between different landfills (see Table 6.7.18). The oxidation rates were estimated at 3.2 – 12.5 % for active sites and 6 – 26.6 % for closed sites. The oxidation rate may have been lower for active, uncapped areas because most of the CH_4 escaped directly into the atmosphere.

The highest oxidation rates were measured in the closed sites of Landfills A, B, and D, and this is attributed to the well-vegetated soil cover and capping of the waste, similar to Abichou et al.'s (2006) finding of the lowest oxidation values from a thin intermediate daily cover areas compared to a thick intermediate well-vegetated soil cover in the landfill. This applied to the active parts of Landfills A and D, and to Landfill C while it was being actively used during the summer 2019 survey.

Previous studies found that oxidation in cover soil increases with decreasing soil moisture content. Czepiel et al. (1996) found an annual whole landfill oxidation rate of 10 % for Nashua landfill in 1994, which depended significantly more on temperature than on soil moisture. Liptay et al. (1998) also found a 10 % annual CH_4 oxidation rate in landfills.

The default oxidation rate for UK landfills is also 10 % (NAEI, 2020). This compares with the oxidation rates for the four landfills studied, which varied between 3.2 and 26.6 %, with an average of 7 % for active and 15 % for closed sites. Thus, we agree with Chanton et al. (2011) that the percentage oxidation rate should not be considered as a constant value, as it depends highly on the activity of the landfill site. Therefore, we recommend using site-specific oxidation rates rather than a default value.

It should be noted that using the stable carbon isotope technique for CH_4 ambient air yields a minimum estimate of CH_4 oxidation (Bourn et al., 2019). Moreover, Gebert et al. (2011) suggest that the reliability of this technique depends significantly on the isotopic fractionation mechanism. For example, flux chamber methods yield highly variable results because of the local fractionations in the topsoil zone. In this work, we measured atmospheric CH_4 plumes that integrated emissions from several cells, thus the average of a statistically significant number of gas wells was used to estimate the oxidation rate. But there is still future work that should ultimately focus on refining the isotope approach to evaluate CH_4 oxidation.

In much earlier studies of the 1990s, the isotopic signature of average landfill sources ranged between -55 and -51 ‰ (Bergamaschi et al., 1998; Levin et al., 1993; Wahlen, 1993), whereas our results ranged from -60 to -54 ‰, with an average of (-57 ± 2) ‰. These indicate a shift to more negative values in recent years influenced partly by the introduction of gas extraction systems and the change of waste composition being sent to landfills. Although landfill CH_4 emissions have decreased since 1990, the

observed changes in the isotopic signature of landfill emissions with changing landfill practice may also make a small contribution to the more negative d^{13}C values observed for global CH_4 over the 2007-2017 period.

6.7.1.2.2.3 Waste sources isotopic signatures

Different waste source types were surveyed using CRDS instruments in a vehicle to identify plumes of CH_4 for sampling and subsequent high precision GC-IRMS measurement. CH_4 mole fractions and $\delta^{13}C$-CH_4 were analysed to investigate variations between different waste sources. The whole site signatures were evaluated to identify the actual emission sources from all processes at the site to the atmosphere. During 39 mobile measurement days, emission plumes from 29 biogas plants, 29 landfills, 14 sewage treatment plants, one water treatment plant, four composting facilities, one landfill leachate treatment plant and a waste recycling facility were measured (see Fig. 6.7.32) to provide a better estimation of the contribution of each waste source to emission inventories and improve the waste source isotopic signature data for modellers to utilize at a regional and global scale. This study can also provide beneficial information to regulatory bodies that develop waste management strategies.

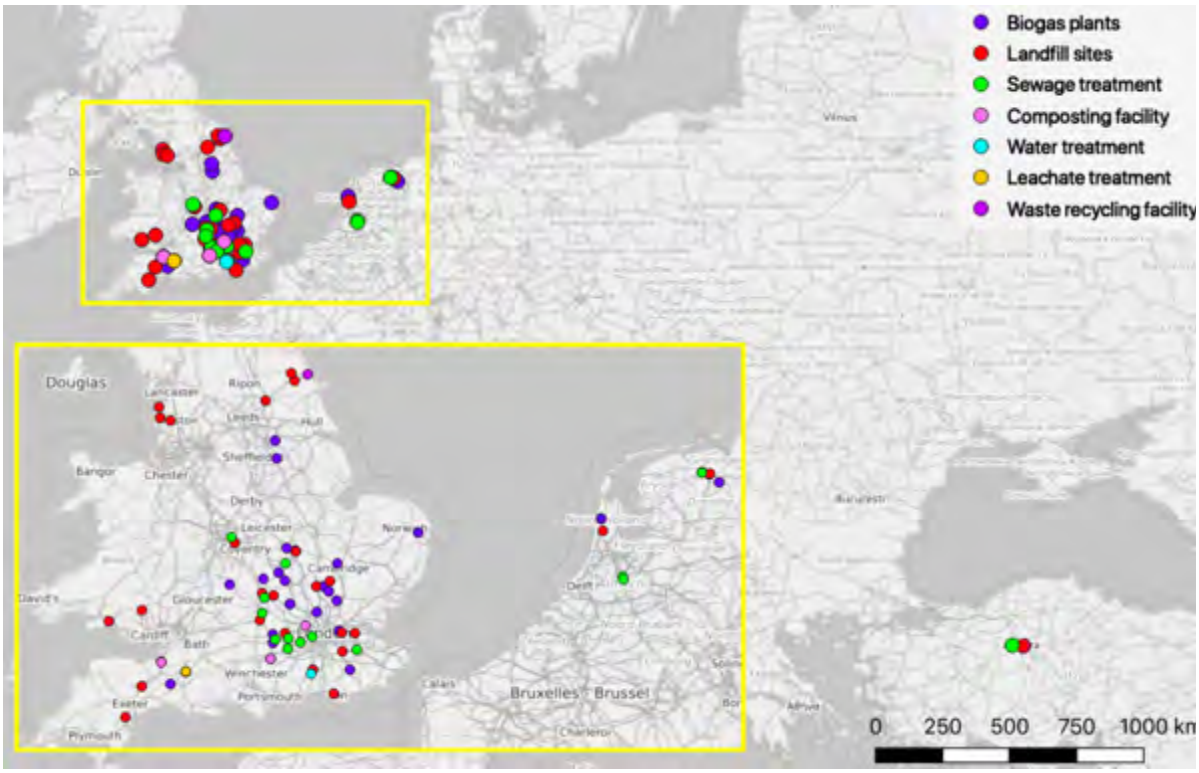

Fig. 6.7.32: Locations and categories of sampling sites

Biogas plants Isotopic Signatures

In biogas plants, methanogenesis produces CH_4 under anaerobic conditions through various metabolic pathways. The isotopic signature of CH_4 in anaerobic digesters depends on the substrate loading rates, the quantity and activity of the methanogenetic community, and operational conditions such as temperature, acidity (pH) and hydraulic retention times (Polag et al., 2015). For example, Polag et al. (2015) propose that $\delta^{13}C$-CH_4 values are depleted by 6 ‰ over a 20- to 35-day period, and the pH is inversely related to $\delta^{13}C$-CH_4 values.

In this study, the $\delta^{13}C$-CH_4 values varied from (-64.4 ± 0.1) to (-44.3 ± 0.1) ‰, with an average of (-54.8 ± 5.5) ‰ (Fig. 6.7.33 and supplementary information S1).

Of these data 82 % of the $\delta^{13}C$- CH_4 values fall between (-64.4 ± 0.1) and (-50.5 ± 0.03) ‰, with an average of (-56.6 ± 4.2) ‰, indicating greater enrichment in ^{13}C than Hoheisel et al.'s (2019) results. The most enriched values came from maize-fed biogas plants (see Fig. 6.7.34). Agricultural maize-waste biogas plants had more enriched signatures, with an average of (-45.7 ± 1.4) ‰. Because maize is a C4 crop with a 10-15 ‰ more ^{13}C-enriched carbon source than C3 vegetation (Levin et al., 1993), this skewed the average isotopic signature for agricultural biogas plants toward ^{13}C-enrichment. Papermill-waste (C3 trees) biogas plants had more depleted signatures than other types of biogas plants (see Fig. 6.7.34).

Food-waste biogas plants and the organic fraction of municipal solid waste (MSW) plants had the larger isotope ranges compared to other feedstocks, with averages of (-56.3 ± 4.0) ‰ and (-54.9 ± 4.5) ‰, respectively (Fig. 6.7.34). This large variability in the $\delta^{13}C$ values indicates that methanogenic pathways may differ according to the type of feedstock, causing changes in carbon isotope value.

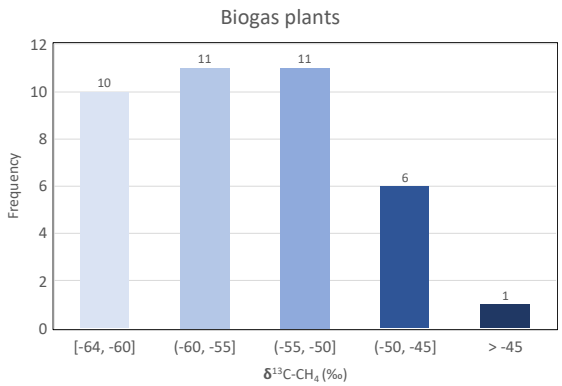

Fig. 6.7.33: Isotopic signature distribution of biogas plants.

Notes: The average of the 39-source signatures is -54.8 ± 5.5‰, with a median value of -55.6‰. Some sites were surveyed more than once. (See the Supplementary information, S1 for details.)

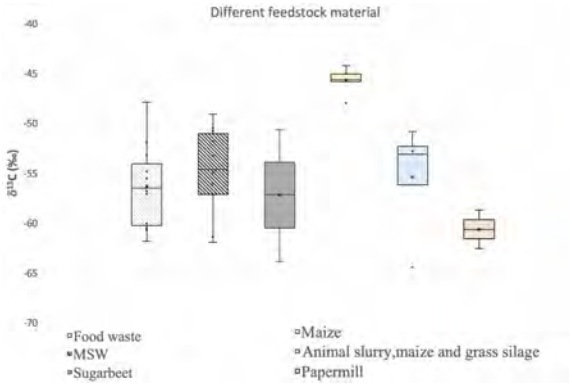

Fig. 6.7.34: Isotopic signature variations between the UK biogas plants relating to different feedstock materials. The figure shows the inner and outlier points with mean marker and line, interquartile calculation includes median value.

Landfill Isotopic Signatures

The isotopic signatures of landfills ranged from -62.1 ± 0.0 to -52.2 ± 0.1‰, with an average of -56.7 ± 2.3‰ (see Fig. 6.7.35 and supplementary information S2). The active landfills (with an averaged value of -58.1 ± 1.7‰) were more depleted in ^{13}C than the closed landfill sites (with an averaged value of -54.8 ± 1.4‰) (see Fig. 6.7.36). The isotopic signatures of landfills may vary with waste composition, temperature and the methanotrophic top-soil oxidation rate (Liptay et al., 1998). Aerobic bacteria in the top cover soil oxidize CH_4 produced in the landfill, causing a shift to more enriched isotopic signatures for CH_4 released into the atmosphere.

Four landfills (LA4, LA5, LA6 and LA11 see supplementary information S2) had previously been surveyed in 2013 by Zazzeri et al. (2015). All of our results, approximately five years later, were more enriched in ^{13}C, with differences of 0.6 to 4.7 ‰ between our results and theirs. This may have been due to changes in the concentration of organic matter and the age of the landfills, because exhaustion of organic matter causes heavier CH_4. The CH_4 mole fractions measured downwind of landfills LA4 and LA5 were much lower than Zazzeri et al. (2015)'s study, which would be expected if the sites were now closed and emissions thus reduced. Monteil et al. (2011) also reported the $\delta^{13}C$ of global landfills/waste is -55 ‰, a slightly more enriched value than this study result.

The average carbon isotopic signature of active landfills from the UK (15), the Netherlands (2), and Turkey (1) were recorded as (-58.5 ± 1.3) ‰, (-56.1 ± 2.4) ‰ and (-55.8 ± 0.8) ‰, respectively.

In Fig. 6.7.36, additional waste source signature values from the Netherlands, Germany, France and Poland were added into this study results. The overall landfill $\delta^{13}C\text{-}CH_4$ results did not change between these countries.

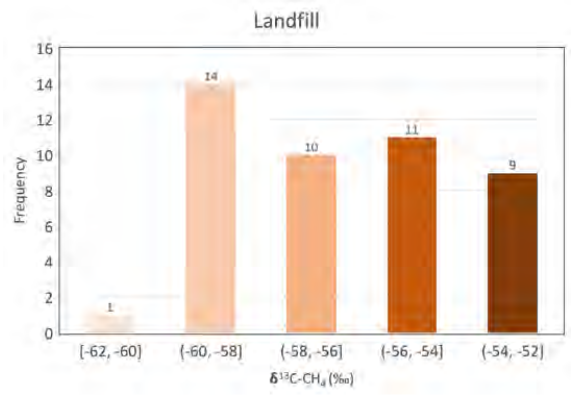

Fig. 6.7.35: Isotopic signature distribution of landfill

Notes: the average of the 45-source signatures is -56.7 ± 2.3‰, with a median value of -56.8‰. Some sites were surveyed more than once. (see supplementary information S2 for details)

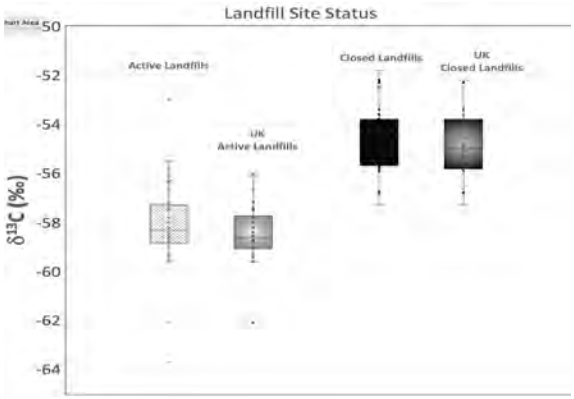

Fig. 6.7.36: Isotopic signature distribution differences between active and closed landfills. Additional data from the Netherlands (3), France (2), Germany (1) were added to current active landfill data from MEMO² database (Menoud et al., 2020). Closed landfills included one additional data from Poland and Netherlands (Menoud et al., 2020). The mean and median isotopic signature of the overall active and closed landfills are (-58.2 ± 2.0) ‰ and -58,4 ‰, (-54.7 ± 1.5) ‰ and -54.6‰, respectively. UK active landfills have (-58.5 ± 1.3) ‰ mean and -58.5 ‰ median values, UK closed landfills have –(54.8 ± 1.4) ‰ mean and -55 ‰ median values.

The greater ^{13}C depletion of active sites is in line with Lowry et al. (2020). However, we found a wider range of isotopic ratios due to investigation of more sources for active sites than Lowry et al. (2020) as nearly all active sites included older enclosed cells in the same area, it was also possible that the sites we surveyed had a larger proportion of closed cells.

Sewage and water treatment plants isotopic Signatures

The isotopic signatures of sewage treatment plants ranged from (-56.8 ± 0.2) to (-47.2 ± 0.1), with an average of (-51.5 ± 2.3) ‰. Nearly 83 % of results lay between -54.4 and -49.3 ‰ (Fig. 6.7.37). These results are comparable with those of Hoheisel et al. (2019), Xueref-Remy et al. (2020) and Toyoda et al. (2011).

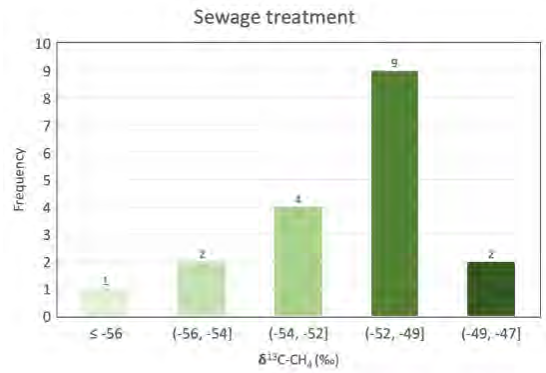

Fig. 6.7.37 Isotopic signature distribution of sewage treatment.

Notes: the average of the 18-source signatures is (-51.5 ± 2.3) ‰, with a median value of -50.8 ‰. Some sites were surveyed more than once. (see supplementary information S3 for details)

Toyoda et al. (2011) show that different stages of sewage treatment produce different isotopic signatures. For example, an aeration tank was more enriched in ^{13}C (-45.5 ‰) than a secondary settling tank (-51.7 ‰). Because we were interested in the overall signature emissions from sewage plants to atmosphere in this study and we had no access to the inside of sewage treatment facilities, we were unable to distinguish the isotopic signatures of each step of the treatment process. However, the results clearly indicate that sludge treatment processes such as anaerobic digestion lead to greater depletion of ^{13}C. It should be noted also that CH_4 emissions from sewage plants highly depend on dissolved oxygen concentration in

aeration basins and water temperature in high density clarifiers (Wang et al., 2011). The isotopic signatures between countries may be due to variation in process treatment, as well as flowrate and organic loading of incoming wastewater, while there were a limited number of sewage treatment works investigated from France, Germany, Poland and Turkey and even the Netherlands.

A CH_4 plume was detected from one water treatment facility because CH_4 emissions are mostly coming from sewage treatment due to higher organic loading. The water treatment process mainly involves the treatment of raw water such as river to produce standardised end-use water like drinking water. The CH_4 emissions from the water treatment had a $\delta^{13}C$-CH_4 signature of (-53.7 ± 0.1) ‰.

Composting facilities and leachate treatment plants isotopic Signatures

The four composting facilities and one leachate treatment plant in the UK surveyed in this study are listed in the supplementary information five (S5), together with the $\delta^{13}C$ signatures of the plumes sampled. The isotopic signatures of the composting facilities calculated a ranged value spanning from (-61.8 ± 0.8) to (-50.8 ± 0.5) ‰, with an average of (-54.7 ± 3.9) ‰ (Fig. 6.7.38). This high isotopic range might be due to the process dependant on the frequency, turnover and aeration of the waste, also the frequency of waterlogging leading back to anaerobic conditions.

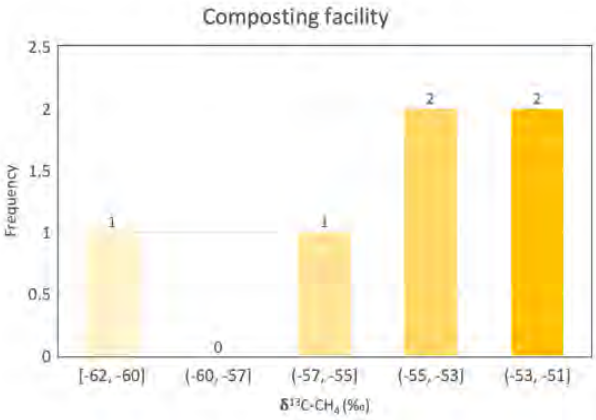

Fig. 6.7.38: Isotopic signature distribution of composting facilities measured in this study.

Notes: the average of the 6-source signatures is -54.7 ± 3.9‰, with a median value of -54.1‰. Some sites were surveyed more than once (See the Supplementary information, S4 for details).

Because most of the composting facilities were in close proximity to other waste sources such as landfill, biogas plants and even farms, it was very challenging to characterize their isotopic signatures. One leachate treatment plant at a landfill site produced signatures between (-58.3 ± 0.5) ‰ in summer and (-55.8 ± 0.1) ‰ in winter. These differences were due to temperature and seasonality changes between the two surveys (see supplementary information S4). Because microbial degradation is highly dependent on temperature variation, the colder weather conditions result in more enrichment in ^{13}C.

Overall waste sources

$\delta^{13}C$ values for all waste sources in Europe ranged between (-64.4 ± 0.1) and (-44.3 ± 0.06) ‰, with an average of (-55.1 ± 4.2) ‰ (see Fig. 6.7.39), and δD values ranged between (-341.3 ± 0.8) and (-251.9 ±14) ‰, with an average of (-295.1 ± 28) ‰ (see Fig. 6.7.40). These results are in line with Sherwood et al. (2017) who reported the mean values of global waste $\delta^{13}C$ and δD value as -56‰ and -298 ‰, respectively. Levin et al. (1993) reported (-55.4 ± 1.4) ‰ for the $\delta^{13}C$-CH_4 value of waste, which is also similar to this study. Yang et al. (2019) described the solid waste management carbon isotopic signature as (-53 to -43.9) ‰, which is a slightly more ^{13}C-enriched range.

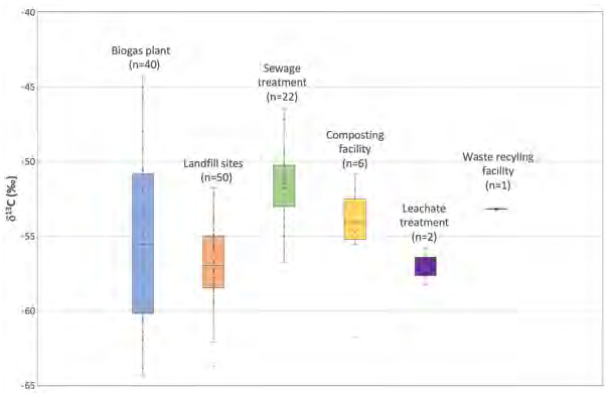

ig. 6.7.39: Isotopic signature distribution of waste sources from Europe. Additional data were included from MEMO² database (Menoud et al., 2020).

The biogas plants had a wider range of isotopic signatures than other sources with more depleted ^{13}C values. This difference may have been due to the variety of feedstock materials and the higher number of sampled sources.

Although all waste-source isotopic signatures originated from biogenic sources, sewage treatment clearly produced more enrichment in ^{13}C, at around -50 ‰ compared with other sources. Our enriched ^{13}C sewage treatment results are in general agreement with Townsend-Small et al. (2012) and Toyoda et al. (2011).

Comparison in deuterium and carbon isotopic signature

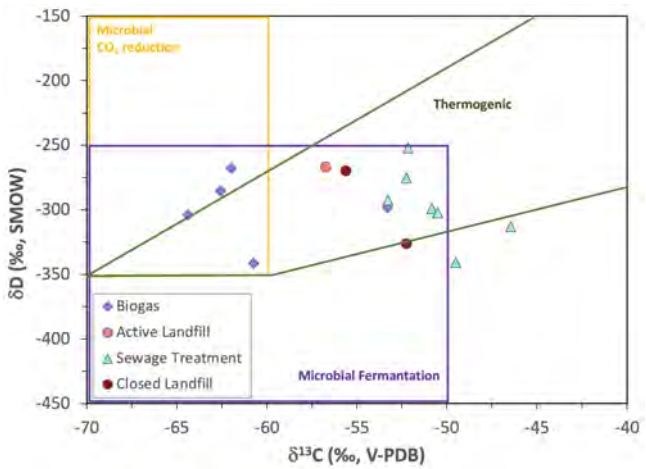

Fig. 6.7.40: δD vs $\delta^{13}C$ of CH_4 from waste sources mainly in the UK and one sewage plant in the Netherlands, measured in this study. The background boxes demonstrate the previous studies range of values (Milkov and Etiope, 2018; Sherwood et al.,2017; Whiticar et al., 1999;1990). The global average atmospheric $\delta^{13}C$ of CH_4 was -47.3 ‰ for the year 2016 (White at al., 2017) and -95.5 ‰ for δD in the year 2015 (Sherwood et al., 2017).

Fig. 6.7.40 demonstrates that the waste category spans a large range, which does not precisely fall into the microbial fermentation category. Biogas plant signatures are slightly more enriched in δD and more depleted in $\delta^{13}C$ compared to other sources. Their methanogenic pathway overlaps with microbial CO_2 reduction (Milkov and Etiope, 2018) and microbial fermentation. The isotopic signatures of landfill and sewage overlapped in some samples through microbial fermentation pathway, but the sewage treatment samples were more enriched in ^{13}C, and the landfill samples were more enriched in D. The deuterium isotopic signatures observed for the five biogas plants studied in the UK (Fig. 6.7.40) span a range from (-341.3 ± 0.8) to (-267.7 ± 49) ‰, with an averaged value of (-299.3 ± 27) ‰ (see Supplementary information S1, for details). In the literature, Levin et al. (1993) only reported one biogas generator deuterium signature for four samples as (-305 ± 49) ‰, which was in line with this study.

Sewage treatment deuterium signatures varied between (-251.9 ± 14) ‰ and (-340.9 ± 21) ‰, with an average of (-296.5 ± 28) ‰ for the seven UK sites, which is similar range in D compared to US sewage treatment plant (-298 ‰) (Townsend-Small et al., 2016). The UK closed landfill sites ((-297.9 ± 40) ‰) had more depleted in deuterium signature compared to the active landfill site ((-266.7 ± 1) ‰). These are more enriched values in comparison with the US active landfill, (-290 ± 4) ‰ (Townsend-S mall et al., 2016).

The isotopic signatures of the biogas plants, composting facilities and active landfills reveal greater ^{13}C depletion than in other waste sources. The Net Zero Commission recommends that all biodegradable waste being sent to landfill sites in the UK will be banned within the next five years and more waste will be diverted to biogas and composting facilities (CCC, 2020). Therefore, isotopic signatures of waste emissions may change in coming years due to variation in waste management strategies.

6.7.1.3 Future plans and expected results

ESR 7 submitted her PhD thesis on December 2020 and passed her VIVA exam on February 2021. Her paper on ”Quantification of CH_4 emissions from UK biogas plant” has been published in Waste Management and is accessible online at https://doi.org/10.1016/j.wasman.2021.01.011.

Her second paper which is titled as "Carbon isotopic characterisation and oxidation of UK landfill CH_4 emissions by atmospheric measurements" was submitted to Waste Management and the paper has been under review since January 19, 2021. Her last paper titled Stable isotopic signatures of CH_4 from waste sources through atmospheric measurements will be submitted to a peer-review journals in 2021.

ESR 7 has been working at the Sustainable Gas Institute in Imperial College London since October, 2020.

6.7.1.4 Collaborations (internal / external)

ESR 7 has been working with the non-academic partner Viridor on landfill monitoring, site access and combined measurement and training in the waste industry. Also, ESR 7 collaborated with Utrecht University to learn deuterium techniques and University of Groningen for her secondments.

ESR 7 contacted Arla Dairy in the UK and had a guided visit of their anaerobic digestion biogas plant.

6.7.1.5 Risks and difficulties

No risks or difficulties reported for this period.

6.7.2. Deliverables

D1.1 - Lightweight CH_4 sensor & AirCore development & deployed on UAV (month 24)

ESR 7 competed her secondment at University of Groningen to learn Aircore deployed on UAV.

D1.4 - Improved emission factors for different source categories from mobile measurement (month 42)

ESR 7 has estimated the 10 different biogas plant emissions in the UK and published the emission rates, losses and emission factors.

D1.5 - Report on harmonized method for mobile CH_4 and $\delta^{13}C$-CH_4 (month 18)

ESR7 has quantified the CH_4 mole fractions and its isotopic signatures from landfill, biogas plants, wastewater treatment plants, farms and city.

D2.1 - Isotopic measurements linked to common scale (month 18)

No contribution reported for this period.

D2.2 Improved isotopic source signatures of local and regional CH_4 (month 36)

ESR7 has contributed to improvement of isotopic signature from different waste sources in the UK and Netherlands by adding new measurements included in the database.

D2.3 - Publication on the use of isotopes for CH_4 source attribution in urban/industrial regions (month 36)

ESR7 has surveyed and contributed measurements for the city of Birmingham.

6.7.3 Training and network activities

6.7.3.1 General training events

ESR 7 has attended or will attend the training events listed below.

Event	Date (start – end)	Location (Host)	Objective / expected skills	ECTS points	Contribution	Comments
Mobile Measurement Training	30.01.2018-31.01.2018	RHUL	To get the skills of using mobile measurement equipment such as CRDS, LGR and sample collection.	2	Participating	
Sample Measurement Training	12.01.2018	RHUL	To learn to how air bag samples are measured on CRDS instrument and mobile LGR	0.5	Participating	
IRMS Analysis Training	02.02.2018	RHUL	To get the skill of laboratory analysis of carbon isotopes using GS-IRMS and interpret the data	0.5	Participating	

MEMO^2 School	05.02.2018-16.02.2018	Holland	Two-week thematic school on methane including courses, practical exercises, field campaigns and data analysis.	6	Presenting a poster and oral presentation	
MEMO^2 annual MEMO^2 Annual Meeting	22.03.2018-23.03.2018	EMPA	To be updated about the project, discuss and evaluate the progress of the first year and give an outlook to the second year.		Presenting a poster and presentation	
Academic Grammar and Vocabulary Course	21.02.2018-14.03.2018	RHUL	Four-week course to enhance basic knowledge of grammar more effectively in writing, to express ideas more clearly and academic in sentences	2	Participating	
Clarity in Academic Writing Course	26.02.2018	RHUL	It is about the importance of logically grouping and sequencing ideas; how to construct clear, cohesion paragraph; how to use sentence/clause connectors; improving clarity though simplified language.	0.5	Participating	
Managing of Research Data and Publication Course	01.03.2018	RHUL	Getting knowledge about open accesses for research publication, introduction to research management	0.5	Participating	
Volunteering in the Science Festival	11.03.2018	RHUL	Guide and show public to how mobile methane measurements are made, make cow mask with kids	0.5	Participating, teaching	
Writing a Literature Review Course	14.03.2018	RHUL	Tips about writing literature review; how to organize and connect to different articles related to sub-subjects.	0.5	Participating	
Networking Workshop	27.02.2018	RHUL	It is about to understanding how to remain your authentic self, whilst building relationships and making helpful contact; giving practical tips and techniques for creating own networking strategy and plan; and Getting the most from digital and online networking	0.5	Participating	
Mentoring and Cultural Awareness Workshop	08.05.2018	RHUL	Couse help to understand cultural differences and the impact on the mentoring relationship; and it gives a chance to work together to identify strategies to manage differences.	0.5	Participating	
MEMO^2 Methane Isotope Workshop	17.09.2018-19.09.2018	RHUL	To learn much more detail about methane isotopes such as global trends. Identification of sources, sampling analysis, measurement techniques and regional /global /temporal modelling of methane isotopes	0	Participating on Skype	
MEMO^2 Plume Workshop Modelling	09.10.2018-10.10.2018	UHEL	To learn how to model plume, make a practice by writing a code on Phyton.	2	Participating	
GIS Course	01.11.2018-06.11.2018	RHUL	To learn ArcGIS programme more effectively to draw methane emission maps	4	Participating	
Introduction to R course	09.11.2018	RHUL	Introduction of some basics of R.	1	Participating	
Emotional Intelligence	08.11.2018	RHUL	To develop my own intelligence profile, using the Emotional Quotient Inventory, understand how to maximize on own emotional strength and improve it.	0.5	Participating	
CV writing and interview Skills Training Course	27.11.2018	RHUL	To learn writing effective CV and interviewing techniques	0.5	Participating	
MEMO^2 School	18.02.2019-22.02.2019	France	To be updated about the project, discuss and evaluate the progress and have a meeting with EU representative.		Presenting a poster and presentation	
Applying for Postdoctoral Fellowships and Research	27.02.2019	RHUL	Getting informed about postdoctoral Fellowships options in the Europe.	0.5	Participating	
Preparing your Viva	28.02.2019	RHUL	Studying strategies and procedure of Viva were learnt.	0.5	Participating	
Volunteering in the Science Festival	07.03.2019	RHUL	Guide and show public to how mobile methane emissions measurement is doing, make cow mask with kids	0.5	Participating, teaching	
Departmental Seminar	13.03.2019	RHUL	Making a presentation during postgrad seminar	0.5	Presenting a presentation	

English language training in Writing Workshops for International PhD Students	03.11.2019	RHUL	Learning writing strategies	1	Participating	
Writing a scientific paper	19.11.2019	RHUL	Evaluating and learning scientific paper	1	Participating	
MEMO² 3rd Annual Meeting	10-11.02.2020	UHEL	To be updated about the project, discuss and evaluate the progress of the project and give an outlook to the future plans		Presenting a presentation	
Departmental Seminar	04.03.2020	RHUL	Poster Presentation at departmental postgrad seminar	0.5	Poster Presentation	

6.7.3.2 Secondments

Secondment	Date (start – end, planned (when))	Location	Host	Description of work / deviations	Scientific / training (skills) objective	Results and future plans
1.	17.09.2018-26.10.2018	Holland	RUG	Mobile measuring of Groningen emission source. Characterization of Groningen Methane Emission Sources	UAV Air core working Principle	Isotopic results and mobile measurement characterization will be done.
2.	27.05.2019-07.06.2019	Holland	UU	Lab working at UU	Learning of deuterium methodology	46 samples were analysed
3.	07.05.2019-Now	UK	Viridor	Mobile measuring of four different landfill, characterization of their isotopic signature and calculation of their oxidation rate.	Seasonal impact on landfill oxidation rate	Summer Fall and Winter surveys were performed, and its results given in result section. Spring survey will be done on April 2020.

6.7.3.3 Conferences

Conference name	Date (start – end, planned (when))	Location	Presentation (oral / poster)	Title of presentation	Authors (main author + co-authors)	Public available (yes / no) / web link
ICOS	11.09.2018-14.09.2018	Czech Republic	Poster	Waste Source in the UK	S. Bakkaloglu + D.Lowry, R. Fisher, E. Nisbet	https://conference.icos-ri.eu/wp-content/uploads/2018/09/ICOS2018SC_Book_of_Abstracts.pdf
BBOS	25.10.2018-26.10.2018	Holland	Poster	Waste Source in the UK	S. Bakkaloglu, + D.Lowry, R. Fisher, E. Nisbet	NO
PFTEC Conference	22.05.2019 24.05.2019	Holland	Poster	Stable Isotopic Signature of Methane from Biogas Sources in the UK and Netherlands	S. Bakkaloglu + D.Lowry, R. Fisher, C, Huilin, E. Nisbet	No
NCGGs Conference	12.06.2019 14.06.2019	Holland	Poster	High Precision Isotope Measurements to Characterize Waste Source of Atmospheric Methane	S. Bakkaloglu + D.Lowry, R. Fisher, C, Huilin, E. Nisbet	No
AGU Conference	09.12.2019 13.12.2019	USA	Poster	The Greenhouse Gas Methane Emissions from Waste Sources in the UK	S. Bakkaloglu + D.Lowry, R. Fisher, C, Huilin, E. Nisbet	No

EGU	04.05.2020 08.05.2020	Austria-online	Pico	Characterization and Quantification of Methane Emissions from Waste in the UK	S. Bakkaloglu + D.Lowry, R. Fisher, H, Chen, E. Nisbet	https://meetingorganizer.copernicus.org/EGU2020/EGU2020-17839.html
AGU	01.12.2020 17.12.2020	USA-online	Talk	Quantifications of methane emissions from UK biogas plants	S. Bakkaloglu + D.Lowry, R. Fisher, H, Chen, E. Nisbet	https://agu.confex.com/agu/fm20/webprogram/Paper702158.html

6.7.3.4 Measurement / sampling campaigns

Campaign	Date (start – end, planned (when))	Location	Host	Description of work	Scientific objective	Samples (nature / number)	Results and future plans
Yorkshire (KM5)	30.01.2018-31.01.2018	Yorkshire	RHUL	Mobile car night measurement	Training on mobile methane measurement	25 bags were collected	
MEMO² School	09.01.2018-12.02.2018	School		Mobile car night measurement	Training on mobile methane measurement	MEMO NL- 35 bags	
Sutton (UNC1)	03.05.2018	Sutton	RHUL	Mobile car night measurement	To quantify methane mole fractions and isotopic signatures	UNC1-1,2,3	Gas leaks have been found
Cambridge	13.05.2018	Cambridge	RHUL	Cow Barn	To quantify methane mole fractions and isotopic signatures	CAM 1,2,3,4,5,6,7,8,9, 10,11,12 13,14,15,16,17,18,19	See 1.2.2
Brighton (UNC2)	14.05.2018	Brighton city	RHUL	Mobile car night measurement	To quantify methane mole fractions and isotopic signatures	UNC2-1,2,3,4,5,6,7,8,9, 10,11,12 13,14,15,16,17,18	See 1.2.2
MEMO-1	22.06.2018	Local Sources	RHUL	Mobile car night measurement	To quantify methane mole fractions and isotopic signatures	MEMO RHUL1-1,2,3,4,5,6	See 1.2.2
MEMO-2	26.06.2018	Oxford, Bicester, Milton Keynes	RHUL	Mobile car night measurement	To quantify methane mole fractions and isotopic signatures	MEMO RHUL2-1,2,3,4	See 1.2.2
MEMO-3	27.06.2018	Local RHUL Sources	RHUL	Mobile car night measurement	To quantify methane mole fractions and isotopic signatures	MEMO RHUL3-1,2,3,4,5	Gas leaks have been found
MEMO-4	28.06.2018	Isle of Grain/Kent	RHUL	Mobile car night measurement	To quantify methane mole fractions and isotopic signatures	MEMO RHUL4-1,2,3,4,5,6,7,8	See 1.2.2
MEMO-5	05.07.2018	Devon	RHUL	Mobile car night measurement	To quantify methane mole fractions and isotopic signatures for Heathfield Landfill, and Exeter region	MEMO RHUL1-1,2,3,4,5,6,7,8,9, 10,11,12	See 1.2.2
RUG-1	25.09.2018	Groningen	RUG	Mobile car night measurement	To quantify methane mole fractions and isotopic signatures for Groningen city and Germany pit fire	GROG1-1,2,3,4,5,6,7,8	Will be evaluated
RUG-2	26.09.2018	Groningen	RUG	Mobile car night measurement	To quantify methane mole fractions and isotopic signatures for Groningen city	GROG2-1,2,3,4,5,6,7,8,9	Will be evaluated
RUG-3	27.09.2018	Groningen	RUG	Mobile car night measurement	To quantify methane mole fractions and isotopic signatures for Groningen city	GROG3-1,2,3,4	Will be evaluated
RUG-4	2.10.2018	Groningen	RUG	Mobile car night measurement	To see the methane emissions and isotopic signatures change during night measurement.	GROG4-1,2,3,4,5,6,7,8,9	Will be evaluated
RUG-5	18.10.2018	Lutjeward	RUG	Observation	Observation of sampling and measurement techniques, taking background samples	ROG5-1,2	Will be evaluated

					for isotopic methane signatures		
RUG-6	19.10.2018	Grijskerk Cow Farm	RUG	Farm- Drone measurement	Observing UAV Aircore Measurement Techniques to quantify methane mole fraction. Figure outing Duct Farm isotopic methane signatures	GROG6-1,2,3,4,5	Will be evaluated
UNC8	21.11.2018	Havering Brough	RHUL	Rainham and Mucking Landfill Survey	To quantify methane mole fractions and isotopic signatures	UNC8,1-22	
UNC10	28.11.2018	Hounslow	RHUL	Mogden Sewage	To quantify methane mole fractions and isotopic signatures	UNC10, 1-13	
BG1	06.12.2018	Various biogas plants at North West of London	RHUL	Biogas Survey	To quantify methane mole fractions and isotopic signatures	BG1,1-19	
BG2	17.12.2018	Reading, Oxford	RHUL	Biogas Survey	To quantify methane mole fractions and isotopic signatures	BG2, 2-22	
TUR	03.01.2019	Ankara, TR	RHUL	Landfill and WWTP	To quantify methane mole isotopic signatures	TUR1,1-9 TUR2,1-6	
UNC16	22.01.2019	Birmingham	RHUL	City Survey	To quantify methane mole fractions and isotopic signatures	UNC16,1-11	
BG3	23.01.2019	SW of Egham	RHUL	Biogas Survey	To quantify methane mole fractions and isotopic signatures	BG3,1-15	
UNC20	05.02.2019	Birmingham	RHUL	City Survey	To quantify methane mole fractions and isotopic signatures	UNC20,1-5	
BG4	11.03.2019	Various waste sources	RHUL	Biogas Survey	To quantify methane mole fractions and isotopic signatures	BG4,1-9	
BG5	14.03.2019	Various biogas plant	RHUL	Biogas Survey	To quantify methane mole fractions and isotopic signatures	BG5,1-5	
NNG2	18.03.2019	North Notts Gas	RHUL	Oil and Gas Survey	To quantify methane mole fractions and isotopic signatures	NNG2,1-7	
UNC23	19.03.2019	Birmingham	RHUL	City Survey	To quantify methane mole fractions and isotopic signatures	UNC23,1-6	
UNC27	02.04.2019	Birmingham	RHUL	City Survey	To quantify methane mole fractions and isotopic signatures	UNC27,1-4	
BG6	15.05.2019	Different waste sources	RHUL	Biogas Survey	To quantify methane mole fractions and isotopic signatures	BG6,1-15	
BG7	23.05.2019	Nottingham, Cranford	RHUL	Biogas Survey	To quantify methane mole fractions and isotopic signatures	BG7,1-23	
UUS-1	03.06.2019	Utrecht	UU	Waste Sources	To quantify methane mole fractions and isotopic signatures	UUS1,1-6	
UUS-2	04.06.2019	Utrecht	UU	Waste Sources	To quantify methane mole fractions and isotopic signatures	UUS2.1-2	
DM1	09.07.2019	Castle Cary	RHUL	Dimmer Landfill Summer Survey	To quantify methane mole fractions and isotopic signatures, to sample gas well	DM-1,1-25	
HF1	16.07.2019	Exeter	RHUL	Heathfield Landfill	To quantify methane mole fractions and isotopic signatures, to sample gas well	HF1,1-8 and 2-5	

BP1	23.07.2019	Broadpath	RHUL	Broadpath Landfill	To quantify methane mole fractions and isotopic signatures, to sample gas well	BP1-15	
WP1	06.08.2019	Pawlett	RHUL	Walpole Landfill	To quantify methane mole fractions and isotopic signatures, to sample gas well	WP1,1-28	
HF2	20.08.2019	Exeter	RHUL	Heathfield Landfill	To quantify methane mole fractions and isotopic signatures and observe process impact	HF2,1-12	
UNC37	23.09.2019	Birmingham	RHUL	City Survey	To quantify methane mole fractions and isotopic signatures	UNC37,1-2	
BG8	01.11.2019	Various biogas plant	RHUL	Biogas Survey	To quantify methane mole fractions for emission rate estimation		
DM2	05.11.2019	Castle Cary	RHUL	Dimmer Landfill Fall Survey	To quantify methane mole fractions and isotopic signatures, to sample gas well	DM-2,1-26	
BG9	03.12.2019	SW of England	RHUL	Broadpath landfill and various biogas plants	To quantify methane mole fractions and isotopic signatures and emission rate estimation		
BG10	21.01.2020	Various biogas plant	RHUL	Biogas Plants	To quantify methane mole fractions for emission rate estimation		
CAM2& BG11	30.01.2020	Cambridge region	RHUL	Cabridye University Cow barn and Biogen Biogas plant	To quantify methane mole fractions and isotopic signatures and emission rate estimation	CAM2,1-17 BG11,1-4	
BG12	17.02.2020	South Petherton	RHUL	Biogas Survey	To quantify methane mole fractions for emission rate estimation		
DM3	17.02.2020	Castle Carry	RHUL	Dimmer Landfill Winter Survey	To quantify methane mole fractions and isotopic signatures	DM3,1-19	
BP2	17.02.2020	Tiverton	RHUL	Broadpath Landfill	To quantify methane mole fractions and isotopic signatures, to observe closure impact	BP2,1-8	
BG13	05.03.2020	Aylesbury region	RHUL	Landfills and Stuchbury Biogas Plant	Arla Dairy site visit and To quantify methane mole fractions and isotopic signatures and emission rate estimation	BG13,1-9	

6.7.4 Dissemination activities

ESR7 is co-author of the following publication

E.G. Nisbet, R.E. Fisher, D. Lowry, J.L. France, G. Allen, **S. Bakkaloglu**, T.J. Broderick, M. Cain, M. Coleman, **J. Fernandez**, G. Forster, P.T. Griffiths, C.P. Iverach, B.F.J. Kelly, M.R. Manning, P.B.R. Nisbet-Jones, J.A. Pyle, A. Townsend-Small, A. al-Shalaan, N. Warwick, G. Zazzeri: Methane Mitigation: Methods to Reduce Emissions, on the Path to the Paris Agreement; Reviews of Geophysics, 58, e2019RG000675, https://doi.org/10.1029/2019RG000675, 2020

https://agupubs.onlinelibrary.wiley.com/doi/epdf/10.1029/2019RG000675

Bakkaloglu, S., Lowry, D., Fisher, R.E., France, J.L., Brunner, D., Chen, H., and Nisbet, E.G.: Quantification of methane emissions from UK biogas plants, Waste Management, 124, 82-93, https://www.sciencedirect.com/science/article/pii/S0956053X21000167, 2021

Supplementary Information

S1. List of biogas plants surveyed with the calculated $\delta^{13}C\text{-}CH_4$ signature. Errors are calculated as standard deviation

Source number	Site location	Feed Stock Material	Sampling date	Number of samples collected	Excess CH_4 (ppb)	$\delta^{13}C\text{-}CH_4$ (‰) (σ)	$\delta D\text{-}CH_4$ (‰) (σ)
B1	Eenigenburg, NL	Food waste	09/02/2018	4	77.01	-60.7 ± 0.1	
B2	Eenigenburg, NL	Food waste	09/02/2018	2	359.7	-56.5 ± 0.1	
B3	West Sussex, UK	MSW	14/06/2018 15/05/2019	4 3	966 318	-49.1 ± 0.3 -53.3 ± 0.0	-298.2 ± 0.4
B4	Cambridgeshire, UK	Food waste	15/06/2018 06/12/2018 30/01/2020	3 2 3	1820.5 192.8 1997.5	-56.8 ± 0.1 -60.1 ± 0.0 -60.6 ± 0.1	
B5	Buckinghamshire, UK	MSW	26/06/2018 05/03/2020	4 3	332.8 823.8	-62.0 ± 0.1 -61.4 ± 0.0	-267.7 ± 49
B6	Hoogezand, NL	MSW	25/09/2018	5	2723.5	-57.2 ± 0.1	
B7	Groningen, NL	MSW	26/09/2018 27/09/2018 02/10/2018	3 3 4	5269.9 968.3 1715.6	-50.5 ± 0.0 -51.9 ± 0.0 -50.8 ± 0.0	
B8	Groningen, NL	Sugar beet	26/09/2018 02/10/2018	2 2	437.1 725.7	-50.7 ± 0.0 -63.9 ± 0.0	
B9	Greater London, UK	Food waste	21/11/2018	3	100.1	-55.6 ± 0.1	
B10	Greater London, UK	Food waste	21/11/2018	3	133	-55.6 ± 0.0	
B11	Hertfordshire, UK	Food waste	06/12/2018	3	208.1	-54.9 ± 0.0	
B12	Hertfordshire, UK	Maize	06/12/2018	3	385.7	-48.0 ± 0.1	
B13	Buckinghamshire, UK	Food waste	06/12/2018 05/03/2020	3 2	1886.7 350.1	-51.9 ± 0.4 -52.0 ± 0.0	
B14	Buckinghamshire, UK	Food waste	06/12/2018	4	1886.7	-61.9 ± 0.0	
B15	Hertfordshire, UK	Food waste	06/12/2018	3	481.2	-53.3 ± 0.1	
B16	Berkshire, UK	Maize	17/12/2018	5	748.9	-45.9 ± 0.1	
B17	Berkshire, UK	Papermill	17/12/2018 15/05/2018	2 4	813.5 152.2	-58.7 ± 0.0 -62.6 ± 0.0	-285.5 ± 0.1
B18	Hampshire, UK	MSW	23/01/2019	6	2877	-57.1 ± 0.9	
B19	South Yorkshire, UK	Sugar beet	22/11/2018	3		-57.2 ± 0.1	
B20	Nottinghamshire, UK	Maize	27/02/2019	2	358.9	-45.1 ± 0.0	
B21	South Yorkshire, UK	Maize	27/02/2019 18/03/2019	3 3	738.5 399.1	-45.7 ± 0.0 -44.3 ± 0.1	
B22	Gloucestershire, UK	MSW	11/03/2019	6	4055	-56.1 ± 0.2	
B23	Northamptonshire, UK	Mixed	14/03/2019	2	107.9	-53.4 ± 0.0	
B24	Middlesex, UK	Mixed	23/05/2019	4	156.4	-64.4 ± 0.1	-303.8 ± 0.1
B25	Northamptonshire, UK	Food waste	23/05/2019	6	808.4	-60.7 ± 0.3	-341.3 ± 0.8
B26	Somerset, UK	Food waste	06/08/2019	10	5960.2	-57.1 ± 0.6	
B27	Cambridgeshire, UK	Food waste	30/01/2020	2	117.1	-47.9 ± 0.0	
B28	Somerset, UK	Mixed	17/02/2020	3	1438	-50.9 ± 0.1	
B29	Oxfordshire, UK	Mixed	05/03/2020	3	334	-52.9 ± 0.2	
Biogas plant, average $\delta^{13}C\text{-}CH_4$: -54.8 ± 5.5‰ (VPDB); $\delta D\text{-}CH_4$: -299.3 ± 27‰ (VSMOW)							

Notes: Mixed feedstock material is the mixture of animal slurry, maize and grass silage.

S2. List of landfills surveyed with the calculated $\delta^{13}C\text{-}CH_4$ signature. Errors are calculated as standard deviation

Source number	Site location	Sampling date	Number of samples collected	Excess CH_4 (ppb)	$\delta^{13}C\text{-}CH_4$ (‰) (σ)	$\delta D\text{-}CH_4$ (‰) (σ)
			Active Landfills			
LA1	Alkmaar, NL	12/02/2018	5	161.8	-53.0 ± 0.1	
LA2	West Sussex, UK	14/06/2018	4	1158	-57.2 ± 0.1	
		15/05/2019	4	807	-56.7 ± 0.2	-266.7 ± 1.0
LA3	East Sussex, UK	14/06/2018	3	322	-58.0 ± 0.5	
LA4	Buckinghamshire, UK[1]	Mar-13	28		-58.5 ± 0.6	
LA5	Kent, UK[1]	Oct-13	8		-57.4 ± 0.5	
LA6	Greater London, UK[1]	Oct-13	11		-56.1 ± 0.5	
LA7	Groningen, NL	26/09/2018	3	1466	-58.6 ± 1.0	
		27/09/2018	2	242.9	-55.5 ± 0.0	
		02/10/2018	3	770.8	-57.3 ± 0.1	
LA8	Greater London, UK	21/11/2018	5	582	-59.6 ± 0.1	
LA9	Oxfordshire, UK	17/12/2018	3	329.5	-62.1 ± 0.0	
		05/03/2020	2	739.5	-59.0 ± 0.0	
LA10	Ankara, TR	03/01/2019	9	21504	-55.8 ± 0.8	
LA11	Warwickshire, UK	Mar-13[1]	26		-58.8 ±0.5	
		21/01/2019	4	708.3	-58.2 ± 0.2	
LA12	Somerset, UK[2]	09/07/2019	11	6939	-59.6 ± 0.1	
		05/11/2019	12	3125	-58.7 ± 0.1	
		17/02/2020	6	19450	-59.6 ± 0.0	
LA13	Devon, UK	23/07/2019	15	13387	-57.5 ± 0.2	
LA14	Somerset, UK[2]	06/08/2019	6	3117	-57.8 ± 0.3	
LA15	Glamorgan, UK[3,4]	23/11/2017	3	857	-58.7	
LA16	North Yorkshire, UK[3,4]	Various dates	4	709	-59.4 ± 1.2	
LA17	North Yorkshire, UK[3,4]	Various dates	13	7568	-58.4 ± 0.2	
LA18	North Yorkshire, UK[3,4]	Various dates	10	883	-59.3 ± 0.4	
LA19	Lancashire, UK[3,4]	Various dates	16	2391	-58.7 ± 0.3	
Active landfill $\delta^{13}C\text{-}CH_4$ mean: -58.1 ± 1.7‰ for overall, -58.5 ± 1.3‰ for UK; $\delta D\text{-}CH_4$: -266.7 ± 1‰						
			Closed Landfills			
LA4	Buckinghamshire, UK	26/06/2018	2	131.3	-53.8 ± 1.4	-172.5 ± 90[5]
LA5	Kent, UK	25/06/2018	5	1152	-55.6 ± 1.3	-269.7 ± 4.0
LA6	Greater London, UK	21/11/2018	8	2601.4	-53.8 ± 0.0	
LA12	Somerset, UK[2]	09/07/2019	6	661	-53.9 ± 0.6	
		05/11/2019	6	669	-53.6 ± 0.3	
		17/02/2020	6	2336	-54.6 ± 0.0	
LA13	Devon, UK[2]	17/02/2019	6	485	-55.9 ± 0.0	
LA14	Somerset, UK[2]	06/08/2019	3	903.4	-55.1 ± 0.1	
LA20	Greater London, UK[2]	21/11/2018	4	230.5	-54.1 ± 0.0	
LA21	Cambridgeshire, UK	15/06/2018	3	448.6	-56.8 ± 0.1	
LA22	Devon, UK	07/05/2018	7	1675	-56.8 ± 0.1	
		16/07/2019	6	2544	-55.7 ± 0.1	
		20/08/2019[3]	7	1649	-57.3 ± 0.2	
LA23	Berkshire, UK	17/12/2018	3	156	-55.8 ± 0.0	
LA24	Middlesex, UK	23/05/2019	3	125	-52.2 ± 0.1	-326.0 ± 0.4
LA25	Bedfordshire, UK	06/12/2018	3	68	-55.9 ± 0.1	
LA26	Oxfordshire, UK	05/03/2020	2	253	-54.9 ± 0.0	
LA27	Glamorgan, UK[4]	27/03/2019	4	4964	-53.4 ± 0.8	
LA28	Lancashire, UK[4]	Various dates		5979	-55.3	
LA29	Somerset, UK[4]	Various dates	16		-52.3 ± 0.9	
Closed landfill $\delta^{13}C\text{-}CH_4$ mean: -54.8 ± 1.4‰(VPDB); $\delta D\text{-}CH_4$: -297.9 ± 40‰ (VSMOW)						

[a] It is an outlier and discarded from the figures and calculations in average. [b] Same landfill site but different areas; [c]Site was partly reopened and dumped with fresh waste; [d]Source signature results were taken from MEMO² database (MEMO² Isotopes, 2020)

[1]Results taken from previous studies (Zazzeri et al., 2015)

S3. List of sewage and water treatment surveyed with the calculated $\delta^{13}C\text{-}CH_4$ signature. Errors are calculated as standard deviation.

Source number	Site location	Sampling date	Number of samples collected	Excess CH_4 (ppb)	$\delta^{13}C\text{-}CH_4$ (‰) (σ)	$\delta D\text{-}CH_4$ (‰) (σ)
S1	Greater London, UK	05/08/2018	5	161.8	-53.0 ± 0.1	
S2	Surrey, UK	22/06/2018 15/05/2019	3 5	958 639	-50.9 ± 0.2 -49.9 ± 0.4	-299.1 ± 1.8 -313.0 ± 1.3
S3	Oxfordshire, UK	26/06/2018	3	4436	-52.3 ± 0.6	-275.6 ± 2.2
S4	Kent, UK	28/06/2018	2	199	-50.7 ± 0.0	-251.9 ± 14
S5	Groningen, NL	26/09/2018 02/10/2018	2 2	421 346	-49.3 ± 0.0 -50.3 ± 0.0	
S6	Middlesex, UK	22/06/2018 28/11/2018	2 7	880 5608	-50.7 ± 0.0 -50.3 ± 0.1	-302.3 ± 7.2
S7	Berkshire, UK	17/12/2018	3	195	-55.0 ± 0.0	
S8	Berkshire, UK	17/12/2018 15/05/2019	4 3	1150 250	-50.3 ± 0.0 -53.3 ± 0.1	-292.4 ± 0.4
S9	Oxfordshire, UK	17/12/2018	3	1153	-51.8 ± 0.0	
S10	Ankara, Turkey	03/01/2019	6	358	-54.4 ± 0.0	
S11	West Midlands, UK	22/01/2019	3	443.9	-51.2 ± 0.1	
S12	Surrey, UK	23/01/2019	5	635.5	-56.8 ± 0.2	
S13	Northamptonshire, UK	23/05/2019	6	9227	-49.5 ± 0.2	-340.9 ± 1.5
S14	Utrecht, NL	03/06/2019	3	157.7	-47.2 ± 0.1	-415.1 ± 21[a]
Sewage Treatment $\delta^{13}C\text{-}CH_4$ mean: -51.5 ±2.3‰(VPDB); $\delta D\text{-}CH_4$: -296.5 ±28‰ (VSMOW)						
W1	West Sussex, UK	14/06/2018	3	285	-53.7 ± 0.1	

[a]Source signature results were taken from MEMO² database (MEMO² Isotopes,2020)

S4. List of composting facility and leachate treatment surveyed with the calculated $\delta^{13}C\text{-}CH_4$ signature. Errors are calculated as standard deviation.

Source number	Site location	Sampling date	Number of samples collected	Excess CH_4 (ppb)	$\delta^{13}C\text{-}CH_4$ (‰) (σ)	$\delta D\text{-}CH_4$ (‰) (σ)
C1	Hampshire, UK	23/01/2019	4	4087	-50.8 ± 0.5	
C2	Somerset, UK	10/07/2019 10/07/2019 05/11/2019	5 4 6	1118 5139 22297	-54.1 ± 0.6 -52.0 ± 2.8 -55.6 ± 0.1	
C3	Somerset, UK	06/08/2018	5	3475	-61.8 ± 0.8	
C4	London, UK[a]	26/08/2018	2	398	-54.1 ± 0.0	
Composting facility: $\delta^{13}C\text{-}CH_4$ mean: -54.7 ± 3.9‰						
LE1	Somerset, UK	10/07/2019 05/11/2019	6 3	899 496	-58.3 ± 0.5 -55.8 ± 0.1	
Leachate Treatment: $\delta^{13}C\text{-}CH_4$ mean: -57.1 ± 1.8 ‰ Recycling Centre[a]: -53.2 ± 0.2 ‰						

6.8 ESR8 – Isotopic characterisation of methane sources in Europe

ESR8

Isotopic characterisation of methane sources in Europe

ESR	Malika Menoud, m.menoud@uu.nl
Supervisor	Thomas Röckmann, T.Roeckmann@uu.nl
Co-supervisor	David Lowry, d.lowry@es.rhul.ac.uk
Non-Academic mentor	Magdalena Hofmann, mhofmann@picarro.com
Official start – end date	15/11/2017 – 15/11/2021

6.8.1 Scientific progress

6.8.1.1 Project introduction and objectives

Methane is a greenhouse gas of major importance, due to its relatively large global warming potential and its potential for driving efficient climate change mitigation policies. From pre-industrial times, atmospheric methane mole fraction has been increased by 150%. From the beginning of the 1990's, its growth rate in the atmosphere slowed down, until a recent rise in 2007. These variations are still not fully understood, as uncertainties remain in the temporal and spatial variability of the emissions sources.

Methane emissions can have three main origins: fossil fuel operations (natural gas, coal, oil) and geological seeps, biogenic formation in wetlands, by animals (ruminants) and through waste management, and biomass burning (wild or anthropogenic). These pathways produce methane with different isotopic ratios in the emitted gas, due to different isotopic fractionations. Measuring carbon and hydrogen isotope ratios in sampled air methane provides useful information about the origin of the methane found at a certain place. These measurements also help to calculate the partitioning of the different methane sources on a larger scale. Isotopic measurements have therefore an important role in reducing the uncertainties in the global methane budget.

This project aims at the characterization of methane sources using isotopic measurements. The measurements are performed at a European scale, with the help of other institutes and by participating in several measurement campaigns. Through the MEMO² network, samples from various locations and diverse sources can be collected and measured. Such data would allow to identify variations in methane source signatures on this continent. The project aims also at investigating the methane sources over an entire region by performing continuous measurements of ambient air at fixed locations, over an extended time period.

6.8.1.2 Project results

6.8.1.2.1 Third year

6.8.1.2.1.1 Measurement campaign at Krakow

From September 2018 to March 2019, the IRMS (Isotope ratio mass spectrometry) system built at Utrecht University (UU) was installed in Krakow. It was measuring ambient air from a mast on the roof of the physics faculty building, at AGH university. The goal was to get a clearer picture of the main methane sources in the Krakow region, and especially to evaluate the influence of emissions from the Silesian coal mines. It was carried out in parallel with sampling campaigns in Silesia (during the CoMet campaign) and in the city and surroundings of Krakow.

In March 2019, the measurement system was packed and sent back to the lab at UU. The data was collected continuously over 5 months, and consists of time series of CH_4 mole fractions ($\chi(CH_4)$), carbon 13 and deuterium in CH_4 ($\delta^{13}C$ and $\delta D\text{-}CH_4$; Fig. 6.8.1).

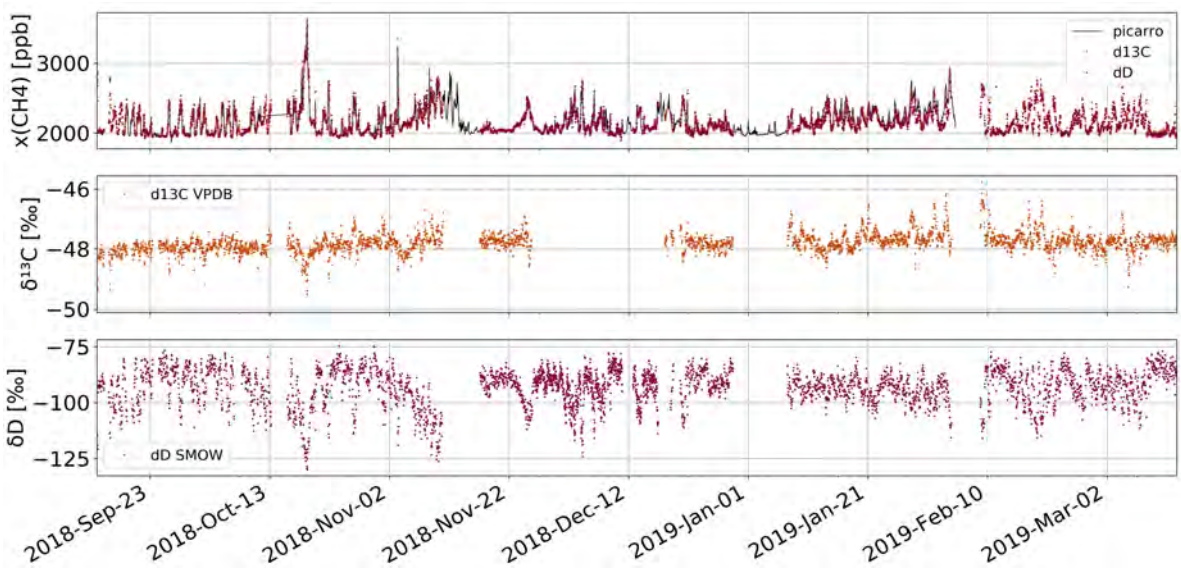

Fig. 6.8.1: Measurements time series at Krakow

We can observe the occurrence of pollution events in the numerous and regular $\chi(CH_4)$ peaks (Fig. 6.8.1). They are correlated with changes in isotopic signatures. The source signatures of these pollution events will be derived from Keeling plots applied on a moving window over the dataset. They can be compared with the source signatures derived from the sampling campaigns (Fig. 6.8.2). A pre-analysis already confirmed the prevalence of thermogenic sources, identified by enriched δD signatures. They differ from the main CH_4 sources in the Netherlands, derived from similar measurements at Cabauw (Röckmann et al. 2016) and Lutjewad (see in the next paragraph).

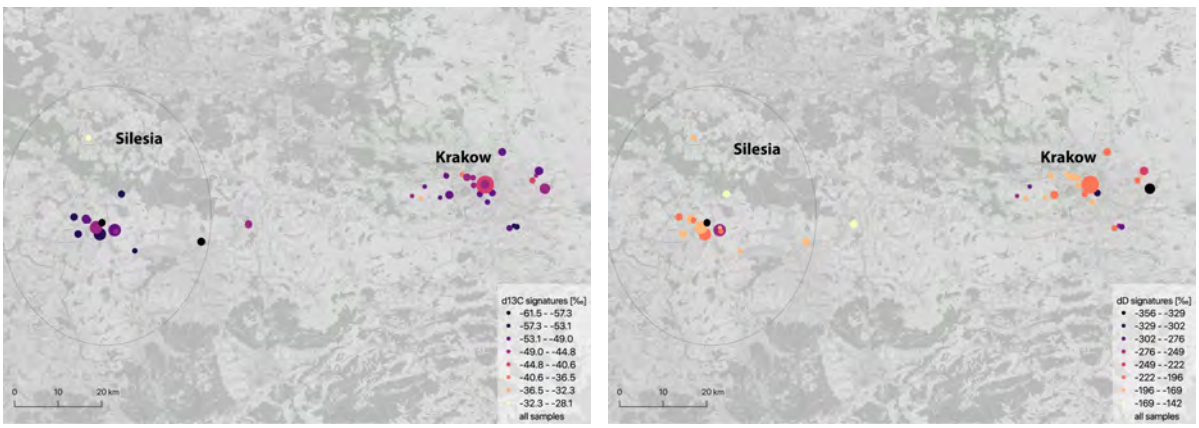

Fig. 6.8.2: Maps of CH_4 source signatures from the sampling campaigns in the Silesia region and the surroundings of Krakow. The left map shows $\delta^{13}C$ signatures, the right map shows δD signatures.

A total of 142 samples, from 55 locations, were taken during the CoMet campaign and my secondment at AGH University of Science and Technology. The source signatures were derived using the Keeling plot approach, and are shown in the map in Fig. 6.8.2. The western part of the map is the Silesia region, from which most sources are coal mines and coal deposits, except one cow farm. Krakow is in the east, where sources were mainly natural gas leaks and the sewage system. South of Krakow, a large landfill was visited and sampled several times. Fossil fuel and microbial sources are better distinguished in the δD signatures.

6.8.1.2.1.2 Lutjewad study

From November 2016 to the end of March 2017, measurements of $\chi(CH_4)$, $\delta^{13}C$ and $\delta D\text{-}CH_4$ were performed continuously on ambient air at Lutjewad, in the North of the Netherlands. The data was analyzed using Keeling plots applied on a moving window over the time series. The resulting signatures are shown in Fig. 6.8.3.

The main conclusions from this study are that methane sources were mostly biogenic, mainly from dairy farms and also from landfills, according to the anthropogenic activities of this region. Some pollution had a higher thermogenic component when the wind came from the east, pointing towards the Groningen gas extraction region or further sources in Germany.

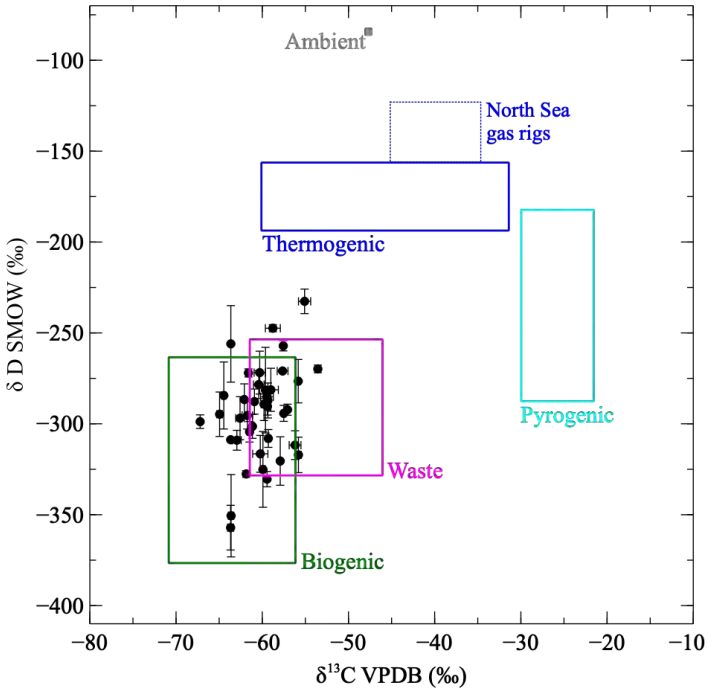

Fig. 6.8.3: Resulting CH_4 source signatures from the moving window Keeling plots applied on the dataset from Lutjewad (2016-2017)

The emissions from the North Sea oil and gas platforms were not detected from the coast during the time of the measurements. This can be due to the distance and the prevalence of southern winds.

Model simulations were performed using two atmospheric models - CHIMERE and FLEXPART-COSMO - and two different emission inventories, EDGAR v4.3.2 and TNO-MACC III. The results are in good agreement with the measurements, as almost all the pollution events are reproduced (Fig. 6.8.4). The source signatures are matching the measurements in general, but some variations appear when looking at individual pollution events (Fig. 6.8.5).

The detailed analysis of individual pollution events was made, as shown in Fig. 6.8.5. By comparing the source signatures derived from the observations and the modelled time series, we noticed that the TNO-MACC III inventory seems to overestimate the share of fossil fuel sources. Model simulations using different input $\delta^{13}C$ source signatures were also compared. The results were significantly improved by adapting the fossil fuel $\delta^{13}C$ signature to the one of the natural gas used in the region. More $\delta D\text{-}CH_4$ measurements are needed to update the input source signatures, and obtain more accurate model results for this isotope.

This work was summarized in a scientific article that is ready to be submitted to the journal Tellus B by the end of March 2020.

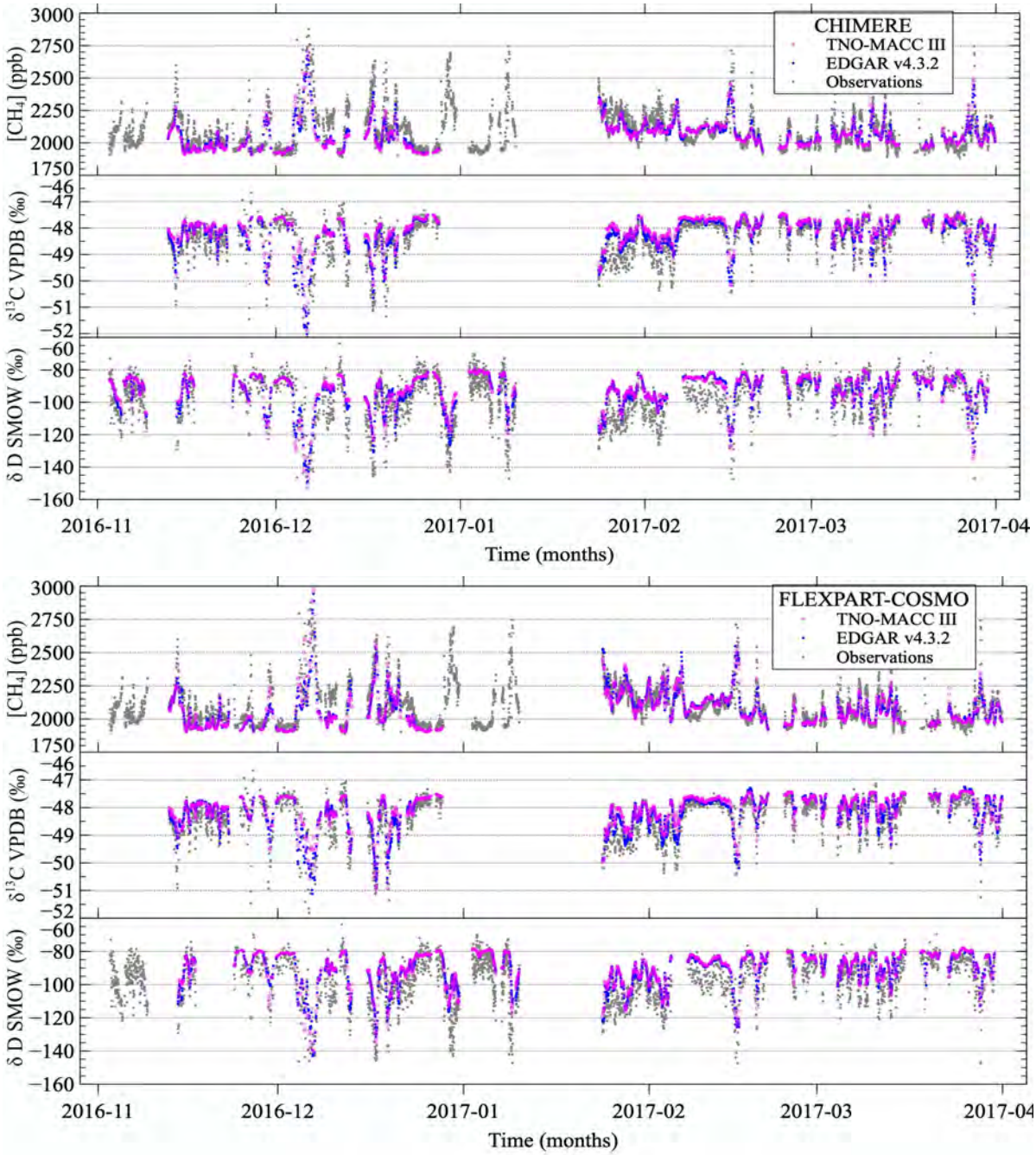

Fig. 6.8.4: Overview of the observed and modelled time series at Lutjewad. Two models were used, CHIMERE (above graph) and FLEXPART-COSMO (below graph), with two different inventories, EDGAR v4.3.2 (blue) and TNO-MACC III (magenta).

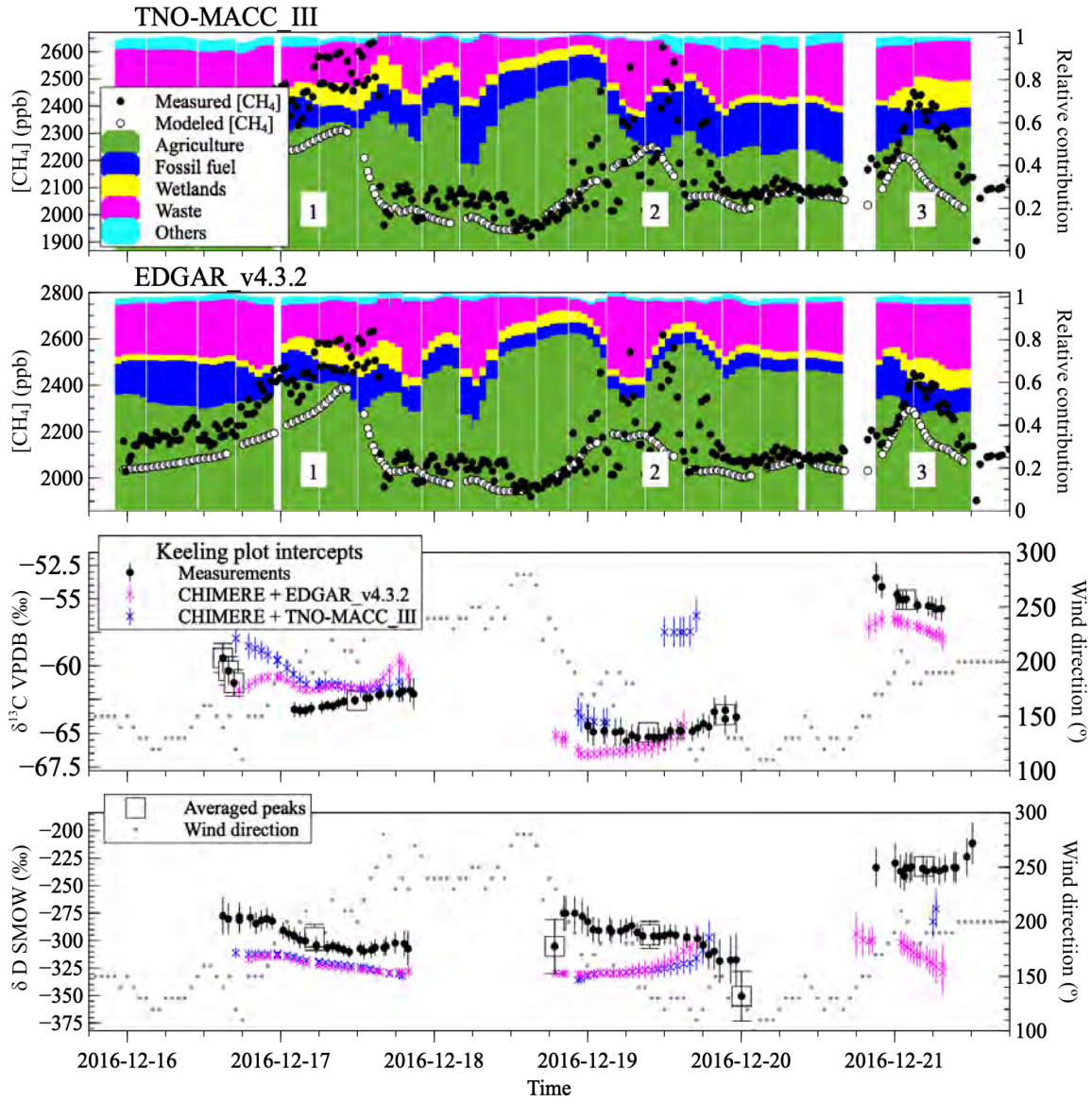

Fig. 6.8.5: Detailed analysis of individual pollution events at Lutjewad. The top panels show the $\chi(CH_4)$ data from observations and the CHIMERE model using the two different inventories (left axis) together with the source contributions providied by the inventories (right axis). The bottom panels show the source signatures from the moving window Keeling plot applied on the observations and the modelled data (left axis), together with the wind direction (right axis)

6.8.1.2.1.3 The ROMEO campaign

More than 300 samples were collected during the ROMEO campaign, from September 28th to October 21st, 2019. Samples were collected from the ground, around individual oil and gas facilities, and also from an aircraft, above oil and gas extraction regions. The first analysis of their isotopic signatures showed large variations in the signatures (Fig. 6.8.6). These variations can partially be explained by the different geology of the visited regions.

During the flights, methane plumes from other sources than the oil and gas extraction activities were sampled. The δD source signatures suggest biogenic origins, from agriculture activities or waste management (Fig. 6.8.6). Source signatures from flight samples have higher uncertainties because the CH_4 elevations were not very high.

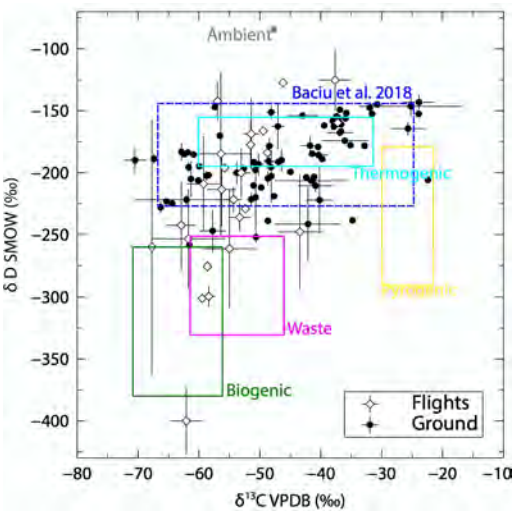

Fig. 6.8.6: Source signatures of all the sites sampled during the ROMEO campaign, from both ground and aircraft teams. The areas show the common signatures assumed for different source sectors from previous literature. Baciu et al. (2016) reported the signatures from geological CH_4 sources in Romania within the dark blue area.

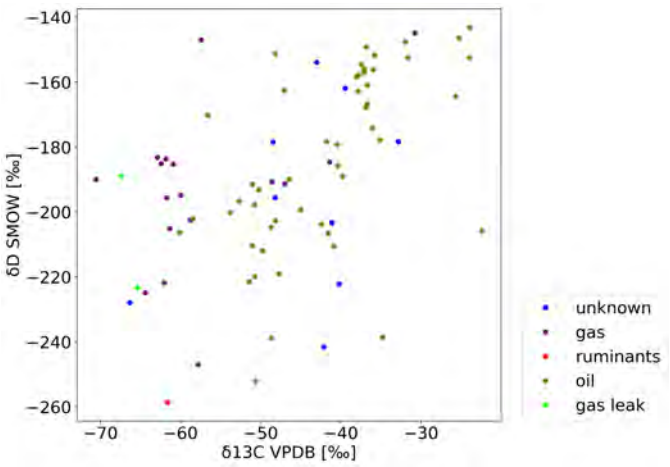

Fig. 6.8.7: Source signatures of the ground samples from the ROMEO campaign, according to different types of sources

When looking closer to the samples from the ground, they can all be identified as of thermogenic origin from their enriched δD source signatures, except the one from ruminants (Fig. 6.8.7). The $\delta^{13}C$ source signatures allow to distinguish from the oil to the gas extraction sites, in almost all the cases. The source signature of the natural gas, sampled in the network leaks, is also very depleted in $\delta^{13}C$, which matches the signatures from most of the gas extraction sites (Fig. 6.8.7).

6.8.1.2.2 Fourth year

The fourth year was dedicated to finalise data evaluation and publication. The ESR prepared D2.2 as a lead author and provided the related isotopic data (https://doi.org/10.5281/zenodo.4062356).

The work of the fourth year is partly an update of the previously reported results.

6.8.1.2.2.1 Measurement campaign in Krakow (update of chapter 6.8.1.2.1.1)

The results from the measurements performed in Krakow in 2018 and 2019 were analysed and presented in a scientific article. The manuscript was submitted to the journal Atmospheric Chemistry and Physics.

The isotopic signatures from sources sampled during mobile surveys in the area allow to distinguish between natural gas leaks, coal mine fugitive emissions, landfill and sewage, and ruminants. The observed time series of CH_4 mole fractions showed regular daily night-time accumulations, sometimes combined with irregular pollution events during the day. The peak source signatures suggest fossil fuel related emissions as a major source - with $\delta^{13}C$ between -55.3 and -39.4 ‰ V-PDB, and δD between -285 and -124 ‰ V-SMOW.

They confirm the influence of Silesian coal mines when the wind is from the west (Fig. 6.8.8), and of natural gas leaks from the network as a local source advected by low wind speed. In the case of Krakow, the use of δD in CH_4 is crucial to distinguish the fossil fuel emissions, as their relatively depleted $\delta^{13}C$ values overlap with the ones of microbial sources (Fig. 6.8.8).

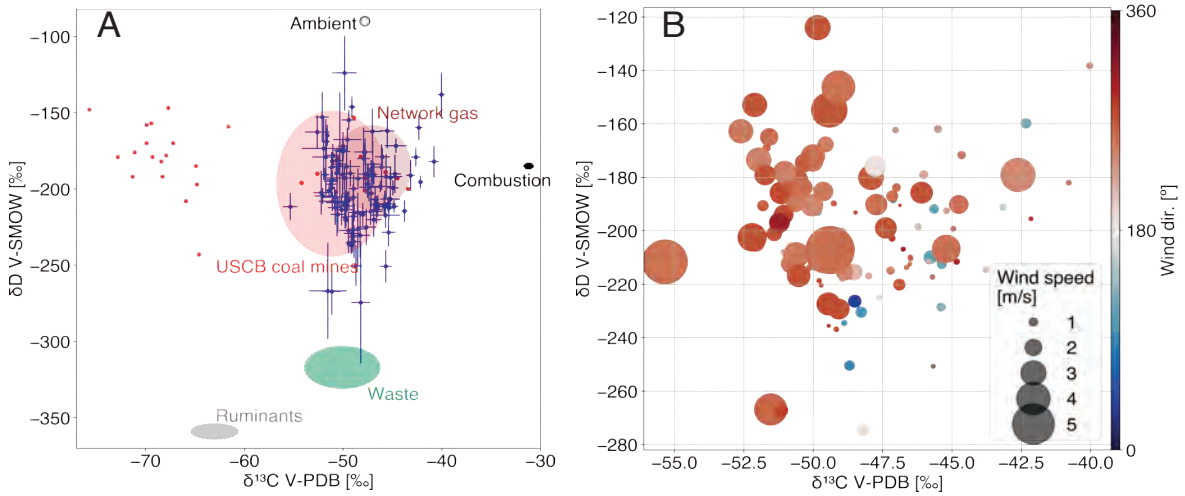

Fig. 6.8.8: Dual isotope plots of the resulting source signatures from the CH_4 peaks identified in the time series. **A.** Dark blue: source signatures with their associated 1σ uncertainties. Coloured areas: ranges of source signatures obtained from the collected samples. Red dots: source signatures of USCB coal gas derived from the literature. The combustion source signature is from coal waste burning samples reported in the MEMO² CH_4 isotopes database. **B.** Source signatures labeled by the average wind direction (colour) and speed (size) measured during the pollution event.

The CHIMERE transport model was used to compute the CH_4 and isotopic composition time series in Krakow, based on two emission inventories. The CH_4 mole fractions are generally underestimated in the model.

The simulated isotopic source signatures, obtained with Keeling plots on each simulated peak using the EDGAR v5.0 inventory, indicate that a higher contribution from fuel combustion sources in EDGAR would lead to a better agreement. The isotopic mismatches between model and observations are mainly caused by uncertainties in the assigned isotopic signatures for each source category, and the way they are classified in the inventory.

These uncertainties are larger for emissions close to the study site, which are more heterogenous than the ones advected from the USCB coal mines (Fig. 6.8.9). Our isotope approach proves to be very sensitive in this region, thus helping to improve emission estimates.

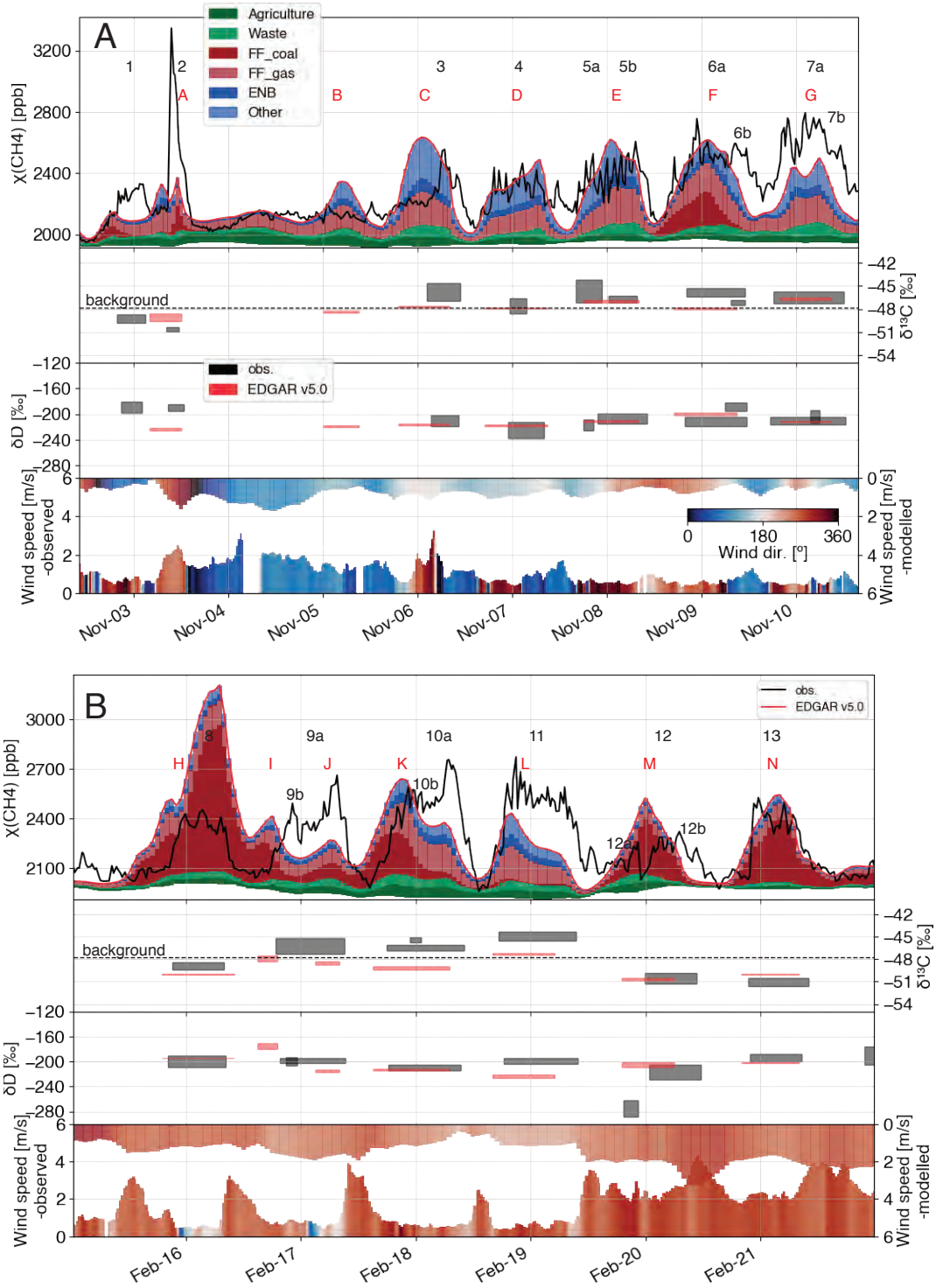

Fig. 6.8.9: Detailed analysis of two subsets of the dataset, **A.** from Nov. 2 to 10, 2018, **B.** from Feb. 15 to 22, 2019. Top panels: observed (grey) and modelled (red) mole fractions and relative source contributions from the EDGAR v5.0 inventory. Middle panels: δ13C and δD source signatures of individual peaks of the observed (grey, from peak 1 to 13) and modelled (red, from peak A to N) time series. Box heights represent ±1σ of each peak isotopic signature. Bottom panels: wind speed and direction measured simultaneously at the study site (pointing up), and used for the CHIMERE simulations (pointing down).

6.8.1.2.2.1 Isotopic measurements during ROMEO (update of chapter 6.8.1.2.1.3)

The Romanian Methane Emissions from Oil and gas (ROMEO) project brought 13 research teams together to Romania in order to quantify emissions from oil and gas exploitation.

A total of 380 air samples were collected in urban areas and around oil and gas extraction sites (Fig. 6.8.10), from ground level vehicles and from an aircraft, for stable isotope analysis. There were measured for δ^{13}C-CH_4 and δD-CH_4 using a continuous flow isotope ratio mass spectrometry (CF-IRMS) system at Utrecht University.

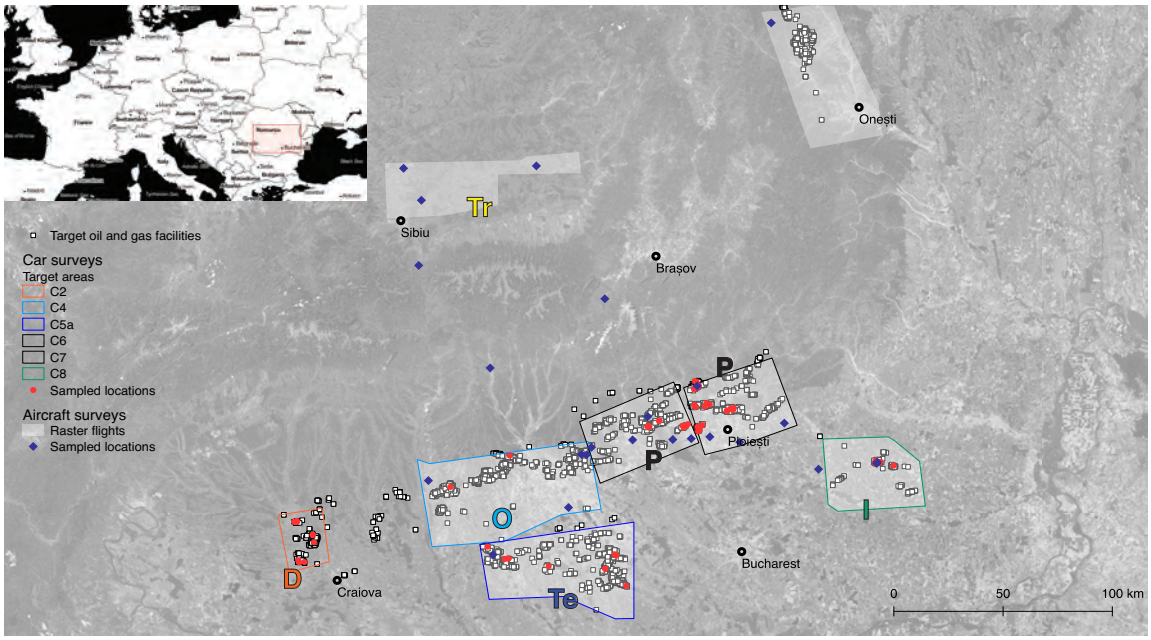

Fig. 6.8.10: Locations of the sampling sites during the entire ROMEO campaign. Isotopic source signatures could be derived at each of the characterised sites. The regions are: P - Prahova, I - Ialomița, Te - Teleorman, O - Olt, D - Dolj, Tr - Transylvania. White symbols: All OMV facilities (confidential), yellow symbols: facilities sampled at the ground, green symbols: samples collected by aircraft, U: undetermined emission source. Basemap: OpenStreetMap contributors.

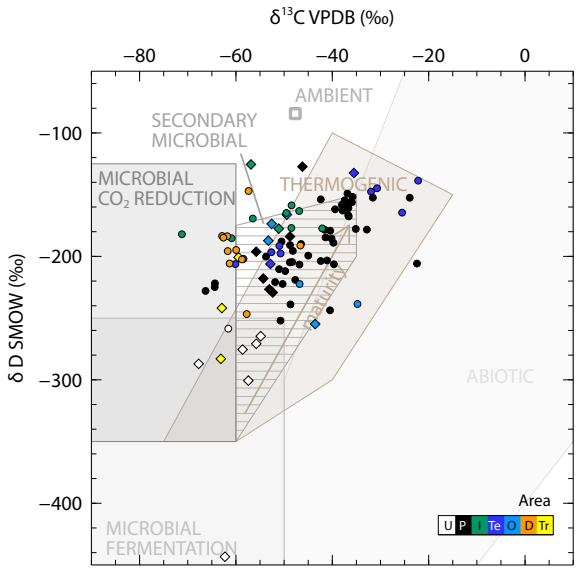

Fig. 6.8.11: Dual isotope plot of the resulting source signatures, for the geographical areas we visited using both ground vehicles and aircraft.

The results were analysed using the Keeling plot approach to derive source signatures at each sampled site. The source signatures obtained for 80 individual oil and gas operation sites range from -71.2 to -22.2 ‰ V-PDB, and from -252 to -139 ‰ V-SMOW, for δ^{13}C and δD respectively (Fig. 6.8.11).

The distinction of emissions from fossil fuel operations is mainly possible using δD signatures, because the wide range of δ^{13}C values overlap with typical signatures of other types of sources (biogenic, pyrogenic). In regions I, D, and P, the lowest δ^{13}C values are associated with gas and condensed gas extraction plants, suggesting the presence of microbial gas formations. To our knowledge, CH_4 of microbial origin was not reported in Wallacean plain deposits until now.

The isotopic signals of plumes sampled from the aircraft ranged from -67.7 to -35.5 ‰ for $\delta^{13}C$ and -443 to -126 ‰ for δD (Fig. 6.8.11). 18 plumes could be linked to oil and gas extraction activities, and 6 plumes were of unknown origin. The isotopic signals of the unknown plumes are typical of CH_4 from microbial fermentation, for example enteric fermentation (cattle farming) or waste degradation (landfills, sewage treatment, etc). Detailed analysis of aircraft isotopic signals and corresponding wind directions allowed us to directly link at least 3 plumes from the aircraft to the underlying oil and gas facilities.

We also studied the ground surface isotopic signatures and ethane content at the different sites in relation with gas composition measurements in the deeper layers reported in the literature. The origin of fossil fuel formations in 5 clusters could be described in detail.

Our results generally help understanding the geology of the region, as well as significantly improving the knowledge of the isotopic signatures of CH_4 emissions in Romania, especially from oil and gas installations.

6.8.1.3 Future plans and expected results

- Publication of the results from ROMEO

We are in the latest stage of the analysis of the results from the ROMEO campaign. I am currently writing a manuscript, with the aim of including it with other ROMEO studies in a special release of the journal Elementa.

- Scientific publication on the update of CH_4 isotopes inventories, including the MEMO2 isotopic database

All CH_4 isotopic signatures from field campaigns within the MEMO^2 projects are publicly available in a data repository. They constitute a significant addition to the global database, which has not recently been fully updated. This could be the aim of a scientific publication that I plan to write in the coming months.

- Analysis of global δD time series, including modelling

Measurement data of δD-CH_4 from the Arctic stations Zeppelin and Alert, and the Antartica station of Neumayer for the last 3 decades will be put together. The aim is to investigate global trends in atmospheric CH_4, with a new constrain brought by the δD time series.

We are collaborating with Heidelberg University (UHEI) and will measure more samples from Neumayer (from 2008 to 2018) to complete the time series (from 1989 to 2019). We plan to analyse the CH_4 mole fraction, $\delta^{13}C$ and δD trends using a relatively simple box model to derive conclusion on the origin of global CH_4 variations in the past decades.

- Finalise my PhD thesis

The end of my contract is in November 2021, and I plan to submit my thesis in time. I need to write an introduction and conclusion to relate the different chapters (consisting of published or submitted scientific articles). I'm planning my defense to be between November 2021 and February 2022.

6.8.1.4 Collaborations (internal / external)

Within MEMO^2:

- Data sharing to build the MEMO^2 isotopic database: collaboration with MEMO^2 partners RHUL UHEI, LSCE, and AGH. We exchanged all our isotopic data to build the database I have published.
- My collaboration with Barbara Szénási (LSCE) was once again successful for the Krakow study. She provided data from the CHIMERE transport model. She is also using the Lutjewad measurement data that I provided, in a study on the model uncertainties.

- ROMEO: the MEMO² partners UHEI, RHUL and AGH contributed in the measurement campaign. The collaboration continues for the analysis of results and writing of publications. I am contributing to the study on Bucharest, and working on the study on isotopes.

Outside MEMO²:

- Contributed to a study from colleagues at NIOZ (Royal Netherlands Institute for Sea Research): I performed measurements of water samples from the North Sea and helped with the interpretation of the results. A scientific publication is currently in preparation.
- Contributed to a study from colleagues in UNSW (University of New South Wales) Sydney: Lu, X., Harris, S. J., Fisher, R. E., France, J. L., Nisbet, E. G., Lowry, D., Röckmann, T., van der Veen, C., Menoud, M., Schwietzke, S., and Kelly, B. F. J.: Isotopic Signatures of Major Methane Sources in the Coal Seam Gas Fields and Adjacent Agricultural Districts, Queensland, Australia, Atmos. Chem. Phys. Discuss. [preprint], https://doi.org/10.5194/acp-2021-76, in review, 2021.
- Ongoing collaboration with Pr. Ingeborg Levin at UHEI for measuring samples they collected in Neumayer, Antartica.

6.8.1.5 Risks and difficulties

Due to the COVID-19 pandemic, the ROMEO phase II campaign was cancelled/postponed several times. It was also not possible to install the IRMS system to another location in Europe to perform continuous measurements as we were planning to.

6.8.2 Deliverables

D2.1 - Isotopic measurements linked to common scale (month 18)

Approved

D2.2 - Improved isotopic source signatures of local and regional CH_4 emissions (month 36)

We didn't start to write up a report on this but appropriate data was collected.

D2.3 - Publications on the use of isotopes for CH_4 source attribution in urban/industrial regions (month 36)

Is taken over by the RHUL group.

D2.4 - Publication on temporal and meteorological influences on CH_4 at fixed sites (month 42)

Started to work on this through the analysis of the Lutjewad data. It will be carried on after analyzing the Krakow data.

D2.5 - Report providing isotopic maps at grid scale from inventories and atmospheric measurements (month 42)

The gathering of all the isotopic signatures from the MEMO² measurements measured at Utrecht University is done. The dataset is completed with the measurements made at RHUL, writing the deliverable has been taken over by the RHUL group. The data I've collected for the MEMO² isotopic database will be included there

6.8.3 Training and network activities.

6.8.3.1 General training events

Event	Date (start – end)	Location (Host)	Objective / expected skills	ECTS points	Contribution	Comments
The art of scientific writing	05/11/2018 – 03/12/2018	Utrecht (UU)	Learning how to write scientific articles in a more effective way	-	Just participating	Still ongoing
Workshop on dispersion modelling	09/10/2018 – 10/10/2018	Heidelberg (UHEI)	Learning how to implement a Gaussian	?	Just participating	Successful training
Workshop on isotopes	17/09/2018 – 19/09/2018	Egham (RHUL)	Learning the techniques for the measurements of CH_4 isotopes,	?	Presenting a poster and	Successful training

			from the sampling to the data interpretation		giving one presentation	
"Climate change in context" bachelor course	09/02/2018 – 12/04/2018	Utrecht (UU)	Experience in teaching	-	Teaching assistant	Positive feedback from the students. I will continue in 2019
1st summer school	5/02/2018 – 16/02/2018	Schoorl, NL	Theoretical training on atmospheric processes and methane. Practical training on mobile measurements, sampling, tracer release, and data analysis	6	Just participating	Successful training
Climate change in context	06/02/2019 – 19/04/2019	Utrecht University	Supporting the students during the exercise session, correcting the essays, tests and exam	-	Teaching assistant	-
The Art of Presenting in Science	20/05/2019 – 17/06/2019	Utrecht University	Learning to present scientific content in an efficient way	1.0	Participant	Very useful, I could directly implement the advices in my next presentations
Optics and Waves	23/04/2020 – 09/07/2020	Utrecht University	Supporting 2 x 3 groups of 2 to 3 students during a small research project in experimental physics	-	Teaching assistant	-
PhACE (PhD Activating Career Event)	08/02/2021 – 09/02/2021	Utrecht University	Exploring career options through discussions with professionals who successfully completed a PhD	-	Participant	Workshops on networking and personal objectives and skills

6.8.3.2 Secondments

Secondment	Date (start – end, planned (when))	Location	Host	Description of work / deviations	Scientific / training (skills) objective	Results and future plans
RHUL	18/06/2018 – 14/07/2018	Egham, UK	RHUL	Isotopic measurement technique, inter-comparison between the labs and mobile surveys	Learning other techniques for isotopic measurements, and for sampling on the field.	The inter-comparison is done, together with the calibration tanks. A dataset of isotopic signatures of various sources in the UK was created. We will work further on the share and use of theis data.
AGH	16/05/2018 – 30/05/2018 (2 weeks, to be continued)	Krakow, PL	AGH	Installation of an in-situ measurement system Participation in the CoMet campaign in Silesia	Learning to install the IRMS and methane extraction system Getting data for isotopic characterisation of methane from the mine exhaust	Continuous data on ambient air is being collected. Other stays in Krakow are planned in December and February, for the sampling of local sources and the de-installation of the system. The results of the CoMet campaign are now available, and will be compared with the data gathered by other groups.
AGH	15/03/2019 – 27/03/2019	Krakow, Poland	AGH	Continuous measurements of ambient air and sampling of local sources	Technical skills: installation and maintenance of the IRMS system Experimental skills: planning and conducting a sampling campaign	The measurements were successful and the resulting dataset is very interesting. It will lead to a scientific publication.
LSCE	17/02/2020 – 13/03/2020	Saint-Aubin, France	UVSQ	No measurements were possible. Objectives changed to	Contributing in the atmospheric modelling work to use the outputs in comparative studies with the observations we've previously collected	We've start to optimize the model input to generate the time series for Krakow. The first simulation of the time series at Svalbard were made, and this work will continue.

6.8.3.3 Conferences

Conference name	Date (start – end, planned (when))	Location	Presentation (oral / poster)	Title of presentation	Authors (main author + co-authors)	Public available (yes / no) / web link
ICOS	10/09/2018 – 14/09/2018	Prague, (CZ)	Poster	Isotopic characterization of methane from mine shafts in the Silesia region	Malika Menoud, Hossein Maazallahi, Mila Stanisavljevic, Thomas Röckmann, Jaroslaw Necki	Yes https://www.researchgate.net/publication/327655309_Isotopic_characterisation_of_methane_from_mine_shafts_in_the_Silesia_region
BBOS	25/10/2018 – 26/10/2018	Soesterberg (NL)	Presentation	Continuous isotopic measurement of atmospheric methane	Malika Menoud, Carina vand der Veen, Thomas Röckmann, Bert Scheeren, Huilin Chen, Jaroslaw Necki	No
NAC	21/03/2019 – 22/03/2019	Utrecht, the Netherlands	Poster	Isotopic characterization of methane sources across Europe	Malika Menoud, Carina van der Veen, Barbara Szenasi, Hossein Maazallahi, Bert Scheeren, Huilin Chen, Jaroslaw Necki, Philippe Bousquet, Thomas Röckmann	No
EGU	08/04/2019 – 12/04/2019	Vienna, Austria	PICO presentation	Using continuous high-precision isotope measurements over several months to characterize sources of atmospheric methane at various European locations	Malika Menoud, Carina van der Veen, Barbara Szenasi, Bert Scheeren, Huilin Chen, Jaroslaw Necki, Philippe Bousquet, Thomas Röckmann	No
EGU	08/04/2019 – 12/04/2019	Vienna, Austria	PICO presentation	Mapping, emission quantification, and attribution of methane enhancements across two European cities; Utrecht, NL and Hamburg, DE	Hossein Maazallahi, Daniel Zavala-Araiza, Stefan Schwietzke, Malika Menoud, Julianne Fernandez, Rebecca Fisher, David Lowry, Euan Nisbet, Hugo Denier van der Gon, Thomas Röckmann	No
EGU	08/04/2019 – 12/04/2019	Vienna, Austria	Oral presentation	Tidal dynamics control microbial methane oxidation in the water column above an active cold seep (Doggerbank, North Sea)	Tim de Groot, Hossein Maazallahi, Thomas Röckmann, Sylvia Walter, Malika Menoud, Bart Meijninger, Chris Mesdag, Darci Rush, Helge Niemann	No
NCGG	12/06/2019 – 14/06/2019	Amsterdam, the Netherlands	Poster	Using long-term high-precision isotope measurements to characterise sources of atmospheric methane at various European locations	Malika Menoud, Carina van der Veen, Bert Scheeren, Huilin Chen, Jaroslaw Necki, Dominik Brunner, Randulph P. Morales, Thomas Röckmann	No
NCGG	12/06/2019 – 14/06/2019	Amsterdam, the Netherlands	Poster	Mobile in situ measurements of methane mixing ratio over Upper Silesian Coal Basin	Mila Stanisavljević, J. Necki, H. Maazallahi, M. Menoud, K. Vinkovic, Piotr Korbeń, M. Schmidt, L. Chmura, J. Bartyzel, M. Gałkowski, W. Wołkowicz, G. Florczyk, S. Defratyka	No
NACGEO	12/03/2020 – 13/03/2020	Utrecht, NL	Oral presentation	Characterisation of methane sources in Lutjewad, the Netherlands, using long-term isotopic composition measurements	M. Menoud, C. van der Veen, B. Scheeren, H. Chen, B. Szénási, R. P. Morales, I. Pison, P. Bousquet, D. Brunner, T. Röckmann	no

EGU	04/05/2020 – 08/05/2020	Online	PICO	CH4 isotopes during ROMEO	M. Menoud, C. van der Veen, T. Röckmann, H. Maazallahi, P. Korben, M. Schmidt, A. Calcan	no
ICOS	15/09/2020 – 17/09/2020	Online	Poster	High temporal resolution measurements of stable CH4 isotopologues in Krakow	M. Menoud, C. van der Veen, J. Necki, B. Szénási, M. Stanisavljevic, I. Pison, P. Bousquet, T. Röckmann	no

6.8.3.4 Measurement / sampling campaigns

Campaign	Date (start – end, planned (when))	Location	Host	Description of work	Scientific objective	Samples (nature / number)	Results and future plans
Krakow	10/12/2018 – 20/12/2018	Krakow, PL	AGH	Sampling of various methane sources in the surroundings of Krakow.	Isotopic characterisation of the main local sources influencing the methane elevations measured in the city.	Air samples in aluminium bags, quantity to be determined	The results will be combined with the continuous in-situ measurements performed through the winter, to potentially identify the sources of methane elevations.
Hamburg	07/11/2018 – 09/11/2018	Hamburg, DE	UU	Sampling of methane sources identified by mobile CRDS measurements	Isotopic characterisation of urban methane sources	Air samples in aluminium bags, 60	The measurements are to be performed.
MEMO^2-RHUL	22/06/2018 – 05/07/2018	England, UK	RHUL	Sampling of methane sources identified by mobile CRDS measurements	Isotopic characterisations of various sources in the UK	Air samples in aluminium bags, 47	The data shows clear agreement between the source types, and the potential of isotopes for source identification. It is now to be shared and combined with RHUL and LSCE data.
CoMet	27/05/2018 – 29/05/2018	Silesia, PL	AGH, DLR	Sampling of plumes from coal mine shafts, identified by mobile CRDS measurements	Isotopic characterisation of methane from Polish coal mines	Air samples in aluminium bags, 43	The data shows a large heterogeneity in the isotopic signatures. It is now to be combined with the data from the other groups to better investigate the formation processes and influencing parameters.
Secondment at AGH (third part)	15/03/2019 – 27/03/2019	Krakow, Poland	AGH	Sampling of various sources around Krakow.	Isotopic characterization of the regional methane sources	110	The signatures from 55 locations were obtained and are used to analyze the continuous measurement dataset.
ROMEO	30/09/2019 – 20/10/2019	Ploiesti, Romania	INCAS	Sampling during ground based and aircraft measurements around oil and gas facilities, as well as the cities of Bucharest and Ploiesti	Isotopic characterization of methane emissions from the oil and gas sector in Romania	336	The first dataset of isotopic signatures from anthropogenic methane emissions in Romania. It will help the isotopic modelling work, and the key findings will be written up in a publication

6.8.4 Dissemination activities

So far, I did not publish my work within this project in a scientific journal. However, I've been doing more dissemination for the general public through social medias.

Other dissemination activities

Dissemination activity	Name	Date	Location	Type of audience	Size of audience
Blog on the MEMO^2 website	My secondment at RHUL	To be published	RHUL, UK	Public	100+
Video on 2 social media platforms (Facebook and Instagram)	MEMO2 in England trailer	24/07/2018	RHUL, UK	Public	100+
Blog on the MEMO^2 website	Installation of a CF-IRMS and methane extraction system	21/09/2018	AGH, PL	Public	100+
Posts on social media during measurement campaigns, with pictures and/or videos	h2020_memo2 (Instagram) and MEMO2 PhDs - H2020 (Facebook)	26/03/2019, 11/10/2019	Poland, Romania	Civil society	World
Lunch talk on the ROMEO campaign at IMAU	A smelly love story	12/12/2019	Utrecht, The Netherlands	Scientists from other fields	Our institute
Blog post	Let's play with the isotopic signatures!	21/04/2020	MEMO^2 website	General public	World
Video	ROMEO	10/09/2020	YouTube, social medias	General public	World

6.9 ESR9 - The isotopic signature of urban CH_4 emissions

ESR9

The isotopic signature of urban CH_4 emissions

ESR	Julianne Mae Fernandez, Julianne.Fernandez@rhul.ac.uk
Supervisor	Dave Lowry, d.lowry@rhul.ac.uk
Co-supervisor	Thomas Rockmann, t.roeckmann@uu.nl
Non-academic mentor	Sam Barker, sam.barker@elementar.com (Elementar)
Official start-end date	08 January 2018 – 31 December 2020

6.9.1 Scientific progress

6.9.1.1 Project introduction and objectives

As atmospheric methane (CH_4) levels continue to increase and the mitigation of greenhouse gases becomes more of a concern, it is important to address CH_4 emissions from large cities. Urban CH_4 emissions include fugitive emissions from natural gas leaks in the distribution network, landfill sites, wastewater treatment plants and sewage system networks. These source locations are normally not identified in national inventories and the plumes from sources often merge, eventually producing a citywide plume of CH_4 that is transported some distance downwind before dispersing.

Street level measurements of CH_4, ethane (C_2H_6), $\delta^{13}C$-CH_4 and $\delta^{2}H$-CH_4 assist in the identification of emissions both from major point sources and from small leaks from natural gas distribution systems. Small leaks can add up: though they are included in emissions inventories such as the UK National Atmospheric Emission Inventory (NAEI), these estimates have high uncertainties due to the lack of measurements.

Mobile CH_4, C_2H_6 concentrations and isotopic measurement surveys were conducted in 3 UK cities with different expected source contributions on a seasonal basis to assess the roles of the sources. The surveyed cities are London, Birmingham, and the coastal city of Swansea in Wales. Swansea was chosen because the region receives coastal Atlantic Ocean background air. Results will be compared to the UK city inventories, assessing source distribution and intensity. Additional opportunities included the large-scale Romanian campaign, ROMEO. Participation in ROMEO allowed for the surveying of Romania's capital city Bucharest. Another objective is to incorporate hydrogen isotope measurements of methane in these studies to further support source determination of methane emissions. Together, the surveying of these cities with multiple source tracers will give us a better understanding of urban methane emissions in Europe.

6.9.1.2 Project results

6.9.1.2.1 Third year

The **Greater London region** was fully covered on a 1 km^2 scale, by October 2019. CH_4 elevations above background levels were determined (Fig. 6.9.1) allowing for the identification of major "hot spots", which will be revisited this summer for emission flux calculations. From the initial full coverage of London, about 150 Flexfoil air sample bags were collected in accessible areas of elevated methane concentrations. These samples and background samples were measured $\delta^{13}C$-CH_4 and $\delta^{2}H$-CH_4 at the RHUL Greenhouse Gas laboratory. The samples were analyzed for source signatures using Keeling plot calculations, which determined 71 source signatures that have a CH_4 elevation greater or equal to 200 ppb CH_4 (Fig. 6.9.2 and 6.9.3). The majority of these sources have signatures ($\delta^{13}C$-CH_4 -35 to -45 ‰) representative of fossil fuel origins (Fig. 6.9.3 and 6.9.4).

Fig. 6.9.1: London methane excess map. Lighter shades indicate greater elevations of methane, whereas darker shades are closer to background levels.

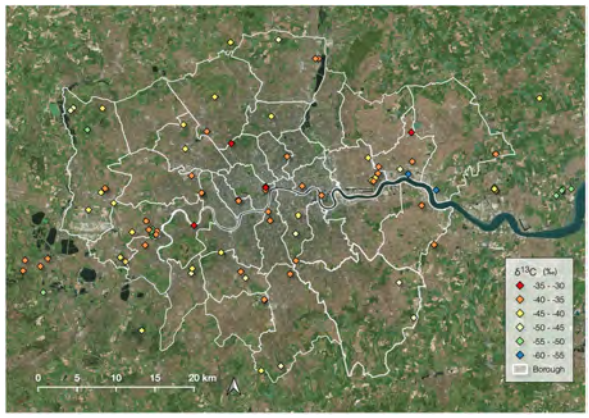

Fig. 6.9.2: δ^{13}C-CH_4 Source Signatures of London. Diamonds indicate plume sample collection locations. Signatures were determined from IRMS measurements and Keeling Plot analysis. Enriched sources are red and orange (thermogenic origins) and the more depleted sources are in blue and light green (biogenic origins).

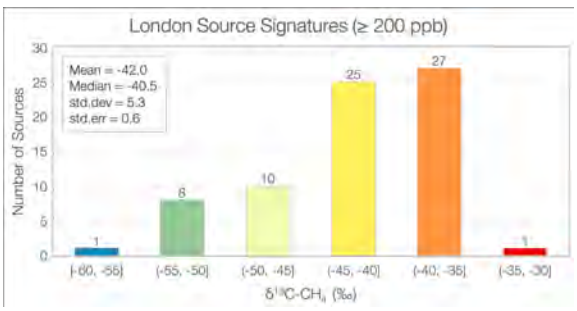

Fig. 6.9.3: Isotopic source category distribution of London. All 71 source signatures are > 200 ppb above CH_4 background levels. Color bars correlate to symbol categories in Fig. 6.9.2

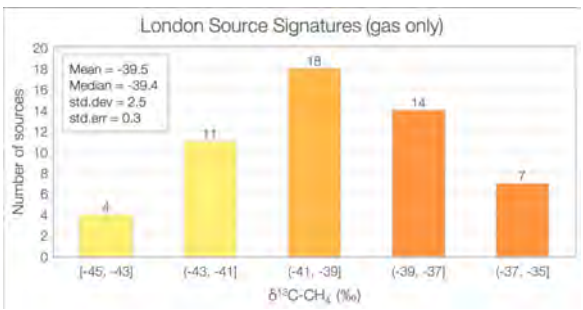

Fig. 6.9.4: Natural gas source distribution. Represents only sources greater or equal to -45 ‰, which is most likely sources of methane from the natural gas distribution system in London.

Swansea was surveyed in March 2019, which consisted of 2 days of mobile measurements. Methane elevations above background levels were calculated (Fig. 6.9.5). Seventeen Flexfoil sample bags were collected which determined 11 source signatures, of which 9 source signatures have methane elevations greater or equal to 200 ppb CH_4 (Fig. 6.9.6).

Though this sample set is much smaller, like London, the majority of the source signatures resemble fossil fuel origins (Fig. 6.9.7 and 6.9.8). Natural gas emissions have been observed from various types of UK National Grid above ground infrastructure (AGI). These include natural gas governors (GG), gas valve compounds (GVC), and gas distribution stations. Other samples that had similar source signatures to these, but were in locations absent of any obvious gas infrastructure have a source of methane that is probably leaking from underground pipes connected to the distribution system.

The **Birmingham surveys** were also completed October 2019, by ESR 7. The Birmingham results will soon be combined and compared with London and Swansea.

Fig. 6.9.5: Swansea methane excess map. Lighter shades indicate greater elevations of methane, whereas darker shades are closer to background levels.

Fig. 6.9.6: δ^{13}C-CH_4 source signatures of Swansea. Diamonds indicate plume sample collection locations. Enriched sources are red and orange (thermogenic origins) and the more depleted sources are in blue and light green (biogenic origins).

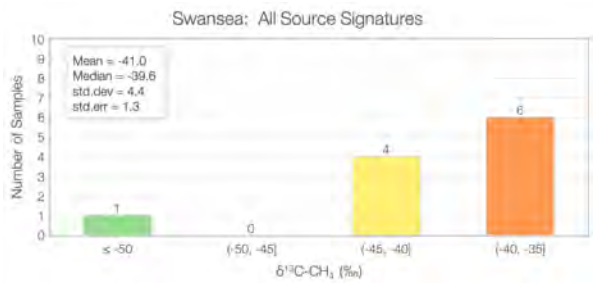

Fig. 6.9.7: Isotopic source category distribution. All 11 source signatures are > 200 ppb above CH_4 background levels. Color bars correlate to figure 11.

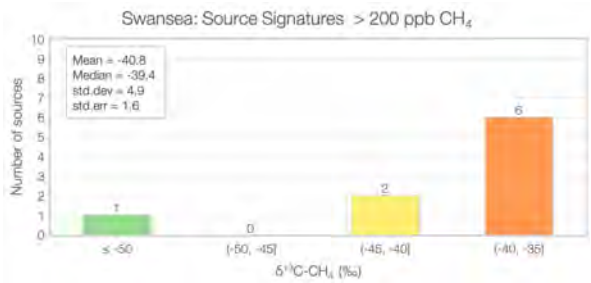

Fig. 6.9.8: Isotopic source category distribution. The 9 source signatures which are > 200 ppb above CH_4 background levels. Color bars correlate to figure 11.

The city of **Bucharest, Romania** was surveyed August 2019. This consisted of 9 full day surveys in collaboration with the National Institute of Aerospace Research (INCAS) and ESR 8 and 10 (UU). Methane elevations were determined using 3 cars and 4 continuous CRDS instruments (Fig. 6.9.9). A total of 90 air samples were collected (51 in August, 39 October). These are combined and result in 65 isotopic source signatures. Samples were measured both at RHUL and UU laboratories. This combination resulted in both carbon and hydrogen measurements of many of the samples (Fig. 6.9.10).

Analysis of Bucharest is currently in process. From the data analysis so far, source determination from δ^{13}C-CH_4 alone is not enough. The addition of δ^2H-CH_4 further helps the source apportionment, but C_2:C_1 measurements are much needed to understand the mixing potential of fugitive municipal wastewater emissions and the natural gas distribution system emissions.

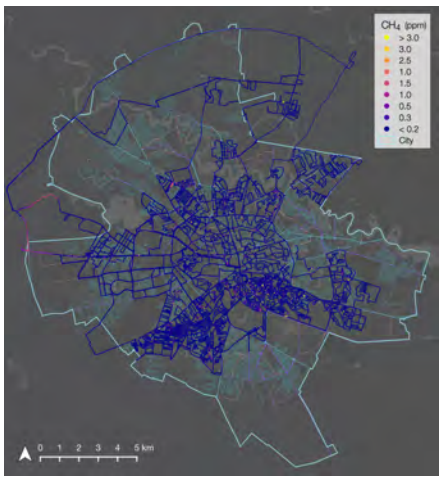

Fig. 6.9.9: Bucharest methane excess map. Elevated CH_4 concentrations (ppm) from 4 various CRDS continuous instruments. Street level measurements were taken from a 60 cm high inlet attached to the bumpers of the cars. Lighter shades indicate greater elevations of methane, whereas darker shades are closer to background levels.

Bucharest's dominant fugitive source still needs to be determined and supported statistically, but overall Bucharest seems to have more sewage-derived emissions compared to London and Swansea. These differences may be due to management and maintenance practices of the municipal facilities. Once all the city results are finalized and published they should be shared with each city and governmental regulators to better understand and manage regulations on mitigating methane emissions from cities.

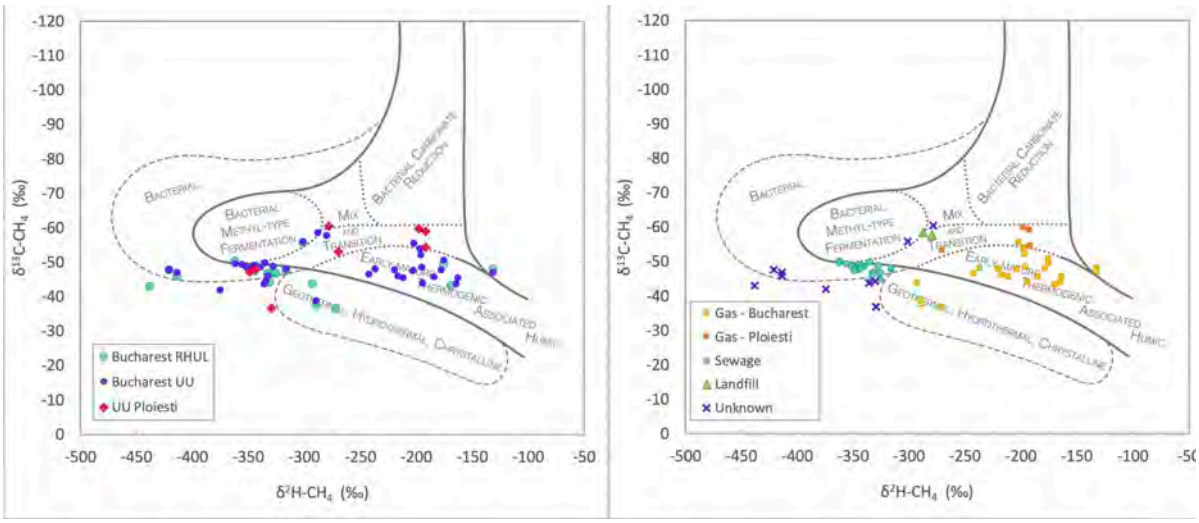

Fig. 6.9.10: Isotopic source signatures of CH_4 emissions in Bucharest and Ploiesti, Romania. sources value of $\delta^{13}C$-CH_4 vs. $\delta^{2}H$-CH_4 are overlaying the classifications of bacterial and thermogenic methane origins (Whiticar, 1999). All values are at least 200 ppb above atmospheric background concentrations. The left plot indicates the samples measured at either RHUL (teal), UU (purple), and the Ploiesti samples. RHUL carbon measurements were paired with dD from UU. Plot on the right indicate the known and unknown source types.

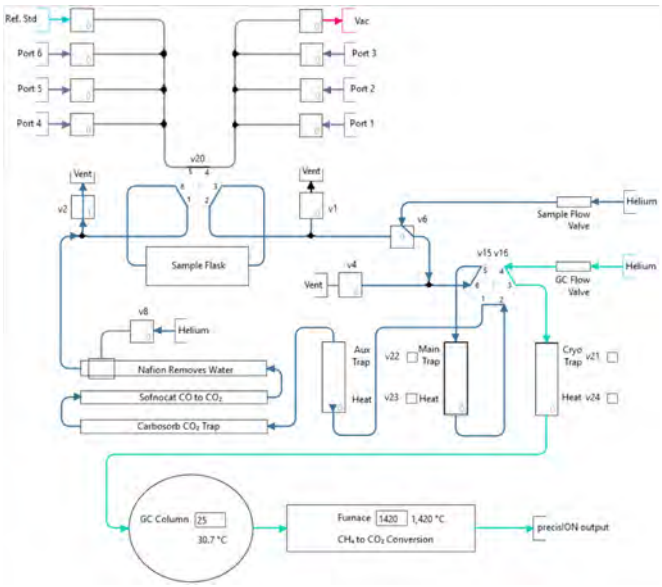

Fig. 6.9.11: RHUL δD Elementar schematic diagram of the 8-port inlet system and sample flow. Sample bags are attached to the ports which fills the sample flask. The sample flows through the nafion, sofnocant and carbasorb traps to remove H_2O, CO, CO_2. Then the sample flows through 3 LN_2 traps followed by a room temperature GC column and Pyrolysis furnace traps to remove more unwanted species in the sample before being measured by the IRMS.

In addition to studying carbon isotopes of methane, it is important to study the less utilized hydrogen isotopes of methane and I have recently started to set up this technique at RHUL. My non-academic partner secondment consisted of one week spent at the Elementar facility near Manchester in September 2019 and an additional week in October.

The first week consisted of developing a system schematic (Fig. 6.9.11) for the ionOS software as well as learning the software system which controls the analysis. The 2nd week consisted of running test samples and ensuring peaks were produced reasonably. Installation of the new RHUL Elementar δD instrument started on the 18th of November. The first issue noticed was that the level of liquid nitrogen (LN_2) significantly had an effect on the produced peak height.

This was solved by connecting an automated liquid nitrogen filler. Samples collected from a Fylde survey this year were measured on the system. Farm, landfill, and gas leak samples were used to determine source signatures (Fig. 6.9.12). When the δD source signatures are matched with their previously measured $\delta^{13}C$ signatures, the data set matches well with known isotopic categories (Fig. 6.9.13). The system is currently still being tested, but has been paused during the UK Covid-19 lockdown.

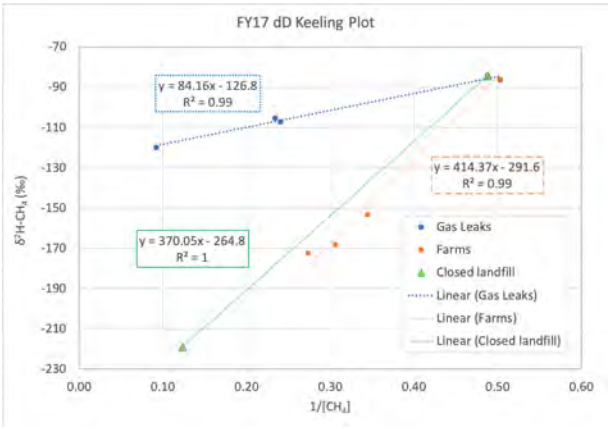

Fig. 6.9.12: δ^2H-CH_4 Keeling plot. Samples were collected February 2020 from 3 different source types in northwestern England. These were measured for δ^2H-CH_4 on the new Elementar instrument to determine source signatures.

6.9.1.2.2 Fourth year

The fourth year was dedicated to finalise data evaluation and publication. The work of the fourth year presented is partly an update of the previously reported results.

During the summer 2019 ESR 10 and I surveyed the **city of Bucharest** in collaboration with INCAS, Romania's National institute for Aerospace Research "Elie Carafoli". Using mobile measurement techniques, we measured street level enhancements, flux rates, and potential source origins (using carbon and hydrogen stable isotopic composition along with ethane:methane ratios) of methane in Bucharest, Romania. We found 969 confirmed locations of methane enhancements, where the maximum mole fraction above background was 38.3 ppm (mean = (0.9 ± 0.1) ppm s.e.; n = 2482). Methane fluxes derived using a previously established empirical relation ranged up to around 290 L min-1 (mean = (3.6 ± 0.4) L min^{-1}, 1 s.e.; n = 969). The total estimated city emission rate is about (1955 ± 71) metric tonnes CH_4 yr^{-1}. More than half (58% to 59%) of the methane enhancements were attributed to biogenic wastewater, mostly from leaking sewer pipelines or wastewater vents.

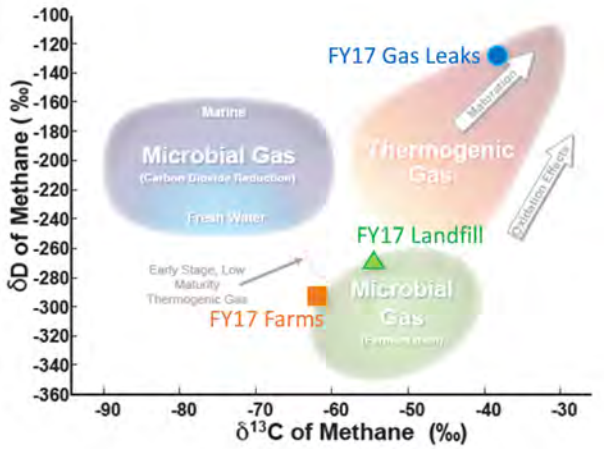

Fig. 6.9.13: δ^{13}C-CH_4 and δ^2H-CH_4 source signatures. Measured sources fall into the appropriate source category of Whiticar & Schaefer (2007).

The hydrogen isotopic composition of methane and ethane:methane ratios were the most useful tracers of methane sources, due to similarities in carbon isotope ratios between sewer wastewater gas and natural gas (Fig. 6.9.14, 6.9.15). This is noticeable from the different source signature population distributions of $\delta^{13}C_{CH4}$ and δ^2H_{CH4} (Fig. 6.9.16). δ^2H_{CH4} shows a more defined separation of the source signatures compared to $\delta^{13}C_{CH4}$.

The Methane from sewer grates, which may represent intentional vents, may be more difficult to mitigate than leaks from gas pipelines, which are often unintentional.

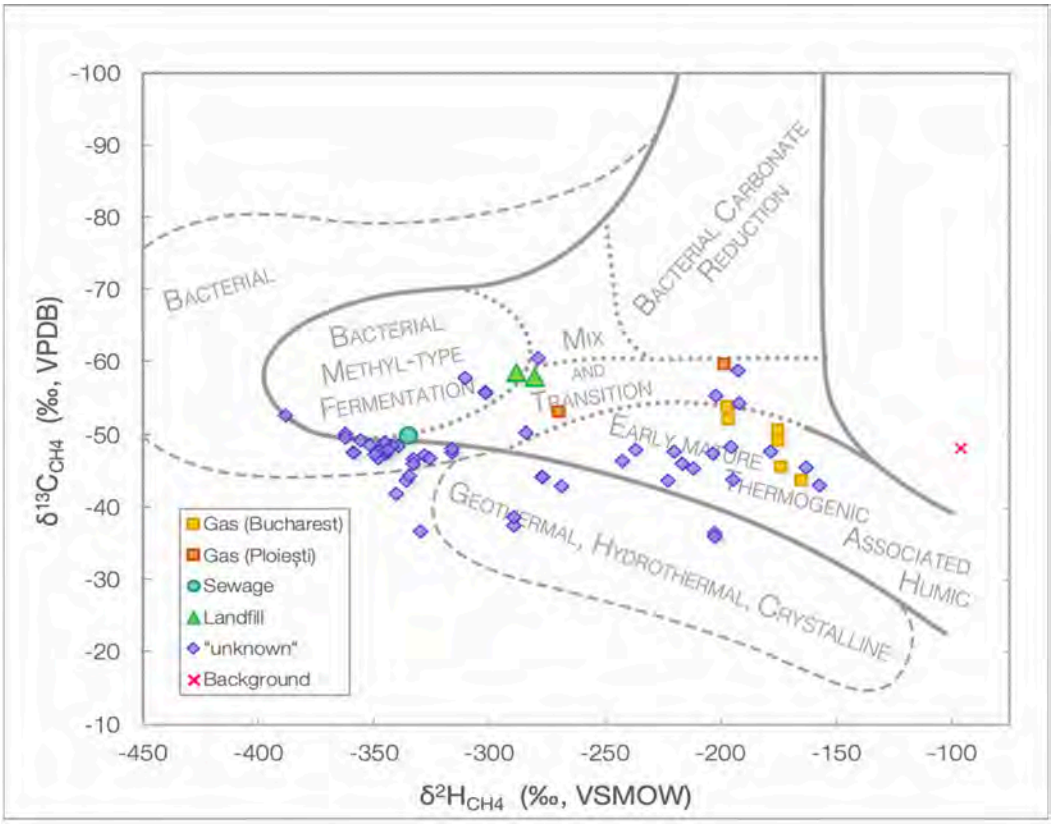

Fig. 6.9.14: Isotopic source signatures of CH_4 enhancements. Comparison between 11 identified and 55 unknown (purple diamond) source signatures. Known source signatures for natural gas is -60 to -46‰ ($\delta^{13}C_{CH4}$) and – 270 to -132‰ ($\delta^{2}H_{CH4}$)(yellow & orange, n=8). Landfills averaged $\delta^{13}C_{CH4}$ to -58‰ (green triangle, n=2), and wastewater is -49.9 ‰ (circle). Points overlay bacterial and thermogenic classifications from Whiticar, 1999

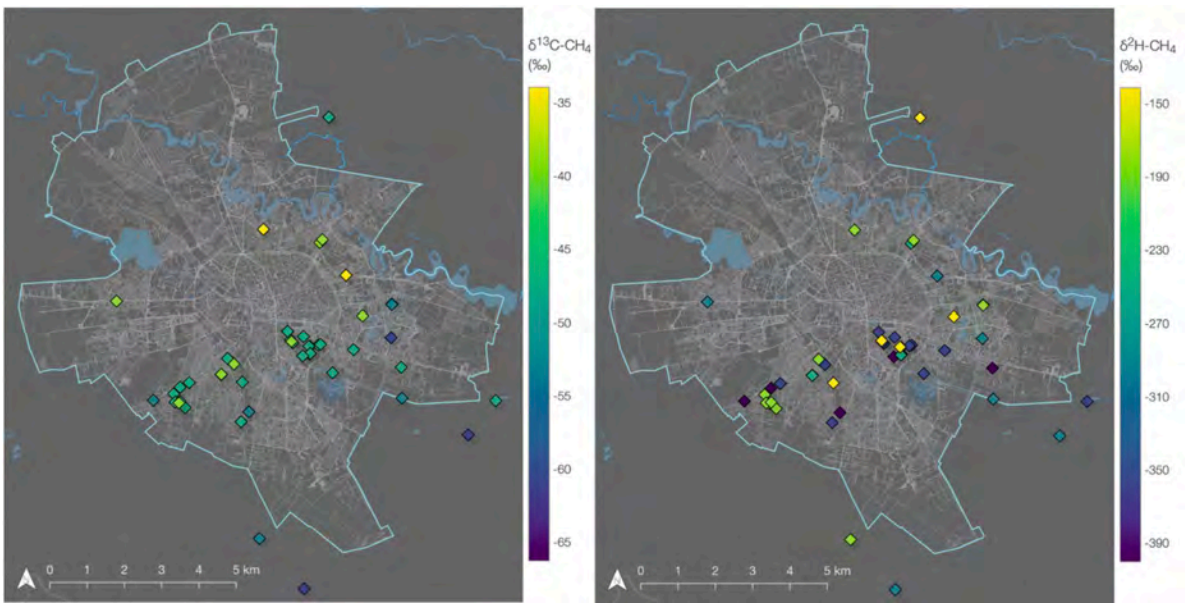

Fig. 6.9.15: Spatial distribution of $\delta^{13}C_{CH4}$ and $\delta^{2}H_{CH4}$ source signatures. $\delta^{13}C_{CH4}$ signatures (left), yellow colors indicate sources of ^{13}C enrichment and blue colors show ^{13}C depletion. $\delta^{2}H_{CH4}$ signatures (right), yellow colors are more enriched and are indicative of thermogenic sources, and purple darker shades indicate ^{2}H depletion and are more likely to be biogenic sources. Less source signature overlap for $\delta^{2}H_{CH4}$ is indicated by the greater color variability.

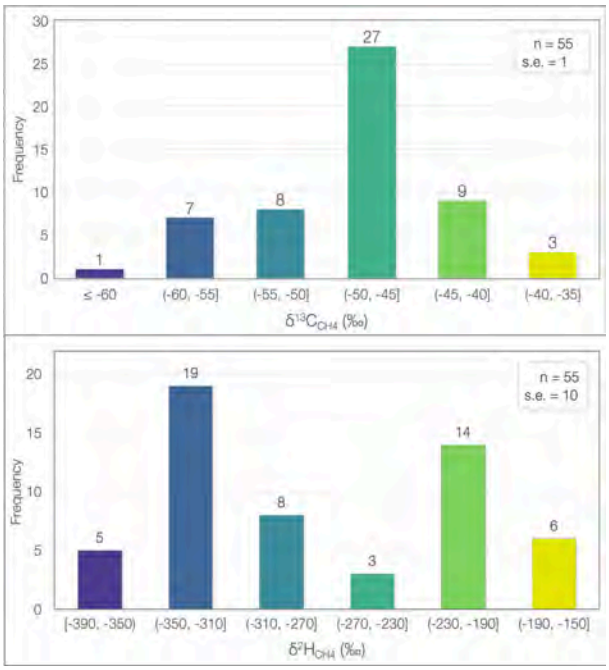

Fig. 6.9.16: City source signature population distribution ($\delta^{13}C_{CH4}$ and $\delta^{2}H_{CH4}$). Combined source signatures of both Bucharest and Ploiești. Histogram showing a normal distribution of $\delta^{13}C_{CH4}$ (top) signatures ranging from -65‰ to -37‰. $\delta^{2}H_{CH4}$ source signatures (bottom) show a bimodal distribution ranging from -388‰ to -157‰.

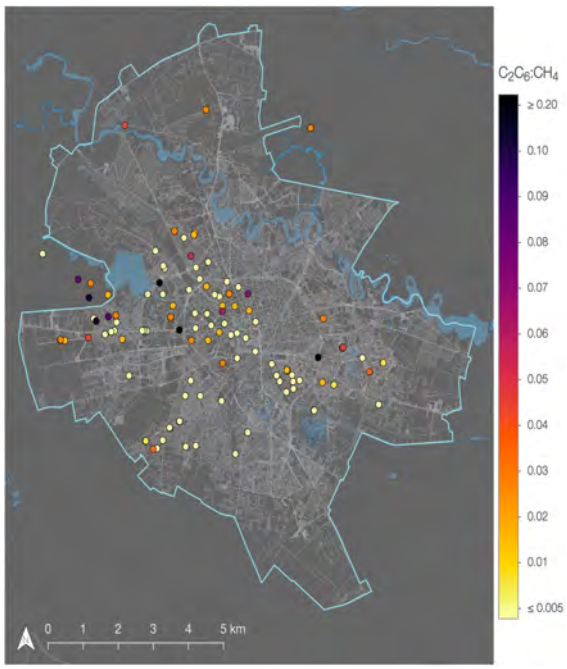

Fig. 6.9.17: Ethane:methane ratios in Bucharest. Map identifies C_2:C_1 ratios where peaks of >0.5 ppm and >3 ppm CH_4 excess over background (for the Picarro G4302 and LGR UMEA analyzers, respectively) were recorded. Lighter colors indicate a relatively low abundance of ethane and darker shades a relatively high abundance.

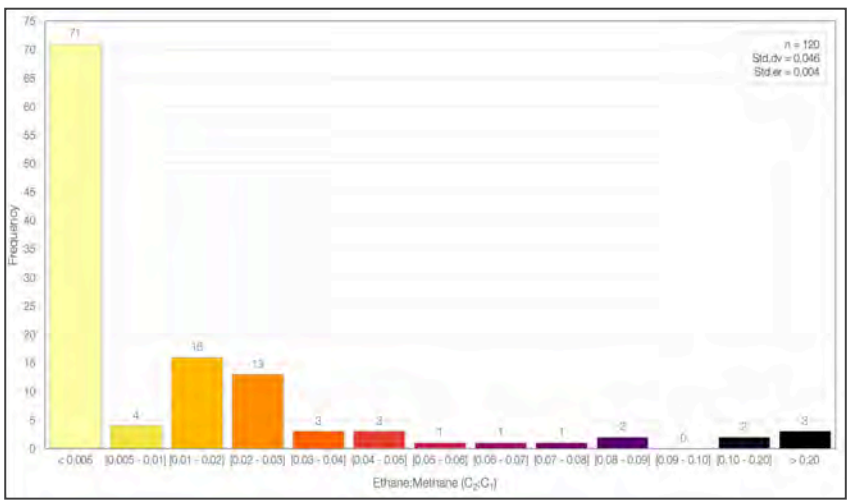

Fig. 6.9.18: Population distribution of ethane:methane ratios. Histogram showing the distribution of determined C_2:C_1 ratios from locations of enhanced CH_4 mole fractions from Bucharest, Romania. Colors correlate to ratios on Fig. 6.9.17. Biogenic sources are < 0.005, thermogenic ranges from > 0.005 to < 0.09 and anything > 0.10 is considered pyrogenic

For my **London** research, most of the isotopic results were already reported during the last reporting period. Data analysis of mobile data was already completed by Felix Vogel, and will be applied to my research with additional detailed analysis of C_2:C_1 to further define sources of enhanced methane.

Draft figures are being produced, with the addition of National Atmospheric Emission Inventory (NAEI) validation incorporating more recently measured isotopes. Fig. 6.9.19 shows the 1 km² 2018 NAEI methane emission estimates with the more $\delta^{13}C_{CH4}$ source signatures. This will be further evaluated by estimating the sectoral emission relations to the isotopic values.

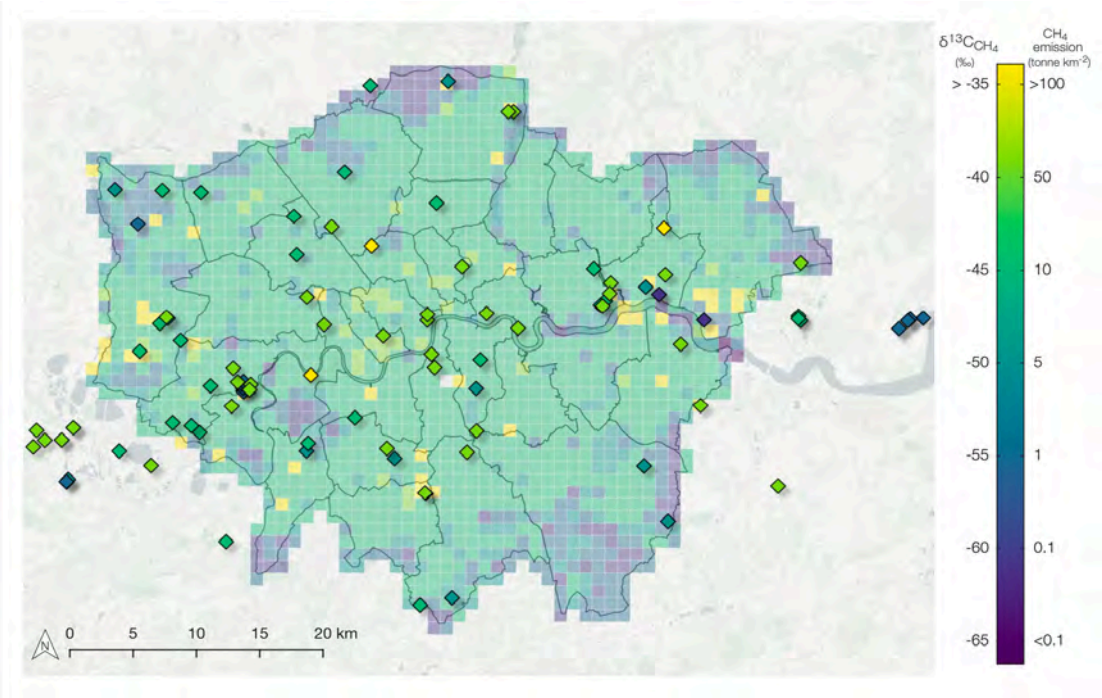

Fig. 6.9.19: Greater London 2018 National Atmospheric Emission Inventory (NAEI) methane estimates (grid, tonnes y^{-1} km^{-2}). Calculated $\delta^{13}C_{CH4}$ source signatures (diamonds) from (2018-2019).

From November 2019 until winter break, the RHUL D/H Elementar system was being tested for optimal measurement settings.

Starting the 2020 spring semester, preliminary $\delta^{2}H_{CH4}$ measurements were conducted on samples collected from the Fylde 14 campaign (northwestern England). Samples of 3 known distinct methane sources (natural gas leak, a farm, and a closed landfill) were analyzed. The Keeling plot results (Figure 8) indicated reasonable source signatures, where the gas signature (-127‰) indicated more enrichment, the farm signature (-265‰) is depleted, and the landfill signature (-292‰) was the most depleted. Comparing these signatures to their $\delta^{13}C_{CH4}$ composition show good relation to their known source type categories (Fig. 6.9.20).

After the first UK lockdown testing and maintenance was put on pause. Upon returning to the lab October 2020, the furnace in the sample extraction system would not heat. Elementar came for maintenance and we found that the heating element was cracked and the ceramic furnace tube was bent. The element was replaced, but the system indicated a decrease of peak sizes from the previous autumn. This was due to leakage between the silica and the ceramic furnace connection, and probably the bent furnace tube itself. Parts were ordered and arrived January 2021. Replacement of the parts started this February and maintenance is still in process.

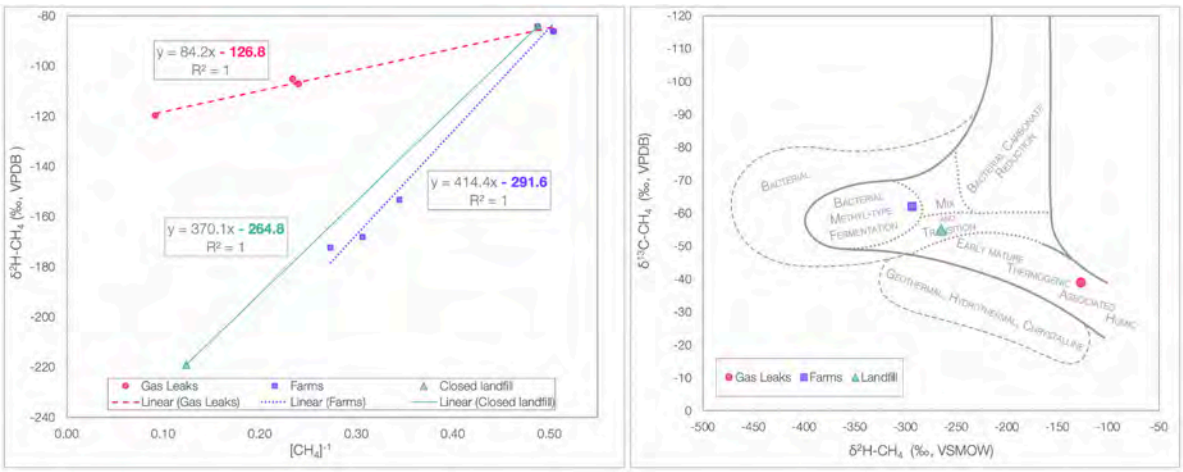

Fig. 6.9.20: Fylde 14 δ^2H_{CH4} Keeling plot (left) and δ^2H_{CH4} vs. $\delta^{13}C_{CH4}$ source signatures (right). Samples were collected February 2020 from 3 different source types in northwestern England. These were measured for δ^2H_{CH4} on the RHUL Elementar instrument. Measured sources fall into the appropriate source categories of Whiticar & Schaefer (2007).

1.3 Future plans and expected results

The Bucharest research is near a second draft and edits from the co-authors are near completion. London paper is on its way. London mobile data has been analyzed for leak locations and emission rates, which are ready for producing map figures. London C_2:C_1 ratios are currently under analysis and will accompany $\delta^{13}C_{CH4}$ for source attribution. Plans for the D/H instrument are to continue testing for optimal measurements by testing discreet furnace temperatures above 1400ºC and measuring with different system flow rates. A calibration method will be developed as well a system measurement protocol to allow more and future team members to utilize the instrument.

6.9.1.4 Collaborations (internal / external)

I've had good communication with Sam Barker from Elementar for establishing and refining RHUL's new δD Elementar instrument measurements and methodology.

Collaborations with Marius Corbu from INCAS has been established during the Bucharest, Romania campaign August 2020. Plans are to collect air samples from the Bucharest gas supply for comparison of isotopic source signatures. Additional communication will continue regularly until the Bucharest paper

I have established collaborations with Malika from UU on building an isotopic database of the MEMO^2 isotopic source signatures that were measured and calculated throughout MEMO^2, which is an ongoing project to be completed this summer.

Collaborations with Felix Vogel have been made to assist with mobile data analysis for CH_4 emission rates since it was already done for the overarching city paper.

6.9.1.5 Risks and difficulties

No risks or difficulties reported.

6.9.2 Deliverables

ESR 9 is involved in the following deliverables: D1.2 / D1.4 / D2.1 / D2.2 / D2.3 / D2.4 / D2.5

D1.2 - Report/publication on CH_4 emissions from wetland and lakes in Sweden (month 30)

No contribution

D1.4 - Improve emissions factors for different source categories from mobile measurements (month 42)

No contribution

D2.1 - Isotopic measurements linked to common scale (month 18)

Approved

I helped fill and measure the tanks used for the laboratory intercomparison. Air samples were collected and measured for CH_4 composition during various mobile surveys in the UK

D2.2 - Improved isotopic source signatures of local and regional CH_4 emissions (month 36)

Measurements and calculations of source signatures in London, Swansea, Bucharest. Attentional sources signatures from Paris & Hamburg.

D2.3 - Publications on the use of isotopes for CH_4 source attribution in urban / industrial regions (month 36)

UK National Atmospheric Emission Inventories are currently being evaluated for London, and will be completed shortly

D2.4 - Publication on temporal and meteorological influences on CH_4 at fixed sites (month 42)

No contribution

D2.5 - Report providing isotopic maps at grid scale from inventories and atmospheric measurements (month 42)

Due to the addition of Bucharest, and more adjusting to the national COVID-19 lockdowns, some analysis and write up delays occurred. Lockdowns restricted the revisiting of London hotspots which were planned for spring/summer 2020. During this period, restrictions have reduced access the RHUL laboratory, preventing testing and maintenance of the new δ^2H system which halted additional δ^2H_{CH4} sample analysis.

6.9.3 Training and network activities

6.9.3.1 General training events

Event	Date (start – end)	Location (Host)	Objective / expected skills	ECTS points	Contribution	Comments
Yorkshire campaign training survey	2018-01-29	RHUL	Lab Field Training		Learned how to prepare and use mobile instruments, collect bag samples, navigate to find methane plumes.	NA
Greenhouse Gas Laboratory training	2018-02-02	RHUL	Laboratory Training		Basic safety training. Introduced to lab instruments to measure [CH_4] and $\delta^{13}C$-CH_4 using Yorkshire samples. Learned how to calibrate mobile instruments.	NA
1st MEMO2 school – Methane measurements and modelling	2018-02-05	MEMO2	External Training Session		The school is part of the European H2020 ITN-ETN project MEMO^2, GA No. 722479. It was a two-weeks school, associated with an intensive measurement campaign, including preparation, lectures and practical.	NA
Greenhouse Gas Laboratory training	2018-02-20	RHUL	Lab Training		Hands on training for air bag samples measuring [CH_4] and $\delta^{13}C$-CH_4.	NA
Data correction training	2018-02-22	RHUL	Lab Training		Data corrections, data management & organization. Introduced to data software and Filezilla and Teamshare.	NA
Department of Earth Sciences Summer Seminar	2018-03-07	RHUL	Poster Presentation		Presented a poster on current research plans.	NA
Writing Literature Reviews	2018-03-14	RHUL	RDP session		Overview of basic steps on writing a literature reviews.	NA

1st MEMO2 Annual Meeting, Dübendorf, Switzerland	2018-03-21	MEMO2	Oral Presentation Poster Presentation		MEMO² Oral presentation on sample results collected during the MEMO² school. Poster presentation summarizing the same results.	NA
FAAM Facility Safety Training	2018-04-11	FAAM	External Training Session		Introduced to North Sea flight research and preparation for flight surveys. Took part in Safety training involving the facility, equipment.	NA
Department of Earth Sciences Postgraduate Research Seminar	2018-06-05	RHUL	Presentation		Presented current research results, progress, and plans for next few months	NA
Isotope workshop	2018-09-17 to 2018-09-19	RHUL	Understand the principles behind mass spectrometry and other isotope measurement techniques. Learn how to collect, analyse and interpret the isotopes of methane			NA
Ploom modeling Workshop	2018-10-08 to 2018-10-10	UH				NA
PGR Seminar Department seminar	29th May 2019	Egham, UK RHUL	Oral presentation, department requirements postgraduate program	?	Update on research presentation	nope
MCAA-UK Workshop Communication & influence	18th Jan 2020	Egham, UK RHUL	Learn how to be a successful and influential speaker.	?	Student participant	Went over basics of giving talks. Lecturer mainly boasted about personal podcast…
MEMO² 3rd Annual Meeting	12th – 13th Feb 2020	Heidelberg, Germany	Update on all MEMO2 work. Organization of papers	?	Oral presentation Update on London research	nope
ROMEO Meeting	12th – 13th Feb 2020	Heidelberg, Germany	Update on all ROMEO campaign. Organization of papers	?	Oral presentation Update on Bucharest city research	nope
Earth Sciences Seminar	2020/03/04	RHUL	Poster Presentation		Presented a poster	
Academic Writing: Planning/Structuring your Essay	2020/10/20	RHUL	Advance writing study skills		Participant	
Time Management Workshop	2020/10/27	RHUL	Advance study skills organization		Participant	
Reading Strategies Workshop	2020/11/02	RHUL	Advance reading study skills		Participant	
Atmospheric Sciences Early Career and Student Networking Event	2020/12/03	AGU2020 Virtual workshop	Learn more about career opportunities in		Participant	Still have no idea what I'd

			Academia, Government and the Private Sector			like to do…
Speak Up: Responding to Everyday Incidents of Bias in STEM	2020/12/04	AGU2020 Virtual workshop	Learned more about Bias in STEM			
Science Policy Networking Mixer	2020/02/10	American Association for the Advancement of Science	Virtually network about science policy, learn about AAAS policy fellowships		Participant and learned about potential career paths and fellowship opportunities	

6.9.3.2 Secondments

Secondment	Date (start – end, planned (when))	Location	Host	Description of work / deviations	Scientific / training (skills) objective	Results and future plans
UU - IMAU	2018-09-24 to 2018-10-21	Utrecht, NL	UU	Training on IRMS system, protocols, surveying		NA
UVSQ	2019-02-25 to 2019-03-22		UVSQ	Mobile survey sampling		NA
LSCE-UVSQ	12th Feb – 23rd March 2019	Gif sur Yvette Cedex LSCE	UVSQ-LSCE	Instrumentation and urban campaign	Campaign around Paris, application of data to models, collect samples for IRMS RHUL	Learned about the Aircore system, sampling methodology, and data analysis. Worked with Polyphemus plume model to estimate emissions. Collected urban, landfill, and gas samples for further analysis.
ELEMENTAR	23rd - 27th Sept 2019 14th - 19th Oct 2019	Isoprime, Cheadle Hulme, UK	Elementar	Assist in new dD instrument development & testing	Introduced to ionOS software. Started running flask samples.	Developed system schematic, and learned basics of the software. Continuing to run tests at RHUL

6.9.3.3 Conferences

Conference name	Date (start – end, planned (when))	Location	Presentation (oral / poster)	Title of presentation	Authors (main author + co-authors)	Public available (yes / no) / web link
1st MEMO2 Annual Meeting	2018-03-21 to 2018-03-23	Dübendorf, Switzerland	Oral & Poster	Isotopic signatures of the 2018 MEMO² school campaign	Fernandez, J.M.	no
PEFTEC-IMMC	22nd - 23rd May 2019	Rotterdam, Netherlands	Poster Presentation	Isotopic signatures of urban methane emission in London	Fernandez J.M., D. Lowry, R. Fisher, E. Nisbet, JL France,	Surf drive

					Colman, S. Bakkaloglu	
Non CO2 Greenhouse Gas Conference 8th	12th - 14th June 2019	Amsterdam, Netherlands	Oral Talk Presentation	Isotopic signatures of urban methane emission	Fernandez JM, D. Lowry, R. Fisher, & E. Nisbet	Surf drive
American Geophysical Union Fall 2019 meeting	9th -13th Dec 2019	San Francisco, CA, USA	Poster presentation	Characteristics of Urban Methane Emissions in London: The Determination of Small Leaks in a Large City	Fernandez J.M., D. Lowry, R. Fisher, E. Nisbet, JL France, P. Nisbet-Jones, M. Colman, S. Bakkaloglu, M. Lanoiselle	Surf drive
EGU 2020	2020/05/04	virtual	presentation	Characteristics of urban methane emissions from Bucharest Romania	J.M. Fernandez, J. France, H. Maazallahi2, M. Corbu, M. Menoud, T. Röckmann, R. Fisher, D. Lowry	https://presentations.copernicus.org/EGU 2020/EGU2020-21759_presentation.pdf
AGU 2020	2020/12/1 – 2020/12/17	virtual		Importance of utilizing multiple methane source tracers when measuring European cities	J.M. Fernandez, James L. France, Hossein Maazallahi, Malika Menoud, Marius-Paul Corbu, Rebecca E. Fisher, Dave Lowry, Thomas Röckmann, Euan G. Nisbet	https://agu.confex.com/agu/fm20/prelim.cgi/Paper/735587

6.9.3.4 Measurement / sampling campaigns

Campaign	Date (start – end, planned (when))	Location	Host	Description of work	Scientific objective	Samples (nature / number)	Results and future plans
Yorkshire	2018-01-xx to 2018-01-xx	Yorkshire, UK	RHUL training	Survey of area to have fracking activity	Conduct and collect data for study on methane before, during and after	3 bag samples for $\delta^{13}C$-CH_4 Continuous measurements of [CH_4], [CO_2], [H_2O], [C_2H_6]	
Schoorl, NL	2018-02-09 to 2018-02-12	Schoorl, NL	MEMO2 1st school	Training survey with MEMO2 group and trace gas release test	Train on working on surveys with all MEMO2 survey vehicles	35 bag samples for $\delta^{13}C$-CH_4 Continuous measurements of [CH_4], [CO_2], [H_2O], [C_2H_6]	See above section 1.2.1
UNC 1	2018-05-03	Sutton, UK	RHUL	Urban city survey	Measure and locate urban CH_4 sources	3 bag samples for $\delta^{13}C$-CH_4	

						Continuous measurements of [CH_4], [CO_2], [H_2O], [C_2H_6]	
UNC 2	2018-06-12	Norfolk / Lincolnshire Terminals, UK	RHUL	LNG terminals survey		18 bag samples for $\delta^{13}C$-CH_4 Continuous measurements of [CH_4], [CO_2], [H_2O], [C_2H_6]	
UNC 3	2018-08-29	Brighton, UK	RHUL	Urban city survey	Measure and locate urban CH_4 sources	15 bag samples for $\delta^{13}C$-CH_4 Continuous measurements of [CH_4], [CO_2], [H_2O], [C_2H_6]	
UNC 4	2018-08-29	Hillingdon, UK	RHUL	Urban city survey	Measure and locate urban CH_4 sources	10 bag samples for $\delta^{13}C$-CH_4 Continuous measurements of [CH_4], [CO_2], [H_2O], [C_2H_6]	
UNC 5	2018-10-25	Ealing, UK	RHUL	Urban city survey	Measure and locate urban CH_4 sources	4 bag samples for $\delta^{13}C$-CH_4 Continuous measurements of [CH_4], [CO_2], [H_2O], [C_2H_6]	Analysis in process
UNC 6	2018-10-25	Harrow, UK	RHUL	Urban city survey	Measure and locate urban CH_4 sources	2 bag samples for $\delta^{13}C$-CH_4 Continuous measurements of [CH_4], [CO_2], [H_2O], [C_2H_6]	Analysis in process
MEMO RHUL 1	2018-0622	Egham/ Staines, UK	RHUL	Local source survey	Measure and locate urban CH_4 sources with visiting UU & UVSQ student	6 bag samples for $\delta^{13}C$-CH_4 Continuous measurements of [CH_4], [CO_2], [H_2O], [C_2H_6]	
MEMO RHUL 2	2018-06-26	Oxford, UK	RHUL	Urban city survey	Measure and locate CH_4 sources of waste facilities with visiting UU & UVSQ student	6 bag samples for $\delta^{13}C$-CH_4 Continuous measurements of [CH_4], [CO_2], [H_2O], [C_2H_6]	Some samples for IRMS RHUL & UU comparison
MEMO RHUL 3	2018-06-27	Spelthorne, UK	RHUL	Urban city survey	Measure and locate urban CH_4 sources with visiting UU & UVSQ student	9 bag samples for $\delta^{13}C$-CH_4 Continuous measurements of [CH_4], [CO_2], [H_2O], [C_2H_6]	Some samples for IRMS RHUL & UU comparison
MEMO RHUL 4	2018-06-28	Kent, UK	RHUL	Urban city survey	Measure and locate urban & waste CH_4 sources with visiting UU & UVSQ student	12 bag samples for $\delta^{13}C$-CH_4 Continuous measurements of [CH_4], [CO_2], [H_2O], [C_2H_6]	Some samples for IRMS RHUL & UU comparison
MEMO RHUL 5	2018-07-05	Devon, UK	RHUL	Heathfield landfill survey	Measure landfill CH_4 with visiting UU & UVSQ student	14 bag samples for $\delta^{13}C$-CH_4 Continuous measurements of [CH_4], [CO_2], [H_2O], [C_2H_6]	Some samples for IRMS RHUL & UU comparison
Ham 1, 2, & 3	2018-10-18 to 2018-10-20	Hamburg, Germany	UU	Urban city survey	Assist and learn protocol of UU surveys to measure and locate urban CH_4 sources.	17 bag samples for $\delta^{13}C$-CH_4 & $\delta^{2}H$-CH_4 Continuous measurements of [CH_4], [CO_2], [H_2O], [C_2H_6]	Analysis in process
Paris_1_City	2019-02-26	Issy-les-Moulineaux & Boulogne, France	LSCE	Secondment, Mobile measurements	Setup & test equipment for upcoming Paris survey	0 bags, Continuous data, (Picarro)	Apply techniques learned to future surveys

Paris_2_City	2019-02-27	Issy-les-Mouline aux & Boulogne, France	LSCE	Secondment Mobile measurements	Survey urban areas of Paris, identify elevations and utilize isotopic samples to determine sources	9	Asses urban signatures for Paris city area
Paris_3_GRTgaz	2019-02-28	GRT gaz distribution station, Fontenay_Mauvoisin, France	LSCE	Secondment Mobile measurements	Sample local gas source, learned aircore methodology, learned data collection protocol for Polyphemus emission estimates	12	Assess local NG distribution signature, Apply gained skills to future surveys
Paris_4_Gonesse_Landfill_Veolia	2019-03-01	Le Plessis-Gassot, France	LSCE	Secondment Mobile measurements	Sample local waste source, learned aircore methodology, learned data collection protocol for Polyphemus emission estimates	10	Assess local Landfill/waste, signature, Apply gained skills to future surveys
France_Etretat	2019-03-02	Etretat, Normandy, France	LSCE	Secondment (mobile measurements for fun & personal interest)	Collect background samples from Northern coastal France	2	Compare BG from sea to BG of City & local sources
Paris_5_City	2019-03-05	NW Paris (8th Arr.)	LSCE	Secondment Mobile measurements & by foot	Located leaks, Collect city isotope samples	5	Asses urban signatures for Paris city area
Paris_6_City	2019-03-06	Western Paris (8th Arr.)	LSCE	Secondment Mobile measurements & by foot	Located leaks, Collect city isotope samples	5	Asses urban signatures for Paris city area
Paris_7_City	2019-03-07	NE Paris (19th Arr.)	LSCE	Secondment Mobile measurements & by foot	Located leaks, Collect city isotope samples	7	Asses urban signatures for Paris city area
UNC24_Swansea	2019-03-26	Eastern England coastal survey, Wales	RHUL	Mobile measurements & sample collection for isotopic signatures	Locate local elevations & identify sources, collect N Atlantic BG air	6	Data to be assessed with London and urban city data. Compare measurements to more inland urban regions
UNC25_Swansea	2019-03-27	Eastern England coastal survey, Wales	RHUL	Mobile measurements & sample collection for isotopic signatures	Locate local elevations & identify sources, collect N Atlantic BG air	12	Data to be assessed with London and urban city data. Compare measurements to more inland urban regions
UNC26_Lambeth & N. Croydon	2019-03-28	London borough survey	RHUL	Mobile measurements & sample collection for isotopic signatures	Locate Greater London elevations & identify sources	4	Measurements and data contribute to greater

							London study.
UNC28_Southwark	2019-04-09	London borough survey	RHUL	Mobile measurements & sample collection for isotopic signatures	Locate Greater London elevations & identify sources	4	Measurements and data contribute to greater London study.
UNC29_Lewisham	2019-04-10	London borough survey	RHUL	Mobile measurements & sample collection for isotopic signatures	Locate Greater London elevations & identify sources	1 BG	Measurements and data contribute to greater London study.
UNC30_Greenwich	2019-06-03	London borough survey	RHUL	Mobile measurements & sample collection for isotopic signatures	Locate Greater London elevations & identify sources	1 BG	Measurements and data contribute to greater London study.
UNC31_Bexely	2019-06-06	London borough survey	RHUL	Mobile measurements & sample collection for isotopic signatures	Locate Greater London elevations & identify sources	4	Measurements and data contribute to greater London study.
UNC32_Hounslow_Heathrow	2019-07-03	London borough survey	RHUL	Mobile measurements & sample collection for isotopic signatures	Locate Greater London elevations & identify sources	2	Measurements and data contribute to greater London study.
UNC33_Waltham_Forest	2019-07-26	London borough survey	RHUL	Mobile measurements & sample collection for isotopic signatures	Locate Greater London elevations & identify sources	1 BG	Measurements and data contribute to greater London study.
UNC34_Redbridge	2019-07-30	London borough survey	RHUL	Mobile measurements & sample collection for isotopic signatures	Locate Greater London elevations & identify sources	1 BG	Measurements and data contribute to greater London study.
UNC35_Congestion Zone	2019-08-07	London City Center survey	RHUL	Mobile measurements & sample collection for isotopic signatures	Locate Greater London elevations & identify sources	4	Measurements and data contribute to greater London study.
UNC36_Barking	2019-08-08	London borough survey	RHUL	Mobile measurements & sample collection for isotopic signatures	Locate Greater London elevations & identify sources	3	Measurements and data contribute to greater London study.
UNC38_Havering	2019-10-09	London borough survey	RHUL	Mobile measurements & sample collection for isotopic signatures	Locate Greater London elevations & identify sources	1 BG	Measurements and data contribute to greater London study.

UNC39_Hackney &Tower Hamlets	2019-10-22	London borough survey	RHUL	Mobile measurements & sample collection for isotopic signatures	Locate Greater London elevations & identify sources	4	Measurements and data contribute to greater London study.
UNC40_Newham	2019-10-23	London borough survey	RHUL	Mobile measurements & sample collection for isotopic signatures	Locate Greater London elevations & identify sources	8	Measurements and data contribute to greater London study.
UNC41_Camden & Islington	2019-10-25	London borough survey	RHUL	Mobile measurements & sample collection for isotopic signatures	Locate Greater London elevations & identify sources	2	Measurements and data contribute to greater London study.
National Physics Laboratory Trace Gas Release	2019-09-09 to 2019-09-13	Bedford Autodrome, Bedford, UK	RHUL	Blind methane & ethane release test. Sampled at various source heights, release rates, concentrations, and inlet heights, in collaboration with ESR05 & NPL	Collect data for methane source emission estimate models. Compare measured data models to known rates.	39	To be assessed for validating RHUL mobile kit, validation and uncertainty of 2 point keeling plots, determine best possible models for RHUL set up.
RHUL Domestic Boilers	2019-06-20	RHUL camupus, Egham, UK	RHUL	Measure output emissions from residential boilers at different stages (starting, warmup, during, and shutoff)	Test significance of methane emissions from domestic boilers.	6	LGRUMEA over saturated with water vapor. Explore alternative measurement techniques. Try tests again.
Local Gas Gov Infrastructure	2020-01-28	Chertsey, Woking	RHUL	Measure local gas governor infrastructure. Measure RHUL gov continuously for 2-3 hours.	Determine nature of gas gov operations to observe any patterns or trends of leaks.	0	No campus emissions seen, leaks mainly were found leaking out of the side panels and not from the ventilation pipes.
ROMEO City Measurements	2019-08-20 to 2019-08-	Bucharest, Romania	ROMEO	Mobile measurements in collaboration with INCAS & UU colleague. Isotopic sample collection of hot spots.	Survey the urban regions of Bucharest, find methane elevations & identify source contributions.	50	Analyze data and write Bucharest paper.
RHUL Environm	2019-11-21	Heathfield	RHUL	Mobile measurements in	To determine surrounding methane levels for	9?	No large elevations seen. Low

ental Project				designated region.	tower measurements		wind. Collected waste samples from Horsham landfill & biogas facilities.

6.9.4 Dissemination activities

ESR9 is co-author of the following publication

E.G. Nisbet, R.E. Fisher, D. Lowry, J.L. France, G. Allen, **S. Bakkaloglu**, T.J. Broderick, M. Cain, M. Coleman, **J. Fernandez**, G. Forster, P.T. Griffiths, C.P. Iverach, B.F.J. Kelly, M.R. Manning, P.B.R. Nisbet-Jones, J.A. Pyle, A. Townsend-Small, A. al-Shalaan, N. Warwick, G. Zazzeri: Methane Mitigation: Methods to Reduce Emissions, on the Path to the Paris Agreement; Reviews of Geophysics, 58, e2019RG000675, https://doi.org/10.1029/2019RG000675, 2020

https://agupubs.onlinelibrary.wiley.com/doi/epdf/10.1029/2019RG000675

6.10 ESR10 – Integration of mobile measurement data in monitoring, reporting, and verification (MRV) of key CH_4 sources in GHG emission reporting across Europe

ESR10

Integration of mobile measurement data in monitoring, reporting, and verification (MRV) of key CH_4 sources in GHG emission reporting across Europe

ESR	Hossein Maazallahi, h.maazallahi@uu.nl
Supervisor	Prof. dr. Thomas Röckmann, t.roeckmann@uu.nl
Co-supervisor	Dr. Hugo Denier van der Gon, hugo.deniervandergon@tno.nl
Non-Academic mentor	Ir. Heijo Scharff, h.scharff@afvalzorg.nl
Official start – end date	01.09.2017 – 31.08.2021

6.10.1 Scientific progress

6.10.1.1 Project introduction and objectives

Climate policies and pragmatic actions are tied closely to the observations, model outputs and inventories. Adding extra greenhouse gases (GHGs) in the atmosphere is equivalent in changing natural condition of atmosphere, thus changing in the climate patterns. The extra GHGs are considerably due to human activities after industrial revolution which is around 1750s. There are wide range of GHGs with different contribution in total extra GHGs.

Among these GHGs there are several gases which are considerably stronger than the others even in small portion. The most important one of these strong GHGs is methane (CH_4). This specie originates from several sources either with natural processes or as results of human activities. The main difference between natural or human activities emissions sit in the fact that natural emissions have been removed by natural removal process over the course of thousands or million years. Thus, any extra amount of GHGs stays in the atmosphere or hardly is more than natural potential to be removed. These extra amount of GHGs gradually increase the Earth ability to absorb incoming radiation and thus enhancing global mean temperature aka global warming. Global warming then alters many characteristics on the planet Earth, e.g. bold example are natural ice reserves melting process in Arctic, Antarctic or glaciers. These maltings then add several other consequences, e.g. sea level rise, change in climate patterns, etc. Sea level rise is then equivalent in loss of many coastal regions and cities.

On the other hand, change in global climate patterns have been already introduced severe impacts, e.g. unusual storms, severe droughts and many other direct or indirect impacts. All in all, adding extra GHGs extremely have been impacted in a short period of time on what had been natural over the course of very long time, thus unknown consequences. To combat these situations, one of the recent proposals is to lower strong and anthropogenic GHGs emissions and CH_4 is the main candidate. However, the contribution of anthropogenic emissions of CH_4 sources is not well known which made it impossible to implement emission reduction plans accordingly.

In the last three years, I have been working with several partners to measure and quantify CH_4 from several different sources, emissions from coal activities in Poland, oil and gas activities in Romania, urban emissions in Hamburg, Utrecht, Munich and Bucharest, big festivals in Munich, oil and gas rigs in North Sea, abandoned oil and gas wells and coal shafts in the Netherlands. All these sources have their own contributions in overall global GHGs emissions which are nested in different inventories, and we intend to prioritise emission sources in EU based on their contribution.

6.10.1.2 Project results

6.10.1.2.1 Third year

6.10.1.2.1.1 Methane emissions evaluation using MATLAB® codes

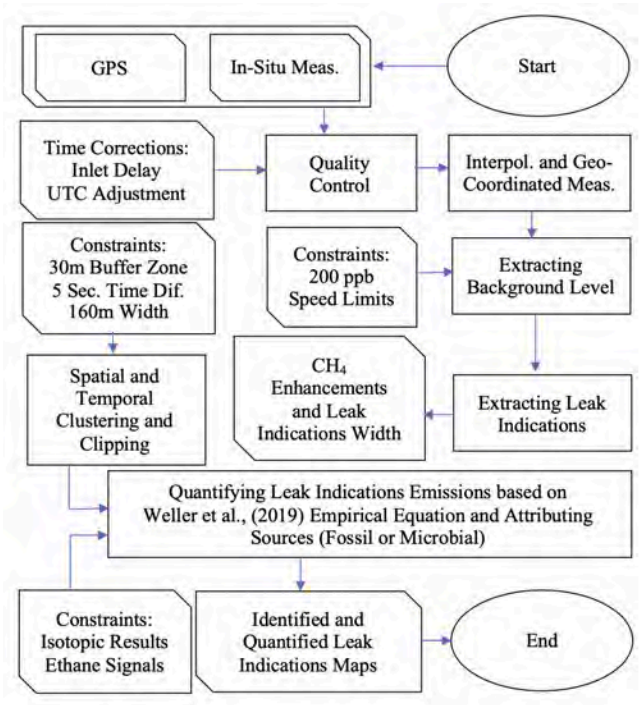

Fig. 6.10.1: MATLAB code flowchart to analyse city measurement surveys

A MATLAB® code was developed by ESR10 to locate and quantify methane emissions from possible gas leaks (leak indications (LIs), i.e. methane enhance-ments above 10% of background level) for city campaign. In this code, in-situ measurement and GPS files get combined, the measurements get timely aggregated and spatially clustered, and all the criteria constraint mentioned in the Weller et al. (2019) were followed.

In Fig. 6.10.1, the flowchart demonstrates the steps taken in the code is provided. The output of this code is mainly quantified methane peaks across a city. However, if ethane signals or isotopic signatures were also collected during the campaign, it is also possible add information on source attribution.

The output of the code can be used to:

- Quantify methane emissions from LIs

The emission quantification output of the algorithm is in unit of volume / time (L/min), and based on the atmospheric ambient temperature and pressure the emissions were converted to unit of mass / time (e.g. tons / year). The output of quantification procedure is useful to update emissions from low pressure pipelines in national inventory reports.

- Report potential gas leaks to local gas distribution companies for further leak repair practices

Attribution process in data evaluation leads in separating emission sources. In Utrecht and Hamburg campaigns information on the source attributions resulted in classifying emissions to fossil, microbial, and pyrogenic. Fossil sources refer to emissions from possible gas leaks from natural gas distribution networks in cities, while microbial emissions refer to emissions mostly from urban swere system, and pyrogenic sources refer to emissions from biomass burning.

Locations were fossil emissions were identified were reported to local gas companies in Utrecht and Hamburg; STEDIN an Gaznets Hamburg respectively. After the reports from Utrecht/Hamburg study submitted to the local gas companies in both cities, repair teams from both companies checked the spots and resulted in fixing major leaks in both cities.

The quantification algorithm was developed at Colorado State University (CSU). At UU we wrote the algorithm in MALTAB® while at CSU they used their own programming code in Python. In order to compare quantified emissions during the Utrecht/ Hamburg campaigns with the US cities, at the first hand we compared the output of the codes with focus on some surveys across city centre of Utrecht and Hamburg. The cross check of the codes resulted in similar outputs (Fig. 6.10.2).

The code will be available on GitHub, and it is possible to customize the code for different instruments, so any institute can run the code and obtain quantified LIs across their study areas. Spatial clustering of the LIs is one of the important steps in the algorithm in which all LIs which belong to a same family are clustered.

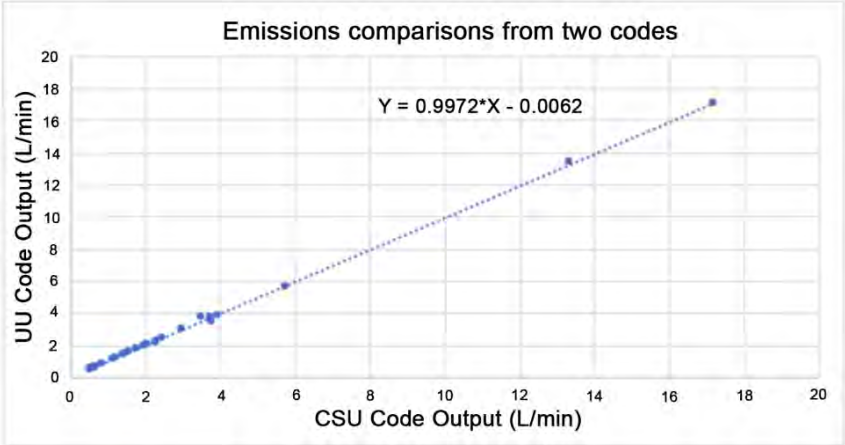

Fig. 6.10.2: Comparison of evaluation code from UU and CSU

In Fig. 6.10.3, an example of the code output is provided from measurement during Hamburg surveys in 2018. As it is shown in top-left part of Fig. 6.10.3, the families are shown in colours and representative of the locations are shown in diamonds. The diamonds are those were reported to the local gas companies to check if there are any leaks from natural gas distribution networks.

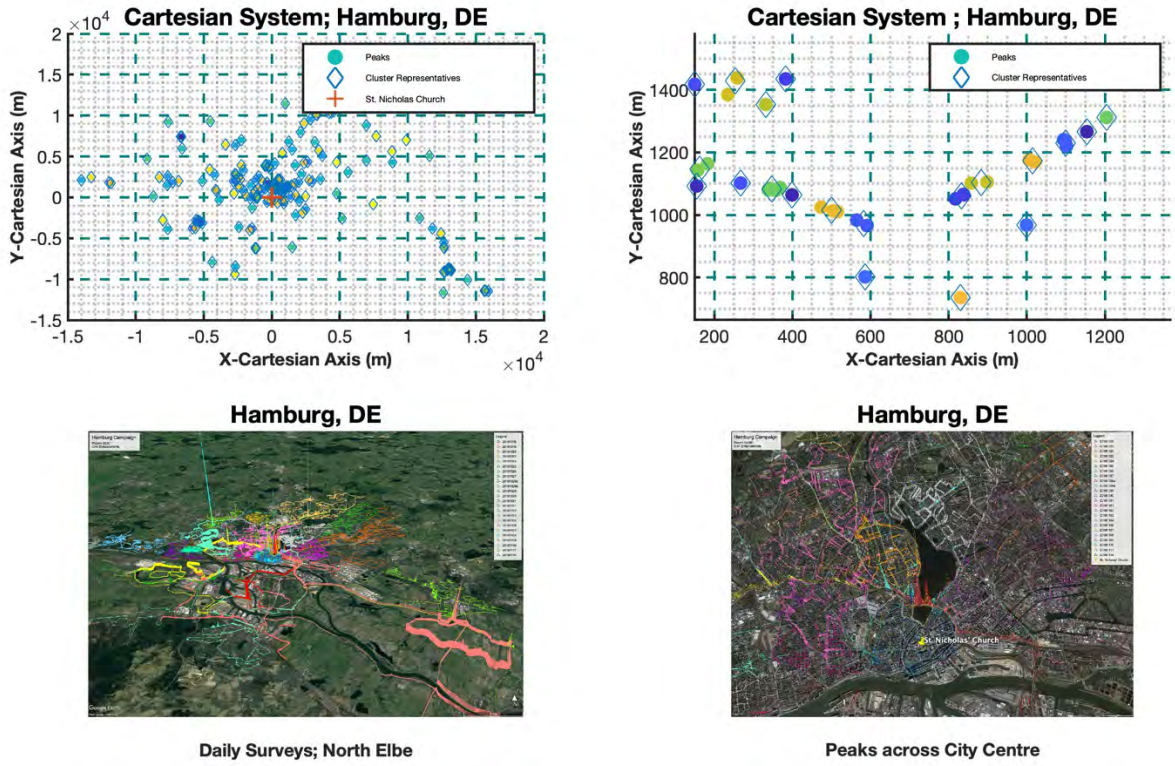

Fig. 6.10.3: Emission locations and clusters. All LIs and clusters in the target area (top-left); LIs and clusters in a smaller region (top-right); complete view of daily surveys across Hamburg (bottom-left); focus of daily surveys across city centre (botton-right)

6.10.1.2.1.2 Campaigns

Fig. 6.10.4: most of ROMEO campaign teams with one of the in-situ measurement plane which belong to Scientific Aviation team

Fig. 6.10.5: Ground team members of ROMEO campaign

Fig. 6.10.6: Checking plans for mobile measurements before departure to field

Fig. 6.10.7: Checking wind conditions with a flag in the field during the ROMEO project

Fig. 6.10.8: UU car used during the ROMEO main campaign for screening and deploying OTM33a method

From February 2019 until February 2020, ESR10 participated in campaigns in the Netherlands, Romania and Germany. The Utrecht and Hamburg measurements were in continuation of the first campaign happened in 2018 and 2019, while the campaigns with TNO/SoDM and the ROMEO project were new.

The campaigns in the Netherlands were in collaboration with TNO to study the status of abandoned oil/gas wells. The results were reported through the TNO to SoDM. In addition to the measurements with TNO, ESR 10 along with his supervisor revisited some of locations where CH_4 enhancements were observed in the main Utrecht campaign. The goal was to check whether the locations identified in the first Utrecht campaign were still present. The findings from this survey were reported to STEDIN and included in the manuscript of Utrecht and Hamburg paper.

In summer 2019, a campaign under title of ROMEO project happened in Romania which was divided into two parts: Bucharest city measurement and field scale measurements from oil and gas activities in Romania which happened between August 2019 until October 2019. The ROMEO campaign was the biggest campaign, ESR 10 participated in 2019.

In January 2020, there was a one-day survey in Hamburg to check locations which had been reported to Gaznets Hamburg (local gas distributor in Hamburg) as the output of first campaign in 2018.

ROMEO main campaign

In October 2019, ESR 10 participated in ROMEO campaign which was designed to quantify CH_4 emissions from oil/gas facilities in Romania. Several groups from several countries participated in this campaign and conducted the measurements with planes, drones, and cars (Fig. 6.10.4).

In the ROMEO campaign, ESR10 participated as a member of ground teams (Fig. 6.10.5) to deploy OTM33a and drive-by methods for quantifying methane emissions from oil and gas facilities. In short explanation, during the OTM33a method, in-situ measurements were carried out in stationary conditions 20-200m downwind a source while in the drive-by method mobile measurements were carried out downwind a source by driving several transects downwind. On 4th of August, UU team headed to the east side of the ROMEO study area to quantify CH_4 emissions from the locations in the east which were mostly related to gas activities. In Fig. 6.10.6, ESR10 is checking the plan with his supervisor; Prof Thomas Röckmann before departure, who was also the coordinator of the ROMEO project. Wind conditions were important factor during the ROMEO campaign. The wind conditions were initially estimated using weather forecast apps but it was important to understand the wind direction in the field to find the most suitable spot to deploy the OTM33a method. In Fig. 6.10.7, ESR10 and his supervisor from TNO; Dr. Hugo Denier van der Gon,

using a flag to check the wind conditions. The wind speed and directions were not favourable during the ROMEO project which means it was either in low speed or the wind directions were changing significantly in a short period of time. This situation made difficulties in for the measurements, however several locations were quantified using different methods including OTM33a and drive-by. The instruments he used was Picarro G2401 and Picarro G4302 onboard a car from host institute INCAS (Fig. 6.10.8). At first step, we screened around oil/gas wells and facilities and later based on the wind direction, most suitable location to deploy the OTM33a method was selected. In Fig. 6.10.9, one day of measurements during the ROEMO campaign is provided in which CH_4 enhancements were observed on several spots. Depending on the wind conditions, topography, time, and possibility of deploying the OTM33a method, for some of the locations methane emissions were quantified. In Fig. 6.10.10, an example of OTM33a deployment is provided, in which the measurements were deployed approximately 25 m downwind of an active oil well with ID of ROM1474. The yellow pins in the Fig. 6.10.10 left shows where the UU car deployed the OTM33a and the red circle shows where the source was. The measurements from this source were plotted against wind direction in the right panel, and a gaussian fit were applied on the average enhancements.

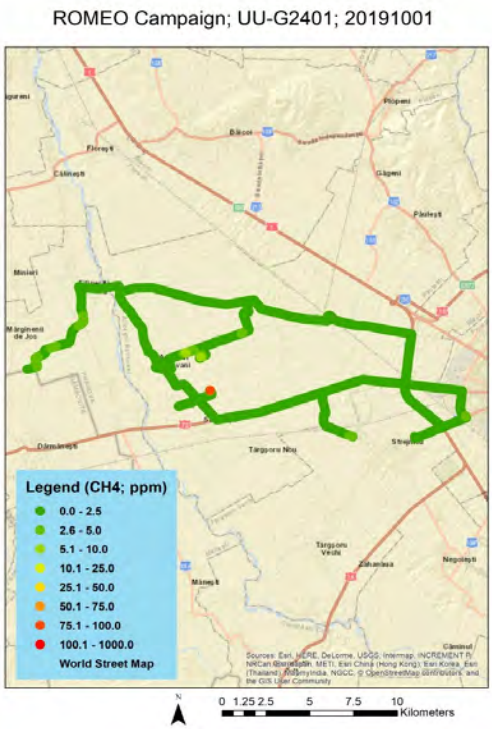

Fig. 6.10.9: UU car used during the ROMEO main campaign for screening and deploying OTM33a method

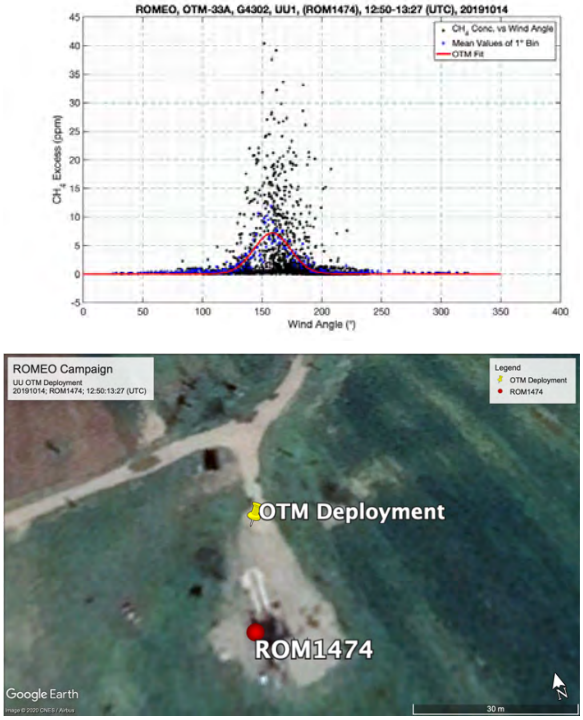

Fig. 6.10.10: In-situ measurements during the OTM-33a application (above), locations of source and the OTM-33a deployment (below)

Emission quantification results from the example in the Fig. 6.10.5 is provided in Table 6.10.1. The quantifications were based on two identifying stability classes based on two methods; stdDW and Turbulent Intensity. As it is shown in the table, the stability classes are different in each method which resulted in different quantifications. The work on quantifications based on the OTM33a method is ongoing and lead by University of Heidelberg. But as a preliminary result the emissions from the wells are about 1 g/s.

Table 6.10.1: OTM33a emission quantifications

Method	Distance	Stability Class	Wind Speed	Methane Emission
stdDW	23 m	1	1.7 m/s	1.3 g/s
Turbulent Int.	23 m	5	1.7 m/s	0.4 g/s

City measurements:

a) Bucharest and Ploiesti, RO

Fig. 6.10.11: Team of the Bucharest city measurement campaign, hosted by INCAS

Bucharest city measurement campaign was conducted from 19th August until 2nd of Sep. 2019 which was hosted by National Institute for Aerospace Research Elie Carafoli (INCAS) (Fig. 6.10.11). The city measurement surveys are part of a campaign called ROmanian Methane Emissions from Oil and gas (ROMEO). MEMO^2 team from Utrecht University (UU), the Netherlands Organisation for applied scientific research (TNO) and Royal Holloway University of London (RHUL) conducted the surveys in collaboration with National Institute for Aerospace Research Elie Carafoli (INCAS). Mobile measurement surveys were carried out using four fast analyzers; Picarro G2301 ($CH_4/CO_2/H_2O$), Picarro G4302 ($CH_4/C_2H_6/H_2O$), Picarro G2401-m ($CH_4/CO/CO_2/H_2O$), and LGRuMEA ($CH_4/C_2H_6/H_2O$) and isotopic samples (including backgrounds) were taken from 36 different spots for further isotopic lab analysis. The instruments were installed in three different cars using inlet from front bumper (60 cm ground level height).

Fig. 6.10.12: Bucharest city measurement devisions

Bucharest city was divided into three sectors and each part was assigned to one of the cars (Fig. 6.10.12). Similar strategies were also applied for Ploiesti but only with one car while the G2401-m were onboard. Car no. 1 covered the sector in blue on which the G4302 were onboard, car no. 2 covered the orange sector on which G2301 and LGRuMEA were onboard, and in red sector car no. 3 covered the roads on which G2401-m were running.

For the Bucharest and Ploiesti measurements four instruments were used. To bring the measurements in one scale, four cylinders were used for the calibration. Calibration of all instruments were done at the beginning and end of campaign using four cylinders (Fig. 6.10.13; Greenland background, low, medium and high methane concentrations). Ploiesti measurements happened after the Bucharest city surveys. In the Ploiesti campaign, ESR10 did not participated physically as the measurements happened when ESR10 left the Romania.

Fig. 6.10.13: Calibrations in the beginning of the Bucharest city measurements

After the calibration procedures, instruments were installed onboard three cars as mentioned before, and surveys started from 20th of August. In Fig. 6.10.14, driving tracks from the three cars are shown which provide the information on the road coverage across the Bucharest city campaign.

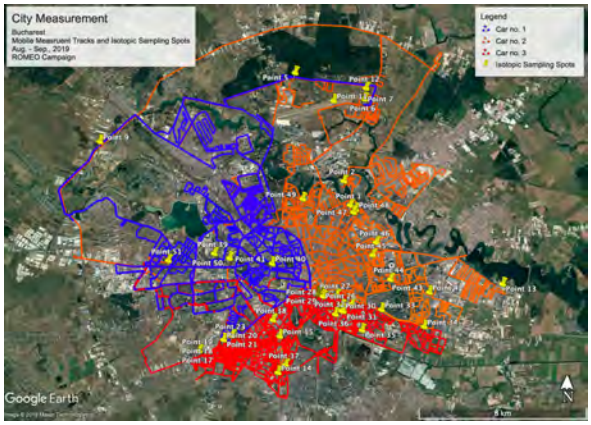

Fig. 6.10.14: Mobile measurement tracks and isotopic sampling spots across Bucharest

b) Utrecht survey, NL

In July 2019, ESR10 along with his supervisor; Prof Thomas Röckmann, visited some of the locations were initially were identified as emission sources in Utrecht surveys (Fig. 6.10.15). The visits resulted in finding the emission sources back and identified some of the sources as microbial emissions from sewer system, as it was also attributed as microbial with the isotopic measurements. The focus was to visit the Joseph Haydnlaan on which several high emission locations were identified in the first Utrecht surveys and reported to the STEDIN. The results of this survey were also reported to the STEDIN and as the STEDIN decided to replace all the gas pipelines beneath this road. The gas pipelines were old and steel and the results from other studies also shown that these conditions make the pipelines prone to leaks more than others.

Fig. 6.10.15: Revisits some of the emission sources in Utrecht (above) and taking samples for lab isotopic measurements (below)

c) Hamburg survey, DE

On 19th of January 2020, ESR10 revisited 10 locations in Hamburg were Gaznets Hamburg fixed the leaks as those were reported from the first Hamburg campaign in 2018. The results showed that in 9 locations there were no leaks and in in close proximity (~100 m) to one of the locations there were enhancements which then was also confirmed by the Gaznets Hamburg as leaks from natural gas distribution network. The company had already planned to replace the pipeline where the enhancements were observed and similar to Utrecht the pipeline was old (dated back to 1930s) and from steel materials.

d) TNO/SoDM project, NL

On 17th of July 2019, ESR10 along with TNO team visited some abandoned gas wells in Rotterdam to check if any enhancements would be observed. The report of this campaign was sent to the SoDM by TNO. The results of this kind of campaigns helps to understand if there are any leaks from sealed abandoned oil/gas wells. The leaks are not only have environmental impact, but also can be result in CH4 accumulation in buildings which were built on top of the abandoned oil/gas wells.

6.10.1.2.2 Fourth year

The fourth year was dedicated to further evaluate and publish the data. Up to now, one first-author publication and two co-author publications are available and briefly summarized below.

6.10.1.2.2.1 PhD publications:

In 2020, I published my first PhD publication titled: *Methane mapping, emission quantification, and attribution in two European cities: Utrecht (NL) and Hamburg (DE)*[1]. This publication was a result of several evaluation stages which are listed as detection, attribution and quantification steps of methane emission sources in Utrecht and Hamburg (see Fig. 6.10.16). A virtual tour of the urban surveys in these two European cities are also available on Leibniz Information Centre for Science and Technology and University Library (TIB) AV portal (https://doi.org/10.5446/49902).

In Fig. 6.10.16, the study area in Utrecht and Hamburg are shown in black polygon; inside the ring in Utrecht and north of Elbe in Hamburg. The driving routs were categorized using information from Open Street Map (OSM) into several levels, see the colours in the maps. Using carbon dioxide (CO_2) and ethane (C_2H_6), CH_4 signals were categorized into fossil (indications for a gas leak), combustion or microbial, and if the signals were not strong enough, CH_4 signals fell into unclassified category. We used an empirical equation from Weller et al. (2019) which was designed to quantify gas leak emissions (Equation 1).

$$\mathrm{Ln}\,(C) = -0.988 + 0.817 * \mathrm{Ln}\,(Q) \qquad (1)$$

In this equation C, represent methane enhancements observed from mobile platform in ppm, and Q is the emission rate in L min^{-1}.

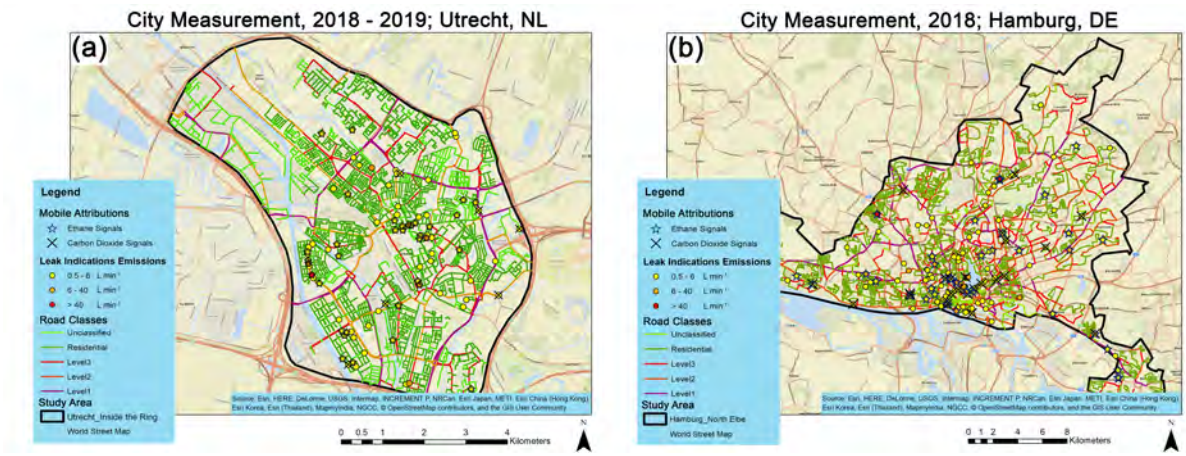

Fig. 6.10.16: Urban surveys in Utrecht and Hamburg study areas

The detection step was based on the campaigns we had earlier in 2018 and 2019 in Utrecht and Hamburg, and then attribution parts relied on either evolution of mobile measurements (Fig. 6.10.16) and/or lab isotopic measurements (Fig. 6.10.17). In Hamburg, in addition to mobile continuous ethane:methane (C_2:C_1) measurements, we took samples from several locations for further attribution practices using hydrogen and carbon methane isotopes ($\delta^{13}C$ and δD) in the lab. In Fig. 6.10.17, attributions from different locations are shown which helps to distinguish CH_4 signals from different sources; fossil, microbial etc.

[1] Maazallahi, H., Fernandez, J. M., Menoud, M., Zavala-Araiza, D., Weller, Z. D., Schwietzke, S., von Fischer, J. C., Denier van der Gon, H., and Röckmann, T.: Methane mapping, emission quantification, and attribution in two European cities: Utrecht (NL) and Hamburg (DE), Atmos. Chem. Phys., 20, 14717–14740, https://doi.org/10.5194/acp-20-14717-2020, 2020.

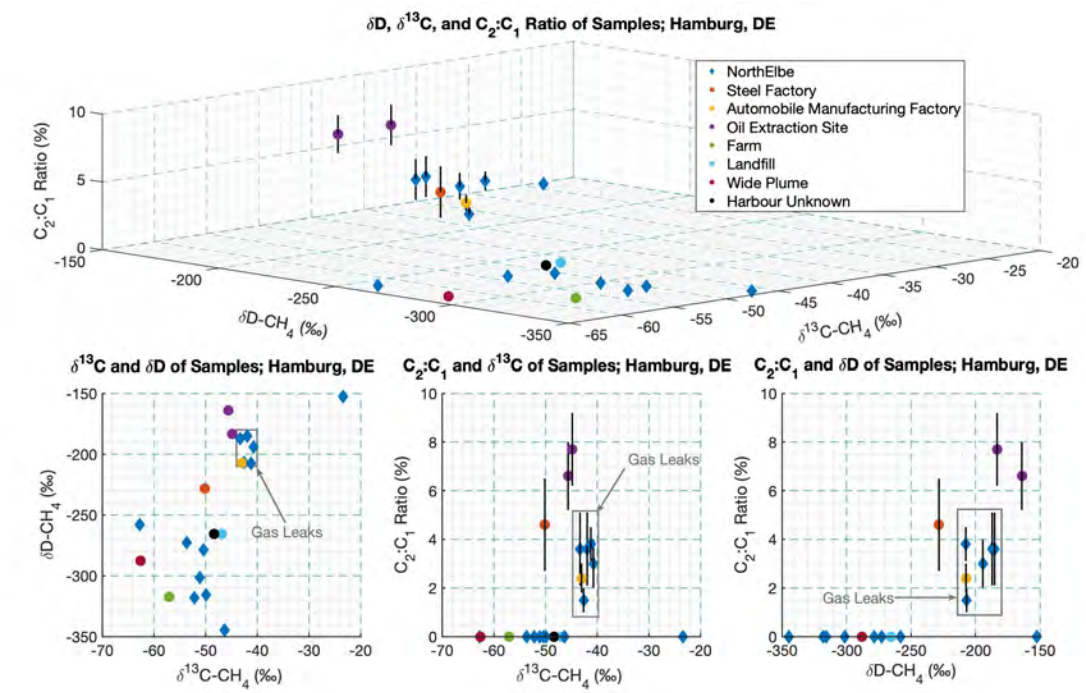

Fig. 6.10.17: C_2:C_1 and isotopic attributions of CH_4 enhanced locations

In Table 6.10.2, a summary of measurements and results is provided. In Utrecht and Hamburg, we drove about 1000 km and 1800 km respectively which account for ~ 450 km and ~ 1200 km coverages in each city. In total we found 81 leak indication (LI, CH_4 enhancement above 10 % of background level) in Utrecht and 145 LI in Hamburg. Attribution practices show that ~ 40% of LIs in Utrecht and ~30 % of LIs in Hamburg are related to gas leaks which in total contribute to about 70 % and 50 % of total CH_4 emission in those study areas respectively. Considering all attribution techniques, we report 0.10 – 0.12 % and 0.04 – 0.07 % of gas loss compare to natural gas consumptions in Utrecht and Hamburg. If we consider the population in the study areas of these two cities, then we can report methane loss from gas leaks in Utrecht and Hamburg as (0.39 ± 0.11) kg yr^{-1} $capita^{-1}$ and (0.15 ± 0.02) kg yr^{-1} $capita^{-1}$ respectively.

Table 6.10.2: Mobile measurements and results summary in Utrecht (NL) and Hamburg (DE)

Study Area			Utrecht (inside the Ring)	Hamburg (North Elbe)
≈ km street driven		Total km driven	1,000 km	1,800 km
		Driven once	220 km	900 km
		Driven more than once	780 km	900 km
≈ km street covered		Total km covered	450 km	1,200 km
		covered once	230 km	900 km
		covered more than once	220 km	300 km
LIs and emissions		Total number	81 LIs	145 LIs
		LI density	5.6 km covered LI^{-1}	8.4 km covered LI^{-1}
		Total emission rate	290 L min^{-1}	490 L min^{-1}
		Average emission rate per LI	3.6 L min^{-1} LI^{-1}	3.4 L min^{-1} LI^{-1}
		Total emission rate per year	107 t yr^{-1}	180 t yr^{-1}
LIs visited	Once	Number	16 LIs	45 LIs
		Emissions	26 L min^{-1}	68 L min^{-1}
		Average emission rate per LI	1.6 L min^{-1} LI^{-1}	1.5 L min^{-1} LI^{-1}
	More than once	Number	65 LIs	100 LIs

		Emissions		264 L min^{-1}	423 L min^{-1}
		Average emission rate per LI		4.1 L min^{-1} LI^{-1}	4.2 L min^{-1} LI^{-1}
Total LIs categorized based on von Fischer et al. (2017) categories	High (>40 L min^{-1})	Number		1 LI	2 LIs
		Emissions		102 L min^{-1}	145 L min^{-1}
		Average emission rate per LI		101.5 (L min^{-1} LI^{-1})	72.4 L min^{-1} LI^{-1}
		% of emissions		35 % of total emissions	30 % of total emissions
	Medium (6-40 L min^{-1})	Number		6 LIs	16 LIs
		Emissions		84 L min^{-1}	176 L min^{-1}
		Average emission rate per LI		14.0 L min^{-1} LI^{-1}	11 L min^{-1} LI^{-1}
		% of emissions		30 % of total emissions	36 % of total emissions
	Low (0.5-6 L min^{-1})	Number		74 LIs	127 LIs
		Emissions		105 L min^{-1}	169 L min^{-1}
		Average emission rate per LI		1.4 L min^{-1} LI^{-1}	1.3 L min^{-1} LI^{-1}
		% of emissions		36 % of total emissions	35 % of total emissions
Total LIs categorized based on OSM road classes	Level 1	Number		6 LIs	29 LIs
		Emissions		5 L min^{-1}	68 L min^{-1}
		Average emission rate per LI		0.76 L min^{-1} LI^{-1}	2.3 L min^{-1} LI^{-1}
	Level 2	Number		16 LIs	34 LIs
		Emissions		145 L min^{-1}	99 L min^{-1}
		Average emission rate per LI		9.0 L min^{-1} LI^{-1}	2.9 L min^{-1} LI^{-1}
	Level 3	Number		3 LIs	23 LIs
		Emissions		10 L min^{-1}	43 L min^{-1}
		Average emission rate per LI		3.4 L min^{-1} LI^{-1}	1.9 L min^{-1} LI^{-1}
	Residential	Number		45 LIs	52 LIs
		Emissions		93 L min^{-1}	274 L min^{-1}
		Average emission rate per LI		2.1 L min^{-1} LI^{-1}	5.3 L min^{-1} LI^{-1}
	Unclassified	Number		11 LIs	7 LIs
		Emissions		38 L min^{-1}	6 L min^{-1}
		Average emission rate per LI		3.4 L min^{-1} LI^{-1}	0.8 L min^{-1} LI^{-1}
Attribution	C_2:C_1 ratio analysis	Fossil (Inc. combustion)	% of emissions	93 % of total emissions	64 % of total emissions
			% of LIs	69 % of LIs	33 % of LIs
		Microbial	% of emissions	6 % of total emissions	25 % of total emissions
			% of LIs	10 % of LIs	20 % of LIs
		Unclassified	% of emissions	1 % of total emissions	11 % of total emissions
			% of LIs	21 % of LIs	47 % of LIs
	$\delta^{13}C$ and δD analysis	Fossil	% of emissions	----------	79 % of total emissions
			% of LIs	----------	38 % of LIs
		Microbial	% of emissions	----------	20 % of total emissions
			% of LIs	----------	54 % of LIs
		Other	% of emissions	----------	1 % of total emissions
			% of LIs	----------	8 % of LIs (Pyrogenic)
	CH_4:CO_2 ratio analysis	Combustion	% of emissions	2 %	10 %
			% of LIs	7 %	17 %
		Other	% of emissions	98 %	90 %
			% of LIs	93 %	83 %
	C_2:C_1 ratio, CH_4:CO_2 ratio, and $\delta^{13}C$ - δD analyses	Fossil	% of emissions	73 %	48 %
			% of LIs	43 %	31 %
		Combustion	% of emissions	2 %	10 %
			% of LIs	7 %	17 %
		Microbial	% of emissions	8 %	35 %
			% of LIs	4 %	33 %
		Unclassified	% of emissions	16 %	7 %
			% of LIs	46 %	19%
Average emission rate per km driven				0.29 L min^{-1} km^{-1}	0.27 L min^{-1} km^{-1}
km driven / total LIs				12.5 km LI^{-1}	12.36 km LI^{-1}

Emission factors to scale-up emissions per km covered			0.64 L min^{-1} km^{-1}	0.40 L min^{-1} km^{-1}
km covered per LIs	km covered / total LIs		5.6 km LI^{-1}	8.4 km LI^{-1}
	km covered / red LIs		454.8 km LI^{-1}	611.4 km LI^{-1}
	km covered / orange LIs		75.8 km LI^{-1}	76.4 km LI^{-1}
	km covered / yellow LIs		6.1 km LI^{-1}	9.6 km LI^{-1}
km road from OSM (≈ km pipeline)			≈ 650 km	≈ 3000 km
Up-scaled methane emissions to total roads			420 L min^{-1} (≈150 t yr^{-1})	1,200 L min^{-1} (≈440 t yr^{-1})
Bootstrap emission rate estimate and error			(420 ± 120) L min^{-1}	(1,200 ± 170) L min^{-1}
Population in study area			≈ 0.28 million	≈ 1.45 million
Average LIs emissions per capita (kg yr^{-1} capita^{-1})			(0.54 ± 0.15)	(0.31 ± 0.04)
Yearly natural gas consumption			≈ 0.16 bcm yr^{-1}	≈ 0.75 bcm yr^{-1}
Fossil emission factors	C_2:C_1 ratio attribution analysis	Average emission rate per km gas pipeline	(0.60 ± 0.2) L min^{-1} km^{-1}	(0.26 ± 0.04) L min^{-1} km^{-1}
		Average emission rates per capita	(0.50 ± 0.14) kg yr^{-1} capita^{-1}	(0.20 ± 0.03) kg yr^{-1} capita^{-1}
	$\delta^{13}C$ and δD attribution analysis	Average emission rates per km gas pipeline	----------	(0.32 ± 0.05) L min^{-1} km^{-1}
		Average emission rates per capita	----------	(0.25 ± 0.04) kg yr^{-1} capita^{-1}
	C_2:C_1 ratio, CH_4:CO_2 ratio, and $\delta^{13}C$ - δD analyses	Average emission rates per km gas pipeline	(0.47 ± 0.14) L min^{-1} km^{-1}	(0.19 ± 0.03) L min^{-1} km^{-1}
		Average emission rates per capita	(0.39 ± 0.11) kg yr^{-1} capita^{-1}	(0.15 ± 0.02) kg yr^{-1} capita^{-1}
		Average emission rates / yearly consumption	0.10 – 0.12 %	0.04 – 0.07 %

In Utrecht and Hamburg, in addition to quantification of urban gas leak locations we also quantified methane emissions from facilities in these two cities. Fig. 6.10.18 shows an example from a wastewater treatment plant in Utrecht for which we quantified total emissions of (160 ± 90) t yr^{-1}.

Table 6.10.3 below summarized all the facilities for which we could quantify CH_4 emissions using gaussian dispersion model. In addition to wastewater treatment plant in Utrecht, we quantified a compost and soil company in Hamburg, and three locations related to oil extraction area of Hamburg.

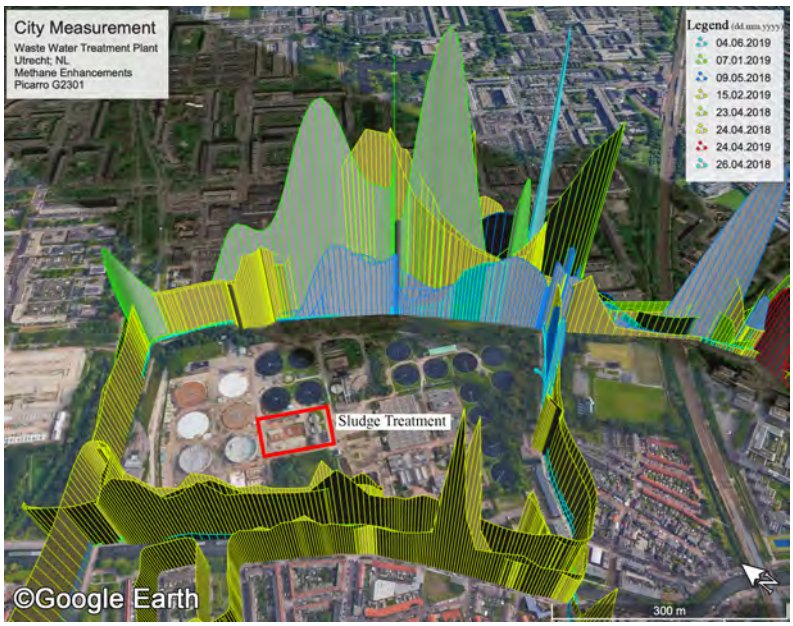

Fig. 6.10.18: CH_4 enhancements measured downwind waste water treatment plant on Brailledreef street and later used for quantifications from this facility in Utrecht; the centre of the area where the sludge treatment is located was considered as the effective CH_4 emission source, the plumes are plotted on the same scale and max CH_4 enhancement is ≈ 0.3 ppm

Table 6.10.3: CH_4 Emissions from larger facilities in Utrecht and Hamburg estimated with the Gaussian Plume model

Facility	Emission rate (t yr^{-1})
Utrecht	
waste water treatment plant (52.109791° N, 5.107605° E)	160 ± 90
Hamburg	
F: compost and soil company (53.680233° N, 10.053751° E)	70 ± 50
Upstream	
D1: 53.468774° N,10.184481° E (separator)	D1: 4.5 ± 3.7
D2: 53.468443° N,10.187408° E (storage tanks)	D2: 5.2 ± 3.0
D3: 53.466694° N,10.180647° E (oil well)	D3: 4.8 ± 4.0

6.10.1.2.2.2 Co-author publications:

a) Methane emissions from the Munich Oktoberfest

As a co-author to a publication led by Technical University of Munich (TUM), Chen et al. (2020)[2], we published an article titled Methane emissions from the Munich Oktoberfest. In 2018, this campaign was carried out around Theresienwiese, where the Oktoberfest happen every year in Munich, Germany. At this festival, there are around 6 million visitors each year and about 8 million L of beer are consumed, about 110 million L of water is used for cleaning, toilet, etc. and approximately 200,000 m^3 of natural gas is used with either cooking (79 %) or heating (21 %). The emissions from this festival could be combination of biogenic or fossil emissions. Emissions from these types of festivals are not included in inventories. We used two Picarro backpacks (G4302) each weight about 15 kg, and we either cycled or walked around Theresienwiese (Fig. 6.10.19).

Fig. 6.10.19: On foot or on bike measurements around the Theresenwisen where Oktoberfest happen with Picarro backpack in-situ instrument, from right to left: Dominik Winkler, Jia Chen, Florian Dietrich and Hossein Maazallahi

We held the measurements around the festival on different days, times and also after the festival to see temporal changes on the emissions. This measurement strategy helped us to understand variability of CH_4 emissions and its correlation to attribute emissions, biogenic and/or thermogenic source of CH_4 emission. To model CH_4 emission, 16 point-sources, representing the tents across the area of festivals, were selected as candidates of CH_4 emission sources (see Fig. 6.10.20).

For the modelling part of the study, gaussian plume modelling was used to explain enhancements observed during the measurement around the area. The enhancements were in scale of about 100 ppb of CH_4 mole fraction above background level. The result show that CH_4 emissions from this festival is (6.7 ± 0.6) µg m^{-2} s^{-1}, with major contribution of fossil emissions. The measurement variability and its correlation with number of visitors could not explain the CH_4 emission were due to biogenic sources. We then concluded that incomplete combustion and/or emission from either heating or cooking or leaks of the temporarily installed gas appliances were the main source of CH_4 emission from this area during the Oktoberfest.

[2] Chen, J., Dietrich, F., Maazallahi, H., Forstmaier, A., Winkler, D., Hofmann, M. E. G., Denier van der Gon, H., and Röckmann, T.: Methane emissions from the Munich Oktoberfest, Atmos. Chem. Phys., 20, 3683–3696, https://doi.org/10.5194/acp-20-3683-2020, 2020.

b) Estimating CH_4, CO_2 and CO emissions from coal mining and industrial activities in the Upper Silesian Coal Basin using an aircraft-based mass balance approach

To achieve the aims of the climate agreement in Paris, intense reduction should be applied from high emitters, thus it is important to have a better understanding of the main emitters. As a co-author to a publication led by German Aerospace Center (DLR), Fiehn et al. (2020)[3], we published a paper related to a campaign held in 2018 under Carbon Dioxide and Methane (CoMet) mission. This campaign was designed to quantify CH_4 emissions from Upper Silesia Coal Basin (USCB) which is one of the hot spots of CH_4 emissions in Europe. This campaign was held in 2018 and designed with two aircraft and three cars equipped with Picarro in-situ measurement analysers continuously measuring CH_4, CO_2, ethane (C_2H_6) and carbon monoxide (CO). In addition to the ins-situ observations, wind data were logged with three Doppler wind lidar Leosphere Wind-cube 200S instruments. In this campaign I participated as contributor to the dataset with mobile measurement with two in-situ instruments (Picarro G2301 and Picarro G4302) onboard a van to continuously measure CH_4, C_2H_6 and CO_2. Fig. 6.10.21 shows the USCB area where the active coal mining shafts are located in red pins, locations of the three wind cubes in yellow and one of the flights on 6th of June. In Fig. 6.10.21, observations from the flight tracks are shown in circles and car measurement are shown in triangles. On this day, two cars drove downwind and one car drove and the aircraft flew on different heights, which all in all gave the required information to apply the mass balance approach to estimate CH_4 emission from the activities across USCB.

Fig. 6.10.20: Measurements around Theresienwiese including 16 emission tracers across the festival area, Munich, Germany

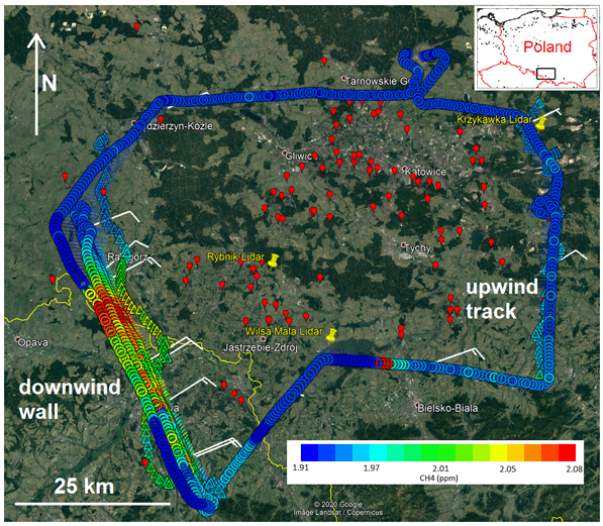

Fig. 6.10.21: Example of flights track around upper Silesia coal basin, Poland

For the two selected flights during the campaign the emissions for CH_4 is (13.8 ± 4.3) and (15.1 ± 4.0) kg s^{-1}, for CO_2 is (1.21 ± 0.75) and (1.12 ± 0.38) t s^{-1}, and for carbon CO was (10.1 ± 3.6) and (10.7 ± 4.4) kg s^{-1}. Comparison of the observed emission with inventories show that for CH_4 estimates from the CoMet and reports from inventories are in the same range while estimates for CO_2 is in the lower range of reports from inventories and estimate of CO emissions are slightly higher than what it is reported in the inventories.

[3] Fiehn, A., Kostinek, J., Eckl, M., Klausner, T., Gałkowski, M., Chen, J., Gerbig, C., Röckmann, T., Maazallahi, H., Schmidt, M., Korbeń, P., Nęcki, J., Jagoda, P., Wildmann, N., Mallaun, C., Bun, R., Nickl, A.-L., Jöckel, P., Fix, A., and Roiger, A.: Estimating CH_4, CO_2 and CO emissions from coal mining and industrial activities in the Upper Silesian Coal Basin using an aircraft-based mass balance approach, Atmos. Chem. Phys., 20, 12675–12695, https://doi.org/10.5194/acp-20-12675-2020, 2020.

6.10.1.3 Future plans and expected results

- We intend to possibly have two follow up campaign with Gasnetz Hamburg and STEDIN in Utrecht. These campaigns are along with previous collaborations we had with these two utilities to detect and quantify gas leaks in these two cities.
- Manuscript submission of Hamburg campaign we had in August, September 2020 (July 2021)
- Possibly participating second phase of ROMEO campaign in Romania fort wo weeks (May – June 2021)
- Manuscript submission on model outputs and aircraft data by December 2021
- Possible extra dataset evaluation: ROMEO-B, Hamburg follow up, or a campaign with STEDIN in Utrecht
- PhD thesis writings start in December 2021
- Finalizing PhD thesis, February 2022

6.10.1.4 Collaborations (internal / external)

- ESR10 and his supervisor; Prof Thomas Röckmann, participated in a meeting in Paris at United Nation venue to exchange knowledge and findings in Utrecht and Hamburg city measurements. In this meeting, all groups active in the city measurement campaigns were involved and collaboration on proceeding evaluation of the city measurements are ongoing.
- During the ROMEO campaign, ESR10 became familiar with several research institutes and groups who are actively involved in quantifying and attributing CH4 emission sources world-wide. The collaboration is ongoing currently with the data evaluation during the ROMEO campaign. Initially it was intended to have second phase of ROMEO in may 2020 but due to the health crisis due to COVID19 pandemic the collaboration for the phase B of ROMEO campaign is postponed for further notice.
- During the campaign with TNO, ESR10 collaborated with colleagues from SoDM and exchanged knowledge and information to understand situation on CH_4 emissions from abandoned oil/gas wells
- ESR10 and his supervisor; Prof Thomas Röckmann, participated in a meeting in Hamburg with Gaznets Hamburg, Environmental Defense Fund (EDF), and Deutscher Verein des Gas- und Wasserfaches (DVGW) which was hosted by Gaznets Hamburg. The meeting resulted in exchanging knowledge and information on mobile measurement and suction method and resulted in planning for a mutual campaign to compare mobile measurement method with suction method used in Germany.

6.10.1.5 Risks and difficulties

Acting on the COVID19 pandemic, I got delays in either conducting a campaign or receiving inputs from partners. We initially planned to conduct a follow up campaign in early summer 2020, but due to the pandemic we could only conduct it in late summer 2020. On the other hand, we faced some delays in receiving some inputs in the evaluation of model outputs related to ROMEO campaign. For these two main reasons I got some delays in the early planning we had.

6.10.2 Deliverables

Within MEMO², ESR 10 is involved in the deliverables D1.4, D1.5, D2.5, D3.2, and D3.4

D1.4 - Improved emission factors for different source categories from mobile measurements (month 42)

No information available.

D1.5 - Report on harmonized method for mobile CH_4 and $13CH_4$ (month 18)

Approved

D2.5 - Report providing isotopic maps at grid scale from inventories and atmospheric measurements (month 42)

No contribution by ESR 10.

D3.2 - Improved bottom-up European CH_4 emissions (month 30)

Submitted

ESR10 participated in related measurement campaigns and delivered / evaluated data.

D3.4 - Top-down estimates of EU-scale CH_4 emissions (month 42)

No contribution by ESR 10.

ESR10 contributed to D3.1 by developing a code to evaluate city surveys.

6.10.3 Training and network activities

6.10.3.1 General training events

Event	Date (start – end)	Location (Host)	Objective / expected skills	ECTS points	Contribution	Comments
Art of Presenting Science	Nov. 2017	UU, Utrecht, NL	Developing scientific presentation skills	2	Participant	
Art of Scientific Writing	Nov. 2017	UU, Utrecht, NL	Developing scientific writing skills	2	Participant	
MEMO2 first summer school	5th–16th February 2018	Schagen, NL	Understanding theoretical background of the plumes, team-work measurements, increasing synergy between students, meeting MEMO2 people for the first time	6	Participant	
Climate change in context	Feb. – April 2018	UU, Utrecht, NL	Assisting in a BSc course	10hr per week	Teaching Assistant	
MEMO2 Annual Meeting	22-23 March, 2018	EMPA, Zurich, CH	Presenting works in the first month of the MEMO2, discussions over the results and how to improve the progress quality and pace.	--	Participant	
National Iranian Gas Company	August 2018	National Iranian Gas Company, Tehran, IR	Introducing MEMO2, with focus on the projects and campaigns held within the MEMO2	--	Giving a Talk	
Plume Modelling Workshop	17-19 Sep., 2018	UHEI, Heidelberg, DE	Understanding the theoretical background of the plume, we also had a programming exercise related to gaussian plume modelling	--	Participant	
Talk at Max-Planck Institute	29 Oct., 2018	MPI-MET, Hamburg, DE	Introducing MEMO2 and the Hamburg campaign	--	Giving a Talk	
Talk at GEOMAR	05 Nov., 2018	GEOMAR, Kiel, DE	Introducing MEMO2 and the Hamburg campaign	--	Giving a Talk	MEMO2 partner
Talk at Meteorological Institute of Hamburg University	13 Nov., 2018	MI, UHH, Hamburg, DE	Introducing MEMO2 and the Hamburg campaign with the first preliminary results	--	Giving a Talk	
TA for Climate Change in Context course	06 February 2019 10 April 2019	UU	Helping students with exercises, grading tests, grading essays written by students,		TA	
NOGEPA meeting	27 September 2019	NOGEPA	Updating the teams participated in campaigns to measure methane emissions from offshore oil and gas platforms		Participated	
UNEP meeting	15 November 2019	UN	Exchange knowledge, information, and understandings from the city surveys		Oral presentation	
Gaznets Hammburg meeting	20 January 2020	Gaznets Hamburg	Exchange knowledge, information, and understandings from the city surveys		Participated	Th emeeting resulted in planning a mutual campaign in Hamburg with Gaznets Hamburg

TA for Climate Change in Context course	05 February 2020 08 April 2020	UU	Helping students with exercises, grading tests, grading essays written by students,		TA	
MEMO2 annual meeting	10 February 2020 11 February 2020	UHEI	Updating the consortium about the activities happened in 2019 and outlooks for 2020		Oral presentation	
ROMEO meeting	12 February 2020 13 February 2020	UHEI	Updating the ROMEO teams about the evaluation carried out from the campaign		Oral presentation	
TA in Climate Change in Context course	5 February – 8 April 2020	Utrecht University	Assisting teaching activities in the course with exercises, exams, homeworks.	-	TA	-

6.10.3.2 Secondments

Secondment	Date (start – end, planned (when))	Location	Host	Description of work / deviations	Scientific / training (skills) objective	Results and future plans
TNO	January 2018	Utrecht	TNO	Working on bottom-up inventories	In progress	In progress
AGH	May-June 2018	Krakow, PL	AGH	Mobile methane measurements, COMET campaign	Improving synergy between MEMO^2 PhDs	Started collaboration with DLR and see how ground base measurements and flights get along with each other

6.10.3.3 Conferences

Conference name	Date (start – end, planned (when))	Location	Presentation (oral / poster)	Title of presentation	Authors (main author + co-authors)	Public available (yes / no) / web link
BBOS	25/10/2017- 27/10/2017	Hotel Erica in Berg en Dal	Poster	Methane Goes Mobile, Measurements and Modelling (MEMO^2)	A. Raznjevic, H. Maazallahi, M. Krol, C. van Heerwaarden, D. Brunner, S. Walter, H. Denier van der Gon, T. Röckmann	No
Industrial Methane Measurements	29/11/2017- 30/11/2017	Antwerp, Belgium	--------	----------	----------	-----
EGU	08/04/2018- 13/04/2018	Vienna, Austria	MEMO^2 Session	Integration of mobile measurement data in monitoring, reporting and verification (MRV) of key methane sources in GHG emission reporting across Europe	H. Maazallahi, H. Denier van der Gon, T. Röckmann	No
ICOS	11/09/2018- 14/09/2018	Prague, Czech Republic	Poster	Methane Emission Mapping and Evaluation across Utrecht City, the Netherlands	H. Maazallahi, M. Menoud, C. van der Veen, H. Denier van der Gon, T. Röckmann	No
EGU	07/04/2019- 12/04/2019	Vienna, Austria	PICO Presentation	Methane Emission Mapping and Evaluation across Utrecht City, the Netherlands	Hossein Maazallahi, Julianne M. Fernandez, Malika Menoud, Rebecca Fisher, Daniel Zavala Araiza, Zachary D. Weller, Stefan Schwietzke, Joseph C. von Fischer, Hugo Denier van der Gon2 and Thomas Röckmann	Yes https://meetingorganizer.copernicus.org/EGU2019/EGU2019-17678-2.pdf
Industrial Methane Measurements	22/05/2019- 23/05/2019	Rotterdam, Netherlands	Oral presentation	Methane Emission Mapping and Evaluation across Utrecht City, the Netherlands	Hossein Maazallahi, Julianne M. Fernandez, Malika Menoud, Rebecca Fisher, Daniel Zavala Araiza, Zachary D. Weller, Stefan Schwietzke, Joseph C. von Fischer, Hugo Denier van der Gon2 and Thomas Röckmann	Yes https://www.ilmexhibitions.com/methane/speakers-list/

Non-CO2 Greenhouse Gases (NCGG)	22/05/2019-23/05/2019	Amsterdam, Netherlands	Oral presentation	Methane Emission Mapping and Evaluation across Utrecht City, the Netherlands	Hossein Maazallahi, Julianne M. Fernandez, Malika Menoud, Rebecca Fisher, Daniel Zavala Araiza, Zachary D. Weller, Stefan Schwietzke, Joseph C. von Fischer, Hugo Denier van der Gon2 and Thomas Röckmann	No
BBOS	23/10/2017–25/10/2017	Den Bosch, Netherlands	Oral presentation	Methane Emission Mapping and Evaluation across Utrecht City, the Netherlands	Hossein Maazallahi, Julianne M. Fernandez, Malika Menoud, Rebecca Fisher, Daniel Zavala Araiza, Zachary D. Weller, Stefan Schwietzke, Joseph C. von Fischer, Hugo Denier van der Gon2 and Thomas Röckmann	No
Attended Nederlands Aardwetenschappelijk Congres (NAC),	12/03/2020-13/03/2020	Utrecht, Netherlands	Oral presentation	Methane Emission Mapping and Evaluation across Utrecht City, the Netherlands	Hossein Maazallahi, Julianne M. Fernandez, Malika Menoud, Rebecca Fisher, Daniel Zavala Araiza, Zachary D. Weller, Stefan Schwietzke, Joseph C. von Fischer, Hugo Denier van der Gon2 and Thomas Röckmann	No
NAC	12 – 13 March	Utrecht	Oral	Methane mapping and emission quantification and attribution in two European cities; Utrecht, NL and Hamburg, DE	**Hossein Maazallahi**, Julianne M. Fernandez, Malika Menoud, Rebecca Fisher, Daniel Zavala Araiza, Zachary D. Weller, Stefan Schwietzke, Joseph C. von Fischer, Hugo Denier van der Gon and Thomas Röckmann	-
vEGU	4 – 8 May 2020	online	-	-	-	-
ICOS	15 – 17 September	Online	-	-	-	-

6.10.3.4 Measurement / sampling campaigns

Campaign	Date (start – end, planned (when))	Location	Host	Description of work	Scientific objective	Samples (nature / number)	Results and future plans
Nauerna Landfill	4 and 15 December 2017	Amsterdam, NL	Afvalzorg	Landfill Measurements	Quantifying methane emission from landfills	--------	--------
Zeeasterweg Landfill	29 November 2017, 5 December 2017	Lelystad, NL	Afvalzorg	Landfill Measurements	Quantifying methane emission from landfills	--------	--------
Braambergen Landfill	29 November 2017, 5 December 2017	Almere, NL	Afvalzorg	Landfill Measurements	Quantifying methane emission from landfills	--------	--------
Campaigns during MEMO2 School	09, 10, 12 February 2018	Schagen, NL	ECN	Farm, Biogas, city measurements	Quantifying and identifying methane emission from different sources	--------	--------
Utrecht	Feb-Apr 2018	Utrecht	UU	City Measurements	Quantifying and identifying methane emission sources across the Hamburg	--------	Comparing the results with other cities.

COMET	May-June 2018	Poland	AGH	Measurements from Coal mining activities	Finding methane emission rate form different shaft in the area	--------	--------
NIOZ/Pelagia	June-July 2018	North Sea	NIOZ	Continuous methane measurements from oil/gas platforms and natural seeps	Understanding methane emissions from anthropogenic and natural sources	13 Glass flask and 37 Bag Samples	--------
TNO/NOGEPA	July 2018	North Sea	TNO/NOGEPA	Continuous methane measurements from oil/gas platforms	Understanding methane emissions from oil and gas extraction platforms	22 Bag samples	--------
Oktoberfest	Sep., Oct. 2018	Munich	Technical University of Munich (TUM)	Stationary and mobile measurements from Oktoberfest festival	Understanding methane emissions from the Oktoberfest	--------	--------
Hamburg	Oct. Nov. 2018	Hamburg	University of Hamburg and Max-Planck Institute	City Measurements	Quantifying and identifying methane emission sources across the Hamburg	104 bag samples (81 UU and 23 RHUL)	--------
Utrecht	01 July 2019	Utrecht	UU	Mobile measurements with Picarro G4302	Revisit to confirm some of the locations identified as LI in the first Utrecht campaign	5	The confirmed locations were reported to STEDIN and included in the Utrecht/Hamburg paper
TNO/SoDM	17 July 2019	Rotterdam	SoDM	Measurements from abandoned oi/gas wells	Screen the status of emissions from abandoned wells	7	Reports were submitted to SoDM by TNO
Bucharest	Aug. – Sep. 2019	Bucharest	INCAS	City Measurements	Quantifying and identifying methane emissions sources across the Bucharest	20 bag samples	Paper will be published and lead by RHUL
ROMEO	Sep. – Oct. 2019	Romania	INCAS	Emissions quantifications from oil and gas activities	Quantifying and identifying methane emissions in Romania	12 bag samples	The synthesis paper will be prepared lead by UU
Hamburg	19 Jan. 2020	Hamburg	--------	Check locations where Gaznets Hamburg fixed leaks reported from the first campaign	Quantifying and identifying methane emissions in Hamburg	--------	Possible leaks were reported to the Gaznets and results used for the Utrecht/Hamburg paper
Hamburg II	2 - 23 August and 12 – 26 September 2020	Hamburg	Gasnetz Hamburg	Urban mobile measurements to detect and quantify gas leaks	Compare different gas leak quantification methods	The focus is now to compare leak quantification from 20 locations	The results will be published as a paper in the next months

6.10.4 Dissemination activities

Type of scientific publication	Title of scientific publication	DOI	Authors	Title of journal or equivalent	Number of ...	Year of publication	Relevant pages	Public/private publication	Peer review [yes/no]	Open access [yes/no],
article in journal	Methane mapping, emission quantification and attribution in two European cities; Utrecht, NL and Hamburg, DE		Hossein Maazallahi, Julianne, M. Fernandez, Malika Menoud, Rebecca Fisher, Daniel Zavala Araiza, Zachary D. Weller, Stefan Schwietzke, Joseph C. von Fischer, Hugo Denier van der Gon and Thomas Röckmann	Atmospheric Physics and Chemistry						
article in journal	Estimating CH4, CO2, and CO emissions from coal mining and industrial activities in the Upper Silesian Coal Basin using an aircraft-based mass balance approach		Alina Fiehn, Julian Kostinek, Maximilian Eckl, Theresa Klausner, Michal Galkowski, Jinxuan Chen, Christoph Gerbig, Thomas Röckmann, Hossein Maazallahi, Martina Schmidt, Piotr Korben, Jarek Necki, Norman Wildmann, Christian Mallaun, Rostyslav Bun, Anna-Leah Nickl, Patrick Jöckel, Andreas Fix, Anke Roiger	Atmospheric Physics and Chemistry						
	Methane emissions from the Munich Oktoberfest	doi.org/10.5194/acp-20-3683-2020	Jia Chen, Florian Dietrich, Hossein Maazallahi, Andreas Forstmaier, Dominik Winkler, Magdalena E. G. Hofmann, Hugo Denier van der Gon, and Thomas Röckmann	Atmospheric Physics and Chemistry	2020					

Dissemination activity	Name	Date	Location	Type of audience	Size of audience
Interview regarding the TNO/NOGEPA cruise, which was broadcasted on youtube	Wat is de rol van het MEMO2 project? - VLOG #9 Offshore Methaan Meetprogramma	7 Oct. 2018	Interview at IMAU, UU, online on youtube: https://www.youtube.com/watch?v=fcsXxEwIF6w&t=1s	General Public	---
University website	Scientists discover more methane leakages in Utrecht's gas distribution network	7 December 2020	https://www.uu.nl/en/publication/scientists-discover-more-methane-leakages-in-utrechts-gas-distribution-network	Public, written in English	public
Atmospheric Chemistry and Physics website	Mobile measurements help quantify and attribute methane emission sources in urban areas	7 December 2020	https://www.atmospheric-chemistry-and-physics.net/about/news_and_press/2020-12-07_mobile-measurements-help-quantify-and-attribute-methane-emission-sources-in-urban-areas.html	Public, written in English	public
Environmental Defense Fund	Scientists Discover 50 Methane Leaks in City of Hamburg's Gas Utility Network	7 December 2020	https://www.edf.org/media/scientists-discover-50-methane-leaks-city-hamburgs-gas-utility-network		
nu.nl	Universiteit ontdekt tientallen lekken in Utrechts aardgasnetwerk	7 December 2020	https://www.nu.nl/utrecht/6095050/universiteit-ontdekt-tientallen-lekken-in-utrechts-aardgasnetwerk.html	Public, written in Dutch	public
duic.nl	Tientallen lekken ontdekt in het Utrechts aardgasnetwerk	7 December 2020	https://www.duic.nl/algemeen/tientallen-lekken-ontdekt-in-het-utrechts-aardgasnetwerk/	Public, written in Dutch	public

gelderlander.nl	Nieuwe meetmethode ontdekt tientallen lekken in Utrechts gasnetwerk	7 December 2020	https://www.gelderlander.nl/utrecht/nieuwe-meetmethode-ontdekt-tientallen-lekken-in-utrechts-gasnetwerk~ae49446f/	Public, written in Dutch	public
utrecht.nieuws.nl	Onderzoekers ontdekken methaanlekken in Utrechts aardgasnetwerk	7 December 2020	https://utrecht.nieuws.nl/onderwijswetenschap/76915/onderzoekers-ontdekken-methaanlekken-in-utrechts-aardgasnetwerk/	Public, written in Dutch	public
Bloomberg.com	Decaying Urban Gas Lines Are Fueling Global Warming	28 January 2021	https://www.bloomberg.com/news/articles/2021-01-28/decaying-urban-gas-lines-leaking-methane-fuel-global-warming?srnd=author	Public, written in English	public

6.11 ESR11 – High-resolution modelling of CH_4 dispersion

ESR11

High-resolution modelling of CH_4 dispersion

ESR	Anja Ražnjević, anja.raznjevic@wur.nl
Supervisor	Chiel van Heerwaarden, chiel.vanheerwaarden@wur.nl
Co-supervisor	Maarten Krol, maarten.krol@wur.nl
Non-Academic mentor	Harm Jonker H.J.J.Jonker@TUDelft.nl
Official start – end date	01/09/2017 – 01/09/2021

6.11.1 Scientific progress

6.11.1.1 Project introduction and objectives

In this project, high-resolution simulations (large-eddy simulations (LES) and direct numerical simulations (DNS)) obtained from the MicroHH model will be used to simulate emissions of methane from various sources (point, line, diffuse). Simulations will be done for different meteorological conditions as well as surface heterogenities and roughnesses. LES and DNS provide detailed temporal and spatial fields of the simulated plume. Therefore, they can be used to set-up virtual experiments to test different measurement techniques. The simulations will be used to test different measurement approaches by mimicking movement of vehicles in the simulations.

An LES will also be done such that it reproduces the measurements in one of the MEMO^2 campaigns in order to compare the modelled results with the measured ones.

6.11.1.2 Project results

6.11.1.2.1 Third year

The Gaussian plume model (GPM) is a simple analytical model which describes dispersion of a plume in a fluid. It can be derived from the advection - diffusion equation after applying many simplifying assumptions, one of the main ones being the stationarity of the plume. The shape of the plume in the 3D space that it is dispersing in is defined by its dispersion coefficients. These coefficients describe the turbulent properties of the flow and vary for different stabilities of the atmosphere as well as the surfaces over which the plume is dispersing (i.e. urban environment or a flat field). Therefore, to properly predict the shape of the plume, these coefficients need to be parametrized. Most of the currently available parametrizations are based on the Pasquill stability classes which divide conditions in the atmosphere into five cases. The most widely used parametrization scheme was given by Briggs and is based on the Prairie Grass experiment, a seminal release experiment performed in 1956 in Nebraska, USA. The experiment has become a standard database for fitting parametrizations and performing model evaluations.

The GPM is very often used in estimations of source strength from measurements of local sources. The two notable mobile measurement techniques are taking plume transects with a measurement device mounted on a moving vehicle and the Other test method (OTM33a) which uses moving platforms to detect plumes after which stationary measurements are performed in the plume centerline. Since the GPM is a simple model used on measurements of plumes in a turbulent flow, there are many possible sources of uncertainties in the source strength estimations. For example, possible sources of uncertainties can be: not knowing the wind speed at the height of the release, orography influences not accounted for in the GPM, atmospheric variability, plume diffusion, stabillity, exact height and location of the source.

We have performed a numerical experiment using direct numerical simulations (DNS) in MicroHH. We simulated turbulent flow over flat terrain and in neutral atmosphere. Into the flow, we released methane

from a point source at four different heights (Fig. 6.11.1). DNS represents the turbulent flows most accurately out of all currently available models. Therefore, we are able to set up a test case in which we have constrained all sources of uncertainties apart from atmospheric variability which has been identified in previous studies (Caulton et al, 2018) as the biggest source of uncertainties.

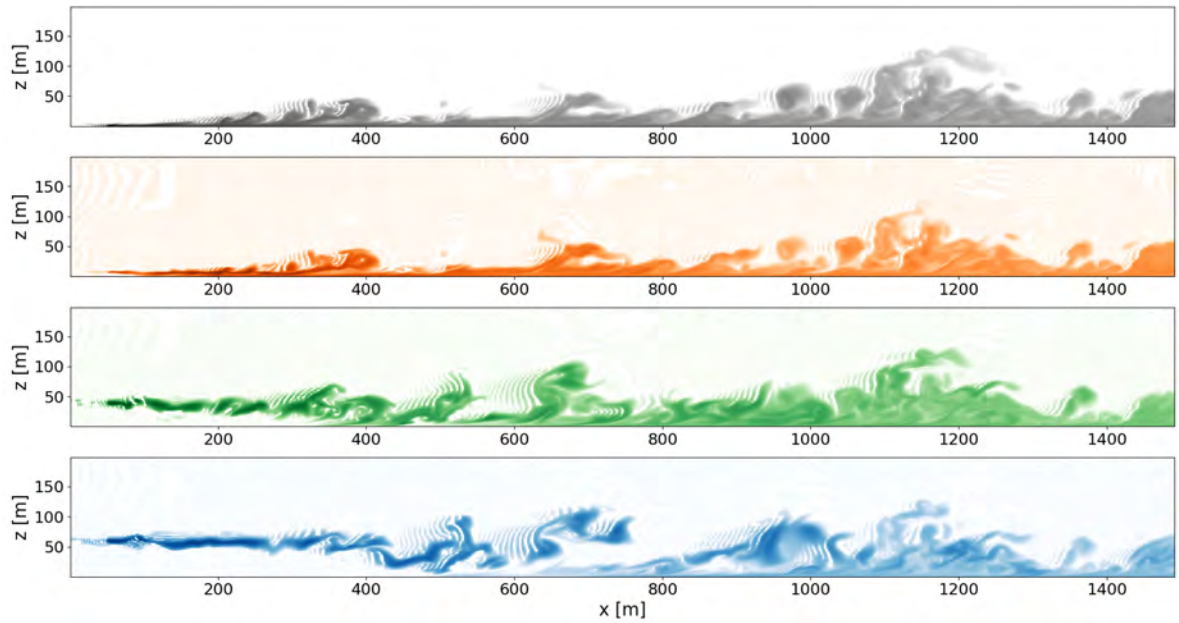

Fig. 6.11.1: Snapshot of x-z transects of the four plumes taken through the plume centerline. Grey plumes correspond with the emission height of 1 m, orange with 7 m, green with 39 m and blue with 60 m.

The analysis has been done only on the emissions from the two highest sources, since the two sources closest to the ground (1 m and 7 m) are in the viscous layer and the buffer layer and the flow does not have the turbulent properties as in the logarithmic layer where the GPM can be applicable.

The theory predicts the average shape of turbulent plumes to be Gaussian. Fig. 6.11.2 shows an average of an hour of simulation for the plume at 60 m. It can be seen that the resulting plume does have the Gaussian shape, but also that the resulting plume is not as dispersed as the GPM predicts. The GPM for the source at the same height and of the same strength as in DNS, with the average wind speed taken from the DNS at the emission height and for dispersion coefficients as defined by Briggs for rural areas and neutral atmosphere is shown with contour lines on Fig. 6.11.2.

As was mentioned, the GPM is too dispersive for this DNS run. Reasons for that can be that the Briggs coefficients have been fitted to the Prairie Grass release experiment, a well-known experiment conducted in Nebraska, USA in 1958, which has become a benchmark for testing dispersion models. The release height for the experiment was 0.5 m, therefore there might be an influence from the ground on the plume for which we are not accounting in our release at 60 m. Another possible reason is that in our run we do not have the influence on the plume from the larger-scale structures, for example from the mesoscale. This discrepancy between dispersion has been reported in the previous studies, but for different atmospheric stabilities (Sharan et al. 2018).

The chosen parametrization of dispersion parameters has a direct influence on the prediction of the source strength using the OTM33a method where the source strength is proportional to their chosen values:

$$Q = 2\pi\sigma_z\sigma_y U c_{max}, \quad (1)$$

where σ_y and σ_z are the dispersion parameters, U is the mean wind measured at the same location as the concentrations. The concentrations are divided into 10° bins according to wind direction on the 100° range. c_{max} is the highest average concentration across the bins.

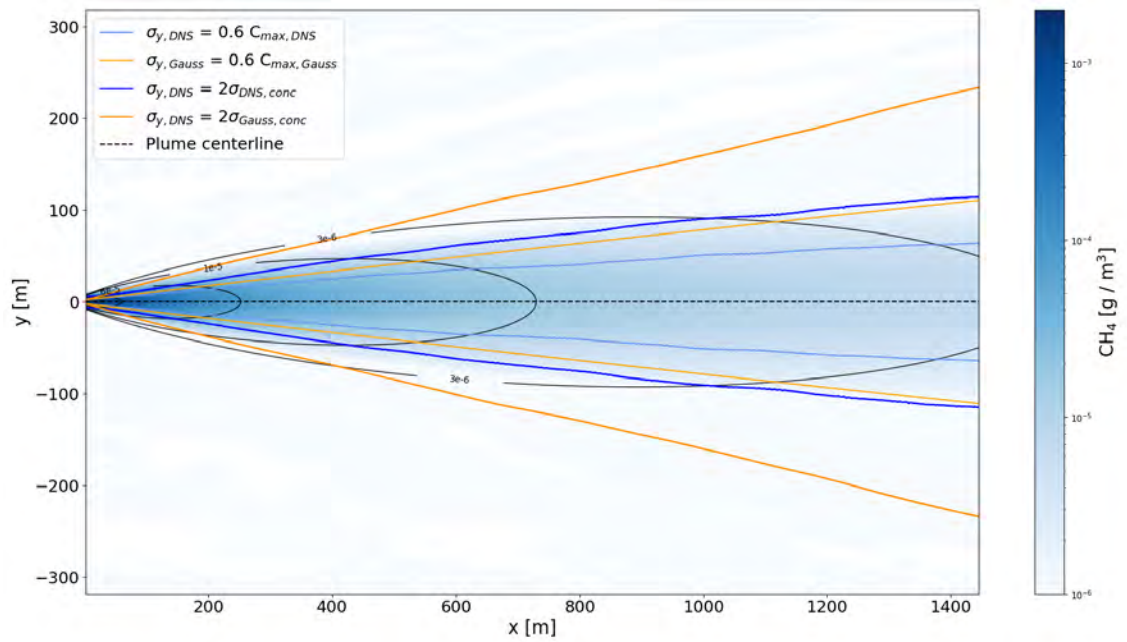

Fig. 6.11.2: Time averaged DNS plume at 60 m height. Averaging was done over the whole hour of the run. Isopleths of concentration show a Gaussian plume released at the same height with the mean wind at the release height. Straight lines denote the edges of the two plumes.

Following the OTM33a procedure we have recorded and analysed concentrations at 4 different downwind distances from the sources. The analysis has been done on a set of 20 half-hour measurements of concentration to achieve viable statistics. Fig. 6.11.3 shows OTM33a predictions for the 4 distances and for the two plumes (39 and 60 m).

First notable result is that the source is highly overestimated for both of the sources. The slightly better results for the lower source are due to the fact that the method also linearly depends on the mean wind, and it is lower for the lower source. It is also visible that the analysis reaches statistical stationarity after 15 min of recording the concentrations which is in line with the theory.

Another result to notice is the low spread of values around the mean value for the high averaging times. This means that the average concentrations all have similar values indicating that either very low concentrations are measured or the concentrations with similar values throughout the plume (on-off plume). As the distance from the source increases so does the spread around the mean, which means the plume is becoming more dispersed further away from the source. This is supported by the results on Fig. 6.11.4 where the time averaged transect through the plume centerline at the emission heights are shown. The time average of plumes aligned by their centers of masses are also shown, as well as fitted Gaussian curves for both of the time averaged plumes. The idea behind this approach is that the dispersion of the plume can be described by two processes: turbulent mixing and plume meandering.

The first process can be seen through the aligned plumes, the wider the time averaged plume is, the stronger is the mixing. Second process is the movement of the whole plume by the larger eddies in the flow. Therefore, the influence of both processes is shown through the time averaged plume.

It can be seen that the dispersion coefficient given by the OTM33a method is too high for this case study, similar to the Briggs parameters shown on Fig. 6.11.2. It can also be seen that the dispersion of the aligned plumes changes slowly with time indicating that the plume shape is not changing rapidly. It can also be seen that the importance of the mixing in the total plume dispersion drops with the distance from the source.

From these results can be taken the importance of knowing the correct dispersion parameters when using these simple methods for estimating the source strength. The other conclusion is that close to the source the plume is keeping its shape dictated by the shape of the source itself and the dispersion of the plume might be too small to use methods which rely on the GPM.

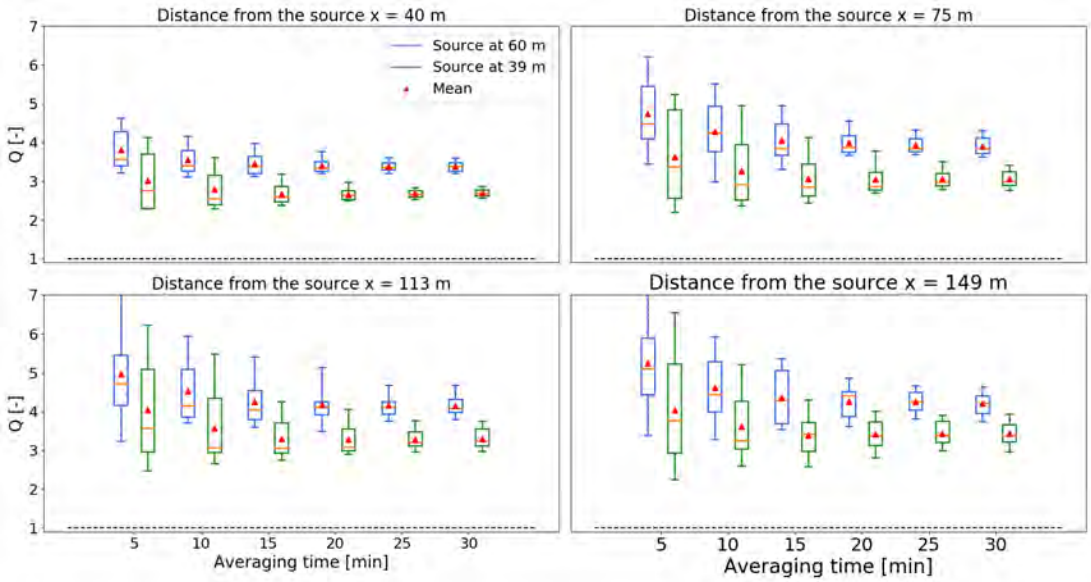

Fig. 6.11.3: Source strength estimations using the OTM33a method at heights 60 m and 39 m for four distances. Boxes show interquartile range, the whiskers span from 5 to 95 percentile of the data. The red triangle denotes the mean and orange line is the median.

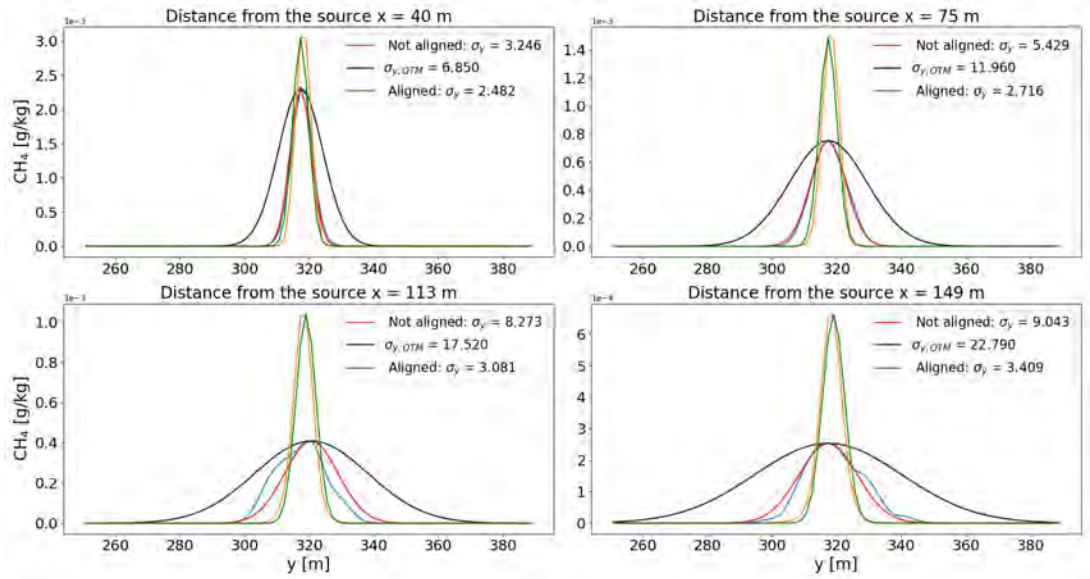

Fig. 6.11.4: Time averages of instantaneous plumes and plumes aligned according to their centers of mass, in the y direction. Emission height is 60 m. The legend shows values of fitted dispersion parameter and the one prescribed by OTM33a.

We have also simulated a car driving through the plume centerline, perpendicular to the mean wind. The car moved infinitely fast (taking the whole transect in one timestep), and with speeds of 7 and 13 ms^{-1} recording the concentrations with frequency of 4 Hz. Each of the measurements were repeated 100 times to get the ensembles.

From the car measurements, the source strength can be inferred using the GPM as

$$Q_{estiim} = \frac{\sum_i c_i}{\sum_i c_{i,Gauss}} Q_{ref} \quad (2)$$

Where Q_{ref} is the source strength set to 1 in the GPM with the same parameters for the source position, wind speed and atmospheric stability as in the measured situation. C_i and $c_{i,Gauss}$ are the measured and modelled concentrations.

To test the influence the atmospheric variability has on estimated source strengths, we compared the variability in source strength estimations from different number of averaged plumes. Therefore, we looked at the source strength estimations from one transect through the plume and from up to 100 averaged transect. The results are shown on Fig. 6.11.5. We can see the clear drop in source strength estimation variability with the increasing number of averages. The decrease is proportional to the square root of the number of averaged transects (~ $1/\sqrt{N}$, where N is the number of averages).

There is also a clear distinction between the transects taken with faster and slower car. The instantaneous transects were taken as the "perfect" measurements, the one to compare the car transects with. It can be seen that the measurements from the faster car are more similar to the instantaneous transects indicating the influence of autocorrelation for the slower car since the faster car has larger spatial step in order to keep the sampling frequency for both speeds at 4 Hz. In general, at least 5 transects should be taken to get within 30% of the true source strength from the car drive-bys. This section showed the most important results of the previous year and will be submitted for review in the very near future.

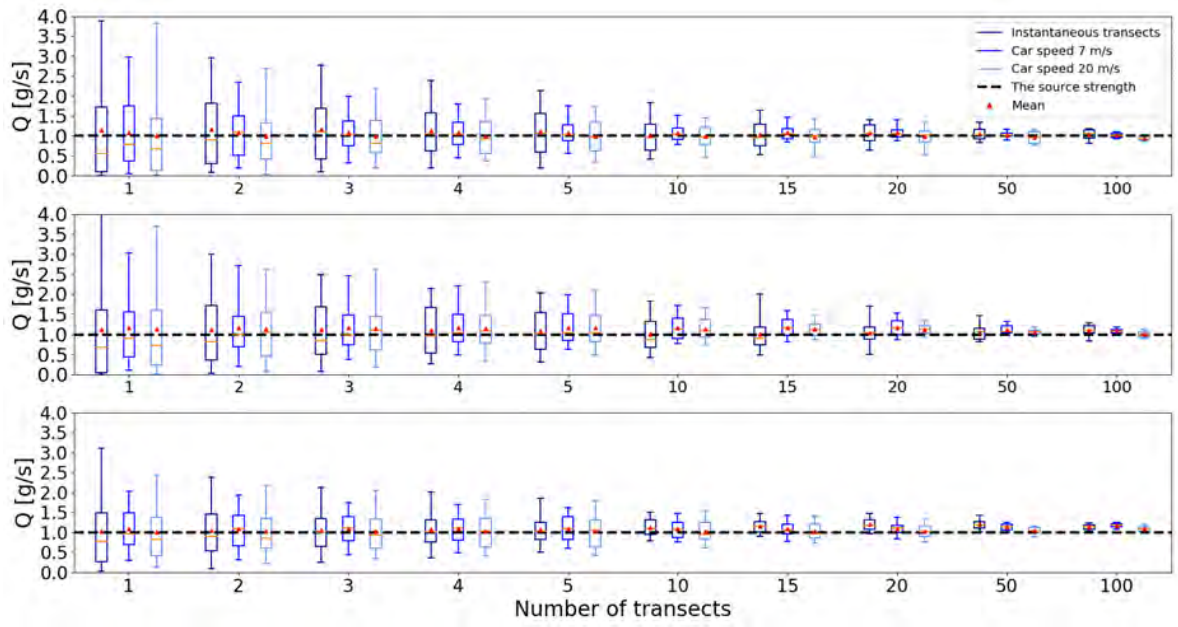

Fig. 6.11.5: Estimation of the source strength for different speeds, the emission height z = 60 m. Boxes show interquartile range, the whiskers span from 5 to 95 percentile, the orange lines are the median. Distances: (top) 225 m, (middle) 454 m, (down) 1213 m.

6.11.1.2.2 Fourth year

High-resolution simulations are an invaluable tool in studying plume dispersion in great detail. They provide detailed 3D fields of the dispersing plume with high temporal resolution while simultaneously resolving the wind that is carrying the plume. LES and DNS have been extensively used in dispersion studies, but those were mostly set in idealistic channel flows which lack explicit connection to boundary layers encountered when measuring plumes in the field (Cassiani, 2020). LES can be paired with the meteorological information (e.g. height profiles of wind, temperature, specific humidity etc.) as forcing in the simulation enabling the reproduction of the boundary layer encountered in the field.

During the October 2019, an extensive measurement campaign on methane emissions from Romanian oil and gas industry (ROMEO) has been performed. During the campaign, on the October 17th, the team from TNO performed extensive measurements of a methane leak from an oil well. The well is situated in the Prahova County, central Romania. The measurement site is situated on a flat plain with little obstacles in the vicinity that could possibly obstruct or distort the plume.

Fig. 6.11.6: Oil well location and the adjacent road the measurements were performed on.

The measurements were performed with an instrument placed in a moving vehicle that drove along the road close to the well recording the concentrations from the well plume together with concentrations of a tracer gas that was emitted from the close vicinity of the well. The geometry of the source location was given on Fig. 6.11.6 and schematic overview of the instrument and vehicle is given on Fig. 6.11.7. The measurements resulted with 40 plume transects over the duration of 3 hours (14 – 17 LT). Simultaneously, the three wind components were recorded at 2 m height with a 3D sonic anemometer placed close to the well. Measured plumes and wind speed and direction are given on Fig. 6.11.8.

Fig. 6.11.7: Instrument set-up used by the TNO group during the ROMEO campaign. Indicated on the figure are the position of the inlet through which the concentrations are led to the instruments used in analysis as well as the position of the GPS on the van. Figure also shows the Gill R3 sonic anemometer.

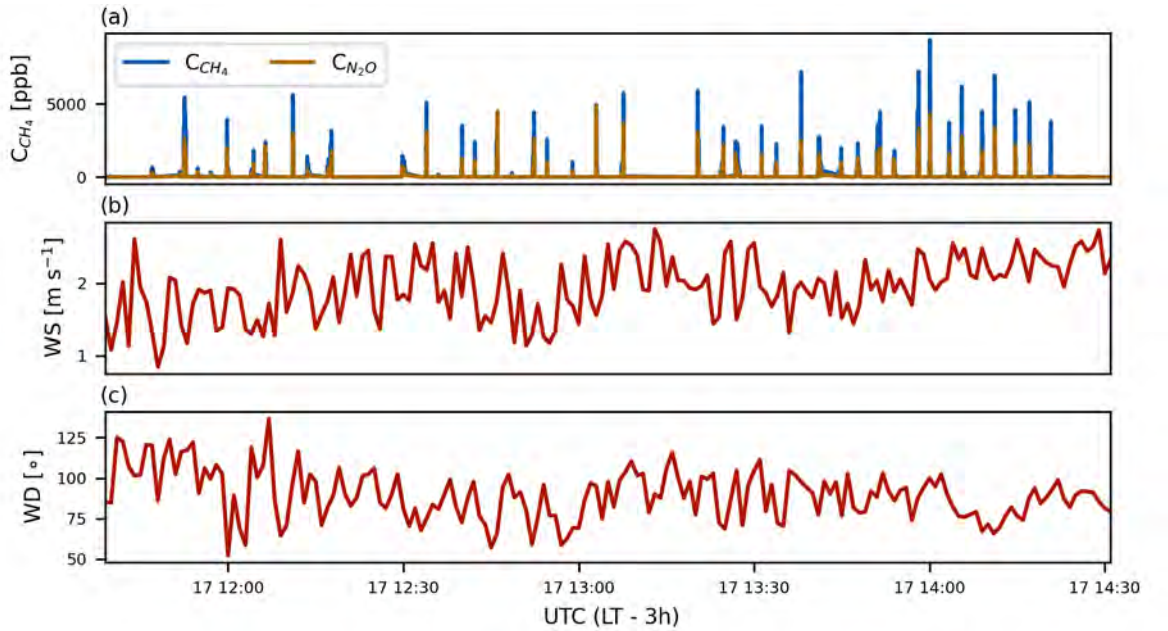

Fig. 6.11.8: (a) CH_4 concentrations measured over the read adjacent to the emitting oil-well and N_2O concentrations emitted from next to the well. (b) Horizontal wind speed measured on the site during the experiment and (c) horizontal wind direction

The LES was performed with ERA5 data (Hersbach et al. 2020) as input to reproduce the conditions encountered in the field. Fig. 6.11.9 shows distribution of geopotential height and temperature over Europe at 12 UTC on October 17th 2019. It can be seen that the area over Romania is characterized with little to no gradient in temperature and geopotential height. This implies that there were no large-scale advection processes that could influence the plume dispersion. Therefore, all the motions of the plume were caused by the local temperature gradients and orography.

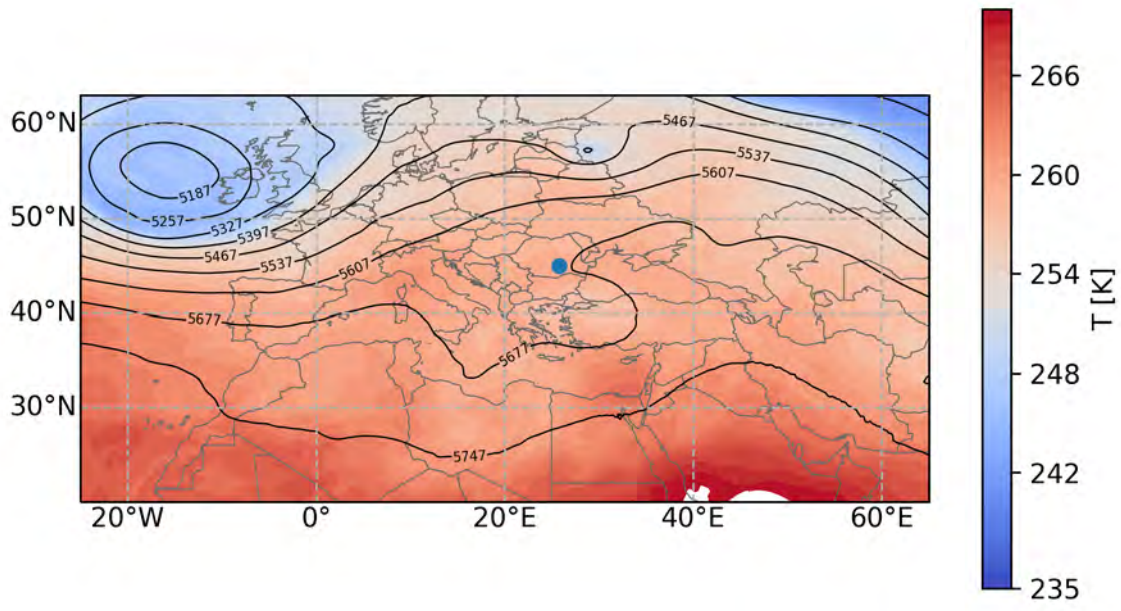

Fig. 6.11.9: Geopotential height (m) and temperature of the 500 hPa pressure level at 12 UTC on 17th October, 2019. Location of the studied region is indicated on the map by a blue circle.

The LES was performed on a 4.8 x 4.8 x 3 km domain with the resolution of 5 x 5 x 2 m close to the ground. Profiles of wind, potential temperature and specific humidity from ERA5 were used as initial conditions. The simulation was also nudged towards hourly profiles of said profiles from ERA5. The resulting plume can be seen of Fig. 6.11.10. It shows large oscillations in wind direction, which is a byproduct of the lack of the large scale forcing. For the simplicity of the analysis of LES results, another simulation was set up in which a mean wind direction was forced in the East direction and the wind sped was made to match the observed one, the rest of the variables were left as in the first run.

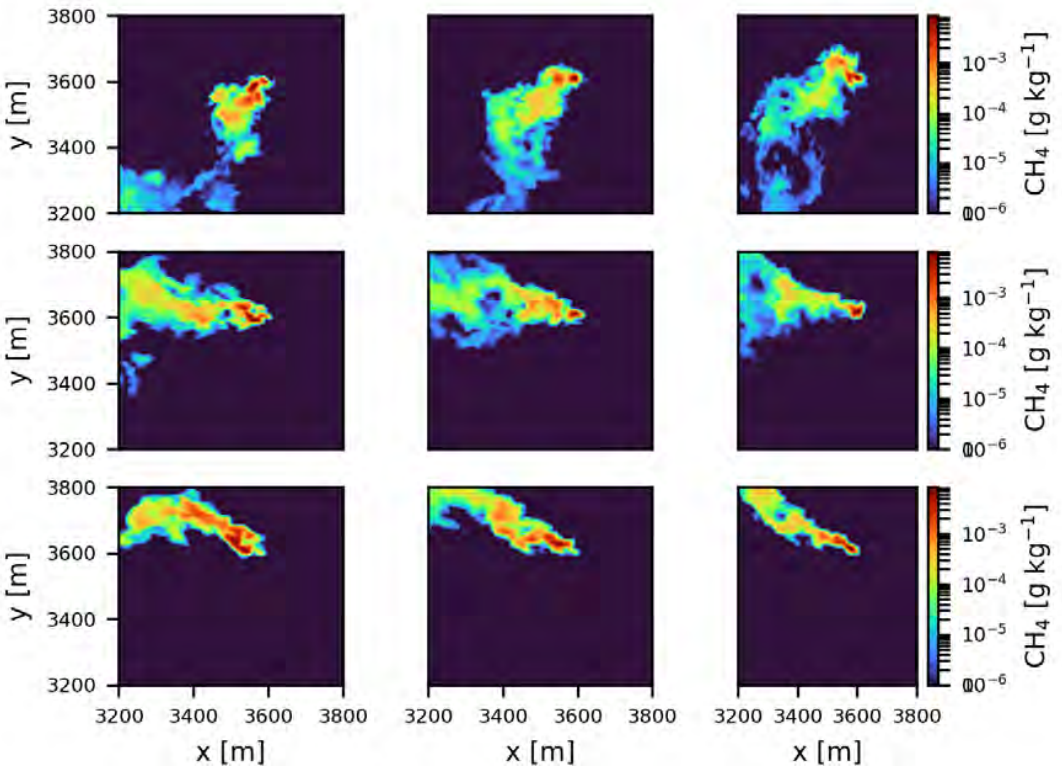

Fig. 6.11.10: Snapshots of instantaneous plumes at 3 m above the surface. Plume at (top) 11:30:00, 11:31:30 and 11:33:00 UTC, (middle) 12:11:30, 12:13:00 and 12:14:30 UTC, (bottom) 13:00:00, 13:01:30 and 13:03:00 UTC.

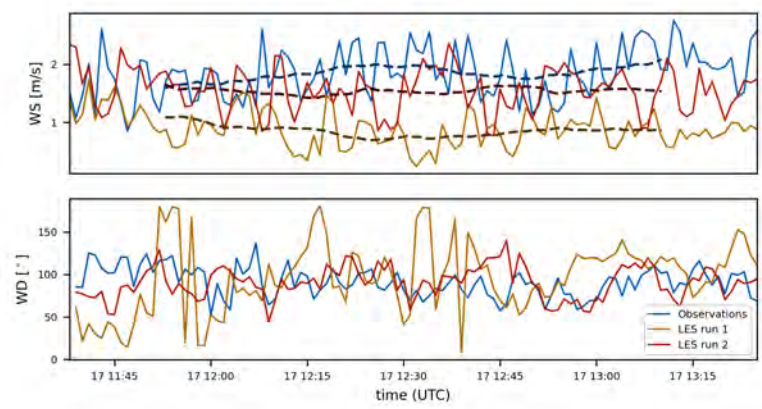

Fig. 6.11.11: Comparison of the observed and simulated (top) horizontal wind speed, (bottom) horizontal wind direction. The values are given as one-minute averages of instantaneous wind. The dotted lines are rolling means of respective wind speeds, shown here for easier interpretation of the mean wind speed.

Comparison of two runs with the data measured in the field is given on Fig. 6.11.11, the variables are given as 1 min averages. Since the mean wind direction in the second run was set to be easterly, it was rotated to match the observations. Much better agreement can be seen between the observations and the second run than the first, not only in the mean wind speed and the magnitude of fluctuations, but also in the magnitude of the wind direction fluctuations.

Firstly, the observed and simulated plumes from the second run were compared and the LES was used to characterize the source strength using the mass balance approach. The method is used by comparing the flux of time-averaged measured plume over a 1D transect through the plume from a source of unknown strength with the time-averaged flux over the same transect from a known source at the same (or similar) position as the unknown one. If the tracer gas is unavailable, generally the Gaussian plume transport model is used. The formula used is

$$Q_{estiim} = \frac{\sum_i c_i}{\sum_i c_{i,ref}} Q_{ref} \quad (3)$$

Where Q_{estim} is the unknown source strength, c_i are the measured concentrations and the subscript *ref* indicates source strength and concentrations on the transect from either the known source of the tracer gas or from the modelled plume. Fig. 6.11.12 gives measured methane and tracer gas plumes shown as half-hour averages, as well as the simulated LES plume, also as half-hour averages.

The insets on the plots show half-hour means of measured and simulated wind direction and speed. The estimation of the unknown source was done with the mean over the whole measurement period of plumes and wind speed (red lines and dots on Fig. 6.11.12). Comparison of the flux of methane from the well with the simulated plume gives the source strength Q_{CH4} = 1.11 g s^{-1}.

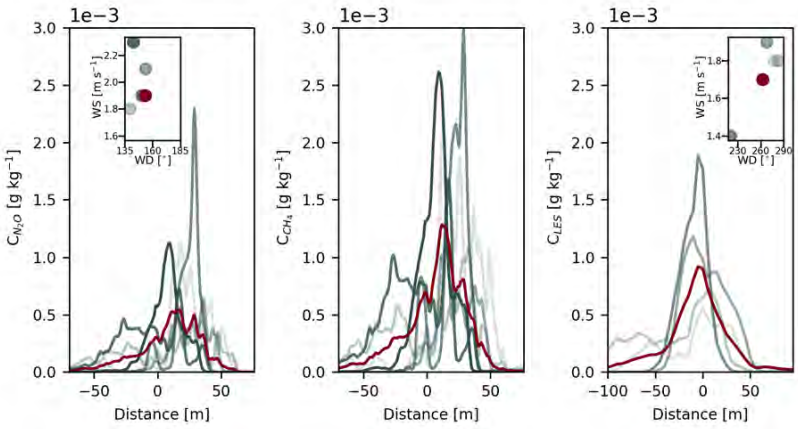

Fig. 6.11.12: Averages of instantaneous plumes over periods of half hour from (left) N_2O, (middle) CH_4 and (right) LES. LES transects were taken at 3 m height and 78 m downwind from the source. Plumes are shown with a color gradient corresponding to the half-hour increments i.e. lightest gray plume is the average of plumes measured in 11.30 - 12.00 UTC, dark grey is the average over 14.00 - 14.30 UTC. Inset shows horizontal wind speed and direction for the corresponding half-hour averages in (left) measurements and (right) LES. Overplotted in red is the average of all the plumes, as well as the averages of horizontal wind speed and direction in the insets.

Following the same principle, LES can be used to estimate the source strength of the tracer gas which results in Q_{tracer} = 0.53 g s^{-1} (the real flow rate was 0.59 g s^{-1}). To evaluate the performance of LES, the tracer gas was used to estimate the unknown source which resulted in Q_{CH4} = 1.23 g s^{-1}. The result show good agreement of LES predicted source strength with the measurements. Therefore it can be concluded that LES can be used as a proxy for the tracer gas for measurements when, for example, the source is unreachable.

Secondly, higher order statistical moments of the measured plume can be studied, which are not obtainable from the field data, but are from the simulated plume. First three statistical moments of the absolute plume were looked at, after which the dispersion processes were separated into relative dispersion and dispersion due to the plume meandering.

Generally, good agreement with the plume behaviour in previous LES studies was observed. Close to the source, the meandering is the driving dispersion mechanism and then at a certain distance from source relative dispersion becomes prevalent. The statistical moments are not shown here for the sake of brevity.

The distance at which the relative dispersion becomes the dominant mechanism can be estimated from the assumption that there exists a downwind distance on which the plume has spent enough time in "flight mode" to be mixed with the eddies of all sizes. That distance can be estimated from the mean horizontal wind speed $\bar{u}$, convective velocity scale w*, and the boundary layer height h_{BL} as

$$L = \frac{\bar{u} h_{BL}}{w*}. \quad (4)$$

All of the variables are available from the LES, and the mixing distance in this case is L = 1360 m. This can be also estimated from the plumes meandering ratio $M = \sigma_{meandering}/\sigma_{relative}$ (where σ is the plume width for the given mechanism) shown on Fig. 6.11.13.

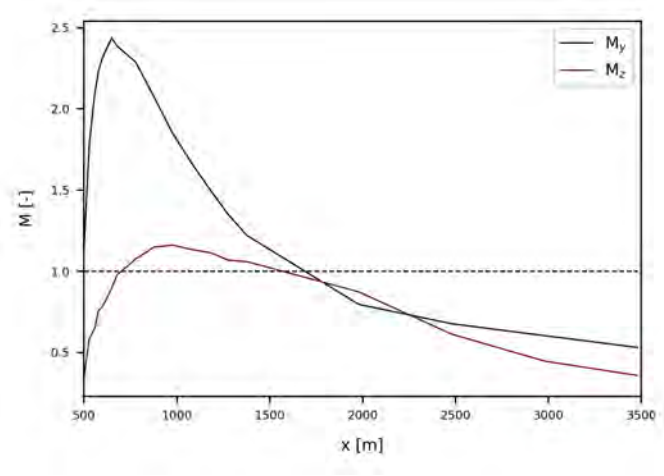

Fig. 6.11.13: Ratio of the relative and meandering component of the total plume width in y and z direction

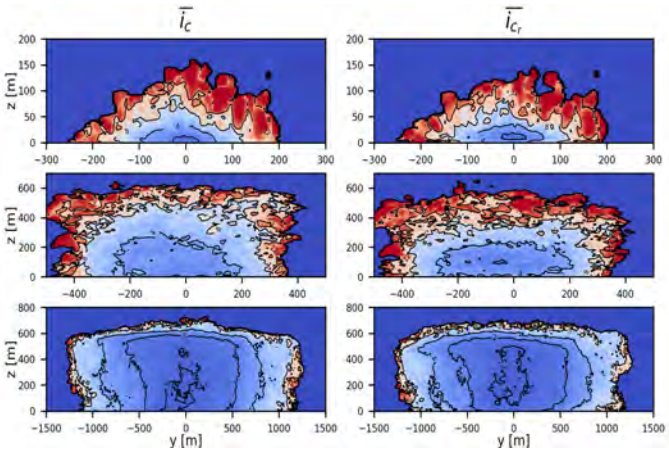

Fig. 6.11.14: Concentration fluctuation intensity in the mean y-z plume in absolute and relative coordinate systems. Distances from source are (top row) 78 m, (middle row) 600 m and (bottom) 1500 m.

When M < 1, then the relative dispersion becomes dominant and strong fluctuations of plumes centerline position die down. The M factor crosses the 1 line at approximately 1400 m from the source (positioned at x = 480 m).

Fluctuations of the simulated plume can be studied through the concentration fluctuation intensity parameter, which is a ratio of the mean plume concentrations, $\bar{c}$ and concentration fluctuations σ_c^2 at a given point. Fig. 6.11.14 gives y-z transect of concentration intensity of the absolute plume (relative and meandering contributions included) and relative plume (instantaneous plumes were centred according to their centres of mass before the statistics was taken). The figure shows highly fluctuating behaviour of the plume close to the source in both cases. For absolute dispersion this was an expected result, while for the relative this indicates that relative dispersion is an important mechanism even close to the source. From theory it is known that relative dispersion is driven by eddies ranging in size from Kolmogorov scale up to the size of the plume itself, which are small eddies close to the source for point sources. In the LES simulating true point sources is not possible due to resolution constraints so these results can be partially influenced by the initial spatial size of the source. Nevertheless, LES with realistic atmospheric conditions have proven to be a good tool for reproduction of conditions encountered in the field.

6.11.1.3 Future plans and expected results

- Paper on LES of measurement day in Romania, results of which are presented above, is close to submission.
- First paper on measurement strategies that was based on a DNS results (presented in the last reporting period) got rejected. It will be re-submitted with the same methodology but on LES data.
- Planned paper on capabilities of DNS to be used in dispersion studies. Comparison of plume and flow statistics from DNS, LES and wind channel experiment if data is available.
- Collaboration with Hossein and Thomas on possible simulation of measurements in Hamburg,
- Defense at the end of the year at the earliest.

6.11.1.4 Collaborations (internal / external)

TNO – Collaboration with Arjan Hensen and his group on data from the ROMEO campaign as presented

EMPA / Randulph – Collaboration with EMPAs student Randulph has started during his secondment to WUR on comparing dispersion in DNS and GRAL model he is using

Planned collaboration with Utrecht group on simulation of Hamburg emissions on street scale

6.11.1.5 Risks and difficulties

Apart the restrictions on travel and homeoffice because of the pandemic, the only possible problem is slower communication with supercomputer used for simulations.

6.11.2 Deliverables

Within the project ESR12 is involved in the deliverables D1.3, D1.4, D3.1, D3.2, D3.3, and D3.4.

D1.3 - Report and publication of the results from the campaign in Silesia (month 36)

Analysis of the measurement strategies in order to help planning of the measurement campaigns.

D1.4 - Report and public on improved emission factors for different source categories from mobile measurements (month 42)

Analysis of the measurement strategies in order to help planning of the measurement campaigns.

D3.1 - New tools to estimate CH_4 source strengths from point sources, including mobile measurements (month 24)

Approved

D3.2 - Improved bottom-up European CH_4 emissions (month 30)

- Simulation of the simplest test case to see the influence of the atmospheric variability
- Analysing two often used measurement techniques of local sources in order to achieve the highest accuracy of source estimations from the measurements.

D3.3 - Forward modelling simulations of CH_4 and isotopologues (month 30)

No contribution to this deliverable yet.

D3.4 - Top-down estimates of EU-scale CH_4 emissions (month 42)

No contribution to this deliverable yet.

6.11.3 Training and network activities

6.11.3.1 General training events

Event	Date (start – end)	Location (Host)	Objective / expected skills	ECTS points	Contribution	Comments
Memo² Gaussian plume workshop	9 – 10 October 2018	Heidelberg	Using Gaussian plume models in estimating source strength of methane	\	ESR helped with the DNS exercise	
SENSE A1 course	17 – 19 October 2018	Soest, the Netherlands	Introduction of the SENSE graduate school to the new PhDs	2	Poster presentation	

Teaching IA	March – May 2019	WUR	Transference of scientific knowledge	-	Teacher assistant	
Career Orientation	October 2019	WUR	Focus on future planning	1.3	Participant	
Teaching IA	March, April 2020	Wageninge n	Transference of knowledge	-	Teaching assistant	
Scientiific wriiting and presenting	20. 3. – 4. .4 2020.	Wageninge n	Improving results presenting skills	1.2	Partiicipant	

6.11.3.2 Secondments

Secondment	Date (start – end, planned (when))	Location	Host	Description of work / deviations	Scientific / training (skills) objective	Results and future plans
1st	**26/03/2018 – 27/04/2018**	**Dubendorf, the Switzerland**	Empa	Planning an OSSE. Looking at the measurements from the first MEMO² school.	Familiarizing with the GRAL dispersion model.	Plans to perform OSSE simulations have been made in order to evaluate performance of both MicroHH and GRAL models.
TNO	July – December 2020	online	Arjan Hensen	Combining DNS simulations with ROMEO measurements, work with TNO data	Interpret real field measurements using 3D simulated dispersion, Learning to deal with field measurements, which differ from model output data	Paper in pre-submission stage
WHIFFLE	Fall of 2020	Delft	Harm Jonker			

6.11.3.3 Conferences

Conference name	Date (start – end, planned (when))	Location	Presentation (oral / poster)	Title of presentation	Authors (main author + co-authors)	Public available (yes / no) / web link
EGU	8 – 13 April 2018	Vienna	Poster	Modeling methane dispersion using three modeling techniques to prepare a field campaign on methane emissions	Anja Ražnjević, Chiel van Heerwaarden , Maarten Krol	Abstract available https://meetingorganizer.copernicus.org/EGU2018/EGU2018-13940.pdf
ICOS	15 – 17 September 2020	Online	Oral	Comparison of large-eddy siimulation of a point source methane plume in a slightly coonvective atmosphere with measurements from MEMO² campaign	Anja Raznjevic, Chiel van Heerwaarden, Bart van Stratum, Arjan Hensen, Ilona Velzeboer, Pim van den Bulk, Maarten Krol	no

6.11.3.4 Measurement / sampling campaigns

ESR11 participated remotely in the ROMEO campaign by providing an evaluation strategy using DNS.

6.11.4 Dissemination activities (March 2017 – February 2019)

Dissemination activity	Name	Date	Location	Type of audience	Size of audience
MEMO² blog	Modeling dispersion of methane	07.11.2018	MEMO² website	scientific, industry, civil society, general public, media	100>

6.12 ESR12 - Inverse modelling of CH_4 and its isotopic composition at European and point source scales

ESR12

Inverse modelling of CH_4 and its isotopic composition at European and point source scales

ESR	Randulph Paulo Morales (randulph.morales@empa.ch)
Supervisor	Dominik Brunner (dominik.brunner@empa.ch)
Co-supervisor	Felix Vogel (felix.vogel@canada.ca)
Non-academic mentor	Arjan Hensen (hensen@ecn.nl)
Official start-end date	1.12.2017 – 31.01.2021

6.12.1 Scientific progress

6.12.1.1 Project introduction and objectives

Methane from facility-scale sources such as landfills and oil and gas production facilities are prone to leakage giving rise to highly uncertain emission flux estimates. To assess the overall impact of these sources, quantification from a representative set of individual sources – from which bottom-up inventories are generated – is necessary. This ESR project aims to improve or validate bottom-up emission inventories using high-resolution dispersion simulations of methane for the investigation of single sources. Moreover, a novel strategy of methane flux quantification with the use of unmanned aerial vehicle (UAV) equipped with a methane sensor is developed. The methods are evaluated in tracer release experiments with known emission rates and applied to quantify emissions from oil and gas wells in Romania as measured during the ROMEO campaign in October 2019.

6.12.1.2 Project results

6.12.1.2.1 Third year

6.12.1.2.1.1 High-resolution dispersion model

The most common approach in dealing with near-field dispersion of pollutants is the use of Gaussian plume models owing to their simplicity and computational efficiency. However, in many situations the underlying assumptions of Gaussian plume models such as stationarity, spatial uniformity, and absence of vertical shear in the flow are violated making their application prone to systematic errors.

In order to benchmark the performance of GRAL, a tracer gas simulation using a Gaussian plume model - formulated with a dispersion parameterization scheme based on the Monin-Obukhov Similarity Theory - was performed. Dispersion coefficients in the horizontal and vertical direction were prescribed by taking 5-minute averages of standard deviation of wind velocity fluctuations in crosswind horizontal and vertical direction. On the other hand, Lagrangian forward dispersion simulations were also conducted using GRAL by prescribing the location of the source and the evolution of the plume were followed within the modelling domain with no obstacles and no topography. Similar to the Gaussian plume simulation, the forcing for GRAL simulations were obtained by averaging locally observed meteorological data including, where available, turbulence parameters every 5 minutes.

Methane concentrations were extracted from the concentration field along certain perpendicular distances downwind of the source and comparison between the horizontal and vertical dispersion of the tracer within the modelling domain were compared (Fig. 6.12.1).

In this ideal case set-up, the source flux was set to 1.0 kg/hr released at a height of 60m above the ground, with a mean wind speed of 8.0 m/s blowing from the west. The atmosphere is under the neutral stability regime with Obukhov length at 1000m and friction velocity of 0.5 m/s. Crosswind horizontal

methane concentrations were extracted 100 meters downwind, and vertical concentration profile was taken at the center of the plume 100 meters downwind.

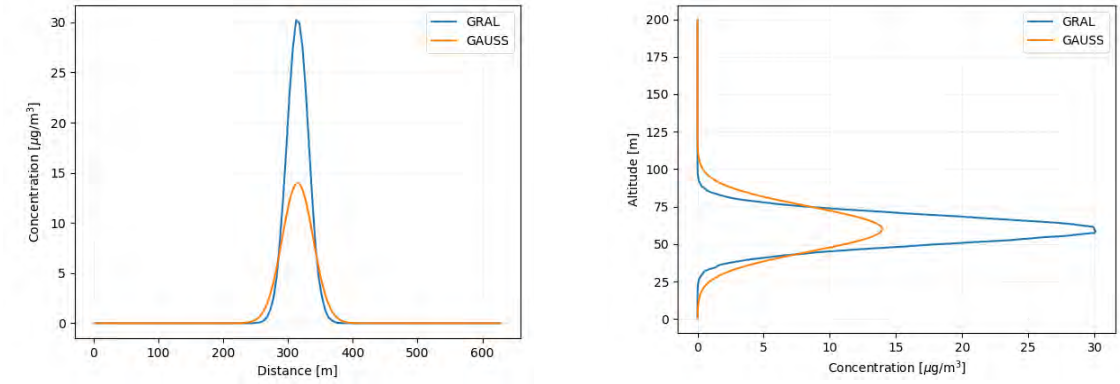

Fig. 6.12.1: Comparison of horizontal and vertical concentrations of methane 100 meters Gaussian plume dispersion model and GRAL model

To assess the performance of GRAL, a forward simulation is being set-up for a tracer release experiment conducted by the National Physical Laboratory (NPL) in the UK where methane molar fractions were measured at different downwind distances of the source (Fig. 6.12.2).

For the next reporting period, a sensitivity analysis to different modelling and measurement configurations will be discussed. More importantly, a demonstration of the suitability of GRAL to quantify methane emissions by combining it with mobile measurements will be presented.

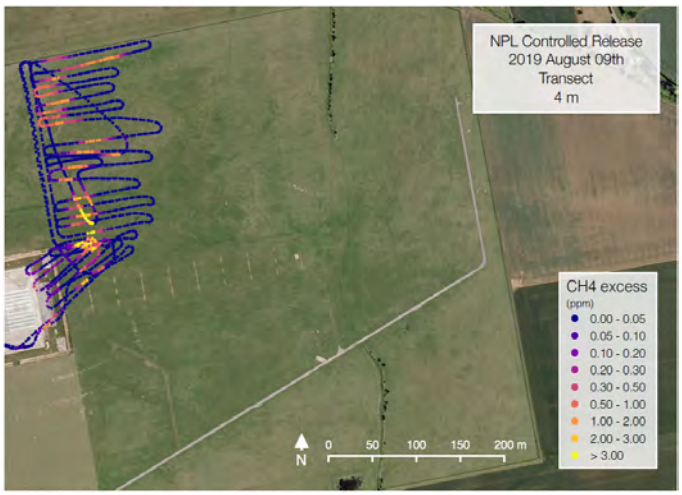

Fig. 6.12.2: Mobile CH_4 measurements at different downwind distances sampled at a height of 4 meters above the ground.

6.12.1.2.1.2 Quantification of methane emissions using Drone based sensors

Deploying unmanned aerial vehicles equipped with methane sensors is a very attractive method in investigating facility-scale methane sources as it allows complete mapping of the spatial and temporal variability of emission plumes within a short period, which are not attainable from conventional ground-based sensors.

We quantify methane emission fluxes from local sources by applying the mass balance method from drone-based QCLAS system measurements. The drone was flown downwind of a given source perpendicular to the main wind direction at different altitudes above ground, while geostatistical interpolation (Kriging) of the measured methane molar fractions was performed to spatially fill the gaps. The interpolated concentrations were multiplied by the cross-sectional area and the mean stream-wise wind profile obtained from a 3D sonic anemometer to get an emission flux.

Illustrated in Fig. 6.12.3 is an example of a flight measurement performed using this measurement set-up. In here, the UAV equipped with a methane sensor was flying 35 meters downwind of the source. Moreover, the plume was sampled at five different altitude, namely, 2.5, 5.0, 7.5, 10.0, and 12.5 meters above ground. Each sampling height was measured twice before moving on to the next height.

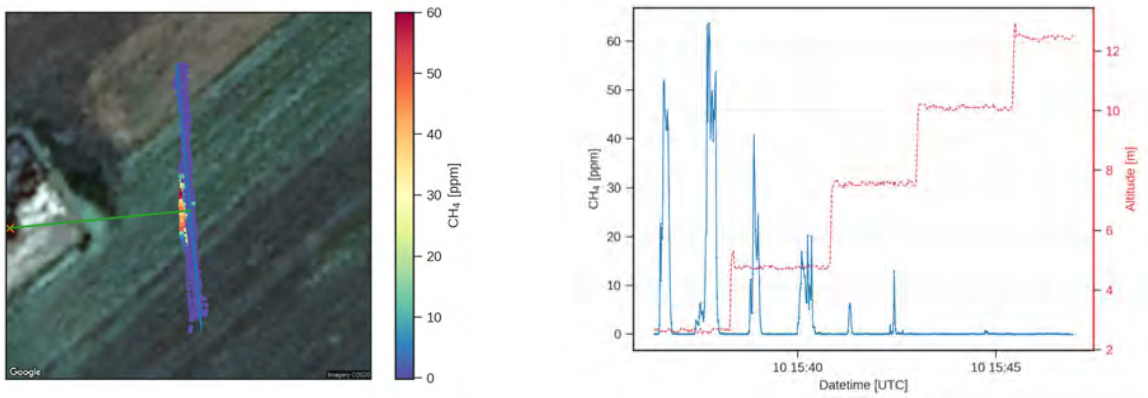

Fig. 6.12.3: Downwind sampling pattern for UAV equipped with methane sensors

Sampled measured molar fractions were then gridded in a single plane, and geostatistical interpolation (Kriging) was applied in the plane, as shown in Fig. 6.12.4, to spatially fill the gaps within the plane.

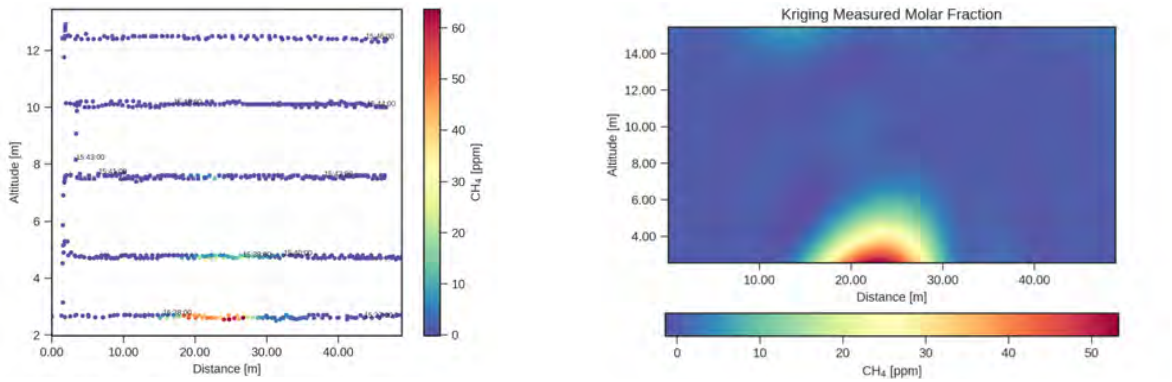

Fig. 6.12.4: Gridded measured methane molar fractions obtained from drone and spatially filled measured methane molar fractions using Kriging

After filling in the gaps, molar fractions were converted into concentrations, and the interpolated concentration field, in units of g/m^3, was multiplied to the cross-sectional area (m^2) and mean streamwise wind profile (m/s) obtained from the 3D sonic anemometer to get emission fluxes (g/s). In this particular example, the emission flux computed is 1.53 g/s. This methodology shall be applied to all applicable measurement sites during the campaign.

Further characterization of the mass balance approach is currently being done by performing controlled release experiments organized at Empa. Preliminary results from a tracer release performed in Dubendorf last October 2019 shows promising results from this quantification set-up. An artificial source from a natural gas bottle was placed in the middle of the field releasing 0.22 g CH_4/s. A mass balance quantification approach was done successively for three times, and emission estimates from the three flights are summarized below:

Table 6.12.1: Summary of emission estimates from three flights performed in a controlled release experiment.

	Flight 1	Flight 2	Flight 3	Mean and S.E.
Emission estimate (g/s)	0.325 ± 0.019	0.124 ± 0.049	0.167 ± 0.009	**0.194 ± 0.044**

During the next reporting period, a detailed discussion on the sensitivity of different measurement configurations, as well as, recommendations for optimal sampling and quantification strategy will be discussed.

6.12.1.2.1.3 Inverse simulations of CH_4 and its isotopologues at European Scale

Lagrangian Particle Dispersion Models (LPDMs) have been applied to atmospheric dispersion modelling in order to derive a time evolution of the concentration field of different pollutants. In an atmospheric setting, LPDMs rely on a pregenerated wind field obtained either from meteorological data or from an output of a separate Eulerian model. In this project, we will be using an LPDM called FLEXPART-COSMO.

FLEXPART-COSMO is a model version of FLEXPART, an offline LPDM, which allows the output of the mesoscale numerical weather prediction model COSMO as the driving meteorology. In this model version, all meteorological fields are preserved on the original COSMO vertical grid which, compared to other versions of FLEXPART, strongly reduces interpolation errors.

Continuous timeseries measurements of methane molar fraction as well as δ^{13}C-CH_4 and δD-CH_4 in ambient air at the Lutjewad station located in the Netherlands were simulated using FLEXPART-COSMO.

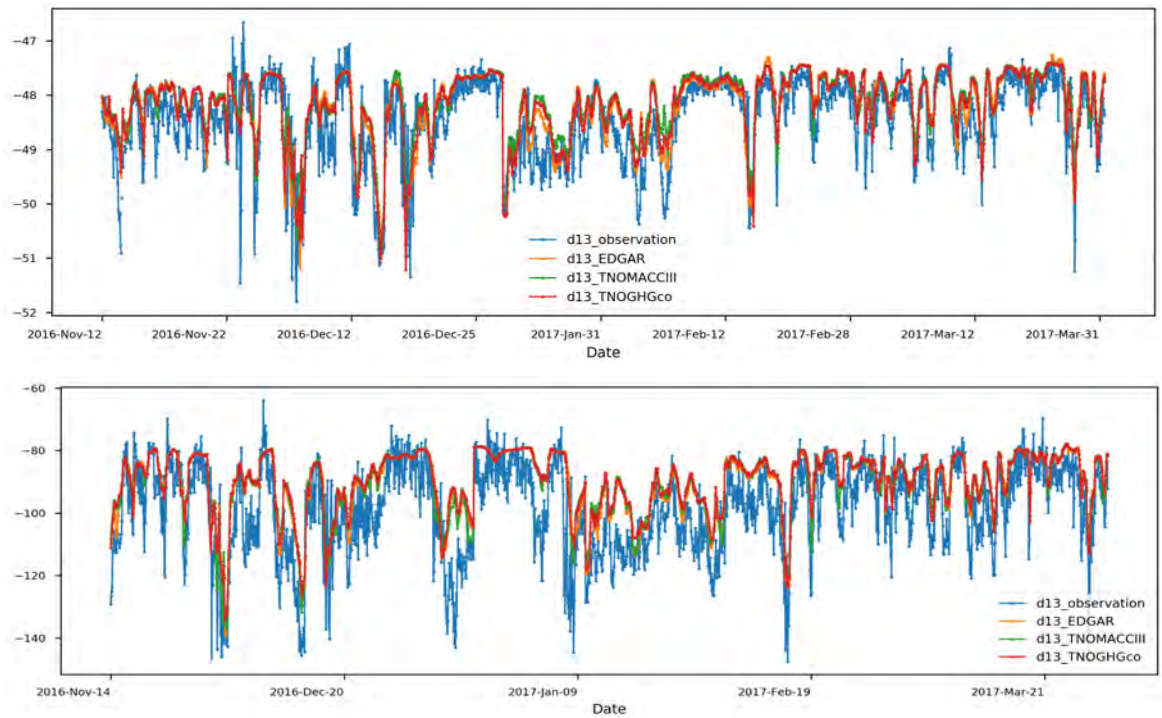

Fig. 6.12.5: Simulated isotopic composition of methane (δ^{13}C-CH4 and δD-CH_4) compared to observed values obtained from Lutjewad station in the Netherlands.

FLEXPART-COSMO was driven by hourly output of the operational COSMO-7 analyses of the Swiss weather service MeteoSwiss at a horizontal resolution of 7 km x 7 km and with 60 vertical levels. 50,000 Lagrangian particles (air parcels) were released from the location of the monitoring site (Lutjewad station) and its inlet at 60 m above surface every 3 hours and followed backwards in time over 4 days in order to derive sensitivity maps or footprints. Methane molar fractions at a specific time were then derived by multiplying the footprints with CH_4 emissions from a gridded emission inventory. Three different inventories were used, namely, the TNO greenhouse gas and co-emitted species emission database (TNO-GHGco) for the year 2015 with a horizontal resolution of approximately 6 km x 6 km, the EDGAR v4.3.2 for the year 2012 with a horizontal resolution of 0.1° x 0.1°, and the TNO monitoring atmospheric composition and climate III (TNO-MACC-III) for the year 2014 with a horizontal resolution of approximately 7 km x 7 km.

The δ^{13}C-CH_4 and δD-CH_4 timeseries were calculated by combining the simulated methane mole fractions for each source category with their respective isotopic signatures taken as one scalar per category based from previous literatures. Background isotopic signatures were obtained from 3-hourly simulations of δ^{13}C and δD using the LMDz model.

Simulation results from FLEXPART-COSMO compared with observed ambient methane isotopic composition is presented in Fig. 6.12.5. The figure shows a qualitative agreement between in-situ measurements of isotopic composition of methane in ambient air and simulated methane isotopic composition using FLEXPART-COSMO. The agreement between the measured and simulated values is a proof-of-concept that continuous high-resolution isotopic data is applicable to constrain source type information on a regional scale better.

6.12.1.2.2 Fourth year

The work during the reporting period Mar 2020 – Feb 2021 focused on the development and application of mass balance methods applied to methane measurements from a drone. An extensive tracer release experiment was organized in Dübendorf, Switzerland from 23 Feb to 14 Mar 2020 to develop, optimize, and evaluate the quantification method. The experiment also involved ESR2 to compare the measurements from the fast in-situ drone analyzer of Empa with the AirCore-system of the University of Groningen. In addition, the source quantifications from the drone were compared for selected cases with results from stationary measurements applying the OTM 33 method as carried out by ESR1. The refined mass balance method was then applied to the drone measurements collected during the ROMEO campaign in 2019 to quantify emissions from individual oil and gas wells in Romania. In the following sections, we provide an overview of the tracer release experiment, an evaluation of the drone-based emission quantifications against the known true release rates, a comparison between measurements from Empa's laser-based sensor with the AirCore system, a comparison with OTM 33 quantifications, and a summary of Empa's drone-based quantifications during ROMEO.

6.12.1.2.2.1 Overview of tracer release experiment

The release experiment was performed in Dübendorf, Switzerland where methane, in the form of natural gas, was released from a bottle at a constant rate. The field is a seasonal crop land with an access road north of the farm mainly used by pedestrians and bicycles.

A dirt road cuts through the middle of the farm and leads to a small concrete platform intended for small tractors. The location is relatively flat, but is shielded by a forested hill in the south. The whole experiment was performed from 23 February to 14 March 2020 with a total of 9 days of active measurements.

The selection of active days was mainly based on favorable weather conditions, i.e. days with no precipitation and with sufficient but not too strong winds. Local wind speeds during the selected days ranged from 1 - 7 ms^{-1}. A total of 35 quantification flights were performed during the whole campaign, of which 18 were suitable for quantification while the rest were discarded mainly due to technical problems with either the drone, one of the analyzers, the tracer release, or the GPS system. A sample quantification flight is presented in Fig. 6.12.6.

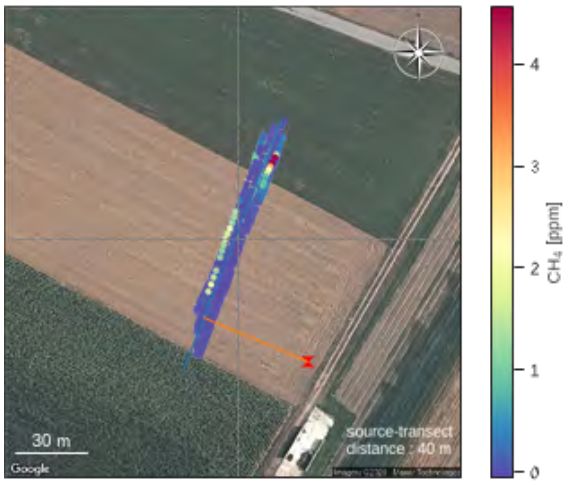

Fig. 6.12.6: Measured methane molar fraction during DüREx with flight code 314_02. The x mark indicates the location of the artificial source, and the source-transect distance is computed as the perpendicular distance between the source and the measurement plane. Meteorology conditions is measured by a 3D sonic anemometer and is located next to the source.

Alongside the drone flights, a second quantification method, called OTM33A, based on stationary measurements with an independent methane analyzer was applied on the first three days of the campaign for comparison. In order to avoid any possible bias in the data processing towards the real tracer release, two of the releases were conducted as blind experiments, where a third-party person released methane at a rate not known to the researchers.

An artificial methane source, in the form of natural gas, was released from a single point during the campaign. Natural gas from a 50 L high-pressure (100 bars) cylinder was directed through a 100 m long tubing to the release point. The end of the tubing was attached to a platform at about 1.5 m above surface. A *Contrec red-y series* mass flow controller (MFC) calibrated for methane up to 100 L/min at normal conditions (i.e., 273.15 K and 101.325 kPa) was used to regulate the releases. A summary of the release rates during the experiment is given in Table 6.12.2. At the start of each measurement day, a suitable location of the release was determined based on prevailing winds. Meteorological conditions were measured using 3D and/or 2.5D anemometers, which were usually placed next to the release point of the source.

Fig. 6.12.7: Lightweight and precise QCLAS developed by Empa, active AirCore developed by RUG, and an accurate RTK-GPS system mounted on the drone system (Matrice 600 DJI)

During controlled-release experiments, we have flown the in-situ Quantum Cascade Laser Absorption Spectrometer (QCLAS) sensor and the active AirCore system together in one integrated system mounted beneath a hexacopter (Matrice 600, DJI) as illustrated in Fig. 6.12.7. The total weight of the system is 13 kg, of which the payload is around 3 kg, and has a total maximum flight time of 20 minutes.

The in-situ airborne sensor, developed in-house, is a compact and lightweight mid-IR laser absorption spectrometer capable of providing real-time atmospheric methane molar fractions measurements at 1 s time resolution. It is highly precise and can achieve a precision (1σ) of 1.1 ppb at 1 s and 0.1 ppb at 100 s averaging time under ideal conditions.

Real-time synchronization between the instrument and a local computer on the ground is made possible by a wireless bi-directional data link that allows real-time access to raw spectral data and all hardware parameters and enables the operator to do real-time spectral fitting and logging and to have full control of the hardware whilst continuously monitoring the status of the instrument.

The active AirCore, designed for airborne sampling, consists of a 50 m thin-wall stainless-steel tubing, a dryer, a micropump, and a data logger. The whole system is enclosed in a carbon fiber box. Similar to the in-situ QCLAS system, the active AirCore system has a light and compact footprint making it suitable for deployment on relatively small commercial drones.

Prior to each quantification flight, the active AirCore is flushed with a calibrated fill gas, spiked with 10 ppm CO, in order to identify the starting point of ambient air sampling. Shortly before the integrated drone system takes off, the micropump is turned on to sample ambient air and as soon as the quantification flight is finished, the pump is turned off to stop sampling ambient air. The active AirCore samples are then immediately analyzed on the ground with a trace gas analyzer (CRDS, Picarro, Inc., CA, USA, model G2401).

Table 6.12.2: Summary of successful measurement flights during DüREx

Date	Flight Code	Release rate [gs^{-1}]	Downwind [m]	Mean WS [ms^{-1}]	Mean WD [° from N]	Stability	Instrument Present
23-Feb	223_01	0.48 ± 0.04	42	4.98 ± 1.41	277 ± 18	N	O, Q
24-Feb	224_01	0.29 ± 0.03	94	5.21 ± 1.61	283 ± 15	N	O, Q
	225_01	0.29 ± 0.03	50	4.53 ± 1.25	304 ± 11	N	A, O, Q
	225_02	0.29 ± 0.03	48	5.68 ± 1.18	304 ± 14	N	A, O, Q
	225_03	0.29 ± 0.03	45	6.08 ± 1.49	304 ± 12	N	A, O, Q
8-Mar	308_02	0.26 ± 0.02	40	1.69 ± 0.76	271 ± 19	U	A, Q
9-Mar	309_01	0.29 ± 0.03	18	2.61 ± 1.31	284 ± 28	N	A, Q
309_02	309_02	0.29 ± 0.03	31	2.65 ± 1.06	284 ± 28	N	A, Q, R
12-Mar	312_01	0.31 ± 0.03	46	3.49 ± 0.83	312 ± 11	N	A, Q, R
	312_03	0.39 ± 0.03	77	3.55 ± 0.71	306 ± 13	N	A, Q, R
13-Mar	313_01	blind	51	3.29 ± 0.97	284 ± 18	U	A, Q, R
	313_02	blind	50	2.88 ± 1.03	282 ± 16	U	A, Q, R
	313_03	0.46 ± 0.04	129	2.34 ± 1.07	257 ± 32	U	A, Q, R
	313_04	0.48 ± 0.04	136	2.63 ± 0.82	282 ± 46	U	A, Q, R
	313_05	0.52 ± 0.05	102	2.15 ± 0.71	280 ± 46	U	A, Q, R
14-Mar	314_01	0.26 ± 0.02	40	0.72 ± 0.33	111 ± 39	U	A, Q, R
	314_02	0.44 ± 0.04	40	0.51 ± 0.22	180 ± 44	U	A, Q, R
	314_03	0.68 ± 0.03	44	0.63 ± 0.27	154 ± 37	U	A, Q, R

O: OTM33A, Q: QCLAS, A: AirCore, R: RTK-GPS

6.12.1.2.2.2 Evaluation of drone-based emission quantifications with QCLAS system

This chapter is an update of the results shown above (6.12.1.2.1.2).

An emerging and attractive approach to quantify emissions from diffusive and leaky sources involves deploying integrated unmanned-aerial-vehicle (UAV) systems capable of measuring methane molar fraction in the atmosphere. The advantages of UAVs are that they are cheap, versatile and easy to deploy. The most common ways of measuring methane from UAVs are: 1) collection of ambient air samples using on-board storage equipment and subsequently analyzing the sample, 2) live analysis of air samples pumping air into long tube connected to a ground-based analyzer, and 3) in-situ reporting of measurements using an analyzer mounted on the drone. Deployment of UAV allows transecting the plume over its entire vertical and horizontal extent, potentially transecting the plume multiple times, which is not possible with car-based or stationary measurements on the ground, which can only sample a small portion of the plume.

We quantify methane emission fluxes from local sources by applying the mass balance method from the drone-based QCLAS system measurements. The drone was flown downwind of a given source perpendicular to the main wind direction at multiple altitudes above ground. Refined geostatistical interpolation (Kriging), accounting for different spatial scales of CH_4 variation of the measured background and enhancements of methane molar fractions was performed to spatially fill the gaps. The interpolated concentrations were multiplied by the cross-sectional area and the mean wind component perpendicular to the measurement plane obtained from a 3D sonic anemometer to get an emission flux.

We have developed a cluster-kriging interpolation algorithm for the in-situ QCLAS measurement. A figure illustrating the process of mapping discreet data points into the whole measurement plane is presented in Fig. 6.12.8. The obtained timeseries was fed into a Gaussian Mixture Model (GMM) to partition the dataset into two clusters with distinctly different spatial correlation length scales, namely, the relatively smooth background and the elevated cluster representing the spatially confined plume signals. The GMM returns the membership probability of a data point belonging to one cluster or the other, as shown in Fig. 6.12.8b.

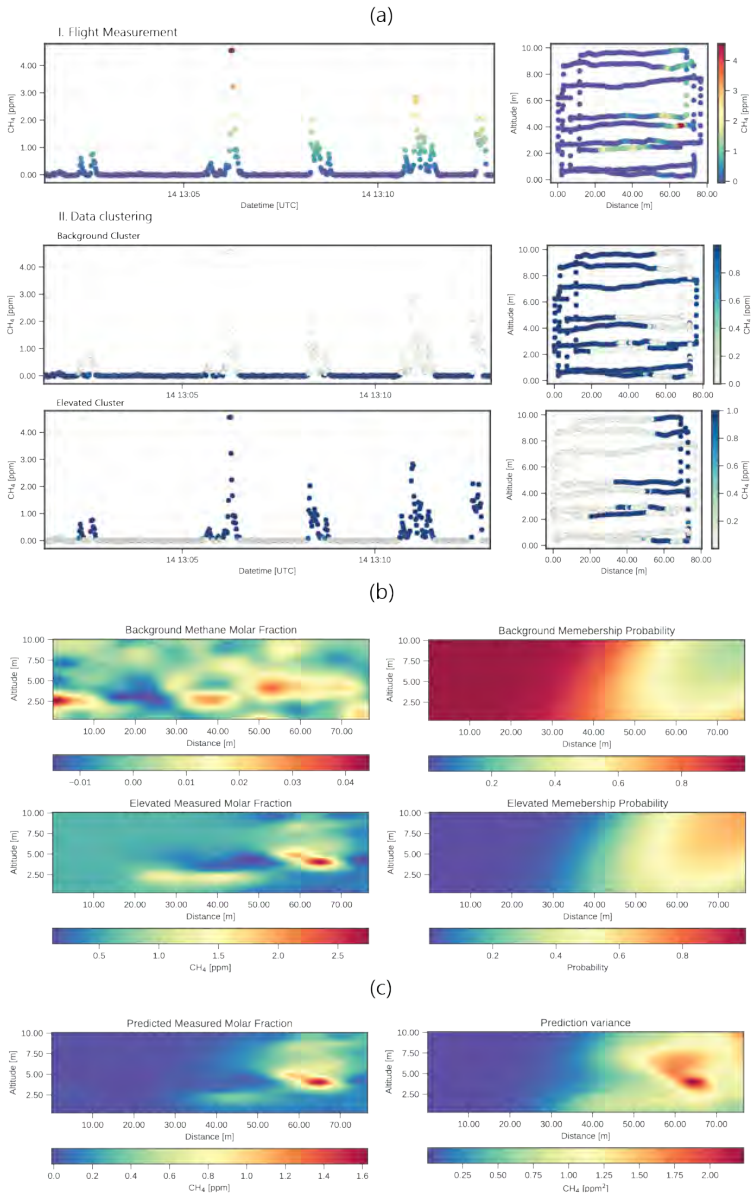

Fig. 6.12.8: (a) I Timeseries and clustering result for DüREx:314_02 after applying GMM with two mixture components. The background and elevated cluster complement each other. The total probability of each data point shared between the two clusters is equal to one. (b) Kriging prediction and membership probabilities of each spatial point within the domain of interest for background and elevated clusters. (c) Expected value and variance of methane molar fractions after combining kriging prediction of the two clusters and their respective membership probabilities

The membership probability of each data point is expanded to the whole domain, and the membership probability at an unobserved location is computed and shown in Fig. 6.12.8c. Optimizing an adequate kriging model for each cluster was performed thereafter, and hyperparameters for each cluster were determined using log-marginal-likelihood (LML) minimization. Optimized hyper-parameters for each cluster were used as input for the kriging model in order to interpolate the values at unobserved locations.

The kriging results for each cluster were combined with their respective membership probability. The resulting kriging field is illustrated in Fig. 6.12.8c where the expected value and variance is computed. The average atmospheric methane mass density during the measurement flight was used to convert the obtained kriging field of methane molar fraction [ppm] into concentrations [gm^{-3}].

Two different treatments for the in-situ QCLAS methane measurements and three different treatments for the wind measurements were applied to all the measurement flights during DüREx.

For the in-situ QCLAS measurements - aside from using cluster-kriging - we have also used ordinary-kriging where obtained methane measurements were not clustered before kriging interpolation.

The three-different treatment for wind data includes: (1) Projecting second-averages of meteorological parameters onto the measurement plane and spatially interpolating the wind field using kriging. (2) Taking the mean normal component of the wind vector. (3) Construction of a theoretical logarithmic wind profile based on the turbulence parameters (i.e. friction velocity and Obukhov length) obtained during the whole duration of the quantification flight.

Combining two in-situ QCLAS methane data treatment (i.e. cluster- and ordinary-kriging) and three wind data treatment (i.e. projection onto measurement plane, mean normal component, and logarithmic profile construction), we have six approaches in quantifying methane emissions.

Measurements from 18 sets of flights were compared to the true release rates to characterize the accuracy of the quantification method. A summary of estimated emission rates using different approaches is summarized in Fig. 6.12.9. Among all the quantification methods applied to all the flights, the best performing approach, characterized by the lowest RMSE compared to other approaches, was obtained by applying the Cluster-Kriging Projected-Wind (CK-PW), where methane measurements were clustered before kriging, and where the normal component of the wind measurements were projected onto the position of the drone. On average, emission estimates obtained using the CK-PW approach tends to underestimate the true-release by 5.10 % with a mean absolute error of 54.7 %. We observed that the worst approach in estimating emissions is by using Ordinary-Kriging Logarithmic-Wind (OK-LW) approach to the dataset. This approach has a mean absolute error of 91.5 % and generally overestimates the true-release by 37.72 %.

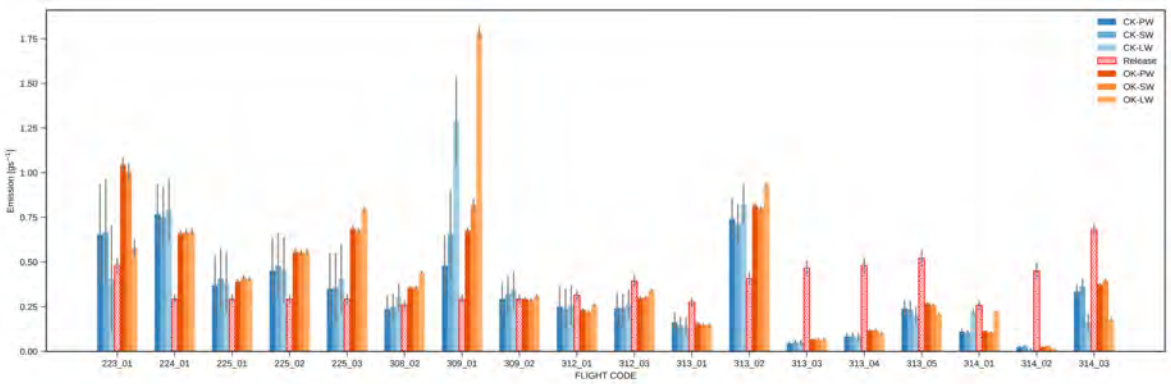

Fig. 6.12.9: Summary of emission estimates using different approaches. CK and OK stands for Cluster-Kriging and Ordinary-Kriging, respectively. PW, SW, and LW refers to the different wind data treatments. PW stands for projected wind, SW for scalar wind, and LW for logarithmic wind.

We have observed a systematic underestimation of emission rates during the last two days of the experiment, specifically for the last six flights (313_03-05- to 314_01-03). In order to analyze the reasons for this underestimation, we compared the predicted kriging fields with a theoretical Gaussian plume dispersion model, in order to test whether the vertical and horizontal distance flown by the drone was sufficient to capture the whole plume. The comparison with the size of the theoretical Gaussian plume suggests that although we managed to detect methane elevations, we were most likely not able to capture the whole extent of the plume during these flights. The reason is that some of these flights were conducted at a rather large distance from the source and under low wind conditions, during which the plume spreads more quickly with downwind distance. For flights 313_03-05, for example, the horizontal and vertical width of the Gaussian plume computed for the meteorological conditions and downwind distance of the flight were on average 75 m and 20 m, respectively. However, the typical cross-sectional plane covered by the drone was of the order of 100 m x 12 m, which is insufficient to fully capture a spread of the calculated plume, especially with respect to the vertical extent.

The average horizontal and vertical spread of the Gaussian plume with respect to windspeed and downwind distance is illustrated in Fig. 6.12.10. The sharp edges in the figure are due to the fact, that the dispersion of the Gaussian plume model depends on stability class, which in turn depends among other factors on wind speed.

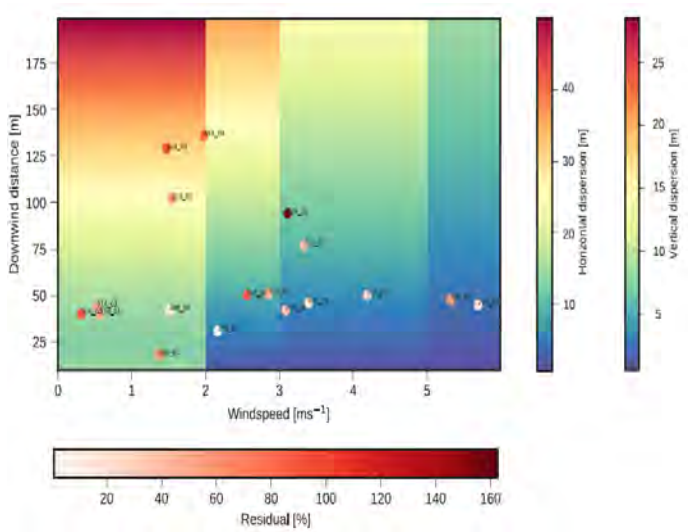

Fig. 6.12.10: Theoretical horizontal and vertical spread of a plume with respect to windspeed and downwind distance. White to red dots refersto the accuracy of each measurement flight.

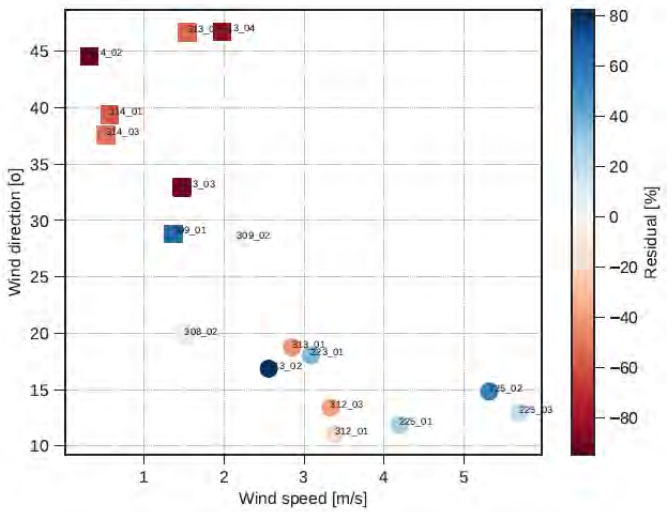

Fig. 6.12.11: Residual plot between true-release rate and estimated-release with respect to wind speed and directional variability. represents the flights that are well within the wind threshold whereas signifies otherwise.

Overlayed are dots ranging from white to red representing the performance of each quantification flight. It can be seen that flights with the highest accuracy are the ones that fall within the blueish region characterized by windspeeds greater than 2 ms^{-1} and a sampling downwind distance between 10 and 75 m. Quantification flights within this region had a higher accuracy mainly because the horizontal and vertical spread of the plume were below 10 m and 5m, respectively, which is a realistic range for the drone to completely map the plume.

Similar to our study, Yang et. al. (2018) performed a rasterized mass balance approach to quantify emissions from individual gas wells in Texas using UAVs. Based on their results, they proposed a minimum threshold of windspeed of 2.3 m s^{-1} and wind direction variability not greater than 33.1° in order to quantify emissions with an accuracy of better than 50 %. Applying the same threshold criteria and additionally restricting the measurements to a maximum downwind distance of a 75 m, we have identified 8 out of 18 flights from our campaign to satisfy these criteria. For these flights, a better mean accuracy of 40 % was obtained (compared to 54.7 % for all flights). Computed emission rates were on average slightly overestimated by 0.06 g s^{-1}, which corresponds to a relative overestimation of 14 %. In contrast, a lower average accuracy was observed when measurement flights were done when the wind is not steady and highly variable. Computed emission rates under these wind conditions were generally underestimated by 21 % with an average error of 66 %.

6.12.1.2.2.3 Comparison between drone measurements from QCLAS and AirCore

A timeseries obtained by simultaneously flying the in-situ QCLAS and the active AirCore is illustrated in Fig. 6.12.12. Methane molar fractions measured using the fast-response QCLAS analyzer are characterized by sharp and instantaneous elevations, whereas methane elevations from the AirCore are rather smooth. Instantaneous methane plumes usually did not have a Gaussian shape but rather showed complex structures with small patches of elevated concentrations due the chaotic nature of turbulence.

These sharp concentration gradients were captured by the fast-response QCLAS system but were significantly smeared out by the AirCore system, which has a much slower response due to mixing in the sampling tube and later in the Picarro analyzer.

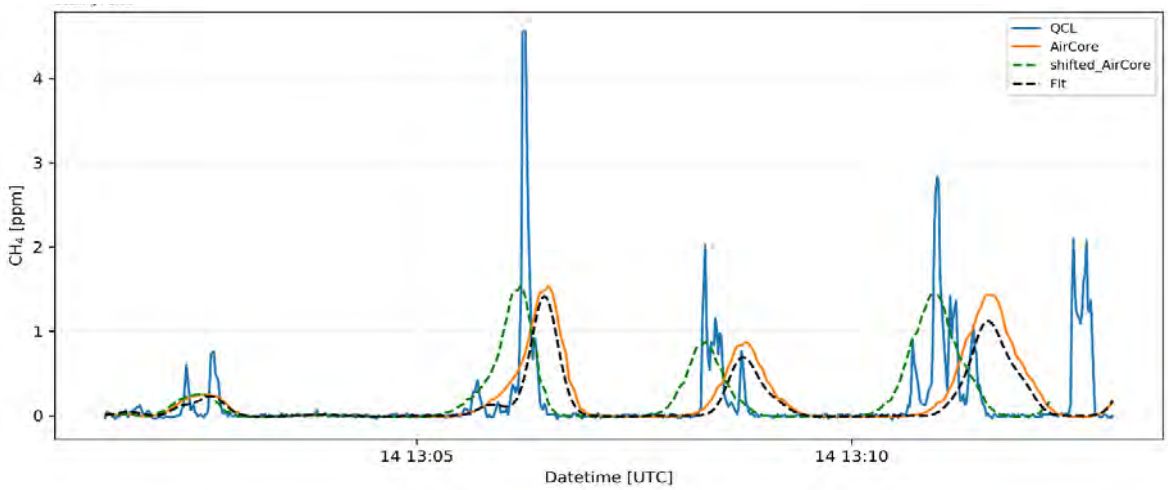

Fig. 6.12.12: Timeseries obtained by simultaneously flying the active AirCore system and the in-situ QCLAS.

To determine the magnitude of the smoothing present in the AirCore measurements, we flew the two instruments simultaneously while measuring the same point source downwind. To mimic the measurements from the AirCore, the QCLAS measurements were transformed using a smoothing, shifting, and stretching (3S) algorithm. The smoothing, shifting and time-stretching parameters were obtained through a non-linear fit to the measurements from the AirCore. On average, we found that AirCore measurements were smoothened by an average of 20 s (1σ) using a Gaussian smoothing function when compared with the QCLAS instrument. Other than smoothing, we also observed that AirCore measurements are temporally shifted and that this shift increases linearly with time at an average rate of 0.07 seconds per second. The smoothing and time-stretching parameters obtained for the individual flights are presented in Table 6.12.3.

Table 6.12.3: Calculated timeshift and smoothing of an AirCore sample as compared to in-situ QCLAS measurements

Flight Code	Shifting rate [QCLAS(s)/AirCore(s)]	Smoothing window [s]
312_01	0.05	20.78
312_03	0.06	23.63
313_03	0.06	19.90
313_04	0.07	18.93
314_01	0.08	18.25
314_02	0.07	17.45
314_04	0.08	18.76
	0.07±0.01	19.67±2.05

Knowing the proper time delay and smoothing of an AirCore sample is essential for a correct localization of the AirCore measurements during the flights. In cases where the time delay and smoothing are not sufficiently well known, the size and location of the plume might not be captured accurately. As an example, a reconstructed plume without applying proper correction is shown in Fig. 6.12.13a. The figure shows the presence of two different plumes, one mid-height and another at the top of the measurement plane. After applying the proper correction (Fig. 6.12.13b), the two plumes collapse into a single plume. We have observed that the emission estimate computed using the corrected timeseries is 30 % higher than the emission estimate computed without applying a correction. Accounting for the time shift of the AirCore data is thus critical when performing a mass-balance quantification approach.

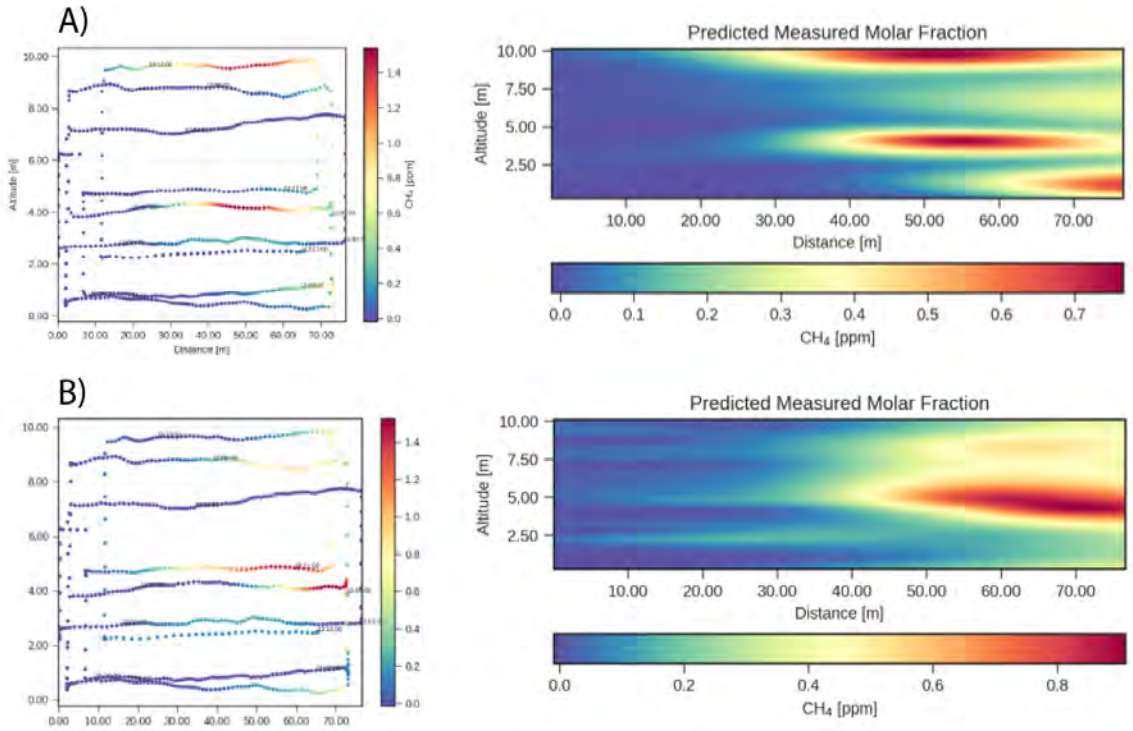

Fig. 6.12.13: Reconstructed methane plume of flight 314_02 using Cluster-based Kriging. A) Reconstructed plume from an AirCore without applying time correction. B) Reconstructed plume from an AirCore after applying time correction.

6.12.1.2.2.4 Comparison of emission estimates using QCLAS and OTM33A

Other Test Methods (OTM) 33A quantification technique were performed, alongside mass-balance quantification flights, during the first three days of the controlled-release experiment. OTM 33A was introduced by U.S. EPA (2014) to quantify emissions of operating natural gas sites emittig at / near ground level without having the need to access the site. This method has been characterized using numerous controlled-release experiments and was eventually used to quantify emissions for oil and gas plants in the US. As our drone-integrated system was used in ROMEO, a large campaign studying the oil and gas emissions in Romania, we have chosen to compare our quantification approach with this quantification technique.

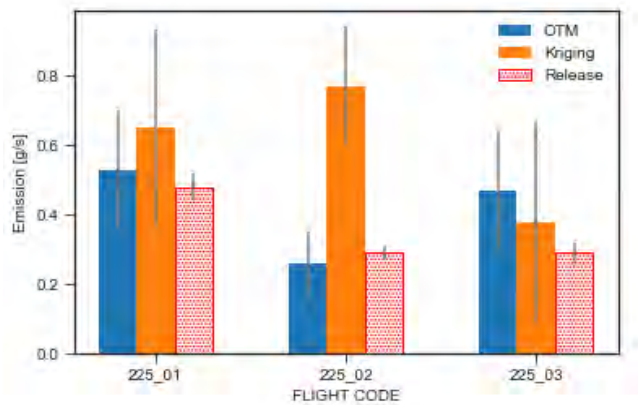

Fig. 6.12.14: Emission bar graph showing the estimated releases using two different quantification techniques and its performance in capturing true emissions.

Quantified releases using OTM33A and our mass-balance approach are presented in Fig. 6.12.14. Although the number of simultaneous quantifications from the drone and with the OTM 33A approach is limited, the results show that both approaches are close to the true-release and that the method uncertainty of both methods usually capture the true-release. This showcases that our quantification technique has a great potential and is at par in measuring methane emissions from oil and gas wells when compared with existing quantification approach, such as OTM33A.

6.12.1.2.2.5 Drone-based emission quantifications during ROMEO

The drone-integrated system was deployed in ROMEO (Romanian Methane Emissions from Oil and Gas) campaign last October 2019 where we performed 41 mass-balance quantification flights spread over 26 sites. We have applied the cluster-kriging projected wind approach (CKPW) in estimating emissions of oil and gas wells. A summary of emission estimates from every investigated site using the in-situ QCLAS presented in Fig. 6.12.15a. Estimated emissions using the AirCore system, completely independent from our system, is also presented in Fig. 6.12.15b.

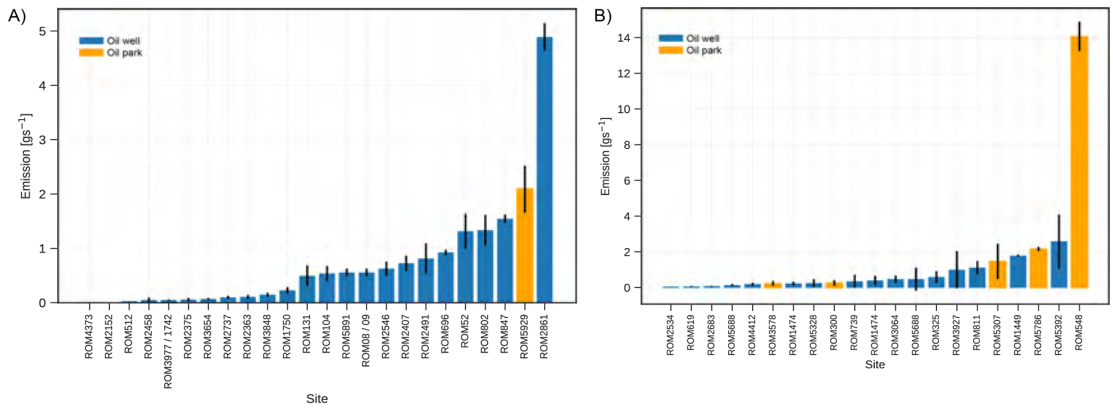

Fig. 6.12.15: Estimated emission rates from oil and gas wells of visited sites in Romania. Reported uncertainty is the standard deviation (1σ) of multiple quantified emissions per site (N>=2) and estimated uncertainty of individual flight (N=1) A) Empa B) Groningen University

We classified obtained emission rates based on the type of facility (i.e., oil-park and oil-well) and fitted a density distribution for estimated emissions from oil-wells, shown in Fig.6.12.16. From the density plot, we have observed a good agreement between computed emissions using the QCLAS and the AirCore even though the two systems were operated independently from one another during the campaign. The average emission of investigated oil wells in Romania using our in-situ QCLAS is 0.66 g s^{-1} with a median of 0.50 g s^{-1}, whereas average emissions obtained using the AirCore system is 0.62 g s^{-1} with a median of 0.39 g s^{-1}. Since most of the quantification flights performed by Empa and Groningen University are biased to high-emitting sites, our quantification suggests that emissions of Romanian oil wells of this type are within the range computed. Continuous efforts to combine all quantification estimates from different ground-based measurement techniques performed during ROMEO is currently being done and we will be supporting further processing and analysis of the data in order to provide a robust bottom-up estimate of oil and gas emissions in Romania.

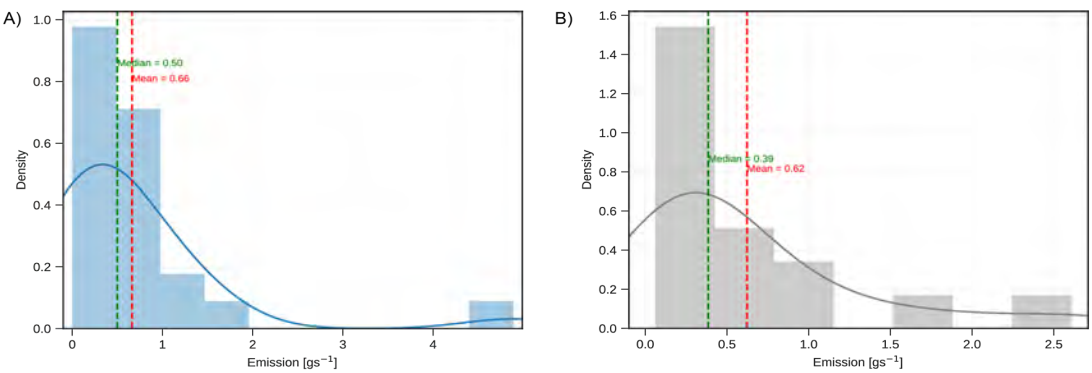

Fig. 6.12.16: Fitted density distribution curve for emission estimates from oil wells using A) Empa's QCLAS and B) Groningen University's AirCore

6.12.1.3 Future plans and expected results

Proposed publications before the end of the project are as follows:

1. *Quantifying localized methane source emissions from mobile sensors using an obstacle-resolving Lagrangian dispersion model*
2. *Estimating local methane sources from drone-based laser spectrometer measurements by mass-balance method*

The date of the PhD defense has not been finalized, but is planned to take place before the end of 2021.

6.12.1.4 Collaborations (internal / external)

The ESR collaborated with WUR to assess the GRAL's performance with respect to MicroHH. This was done during a secondment.

Further was a joint control release experiment conducted (February – March 2020) together with three partner organizations within the network.

Quantification results from the ROMEO campaign were already submitted and we will support the writing of the overview paper discussing the quantification of methane emissions from oil and gas-wells from Romania using different ground-based quantification techniques.

6.12.1.5 Risks and difficulties

No administrative problems or difficulties have occurred within the reporting period.

6.12.2 Deliverables

D1.3 - Report/publication on CH_4 emissions from wetland and lakes in Sweden (month 30)

No significant progress has been made for this deliverable

D3.1 - New tools to estimate CH_4 source strengths from point sources, including mobile measurements (month 24)

Approved – Implementation of tools ongoing

The GRAL dispersion model has been set-up flexibly to simulate methane sources on simple and complex model configurations. Sensitivity of the model set-up to different measurement configuration is currently being against mobile measurements taken during the duration of the campaign

Quantification of methane emissions from local sources using drone-based measurements by applying a refined Kriging algorithm, which accounts for different spatial scales of methane variation in the background and the plume.

D3.2 - Improved bottom-up European CH_4 emissions (month 30)

Mobile measurements from vehicles and drones taken during the whole duration of the project is currently being processed using different tools and a distribution function for each source category will be generated and compared / incorporated to existing bottom-up estimates.

D3.3 - Forward modelling simulations of CH_4 and isotopologues (month 36)

Approved – implementation of modelling simulations ongoing

Inverse simulations using FLEXPART-COSMO were run to obtain methane molar fractions for the site in Lutjewad in the Netherlands. The simulation period covers November 2016-March 2017, and was compared to a continuous timeseries measurements of methane molar fractions obtained for the same period.

Simulated molar fractions were grouped for different source categories, and by associating each source category to a respective isotopic signature taken from literature. The isotopic composition of ambient CH_4 was calculated.

D3.4 - Top-down estimates of EU-scale CH_4 emissions (month 42)

Top-down CH_4 emission estimates for whole Europe for the years 2005-2017 have been produced in the framework of the VERIFY project using FLEXPART-IFS and is currently being adapted on inversions with FLEXPART-COSMO.

6.12.3 Training and network activities

6.12.3.1 General training events

Event	Date (start – end)	Location (Host)	Objective / expected skills	ECTS points	Contribution	Comments
MEMO2 Winter School	5-16 February 2018	Schoorl, Netherlands	Lectures on atmospheric modelling specifically on modelling methane species using large eddy simulations. Lectures on the fundamental of atmospheric physics and chemistry, atmospheric isotopes, and methane measurement techniques Practical lectures on methane measurements	6	Participation in classes, Poster presentatiions, and modelling exercises	
Tropospheric Chemistry	Spring Semester 2018	ETH Zurich, Switzerland	Aims to provide an overview on tropospheric chemistry, which includes laboratory studies and numerical modelling. The focus of the course covers the sources and sinks of aerosols and oxidants at different scales.	3	Participation in classes as well as written exercise and oral exam	
Basic German A1.1	Spring Semester 2018	University of Zurich, Switzerland	Aims to teach students how to communicate in German at a basic level.	2	Participation in classes with written and oral exercises	
Basic German A1.2	Summer School 2018	University of Zurich, Switzerland	Continuation of the course basic German A1.1 which aims to teach students how to communicate in German at a conversational level.	1	Participation in classes with written and oral exercises	
Reproducibility in Computational Sciences	9-13 September (Summer School)	École polytechnique fédérale de Lausanne, Switzerland	Introduced the best practices and tools for reproducing research in computational sciences. Strategies on data management as well as maintenance of code and software were discussed in the session.	1	Participation in classes, computational exercises, and oral presentation	
MEMO2 Isotope Workshop	17-19 September 2018	Royal Holloway, University of London, UK	Aims to introduce the fundamental knowledge of methane isotopologues and its significance in the apportionment of methane ources and sinks in the atmosphere.		Participation in classes and data analysis	
MEMO2 Modelling Workshop	9-10 October 2018	Institut fuer Umweltphysik, Universitaet Heidelberg, Germany	Aims to introduce the different type of models whic are typically used in the field of atmospheric sciences. Different models ranging from a high resolution small scale simulations up to regional scale models were discussed during the workshop.		Participation, computational exercises, and presentation	
Boundary Layer Meteorology	Fall Semester 2018	ETH Zurich, Switzerland	The aim of the course is to acquire basic knowledge on atmospheric turbulence. It offers theoretical as well as practical approaches to treat atmospheric boundary layer flows.	4	Participation in classes. Written exercises, and oral examination	
Boundary Layer Meteorolgy	21.09.2020 – 23.12.2020	ETH Zurich	ESR gained basic knowledge on atmospheric turbulence and theoretical as well as practical approaches to treat Planetary Boundary Layer flows. ESR gained familiarity with the relevant processes (turbulent transport, forcing) within, and typical states of the Planetary Boundary Layer.	3	Participated in the lecture	

6.12.3.2 Secondments

Secondment	Date (start – end, planned (when))	Location	Host	Description of work / deviations	Scientific / training (skills) objective	Results and future plans
	29.10.2018-23.11.2018	Paris, France	LSCE-UVSQ	The work of the ESR during the duration of his secondment is divided into 2 main tasks. The	The objective of the first task is to be able to compare measured CH_4 peaks with a local source	Future plans include the application of GRAL model in all the measurement

				firs one is to be able to set-up GRAL model for a wastewater treatment plant in Paris. The secondment is to be able to be able to set-up FLEXPART=COSMO simulations	scale model such as GRAL. The second task is to be able to do an inter-comparison between PYVAR-CHIMERE model and FLEXPART-COSMO	campaigns made by ESR3. A joint publication with ESR 13 about the results of comparing the two models has also been planned.
Point Source Scale Modelling	10.11.2019 – 07.12.2019	Wageningen, Netherlands	WUR	Benchmarking of GRAL with respect to MicroHH	Learn how atmospheric DNS models work, and how it compares to existing models	Simulations under different will be run using GRAL and MicroHH and comparion between the two shall be done

6.12.3.3 Conferences

Conference name	Date (start – end, planned (when))	Location	Presentation (oral / poster)	Title of presentation	Authors (main author + co-authors)	Public available (yes / no) / web link
NCGG Conference	12-14.06.2019	Amsterdam, the Netherlands	oral	Quantifying localized methane source emissions from mobile sensors using an obstacle-resolving Lagrangian dispersion model	Randulph Morales, Lukas Emmenegger, Dominik Brunner	
EGU 2020	4-8.05.2020	Austria (Virtual)	PICO	Estimating local methane sources from drone-based laser spectrometer measurements by mass-balance method	Randulph Morales, Jonas Ravelid, Killian Brennan, Bela Tuzson, Lukas Emmenegger, and Dominik Brunner	
ICOS Science Conference	15-17.09.2020	Sweden (Virtual)	Oral	Cluster-based Ordinary Kriging for estimating local methane sources from drone based laser spectrometer. measurements	Randulph Morales, Jonas Ravelid, Béla Tuzson, Lukas Emmenegger, and Dominik Brunner	
Empa PhD Symposium 2020	30.11.2020	Switzerland (Virtual)	Poster	Quantification of methane emissions from local sources using drone-based laser spectrometer measurements	Randulph Morales, Jonas Ravelid, Béla Tuzson, Lukas Emmenegger, and Dominik Brunner	

6.12.3.4 Measurement / sampling campaigns

Campaign	Date (start – end, planned (when))	Location	Host	Description of work	Scientific objective	Samples (nature / number)	Results and future plans
ROMEO	01 – 20.10.2019	Romania		Measurement of oil and gas wells using drones equipped with methane sensor	Quantification of methane emissions from drone-based measurements using a mass balance approach	35 flights	
DUREX	17.2 – 15.3.2020	Stettbach		Control release experiment	Characterization of the mass balance approach	35 flights	

6.12.4 Dissemination activities

Scientific publications

Type of scientific	Title of scientific publication	DOI	ISSN or eSSN	Authors	Title of journal or equivalent	Number of journal, mont	Publisher	Place of publication	Year of publication	Relevant pages	Public/ private publication	Peer review	Open access

publication						h and year of publication					[yes/no]	[yes/no]	[yes/no],
Abstract in conference proceedings	Estimating local methane sources from drone-based laser spectrometer measurements by mass-balance method	doi.org/10.5194/egusphere-egu2020-14778		Randulph Morales, Jonas Ravelid, Killian Brennan, Bela Tuzson, Lukas Emmenegger, and Dominik Brunner	EGU Assembly 2020				2020			Yes	Yes
Article in journal	Three-dimensional radiative transfer effects on airborne, satellite and ground-based trace gas remote sensing			Marc Schwaerzel, Claudia Emde, Domnik Brunner, Randulph Morales, Alexis Berne, Brigitte Buchmann, Gerrit Kuhlman	Atmospheric Measurement Techniques				2020			Yes	Yes
Article in journal	Characterisation of methane sources in Lutjewad, the Netherlands, using long-term isotopic composition measurements			Malika Menoud, Carina van der Veen, Bert Scheeren, Huilin Chen, Barbara Szenasi, Randulph Morales, Isabelle Pison, Philippe Bousquet, Dominik Brunner, Thomas Roeckmann	Tellus B: Chemical and Physical Meteorology				2020			Yes	Yes
Article in journal	A compact QCL spectrometer for mobile, high-precision methane sensing aboard drones			Bela Tuzson, Manuel Graf, Jonas Ravelid, Philipp Scheidegger, Andr	Atmospheric Measurement Technique Discussions				2020			Yes	Yes

6.13 ESR13 - Atmospheric monitoring of the CH_4 emissions at the European scale

ESR13

Atmospheric monitoring of the CH_4 emissions at the European scale

ESR	Barbara Szénási, barbara.szenasi@lsce.ipsl.fr
Supervisor	Philippe Bousquet, philippe.bousquet@lsce.ipsl.fr
Co-supervisor	Maarten Krol, maarten.krol@wur.nl
Non-academic mentor	Renato Winkler, rwinkler@picarro.com, Magdalena Hofmann, mhofmann@picarro.com
Official start-end date	01.10.2017 – 30.09.2020

6.13.1 Scientific progress

6.13.1.1 Project introduction and objectives

This project aims at improving our understanding of CH_4 emissions at the European scale by addressing various sources of uncertainties. We explore the potential of emission uncertainty reduction by top-down atmospheric inversions of methane emissions. Atmospheric inversions make it possible to obtain top-down emissions which represent the best knowledge, including the information from both bottom-up emission inventories and atmospheric measurements. Through three studies, we focus on different sources of uncertainties that must be specified in atmospheric inversions. In the first study, we use several bottom-up anthropogenic emission inventories of CH_4 to simulate the atmospheric mixing ratio of CH_4 over Europe. The simulations are used for estimating errors for atmospheric inversions of CH_4 emissions over Europe. The second study targets other possible causes for misfits between measured and simulated atmospheric CH_4 mixing ratios, as well as isotopic ratios $\delta^{13}C$ and $\delta^{2}H$. This work demonstrates that information gained from isotopic measurements within MEMO^2, in addition to measurements of CH_4 mixing ratios, can be valuable for evaluating emission inventories and estimating emissions by atmospheric inversions.

The potential of $\delta^{13}C$ and $\delta^{2}H$ measurements in atmospheric inversions is investigated by determining the instrument precision needed to detect signals $\delta^{13}C$ and $\delta^{2}H$ from various CH_4 sources. This is examined at the location of monitoring sites in the Integrated Carbon Observation System (ICOS) network. Our results indicate high precision requirements on instruments measuring $\delta^{13}C$ and $\delta^{2}H$. However, they reveal that isotopic information, on top of mixing ratios, could improve discrimination of CH_4 sources when implemented in atmospheric inversions of CH_4 emissions. This project offers insights into how inversion frameworks could be configured and what the essentials are to reliably estimate CH_4 emissions at the European scale.

6.13.1.2 Project results

6.13.1.2.1 Third year

6.13.1.2.1 Simulations using the atmospheric transport model CHIMERE

Simulations of CH_4 mixing ratios have been performed at the European scale with the CHIMERE chemistry transport model (CTM) using annual anthropogenic emissions from the EDGAR version 4.3.2, TNO-MACC_III and ECLIPSE V_5a emission inventories from the years, respectively, 2011, 2011 and 2010. Simulations have been carried out for 2015 with a horizontal resolution of 0.5° x 0.5° (~50x50 km) using the meteorology of ECMWF and the boundary and initial conditions of the MACC product (Marécal et al., 2015) as the reference simulations. Table 6.13.1 lists all the simulations used in this reporting period.

Table 6.13.1: Simulation set-ups of the CTM CHIMERE used in this report period

Horizontal resolution	0.5° x 0.5°	0.25° x 0.25°	0.5° x 0.25°	0.1° x 0.1°
Simulated year	2015	2015	2015	2016-2017
Boundary condition	LMDz & MACC	MACC	MACC	MACC
Emission inventory	EDGARv4.3.2 & TNO-MACC_III & ECLIPSE_V5a	EDGARv4.3.2 & TNO-MACC_III & ECLIPSE_V5a	EDGARv4.3.2 & TNO-MACC_III & ECLIPSE_V5a	EDGARv4.3.2 & TNO-MACC_III
Emission sector	Total & sectoral CH_4	Total & sectoral CH_4	Total & sectoral CH_4	Total & sectoral CH_4
Type of emission	Anthropogenic & Wetland	Anthropogenic	Anthropogenic	Anthropogenic & Wetland

6.13.1.2.2 Error estimation for atmospheric inversions of CH_4 over Europe

We follow the method of Wang et al. (2017) to obtain estimates for errors which must be considered in atmospheric inversions of CH_4 emissions in Europe. With the previously described set of simulations (Table 6.13.1), we estimate the following errors:

- Representation error ε_{repr}: error of a model not perfectly representing the measured values due to the difference between a grid cell in the model and the actual scale at which a measurement is representative. Simulations with a horizontal resolution of 0.25° x 0.25° were compared to the reference simulations to obtain this error.
- Boundary condition error ε_{LBC}: the background error associated with the lateral boundary conditions (LBCs), due to the choice of the lateral (sides and top of the domain) and initial conditions. Simulations performed using another set of boundary conditions (made by Bousquet et al. (2006) with the Laboratoire de Météorologie Dynamique (LMDz) model) were compared to the reference simulations to obtain this error.
- Transport error ε_{transp}: error that is due to discretisations with sub-grid scale parametrisations and other approximations of the fundamental equations of the atmospheric transport used in a model. Simulations with a horizontal resolution of 0.5° x 0.25° were compared to the simulations of the CTM LOTOS-EUROS (Manders et al., 2017) to obtain this error.
- Emission induced error ε_b: error that is due to the misrepresentation of emissions on the spatial and temporal grid of the model. Simulations made with the emissions of the three inventories were compared to each other to obtain this error.

The above-mentioned errors are computed from afternoon values (12h and 18h UTC included), either in all the grid cells of the European domain or at the locations of the 31 measurement sites which could be used for the inversion of fluxes (i.e. site providing hourly measurements of CH_4 atmospheric mixing ratios for at least six months in 2015). Since the horizontal resolutions used for the simulations are coarser than the scale at which CH_4 emission patterns actually vary, steep gradients of concentrations induced by steep gradients of emissions encountered in certain types of activity sectors (e.g. waste) cannot be well represented. Therefore, the representation error and the transport error may be underestimated close to hot-spots and large emitting areas. Even though these are key-regions in which a reduction of uncertainties on emissions brought by the inversions would be very useful, our quick study shows that observations near these areas should be used with caution with our horizontal resolutions (Fig. 6.13.1). The emission induced error ε_b is a reference error that indicates how an inversion framework should be built. To evaluate whether an atmospheric inversion is relevant to tackle an issue about CH_4 fluxes, we compare the magnitudes and structures of all the other errors to the emission induced error. Several strategies are available for obtaining meaningful top-down flux estimates:

- the emission induced error dominates all other types of error: most inversion set-ups are able to bring information on the fluxes
- some errors are the same magnitude as the emission induced error: the inversion framework is able to make use of the available observations to optimize fluxes but may lead to inconclusive results

some errors are large compared to the emission induced error: it may be possible to control the sources of these errors alongside the CH_4 fluxes. For instance, regional inversions classically include LBCs in their control vector to avoid impacting emission estimates by biases of the LBCs. Otherwise, the inversion is not relevant for the problem of interest.

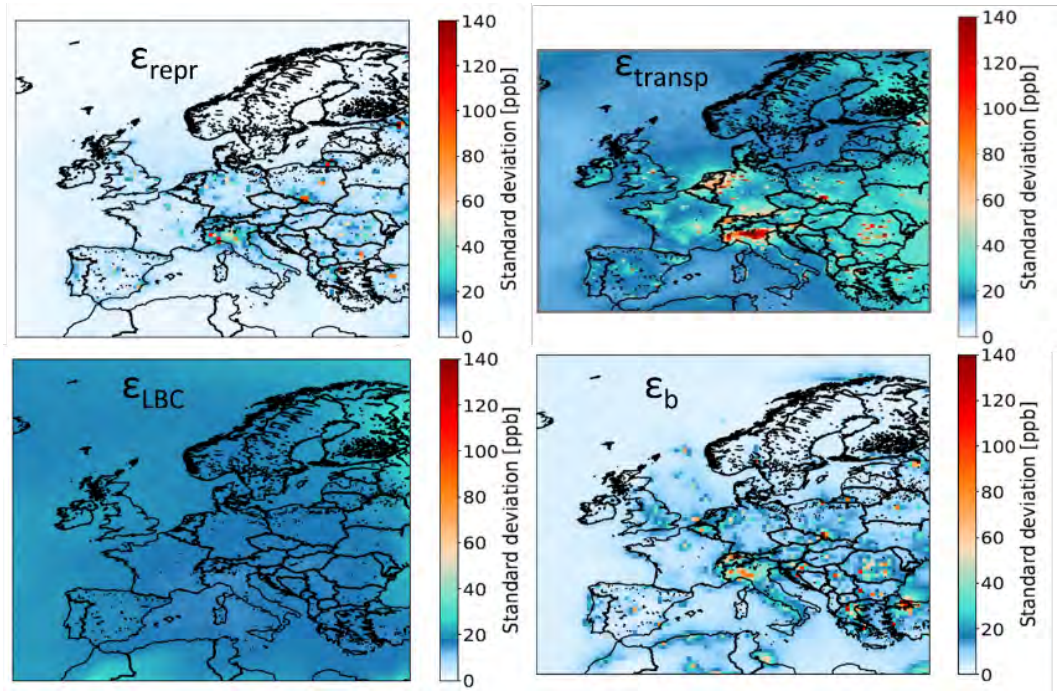

Fig. 6.13.1: Annual mean standard deviation of the estimated errors over the European domain for 2015

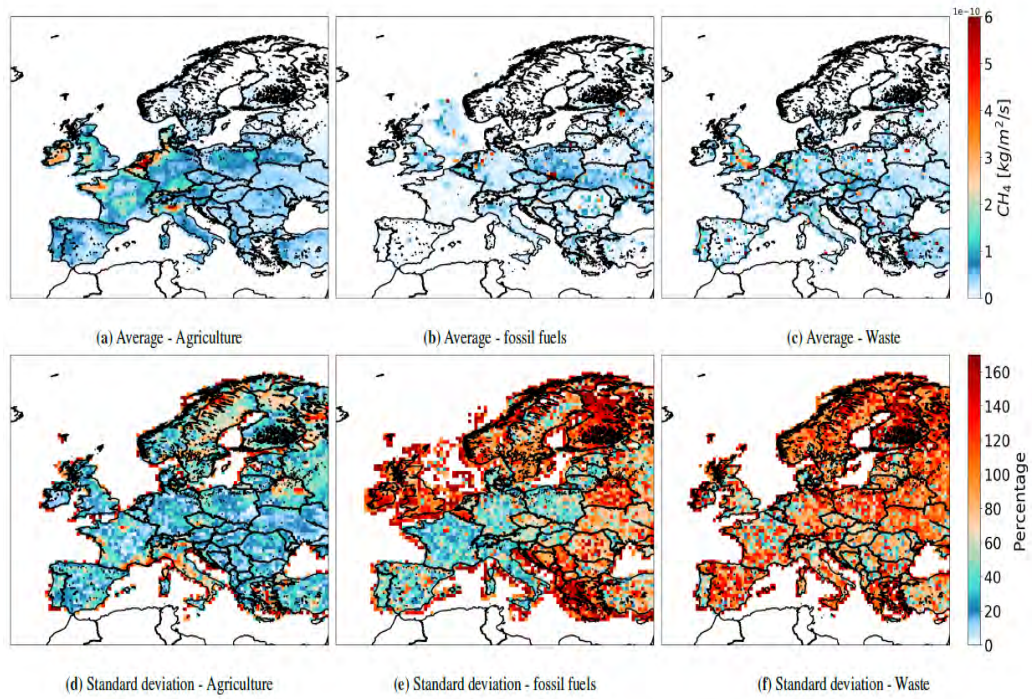

Fig. 6.13.2: Average (a-c) and standard deviation (d-f) of yearly emissions of the TNO-MACC_III, EDGARv4.3.2 and ECLIPSE V5a anthropogenic inventories in the main emission sectors of CH_4

In Fig. 6.13.2, the relative magnitudes of the representation, the transport and the boundary condition errors are compared to the emission induced error. It indicates that the representation error can be treated in the inversion with the observation error statistics whereas the sources of the transport and the boundary condition errors may better be controlled alongside the emission fluxes in the inversion. Including LBCs in the control vector is usually done in regional inversions, but optimising the transport at the same time as emissions remains challenging in most state-of-the-art inversion systems.

To gain some insights on the prior knowledge on CH_4 emissions, we also look into the prior error, which is the error in the inventories, particularly due to the spatial distribution of the emissions at the sectoral scale. It includes the errors due to the projection of the inventories on the model's grid. We find that the emissions in the inventories differ most in the waste and fossil fuel related emission sectors with about 49 % over the whole European domain (see Fig. 6.13.3). The agriculture sector is the most certain sector with only 23 % uncertainty over Europe. Some high emitting areas or hot-spots are not represented consistently, i.e. their locations and/or emissions are not in agreement in the three inventories. Discrepancies also arise from the projection of emissions onto the model's grid along the coasts, which may impact specifically the inversion of data from coastal measurement sites. All cases where emission gradients between two neighbouring types of land-use are steep will lead to such an issue.

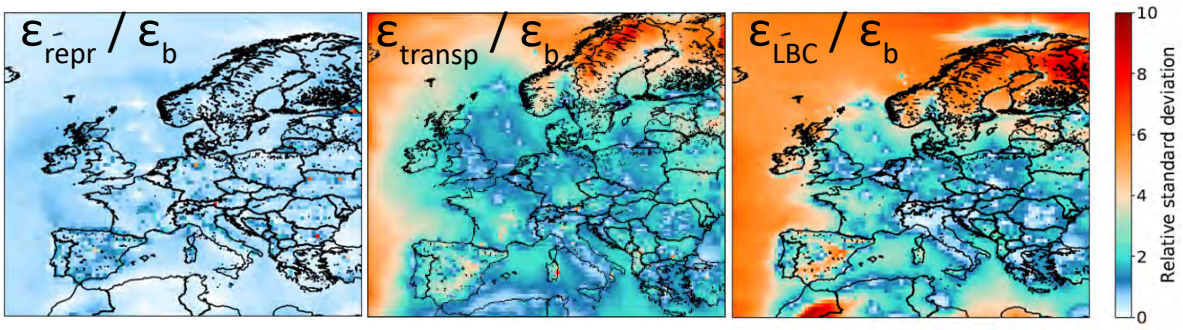

Fig. 6.13.3: Annual mean of the standard deviation of the errors relative to the emission induced error over the European domain for 2015

6.13.1.2.3 Analysis of simulated isotopic signatures

Isotopologues are useful to discriminate sector contributions of CH_4 emissions as the isotopic composition varies highly depending on the source type. For instance, the signature is different depending on whether CH_4 is produced by thermogenic (e.g. natural gas), biogenic (e.g. domestic animals, landfills, wetlands) or pyrogenic (combustion) sources. The comparison between measured and simulated CH_4 mixing ratios and isotopic composition can be used for evaluating flux measurement methods and other data gained from measurements, such as isotopic source signatures or emissions estimated from measurements. Simulations allow a broad investigation of the magnitude, the sectoral and spatial distribution of atmospheric CH_4 mixing ratios, and how the simulated mixing ratios depend on emissions. The aim of this task is to study how the various CH_4 sources, with different isotopic signatures, in different areas and environments in Europe, such as the regional or city scale, blend into larger-scale concentration fields.

Forward simulations of atmospheric CH_4 mixing ratios and isotopes have been carried out for the period between November 2016 and March 2017 at the European scale and at the city-scale.

As CHIMERE is not set up to simulate isotopic composition, we computed the ^{13}C and ^{12}C (D and H), as well as the atmospheric isotopic ratios of $\delta^{13}C$ (δD), from the sectoral forward simulations of CH_4.

Sectoral simulated CH_4 mixing ratios and signatures of $\delta^{13}C$ and δD obtained from various literature sources were used as input to determine the simulated $\delta^{13}C$ and δD ratios through the following steps (shown for $\delta^{13}C$ only, analogue for δD):

1) Obtain sectoral ^{13}C and ^{12}C: $\frac{^{13}C}{^{12}C} = \left(\frac{\delta^{13}C}{1000‰} + 1\right) * PDB_{std} * CH_4$

2) Sum the sectoral ^{13}C and ^{12}C to get the totals

3) Compute modelled $\delta^{13}C$: $\delta^{13}C = \left(\frac{13C/12C}{PDB_{std}} - 1\right) * 1000$

For the background, the simulations of $\delta^{13}C$ and δD made by the LMDz model by Thanwerdas et al. (2019) were used as input signatures.

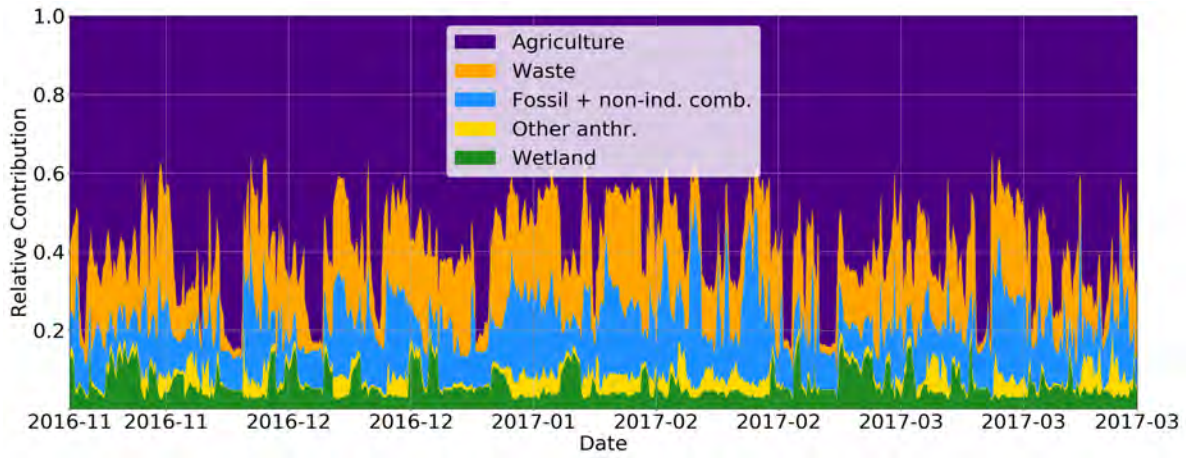

Fig. 6.13.4: Sectoral discrimination of CH_4 mixing ratios above background at Lutjewad. The emissions from TNO-MACC_III were used to simulate the sectoral contributions of CH_4 by CHIMERE that are shown in this figure. Only the results for TNO-MACC are shown as the results for EDGAR are very similar.

Simulated CH_4 total mixing ratios and isotopic ratios of $\delta^{13}C$ and δD have been compared to measurements provided by the MEMO² partners at Lutjewad (NL) and isotopic ratios of $\delta^{13}C$ at Heidelberg (DE). The CHIMERE model is able to represent the average isotopic signature and to capture the temporal variability of the measured ratios. The performances of the models have been evaluated with the aid of the Pearson correlation (Pearson, 1895) and the RMSE (root mean square error) (Armstrong and Collopy, 1992). Generally, the simulated isotopic compositions are well correlated, i.e. $R^2 \geq 0.55$, to the measurements and the RMSE of 0.5-0.8 shows a good agreement of the simulated signatures to the measured ones.

The simulations enable us to explore the sectoral contributions: Fig. 6.13.4 shows the results of the sectoral discrimination at Lutjewad. For this figure, we took the simulated CH_4 mixing ratios from the anthropogenic and wetland emission sources, as well as the total CH_4 mixing ratios without the background into account. The background here is neglected as we are interested in the sectoral contributions above the background. We compared the contribution of each emission sector to the total contribution in relative terms, which showed that 40-60 % of the simulated mixing ratios above the background is due to the agriculture sector.

The combination of the isotopic signatures of the source sectors is important for the computation of the total $\delta^{13}C$ and δD so that the sensitivity analyses explore the impact of the change in the input source signatures (decrease by 10 %) and the relative contribution of the source sectors (increase by 20 %). The comparison of simulated signatures to measured signatures combined with the sensitivity analyses shows that the background CH_4 in the model is underestimated which causes an overall underestimation of the measured CH_4 mixing ratios by the model.

Furthermore, the simulated total $\delta^{13}C$ and δD time series compare better to the measured ones when the simulated background $\delta^{13}C$ and δD by LMDz is decreased by 0.4 ‰ and increased by 8 ‰, respectively.

Fig. 6.13.5 a) shows that the increase of the relative contribution of the biogenic sources (agriculture, waste, wetland) by 20 % (exception: background increased by 2 %) improves the fit between the simulation outputs and the measurements. The improvement is defined by a lower RMSE and a higher correlation between simulation outputs and measurements, and a standard deviation of the simulation output that is closer to that of the measurements. This improvement due to the increase of the relative contribution of CH_4 mixing ratios of the biogenic sources is connected to the fact that their signatures are lower than that of other sources, making the total $\delta^{13}C$ and δD more depleted. In another sensitivity analyses (Fig. 6.13.5 b)), the simulated isotopic ratios compared to the measured ones improved when decreasing the input signatures of all source sectors used for the simulations by 10 % (exception: background not included in this analysis). This is due to the measured CH_4 mixing ratios being underestimated by the simulated ones and thus the measured isotopic ratios being overestimated by the simulated ones. Decreasing the input signatures of the sources used for the simulations leads to more depleted simulated total $\delta^{13}C$ and δD that are closer to the measured $\delta^{13}C$ and δD.

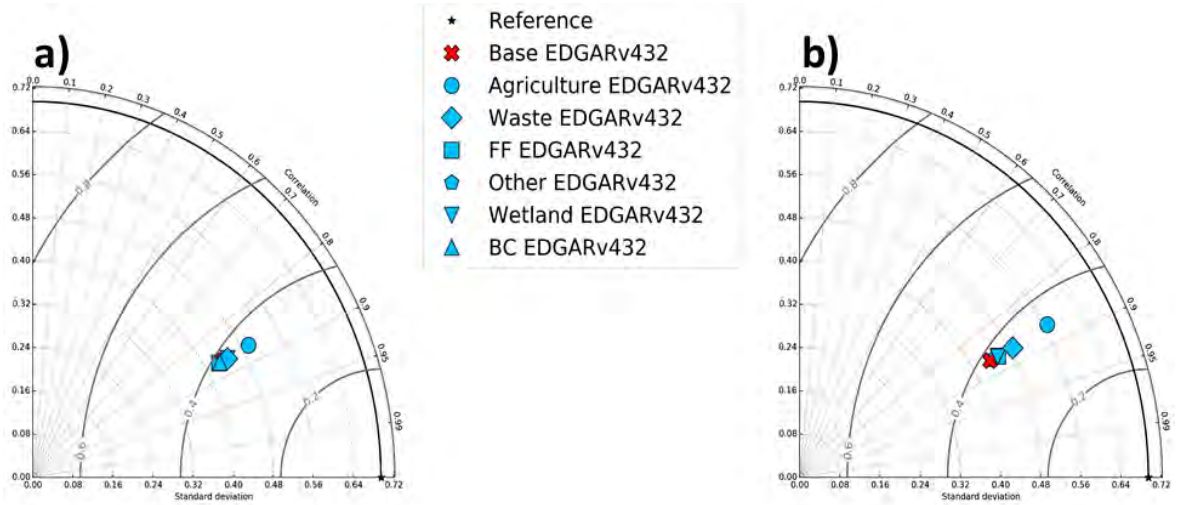

Fig. 6.13.5: Results of the sensitivity analysis as comparison of simulated and measured $\delta^{13}C$ in Taylor diagrams. a) Results of the sensitivity analysis when increasing the relative contribution of the source sectors by 20 %. b) Results of the sensitivity analysis when decreasing the input signatures of the source sectors by 10 %. Conclusions for δD are similar and thus only $\delta^{13}C$ is shown.

6.13.1.2.2 Fourth year

The fourth year focussed on further evaluating and publication of data and the defense of the thesis. The results presented for the fourth year are partyl an update of those of the third year.

Simulations of CH_4 mixing ratios have been performed at the European scale with the CHIMERE chemistry transport model (Menut et al., 2013; Mailler et al., 2017, Fortems-Cheiney et al., 2012) using annual anthropogenic emissions from the EDGAR version 4.3.2 (Janssens-Maenhout et al., 2018) and TNO-MACC_III (Kuenen et al., 2014) emission inventories for the year 2011. Natural wetland emissions are taken from the ORCHIDEE process model (Ringeval et al., 2011) for the year 2009, which was the last available year at the beginning of this study. Simulations have been carried out for 2015 with a horizontal resolution of 0.5° x 0.5° (~50x50 km) over Europe and of 0.1° x 0.1° (~10x10 km) over a smaller domain covering parts of North-western Europe (Fig. 6.13.6).

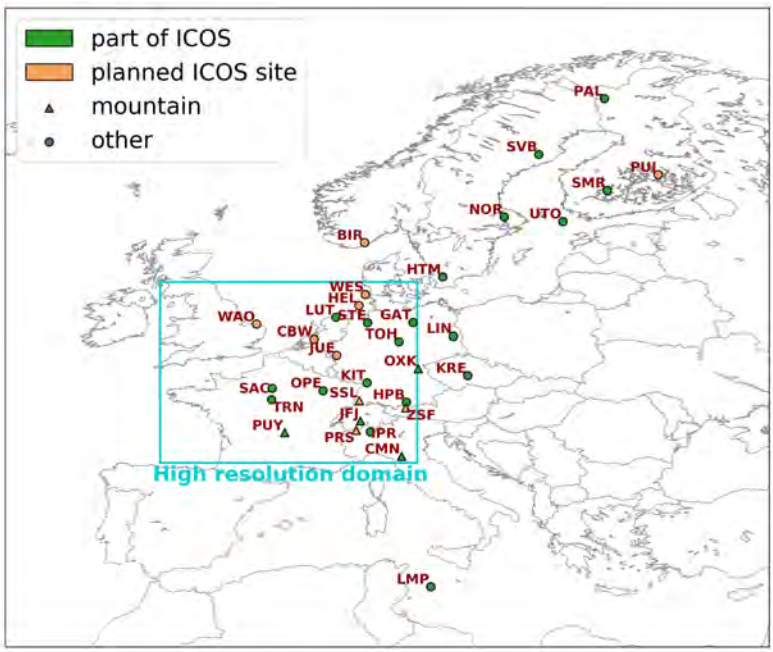

Fig. 6.13.6: Domains used for simulating atmospheric CH_4 mixing ratios and isotopologues, including the monitoring sites of the ICOS network.

The meteorological forcing's are obtained from the European Centre for Medium-Range Weather Forecasts (ECMWF) and the boundary and initial conditions from the analysis and forecasting system developed in the Monitoring Atmospheric Composition and Climate (MACC) project (Marécal et al., 2015).

Time series of atmospheric $\delta^{13}C$ and $\delta^{2}H$ isotope ratios are computed with an hourly temporal resolution based on simulated CH_4 mixing ratios for the four main CH_4 source categories: agriculture, waste, fossil fuel related emissions and wetland emissions (Table 6.13.2).

The simulated CH_4 mixing ratios per source are combined with their corresponding $\delta^{13}C$ and $\delta^{2}H$ isotopic source signatures (Table 6.13.2). The atmospheric CH_4 mixing ratios, as well as $\delta^{13}C$ and $\delta^{2}H$ isotope ratios are computed for the locations of measurement sites and for the domain using emissions from the two anthropogenic emission inventories to tackle uncertainties in emissions and their impact on the simulations of atmospheric CH_4 mixing ratios and $\delta^{13}C$ and $\delta^{2}H$ isotope ratios. To represent background isotopic values, we use the $\delta^{13}C$ and $\delta^{2}H$ simulations made with the Laboratoire de Meteorologie Dynamique (LMDz) global model (Hourdin et al., 2006) by Thanwerdas et al. (2019), which have a 3-hourly temporal resolution.

Table 6.13.2: Source isotopic signatures used as input for the computation of the atmospheric isotopic compositions $\delta^{13}C$ for Heidelberg (Hoheisel et al. 2019) and $\delta^{13}C$ and $\delta^{2}H$ for the ICOS network, including the ranges of values found in the listed references. The $\delta^{13}C$ and $\delta^{2}H$ values for the boundary mixing ratios demonstrate the mean value as they vary over time.

Source sector	Heidelberg $\delta^{13}C$ [‰] (Hoheisel et al. 2019)	Europe $\delta^{13}C$ [‰]	Europe $\delta^{2}H$ [‰]	References
Agriculture (SNAP 10)	-64.0	-63.5 [-74.4 – -50.3]	-306 [-442 – -168]	Menoud et al. (2020a), Sherwood et al. (2017), Levin et al. (1993), Klevenhusen et al. (2010), Bréas et al. (2001), Bilek et al. (2001), Röckmann et al. (2016), Uzaki et al. (1991), Tyler et al. (1997)
Waste (SNAP 9)	-55.0	-54.9 [-73.9 – -45.4]	-290 [-347 – -172]	Bergamaschi et al. (1998b), Levin et al. (1993), Zazzeri et al. (2015), Röckmann et al. (2016), Menoud et al. (2020a), Games and Hayes (1976), Sherwood et al. (2017)
Fossil fuel related emissions (SNAP 2 & 5)	-47.0	-46.4 [-87.0 – -14.8]	-185 [-415 – -56]	Levin et al. (1999), Röckmann et al. (2016), Menoud et al. (2020a), Sherwood et al. (2017), Lowry et al. (2001), Thielemann et al. (2004), Zazzeri et al. (2016)

Other anthropogenic sources (SNAP 1, 3, 4, 6, 7, 8)	-35.0	-38.3 [-64.4 – -12.5]	-206 [-308 – -110]	Menoud et al. (2020a), Röckmann et al. (2016), Levin et al. (1999), Chanton et al. (2000), Nakagawa et al. (2005), Sherwood et al. (2017)
Wetlands (SNAP 11)	-71.0	-68.2 [-96.5 – -48.0]	-337 [-450 – -288]	Menoud et al. (2020a), Sherwood et al. (2017), Tyler et al. (1987), Smith et al. (2000), Fisher et al. (2017), Galand et al. (2010), Happell et al. (1995), Martens et al. (1992), Bilek et al. (2001), Sugimoto and Fujita (2006), Quay et al. (1999)
Boundary mixing ratios	-47.4	-47.0	-86	Thanwerdas et al. (2019)

In this reporting period, we have carried out two analyses on simulated isotopic ratios. One of these analyses focuses on reasons for misfits between measured and simulated CH_4 mixing ratios and isotope ratios, by comparing simulated atmospheric $\delta^{13}C$ isotope ratios to ones measured at the German monitoring site Heidelberg. In the other analysis, we study the potential of long-term (> 1 year) isotopic measurements for CH_4 source detection at monitoring sites of the European ICOS network. The potential of isotopic measurements is determined by two aspects in this study: realistic instrument precision and placement of monitoring sites. As the instrument uncertainty sets limitations on CH_4 emission estimates, we examine the instrument precision needed to detect signals of $\delta^{13}C$ and $\delta^{2}H$. By combining atmospheric modelling and measurements, these studies explore different constraints on the CH_4 budget and the potential of isotopic ratio measurements to improve estimates of CH_4 emissions at the European scale.

For the first study, source isotopic signatures from the study of Hoheisel et al. (2019) are used as input for computing atmospheric $\delta^{13}C$ isotope ratios. For the computation of $\delta^{13}C$ and $\delta^{2}H$ isotope ratios in the ICOS network study, the $\delta^{13}C$ and $\delta^{2}H$ isotopic source signatures are assumed homogeneous in time and space over the domain covering entire Europe. They are chosen with the aid of several literature studies and the MEMO² measurements (Menoud et al., 2020a) and are summarised in Table 6.13.2. Although MEMO² campaigns have been carried out at several locations in Europe and they have brought valuable information on typical isotopic source signatures, the locations of the measurement sites we focus on do not overlap with the MEMO² campaign locations. The areas of interest in MEMO² are large emission areas, whereas the sites of the ICOS network are located in rather low emission areas to be representative at large spatial scales. Table 6.13.2 lists the isotopic source signatures used in both studies.

6.13.1.2.2.1 Analysis of simulated isotopic ratios at the Heidelberg monitoring site

Isotopologues are useful to discriminate sector contributions of CH_4 emissions as the isotopic composition varies highly depending on the source type. For instance, the signature is different depending on whether CH_4 is produced by thermogenic (e.g. natural gas), biogenic (e.g. domestic animals, landfills, wetlands) or pyrogenic (combustion) sources. The comparison between measured and simulated CH_4 mixing ratios and isotopic composition can be used for evaluating flux measurement methods and other data gained from measurements, such as isotopic source signatures or emissions estimated from measurements. Simulations allow a broad investigation of the magnitude, the sectoral and spatial distribution of atmospheric CH_4 mixing ratios, and how the simulated mixing ratios depend on emissions. The aim of this task is to investigate the value of quasi-continuous isotopic composition measurements for CH_4 source attribution.

Material and methods

Forward simulations of atmospheric CH_4 mixing ratios and $\delta^{13}C$ isotopic ratios have been carried out for the period between November 2016 and March 2017 at the location of the monitoring site Heidelberg,

located in South-West Germany (Fig. 6.13.6). These simulations have been used, among others, to determine the dominant source type around Heidelberg and have been compared to measurements provided by the Heidelberg University. The dominant source type for the five-month study period is determined by the Miller-Tans approach (Miller and Tans, 2003), combined with an orthogonal distance regression fit that takes the uncertainties in the X and Y variables into account.

Results

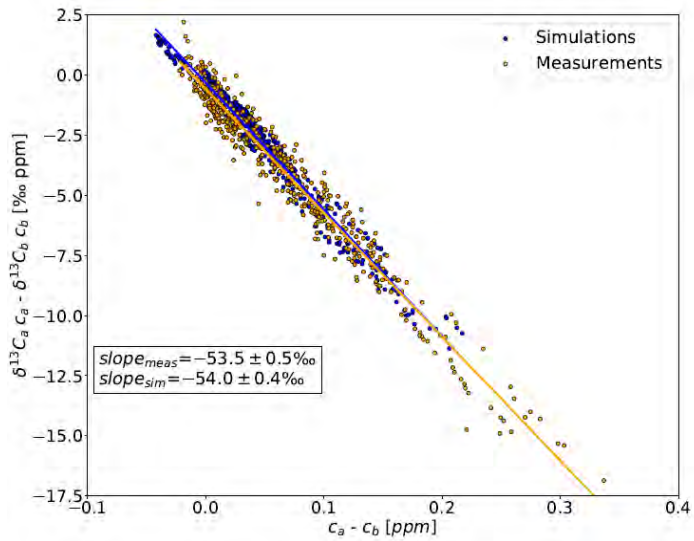

Fig. 6.13.7: Miller-Tans plots based on modified simulated CH_4 mixing ratios used for simulating the background for the period November 2016 - March 2017. The Miller-Tans plots are made by using simulations with the TNO-MACC_III inventory

The Miller-Tans plots used for determining the dominant source type around Heidelberg are shown in Fig. 6.13.7. The average $\delta^{13}C$ isotopic source signature derived from the measurements is (-53.5 ± 0.5) ‰, implying that the dominant source around Heidelberg is of microbial origin, possibly waste. However, this $\delta^{13}C$ source isotopic signature could also be due to a mixing of microbial and thermogenic sources. The $\delta^{13}C$ isotopic source signatures defined from the simulations with EDGARv4.3.2 and TNO-MACC_III are (-55.0 ± 0.3) ‰ and (-54.2 ± 0.4) ‰, respectively. They could also imply a microbial origin. The $\delta^{13}C$ source isotopic signatures used as input for the source sectors (Table 6.13.2) and the source contributions to the simulated total CH_4 mixing ratios (not shown), however, imply a mixing of agriculture and fossil fuel related sources: agricultural sources have a larger contribution to the simulated total CH_4 mixing ratios with both inventories than waste sources.

The measured source signature is underestimated by both simulations. However, the derived $\delta^{13}C$ source signature with TNO-MACC_III is higher and thus closer to the measured isotopic source signature than that with EDGARv4.3.2. The difference between the regression lines of the measurements and simulations is likely due to issues with the simulated CH_4 boundary mixing ratios used for the background in this study. We test this hypothesis with a simplified method for simulations with the TNO-MACC_III inventory, in which we replace the simulated CH_4 boundary mixing ratios by the lowest 10th percentile of the measured CH_4 mixing ratios in a 10-day running window. The 10-day running window is chosen as this amount of days exceeds the synoptic time scale (about 5 days) and can be considered representative of background conditions. The modification of the CH_4 boundary mixing ratios (Fig. 6.13.8) leads to a higher average simulated $\delta^{13}C$ source isotopic ratio of (-54.0 ± 0.4) ‰. This is even in the range of the uncertainty of the average $\delta^{13}C$ source isotopic ratio derived from the measurements. The improvement caused by replacing the CH_4 boundary mixing ratios indicates that there are issues with the simulated CH_4 boundary mixing ratios. Therefore, the simulated CH_4 boundary mixing ratios need further, in-depth analyses to learn more about the underlying issues. Nevertheless, it can be shown that isotopologue measurements are a great asset for determining the origin of atmospheric CH_4.

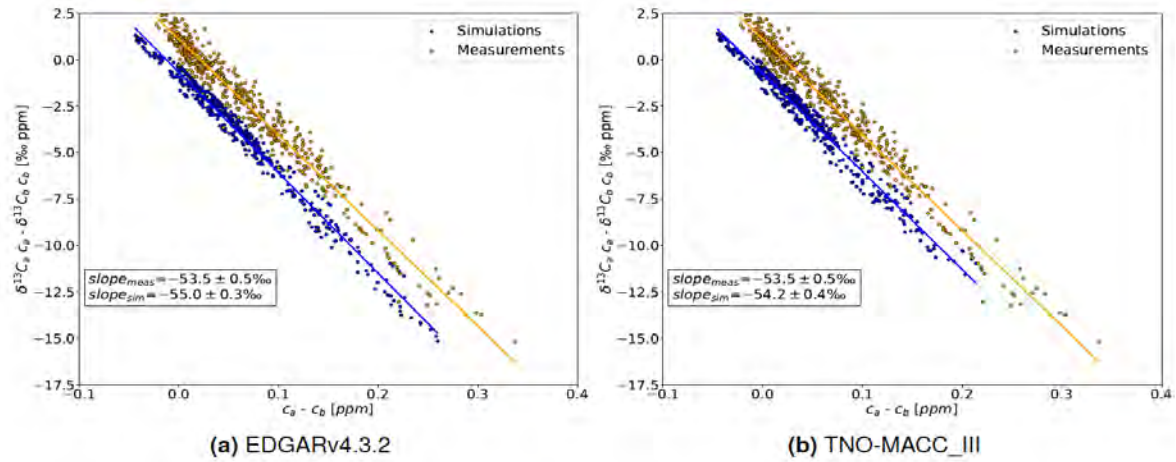

Fig. 6.13.8: Miller-Tans plots based on measured and simulated CH_4 mixing ratios and $\delta^{13}C$ isotopic ratios for the period November 2016 -- March 2017.

6.13.1.2.2.2 Investigating the potential of isotopic measurements for CH_4 source detection in a modelling framework

Further analyses of atmospheric CH_4 mixing ratios and isotopologues (not shown here) have revealed that inaccurate magnitudes and placement of methane emissions in the inventories is the main reason for the differences between measured and modelled $\delta^{13}C$ and $\delta^{2}H$ and that measurements of isotopologues in addition to mixing ratios can be an asset for gaining more information about CH_4 emissions. $\delta^{13}C$ and $\delta^{2}H$ measurements are usually available as flask-sampled data with a low frequency of several days to weeks, while high-frequency (~hourly) data of isotopic composition have been demonstrated to be able to reduce uncertainties on emissions estimated through atmospheric inversions (Rigby et al., 2012). However, the global scarcity of high-frequency, long-term measurements of $\delta^{13}C$ and $\delta^{2}H$ limits their application in emission estimation methods, such as atmospheric inversions.

Therefore, we investigate, through experiments with synthetic data, the importance of high-frequency $\delta^{13}C$ and $\delta^{2}H$ data to be assimilated in atmospheric inversions, alongside with CH_4 mixing ratios, to improve CH_4 emission estimates. While awaiting availability of more high-frequency atmospheric isotopic measurements of several months or years in Europe, the evaluation is made at monitoring sites of the ICOS network. ICOS is chosen as the sites in this network already provide measurements of atmospheric CH_4 mixing ratios and it could represent a possible CH_4 isotopologue monitoring network. Furthermore, we address the limitation on CH_4 source detection due to limited precisions of instruments measuring atmospheric isotopic composition (Schaefer et al., 2019). Following Thonat et al. (2019), we analyse four reasonable instrument precisions for $\delta^{13}C$ and $\delta^{2}H$ analyses (Table 6.13.3) and investigate from what type of CH_4 sources atmospheric $\delta^{13}C$ and $\delta^{2}H$ signals would be detectable with given instrument precisions. A further aim of this analysis is to provide ICOS sites or alternative locations that would be best suited for long-term monitoring of CH_4 isotopologues. Moreover, we analyse seasonal variations in the detectability of sources.

Table 6.13.3: Instrument precisions used as thresholds for $\delta^{13}C$ and $\delta^{2}H$ signal detection from CH_4 sources, including studies carried out with instruments of these precisions.

$\delta^{13}C$ [‰]	References	$\delta^{2}H$ [‰]	References
0.02	Lowe et al. (2002)	0.5	Bergamaschi et al. (1998a)
0.05	Lowe et al. (2002), Fisher et al. (2006)	1.0	Röckmann et al. (2016), Menoud et al. (2020b), Lowe et al. (2002)
0.1	Röckmann et al. (2016), Menoud et al. (2020b), Lowe et al. (2002)	3.0	Lowe et al. (2002)
0.2	WMO (2018)	5.0	WMO (2018)

Material and methods

Table 6.13.4: Selected monitoring sites of the ICOS network within Europe

3-letter code of site	Name of site	Country	Part of ICOS
BIR	Birkenes Observatory	Norway	In process
CBW	Cabauw	The Netherlands	In process
CMN	Monte Cimone	Italy	Yes
GAT	Gartow	Germany	Yes
HEL	Helgoland	Germany	In process
HPB	Hohenpeissenberg	Germany	Yes
HTM	Hyltemossa	Sweden	Yes
IPR	Ispra	Italy	Yes
JFJ	Jungfraujoch	Switzerland	Yes
JUE	Jülich	Germany	In process
KIT	Karlsruhe	Germany	Yes
KRE	Krešín u Pacova	Czech Republic	Yes
LIN	Lindenberg	Germany	Yes
LMP	Lampedusa	Italy	Yes
LUT	Lutjewad	The Netherlands	Yes
NOR	Norunda	Sweden	Yes
OPE	Observatoire Pérenne de l'Environnement	France	Yes
OXK	Ochsenkopf	Germany	Yes
PAL	Pallas	Finland	Yes
PRS	Plateau Rosa	Italy	In process
PUI	Puijo	Finland	In process
PUY	Puy de Dome	France	Yes
SAC	Saclay	France	Yes
SMR	Hyytiälä	Finland	Yes
SSL	Schauinsland	Germany	In process
STE	Steinkimmen	Germany	Yes
SVB	Svartberget	Sweden	Yes
TOH	Torfhaus	Germany	Yes
TRN	Trainou	France	Yes
UTO	ICOS Utö - Baltic sea	Finland	Yes
WES	Westerland	Germany	In process
WAO	Weybourne Atmospheric Observatory	United Kingdom	In process
ZSF	Zugspitze	Germany	In process

The simulations for this study are carried out for a year between 1 July 2016 and 30 June 2017. Presently, there are 23 monitoring sites in our European domain that are part of the ICOS network. We also include ten additional sites that are in the labelling process to become part of the ICOS network (Table 6.13.4).

Following Thonat et al. (2019), we compute the standard deviations (SD) of simulated daily (1-day mean) total atmospheric δ^2H and $\delta^{13}C$ time series over a 3-day running window, i.e. running time interval, to be in the range of the synoptic time scale (about 5 days). We test a set of instrument precisions, i.e. thresholds for signal detection. If a threshold is exceeded by the running SDs of the total atmospheric δ^2H and $\delta^{13}C$ signals, we compute the SDs of the individual CH_4 sources over the same running window. Even though total atmospheric signals consist of various sources that have different isotopic signatures, we consider only the source with the highest running SD as detectable for a given day. The exceedance of a threshold indicates that the synoptic variability of atmospheric signals can be detected, in which case a measuring instrument is considered to be able to provide useful information for regional atmospheric inversions. To conclude on how often signals from CH_4 sources are detectable in a year, the number of days when signals are detectable are added up over the one-year study period.

The thresholds for δ^2H and $\delta^{13}C$ are chosen according to precisions of current instruments and compatibility targets defined by the WMO IAEA (World Meteorological Organization - International Atomic Energy Agency) (WMO, 2018), which can be found in Table 6.13.3.

We also analyse in which season the various sources are more expected to be detected. Doing so can reveal which season is most suited to perform intensive measurement campaigns of several days to weeks or quasi-continuous measurements (e.g. Röckmann et al., 2016; Menoud et al., 2020b) if there is no possibility for measurements of at least a year. This is especially helpful if the source of interest is detectable only on a low number of days (~ one month or less) during a year.

It should be noted that the source detection method used in this study is optimistic as we consider only the source with the highest SD as detectable, while atmospheric signals consist of contributions from different sources. The number of detection events can be lower than in our study as signals can cancel each other out for some events. Furthermore, sources that have been indicated as detectable in our study highly depend on the emissions' magnitude and spatial distribution in the inventories used.

Results

The precision targets defined by the WMO IAEA (WMO, 2018) for $\delta^{13}C$ and $\delta^{2}H$ are 0.2 ‰ and 5 ‰, respectively, for regionally oriented studies. However, our analysis implies that the 0.2 ‰ and 5 ‰ precisions are sufficient for detecting sources only from large emitting areas, such as the Po-Valley in Italy or the Silesian coal basin in Poland, during about six months of the year (Fig. 6.13.9, showing an example using the TNO-MACC_III inventory for simulations). The second highest precisions of 1 ‰ for $\delta^{2}H$ analyses and 0.05 ‰ for $\delta^{13}C$ analyses have been demonstrated to be more useful for providing information on CH_4 sources in regional atmospheric inversions: sources could be detected at about half of the ICOS sites during 85% of the year. The highest precisions of 0.5 ‰ for $\delta^{2}H$ analyses and 0.02 ‰ for $\delta^{13}C$ analyses could yield even more days on which sources can be detected. Such precisions, however, are quite ambitious and require strict laboratory protocols.

Our analyses demonstrate that mainly background and agricultural sources would be detectable at most ICOS sites (Fig. 6.13.9). Therefore, we have investigated at which ICOS sites it would be most beneficial to carry out isotopic measurements. The sites Steinkimmen (DE), Cabauw (NL), Lutjewad (NL) and IPR (IT) have been implied by simulations with both inventories as potential sites for signal detection during at least six months in a year (Fig. 6.13.10). However, areas around the first three sites are known for large emissions originating from agricultural activities and thus the main detectable confirmed source at these sites is agriculture. At IPR, waste sources are the dominant detectable source. The sites KRE (CZ) and LIN (DE) appear to be promising for the detection of fossil fuel related sources for about a month.

While background sites are valuable for monitoring the general atmospheric evolution of sources and sinks of greenhouse gases at larger regional scales, sites and regions where signals from CH_4 sources would be detectable, could be useful to improve our understanding on specific methane sources and their temporal and spatial distribution. For example, sites and regions with controversial source detectability for EDGARv4.3.2 and TNO-MACC_III (results not shown) could be considered for long-term monitoring of $\delta^{2}H$ and $\delta^{13}C$ isotope ratios. A good example is the monitoring site Steinkimmen (STE) in Germany, at which simulations with TNO-MACC_III suggest that fossil fuel related sources are detectable, whereas simulations with EDGARv4.3.2 do not indicate fossil fuel related sources as detectable.

Moreover, it would be advantageous to measure CH_4 isotopic composition in further regions where waste and fossil fuel related sources can be detectable. Such regions are, for example, Southern part of the UK and Eastern Europe (such as Greece or Romania), respectively (Fig. 6.13.10 and 6.13.11). As none of the ICOS sites is indicated to be a potential site for detecting signals from wetlands, other higher latitude regions, such as Southern Finland, could be a good target for measuring $\delta^{2}H$ and $\delta^{13}C$ isotope ratios and CH_4 mixing ratios from wetlands.

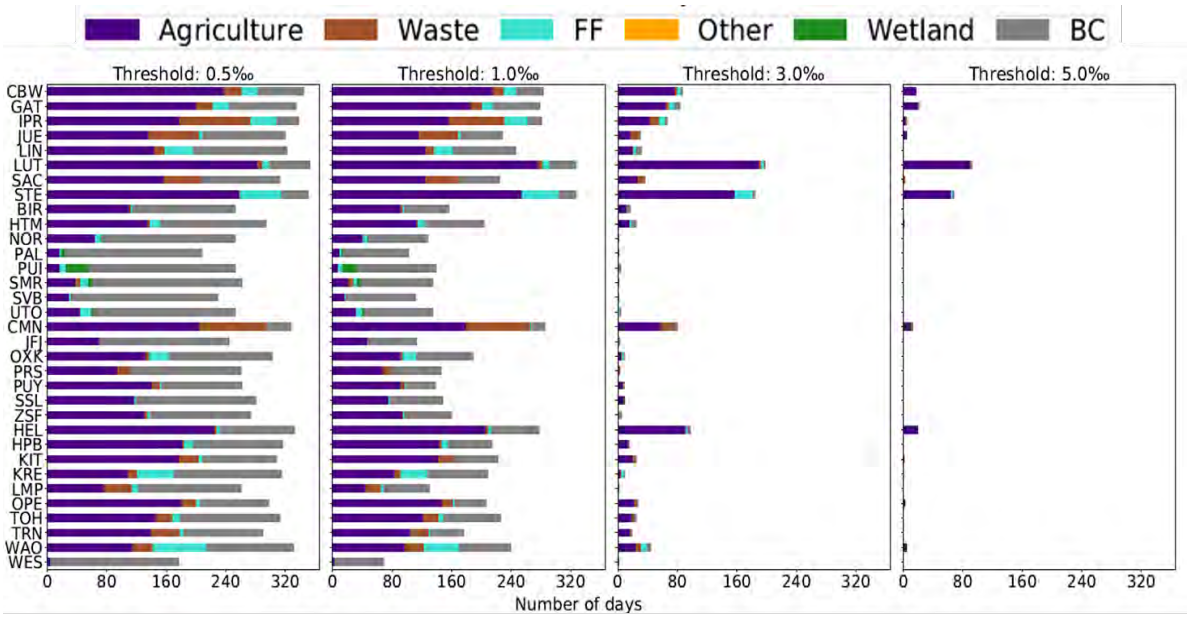

(a) δ^2H, TNO-MACC_III

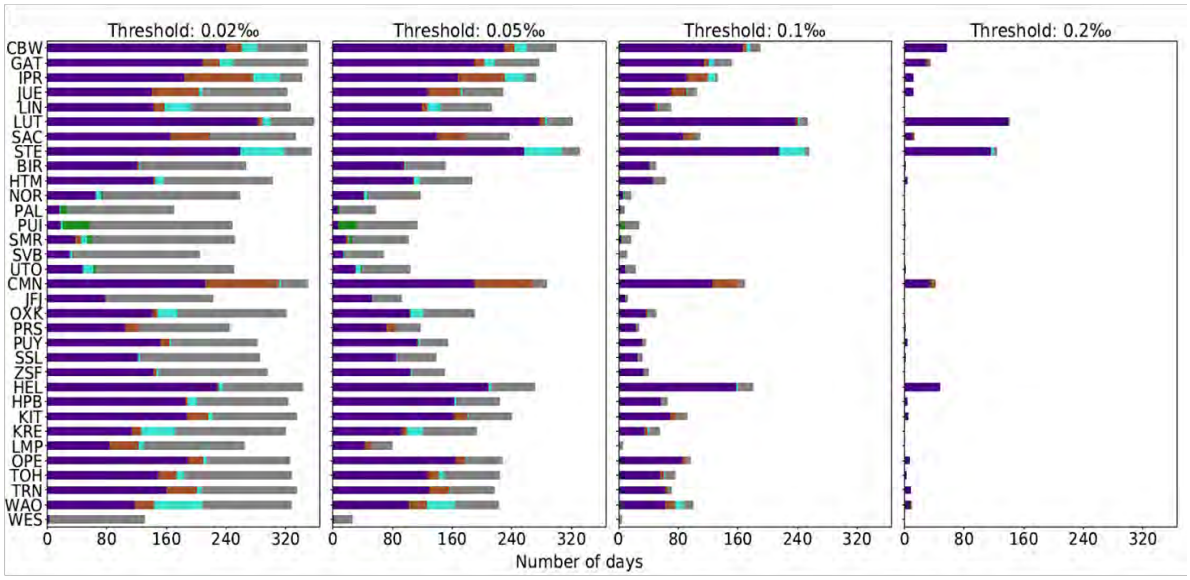

(b) δ^{13}C, TNO-MACC_III

Fig. 6.13.9: Number of days in the study year when simulated daily source contributions to (**a**) δ^2H and (**b**) δ^{13}C at ICOS sites are above given thresholds, computed from standard deviations over the 3-day running windows, for the TNO-MACC_III inventory in the domain covering whole Europe. Colours indicate detectable source types.

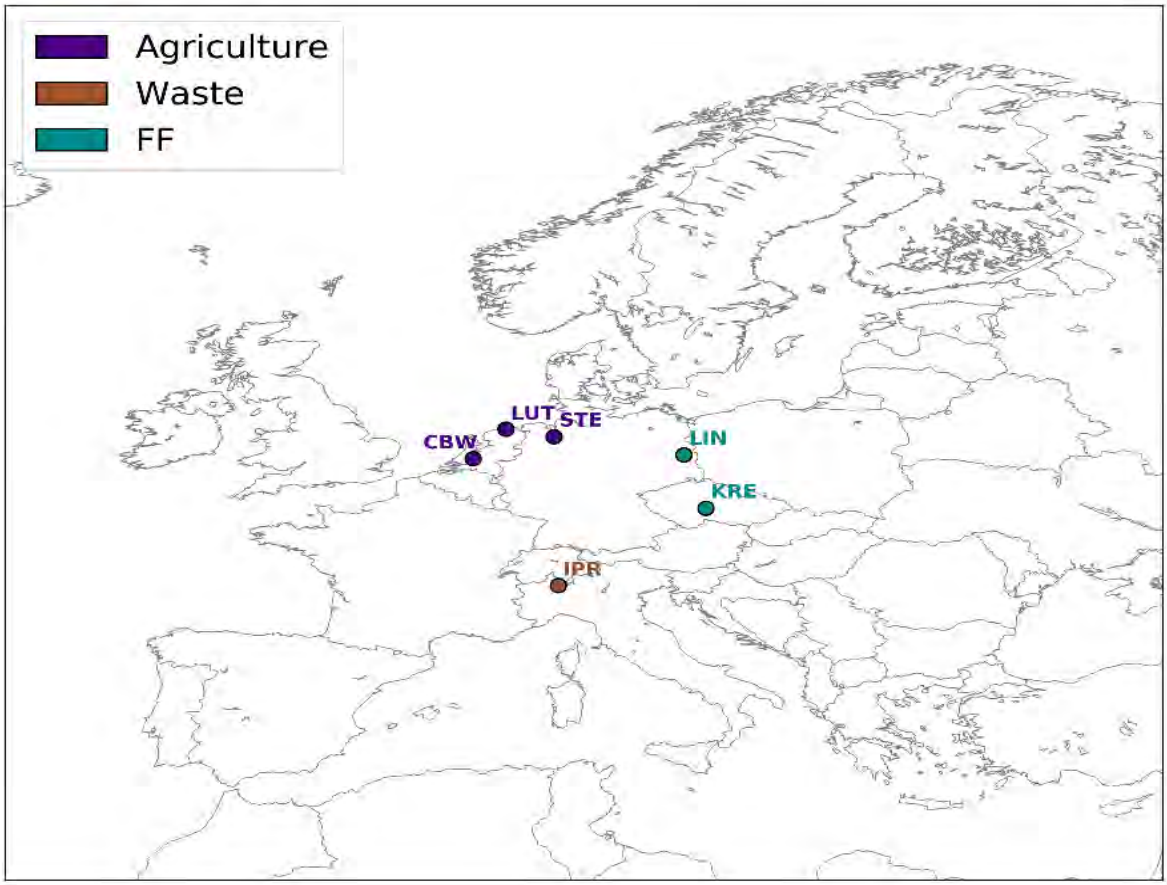

Fig. 6.13.10: Sites and areas that could be targeted for monitoring atmospheric δ^2H and $\delta^{13}C$ isotope ratios from different CH_4 sources.

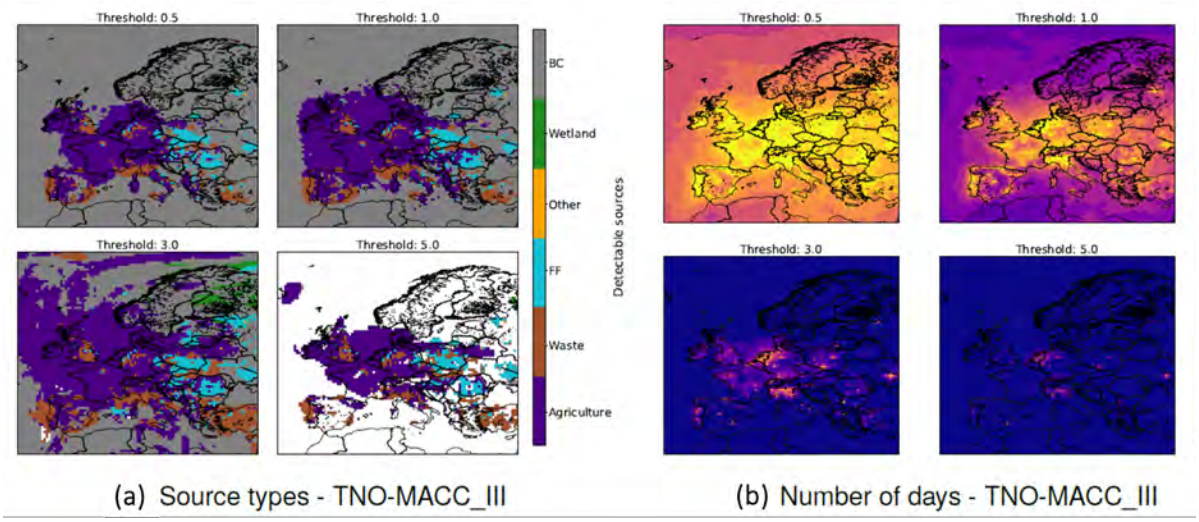

Fig. 6.13.11: Number of days in the study year (**b**) and source types (**a**) when simulated daily source contributions to δ^2H at ICOS sites are above given thresholds, computed from 3-day running standard deviations. Results are shown for the TNO-MACC_III inventories in the domain covering whole Europe.

Seasonal variations are observable in the detectability of sources (Fig. 6.13.12). Agriculture and waste sources are primarily detectable in autumn, while fossil fuel related sources and boundary conditions are detectable on most days in winter and autumn. Although wetlands were found detectable only at a few high-latitude sites on a few days of the year, the highest possibility to detect signals from them would be during summer and autumn. This suggests that possibly an even higher precision than 0.02 ‰ for $\delta^{13}C$ and 0.5 ‰ for $\delta^{2}H$ would be necessary for wetland source detection and possibly at other locations than those at which the current ICOS sites are installed.

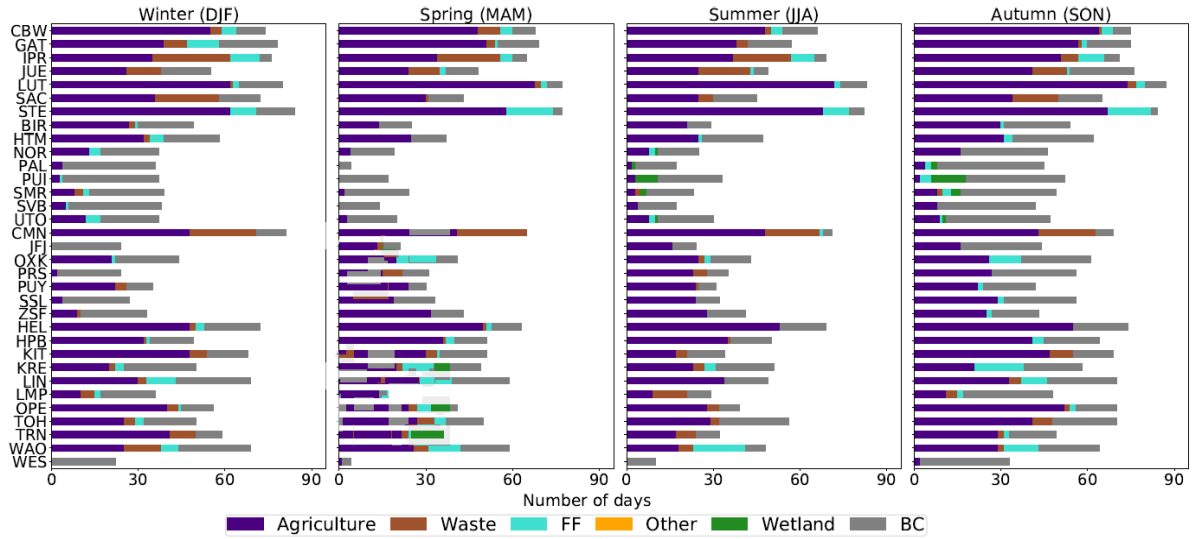

Fig.6.13.12: Seasonality of simulated daily source contributions to $\delta^{2}H$ at ICOS sites being above the 1‰ threshold, computed from 3-day running standard deviations. Colours indicate detectable source types. Results are shown for using the TNO-MACC_III inventory in the domain covering Europe.

Even though this study has been performed for one year only, we assume that the results apply for the years after 2017 as emission hot-spots and large emission areas will likely remain at similar locations in Europe. Moreover, most CH_4 emissions in Europe do not have a high inter-annual variability, due to which we can assume that our results will still apply in the near future. Hence, $\delta^{2}H$ and $\delta^{13}C$ data sets can be implemented in atmospheric inversions of CH_4 emission over Europe, once a sufficient amount of $\delta^{2}H$ and $\delta^{13}C$ data with sufficient instrument precision are available. However, as our study showed, even higher precisions than 0.02 ‰ for $\delta^{13}C$ and 0.5 ‰ for $\delta^{2}H$ may be necessary to detect sources. This may be the case especially for wetland and fossil fuel related sources. Alternatively, atmospheric inversions could further investigate the value of long-term isotopic data by using synthetic measurements of $\delta^{2}H$ and $\delta^{13}C$ over multiple years.

6.13.1.2.2.3 General conclusions of the studies in this reporting period

We found that a possible reason for the low model performance for atmospheric $\delta^{13}C$ isotopic ratios is improper $\delta^{13}C$ source isotopic signatures used for the area around Heidelberg. Moreover, we determined the average measured $\delta^{13}C$ source isotopic signature, which suggests microbial sources or a mix of microbial and thermogenic sources as dominant in the region. The simulations with both inventories are in agreement with that.

Through the investigation of the instrument precision, we found that a precision of at least 1 ‰ for $\delta^{2}H$ analyses and 0.0 5‰ for $\delta^{13}C$ analyses would be needed to detect sources at most sites during at least six months. The sites Steinkimmen (DE), Cabauw (NL), Lutjewad (NL) and IPR (IT) have been implied by simulations with both inventories as potential sites for signal detection during at least six months in a year. At IPR, waste sources are the dominant detectable source.

The sites KRE (CZ) and LIN (DE) appear to be promising for the detection of FF related sources for about a month. In order to learn more about CH_4 sources and sinks, it would be advantageous to measure CH_4 isotopic composition in further regions where waste and fossil fuel related sources can be detectable. Such regions are, for example, Southern part of the UK and Eastern Europe, respectively. As none of the ICOS sites is indicated to be a potential site for detecting signals from wetlands, other higher latitude regions, such as Southern Finland, could be a good target for measuring δ^2H and $\delta^{13}C$ isotope ratios and CH_4 mixing ratios from wetlands.

6.13.1.3 Future plans and expected results

The work in this project has been finished and the PhD thesis has been defended on 17 December 2020. We have recently submitted a revision of an article, presenting a study about estimating errors for atmospheric inversions of CH_4 emissions over Europe (described in the report for the period 01.03.2019-28.02.2020). Currently, we are working on a second publication, focusing on possible causes for misfits between measured and simulated atmospheric CH_4 mixing ratios, as well as isotopic ratios $\delta^{13}C$ and δ^2H, at the Lutjewad monitoring site (described in the report for the period 01.03.2019-28.02.2020). A third publication is planned, which will focus on the theoretical study for determining the instrument precision needed to detect signals of $\delta^{13}C$ and δ^2H from various CH_4 sources at the monitoring sites of the ICOS network (described further above in this report).

Furthermore, we may carry out atmospheric inversions of CH_4 emissions at the European scale, following the results of the three studies, once the tasks connected to the planned new European CH_4 emission inventory, based on the measurement campaigns carried out by other PhD students in the MEMO^2 project, will be completed.

6.13.1.4 Collaborations (internal / external)

There is a close collaboration with ESR8 for the modelling of isotopic ratios. ESR8 provided us with approx. 5 months of in-situ measurements of $\delta^{13}C$ and δD at the sites Lutjewad (NL) and Krakow (PL). Furthermore, the measurements of isotopic ratios of $\delta^{13}C$ at the site Heidelberg (DE) have been shared with us for modelling purposes.

Furthermore, we collaborate with TNO via using the model outputs of the LOTOS-EUROS model and discussing planned tasks for ESR13's PhD project.

6.13.1.5 Risks and difficulties

One of the initially planned deliverables was to make an updated European CH_4 emission inventory, based on the measurement campaigns carried out by other PhD students in the MEMO^2 project. Unfortunately, this has not been implemented during ESR 13's PhD project. This lead for ESR 13 to deviate from the original plan, which was to carry out atmospheric inversions, including new knowledge gained from the MEMO^2 measurements. Instead, we decided to focus on the main uncertainties of atmospheric inversions and the advantages of using CH_4 isotopologues in inversion studies.

The obligations in the MEMO^2 project during a PhD of three years is demanding due to the amount of training events and meetings. Thus, there was a need to extend the PhD project by three months.

6.13.2 Deliverables

D2.5 - Report providing isotopic maps at grid scale from inventories and atmospheric measurements (month 42)

ESR13 did not contribute to this deliverable but an inventory of isotopic signatures of $\delta^{13}C$ and δ^2H has been provided to us by ESR8, which we used as input for our study on the ICOS network.

D3.1 - New tools to estimate CH_4 source strengths from point sources, including mobile measurements (month 24)

The deliverable report was submitted by ESR11. ESR13 did not contribute to this deliverable as the scale of interest (local scale) for this deliverable differs from ESR13's work scale (European scale).

D3.2 - Improved bottom-up European CH_4 emissions (month 30)

As the work for this deliverable has been postponed to 2021, ESR13 can't contribute to this work as she has finished her PhD before the work for this deliverable will be started.

D3.3 - Forward modelling simulations of CH_4 and isotopologues (month 30)

The report was submitted in September 2019. The simulations in this deliverable are the basis for the estimation of errors in transport models and emission fluxes that are required to derive top-down estimates of emissions from atmospheric measurements of CH_4.

D3.4 - Top-down estimates of EU-scale CH_4 emissions, (month 42)

ESR13 could not contribute to this deliverable as there were not enough data available in the end to perform novel atmospheric inversions of CH_4 emissions over Europe.

6.13.3 Training and network activities (March 2017 – February 2019)

6.13.3.1 General training events

Event	Date (start – end)	Location (Host)	Objective / expected skills	ECTS points	Contribution	Comments
Greenhouse gases (GHG) challenges and observations	October–December 2017	Ecole Polytechnique, Palaiseau, France	The course makes one aware of the main climate effects of the increase of the atmospheric burden of GHGs, as well as of the various emission scenarios, including their ties to regional policy and economy, and the link between emissions and atmospheric concentration. The methodologies used to improve the knowledge on GHG sources and sinks were detailed and various observation techniques were presented.	4	Participation in classes and written exam	
Biogeochemical cycles and interactions with the biosphere at global scale	October–December 2017	AgroParisTech, Paris, France	The course aims the understanding of pollutant and greenhouse gas global budgets but also to establish relevant climate scenarios for the future. This teaching unit gives a basic knowledge on the major global biogeochemical cycles (carbon, nitrogen, ...) and to provide highlights on few biosphere - atmosphere interactions from regional scale to global scale.	3	Participation in classes and writing of two reports for the exam	
1st MEMO^2 school	5-16 February 2018	Schoorl, Netherlands	The school's objective was to present the basics of atmospheric physics and chemistry, greenhouse gases (especially methane), isotopes and several measurement techniques. The latter did not only include theoretical training but it was demonstrated in a measurement campaign. The gathered data from the measurements were analysed.	6	Participation in classes, helping in modelling exercise, preparation of a poster, data analyses	
Isotope workshop	17-19 September 2018	Royal Holloway, University of London, UK	The workshop was dedicated to the fundamentals in detail on methane isotopes. It included theoretical lessons, an experimental training in the laboratory and analysis of the collected data. Furthermore, the training included the modelling concepts of isotopes.		Participation and data analysis	
Dispersion modelling workshop	9-10 October 2018	Institut fuer Umweltphysik, Universitaet Heidelberg, Germany	This workshop was designed to understand the essential know-how on dispersion modelling and to be able to use Gaussian plume models.		Participation	
French language course	March 2019 – November 2019	LSCE	Grammar and speaking skills	0	Participating, taking small exams	
LOTOS-EUROS modelling workshop	15-16 January 2020	TNO Utrecht	Updates about the LOTOS-EUROS model, updates of the users' modelling activities	0	Participating, giving an oral presentation	
MEMO^2 annual meeting	10-11 February 2020	University Heidelberg	Updates about the project partners activities and progress	0	Participating, giving an oral presentation	
MEMO^2 meeting	12.10.2020	Online (UU)	General project progress		Presentation	

6.13.3.2 Secondments

Secondment	Date (start – end, planned (when))	Location	Host	Description of work / deviations	Scientific / training (skills) objective	Results and future plans
WUR	19 February 2018 – 19 March 2018	Wageningen, the Netherlands	WUR	The goal of the secondment was an inter-model comparison using the MicroHH model, a computational fluid dynamics code for the simulation of turbulent flows in the atmosphere, and the CHIMERE chemistry-transport model.	For inverse modelling, we need to obtain the representation error of the vertical mixing and the transport error. These errors can be assessed when comparing the simulation results to those of another model (MicroHH). To learn more about MicroHH, I spent a month at WUR.	I have learnt to run MicroHH. Simulations of CH_4 have been performed for one day only as the simulations are costly. Comparisons of one day only does not provide statistically significant results and thus we are thinking about whether it is advisable to use the simulation results.
Secondment 2	17 June – 12 July 2019	Utrecht, Netherlands	TNO	Compute the errors in transport models and emission inventories that are needed for performing atmospheric inversions of CH_4 with the aid of the TNO team	Estimate errors in transport models and emission inventories. And get more insight in the emission sectors and their uncertainties	The errors have been estimated and a scientific paper has been written about it
Secondment 3 (part 1)	9 – 20 Dec 2019	Utrecht, Netherlands	UU	Carry out sensitivity analyses for modelling isotopic ratios	Gain knowledge about isotopic ratios	The sensitivity analyses have been carried out and their preliminary results discussed with ESR 8 and her supervisor.
Secondment 3 (part 2)	13 – 24 January 2020	Utrecht, Netherlands	TNO	Design an Observation System Simulation Experiment (OSSE) to answer the question if there's a need for measuring isotopic ratios of $\delta^{13}C$ and δD at already existing ICOS sites in a sub-European domain	Gain more insight in designing an OSSE	A plan has been made and the OSSE study will be carried out based on the results of the sensitivity analyses within the next weeks.

6.13.3.3 Conferences

Conference name	Date (start – end, planned (when))	Location	Presentation (oral / poster)	Title of presentation	Authors (main author + co-authors)	Public available (yes / no) / web link
EGU	9-13 April 2018	Vienna, Austria	Poster presentation	Atmospheric monitoring of methane emission at the European scale	B. Szénási, I. Pison, G. Broquet, M. Saunois, P. Bousquet, A. Berchet	https://presentations.copernicus.org/EGU2018-14964_presentation.pdf
EGU	9-13 April 2018	Vienna, Austria	Presentation during the MEMO^2 session	Atmospheric monitoring of methane emission at the European scale	B. Szénási, I. Pison, G. Broquet, M. Saunois, P. Bousquet, A. Berchet	
EGU 2019	7 – 12 April 2019	Vienna, Austria	PICO presentation	Evaluation of methane emission inventories at the European scale by comparing atmospheric transport models and measurements	Barbara Szenasi, Isabelle Pison, Antoine Berchet, Gregoire Broquet, Philippe Bousquet, Marielle Saunois, Hugo Denier van der Gon, Arjo Segers, Randulph Morales and Dominik Brunner	no
NCGG8	12-14 June 2019	Amsterdam, Netherlands	Oral presentation	Atmospheric monitoring of methane emissions at the European scale	Barbara Szenasi, Isabelle Pison, Antoine Berchet, Gregoire Broquet, Philippe Bousquet, Marielle Saunois, Hugo Denier van der Gon, Arjo Segers, Randulph Morales and Dominik Brunner	no

6.13.3.4 Measurement / sampling campaigns

Campaign	Date (start – end, planned (when))	Location	Host	Description of work	Scientific objective	Samples (nature / number)	Results and future plans
MEMO^2 school	5-16 February 2018	Schoorl, NL	ECN, Petten, NL	Mobile measurements of methane and methane isotopes in and around Schrool. The targeted areas were around farms and agricultural fields.	It was within the framework of the MEMO^2 school with the objective of acquiring some measurement skills and techniques.	The measurements of our team were carried out using a Picarro analyser. It measures CH_4 and CO_2.	These measurements might be included in later model evaluation work.

6.13.4 Dissemination activities

Publications are in progress, the thesis (B. Szénási: Atmospheric monitoring of methane emissions at the European scale, thesis nr. 2020UPASJ006) will be publicly available soon.

Dissemination activity	Name	Date	Location	Type of audience	Size of audience
Blog entry on the MEMO^2 website		05 September 2018	https://h2020-memo2.eu/category/blog/	General public interested in science	

7. References

ADBA, 2019. Anaerobic Digestion Policy Report. Anaerobic Digestion & Bioresources Association, London.

Abichou, T., Powelson, D., Chanton, J., Escoriaza, S., Stern, J., 2006. Characterization of methane flux and oxidation at a solid waste landfill. J. Environ. Eng. 132, 220–228. https://doi.org/10.1061/(ASCE)0733-9372(2006)132:2(220)

AIRPARIF. 2005. "Analyss of Inventory and Emissions' Cadastres of Principal Greenhouse Gasses in Ile-de-France Region."

Armstrong and Collopy, 1992: Error Measures For Generalizing About Forecasting Methods: Empirical Comparisons, International Journal of Forecasting, 8, 69-80, 1992

Ars, S., Broquet, G., Yver Kwok, C., Roustan, Y., Wu, L., Arzoumanian, E., and Bousquet, P.: Statistical Atmospheric Inversion of Local Gas Emissions by Coupling the Tracer Release Technique and Local-Scale Transport Modelling: A Test Case with Controlled Methane Emissions, Atmos. Measure. Tech. 10 (12): 5017–37. https://doi.org/10.5194/amt-10-5017-2017

Assan, S., Baudic, A., Guemri, A., Ciais, P., Gros, V., and Vogel, F.R.: Characterization of Interferences to in Situ Observations of Delta13CH4 and C2H6 When Using a Cavity Ring-down Spectrometer at Industrial Sites, Atmos. Measure. Tech. 10 (6): 2077–91. https://doi.org/10.5194/amt-10-2077-2017

Assan, Sabina. 2017. "Towards Improved Source Apportionment of Anthropogenic Methane Sources." PhD thesis, LSCE: UVSQ.

Baldé, H., VanderZaag, A.C., Burtt, S.D., Wagner-Riddle, C., Crolla, A., Desjardins, R.L., MacDonald, D.J., 2016. Methane emissions from digestate at an agricultural biogas plant. Bioresour. Technol. 216, 914–922. https://doi.org/10.1016/j.biortech.2016.06.031

Bakkaloglu, S., Lowry, D., Fisher, R.E., France, J.L., Brunner, D., Chen, H., and Nisbet, E.G.: *Quantification of methane emissions from UK biogas plants,* Waste Management, 124, 82-93, https://www.sciencedirect.com/science/article/pii/S0956053X21000167, 2021

Bansal, S., Tangen, B., & Finocchiaro, R. (2016). Temperature and Hydrology Affect Methane Emissions from Prairie Pothole Wetlands. Wetlands, 36(2), 371–381. https://doi.org/10.1007/s13157-016-0826-8

Bergamaschi, P., Lubina, C., Konigstedt, R., Fischer, H., Veltkamp, A.C., Zwaagstra, O., 1998. Stable isotopic signatures (delta C13, delta D) of methane from European landfill sites. J. Geophys. Res. Atmos. 103, 8251–8265. https://doi.org/10.1029/98JD00105

P. Bergamaschi, C. A. M. Brenninkmeijer, M. Hahn, T. Röckmann, D. H. Scharffe, P. J. Crutzen, N. F. Elansky, I. B. Belikov, N. B. A. Trivett, and D. E. J. Worthy. Isotope analysis based source identification for atmospheric CH_4 and CO sampled across Russia using the Trans-Siberian railroad. Journal of Geophysical Research: Atmospheres, 103(D7):8227–8235,1998a.doi:10.1029/97JD03738., https://agupubs.onlinelibrary.wiley.com/doi/abs/10.1029/97JD03738.

R. S. Bilek, S. C. Tyler, M. Kurihara, and K. Yagi. Investigation of cattle methane production and emission over a 24-hour period using measurements of d13C and dD of emitted CH4 and rumen water. Journal of Geophysical Research: Atmospheres, 106(D14):15405–15413, 2001, https://agupubs.onlinelibrary.wiley.com/doi/abs/10.1029/2001JD900177

Börjesson, G., Samuelsson, J., Chanton, J., 2007. Methane oxidation in Swedish landfills quantified with the stable carbon isotope technique in combination with an optical method for emitted methane. Environ. Sci. Technol. 41, 6684–6690. https://doi.org/10.1021/es062735v

Börjesson G., Samuelsson J., Chanton J., Adolfsson R., Galle B. and Svensson B.H. A national landfill methane budget for Sweden based in field measurements, and an evaluation of IPCC models, Tellus, 61B, 424-435 (2009).

Bousquet, P., Ciais, P., Miller, J. B., Dlugokencky, E. J., Hauglustaine, D. A., Prigent, C., Van der Werf, G. R., Peylin, P., Brunke, E.-G., Carouge, C., Langenfelds, R. L., Lathière, J., Papa, F., Ramonet, M., Schmidt, M., Steele, L. P., Tyler, S. C., and White, J.: Contribution of anthropogenic and natural sources to atmospheric methane variability, Nature, 443, 439–443, https://doi.org/doi:10.1038/nature05132, 2006

Brantley, H. L.; Thoma, E. D.; Squier, W. C.; Guven, B. B.; Lyon, D. Assessment of methane emissions from oil and gas production pads using mobile measurements. Environ. Sci. Technol. 2014, 48, 14508– 14515, DOI:10.1021/es503070q

Brass M. and Röckmann, T.: Continuous-flow isotope ratio mass spectrometry method for carbon and hydrogen isotope measurements on atmospheric methane, Atmos. Meas. Tech., 3, 1707- 1721, doi:10.5194/amt-3-1707-2010, 2010

O. Bréas, C. Guillou, F. Reniero, and E. Wada. The Global Methane Cycle: Isotopes and Mixing Ratios, Sources and Sinks. Isotopes in Environmental and Health Studies, 37(4):257–379, 2001, https://doi.org/10.1080/10256010108033302

CCC, 2019. Net Zero Technical Report. Committee on Climate Change, London.

CCC, 2020. Reducing UK Emissions: 2020 Progress Report to Parliament. Committee on Climate Change, London.

Caulton, D.R., Qi L., Bou-Zeid, E., Lu, J., Lane, H.M., Fitts, J.P., and Buchholz, B.: Improving Mobile Platform Gaussian-Derived Emission Estimates Using Hierarchical Sampling and Large Eddy Simulation, Atmos. Chem. Phys. Dis., November, 1–39. https://doi.org/10.5194/acp-2017-961

Caulton, Dana R, Qi Li, Elie Bou-zeid, Jeffrey P Fitts, Levi M Golston, Da Pan, Jessica Lu, et al. 2018. "Quantifying Uncertainties from Mobile-Laboratory-Derived Emissions of Well Pads Using Inverse Gaussian Methods," 15145–68.

Chanton, J.P., Rutkowski, C.M., Mosher, B., 1999. Quantifying methane oxidation from landfills using stable isotope analysis of downwind plumes. Environ. Sci. Technol. 33, 3755–3760. https://doi.org/10.1021/es9904033

Chanton, J., Liptay, K., 2000. Seasonal variation in methane oxidation in a landfill cover soil as determined by an in situ stable isotope technique. Global Biogeochem. Cycles 14, 51–60. https://doi.org/10.1029/1999GB900087

Chanton, J.P., Abichou, T., Langford, C., Spokas, K., Hater, G., Green, R., Goldsmith, D., Barlaz, M.A., 2011. Observations on the methane oxidation capacity of landfill soils. Waste Manage. 31, 914–925. https://doi.org/10.1016/j.wasman.2010.08.028

Jeffrey Chanton, Christine Rutkowski, Candace Schwartz, D. Ward, and Lindsay Boring. Factors influencing the stable carbon isotopic signature of methane from combustion and biomass burning. Journal of Geophysical Research, 105:1867–1877, Jan. 2000. doi:10.1029/1999JD900909

Chen, J., Dietrich, F., Maazallahi, H., Forstmaier, A., Winkler, D., Hofmann, M. E. G., Denier van der Gon, H., and Röckmann, T.: *Methane emissions from the Munich Oktoberfest,* Atmos. Chem. Phys., 20, 3683–3696, https://doi.org/10.5194/acp-20-3683-2020, 2020

Christensen, T. R., Ekberg, A., Ström, L., Mastepanov, M., Panikov, N., Öquist, M., Oskarsson, H. (2003). Factors controlling large scale variations in methane emissions from wetlands. Geophysical Research Letters, 30(7). https://doi.org/10.1029/2002GL016848

Craig, Harmon. 1957. "Isotopic Standards for Carbon and Oxygen and Correction Factors for Mass-Spectrometric Analysis of Carbon Dioxide." Geochemica et Cosmochemica Acta 12: 133–49.

Crippa, Monica, et al. "Gridded Emissions of Air Pollutants for the Period 1970–2012 within EDGAR V4.3.2." Earth System Science Data, vol. 10, no. 4, 26 Oct. 2018, pp. 1987–2013, 10.5194/essd-10-1987-2018

Czepiel, P.M., Mosher, B., Crill, P.M., Harriss, R.C., 1996. Quantifying the effect of oxidation on landfill methane emissions. J. Geophys. Res. Atmos. 101, 16721-16729. https://doi.org/10.1029/96JD00222

De Visscher, A., De Pourcq, I., Chanton, J., 2004. Isotope fractionation effects by diffusion and methane oxidation in landfill cover soils. J. Geophys. Res. Atmos. 109, D18111. https://doi.org/10.1029/2004JD004857

Defratyka, Sara, Jean-Daniel Paris, Camille Yver-Kwok, Julianne M. Fernandez, Piotr Korben, and Philippe Bousquet. 2020. "Mapping Urban Methane Sources in Paris, France." Manuscript Submitted for Publication.

Defratyka, S. M., Paris, J.-D., Yver-Kwok, C., Loeb, D., France, J., Helmore, J., Yarrow, N., Gros, V., and Bousquet, P.: *Ethane measurement by Picarro CRDS G2201-i in laboratory and field conditions: potential and limitations*, Atmos. Meas. Tech. Discuss. [preprint], https://doi.org/10.5194/amt-2020-410, under review, 2020

Delre, A., Hensen, A., Velzeboer, I., van den Bulk, P., and Scheutz, C.: Fugitive methane and ethane emission quantifications from onshore oil and gas sites in Romania, using a tracer gas dispersion method, Elementa Science, in preparation

Dlugokencky, E. J., E. G. Nisbet, R. Fisher, and D. Lowry. 2011. "Global Atmospheric Methane: Budget, Changes and Dangers." Philosophical Transactions of the Royal Society A: Mathematical, Physical and Engineering Sciences 369 (1943): 2058–72. https://doi.org/10.1098/rsta.2010.0341

Duren, Riley M., and Charles E. Miller. 2012. "Measuring the Carbon Emissions of Megacities." Nature Climate Change 2 (8): 560–62. https://doi.org/10.1038/nclimate1629

"E-PRTR." Europa.eu, 2019, prtr.eea.europa.eu/.

Fabiańska M.J., Ciesielczuk J., Kruszewski Ł., Misz-Kennan M., Blake D.R., Stracher G., Moszumańska I., Gaseous compounds and efflorescences generated in self-heating coal-waste dumps – a case study from the Upper- and Lower Silesian Coal Basins (Poland), Int. J. of Coal Geology; 116–117:247–261, doi: 10.1016/j.coal.2013.05.002, 2013

Fernandez, J.M., Maazallahi, H., France, J.L., Menoud, M., Corbu, M., Ardelean, M., Calcan, A., van der Veen, C., Röckmann, T., Fisher, R.E., Lowry, D., and Nisbet, E.G.: Street-level methane emissions of Bucharest, Romania and the influence of urban wastewater, Atmospheric Environment, in preparation

Fiehn, A., Kostinek, J., Eckl, M., Klausner, T., Gałkowski, M., Chen, J., Gerbig, C., Röckmann, T., Maazallahi, H., Schmidt, M., Korben, P., Neçki, J., Jagoda, P., Wildmann, N., Mallaun, C., Bun, R., Nickl, A.-L., Jöckel, P., Fix, A., and Roiger, A.: *Estimating CH_4, CO_2 and CO emissions from coal mining and industrial activities in the Upper Silesian Coal Basin using an aircraft-based mass balance approach*, Atmos. Chem. Phys., 20, 12675–12695, https://doi.org/10.5194/acp-20-12675-2020, 2020

Fischer, Joseph C. von, Daniel Cooley, Sam Chamberlain, Adam Gaylord, Claire J. Griebenow, Steven P. Hamburg, Jessica Salo, Russ Schumacher, David Theobald, and Jay Ham. 2017. "Rapid, Vehicle-Based Identification of Location and Magnitude of Urban Natural Gas Pipeline Leaks." Environmental Science & Technology 51 (7): 4091–99. https://doi.org/10.1021/acs.est.6b06095

Fisher, R., France, J., Lowry, D., Lanoisellé, M., Brownlow, R., Pyle, J., Cain, M., Warwick, N., Skiba, U., Drewer, J., Dinsmore, K., Leeson, S., Bauguitte, S., Wellpott, A., O'Shea, S., Allen, G., Gallagher, M., Pitt, J., Percival, C., and Nisbet, E.: Measurement of the 13C isotopic signature of methane emissions from northern European wetlands. Global Biogeochemical Cycles, 31, Mar. 2017. doi: 10.1002/2016GB005504.

Fisher, R., Lowry, D., Wilkin, O., Sriskantharajah, S., and Nisbet, E.G.: 2006. "High-Precision, Automated Stable Isotope Analysis of Atmospheric Methane and Carbon Dioxide Using Continuous-Flow Isotope-Ratio Mass Spectrometry." Rapid Communications in Mass Spectrometry 20 (2): 200–208. https://doi.org/10.1002/rcm.2300

Flesch, T., Desjardins, R., Worth, D., 2011. Fugitive methane emissions from an agricultural biodigester. Biomass Bioenerg. 35, 3927–3935. https://doi.org/10.1016/j.biombioe.2011.06.009.

A. Fortems-Cheiney, I. Pison, G. Dufour, G. Broquet, A. Berchet, E. Potier, A. Coman, G. Siour, and L. Costantino. Variational regional inverse modeling of reactive species emissions with PYVAR-CHIMERE. Geoscientific Model Development Discussions, 2019:1–22, 2019. doi: 10.5194/gmd-2019-186. URL https://www.geosci-model-dev-discuss.net/gmd-2019-186/

Pierre Galand, Kim Yrjälä, and R. Conrad. Stable carbon isotope fractionation during methanogenesis in three boreal peatland ecosystems. Biogeosciences, 7, Nov. 2010. doi: 10.5194/bg-7-3893-2010.

Gałkowski, Michał, et al. "In Situ Observations of Greenhouse Gases over Europe during the CoMet 1.0 Campaign Aboard the HALO Aircraft." Atmospheric Measurement Techniques Discussions, 17 Aug. 2020, pp. 1–29, amt.copernicus.org/preprints/amt-2020-287/, 10.5194/amt-2020-287.

L. M. Games and J. M. Hayes. On the mechanisms of CO_2 and CH_4 production in natural anaerobic environments. Environmental Biogeochemistry, pages 51–73, 1976.

Gardiner, Tom, Jon Helmore, Fabrizio Innocenti, and Rod Robinson. 2017. "Field Validation of Remote Sensing Methane Emission Measurements." Remote Sensing 9 (9): 956. https://doi.org/10.3390/rs9090956

Gebert, J., Röwer, I.U., Scharff, H., Roncato, C.D., Cabral, A.R., 2011. Can soil gas profiles be used to assess microbial CH4 oxidation in landfill covers? Waste Manage. 31, 987–994. https://doi.org/10.1016/j.wasman.2010.10.008

Gioli, B., P. Toscano, E. Lugato, A. Matese, F. Miglietta, A. Zaldei, and F.P. Vaccari. 2012. "Methane and Carbon Dioxide Fluxes and Source Partitioning in Urban Areas: The Case Study of Florence, Italy." Environmental Pollution 164 (May): 125–31. https://doi.org/10.1016/j.envpol.2012.01.019

James D. Happell, Jeffrey P. Chanton, and William J. Showers. Methane transfer across the water-air interface in stagnant wooded swamps of Florida: Evaluation of mass-transfer coefficients and isotropic fractionation. Limnology and Oceanography, 40(2):290–298, 1995, https://aslopubs.onlinelibrary.wiley.com/doi/abs/10.4319/lo.1995.40.2.0290

Hensen. Methods for Observation and Quantification of Trace Gas Emissions from Diffuse Sources. Amsterdam: Vrije Universiteit -01-12, 2012

Hoheisel, A., Yeman, C., Dinger, F., Eckhardt, H., Schmidt, M., 2019. An improved method for mobile characterisation of delta (CH_4)-C-13 source signatures and its application in Germany. Atmos. Meas. Tech. 12, 1123–1139. https://doi.org/10.5194/amt-12-1123-2019

Hourdin, F., Musat, I., Bony, S., Braconnot, P., Codron, F., Dufresne, J.-L., Fairhead, L., Filiberti, M.-A., Friedlingstein, P., Grandpeix, J.-Y., Krinner, G., Levan, P., Li, Z.-X., and Lott, F.: The LMDZ4 general circulation model: climate performance and sensitivity to parametrized physics with emphasis on tropical convection. Climate Dynamics, 27(7-8):787–813, Dec. 2006. doi: 10.1007/s00382-006-0158-0.

INSEE. 2019. "INSEE." (https://www.insee.fr/fr/statistiques/1893198)

Jackowicz-Korczyński, M., Christensen, T. R., Bäckstrand, K., Crill, P., Friborg, T., Mastepanov, M., & Ström, L. (2010). Annual cycle of methane emission from a subarctic peatland. Journal of Geophysical Research: Biogeosciences, 115(G2). https://doi.org/10.1029/2008JG000913

Jackson, Robert B., Adrian Down, Nathan G. Phillips, Robert C. Ackley, Charles W. Cook, Desiree L. Plata, and Kaiguang Zhao. 2014. "Natural Gas Pipeline Leaks Across Washington, DC." Environmental Science & Technology 48 (3): 2051–58. https://doi.org/10.1021/es404474x.

Jammet, M., Dengel, S., Kettner, E., Parmentier, F.-J. W., Wik, M., Crill, P., & Friborg, T. (2017). Year- round CH4 and CO2 flux dynamics in two contrasting freshwater ecosystems of the subarctic. Biogeosciences, 14(22), 5189–5216. https://doi.org/10.5194/bg-14-5189-2017

Jammet, M., Crill, P., Dengel, S., & Friborg, T. (2015). Large methane emissions from a subarctic lake during spring thaw: Mechanisms and landscape significance. Journal of Geophysical Research: Biogeosciences, 120(11), 2289–2305. https://doi.org/10.1002/2015JG003137

G. Janssens-Maenhout, M. Crippa, D. Guizzardi, M. Muntean, E. Schaaf, F. Dentener, P. Bergamaschi, V. Pagliari, J. G. J. Olivier, J. A. H. W. Peters, J. A. van Aardenne, S. Monni, U. Doering, and A. M. R. Petrescu. EDGAR v4.3.2 Global Atlas of the three major Greenhouse Gas Emissions for the period 1970–2012. Earth System Science Data, 10.5194/essd-11-959-2019, https://essd.copernicus.org/articles/11/959/2019/.

Keeling, Charles D. "The Concentration and Isotopic Abundances of Atmospheric Carbon Dioxide in Rural Areas." Geochimica et Cosmochimica Acta, vol. 13, no. 4, Jan. 1958, pp. 322–334, 10.1016/0016-7037(58)90033-4

Keeling: The Concentration and Isotopic Abundances of Carbon Dioxide in the Atmosphere, Tellus, 12:2, 200-203, 1960, DOI: 10.3402/tellusa.v12i2.9366, 1960

Klevenhusen, F., Bernasconi, S., Kreuzer, M., and Soliva, C.: Experimental validation of the Intergovernmental Panel on Climate Change default values for ruminant-derived methane and its carbon-isotope signature. Animal Production Science - ANIM PROD SCI, 50, Jan. 2010. doi: 10.1071/AN09112.

Korben, P., Jagoda, P., Maazallahi, H., Kammerer, J., Necki, J.M., Bartyzel, J., Radovici, A., Schmidt, M., Röckmann, T., and other ROMEO team members: Quantification of methane emission from oil and gas wells using Other Test Method - 33a and Gaussian Plume Model during ROMEO campaign, Romania, in preparation

J. J. P. Kuenen, A. J. H. Visschedijk, M. Jozwicka, and H. A. C. Denier van der Gon. TNO-MACC_II emission inventory; a multi-year (2003-2009) consistent high-resolution European emission inventory for air quality modelling. Atmospheric Chemistry and Physics, 14(20):10963–10976, 2014. doi:10.5194/acp-14-10963-2014. URL https://www.atmos-chem-phys.net/14/10963/2014/.

Łakomiec, P., Holst, J., Friborg, T., Crill, P., Rakos, N., Kljun, N., Olsson, P.-O., Eklundh, L., and Rinne, J.: Field-scale CH_4 emission at a sub-arctic mire with heterogeneous permafrost thaw status, Biogeosciences Discuss. [preprint], https://doi.org/10.5194/bg-2021-81, in review, 2021

Lamb, B.K., Cambaliza, M., Davis, K., Edburg, S., Ferrara, T., Floerchinger, C., Heimburger, A.: Direct and Indirect Measurements and Modeling of Methane Emissions in Indianapolis, Indiana." Environmental Science & Technology 50 (16): 8910–17, 2016, https://doi.org/10.1021/acs.est.6b01198

Levin, I., Bergamaschi, P., Dorr, H., Trapp, D., 1993. Stable isotopic signature of methane from major sources in Germany. Chemosphere 26, 161–177. https://doi.org/10.1016/0045-6535(93)90419-6

Levin, I., Glatzel-Mattheier, H., Marik, T., Cuntz, M., Schmidt, M., Worthy, D.E., 1999. Verification of German methane emission inventories and their recent changes based on atmospheric observations. J. Geophys. Res. Atmos. 104, 3447–3456. https://doi.org/10.1029/1998JD100064

Liptay, K., Chanton, J., Czepiel, P., Mosher, B., 1998. Use of stable isotopes to determine methane oxidation in landfill cover soils. J. Geophys. Res. Atmos. 103, 8243–8250. https://doi.org/10.1029/97JD02630

"Local Weather Forecast, News and Conditions | Weather Underground." Wunderground.com, 2014, www.wunderground.com/.. Accessed 12 Feb. 2021.

Lopez, M., O.A. Sherwood, E.J. Dlugokencky, R. Kessler, L. Giroux, and D.E.J. Worthy. 2017. "Isotopic Signatures of Anthropogenic CH4 Sources in Alberta, Canada." Atmospheric Environment 164 (September): 280–88. https://doi.org/10.1016/j.atmosenv.2017.06.021

D. Lowe, J. White, I. Levin, M. Wahlen, J.B. Miller, and P. Bergamaschi. Isotope measurement techniques for atmospheric methane (IAEA-TECDOC–1268), Jan. 2002. ISSN 1011-4289. International Atomic Energy Agency (IAEA).

Lowry, David, Craig W. Holmes, Nigel D. Rata, Phillip O'Brien, and Euan G. Nisbet. 2001. "London Methane Emissions: Use of Diurnal Changes in Concentration and δ 13C to Identify Urban Sources and Verify Inventories." Journal of Geophysical Research: Atmospheres 106 (D7): 7427–48. https://doi.org/10.1029/2000JD900601

Lowry, D., Fisher, R.E., France, J.L., Coleman, M., Lanoisellé, M., Zazzeri, G., Nisbet, E.G., Shaw, J.T., Allen, G., Pitt, J., Ward, R.S., 2020. Environmental baseline monitoring for shale gas development in the UK: Identification and geochemical characterisation of local source emissions of methane to atmosphere. Sci. Total Environ. 708, 134600. https://doi.org/10.1016/j.scitotenv.2019.134600

Lu, X., Harris, S.J., Fisher, R.E., France, J.L., Nisbet, E.G., Lowry, D, Röckmann, T., van der Veen, C., Menoud, M., Schwietzke, S., and Kelly, B.F.J.: Isotopic signatures of major methane sources in the coal seam gas fields and adjacent agricultural districts, Queensland, Australia, Atmos. Chem. Phys. Discuss. [preprint], https://doi.org/10.5194/acp-2021-76, in review, 2021

Luther, A., Kleinschek, R., Scheidweiler, L., Defratyka, S., Stanisavljevic, M., Forstmaier, A., Dandocsi, A., Wolff, S., Dubravica, D., Wildmann, N., Kostinek, J., Jöckel, P., Nickl, A.-L., Klausner, T., Hase, F., Frey, M., Chen, J., Dietrich, F., Nęcki, J., Swolkień, J., Fix, A., Roiger, A., and Butz, A.: *Quantifying CH_4 emissions from hard coal mines using mobile sun-viewing Fourier transform spectrometry*, Atmos. Meas. Tech., 12, 5217–5230, https://doi.org/10.5194/amt-12-5217-2019, 2019.

Maazallahi, H., Fernandez, J.M. , Menoud, M., Zavala-Araiza, D., Weller, Z.D., Schwietzke, S., von Fischer, J.C., Denier van der Gon, H., and Röckmann, T.: *Methane mapping, emission quantification, and attribution in two European cities: Utrecht (NL) and Hamburg (DE)*, Atmos. Chem. Phys., 20, 14717–14740, https://doi.org/10.5194/acp-20-14717-2020, 2020

Maciej J. Kotarba, Jerry L. Clayton. "Coalbed Gases and Hydrocarbon Source Rock Potential of Upper Carboniferous Coal-Bearing Strata in Upper Silesian Coal Basin, Poland: ABSTRACT." AAPG Bulletin, vol. 80, 1996, 10.1306/522b3141-1727-11d7-8645000102c1865d.

S. Mailler, L. Menut, D. Khvorostyanov, M. Valari, F. Couvidat, G. Siour, S. Turquety, R. Briant, P. Tuccella, B. Bessagnet, A. Colette, L. Létinois, K. Markakis, and F. Meleux. CHIMERE-2017: from urban to hemispheric chemistry-transport modeling. Geoscientific Model Development, 10(6):2397–2423, 2017. https://www.geosci-model-dev.net/10/2397/2017/.

Mallet, V, D Quelo, B Sportisse, M Ahmed de Biasi, E Debry, I Korsakissok, L Wu, et al. 2007. "Technical Note: The Air Quality Modeling System Polyphemus." Atmos. Chem. Phys., 9.

McKain, Kathryn, Adrian Down, Steve M. Raciti, John Budney, Lucy R. Hutyra, Cody Floerchinger, Scott C. Herndon, et al. 2015. "Methane Emissions from Natural Gas Infrastructure and Use in the Urban Region of Boston, Massachusetts." Proceedings of the National Academy of Sciences 112 (7): 1941–46. https://doi.org/10.1073/pnas.1416261112

Manders, A., Builtjes, P., Curier, L., Gon, H., Hendriks, C., Jonkers, S., Kranenburg, R., Kuenen, J., Segers, A., Timmermans, R., Visschedijk, A., Wichink Kruit, R., Pul, W., Sauter, F., Swaluw, E., Swart, D., Douros, I., Eskes, H., Meijgaard, E., and Schaap, M.: Curriculum Vitae of the LOTOS-EUROS (v2.0) chemistry transport model, Geoscientific Model Development Discussions, pp. 1–53, https://doi.org/10.5194/gmd-2017-88, 2017

Marécal, V., Peuch, V.-H., Andersson, C., Andersson, S., Arteta, J., Beekmann, M., Benedictow, A., Bergström, R., Bessagnet, B., Cansado, A., Chéroux, F., Colette, A., Coman, A., Curier, R. L., Denier van der Gon, H. A. C., Drouin, A., Elbern, H., Emili, E., Engelen, R. J., Eskes, H. J., Foret, G., Friese, E., Gauss, M., Giannaros, C., Guth, J., Joly, M., Jaumouillé, E., Josse, B., Kadygrov, N., Kaiser, J. W., Krajsek, K., Kuenen, J., Kumar, U., Liora, N., Lopez, E., Malherbe, L., Martinez, I., Melas, D., Meleux, F., Menut, L., Moinat, P., Morales, T., Parmentier, J., Piacentini, A., Plu, M., Poupkou, A., Queguiner, S., Robertson, L., Rouïl, L., Schaap, M., Segers, A., Sofiev, M., Tarasson, L., Thomas, M., Timmermans, R., Valdebenito, Á., van Velthoven, P., van Versendaal, R., Vira, J., and Ung, A.: A regional air quality forecasting system over Europe: the MACC-II daily ensemble production, Geosci. Model Dev., 8, 2777–2813, https://doi.org/10.5194/gmd-8-2777-2015, 2015.

Martens, C.S., Kelley, C.A., Chanton, J.P., and Showers, W.J.: Carbon and hydrogen isotopic characterization of methane from wetlands and lakes of the Yukon-Kuskokwim delta, western Alaska, J. Geophys. Res. Okt.1992, https://doi.org/10.1029/91JD02885

Menoud, M., van der Veen, C., Scheeren, B., Chen, H., Szénási, B., Morales, R.P., Pison, I., Bousquet, P., Brunner, D., and Röckmann, T.: *Characterisation of methane sources in Lutjewad, The Netherlands, using quasi-continuous isotopic composition measurements*, Tellus B: Chemical and Physical Meteorology, 72, 1–19, https://doi.org/10.1080/16000889.2020.1823733, 2020

*Menoud, M., Röckmann, T., Fernandez, J., Bakkaloglu, S., Lowry, D., Korben, P., Yver Kwok, C.: mamenoud/MEMO2_isotopes: v8.1 complete (Version v8.1.0) [Data set]. Zenodo. http://doi.org/10.5281/zenodo.4062356, 2020

Menoud, M., van der Veen, C., Maazallahi, H., Hensen, A., Velzeboer, I., van den Buk, P., Delre, A., Korben, P., Schwietzke, S., Ardelean, M., Calcan, A., Baciu, C., Scheutz, C., Schmidt, M., and Röckmann, T.: CH_4 isotopic signatures of emissions from oil and gas extraction sites in Romania, in preparation

L. Menut, B. Bessagnet, D. Khvorostyanov, M. Beekmann, N. Blond, A. Colette, I. Coll, G. Curci, G. Foret, A. Hodzic, S. Mailler, F. Meleux, J.-L. Monge, I. Pison, G. Siour, S. Turquety, M. Valari, R. Vautard, and M. G. Vivanco. CHIMERE 2013: a model for regional atmospheric composition modelling. Geoscientific Model Development, 6(4):981–1028, 2013. doi:10.5194/gmd-6-981-2013. URL https://www.geosci-model-dev.net/6/981/2013/.

Milkov, A.V., Etiope, G., 2018. Revised genetic diagrams for natural gases based on a global dataset of >20,000 samples. Organic Geochemistry 125, 109–120. https://doi.org/10.1016/j.orggeochem.2018.09.002

Miller, John B., and Pieter P. Tans. 2003. "Calculating Isotopic Fractionation from Atmospheric Measurements at Various Scales." Tellus B: Chemical and Physical Meteorology 55 (2): 207–14. https://doi.org/10.3402/tellusb.v55i2.16697

Monteil, G.A., Houweling, S., Dlugockenky, E.J., Maenhout, G., Vaughn, B.H., White, J.W.C., Rockmann, T., 2011. Interpreting methane variations in the past two decades using measurements of CH4 mixing ratio and isotopic composition. Atmos. Chem. Phys. 11, 9141–9153. https://doi.org/10.5194/acp-11-9141-2011

Moser, R.D., Kim, J., Mansour, N.N. (1999): Direct numerical simulation of turbulent channel flow up to Re(τ)=590. Physics of fluids, Vol.11, No.4, 943-945.

NAEI, 2020. National Atmospheric Emissions Inventory in 2018. NAEI, London.

Fumiko Nakagawa, Urumu Tsunogai, Daisuke Komatsu, Keita Yamada, Naohiro Yoshida, Jun Moriizumi, Koichiro Nagamine, Takao Iida, and Yukimasa Ikebe. Automobile exhaust as a source of 13C- and D-enriched atmospheric methane in urban areas. Organic Geochemistry, 36:727–738, May 2005. doi: 10.1016/j.orggeochem.2005.01.003

Ni, Yunyan, et al. "Hydrogen Isotope of Natural Gas from the Xujiahe Formation and Its Implications for Water Salinization in Central Sichuan Basin, China." Journal of Natural Gas Geoscience, vol. 4, no. 4, Aug. 2019, pp. 215–230, 10.1016/j.jnggs.2019.08.003.

Nisbet, E.G., Fisher, R.E., Lowry, D., France, J.L., Allen, G., Bakkaloglu, S., Broderick, T.J., Cain, M., Coleman, M., Fernandez, J., Forster, G., Griffiths, P.T., Iverach, C.P., Kelly, B.F.J., Manning, M.R., Nisbet-Jones, P.B.R., Pyle, J.A., Townsend-Small, A., al-Shalaan, A., Warwick, N., and Zazzeri, G.: *Methane Mitigation: Methods to Reduce Emissions, on the Path to the Paris Agreement*;Reviews of Geophysics, 58, e2019RG000675, https://doi.org/10.1029/2019RG000675, 2020

NNFCC, 2019. Biogas map. Anaerobic Digestion [website]. http://www.biogas-info.co.uk/resources/biogas-map/

Omara, M., Zimmerman, N., Sullivan, M.R., Li, X., Ellis, A., Cesa, R., Subramanian, R., Presto, A.A., and Robinson, A.L.: Methane Emissions from Natural Gas Production Sites in the United States: Data Synthesis and National Estimate, Environ. Sci. Technol. 52, 12915−12925, 2018, DOI:10.1021/acs.est.8b03535

Pasquill, F. 1961. "Estimation of the Dispersion of Windborne Material" 90 (Meteorol. Mag.): 33–49.

Pataki, D. E., J. R. Ehleringer, L. B. Flanagan, D. Yakir, D. R. Bowling, C. J. Still, N. Buchmann, J. O. Kaplan, and J. A. Berry. 2003. "The Application and Interpretation of Keeling Plots in Terrestrial Carbon Cycle Research: APPLICATION OF KEELING PLOTS." Global Biogeochemical Cycles 17 (1). https://doi.org/10.1029/2001GB001850

Pearson, 1895: Karl Pearson: Notes on regression and inheritance in the case of two parents, Proceedings of the Royal Society of London, 1895

Phillips, Nathan G., Robert Ackley, Eric R. Crosson, Adrian Down, Lucy R. Hutyra, Max Brondfield, Jonathan D. Karr, Kaiguang Zhao, and Robert B. Jackson. 2013. "Mapping Urban Pipeline Leaks: Methane Leaks across Boston." Environmental Pollution 173 (February): 1–4. https://doi.org/10.1016/j.envpol.2012.11.003

Polag, D., May, T., Müller, L., König, H., Jacobi, F., Laukenmann, S., Keppler, F., 2015. Online monitoring of stable carbon isotopes of methane in anaerobic digestion as a new tool for early warning of process instability. Bioresour. Technol. 197, 161–170. https://doi.org/10.1016/j.biortech.2015.08.058

Pugh, C. A., Reed, D. E., Desai, A. R., & Sulman, B. N. (2018). Wetland flux controls: how does interacting water table levels and temperature influence carbon dioxide and methane fluxes in northern Wisconsin? Biogeochemistry, 137(1), 15–25. https://doi.org/10.1007/s10533-017-0414-x

Paul Quay, Johnny Stutsman, David Wilbur, Amy Snover, Ed Dlugokencky, and Tom Brown. The isotopic composition of atmospheric methane. Global Biogeochemical Cycles, 13:445–461, Jun. 1999. doi: 10.1029/1998GB900006.

Ražnjevic, A., van Heerwaarden, C., van Stratum, B., Hensen, A., Velzeboer, I,, van den Bulk, P., and Krol, M.: Large-eddy simulation of a point source methane plume in a realistic convective atmospheric boundary layer, in preparation

Ražnjevic, A., van Heerwaarden, C., and Krol, M.: Evaluation of OTM33A and car sampling plume measurement strategies under neutral conditions using direct numerical simulation, in preparation

Rella, C. W., Hoffnagle, J., He, Y., Tajima, S.: Local- and regional-scale measurements of CH_4, $\delta 13CH_4$, and C_2H_6 in the Uintah Basin using a mobile stable isotope analyzer, Atmos. Meas. Tech., 8, 4539–4559, https://doi.org/10.5194/amt-8-4539-2015, 2015.

Rella, Chris W., Tracy R. Tsai, Connor G. Botkin, Eric R. Crosson, and David Steele. 2015. “Measuring Emissions from Oil and Natural Gas Well Pads Using the Mobile Flux Plane Technique.” Environmental Science & Technology 49 (7): 4742–48. https://doi.org/10.1021/acs.est.5b00099

Richardson, S.J., Miles, N.L., Davis, K.J., Lauvaux, T., Martins, D.K., Turnbull, J.C., McKain, K., Sweeney, C., Cambaliza, M.O.L.: Tower measurement network of in-situ CO_2, CH_4, and CO in support of the Indianapolis FLUX (INFLUX) Experiment. Elem Sci Anth, 5, p.59. 2017

M. Rigby, A. J. Manning, and R. G. Prinn. The value of high-frequency, highprecision methane isotopologue measurements for source and sink estimation. Journal of Geophysical Research: Atmospheres, 117(D12), 2012. doi: 10.1029/2011JD017384. URL https://agupubs.onlinelibrary.wiley.com/doi/abs/10.1029/2011JD017384.

B. Ringeval, Pierre Friedlingstein, Charles Koven, Philippe Ciais, Nathalie de NOBLET, B. Decharme, and P. Cadule. Climate-CH4 feedback from wetlands and its interaction with the climate-CO2 feedback. Biogeosciences, 8:2137–2157, Aug. 2011. doi: 10.5194/bg-8-2137-2011

Rinne, J., Tuittila, E.-S., Peltola, O., Li, X., Raivonen, M., Alekseychik, P., … Vesala, T. (2018). Temporal Variation of Ecosystem Scale Methane Emission From a Boreal Fen in Relation to Temperature, Water Table Position, and Carbon Dioxide Fluxes. Global Biogeochemical Cycles, 32(7), 1087–1106. https://doi.org/10.1029/2017GB005747

Rinne, J., Tuovinen, J.-P., Klemedtsson, L., Aurela, M., Holst, J., Lohila, A., Weslien, P., Vestin, P.,Łakomiec, P., Peichl, M., Tuittila, E.-S., Heiskanen, L., Laurila, T., Li, X., Alekseychik, P., Mammarella, I., Ström, L., Crill, P., and Nilsson, M.B.: *Effect of the 2018 European drought on methane and carbon dioxide exchange of northern mire ecosystems*, Phil. Trans. R. Soc. B, 375: 20190517, http://dx.doi.org/10.1098/rstb.2019.0517, 2020

Röckmann, Thomas, Simon Eyer, Carina van der Veen, Maria E. Popa, Béla Tuzson, Guillaume Monteil, Sander Houweling, et al. 2016. “In Situ Observations of the Isotopic Composition of Methane at the Cabauw tall Tower Site.” Atmospheric Chemistry and Physics 16 (16): 10469–87. https://doi.org/10.5194/acp-16-10469-2016.

Roscioli, J. R., T. I. Yacovitch, C. Floerchinger, A. L. Mitchell, D. S. Tkacik, R. Subramanian, D. M. Martinez, et al. 2015. “Measurements of Methane Emissions from Natural Gas Gathering Facilities and Processing Plants: Measurement Methods.” Atmospheric Measurement Techniques 8 (5): 2017–35. https://doi.org/10.5194/amt-8-2017-2015

Satterthwaite, David. 2008. “Cities’ Contribution to Global Warming: Notes on the Allocation of Greenhouse Gas Emissions.” Environment and Urbanization 20 (2): 539–49. https://doi.org/10.1177/0956247808096127

Hinrich Schaefer. On the Causes and Consequences of Recent Trends in Atmospheric Methane. Current Climate Change Reports, Aug. 2019. doi:10.1007/s40641-019-00140-z.

Scheutz, C., Fredenslund, A.M., 2019. Total methane emission rates and losses from 23 biogas plants. Waste Manag. 97, 38–46. https://doi.org/10.1016/j.wasman.2019.07.029

Sherwood, O.A., Schwietzke, S., Arling, V.A., Etiope, G., 2017. Global inventory of gas geochemistry data from fossil fuel, microbial and burning sources, version 2017. Earth Syst. Sci. Data 9, 639–656. https://doi.org/10.5194/essd-9-639-2017

L.K. Smith, W.M. Lewis, J.P. Chanton, Greg Cronin, and Stephen K. Hamilton. Methane emissions from the Orinoco River floodplain, Venezuela. Biogeochemistry, 51:113–140, 2000. doi: https://doi.org/10.1023/A:1006443429909.

Sokal, R. R., and F. J. Rohlf. 1995. Biometry: The Principles and Practice of Statistics in Biological Research. 3rd ed. W.H. Freeman and Company.

Stanisavljević, M., Nęcki, J., Swolkień, J., Gałkowski, M., Maazallahi, H., Korbeń, P., Menoud, M., van der Veen, C., Röckmann, T., Schmidt, M., Wietzel, J., Vinković, K., Defratyka, S., Zieba, D., Chmura, L., and Wołkowicz, W.: Determination of methane emission rates and isotopic signatures from coal mine ventilation shafts in Upper Silesia, Poland, in preparation

Atsuko Sugimoto and Noboru Fujita. Hydrogen Concentration and Stable Isotopic Composition of Methane in Bubble Gas Observed in a Natural Wetland. Biogeochemistry, 81:33–44, Oct. 2006. doi: 10.1007/s10533-006-9028-4.

Swolkień, Justyna. "Polish Underground Coal Mines as Point Sources of Methane Emission to the Atmosphere." International Journal of Greenhouse Gas Control, vol. 94, Mar. 2020, p. 102921, www.sciencedirect.com/science/article/pii/S175058361930266X, 10.1016/j.ijggc.2019.102921

Szénási, B., Berchet, A., Pison, I., Broquet, G., Menoud, M., van der Veen, C., Scheeren, B., Chen, H., Röckmann, T., and Bousquet, P.: What can we learn about methane emissions from the comparison of measured and simulated methane isotopic ratios at a coastal monitoring site?, in preparation

Thanwerdas, J., Saunois, M., Berchet, A., Pison, I., Hauglustaine, D., Ramonet, M., Crevoisier, C., Baier, B., Sweeney, C., and Bousquet, P.: Impact of atomic chlorine on the modelling of total methane and its $^{13}C:{}^{12}C$ isotopic ratio at global scale, Atmos. Chem. Phys. Discuss., https://doi.org/10.5194/acp-2019-925, in review, 2019.

Thielemann, Thomas, et al. "Methane Exchange between Coal-Bearing Basins and the Atmosphere: The Ruhr Basin and the Lower Rhine Embayment, Germany." Organic Geochemistry, vol. 31, no. 12, Dec. 2000, pp. 1387–1408, 10.1016/s0146-6380(00)00104-2.

Thomas Thielemann, Bernhard Cramer, and Axel Schippers. Coalbed methane in the Ruhr Basin, Germany: A renewable energy resource? Organic Geochemistry, 35:1537–1549, Nov. 2004. doi: 10.1016/j.orggeochem.2004.05.004.

T. Thonat, M. Saunois, I. Pison, A. Berchet, T. Hocking, B. F. Thornton, P. M. Crill, and P. Bousquet. Assessment of the theoretical limit in instrumental detectability of northern high-latitude methane sources using d13cCH4 atmospheric signals. Atmospheric Chemistry and Physics, 19(19):12141–12161, 2019. https://acp.copernicus.org/articles/19/12141/2019/.

Townsend-Small, A., Tyler, S.C., Pataki, D.E., Xu, X., Christensen, L.E., 2012. Isotopic measurements of atmospheric methane in Los Angeles, California, USA: Influence of "fugitive" fossil fuel emissions. J. Geophys. Res. Atmos. 117(D7). https://doi.org/10.1029/2011JD016826

Townsend-Small, A., et al., 2016. Using stable isotopes of hydrogen to quantify biogenic and thermogenic atmopsheric methane sources: A case study from the Colorado Front Range, Geophys. Res. Lett. 11,462-11,471. https://doi:10.1002/ 2016GL071438

Toyoda, S., Suzuki, Y., Hattori, S., Yamada, K., Fujii, A., Yoshida, N., Kouno, R., Murayama, K., Shiomi, H., 2011. Isotopomer analysis of production and consumption mechanisms of N_2O and CH_4 in an advanced wastewater treatment system. Environ. Sci. Technol. 45, 917–922. https://doi.org/10.1021/es102985u

Turner, 1994; The Long Lifetime of the Dispersion Methods of Pasquill in U.S. Regulatory Air Modeling, 1994

Tuzson, B., Graf, M., Ravelid, J., Scheidegger, P., Kupferschmid, A., Looser, H., Morales, R. P., and Emmenegger, L.: *A compact QCL spectrometer for mobile, high-precision methane sensing aboard drones*, Atmos. Meas. Tech., 13, 4715–4726, https://doi.org/10.5194/amt-13-4715-2020, 2020.

Stanley C. Tyler, Donald R. Blake, and F. Sherwood Rowland. $^{13}C/^{12}C$ ratio in methane from the flooded Amazon forest. Journal of Geophysical Research: Atmospheres, 92(D1):1044–1048, 1987. doi: 10.1029/JD092iD01p01044. URL https://agupubs.onlinelibrary.wiley.com/doi/abs/10.1029/JD092iD01p01044

S. C. Tyler, R. S. Bilek, R. L. Sass, and F. M. Fisher. Methane oxidation and pathways of production in a Texas paddy field deduced from measurements of flux, d13C, and dD of CH4. Global Biogeochemical Cycles, 11(3):323–348, 1997. doi:10.1029/97GB01624. https://agupubs.onlinelibrary.wiley.com/doi/abs/10.1029/97GB01624.

M. Uzaki, H. Mizutani, and E. Wada. Carbon isotope composition of CH_4 from rice paddies in Japan. Biogeochemistry, 13:159–175, Apr. 1991. doi: https://doi.org/10.1007/BF00002775

Van Heerwaarden, C., van Stratum, B. J. H., Heus, T., Gibbs, J.A., Fedorovich E., Mellado, J.P. (2017): MicroHH 1.0: A computational fluid dynamics code for direct numerical simulation and large-eddy simulation of atmospheric boundary layer flows. Geosci. Model Dev.

Vinkovic, K., Andersen, T., de Vries, M., Kers, B., van Heuven, S., Peters, W., Hensen, A., and Chen, H.: Quantification of methane emissions from dairy cows using an Unmanned Aerial Vehicle (UAV) based active AirCore system and mobile van, in preparation

Wahlen, M., 1993. The global methane cycle. Annual Review of Earth and Planetary Sciences, 21(1), pp.407-426.

Wang, J., Zhang, J., Xie, H., Qi, P., Ren, Y., Hu, Z., 2011. Methane emissions from a full-scale A/A/O wastewater treatment plant. Bioresource Technology, 102(9), pp.5479-5485. https://doi.org/10.1016/j.biortech.2010.10.090

Wang, Y., Broquet, G., Ciais, P., Chevallier, F., Vogel, F., Kadygrov, N., Wu, L., Yin, Y., Wang, R., and Tao, S.: Estimation of observation errors for large-scale atmospheric inversion of CO2 emissions from fossil fuel combustion, Tellus B: Chemical and Physical Meteorology, 69, 1325 723, https://doi.org/10.1080/16000889.2017.1325723

Weller, Z. D., Yang, D. K. and von Fischer, J. C.: An open source algorithm to detect natural gas leaks from mobile methane survey data, edited by M. Mauder, PLoS One, 14(2), e0212287, doi:10.1371/journal.pone.0212287, 2019

Whiticar, Michael J. "A Geochemial Perspective of Natural Gas and Atmospheric Methane." Organic Geochemistry, vol. 16, no. 1-3, Jan. 1990, pp. 531–547, 10.1016/0146-6380(90)90068-b.

WMO. 19th WMO/IAEA Meeting on Carbon Dioxide, Other Greenhouse Gases, and Related Measurement Techniques (GGMT-2017) 27–31 August 2017, Dübendorf, Switzerland, Technical publications GAW Report No. 242, 2018. World Meteorological Organization, Geneva, Switzerland.

Wutzler, T., Lucas-Moffat, A., Migliavacca, M., Knauer, J., Sickel, K., Šigut, L., … Reichstein, M. (2018). Basic and extensible post-processing of eddy covariance flux data with REddyProc. Biogeosciences, 15(16), 5015–5030. https://doi.org/10.5194/bg-15-5015-2018

Xinyi, L., Harris, S.J., Fisher, R.E., France, J.L., Nisbet, E.G., Lowry, D., Röckmann, T., van der Veen, C., Menoud, M., Schwietzke, S., and Kelly, B.F.: *Isotopic Signatures of Major Methane Sources in the Coal Seam Gas Fields and Adjacent Agricultural Districts, Queensland, Australia;* ACP discussions preprint discussion started: 5 February 2021, https://doi.org/10.5194/acp-2021-76

Xueref-Remy, I., G. Zazzeri, F.M. Bréon, F. Vogel, P. Ciais, D. Lowry, and E.G. Nisbet. 2019. "Anthropogenic Methane Plume Detection from Point Sources in the Paris Megacity Area and Characterization of Their Δ13C Signature." Atmospheric Environment, October, 117055. https://doi.org/10.1016/j.atmosenv.2019.117055

Yacovitch, Tara I., Scott C. Herndon, Gabrielle Pétron, Jonathan Kofler, David Lyon, Mark S. Zahniser, and Charles E. Kolb. 2015. "Mobile Laboratory Observations of Methane Emissions in the Barnett Shale Region." Environmental Science & Technology 49 (13): 7889–95. https://doi.org/10.1021/es506352j

Yang, S., Lan, X., Talbot, R., Liu, L., 2019. Characterizing anthropogenic methane sources in the Houston and Barnett Shale areas of Texas using the isotopic signature $\delta^{13}C$ in CH_4. Sci. Total Environ. 696, 133856. https://doi.org/10.1016/j.scitotenv.2019.133856

Zazzeri, G., D. Lowry, R. E. Fisher, J. L. France, M. Lanoisellé, C. S. B. Grimmond, and E. G. Nisbet. 2017. "Evaluating Methane Inventories by Isotopic Analysis in the London Region." Scientific Reports 7 (1). https://doi.org/10.1038/s41598-017-04802-6.

Zazzeri, G., D. Lowry, R.E. Fisher, J.L. France, M. Lanoisellé, and E.G. Nisbet. 2015. "Plume Mapping and Isotopic Characterisation of Anthropogenic Methane Sources." Atmospheric Environment 110 (June): 151–62. https://doi.org/10.1016/j.atmosenv.2015.03.029

G. Zazzeri, Lowry, D., Fisher, R., France, J., Lanoisellé, M., Kelly, B., Necki, J., Iverach, C., Ginty, E., Zimnoch, M., Jasek-Kami´nska, A., and Nisbet, E.: Carbon isotopic signature of coalderived methane emissions to the atmosphere: From coalification to alteration. Atmospheric Chemistry and Physics, 16:13669–13680, Nov. 2016. doi: 10.5194/acp-16-13669-2016.